



New Scientific and News Editors from 2004

Scientific Editor



Walter Leitner was born in Pfarrkirchen, Bavaria, on 2 February 1963. He is married to Andrea Leitner and they have two children (Eva-Maria, 10, and Johannes, 8). He is Professor for Technical Chemistry and Petrochemistry at the RWTH Aachen (successor to Willi Keim) and External Scientific Member of the Max-Planck-Institute for Coal Research, Mülheim, Germany. His research interests are focused on transition metal complexes as catalysts for chemical transformations and the use of supercritical fluids as benign reaction media. The scientific achievements of his group have been recognized *inter alia* with the Gerhard-Hess-Award of the German Science Foundation, the Carl-Zerbe-Award, the 2nd International Messer Innovation Award and the Otto-Roelen-Medal. He is co-editor (with P. G. Jessop) of the book "Chemical Synthesis using Supercritical Fluids" and chairman of the conference series "Green Solvents for Synthesis".

News Editor



Markus Hölscher received his Ph.D. from the RWTH-Aachen for the synthesis and characterization of microporous heteropolytungstates and -molybdates with Professor W. Hölderich in 1995. From 1995 he worked as editor and interpreter for *Angewandte Chemie*, but in 2000 he joined Professor Höcker's group, investigating the mechanisms of zirconocene-catalyzed polymerisations of acrylates by means of quantum chemical calculations. In 2002 he moved to Professor Leitner's group, exploring the mechanisms of transition metal-catalyzed reactions using theoretical calculations.

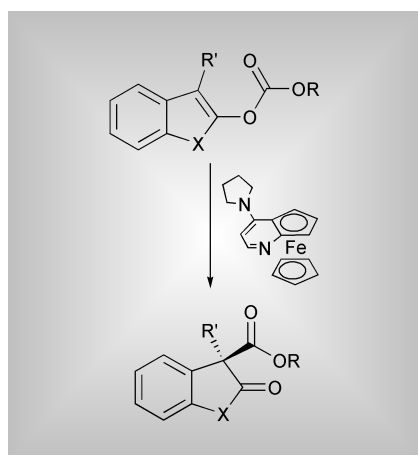


Highlights

Duncan Macquarrie reviews some of the recent literature in green chemistry

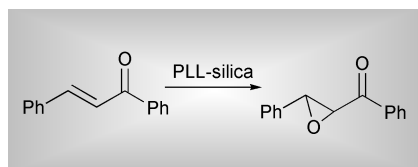
Enantioselective synthesis

The catalytic enantioselective synthesis of chiral quaternary carbons is a very difficult task. Ivory Hills and Greg Fu of MIT have now published a very efficient route to one class of these compounds (*Angew. Chem., Int. Ed.*, 2003, **42**, 3921). A series of oxindoles and benzofurans



with chiral quaternary centres are of interest as bioactive compounds, and they can be prepared using a chiral base-catalysed rearrangement of *O*-acylated precursors. Using the chiral analogue of DMAP shown in the scheme, they found that excellent ee's (up to 98%) could be achieved, with bulky R groups being preferred.

The use of silica-supported poly (*L*)-leucine for the enantioselective Julia-Colonna epoxidation of electron-deficient alkenes is one of the most effective and green methods for this transformation. Now Stan Roberts and his

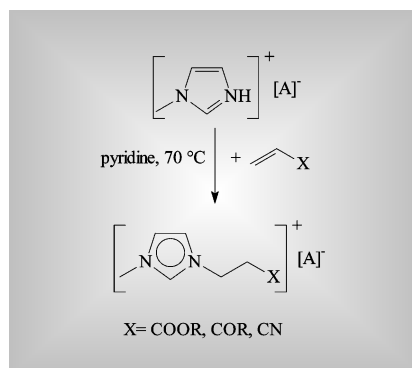


team at the University of Liverpool and Degussa have published details of a large-scale preparation and use of this material (*Org. Proc. Res. Dev.*, 2003, **7**, 509). It is now possible to prepare the catalyst on a multi-hundred-gram scale and the new

route is considerably more efficient than the old one. Fewer details were given about the epoxidations (except the expected effects of stirrer speed)—these will be given elsewhere.

Ionic liquids

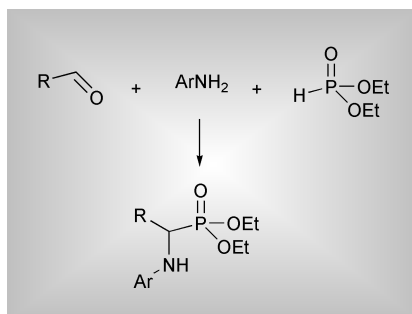
Functional ionic liquids (where one of the chains contains a functional group) have attracted little attention despite their potential for improved solubility. This is partly due to complex syntheses. Now Peter Wasserscheid and colleagues from the RWTH Aachen have described a



simple approach to their preparation (*Chem. Commun.*, 2003, 2038). This involves the protonation of *N*-methylimidazole and subsequent Michael addition to acrylonitrile or methyl vinyl ketone, amongst others. Yields are essentially quantitative.

Solvent-free reactions

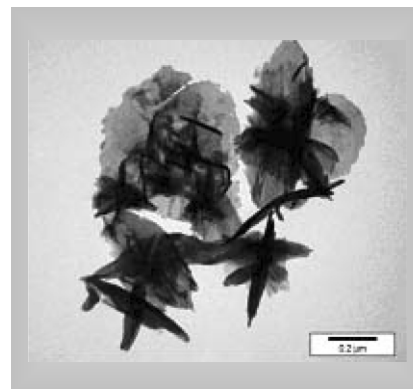
A solvent-free three-component reaction has been published by the group led by Takahiko Akiyama at Gakushuin University in Tokyo (*Synlett*, 2003, 1463). They have shown that the coupling of an



aldehyde, an amine and diethyl phosphite using trifluoroacetic acid as catalyst leads directly to the aminophosphonate product in essentially quantitative yield, considerably higher than when typical organic solvents are used (yields range from 13–83% compared to 96% with no solvent). A range of aromatic amines all give excellent yields at room temperature.

Materials synthesis

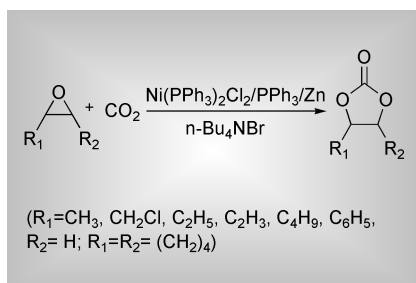
The synthesis of bismuth selenide has been approached from many angles in attempts to make the material, which has potential in a range of applications involving thermomechanical or electromechanical measurement and other



sensing applications. R. Harpeness and A. Gedanken of the Bar-Ilan University in Ramat-Gan, Israel, have now applied a microwave route to its synthesis (*New J. Chem.*, 2003, **27**, 1191). They utilise a combination of a polyol as solvent and reducing agent along with bismuth oxynitrate and elemental selenium. The process yields good quality Bi₂Se₃ in a less wasteful manner compared to other routes. The synthesis of other analogous materials is being investigated.

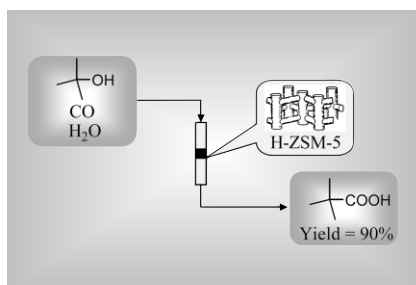
Insertion reactions

The coupling of epoxides and carbon dioxide to give cyclic carbonates represents a nice way to generate useful functionality and to utilise carbon dioxide. While several catalytic systems have been described, Chungu Xia and co-workers from the State Key University of the Chinese Academy of Sciences at Lanzhou is claimed to be amongst the



best (*Chem. Commun.*, 2003, 2042). They have developed a complex Ni/Zn system which is air-stable and simple to prepare. It doesn't require any co-solvents and has excellent activity. Excellent yields and selectivities are obtained along with very high activity.

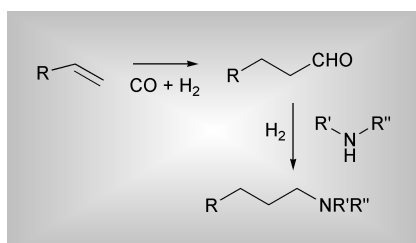
The insertion of carbon monoxide is also an interesting transformation and here the Koch reaction is important. This reaction converts alcohols to carboxylic acids using CO insertion. Normally this requires considerable amounts of very strong acids, but now it has been shown



that zeolites can replace the liquid acids and improve the recoverability of the acid component. Qiang Xu and colleagues at the AIST in Osaka have demonstrated that H-ZSM5 will convert *t*-BuOH to the acid in excellent yield and high selectivity with no deactivation even after 120 h on stream in a continuous gas-phase process (*Chem. Commun.*, 2003, 2070).

Amine synthesis

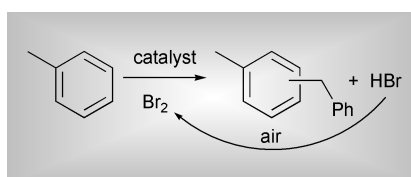
A clean and simple synthesis of amines has been developed by Matthias Beller and his colleagues at the University of Rostock (*J. Am. Chem. Soc.*, 2003, **125**, 10311). They have extended the hydroformylation methodology to include



imine formation and reduction of the aldehyde product. All this is achieved in one step, utilising a cationic Rh catalyst, an alkene, CO, an amine and hydrogen. It proved possible to tune conditions such that the desired sequence proceeds with minimal formation of undesired side products.

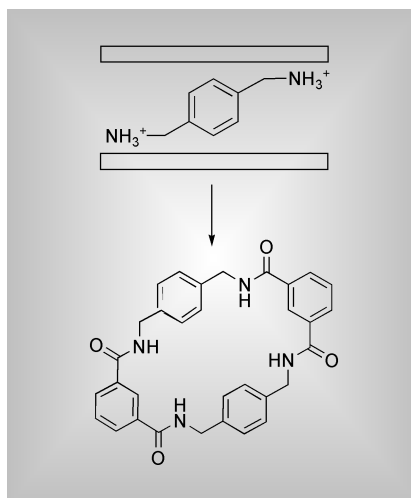
Clays

The Friedel–Crafts reaction remains a popular target for improved catalytic systems. One interesting paper which has recently been published by Benita Barton and colleagues from the Catalysis Research Unit at the Port Elizabeth Technikon (*Org. Proc. Res. Dev.*, 2003, **7**,



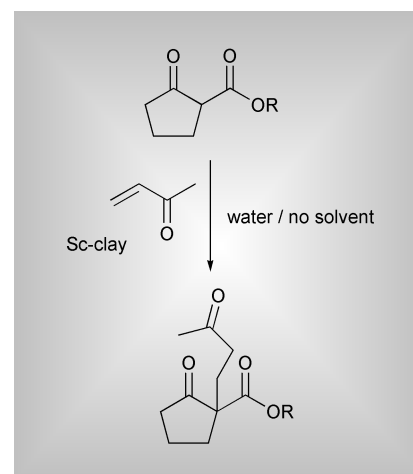
571) relates to the use of modified clays as catalysts for the coupling of toluenes *via* bromination–Friedel–Crafts reaction. The HBr formed is then re-oxidised to bromine and reused, making the process catalytic in bromine. Careful control of clay activation, the nature and loading of the metal exchanged into the clay, and final catalyst activation is critically important to the selectivity (primarily avoiding ring bromination), but the best systems gave complete selectivity towards the Friedel–Crafts product.

Clays have been used as host templates for the efficient synthesis of macrocycles. Dimitrios Petridis and co-workers at the Institute of Materials Science, NCSR Demokritos in Athens and the University of Ioannina have shown that the interlayer galleries can serve to organise on



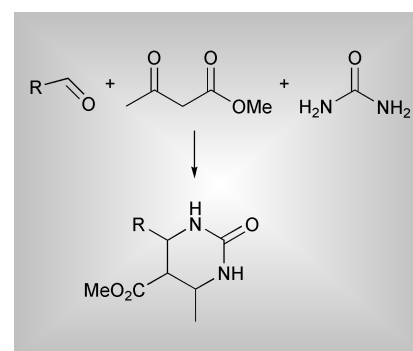
coupling partner in such a way as to encourage the selective formation of rings rather than linear oligomers (*Chem. Eur. J.*, 2003, **9**, 3904). In this way, high dilution can be avoided and the catalyst can be recovered and reused. Yields are typically 60–65%.

A very simple procedure for the Michael addition reaction has been described by Kiyotomo Kaneda and his groups at Osaka University (*J. Am. Chem. Soc.*, 2003, **125**, 10486). They have used



a Sc-exchanged montmorillonite clay as a reusable catalyst for the Michael addition. Yields are excellent at a 1:1 stoichiometry, and the reactions can be carried out either in water or solvent-free. Interestingly, the catalyst is significantly more active than scandium triflate itself.

A further use of clays has been detailed by Alok Kumar Mitra and Krishna Banerjee of the University of Calcutta in



India (*Synlett*, 2003, 1509). They have shown that clays can be used as hosts and catalysts for the solvent-free, microwave-induced conversion of ketoesters, aldehydes and urea into pyrimidines. Yields are excellent and times are short. While extraction of the product is



required, novel reaction engineering combined with these reactions would potentially lead to a very simple and clean method.

Reviews

- Ryoji Noyori at Nagoya University and colleagues from Tokyo Institute of Technology and the National Institute of Advanced Industrial Science and Technology in Ibaraki have published a feature article concerning the use of hydrogen peroxide as a green oxidant for a variety of processes. (*Chem. Commun.*, 2003, 1977).
- Abraham Stroock and George Whitesides of Harvard University have published a review entitled 'Controlling Flow in Microchannels with Patterned Surface/Charge and Topography' which will be of interest to those working in miniaturisation (*e.g.* analytical, high-throughput and microreactors) (*Acc. Chem. Res.*, 2003, **36**, 597).
- Marcel Moreño-Manas and Roser Pleixats of the Universitat Autònoma de Barcelona in Spain have published an overview of the use of metal nanoparticles in the catalysis of C–C bond forming reactions (*Acc. Chem. Res.*, 2003, **36**, 638).
- Issue 8 of *Chemical Reviews* is dedicated to the theme of enantioselective catalysis, with 22 reviews covering a wide range of topics (*Chem. Rev.*, 2003, **103**, 8).
- Jean-Marie Brégeault of the Université Pierre et Marie Curie in Paris has published a review covering liquid-phase oxidation reactions catalysed by transition metal complexes, focussing on industrially important reactions (*Dalton Trans.*, 2003, 3289).
- Richard Hsung and colleagues at the University of Minnesota, USA, have published a short review entitled 'In search of an Atom-Economical Synthesis of Ynamides' which looks at various approaches to these versatile but awkward to prepare compounds (*Synlett*, 2003, 1379).

Green Chemistry

An Introductory Text

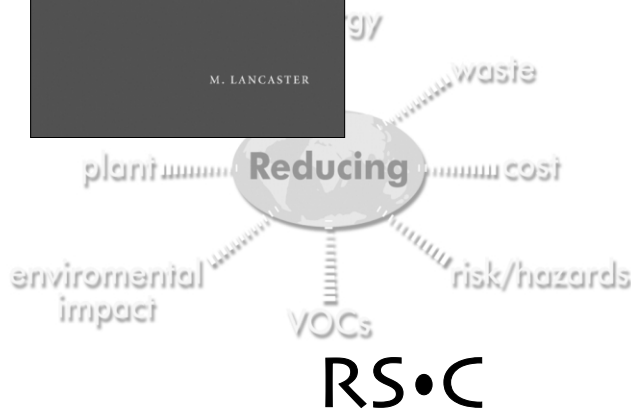
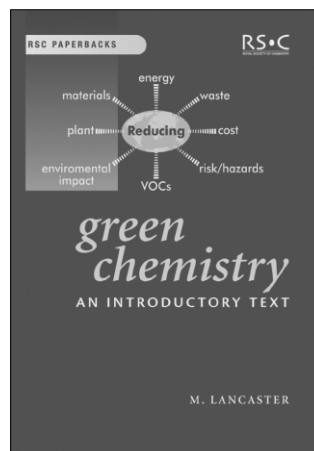
BY M LANCASTER

University of York, UK

The challenge for today's new chemistry graduates is to meet society's demand for new products that have increased benefits, but without detrimental effects on the environment. **Green Chemistry: An Introductory Text** outlines the basic concepts of the subject in simple language, looking at the role of catalysts and solvents, waste minimisation, feedstocks, green metrics and the design of safer, more efficient, processes. The inclusion of industrially relevant examples throughout demonstrates the importance of green chemistry in many industry sectors.

Intended primarily for use by students and lecturers, this book will also appeal to industrial chemists, engineers, managers or anyone wishing to know more about green chemistry.

Softcover | 2002 | viii + 310 pages | ISBN 0 85404 620 8 | £25.00
RSC members' price £16.25



advancing the chemical sciences

Orders & further details Sales & Customer Care Dept
Royal Society of Chemistry · Thomas Graham House
Science Park · Milton Road · Cambridge · CB4 0WF · UK

T +44(0)1223 432360 · F +44(0)1223 426017 · E sales@rsc.org
Or visit our websites: www.rsc.org and www.chemsoc.org
Registered Charity No. 207890



GSC TOKYO 2003

Makoto Misono, Chair of the Planning Committee, introduces this special issue on The First International Conference on Green & Sustainable Chemistry, held in Tokyo during March 2003.



From 13–15 of March, 2003, when the cherry started to bloom in Japan, the First International Conference on Green and Sustainable Chemistry, GSC TOKYO 2003, was held at the Waseda University International Conference Center, Tokyo (the funding for the center's main hall was a donation from Dr. Ibuka, the founder of SONY Corp. and a graduate of the university).

The conference was organized by the GSC Network, Japan, in collaboration with foreign and domestic organizations, including GCI/ACS (USA), GCN/RSC (UK), DECHEMA (Germany), CEFIC, several embassies, OECD, and many Japanese organizations such as the three Ministries, the Science Council, the Chemical Industry Association, and several academic societies. We had about 760 participants from 21 countries (*ca.* 120 from overseas), and 27 lectures, two panel discussions, 120 posters and 49 exhibitions. In addition, a student forum was organized on the 12th and 16th of March. During the conference, three GSC awards from the Japanese Ministers (Ministers of Economics, Trade and Industry, Minister of Education, Culture, Sports, Science and Technology, Minister of Environment) were presented and the achievements of the awardees were celebrated.

GSC is defined as innovative chemical technology to minimize the consumption of depletive resources and the discharge of wastes through the life cycle of chemical products and processes, and to secure the health and safety of mankind and the environment. Green, or sustainable, chemistry (GC or SC) has similar aims and may be regarded as the same.

The organizing committee (chairman; K. Yamamoto, Asahi Chemical) attempted to make this conference remarkable in three aspects. Firstly, the conference was organized truly internationally. During the preparations, we closely communicated with foreign key people and organizations, and tried to reflect the results of these communications in the program. This may be evident from the fact that the number of speakers from abroad was greater than that of domestic speakers. In addition to the Japanese GSC awardees, recipients of GC awards in Australia, the UK and the US also gave lectures. Secondly, the conference was supported strongly and equally by academia, industry and governments, as seen by the top-class

speakers and participants from all of these sectors. Thirdly, the program covered a very broad range of topics from basic research to real industry and also included education and metrics. For education and metrics, we organized two special symposia and a student forum. The latter was held with great success. We believe these issues are very important for the sound development of green and sustainable chemistry in the future.

The next GSC conference will be held in 2005 in the United States. We hope that the basic ideas of this conference will be followed and further developed.

To end this Foreword, let me cite words from my closing remarks of the conference.

“We all know the important roles that the chemical sciences and technology have played in the past and will play in the future. We also know that the chemical science and technology of the future should not be the same as that we had in the last century.

Although we have different opinions from ecological, sociological and economical viewpoints about what kind of chemistry should be pursued and how to establish it, through the GSC conference, we were able to identify to a significant degree the problems we must solve and the direction we must proceed in. Now we share a common idea that the chemistry we pursue must be friendly and at the same time beneficial to the environment and human beings, and that this chemistry is indispensable for the sustainable development of our society. This chemistry is GSC. In short, GSC is the chemical science and technology for society, or that trusted and relied upon by the general public.

GSC will be achieved only by the integration of continuing efforts of chemists and chemical engineers to approach this goal, while the goal is not easy to reach. Here international collaborations and collaborations between academia, industry and government are very necessary. Collaboration should also occur outside the chemical community, for example, with mass media, NGO, and school teachers. All of these concepts are included in the Tokyo Statement which was declared at the end of the conference. Let us strengthen our efforts directed towards this goal and make strong strides to it, individually and as a whole.

Finally, the organizing committee wishes to express sincere thanks to all for the wonderful lectures and discussions. Thanks are also given for the support from many people and institutions.”

In this issue, the major achievements of the conference, including the Tokyo Statement and discussions on metrics and education, are reported. Several outstanding scientific presentations are also collected. We hope these are of interest to all who are concerned about GSC/GC/SC and are useful for its progress.



1st International Conference on Green & Sustainable Chemistry (GSC TOKYO 2003)

Kohichi Segawa, Chairman of the Local Committee for GSC TOKYO 2003 describes this important new event

In March 13–15, 2003, GSC TOKYO 2003 was held at the International Conference Center of Waseda University, organized by the Green & Sustainable Chemistry Network, Japan (<http://www.gscn.net>). There were about 760 participants at the conference, including 120 overseas participants from 20 countries.

There were 12 sessions of oral presentations and 130 poster presentations at the conference. These presentations, together with the accompanying exhibition, showed the full range of industrial and scientific developments in green and sustainable chemistry (GSC). Lectures at the plenary, keynote and general session at GSC TOKYO 2003 are summarized follows:

Session 1 (Plenary Lecture)

M. Fitzpatrick (Rohm & Haas, USA) – *Green and Sustainable Chemistry: Driving Success through Collaboration*. The importance of collaborations between various sectors was stressed; e.g. external collaborations between industry and NGO, and internal collaborations within the industrial sectors.

T. Nishide (Ministry of Economy, Trade and Industry, Japan) – *Green & Sustainable Chemistry in Japan*. The following subjects were discussed with many figures and examples:

- Maintenance of legal system related to environment and administration of chemical substances
- History of industrial technology and industrial ecology policy
- R&D activities related GSC
- GSC activities in domestic companies
- International collaboration
- GSC Award

Session-2 (Keynote Lecture : Industry's Vision toward GSC)

B. Cue (Pfizer Inc, USA) – *Pfizer's*

Vision on Green and Sustainable Chemistry. The benefits of practicing the principles of green chemistry include lower costs, more robust manufacturing processes, easier technology transfer leading to product launch readiness and sustained supply, higher level of regulatory compliance and positive public image. Examples of products introduced recently by the company were discussed from the viewpoint of GSC.

D. Nissen (BASF, Germany) – *Sustainable Development and Profitable Growth—Challenges for a Global Chemical Corporation*. Sustainable development over the long term is a necessary precondition for profitable growth of a company. In addition, chemical industry has a responsibility to contribute to meeting future challenges posed by sustainable development. Activities by BASF in this area were presented, including eco-efficiency analysis.

A. Kosai (Sumitomo Chemicals, Japan) – *Sumitomo Chemical and Sustainable Development*. The history and background of a Japanese chemical industry, Sumitomo Chemical, was described from the viewpoint of sustainable development and illustrative examples of the company's achievements and the role of chemical industry in the future were presented.

Session 3 (Keynote Lecture: Science & Technology for GSC)

R. Sheldon (Delft University of Technology, Netherlands) – *Green Chemistry and Catalysis for Sustainable Organic Synthesis*. It was stressed that catalysis is the key technology in developing innovative organic synthesis based on the concept of GSC. Recent developments in homogeneous, heterogeneous and biocatalysis were reviewed in the context of fine chemical synthesis with emphasis on chemo-,

regio- and stereo- selectivity issues and the use of novel reaction media and catalyst recycling.

A. Steinbuechel (Muenster University, Germany) – *Microbial Systems for Production of Polyesters and Polyamides from Renewable Resources*. The currently available technically relevant PHAs and polyamides from microorganisms, as well as on the production, properties and applications of these biopolymers, were reviewed and the concept and potential of biotechnology in synthesis of a wide variety of polyesters and polyamides by recombinant DNA were discussed. It was stressed that control of reactivity and specificity of polymerases is possible by optimizing reaction conditions and molecular transformation reactions.

H. Komiyama (University of Tokyo, Japan) – *Sustainable Chemical Technology and the Importance of Information Infrastructure*. The current status of the chemical industry was analyzed from the viewpoint of environment and energy. It was shown that designing the complexity of systems is a fundamental issue, and the background, recent research and future perspective on the structure of information infrastructure were discussed. The importance and conditions for constructing chemical information infrastructures, as a base of GSC in the chemical industry were emphasized.

Session 4 (Panel Discussion, Education & Enlightenment for GSC)

This session was organized to improve the reliability of society on chemistry by promoting information exchange, enlightenment and communications among students, high school teachers, researchers in academic and industrial sectors. Although the number of participants was not large, the discussions



were quite active and the importance of education, especially communications between chemists and society and GSC oriented education for children, was emphasized.

H. Tsuge, (Keio University) chaired the session consisting of the following lectures and panel discussion. This session was open to non-registrants.

Lectures by the panelists:

- H. Tsuge (Keio University, Japan) – *Perspectives of Green & Sustainable Chemistry Education in the World*
- J. Warner (University of Massachusetts, Boston, USA) – *Green Chemistry and Science Education for Everyone*
- J. Clark (University of York, UK) – *Green Chemistry and the Consumer*
- T. H. Lee (Yonsei University, Korea) – *A Current Statuses of GSC Research & Education Program in Korea*
- K. Ogino (Tohoku University, Japan) – *Green & Sustainable Chemistry Education in Japan*

Session 5 (Presentation by GC/GSC Award Winners)

Past GC/GSC Award winners from 4 countries presented their work:

- S. Konishi (Nippon Paint, Japan) – *Development of Recyclable Waterborne Coating System Aiming for Green Sustainable Market*
- H. Tsuzuki (Fuji Photo Film, Japan) – *Development of the Aquo-coated Photo-thermographic Material*
- K. Kaneda (Osaka University, Japan) – *Development of Environmentally Friendly Heterogeneous Metal Catalysts using Inorganic Crystallines as Macroligands*
- C. Strauss (Monash University, Australia) – *Thermal Green Chemistry*
- I. Dobson (British Petroleum, UK) – *Leaps of Innovation*

Session 6 (Accomplishments by Academia/Industry Collaboration)

P. G. Rieger (Stuttgart University, Germany) – *From End of Pipe to Product Integrated Environmental Protection*

X. H. Wang (CIAC, P. R. China) – *Fixation of Carbon Dioxide into*

Biodegradable Plastics, From Lab Curiosity to Industrial Practice

L. Rothman (SC Fluids, USA) – *Cleaning Semiconductor Wafers with Supercritical Fluids*

N. Sayo (Takasago International, Japan) – *Practical Asymmetric Synthesis in Takasago*

Session 7 (Implementation of GSC by Industry)

J. Joosten (DSM, Netherlands) – *The Importance of Sustainability for DSM*

E. Tanaka (Mitsubishi Chemicals, Japan) – *The Environmentally Friendly Plastic Products and Eco-System in Mitsubishi Chemical Group.*

E. Ohno (Toyota Motor, Japan) – *TOYOTA's Challenge on Environmental Issue*

D. Bhasker (Ondeo-Nalco, USA) – *Holistic Approach to Sustainable Development in Pulp and Paper Industry*

Session 8 (Panel Discussion, Metrics for GSC)

I. Yasui, (The University of Tokyo, Japan) chaired the session consisting of the following lectures and panel discussion:

Panelists:

- H. J. Klueppel (Henkel, Germany) – *From Vision to Measurement*
- S. Sikdar (EPA, USA) – *Scope and Limitation of Sustainability Metrics for Products and Processes*
- T. Ibusuki (AIST, Japan) – *Introduction and Evaluation of GSC Related R&D Projects in AIST*
- P. Norling (RAND, USA) – *Green Chemistry: How Do We Measure Success?*
- A. Curzons (Glaxo Smith Kline, UK) – *Metrics to Green Chemistry- Selection and Their Use*
- I. Yasui (The University of Tokyo, Japan) – *Green and Sustainable Indices for the Evaluation Process of GSC Awards in Japan*

Session 10 (Frontiers of GSC)

Challenges and recent progress in the frontiers of GSC were discussed by four specialists in organic chemistry:

- C. J. Li (Tulane University, USA) – *The Taoism of Developing Green*

Chemistry for Multi-step Synthesis

- H. Puetter (BASF, Germany) – *Recent Electrochemical Contributions to Green Chemistry- Will They Enhance Sustainability?*
- Neil Bruce (University of York, UK) – *Novel Biocatalytic Processes for the Production of Semi-synthetic Opiate Drugs*
- G. Francio (ITMC Aachen, Germany) – *Green Catalytic Processes with Ionic Liquids/Supercritical Carbon Dioxide Media*

Session 11 (Keynote Lecture: GSC, Present and Future)

R. Breslow (Columbia University, USA)

– *Greening of Chemistry: Environmental Challenges for Chemists.* First his recent work on “Beyond the Molecular Frontier—Challenges for Chemistry and Chemical Engineering in the 21st Century” was briefly introduced. His work on Green Chemistry was presented. Use of benign solvents, organic reactions in water, the hydrophobic effect including increasing rates and promoting useful selectivity and finally results of his recent works were also discussed.

T. Connelly (DuPont, USA) – *DuPont's R&D Strategy for Green Chemistry for Sustainable Growth.* For sustainability to become a reality it must be part of the everyday life and action of a company. At DuPont, sustainable growth objectives are incorporated into the overall program of scientific research, product innovation and business development. Examples such as a catalysis for waste free synthesis of fluoroaromatics, Nafion's catalytic activities and immobilized biocatalyst for manufacturing a starting material for agricultural product were presented.

Session 12 (GSC, Tokyo Statement)

P. Anastas (OSTP, USA) and S.

Murahashi (Okayama University of Science, Japan). The Tokyo Statement was declared by the participants of GSC TOKYO 2003 to promote ‘Green and Sustainable Chemistry (GSC)’ as a key initiative in the ongoing efforts to achieve sustainable development.



Metrics for Green and Sustainable Chemistry

Itaru Yasui, from the Institute of Industrial Science at the University of Tokyo, reports from a Panel Discussion at the First International Conference on Green & Sustainable Chemistry held in Japan

The first trial to discuss the metrics of Green and Sustainability Chemistry (GSC) took place at the First International Conference on GSC as a panel discussion. The panelists tried to clarify what is green and what is sustainability. They all pointed out the importance of metrics, and some direction for further discussion was fixed. It was not an easy task to reach one conclusion with full agreement, so it will need future trials at the next conference to find common metrics for green and sustainability.

Outlines of the presentations

Six presentations with different topics are summarized very briefly as follows:

Hans-Jørgen Klüppel, Henkel KGaA, 'From Vision to Measurement'

This presentation started with the definition of green and sustainability, followed by an introduction to the activities of DECHEMA. An industry-specific definition of sustainability for the detergent industry was discussed. Nine topics for sustainability, to be used in the reports as a consumer communication tool, were defined, and corresponding indicators for each were discussed. See Fig. 1 for Klüppel's chosen slide.

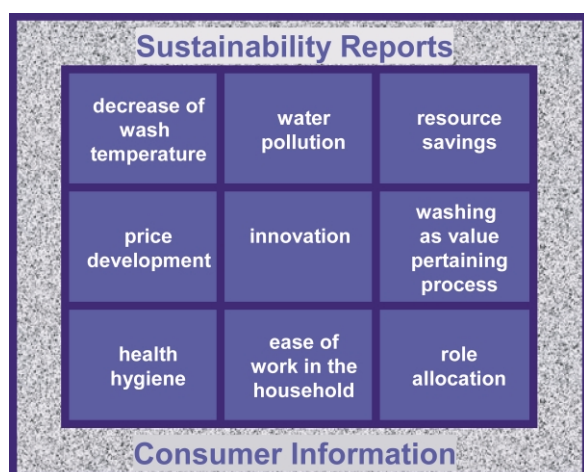


Fig. 1 Nine topics for sustainability.

Subhas K. Sikdar, National Risk Management Research Laboratory, US EPA, 'Scope and Limitations of Sustainability Metrics for Products and Processes'

The definition of sustainability was discussed first. The original definition in the Brundtland Report was modified to include ecological capabilities by US EPA.

The triple bottom line concept, with three kinds of aspects was interpreted. We are still in the very preliminary stage of Metrics. A very impressive figure 'Road to Metrics' was presented. See Fig. 2 for Sikdar's chosen slide.

Takashi Ibusuki, National Institute of Advanced Industrial Science and Technology, 'Introduction and Evaluation of GSC Related R&D Projects in AIST'

Several research activities, including developing minimum energy chemical process or emission control technology with lower energy and resource consumption, were explained; e.g. a one-step propylene oxide synthesis can improve the E-factor from 2.2 to 0.3. The effects of improvement were schematically expressed by the use of the Four Axes Method proposed by Yasui. See Fig. 3 for Ibusuki's chosen slide.



Fig. 2 The Road to Sustainability.

Parry M. Norling, 'Green Chemistry: How Do We Measure Success?'

A trial to evaluate activities for research and development in the field of Green Chemistry was introduced. Performance of a research system can be measured with input, in-process, output and outcome metrics. For example, input metrics might include the number of students studying green chemistry, or the size of grants in green chemistry, or the number of environmental problems being attacked. See Fig. 4 for Norling's chosen slide.

Alan Curzons, GlaxoSmithKline, 'Metrics to Green Chemistry — Selection and Use'

First he explained that metrics are essential for a variety of reasons. They help scientists understand issues, enable benchmarking, and allow improvement targets to be set. A set of core 'sustainable metrics' were identified: Mass, Energy, Toxic dispersion, Natural resource utilization, Solvents, Economics. Yield remains a very good metric from an economic standpoint. Several systems to choose solvents, for example, were explained. See Fig. 5 for Curzon's chosen slide.



One Step Propylene Oxide (PO) Synthesis Improvement of E-factor

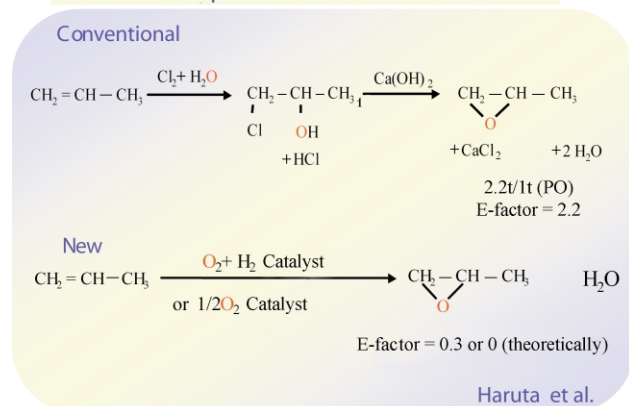


Fig. 3 One-step propylene oxide synthesis.

Itaru Yasui, IIS, University of Tokyo, 'Green and Sustainable Indices for the Evaluation Process of GSC Awards in Japan'

GSC Awards started in FY2001, and LCA-based metrics have been introduced to express environmental aspects for sustainability. The Four axes method was proposed as a method to evaluate relative improvement of products/processes from an environmental viewpoint. Another criterion is used by the selection committee for evaluation or reduction of risks by the avoidance of highly hazardous substances. The third category of the award is for educational/communication activities which enhance public acceptance of Green and Sustainable Chemistry. See Fig. 6 for Yasui's chosen slide.

technologies that reduce or eliminate the use or generation of hazardous substances in the design, manufacture and use of chemical products."

Definition of sustainability

The definition of sustainability is difficult, but it is the most important issue to be discussed. The original definition by Brundtland Report was generally accepted. If metrics is discussed to meet the original definition, there is no single agreement and the 'triple bottom line approach' is most common these days. In the panel, Sikdar and Klüppel both explained the definition of sustainability as follows:

Sikdar

There are three aspects to the sustainability debate: economic

Several important points for future discussion

Definition of green

The following definition adopted by Klüppel, which can be seen on the Internet page of US Environmental Protection Agency (EPA), seems to be accepted by the panelists.

Green Chemistry Mission: "to promote innovative chemical

development, ecological (or environmental) preservation, and social good. Sustainable development is an optimization of the three dimensions. Suppose we could quantify pollution avoidance, economic value added, and societal good of a product, process, or a system, we could show that taking a system from the old to the new would be progress. The social aspect of sustainability is the hardest target to quantify, and little quantitative work is found. On economic development and ecology (or environment), significant work has come from ecologists and economists. Technologists and businesses are beginning to adopt these ideas. For instance, BASF has created eco-efficiency metrics to evaluate industrial processes or products to optimize resource use (such as material and energy), waste minimization, and elimination of toxic or hazardous materials in production.¹ Eco-efficiency does not tackle the social dimension of sustainability; yet it is important progress.

Klüppel

Many publications, discussions and the US-EPA Internet page give the impression that green and sustainable chemistry are the same. But the equation green = sustainable is misleading. Sustainability is more than ecology. It does not only include ecological aspects, but also economical and social aspects.

In general the term sustainability is very often used as headline, but only parts are covered, *i.e.* we find the well known discussions on ecological aspects under

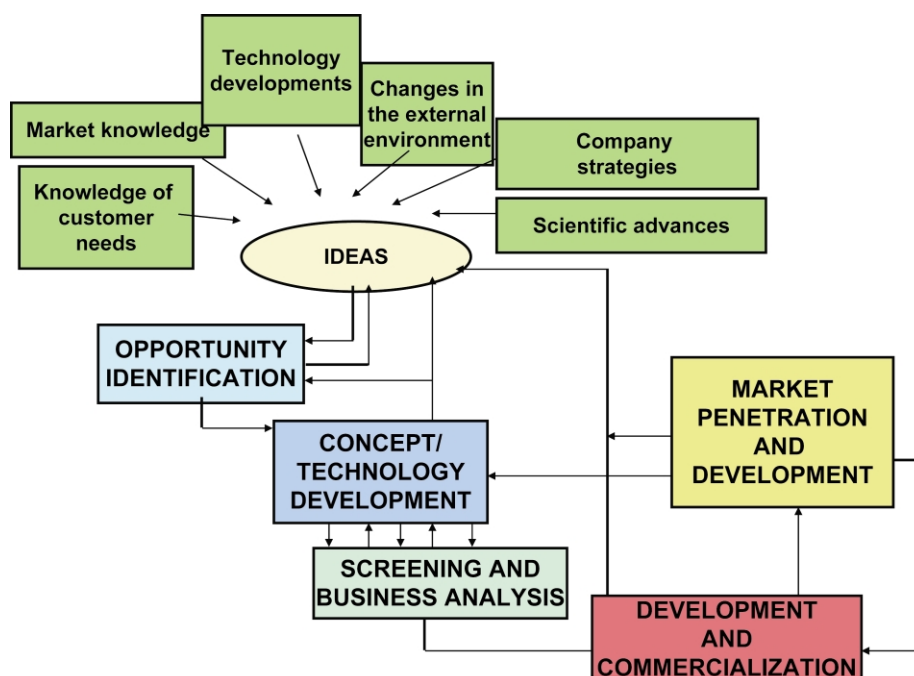


Fig. 4 Innovation – not a linear process.



Solvent Selection Guide - Home Page - Microsoft Internet Explorer provided by SmithKline Beecham WSD IR

Address: s:\joe\web\Intranet Sites (development)\Ssg\default.htm

© Copyright 2002, GlaxoSmithKline

Home/Solvent Selection Guide

How to use Introduction Background Case Study Economics Life Cycle Printable Version Order form Key Site Info

SOLVENT		Waste	Impact	Health	Safety	LifeCycle	GMS use
Alcohols	Ethylene glycol	4	9	8	9	9	
	1-Butanol	5	8	9	8	5	Ir
	Diethylene glycol mono butyl ether	5	7	8	9	7	
	Isoamyl alcohol [3-methyl-1-butanol]	7	7	7	8	6	
	2-Ethyl hexanol	9	6	6	7	6	U
	1-Propanol	4	7	7	8	7	D
	Ethanol/IMS	3	8	10	7	9	C,D,Ir,T,U
	2-Propanol [isopropanol]	3	9	8	7	5	A,C,D,Ir,T,I
	t-Butanol	3	10	7	7	8	T
	Methanol	3	10	5	8	9	A,C,D,Ir,T,I
Esters	Butyl acetate	7	8	7	8	5	
	Propyl acetate	6	7	7	7	5	
	Isopropyl acetate	5	8	7	7	6	A,U
	Ethyl acetate	4	8	7	4	6	A,C,D,Ir,T,I
	Methyl acetate	2	10	6	5	7	W
	Dimethyl carbonate	3	7	5	7	8	
	Mesitylene [1,3,5-trimethylbenzene]	9	2	6	5	7	
	n-Xylene	9	2	5	5	7	

Fig. 5 Solvent Selection Guide.

this headline, giving the impression of news. This might only be justified if the discussed aspects are extremely important in the sense of a precondition for sustainability or knock out criteria blocking the way to sustainability.

Defining sustainability or sustainable development is not an easy task. In the Brundtland Report of 1987 sustainable development is described as follows: 'Sustainable development meets the needs of the present without compromising the abilities of the future generations to meet their own needs.' The key issue is the term 'needs.' We have problems in understanding and agreeing the needs of the present generations, it is even more complicated to describe the needs of future generations.

An additional problem is raised when

observing different levels, e.g. global, regional or local aspects. Similar problems occur when defining the responsibility of the different actors, e.g. of society, of one stakeholder, of one company or, even more complicated, the requirements for one product of a company.

Related to the topic of the presentation: What should be the scope of sustainable chemistry? Should we consider chemical reactions, processes, manufacturing, products, or product systems?

Different view of green and sustainability

In the discussion on 'What is Sustainable Consumption in the WSSD Plan of Implementation', Yasui already claimed that the basic condition for sustainability is environmental aspect, and that economical and social aspects provide only additional conditions.²

Yasui

A more complex definition of green and sustainability was discussed. Environmental aspects are the most basic and essential concepts for both green and sustainability. We have to limit our discussion

within the area where environmental aspects with and without cross section with economic and social aspects. It must also be recognized that even within the environmental aspects, colour of green is not uniform, varying from pale green to deep green.

Factors to be taken into account in the metrics for environmental aspects

In these days, LCA has been recognized as a powerful method to express the environmental burden caused by any products/processes. It is the first step to determining what the environmental burden is and which items should be included in the discussion. The panelists listed the following as items to be considered as environmental burdens:

Klüppel: energy, resource, water, waste, etc.

Sikdar: (a) resource type: energy, material, water, land, (b) impacts type: acidification, global warming, human health, ozone depletion, photochemical smog, wastes, and ecological health.

Ibusuki: energy, material in E-factor, solvent reduction, NO_x, SPM, photochemical smog, VOC.

Norling: Solvent, waste reduction, hazardous chemical reduction, energy saving, ozone depletion, NO_x.

Curzons: mass, energy, toxic dispersion, natural resource utilization, solvents.

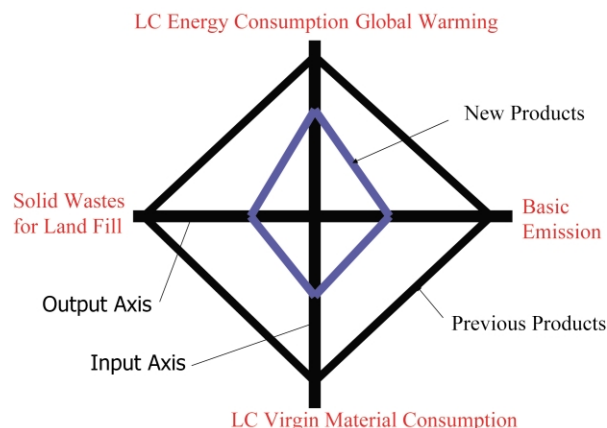


Fig. 6 The Four-axes method.



Yasui: energy (global warming), environmental emission, resource, landfills, if limited only four items.

There seemed to be no large differences between the lists proposed by the panelists.

Approach to be used in metrics

It is necessary to have some kind of analytical method to evaluate environmental aspects of sustainability. The following are the list of effective methodologies proposed by panelists to be used in metrics. Life Cycle Assessment is a common method to cover wide issues, and the E-factor or Atom Economy and related methods are metrics to be used in some area of chemistry, in which yield is rather low.

Klüppel: Life Cycle Data, Energy Balance Analysis, and Stakeholder Workshop.

Sikdar: Life Cycle Assessment, Risk Assessment, Risk Management, Industrial Ecology.

Ibushuki: E-factor, Life Cycle Assessment.

Norling: —

Curzons: Effective Mass Yield, E-factor, Atom Economy, Mass Productivity, Reaction Mass Efficiency, Life Cycle Assessment, Solvent Selection

Yasui: Life Cycle Assessment, Risk Assessment

Discussions after the presentations

Q: Norling to Yasui: How easy is it for the applicant of GSC award to describe their product/process in the form of the Four Axes Method? Is it necessary to support them to make the figures?

A: by Yasui: No. Not really. In Japan, most companies have some LCA data concerning their products/processes. LCA has already spread widely in Japan.

Comment by Curzons: It is crucial to share LCA data.

Q: Ibusuki to Klüppel: In the evaluation process for sustainability, you have nine factors. How do you make a total point considering nine factors?

A: by Klüppel, The weighting problem is difficult. Therefore it is very important to create a dialog process involving all stakeholders.

Q: Ibusuki to Klüppel: Do you have a selection process for the best available technology?

A: by Klüppel: We use extent of improvement is a the measure for selection.

Q: Yasui to Klüppel: Weighting is difficult. But if you try to use only improvement, i.e. relative value, will the situation be improved?

A: by Klüppel: No, but linking it may be OK. In reality, there is a lot of cross-linking.

Q: Paul Anastas to all panelists: Not everything can be counted. Sustainability metrics are not so effective, because the boundary problem is unsolved and important. How do we avoid the pitfalls? Bad analysis is worse than no analysis at all.

A: by Sikdar: We are at a very early stage of handing sustainability. We now know how to reduce environmental impacts. In principle, I think it is possible to consider several factors. The metrics we choose must undergo such a refinement process.

A: by Norling: It is true we cannot measure all the processes. In such cases it is useful to construct models for evaluation. We can partly do it.

References

- 1 P. Saling, Eco-efficiency analysis by BASF: The Method, *J. Life Cycle Anal.*, 2002, 7(4), 203.
- 2 Itaru Yasui, 'Research of the CREST Team toward Sustainable Consumption', *The 1st International Workshop on 'Sustainable Consumption'*, Tokyo, March 19–20, 2003.



GSC Tokyo Statement

Paul Anastas (UPA) and Shun-Ichi Murahashi (Okayama Univ. of Science) report on the declaration statement which resulted from discussions at the First International Conference on Green and Sustainable Chemistry held at Tokyo in 2003

Introduction

The First International Conference on Green and Sustainable Chemistry, (GSC TOKYO 2003, Chairman: Dr. K. Yamamoto) was held from March 13 to 15, 2003 in Tokyo. The participants of the conference made the following declaration to promote 'Green and Sustainable Chemistry (GSC)' as a key initiative in the ongoing efforts to achieve sustainable development.

The first draft of the statement was written by a task group of the Organizing Committee headed by Professor M. Misono and Mr. S. Seta. The draft was then sent to the members of International Advisory Board (23 members from 17 countries) and was amended reflecting the comments from the IAB members. The statement was adopted at a joint meeting of the Organizing committee and the International Advisory Board and reported at the conference by Dr. P. Anastas and Professor S.-I Murahashi and adopted by the participants. The statement was disseminated as a message from the GSC TOKYO 2003 to the public *via* journals and mass media which include the University on the Air.

The IAB committee agreed that GSC international conference will be held continuously in every two years, and the next conference will be hosted by US UPA and ACS in 2005 in Washington, D.C.

GSC Tokyo Statement

Today, chemistry and chemical technology are the foundation of our modern civilization, serving many of society's vital needs while providing numerous benefits. The contribution of chemistry to people's lives in the 21st century will continue to be wide-ranging in a variety of positive ways. However, to fulfill this role, we recognize that it is of the utmost importance for chemistry and chemical technology to be safe, useful, and also to enjoy public trust. Moreover, respect for the environment and consideration of the limited availability of resources and energy must become integral components of the planning, development and application of chemical technologies. This is a common issue for all sciences in the modern age.

The 2002 World Summit on Sustainable Development in Johannesburg, the first follow-up to the 1992 Earth Summit held in Rio de Janeiro, made communicating progress on sustainability a priority, and pledged a strong commitment to protect health, safety, and the environment. Social responsibility was also called upon in contributing to the economic well-being of nations.

We believe that 'Green and Sustainable Chemistry (GSC)' can make a major contribution to a sustainable society, and provides the platform to work for a more

sustainable future. Sustainability can only be achieved if enthusiastically promoted by all persons associated with chemistry and chemical technology on a global scale. As a means of finding real solutions to improve and protect both human health and the planet we all share, 'GSC' will play an integral part in this vital effort by providing the tools necessary for a new paradigm.

'GSC' activities will focus on education, research and development. 'GSC' education will inspire young scientists with the ethical and practical skills needed for reorienting chemical technology to favor sustainability. 'GSC' R&D will establish processes, products and methods that minimize the adverse effects of chemicals, throughout their life cycle, on human health and the environment. This will entail the utmost effort for developing science-based risk management practices as the foundation of sustainable development. The GSC Tokyo 2003 will greatly accelerate the bringing together of all sectors, including industry, academia, government, as well as non-governmental and international organizations, to coordinate activities and share expertise globally. This will achieve the maximum level of performance for sustainable development.

March 15, 2003.



Sustainable development and profitable growth – challenges for a global chemical corporation

The following is an abstract of the lecture given by Dr Dietmar Nissen, President of the BASF East Asia Regional Headquarters, at the First International Conference on Green & Sustainable Chemistry held in Tokyo in March 2003.

Sustainable Profitable Performance is the very first concept in BASF's code of conduct named *Values and Principles*. This concept reflects the goals which a modern, global company has to pursue. A corporation must not live off its capital. It must not deplete its own resources, nor the resources of the environment or of society. BASF sees absolutely no contradiction between sustainable

development and profitable growth. We are, on the contrary, convinced that over the long term sustainable development is a necessary precondition for profitable growth.

When it comes to sustainably developing civilization, the chemical industry is not the problem, but rather is part of the solution to overcoming future challenges. Although many consumers are

unaware of it, our products make a major contribution to sustainable development. In modern cars, for instance, innovative polymer materials reduce the weight and thereby increase the cars' energy efficiency. In Germany alone, the use of plastics in cars saves almost 500 million litres of fuel each year (Fig. 1). The building and construction sector is another excellent example: Styropor®, the

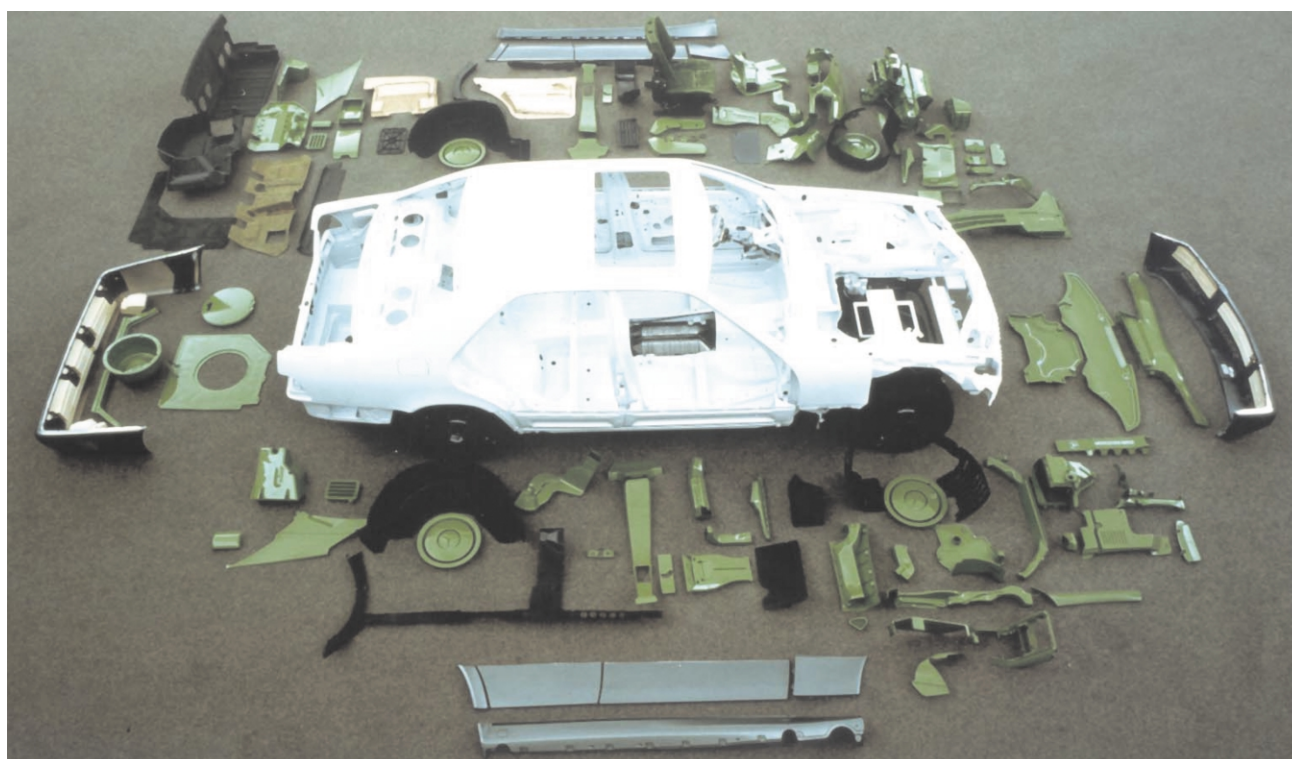


Fig. 1 A high proportion of modern cars consist of plastics, which reduce weight and help to save fuel.

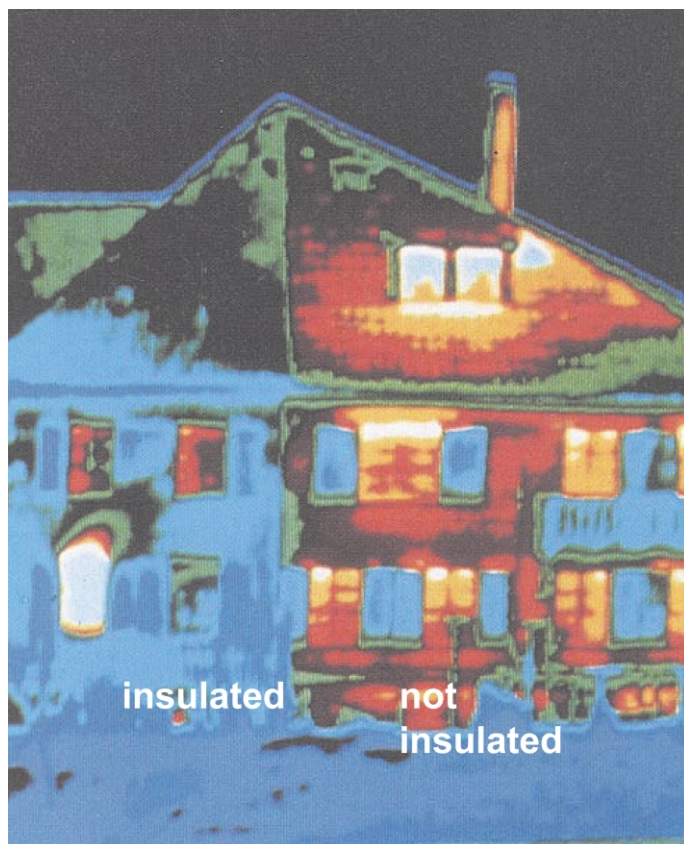


Fig. 2 In a single European family home insulated with Styropor®, 1900 liters of heating oil can be saved per year.

expandable polystyrene foam plastic invented by BASF in the early 1950s, is used for housing insulation and help save energy all over the world (Fig. 2).

Innovations will play an important role in the chemical industry's contribution to sustainable development. Today, society demand is an increasingly important motive force for innovations. One innovative contribution to contain global warming is BASF's 'Three-Liter-House'. Through the use of a wide variety of measures to improve insulation and through innovative energy concepts such as the fuel cell, it is possible to drastically reduce the amount of fossil fuel for heating a house.

Another innovation of BASF could help to tackle the problem of plastic waste. Ecoflex®, our biodegradable plastic, has been a great success in the past years (Fig. 3) and is expected to continue showing double-digit growth rates in the long term. To make mobility more sustainable, intensive research is conducted to find new drive systems. One of the most promising alternatives to the conventional combustion engine is the fuel cell. Through the development of a new high-performance catalyst by BASF, hydrogen can be obtained from methanol.

This hydrogen is then used in the fuel cell to generate electrical power.

Sustainable development, however, means more than creating environmentally friendly products. The other dimensions of sustainability must not be ignored. For a financial analyst, for instance, sustainability means that a company will still be successful in 10 or 20 years. Over the last decade, BASF has shown that it can successfully implement its strategy and achieve stable growth even in a difficult economic environment. This is also reflected in the company's shares. Even in the difficult environment of 2002, BASF shares outperformed both the German and the European index.

For a business to remain competitive, flexibility is a key success factor. In recent years the chemical industry has responded, through a series of structural adjustments, to the challenges of globalization and the need to concentrate on its core competencies. In view of the many different directions being pursued by individual companies, it is clear that there is no single right way, no universally valid strategy. Although BASF has made less drastic changes than some competitors, the company has nevertheless constantly optimised its

portfolio. With this pro-active portfolio management, the company increased its return on investment and reduced its cyclicity. Today, BASF's business is more innovation-driven than ten years ago.

The long-term competitiveness within the chemical industry depends on innovation. The only way to ensure a unique selling proposition in the market is through outstanding product characteristics, excellent customer relationships and continual innovation. This means that more new products and processes must be generated through



One week



Two weeks



Four weeks

Fig. 3 Ecoflex® makes plastic waste disappear.



R&D than old products lost through 'commoditization.' Innovations will make the chemical industry an even more potent force for sustainable development.

To firmly integrate sustainable development in a corporation, it is critical that it becomes part of the everyday activities of the company. Two things are needed for this to occur: efficient corporate structures, and effective management systems in which the principle of sustainable development is firmly rooted. BASF developed a sustainability management structure, which is led by a Sustainability Council of chief executives.

An excellent example of an effective management instrument is the eco-

efficiency analysis that has been developed by BASF. This tool is a unique strategic instrument to evaluate the sustainability of BASF products in a very transparent way. It allows assessing economic and environmental issues in developing products and processes.

BASF's eco-efficiency analysis is a good example of how well measures that are not regulated by the government, but rather voluntary measures, can help create a balance between sustainable development and profitable growth in the chemical industry. Other examples include the Responsible Care initiative of the chemical industry worldwide as well as Global Compact, a network of UN organizations, companies and non-

governmental organizations initiated by U.N. Secretary General Kofi Annan. These voluntary measures demonstrate that the chemical industry is playing an active role in responding to the challenges of a growing and ageing world society. As we move forward toward meeting demanding objectives, however, it is important to preserve an acceptable framework of self-determination in which companies can operate responsibly.

For BASF, there is no viable alternative to the principle of sustainable development in order to achieve sustained economic success.

For further information contact Cordelia Krooss, email: kroossc@basf-east-asia.com.hk, Tel: (+852) 27313 792.



Leaps of innovation

Dr. Ian D. Dobson (UPA) General Manager, Technology, BP Chemicals, Sunbury on Thames, Middlesex, UK, describes sustainability applied to chemicals manufacturing in the UK

Background

The redeployment of BP Chemicals' manufacturing capacity around Europe at fewer and more efficient sites in the 1990s sounded like trouble for some product areas. Uncertain futures loomed for vinyl acetate (VAM) and ethyl acetate production as their facilities at Baglan Bay in the UK and the Italian sites of Porto Maghera and Priollo were targeted for closure.

The solvents business unit had to make a choice:

- it could try to justify staying put
- it could move production to one of the advantaged production sites
- it could choose to exit the Vinyl acetate and ethyl acetate businesses.

Staying with production in Baglan Bay in South Wales was not a real option because the site was scheduled for eventual shutdown. But moving to BP's chemical complex at Saltend near Hull in the north of England implied heavy investment in new plant – too costly if a manufacturing facility were to be built based on a traditional fixed bed reactor for the VAM chemical process. And the exit route was the least attractive of all for BP.

At the same time, the orders from senior management in BP Chemicals were clear: 'No repeats in technology.' This meant that any facilities being rebuilt would have to incorporate significantly improved production processes. The decision was clear – new technology was needed to unlock the next generation of production and rationalize the Baglan bay production situation.

We decided to ramp up the development of two new technologies which we already had under way. We were able to demonstrate the economic case for state-of-the-art facilities in Hull—where they could find the required acetic acid feedstock plus competitively-priced power and heat from the newly built on-site combined cycle gas turbine power station owned by the Saltend Cogeneration Company. But it was not to be an easy task.

Award-winning processes



In June, the Leap and Avada processes were acknowledged by the industry with two prestigious awards in the highly competitive 2002 Institution of Chemical Engineers Awards programme in the UK. Leap won the AspenTech Award for Business Innovation, given for a new process, design technology, or way of working which generates significant business value. Avada netted the AstraZeneca Award for Excellence in Green Chemistry and Engineering – new this year – presented for the best development, design and use of a new process, showing an interdisciplinary approach, which is robust and viable while minimising or eliminating pollution at source and risk to health and the environment.

The two chemical products serve related markets. VAM, which is in the company's acetyls business unit, is essential to emulsion-based paints, wallpaper paste and wood glue. Ethyl acetate is also in the acetyls business unit, and is used in surface coatings, inks and pharmaceuticals.

To achieve today's end result of two sophisticated full-scale operating chemical processes demanded seven years of highly focused effort. To the outside world, a time scale of seven years from the first glimmer of an idea to commercial production may seem extensive. But developing new chemical manufacturing processes and taking them to full commercial operation is a step-wise procedure involving many interlinking stages, one of these being a demonstration plant, to check that the process works at large scale. Ensuring that the very large capital sums required for a new manufacturing plant are being invested wisely is critical—many new processes in

the petrochemical industry take as long as 10–15 years to bring to fruition.

Baglan Bay's conventional VAM facility used a fixed bed reaction process, as do all other VAM plants worldwide, to bring together the three feedstocks required to make VAM – acetic acid, ethylene and oxygen. In the late 1980s BP Chemicals was already looking to the future and had developed a new fixed bed catalyst, incorporating this into a proprietary fixed bed process design for a joint venture plant in Ulsan, Korea. But the cost of building such a VAM plant in the higher-cost environment of Europe did not generate investment economics attractive enough to compete with other available BP investment projects.

Consequently the team called on a wide range of resources to work on developing the VAM fluidised bed route as a more cost-effective solution. The savings in the new process – branded as LEAP technology—come from process simplification and intensification made



possible by the use of a fluidised bed process, requiring only a single reactor compared with the two reactors usually needed by fixed bed processes. The research and development work was based in Hull but drew on expertise from BP Chemicals in the USA, Sunbury in the UK, and Lavéra in France, with significant input from BP's acrylonitrile and polyethylene businesses, both of which have fluid bed expertise.

Hull proved to be the optimum location for the commercial-scale plant. Acetic acid was already produced there, an ethylene supply pipeline from Teesside was approved for construction, and industrial gas specialist Air Products, already on site for acetic acid production, was brought in to build an air separation unit to produce the oxygen.

We were determined to access the right skills wherever they existed in the BP group and not try to recreate them at one research centre. We reached out not only to chemical stream technologists but also to our colleagues in downstream refining, where there were fluid catalytic cracker experts.

Fluid bed solution

What provided the breakthrough for LEAP was progress in two areas: fluidised bed technology, led by engineering technology, based in Sunbury, and work on a new precious metals catalyst.

In a fixed bed reactor, the catalyst, which promotes the reaction, is in the form of spheres which are packed into tubes. The reaction gases pass through the tubes and around the catalyst particles in the spaces between the spheres without moving them. In a fluidised bed reactor the catalyst is in the form of a fine powder, similar to talcum powder, and as the reaction gases flow upwards through the reactor they blow the fine catalyst around, rather like the balls in a 'lottery blower'. This gives much better mixing and contact between the gases and the catalyst, improving heat transfer and allowing the catalyst to be removed and replenished without having to shut down the reactor.

While fluidised beds are cheaper and easier to build, they are very difficult to scale up from laboratory tests. In the case of VAM, we employed full scale X-ray imaging in BP's unique VIPA (visualisation, imaging and process analysis) centre at Hull. This allowed us to view and understand the fluid dynamics of a commercial-scale reactor. Fluid dynamics are affected by the

reactor's geometry and the internal equipment such as cooling coils and baffles. Optimising the process scale-up required meticulous, frame-by-frame inspection of the X-ray video.

Without the X-ray data, a \$20–30 million demonstration plant would have been necessary, along with another 3–4 years of development experience before attempting the commercial stage.

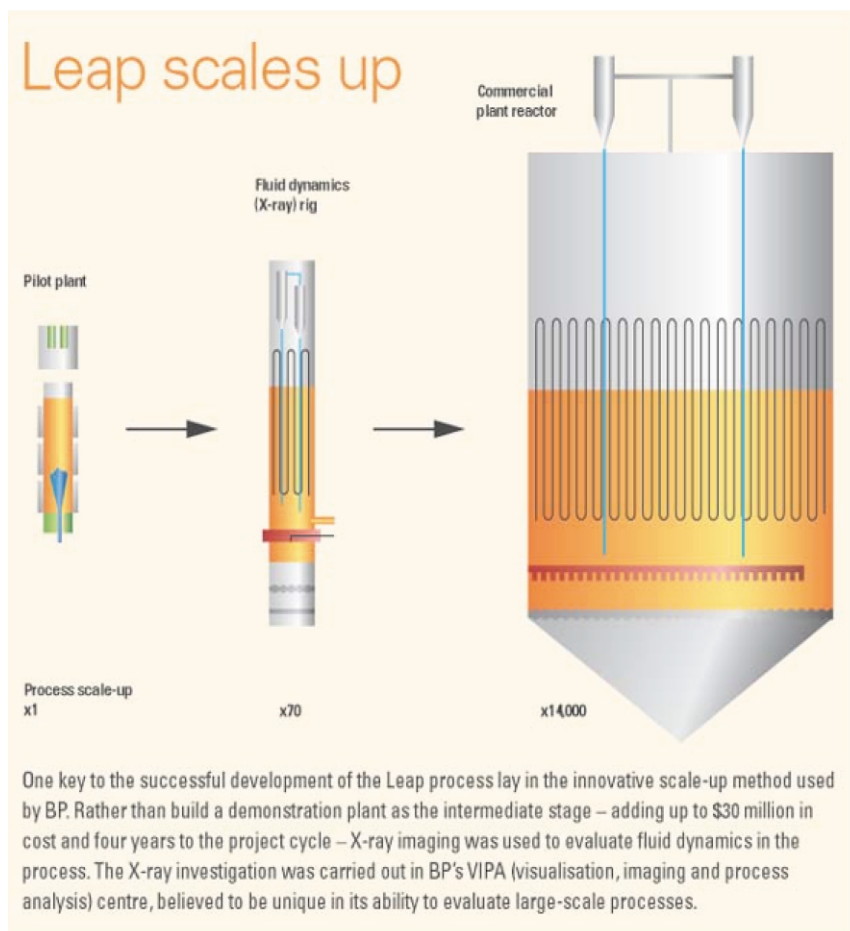
Moving from a fixed to fluidised operation also required a new catalyst. The VAM catalyst development programme employed a virtual-team approach, with BP technologists in Hull and Sunbury in the UK, and Warrensville (and later in Naperville) in the USA, working on different aspects of catalyst screening, preparation and testing. By exchanging results electronically, with email and audio/video conferencing, the team selected promising catalyst formulations and prepared them in fluidised bed form for testing at larger scale. Having selected the preferred catalyst – a precious metal mix in the form of very fine spheres, so minuscule that they seem to flow almost as a liquid – the next step was to scale up the catalyst preparation to commercial batch size.

In collaboration with leading catalyst manufacturer Johnson Matthey, the BP technologists worked out new techniques to prepare the catalyst at commercial scale and control the location of the active metals in the support material.

A small pilot plant for the Leap technology made clear the viability of the chemistry, but to put the chemistry and the large-scale process dynamics together, the team relied solely on a computer model. This meant directly scaling up by a size factor of 14,000 without intermediate stages of expansion. We put our faith in the modelling techniques and our ability to manipulate and understand the data.

The first time the full process was put to the test was when the plant was started up at the end of 2001, and naturally tensions ran high even though we had high confidence in our modeling. Monitoring data on six screens, including a wall-sized display, the team held its breath. We added the oxygen, watched the temperatures rise, and within two hours we were making on-specification vinyl acetate and moving it into bulk storage.

The decision to go to a fluidised bed process had saved 30% in capital costs. This helped turn a difficult investment





decision into a much easier one.

The plant, the world's first fluidised bed process for VAM, is rated at an annual capacity of 250,000 tonnes, and output volume can be boosted further in line with market penetration. Research work has continued, and options for further capacity increases are being developed. With over 80% of today's VAM plants being more than 20 years old, the LEAP competitive edge will continue to increase as other VAM producers face similar decisions on investing in new plant, based on costly fixed bed facilities.

Eliminating ethanol as an intermediate

Separately the Solvents business research team also came up with a new solution for ethylacetate production, trademarked AVADA (for AdVanced Acetates by Direct Addition). The new technology converts ethylene and acetic acid gases directly into ETAC using a heteropolyacid (HPA) catalyst, without the usual intermediate stage of esterification – this

would have required another feedstock chemical, ethanol.

By avoiding the need to build new ethanol production facilities, capital costs were kept down and the transport logistics significantly simplified. The resultant technology represents a significant advance in chemistry terms, a true step change.

The AVADA plant was constructed under such time pressure that the commercial engineering design was carried out in parallel with the commissioning of a fully integrated pilot plant at BP's Hull research centre. The design was then modified in real time as experience from the pilot plant was logged.

The ethyl acetate development work was also widely collaborative like that on the VAM project, calling on the cooperation of chemists, chemical engineers, process developers, catalyst manufacturers and research departments in several universities, particularly the Leverhulme centre of Liverpool University in the UK and Waterloo University in Canada.

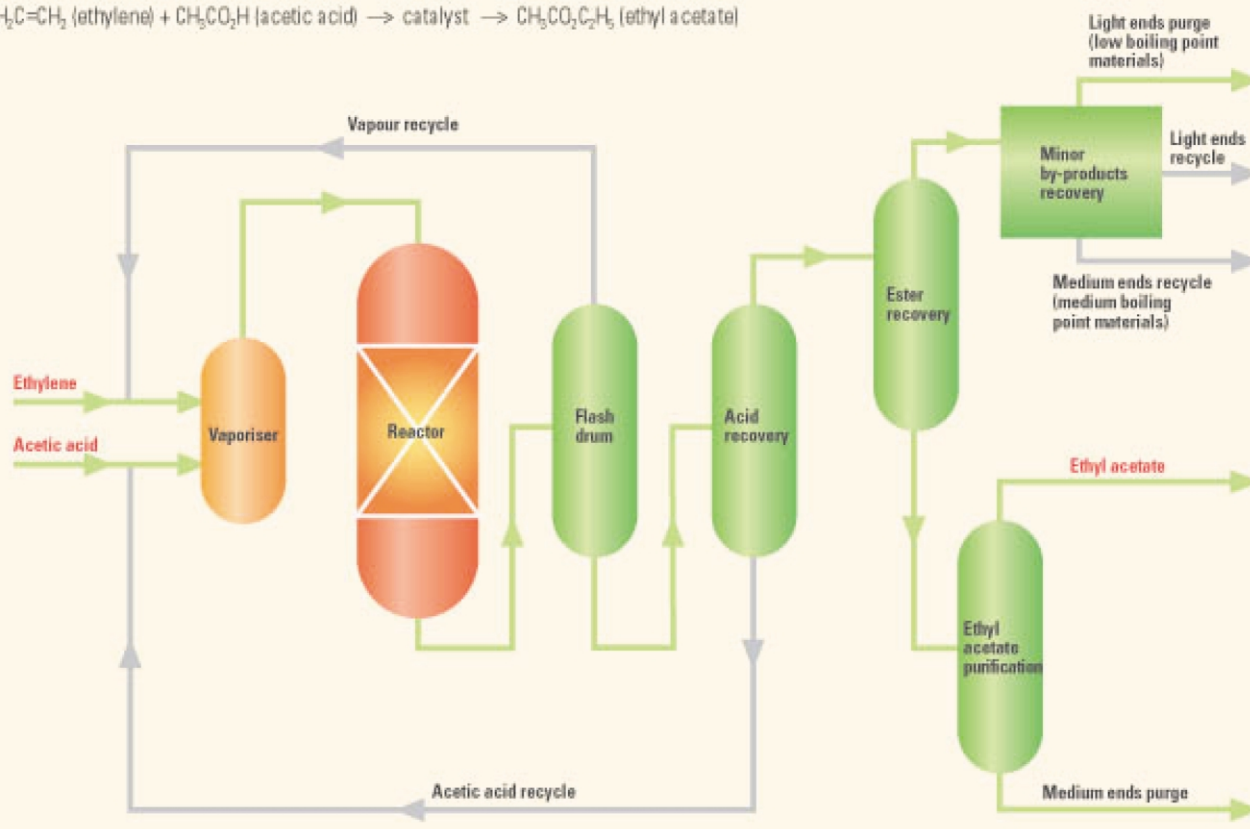
Long life catalyst

Interestingly, the chemistry of using HPAs for this type of reaction was well known but there had always been obstacles to its commercialisation. The problem had always been catalyst lifetime, since the heteropolyacids typically suffered rapid ageing and loss of activity. The new AVADA catalyst consists of a bed of silica beads, in the surface pores of which sits the HPA liquor. The HPA itself is an optimal balance of low-volatility silico-tungstic acid, known as a superacid, which in combination with the ideal silica bead produces long-term activity. The low volatility of the HPA helps the catalyst survive the reactor's extremes of heat and pressure, thus allowing long periods of uninterrupted operation for the plant. The Hull plant has achieved continuous sustained operation during its first year in commercial production.

Along the road to operation, the AVADA team introduced several improvements and innovations, including a method for reducing the reactor's pressure drop and thus saving on gas recompression costs, and further

BP's new Avada process

Avada enables ethylene and acetic acid to be combined directly using a heteropolyacid catalyst, to produce ethyl acetate without an intermediate esterification stage. The reaction is:
 $\text{H}_2\text{C}=\text{CH}_2$ (ethylene) + $\text{CH}_3\text{CO}_2\text{H}$ (acetic acid) $\xrightarrow{\text{catalyst}}$ $\text{CH}_3\text{CO}_2\text{C}_2\text{H}_5$ (ethyl acetate)





improving the energy efficiency of the process.

The start-up was as dramatic as that of the LEAP team but stretched over two weeks while the control system on the ethylene feed and a few other teething problems were resolved. But on a warm afternoon in June 2001 the plant went live, and the commissioning team monitored its progress.

When we saw the temperature gains across the beds, we knew we were making ethyl acetate. The purity of the product was excellent – 99.98%, the best ever. The commissioning team were very emotional and very relieved as well as being enormously pleased and proud.

The AVADA process beats conventional processes in environmental friendliness. Traditional esterification units produce as much water as they do ethyl acetate and therefore require treatment and disposal of this aqueous effluent waste stream. The other main technology in the market, Tischenko condensation, uses an acetaldehyde feedstock. This is less efficient than

producing ethylacetate directly from a modern ethylene cracker, and Tischenko processing also produces waste streams from the aluminium salts used as catalyst.

Already the world leader in ethylacetate production, BP Chemicals will now extend its lead with the high efficiency AVADA plant, designed to produce 220,000 tonnes per year, making it approximately 50% larger than its nearest competitor. In the first ten months of operation the plant at Hull produced around 100,000 tonnes of ethylacetate. At full capacity it will produce about two-and-a-half times as much ethylacetate as does conventional technology, as measured in tonnes produced per operating employee. Compared to conventional processes, energy consumption is about 20% lower and feedstock losses are some 35% less than in conventional esterification.

So overall, we managed to exit the old facilities at Baglan Bay and move our Vinyl acetate process to Hull. We closed the old ethanol production unit at Baglan bay, which had been reliant on ethylene delivered by ship from Grangemouth. We

focused two processes which needed acetic acid feedstock at our Hull site where that acetic acid is produced eliminating rail movements of acetic between Hull and Baglan Bay. We connected the Hull site to the Wilton cracker to supply ethylene by pipeline. This eliminated the trucking of some 60,000 tonnes of ethanol by road. We eliminated more than 100,000 tonnes of wastewater stream. We reduced our energy consumption and feedstock wastage significantly with benefits to our CO₂ emissions. All this was achieved with much lower capital cost than the traditional processing.

BP expects that the superior performance of its new LEAP and AVADA plants will begin to distinguish the company's technology in the marketplace even more as various competitors older chemical manufacturing facilities reach the end of their days.

The technology is potentially interesting for other acid-catalysed processes such as the manufacturing of fuels, detergents and lubricants.



Cetylpyridinium dodecatungstate on fluorapatite: efficient and reusable solid catalyst for solvent-free epoxidation†

Junko Ichihara,^{*a} Akihiro Kambara,^b Katsuma Iteya,^b Eiko Sugimoto,^b Takeshi Shinkawa,^b Aki Takaoka,^b Shunro Yamaguchi^a and Yoh Sasaki^{*b}

^a The Institute of Scientific and Industrial Research, Osaka University, Mihogaoka, Ibaraki, Osaka 567-0047, Japan. E-mail: ichihara@sanken.osaka-u.ac.jp

^b Faculty of Science and Engineering, Kinki University, Kowakae, Higashiosaka, Osaka 577-8502, Japan. E-mail: sasaki@meta.kindai.ac.jp

Received 25th March 2003

First published as an Advance Article on the web 27th May 2003

We have developed a new catalytic solid phase system for epoxidations using urea–hydrogen peroxide complex (urea–H₂O₂) and cetylpyridinium dodecatungstate ((CetylPy)₁₀[H₂W₁₂O₄₂]) catalyst on fluorapatite. In the solid phase system epoxidations of cyclic alkenes and allylic alcohols proceeded without solvent at room temperature to afford the corresponding epoxides in good yields. The recovered solid catalyst phase was reusable for the reaction.

Introduction

The search for environmentally benign alternatives to the conventional reaction process using organic solvents has been of great significance in green, sustainable chemistry.¹ Green solvents such as supercritical liquids, solvent-free reaction systems, and reusable solid-supported reagents and catalysts are examples of green processes.² We have developed a new solvent-free catalytic reaction system by using a solid disperse phase which is harmless to the environment and easily handled. Fluorapatite (FAP) was effective as a solid disperse phase for assisting tungstic acid (H₂WO₄)-catalyzed epoxidation of alkenes and allylic alcohols with solid urea–H₂O₂ without solvent.³ In our system, the apatite phase has been used as a solid disperse phase instead of an organic solvent. As a catalyst in our solid-phase-system, a variety of nanosized clusters of polyoxometalates such as heteropoly- and isopoly-tungstates or molybdates were examined and enhancement of their catalytic activities by FAP was also found.⁴ Taking into account the stabilities of the solid catalysts for reuse, modification of polyoxometalates by organic cations was carried out and examined in the solid-phase-system. In this paper, we report a highly active and reusable solid-phase-system using cetylpyridinium dodecatungstate catalyst on fluorapatite for the solvent-free epoxidations.

Results and discussion

Catalytic activities of various polyoxometalates simply mixed with FAP powders (polyoxometalates/FAP) were examined in the solvent-free epoxidation of cyclooctene with urea–H₂O₂ at 25 °C under solid phase conditions. Cetylpyridinium salts and ammonium salts of heteropoly- and isopoly-tungstates or molybdates were used as polyoxometalates. The cetylpyridinium salts were prepared from the inorganic salts by ion-exchange with cetylpyridinium chloride. The results are shown in Fig. 1. The catalytic activities of cetylpyridinium tungstates and molybdates greatly varied by the cluster structures, compared with those of the ammonium salts. Among them

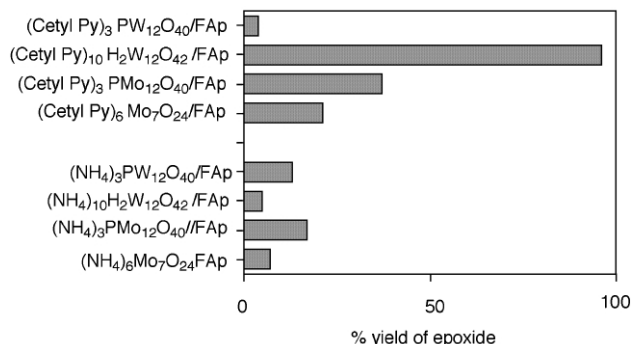


Fig. 1 Catalytic activities of polyoxometalates/FAP in the epoxidation of cyclooctene (at 25 °C after 6 h).

cetylpyridinium dodecatungstate (CetylPy)₁₀[H₂W₁₂O₄₂] showed outstandingly high catalytic activity in the solid phase system. The corresponding epoxide was formed in over 90% yield after 6 h at 25 °C. Such high activities of dodecatungstate have rarely been reported to the best of our knowledge.^{5–7} In the liquid–liquid biphasic reaction it is well-known that cetylpyridinium phosphotungstate (CetylPy)₃[PW₁₂O₄₀] is the most

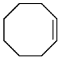
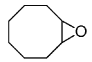
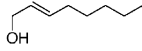
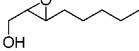
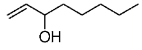
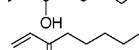
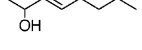
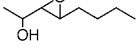
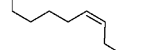
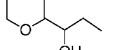
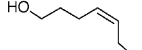
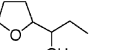
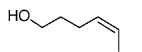
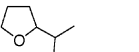
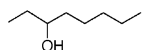
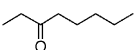
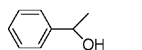
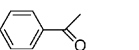
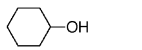
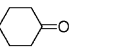
Green Context

Epoxidations are among the most useful reactions in synthetic organic chemistry. While active epoxidation reagents such as percarboxylic acids are available they present serious safety problems and leave acid waste. Apart from oxygen itself, hydrogen peroxide is the most benign and low waste reagent for epoxidations and it is important that we develop effective catalytic methods for activating aqueous and non-aqueous hydrogen peroxide systems (see Green Chemistry for a recent review on this subject). This article reports a novel catalytic method for activating the easy to handle urea H₂O₂ complex. The solid catalyst is efficient and reusable. Reactions are also run under ambient conditions and in the absence of solvent.

JHC

† Presented at The First International Conference on Green & Sustainable Chemistry, Tokyo, Japan, March 13–15, 2003.

Table 1 Solvent-free oxidations using $(\text{CetylPy})_{10}[\text{H}_2\text{W}_{12}\text{O}_{42}]/\text{urea-H}_2\text{O}_2/\text{FAP}$ system^a

Substrate	Time/h	Product	Isolated yield (%)	(selectivity) ^b
	24		86	(97)
	6		72	(98)
	48		46 cs 4.4	(99) ds 2.1
	24		73	(100) ds 1.8
	45		42	(95)
	29		78	(99)
	28		56	(99)
	24 24 (50 °C)		10 ^b 21 ^b	
	360		94	(83)
	144		44	(93)

^a Substrate, 2.5 mmol; cat. 0.025 mmol; urea-H₂O₂, 6.25 mmol; FAp, 1.25 g at 25 °C. cs : epoxide/enone chemoselectivity, ds: erythro/threo selectivity.

^b Determined by GC.

efficient catalyst.^{8–12} In our solid phase system, in contrast, $(\text{CetylPy})_3[\text{PW}_{12}\text{O}_{40}]$ was not effective.

Typical epoxidations of cyclic alkenes and allylic alcohols using $(\text{CetylPy})_{10}[\text{H}_2\text{W}_{12}\text{O}_{42}]/\text{FAP}$ and urea-H₂O₂ are summarized in Table 1. The epoxidations of C=C double bonds of these compounds proceeded at room temperature to afford the corresponding epoxides in good yields. Oxidations of alkenyl alcohols which have a 3 or 4 methylene chain between C=C double bond and hydroxyl group also proceeded at room temperature to give the cyclic compounds containing oxygen selectively *via* the epoxides. Under similar reaction conditions, secondary alcohols were slowly oxidized to the ketones.

For our solid reaction system using $(\text{CetylPy})_{10}[\text{H}_2\text{W}_{12}\text{O}_{42}]/\text{FAP}$ and urea-H₂O₂, it is important that the solid catalyst phase was repeatedly usable. The repeated epoxidations using the solid-catalyst-phase recovered after the reaction were carried out under the simple procedures as shown in the flowchart (Fig. 2). To the solid mixture of $(\text{CetylPy})_{10}[\text{H}_2\text{W}_{12}\text{O}_{42}]$ (0.074 mmol, 3.2 mol%) and FAP (2.50 g) in a test tube with screw-cap, was added solid urea-H₂O₂ (5.10 mmol), and the solid mixture was permeated by liquid cyclooctene (2.3 mmol). Then, in the closed test-tube, the mixture was left without stirring at 25 °C for 6 h. The solid reaction mixture was extracted with pentane and the solvent was evaporated. A colorless solid of epoxycyclooctane was obtained in 85% yield. The GC purity was about 99% without purification. The solid moiety remained after the isolation of the epoxide was washed with a small amount of 5% water-acetone solution to remove urea-complexes, and dried under vacuum over P₂O₅. To the recovered solid-catalyst-phase was added cyclooctene and urea-H₂O₂, and the reaction was carried out at rt for 6 h in a similar way. After the same experimental procedures (isolation and recovery) the reaction was repeatedly carried out. $(\text{CetylPy})_{10}[\text{H}_2\text{W}_{12}\text{O}_{42}]/\text{FAP}$ was reused for the epoxidation of cyclooctene with urea-H₂O₂ over 5 times to keep high catalytic activity. Urea-H₂O₂ can be easily prepared from 30% aq. H₂O₂ and the

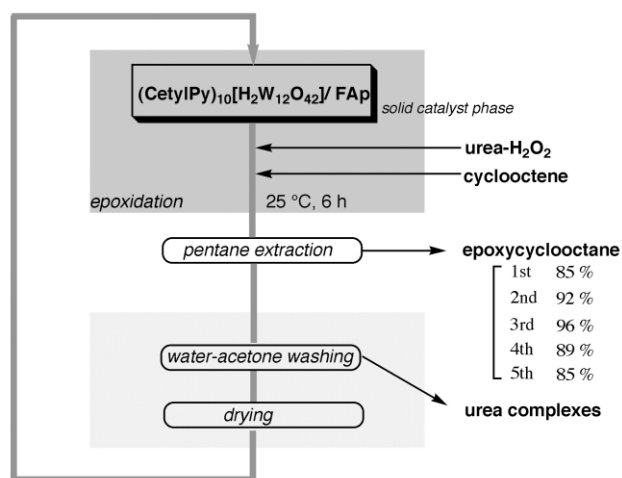


Fig. 2 Recycling system of cyclooctene-epoxidation using $(\text{CetylPy})_{10}[\text{H}_2\text{W}_{12}\text{O}_{42}]/\text{FAP}$.

urea-complexes removed by washing, and then atom efficiency is 87.5% in our cyclooctene-epoxidation.¹³

Conclusions

$(\text{CetylPy})_{10}[\text{H}_2\text{W}_{12}\text{O}_{42}]$ on FAP is an efficient, reusable solid catalyst for the epoxidations with urea-H₂O₂ without solvent. The catalyst was easily prepared by ion exchange of commercially available ammonium paratungstate with cetylpyridinium chloride. Our solid phase system is convenient and a green process in the following points: solvent-free, catalytic reaction, using a harmless solid disperse phase and reusable solid catalyst

phase, without heating or cooling, without special apparatus.¹⁴

References

- 1 *Handbook of Green Chemistry & Technology*, ed. J. Clark and D. Macquarrie, Blackwell, Oxford, 2002.
- 2 G. Grigoropoulou, J. H. Clark and J. A. Elings, *Green Chem.*, 2003, **5**, 1–7.
- 3 J. Ichihara, *Tetrahedron Lett.*, 2001, **42**, 695–697.
- 4 J. Ichihara, S. Yamaguchi, T. Nomoto, H. Nakayama, K. Iteya, N. Naitoh and Y. Sasaki, *Tetrahedron Lett.*, 2002, **43**, 8231–8234.
- 5 C. Aubry, G. Chottard, N. Platzner, J.-M. Bregeault, R. Thouvenot, F. Chauveau, C. Huet and H. Ledon, *Inorg. Chem.*, 1991, **30**, 4409–4415.
- 6 L. Salles, C. Aubry, R. Thouvenot, F. Rober, C. Doreix-Morin, G. Chottard, H. Ledon, Y. Jeannin and J.-M. Bregeault, *Inorg. Chem.*, 1994, **33**, 871–878.
- 7 N. J. Campbell, A. C. Dengel, C. J. Edwards and W. P. Griffith, *J. Chem. Soc., Dalton Trans.*, 1989, 1203–1208.
- 8 C. Venturello and R. D'Aloiso, *J. Org. Chem.*, 1988, **53**, 1553–1557; C. Venturello, R. D'Aloiso, J. C. Bart and M. Ricci, *J. Mol. Catal.*, 1985, **32**, 107–110.
- 9 Y. Ishii, K. Yamawaki, T. Ura, H. Yamada, T. Yoshida and M. Ogawa, *J. Org. Chem.*, 1988, **53**, 3587–3593.
- 10 Y. Ishii, K. Yamawaki, T. Yoshida, T. Ura and M. Ogawa, *J. Org. Chem.*, 1987, **52**, 1868–1870.
- 11 D. C. Duncan, C. Chambers, E. Hecht and C. L. Hill, *J. Am. Chem. Soc.*, 1995, **117**, 681–691.
- 12 J. Ichihara and S. Yamaguchi, *Phosphorus Research Bull.*, 1998, **8**, 143–146; Y. Sasaki, T. Nomoto, S. Yamaguchi and J. Ichihara, *Phosphorus Research Bull.*, 1999, **9**, 87–90; Y. Yasuhara, S. Yamaguchi, J. Ichihara, T. Nomoto and Y. Sasaki, *Phosphorus Research Bull.*, 2000, **11**, 43–46.
- 13 C. Lu, E. W. Hughes and P. Giguere, *J. Am. Chem. Soc.*, 1941, **63**, 1507.
- 14 When the catalyst on solid phase was deactivated, the tungstate and the apatite phase can be separately recovered by high temperature-heating and washing with water. Fluorapatite is more stable than hydroxyapatite at about 900 °C. When the apatite phase is converted to calcium phosphate by sintering above this temperature, the solid phase can be regenerated by hydrothermal reaction at basic conditions.



Novel supporting materials of lipase PS suitable for use in an ionic liquid solvent system†

Toshiyuki Itoh,^a Nozomi Ouchi,^a Yoshihito Nishimura,^a Han Shi Hui,^a Naonobu Katada,^a Miki Niwa^a and Makoto Onaka^b

^a Department of Materials Science, Faculty of Engineering, Tottori University, 4-101 Koyama Minami, Tottori 680-8552, Japan

^b Graduate School of Arts and Sciences, The University of Tokyo, Komaba, Meguro-ku, Tokyo 153-8902, Japan. E-mail: titoh@chem.tottori-u.ac.jp; Fax: 81-857-31-5259; Tel: 81-857-31-5259

Received 24th April 2003

First published as an Advance Article on the web 11th July 2003

Seven types of immobilized lipase PS were prepared using supporting materials such as metal oxides, ceramics, and mesoporous silica. They were then evaluated for use in an ionic liquid solvent system. The reaction rate was significantly dependent on the combination of the source of the supporting materials and solvent system. Tungsten(vi) oxide coated-metal oxides were thus found as novel supporting materials for lipase PS.

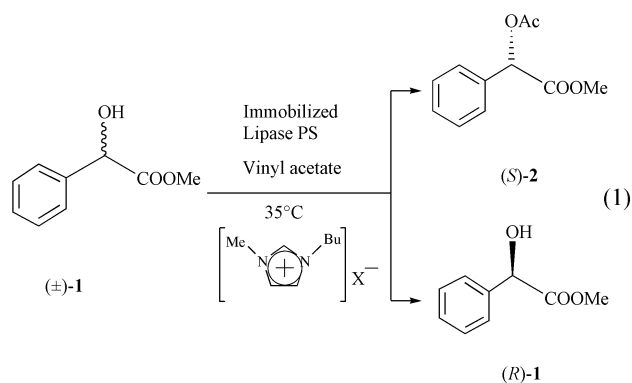
We have been investigating the lipase-catalyzed enantioselective transesterification of secondary alcohols in an ionic liquid solvent system.^{1–5} In these reactions, we found that the suitable immobilization of lipase was essential for realizing the reaction, and Toyonite 200P⁶ and methacrylpropyl SBA-15⁷ were found to be good supporting materials; this makes it possible to use lipase PS in an ionic solvent system.³ In this paper, we report the results of our further investigation of finding novel immobilized lipase PS suitable for use in an ionic liquid solvent system.

Lipase PS is well respected and is one of the most widely used enzymes applicable for various substrates,¹⁰ however, poor reactivity was obtained when commercial lipase PS was used for the reactions in an ionic liquid solvent system.^{1,3} Initially, we prepared three types of immobilized lipase PS supported by Zeolite USY,¹² aluminium(III) oxide (Al₂O₃),¹³ and tungsten(vi) oxide coated-aluminium(III) oxide (WO₃/Al₂O₃)^{14a} for use as catalysts; it was found that only WO₃/Al₂O₃ showed activity. Hence, we focused our attention on tungsten(vi) oxide coated-metal oxides (WO₃/M_xO_y) as supporting materials for the immobilization of lipase PS. Since these immobilized lipases readily precipitate in an ionic liquid solvent, it is easy to separate them during the extraction process of the products from the reaction mixture.

Immobilized lipase PS was prepared as follows according to the method reported by Sakai *et al.*⁸ Lipase PS (3.75 g) was dissolved in a 0.1 M phosphate buffer (pH 7.2) (10 ml) and the mixture was incubated at 25 °C for 6 h and then centrifuged at 3 000 rpm for 5 min. To the resulting supernatant was added a supporting material (0.31 g) and the mixture was incubated for 16 h at 35 °C. The immobilized-lipase PS was collected by filtration through a sintered glass filter and pre-dried in a desiccator for 24 h at room temperature in the presence of fresh dried silica gel, and finally desiccated under reduced pressure at 50 hPa at room temperature for 24 h.⁹

We chose methyl (±)-mandelate ((±)-**1**) as the model substrate for the present immobilized lipase PS-catalyzed reaction, because Novozym 435, which is the most promising enzyme for an ionic liquid solvent system,^{1–5} cannot acetylate ((±)-**1** with enantioselectivity.³ Typically, the reaction was

carried out as follows: to a solution of ((±)-**1**) (50.0 mg, 0.30 mmol) and vinyl acetate (31 mg, 0.45 mmol) in 1.5 ml of 1-butyl-3-methylimidazolium tetrafluoroborate ([bmim]BF₄) or hexafluorophosphate ([bmim]PF₆) was added an immobilized lipase PS (25 mg), and the mixture was incubated at 35 °C with shaking at a speed 120 cycles per min. (eqn. (1)). The product and remaining substrate were extracted with ether (ten times) from the reaction mixture and the combined organic layer was evaporated and subsequent silica gel thin layer chromatography (TLC) (hexane–ethyl acetate, 4:1) gave the acetate (*S*)-**2** and alcohol (*R*)-**1** in good yield. The enantiomeric excess was determined by capillary GC analysis on chiral phase (G-Ta) as the acetate **2**.



As shown in Table 1, the reaction rate was strongly dependent on the supporting materials and an interesting contrast in

Green Context

The use of lipases in ionic liquids is an attractive method for enantioselective esterification and related reactions. However, results in ionic liquids can be mixed, and this paper looks at supported enzymes as a way of overcoming these difficulties. This approach is strongly dependent on the nature of the support used, but the correct system can extend the utility of the enzymes in ionic liquid systems, as well as making recovery simpler. *DJM*

† Presented at The First International Conference on Green & Sustainable Chemistry, Tokyo, Japan, March 13–15, 2003.

Table 1 Lipase-catalyzed enantioselective transesterification using various types of immobilized Lipase PS in the ionic solvent system

Entry	Supporting materials	Ionic liquid	Time/h	% ee of (<i>S</i>)- 2 (% Yield ^b)	% ee of (<i>R</i>)- 1 (% Yield ^b)	Conv./c	Relative rate ^c	<i>E</i> value ¹¹
1	WO ₃ /TiO ₂	[bmim]PF ₆	24	> 99 (5)	13 (83)	0.12	0.50	> 200
2	WO ₃ /SnO ₂	[bmim]PF ₆	24	79 (22)	10 (73)	0.31	1.3	9
3	WO ₃ /SnO ₂	[bmim]PF ₆	5	> 99 (5)	11 (83)	0.10	0.42	> 200
4	WO ₃ /Al ₂ O ₃	[bmim]PF ₆	24	> 99 (20)	11 (65)	0.22	0.92	> 200
5	WO ₃ /Fe ₂ O ₃	[bmim]PF ₆	24	> 99 (4)	4 (87)	0.04	0.17	> 200
6	WO ₃ /ZrO ₂	[bmim]PF ₆	24	> 99 (3)	8 (83)	0.07	0.29	> 200
7	WO ₃ /TiO ₂	[bmim]BF ₄	24	88 (6)	8 (83)	0.11	0.46	17
8	WO ₃ /SnO ₂	[bmim]BF ₄	24	94 (10)	15 (77)	0.14	0.58	37
9	WO ₃ /Al ₂ O ₃	[bmim]BF ₄	24	92 (8)	8 (90)	0.08	0.33	26
10	WO ₃ /Fe ₂ O ₃	[bmim]BF ₄	24	93 (16)	9 (80)	0.09	0.38	30
11	WO ₃ /ZrO ₂	[bmim]BF ₄	24	69 (3)	8 (83)	0.10	0.42	6
12	WO ₃ /SnO ₂	[bmim]N(Tf) ₂	24	> 99 (15)	18 (80)	0.15	0.63	> 200
13	WO ₃ /Al ₂ O ₃	[bmim]N(Tf) ₂	24	> 99 (11)	15 (71)	0.13	0.54	> 200
14	Toyonite 200P	[bmim]PF ₆	24	> 99 (10)	13 (85)	0.20	0.83	> 200
15	Toyonite 200P	[bmim]BF ₄	24	> 99 (35)	78 (58)	0.44	1.8	> 200
16 ^d	SBA-15	[bmim]PF ₆	48	> 99 (14)	22 (71)	0.22	0.46	> 200
17 ^d	SBA-15	[bmim]BF ₄	48	> 99 (27)	21 (60)	0.38	0.79	> 200
18	noPS/WO ₃ /SnO ₂	[bmim]PF ₆	24	0 (27)	0 (57)	—	—	—
19	noPS/WO ₃ /SnO ₂	[bmim]BF ₄	24	0 (0)	0 (97)	—	—	—
20	WO ₃ /TiO ₂	<i>i</i> -Pr ₂ O	120	> 99 (14)	21 (67)	0.18	0.15	> 200
21	WO ₃ /SnO ₂	<i>i</i> -Pr ₂ O	24	> 99 (16)	24 (53)	0.20	0.83	> 200
22	WO ₃ /Al ₂ O ₃	<i>i</i> -Pr ₂ O	24	> 99 (5)	5 (77)	0.05	0.2	> 200
23	WO ₃ /Fe ₂ O ₃	<i>i</i> -Pr ₂ O	24	> 99 (22)	39 (57)	0.28	1.2	> 200
24	WO ₃ /ZrO ₂	<i>i</i> -Pr ₂ O	24	> 99 (6)	13 (77)	0.12	0.5	> 200

^a The reaction was carried out at 35 °C in the presence of 1.5 equiv. of vinyl acetate as acyl donor. ^b Isolated yield. Enantiomeric excess was determined by capillary GC analysis using a chiral column (Chiraldex G-TA); > 99% ee means that no isomer is detected in the analysis conditions. ^c Relative Rate: %conv./reaction time (h). ^d The reaction was carried out in the absence of the catalyst.

enantioselectivity was found for the solvent systems employed. However, we found no significant relationship between the results and physical properties of these metal oxides.¹⁴ For example, the reactions of lipases immobilized by the WO₃/M_xO_y catalyzed reaction proceeded with perfect enantioselectivity (*E* > 200) in [bmim]PF₆ (Entries 1, 3–6), while those in [bmim]BF₄ gave the product (*S*)-**2** with reduced enantioselectivity (Entries 7–11). The most rapid reaction was recorded when WO₃/SnO₂-supported lipase PS was used as the catalyst in [bmim]PF₆ with poor enantioselectivity (Entry 2). We carefully reinvestigated this reaction and found that optically pure acetate (*S*)-**2** was obtained if the reaction was stopped for 5 h (Entry 3), and the reaction mixture was gradually acidified during the reaction. The esterification of (*±*)-**1** took place even when the reaction was carried out in the presence of WO₃/SnO₂ without lipase (Entry 18). Therefore, it was concluded that this drop in the enantioselectivity of Entry 2 was caused by the acid- or WO₃/SnO₂-catalyzed acylation independent of the enzymatic reaction. This was supported by the facts that excellent enantioselectivity was obtained when WO₃/SnO₂- or WO₃/Al₂O₃-supported lipase PS catalyzed reaction was conducted in [bmim]N(Tf)₂ which was respected to be the most stable ionic liquid for hydrolysis (Entries 12 and 13). We assumed that partial hydrolysis of [bmim]PF₆ with the moisture was mediated by WO₃/SnO₂.¹⁵ Interestingly, no reaction took place in the presence of WO₃/SnO₂ without enzyme in [bmim]BF₄ solvent system (Entry 19), although we anticipated that the reduced enantioselectivity in [bmim]BF₄ (Entries 7–11) was caused by the acid-catalyzed reaction due to the partial hydrolysis of [bmim]BF₄ with the moisture.

Lipase PS supported by WO₃/Al₂O₃ gave the best result in the [bmim]PF₆ solvent system (Entry 4), while lipase PS supported WO₃/SnO₂ worked the best in the [bmim]BF₄ solvent system (Entry 8). It is interesting that there was a clear contrast in the activity of the WO₃/M_xO_y supported lipase enzyme with the Toyonite 200P or methacryloxypropyl SBA-15 supported one; lipase PS supported by WO₃/M_xO_y gave better results in the [bmim]PF₆ solvent system than those in [bmim]BF₄ (Entries 1–11), while Toyonite 200P or methacryloxypropyl SBA-15

supported lipase PS worked better in the [bmim]BF₄ solvent system (Entries 14 and 17). Lipase PS supported by WO₃/M_xO_y also worked well in the ordinary diisopropyl ether (*i*-Pr₂O) solvent system, and the best result was obtained for WO₃/Fe₂O₃ in this solvent system (Entry 23).

In summary, we established that the proper immobilization of enzyme makes it possible to extend its applicability. Tungsten(vi) oxide-coated metal oxides were suitable as supporting materials for lipase PS, though it is still unclear how these supporting materials affect the enzyme activity in an ionic liquid solvent system. Further investigation of the scope and limitations of this reaction will allow optimization of the lipase-catalyzed reaction in an ionic solvent system.

References

- 1 T. Itoh, E. Akasaki, K. Kudo and S. Shirakami, *Chem. Lett.*, 2000, 262.
- 2 T. Itoh, E. Akasaki and Y. Nishimura, *Chem. Lett.*, 2002, 154.
- 3 T. Itoh, Y. Nishimura, M. Kashiwagi and M. Onaka, *Ionic Liquids as Green Solvents: Progress and Prospects*, ACS Symposium Series, ed. R. D. Rogers and K. R. Seddon, American Chemical Society, 2003, ch. 21.
- 4 T. Itoh, N. Ouchi, S. Hayase and S. Nishimura, *Chem. Lett.*, 2003, **32**, 654.
- 5 T. Itoh, Y. Nishimura, N. Ouchi and S. Hayase, *J. Mol. Catal. B: Enzymatic*, 2003, **12**, in press.
- 6 Toyonite is a porous ceramic prepared from a kaolinite: Toyodenka Co., Ltd. Phone: +81-888-31-1241. m-kamori@toyodenka.com. Toyonite 200P immobilized lipase PS is now commercially available from Amano Enzyme, Ltd.
- 7 D. Zhao, J. Feng and G. D. Stucky, *Science*, 1998, **279**, 548.
- 8 T. Sakai, K. Hayashi, F. Yano, M. Takami, M. Ino, T. Korenaga and T. Ema, *Bull. Chem. Soc. Jpn.*, 2003, (7), 1441.
- 9 We used the same immobilized enzyme for the three reactions in [bmim]PF₆, [bmim]BF₄, and *i*-Pr₂O.
- 10 For reviews see: (a) C. H. Wong and G. M. Whitesides, *Enzymes in Synthetic Organic Chemistry*, in *Tetrahedron Organic Chemistry Series*, Vol. 12, ed. J. E. Baldwin and P. D. Magnus, Pergamon, 1994; (b) F. Theil, *Chem. Rev.*, 1995, **95**, 2203; (c) T. Itoh, Y. Takagi and

- H. Tsukube, *Trends Org. Chem.*, 1997, **6**, 1; (d) F. Theil, *Tetrahedron*, 2000, **56**, 2905.
- 11 C.-S. Chen, Y. Fujimoto, G. Girdauskas and C. J. Sih, *J. Am. Chem. Soc.*, 1982, **102**, 7294.
- 12 USY was provided by Catalysts and Chemicals Industry, Co. Ltd.
- 13 Provided by the Catalysis Society of Japan as a reference catalyst JRC-ALO4.
- 14 N. Naito, N. Katada and M. Niwa, *J. Phys. Chem., B*, 1999, **103**, 7206. Selected physical properties of these metal oxides are listed as follows. (a) Order of the content of WO_3 : WO_3/TiO_2 (40 wt%) > $\text{WO}_3/\text{Al}_2\text{O}_3 = \text{WO}_3/\text{ZrO}_2$ (20 wt%) > $\text{WO}_3/\text{Fe}_2\text{O}_3$ (8 wt%) > WO_3/SnO_2 (6 wt%). (b) Order of the BET (Brunauer-Emmett-Teller) surface area ($\text{m}^2 \text{g}^{-1}$): $\text{WO}_3/\text{Al}_2\text{O}_3$ (125) > WO_3/ZrO_2 (99) > WO_3/TiO_2 (82) > $\text{WO}_3/\text{Fe}_2\text{O}_3$ (66) > WO_3/SnO_2 (30). (c) Order of the acid content (mol kg^{-1}): $\text{WO}_3/\text{Al}_2\text{O}_3$ (0.247) > WO_3/TiO_2 (0.215) > WO_3/ZrO_2 (0.190) > $\text{WO}_3/\text{Fe}_2\text{O}_3$ (0.079) > WO_3/SnO_2 (0.031). (d) Tungsten density of the surface/ nm^{-2} : WO_3/TiO_2 (6.3), WO_3/SnO_2 (5.3), $\text{WO}_3/\text{Al}_2\text{O}_3$ (4.1), $\text{WO}_3/\text{Fe}_2\text{O}_3$ (3.1), WO_3/ZrO_2 (5.1).
- 15 Partial hydrolysis of $[\text{bmim}]\text{PF}_6$ was confirmed by the fact that the pH value of the water layer obtained after shaking with the reaction mixture reached *ca.* pH 3, while it showed neutral for those obtained from a fresh $[\text{bmim}]\text{PF}_6$.



A novel non-phosgene polycarbonate production process using by-product CO₂ as starting material†

Shinsuke Fukuoka,^{*a} Mamoru Kawamura,^b Kyosuke Komiya,^c Masahiro Tojo,^d Hiroshi Hachiya,^e Kazumi Hasegawa,^f Muneaki Aminaka,^f Hirosige Okamoto,^f Isaburo Fukawa^d and Shigenori Konno^g

^a Corporate Research & Development Administration, Asahi Kasei Corporation, Hibiya-Mitsui Bld, Yurakucho 1-1-2, Chiyoda-ku, Tokyo 100-8440, Japan.

E-mail: fukuoka.sb@om.asahi-kasei.co.jp; Fax: +81-3-3507-2426; Tel: +81-3-3507-2432

^b Environment, Safety & Production Technology Administration, Asahi Kasei Corporation, Hibiya-Mitsui Bld, Yurakucho 1-1-2, Chiyoda-ku, Tokyo 100-8440, Japan

^c Organic Chemicals Development Dept., Chemicals & Plastics Company, Asahi Kasei Corporation, Yako 1-3-1, Kawasaki-ku, Kawasaki, Kanagawa 210-0863, Japan

^d Central Research Laboratory, Asahi Kasei Corporation, Samejima 2-1, Fuji, Shizuoka 416-8501, Japan

^e PC Development Group, PC Division, Chemicals & Plastics Company, Asahi Kasei Corporation, Yako 1-3-1, Kawasaki-ku, Kawasaki, Kanagawa 210-0863, Japan

^f Chemistry & Chemical Process Laboratory, Asahi Kasei Corporation, Niihama 2767-11, Kojima-Shionasu, Kurashiki, Okayama 711-8510, Japan

^g PC Division, Chemicals & Plastics Company, Asahi Kasei Corporation, Hibiya-Mitsui Bld, Yurakucho 1-1-2, Chiyoda-ku, Tokyo 100-8440, Japan

Received 2nd May 2003

First published as an Advance Article on the web 24th July 2003

Asahi Kasei Corp. has succeeded in the development of a new green process for producing an aromatic polycarbonate based on bisphenol-A (hereafter usually abbreviated as PC) without using phosgene and methylene chloride.¹ The new PC production process is the world's first to use carbon dioxide (CO₂) as a starting material. Until Asahi Kasei's new process was revealed, all of the PC in the world has been produced using carbon monoxide (CO) made from cokes or lower hydrocarbons and oxygen as a starting material. Furthermore, more than about 93% of the PC has been produced by the so-called "phosgene process" which uses phosgene made from CO and chlorine (Cl₂) as a monomer. However, the phosgene process inherently involves a number of environmental and economic shortcomings in addition to the high toxicity of phosgene itself and the high carcinogenic probability of methylene chloride itself. Asahi Kasei's new process enables high-yield production of the two important products for our citizens' lives, high-quality PC and high-purity monoethylene glycol (MEG), starting from ethylene oxide (EO), carbon dioxide (CO₂) and bisphenol-A. This new technology not only overcomes the environmental and economic problems existing in the phosgene process, but also achieves resource conservation, and energy conservation. Furthermore, the new process contributes to the earth environment by the reduction of CO₂ emissions (173 tons per thousand tons of product PC). Commercial application of the new process was carried out at the 50,000 ton year⁻¹ PC plant of Chimei-Asahi Corporation, a joint venture between Asahi Kasei Corporation and Chi Mei Corporation, which was newly constructed in Taiwan and has been successfully operating since June 2002. In recognition of the outstanding advance in ecological and sustainable performance that this technology represents, Japan's Minister of Economy, Trade and Industry conferred the Green and Sustainable Chemistry Award of 2003 on us. Furthermore, the Chairman of Japan Chemical Industry Association also conferred the 35th Japan Chemical Industry Association Award of 2003 on us as an outstanding chemical technology. An outline of this new non-phosgene PC process embodying the spirit of Green and Sustainable Chemistry is given here.

1 Introduction

An aromatic polycarbonate based on bisphenol-A (PC) has been widely employed as an engineering plastic in various applications basic to the modern lifestyle including automobiles, electric & electronic appliances, office equipments, and sheets, etc. Especially, PC is important as an indispensable resin for the optical disks of music or data and image storage, such as CDs and DVDs. This is because of the excellent properties of PC

such as outstanding impact resistance, transparency, heat resistance, and dimensional stability. About 2.7 million tons of PC have been produced annually worldwide, and until now all production has used carbon monoxide (CO) as a starting material. The vast majority of PC has been produced in the phosgene process where CO and chlorine are combined to form phosgene, a toxic gas, as an intermediate raw material. However, the phosgene process (see Fig. 1) entails a number of drawbacks in environmental terms as follows:

(1) It is necessary to use a large quantity (more than 4.3 ton/PC 10 ton) of very dangerous phosgene as a monomer. (2) It is necessary to use a very large quantity (more than 10 times by

† Presented at The First International Conference on Green & Sustainable Chemistry, Tokyo, Japan, March 13–15, 2003.

weight of the PC to be produced) of methylene chloride as a polymerization solvent. Methylene chloride is a low-boiling-point solvent with an exposure limit reflecting its carcinogenic properties (IARC classification: group-2B, possibly carcinogenic to humans; EPA classification: group-B2, probable human carcinogen). (3) A very large quantity of waste water must be treated before discharging. This process consists of an interfacial polymerization step using water and methylene chloride and also requires a very large quantity of water (more than 10 times by weight of the PC to be produced). Furthermore, a very large quantity of water is used for washing and purification of the obtained methylene chloride solution of PC to remove the contaminants, such as the NaCl produced, the unreacted sodium salt of bisphenol-A, the low molecular weight oligomers, and polymerization catalysts used *etc.* After the polymerization and purification steps, the water layer is separated from the methylene chloride layer by the phase separation step. However, the water layer contains methylene chloride due to its high solubility in water (20 g l^{-1}) in addition to the above contaminants. (4) It is very difficult to prevent completely the release of the methylene chloride to the atmosphere due to its low boiling point (40°C). (5) It is easy for corrosion of the equipment to occur due to the hydrochloric acid

and aqueous solution of NaCl produced. (6) The raw materials, chlorine and NaOH which are produced by electrolysis of aqueous NaCl using a large quantity of electric power, are consumed and converted to NaCl and ultimately require the disposal of waste salt water.

Many attempts have been made to overcome the environmental and cost disadvantages of the phosgene process, but faced with significant technological barriers, both for a production step for a safe monomer of diphenyl carbonate (DPC) to replace phosgene and for a polymerization step to produce polycarbonate, success has been limited.

Based on a strong mission which contributes to society by creating a "benign process to the earth", a mission which is similar to the concept of green and sustainable chemistry, we, Asahi Kasei's researchers and engineers, have made substantial endeavors to develop new non-phosgene technology for the production of PC necessary for the modern lifestyle for the long term of more than 20 years. As a result, we have succeeded in developing an innovative non-phosgene process for producing PC, in which the carbonyl group of CO_2 is incorporated into the main chain of PC. This is the world's first polycarbonate process which uses CO_2 as a starting material, in contrast to all other existing processes which use CO as a starting material.

Green Context

Polycarbonate is a very widely used engineering plastic with applications in areas including electronic appliances and automobiles. To date all of this material has been prepared using CO as the feedstock – most of it *via* the highly dangerous phosgene. Here we see described the first polycarbonate manufacturing process using carbon dioxide as the C1 feedstock. This award-winning development has many major green chemistry advantages compared to traditional processes. *JHC*

2 Asahi Kasei's green and innovative process for producing PC (Fig. 2)

Asahi Kasei's new technology uses ethylene oxide (EO), its by-product CO_2 , and bisphenol-A as starting materials to produce high-quality polycarbonate (PC) and high-purity monoethylene glycol (MEG) in high yields respectively. Because CO_2 has low chemical reactivity, it was considered to be difficult to incorporate it into the polycarbonate main chain. However, this technology successfully integrates all of the CO_2 used into the products by developing technologies which enable the desired reactions to proceed effectively and selectively.

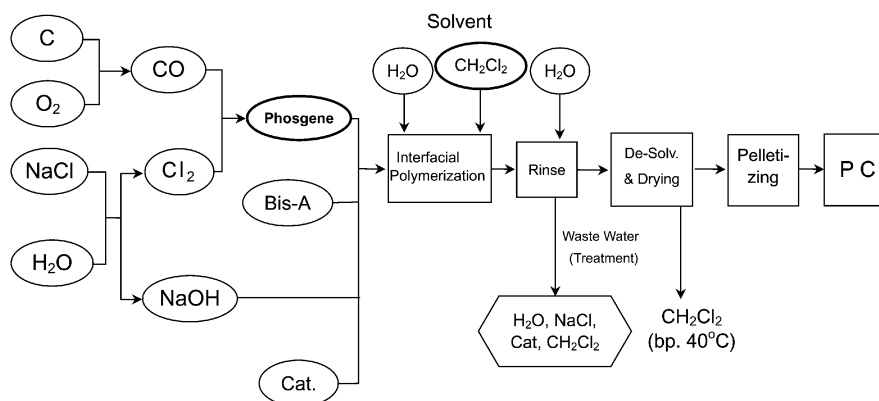


Fig. 1 Phosgene PC process.

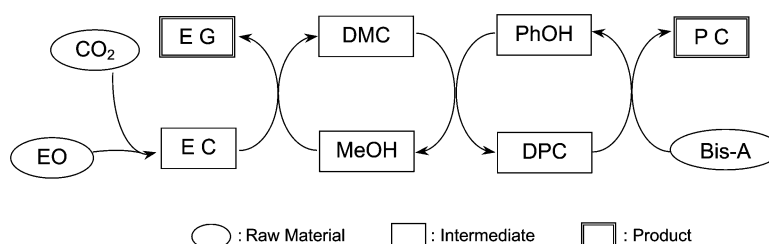


Fig. 2 Asahi Kasei's new non-phosgene PC process.

The main characteristic features of Asahi Kasei's new process are as follows:

(1) This process has no environmental drawbacks existing in the phosgene process described above. (Phosgene free, methylene chloride free, and process water free) (2) The CO₂ used as starting material is a by-product generated in the production of ethylene oxide (generally used to make ethylene glycol for PET bottles, films, and fibers, *etc.*), and is usually released to the atmosphere. (3) High yields and high selectivity are achieved in both the monomer production step and the polymer production step. (4) All intermediate products, ethylene carbonate (EC), dimethyl carbonate (DMC), methanol, diphenyl carbonate (DPC), and phenol are completely used or recycled as raw materials of the next reaction step or the preceding reaction step. (5) There are no wastes, and no waste process water to have to be treated. (6) Monoethylene glycol (MEG) can be selectively produced in high yield by the energy-saving process because of using no process water. (7) The polymerization step uses a unique original reactor which utilizes gravity without using mechanical stirring used in the usual melt polymerization. (8) Purification and separation steps for the PC are unnecessary. The molten PC obtained from the polymerization step can be directly palletized to conserve energy compared with the phosgene process wherein the PC is produced in powder form and it must be made to pellet by heating and melting.

The CO₂ used as starting material is a by-product generated in the production of ethylene oxide, and is usually released to the atmosphere. Therefore, this process is thought to be totally green, because not only is the wasted CO₂ effectively utilized but also there are no waste and no waste process water, and both savings of materials and energy are achieved.

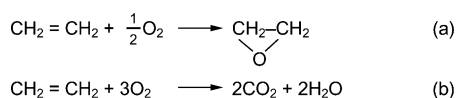
2.1 Monomer production process

In order to produce high-purity and high-performance polycarbonate (PC) by non-phosgene processes, it is indispensable to use very high purity bisphenol-A and diphenyl carbonate (DPC). High-purity bisphenol-A is commercialized in large quantity and can be available for producing PC on an industrial scale. However, DPC was not commercialized for industrial scale production of PC; only several hundred tons of DPC containing Cl-compound impurities were produced from phosgene and were on the market as a specialty chemical, but the price was several times as high as that of PC itself. It has been well known that DPC synthesis is very difficult except the reaction of phosgene with phenol. Therefore, it is very important to develop non-phosgene and high-purity DPC production technology suitable for industrialization. Especially, the impurities, such as chloride compounds, alkali and alkaline earth metal compounds, must not be contained in DPC, because even in very small amounts, such as less than 0.1 ppm, they exert a bad effect on the polymerization step or on the properties of the PC produced.

We have succeeded in development of a new process which can produce very high-purity DPC containing none of these impurities in high yield with high selectivity from CO₂, ethylene oxide (EO) and phenol, and which can be commercialized. This new process for monomer production consists of three steps, an ethylene carbonate (EC) production step, a dimethyl carbonate (DMC) and monoethylene glycol (MEG) production step, and a DPC production step.

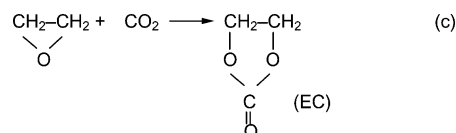
2.1.1 Ethylene carbonate (EC) production step. There are a lot of EOG (ethylene oxide and ethylene glycol) plants, and about 13 million tons of EO are produced annually all over the world. In all the EO plants, EO is produced by the oxidation of ethylene with oxygen. The yield of EO in this process cannot exceed about 80%, because this oxidation reaction using oxygen at high temperature in the presence of an Ag catalyst

necessarily produces CO₂ as a by-product in about 20% yield.² Almost all of the CO₂ produced as a by-product in the EOG plants is usually released to the atmosphere.



Scheme 1 Reactions (a) and (b).

However, in Asahi Kasei's new process, the CO₂ produced as a by-product in the EO plant is effectively utilized as a raw material, and EC can be produced almost quantitatively by the reaction of the CO₂ with the EO in the liquid phase or super critical phase.



Scheme 2 Reaction (c).

This reaction (c) is well known to proceed smoothly using a catalyst, such as alkali or alkaline earth metal halides, amines, quaternary ammonium or phosphonium salts, guanidine, Lewis acid-amine complex compounds, and anion-exchange resins containing quaternary ammonium salts, to give EC continuously in a high yield.³ Although the commercial production of EC is performed by this method, several process improvements for the new EC plant have been enforced to produce high-quality EC quantitatively. For DPC production, the new EC plant has been constructed near the EO plant and has been smoothly operating.



Scheme 3 Reaction (d).

2.1.2 Dimethyl carbonate (DMC) and monoethylene glycol (MEG) production step. We have developed a process that enables us to produce high-purity DMC and high-purity MEG from EC and methanol (MeOH), respectively, in quantitative yields.

Until our development, three methods had been proposed to progress this reaction.

The first one is a complete batch method in which the reaction is conducted in an autoclave at a temperature higher than the boiling point of MeOH in the presence of a catalyst under pressure.⁴

The second one is a batch reaction method which uses a batch reactor fitted with a distillation column on the reactor. In this method, the reaction occurs only in the reactor batch-wisely in the presence of a catalyst, while the distillation column works to separate the vaporized DMC from the azeotropic mixture of DMC-MeOH and to return the DMC to the reactor.⁵ However, it is very difficult to get DMC and MEG in high yields by this method, because the MEG produced easily reacts with the unreacted EC in the reactor to give the higher molecular weight by-products, such as diethylene glycol (DEG), triethylene glycol (TEG) *etc.* Although the selectivity of MEG can be improved to some degree by use of a large excess of MeOH, the degree of the improvement is not enough.

The third one is a continuous method which uses a tubular reactor.⁶ However, this method can not achieve the high

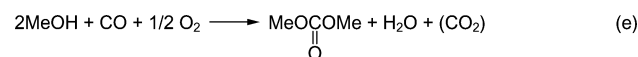
conversion of EC, because this reaction is an equilibrium reaction, even if an excess of MeOH is used such as MeOH : EC = 4 : 1 (molar ratio), the conversion of EC is about 40–60% at 80–120 °C.

Thus, these three methods proposed until now have had several drawbacks in that the reaction time is long, a large excess of MeOH must be used to lower the production of high boiling point by-products, high yields of DMC and MEG with high selectivity cannot be achieved, the complete recovery of the unreacted EC in the presence of EG is difficult, *etc.* Therefore, it is difficult to use these methods on a commercial scale. In the above-described situation, we have made extensive and intensive studies to develop a process free of the drawbacks of the various hitherto proposed processes. As a result, it has surprisingly been found that high-purity DMC and high-purity MEG can be continuously produced in quantitative yields (more than 99%) respectively at a high production rate using a new method.

In the new method, the inherent characteristics of the reaction of EC with MeOH (such as the equilibrium reaction, easy reactivity of EC with the hydroxy compounds, azeotrope formation of the raw materials and the products *etc.*) are fully considered, and the facilities and the operation conditions are designed to achieve almost complete conversion avoiding the side reactions.

In order to establish the new technology at a level capable of industrialization, a lot of experiments using a variety of conditions and many times of continuous operation for the long term had to be practiced using several kind of facilities combined with several apparatus, and further many improvements also had to be enforced. Thus, in the second step of the monomer process, very high-purity DMC containing no chlorides impurities can be produced compared with the other conventional DMC processes.

For PC production, another process for production of DMC has been already commercialized, in which the oxidative carbonylation reaction (e) of MeOH with CO and oxygen is used in the presence of a CuCl-slurry catalyst system.⁸



Scheme 4 Reaction (e).

However, it is said that this oxidative carbonylation process has several shortcomings and has to be further improved to establish it as a greener process:⁹

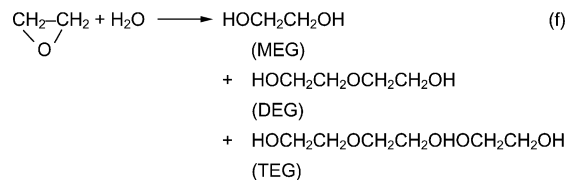
(1) The selectivity of DMC is low, 65–70% and >95% based on CO and MeOH used, respectively, and significant amounts of CO₂ (about 30%) by-production is unavoidable. (2) The reaction system is highly corrosive and erosive, because it contains highly concentrated CuCl-slurry and the water produced. (3) The DMC contains chloride impurities derived from the catalyst system which are difficult to separate. It is well known that very small amounts (<0.1 ppm) of chloride impurities exert bad effects not only on the polymerization reaction but also on the performance of the polycarbonate

produced. In order to get high-purity DMC, precise separation steps are necessary. However, these steps lead to a lowering of the DMC yield and to an increase in energy consumption. (4) The water, another product, must be separated from the reaction mixture and treated before discharging.

The DMC production step of Asahi Kasei's new process has none of these shortcomings, therefore, it is greener than the conventional process.

Furthermore, in the second step, attention must be paid to the EG production. High-purity MEG can also be produced in high yield. All of the ethylene glycol (EG) in the world (14.5 million tons year⁻¹) has been produced by the reaction of EO with water. However, this process has at least two big problems to be solved as follows:²

(1) The yield of MEG is low, and the oligomers such as diethylene glycol (DEG), triethylene glycol (TEG) are necessarily produced as by-products in more than 10% yield. It is necessary to use large quantities of energy to separate these by-products by distillation. (2) In order to produce MEG with about 90% selectivity, a very large excess of H₂O, as much as 22–25 times in mol to EO, must be used. This means that the very large amounts of H₂O remaining in the reaction mixture must be separated by distillation from the products. As a result a very large quantity of energy must be consumed for the distillation because the latent heat of H₂O for vaporization is very large (540 kcal kg⁻¹).



Scheme 5 Reaction (f).

In contrast with the conventional EG process, the second step of Asahi Kasei's new process can produce high-purity MEG in a high yield with high selectivity (more than 99%, respectively) using MeOH instead of H₂O, wherein the molar ratio of MeOH to EC is not so large. This means that the new process can achieve energy-saving in a high level, because there are no H₂O and by-products such as DEG to be distilled off, and the amount of MeOH to be distilled off is not so much, and further both values of the latent heat for vaporization and the specific heat of MeOH are only about half those of H₂O.

The world's first commercial plant for co-producing DMC and MEG has been smoothly operating since June 2002 in Taiwan.

2.1.3 Diphenyl carbonate (DPC) production step. In the third step of Asahi Kasei's new monomer process, DPC is produced by using the combination of two reactions from DMC and PhOH. The main reactions occurring in the process are as follows. At first, methylphenyl carbonate (MPC) is produced by the transesterification reaction of DMC with PhOH, then 2 moles of MPC are disproportionated to DPC and DMC by the

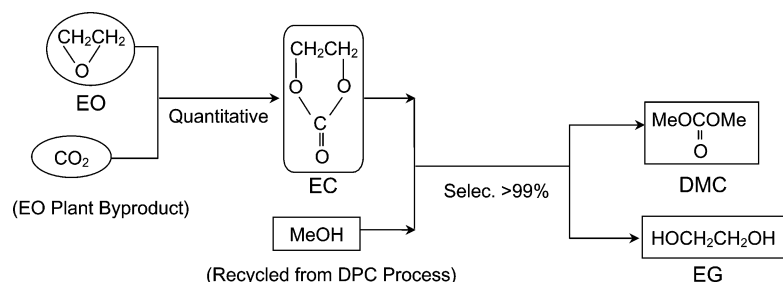
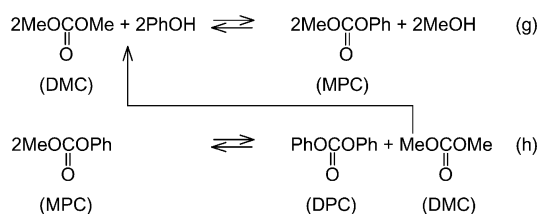


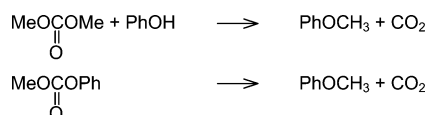
Fig. 3 Asahi Kasei's PC Monomer Process — EC, DMC —.

self-transesterification reaction (disproportionation reaction). The DMC produced in the reaction (h) is recycled to the first transesterification reaction (g), and the MeOH produced in the reaction is recycled to the DMC and MEG production step.



Scheme 6 Reactions (g) and (h).

Both of these two reactions are equilibrium reactions having low equilibrium constants. Especially, reaction (g) has an extremely small equilibrium constant ($K = 10^{-3}-10^{-4}$), and furthermore the reaction is very slow. Also, side reactions such as etherification and decarboxylation easily occur to give anisole and CO_2 .¹⁰ So, there were a lot of difficulties and problems in developing a feasible process for commercialization using these reactions.



Scheme 7 Reactions of DMC with PhOH and decarboxylation of methyl phenyl carbonate to produce anisole and CO_2 .

We have developed an innovative process which can produce very high-purity DPC, which is indispensable for high performance polycarbonate, in a high production rate with high selectivity (>99%). In this process, the two reactions described above ((g) and (h)) are conducted using the two continuous multi-stage distillation columns combined each other, and the reactions and separations of the products by distillation are carried out simultaneously in those columns (Fig. 4).

The technology where the reaction and the separation of the products by distillation are carried out simultaneously in the same distillation column is called a reactive distillation. This reactive distillation technology for producing DPC was first disclosed to the world by our patents.¹¹ Before the disclosure of our patents, all efforts for producing DPC had been focusing on development of the catalyst to raise the very slow reaction rate of DMC with PhOH and on prevention of taking away of DMC from the reaction system by azeotrope formation with produced MeOH. In these research and developments, the reactions were carried out batch-wisely in the reactor (tank or flask) fitted with a distillation column on the reactor, in which the reaction occurred only in the reactor containing the catalyst.¹² At that time, none of the proposals for producing DPC continuously had been published, except one process¹³ using a tube reactor packed with molecular sieves to absorb produced MeOH, which is completely different from the reactive distillation method. After disclosure of our patents, a lot of patent applications in DPC production using the reactive distillation technology have been carried out.¹⁴

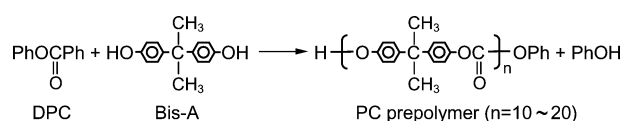
In this step, at least two reactive distillation columns combined with each other must be used, therefore, it is more complicated and difficult to produce high-purity DPC smoothly. We had to construct the pilot scale facilities several times, which were capable of both the two reactions and the two distillations under pressure and under reduced pressure respectively. And we had to practice the long term operations under different conditions many, many times, because it is very difficult to create the steady states required to operate the two or more combined distillation columns when conducting many reactions, many distillations and many recyclings of the

materials. Such hard and long term endeavors led to the establishment of this technology capable for commercialization.

The commercial plant for producing high-purity DPC from DMC and PhOH using the reactive distillation method developed by Asahi Kasei has been smoothly operating.

2.2 Polymer production process

When we try to produce PC on a large scale by transesterification reaction of bisphenol-A (Bis-A) with DPC, removing the by-product PhOH from the reaction mixture under high vacuum becomes a difficult problem. This problem is particularly troublesome, because it is based on the substantial characteristics existing in the polycondensation reaction of PC itself. In order to advance the polymerization, it is necessary to remove the PhOH produced by the equilibrium reaction effectively from the reaction mixture through the surface of the polymer.



Scheme 8 Reaction of DPC with Bis-A.

However, in the case of PC, an extreme increase of melt viscosity occurs with progression of the polymerization and the surface renewal of the polymer by mechanical stirring for removing the PhOH becomes very difficult before reaching the required molecular weight. As a result, the polymerization becomes harder to progress. In order to lower the melt viscosity and to progress the polymerization, it is necessary to make the reaction conditions more severe; that is, a higher reaction temperature of greater than about 300 °C under high vacuum of less than about 13 Pa for a fairly long time. However, these severe reaction conditions easily result in fatal damages to the PC produced, such as discoloration, deterioration of the physical properties. Thus, the difficult problems encountered in progressing the melt polymerization reaction of PC without causing fatal damages to the polymer have remained for a long time. In this respect, the polycondensation reaction of PC is essentially different from the others, such as polyethylene terephthalate (PET) and polyamides (Nylons). One of the reasons why none of the newcomers could enter the production of PC for a long time until now is because of the presence of substantial difficulty in the polymerization step. The latest newcomer entered into PC commercialization in 1985 using the phosgene process in the USA.

In the pre-polymerization step, the PC prepolymer having a polymerization degree of about 10–20 can be obtained from the molten mixture of Bis-A and DPC without such difficulty because of the relatively low melt viscosity, however, when the polymerization degree becomes more than about 20, the melt behavior rapidly changes from the previous one and a drastic increase in the melt viscosity occurs. The required polymerization degrees of PC as an engineering plastic are about 30–60, so a further-polymerization step is necessary. For this further-polymerization step, we have successfully developed two different processes capable of industrialization to overcome the difficult problem based on the extremely high viscosity of PC.¹ One is a solid-state polymerization process, and the other is a melt polymerization using a unique reactor without mechanical stirring.

2.2.1 Solid-state polymerization process. This further-polymerization process of PC is based on the new concept developed by us for the amorphous polymer, and was published

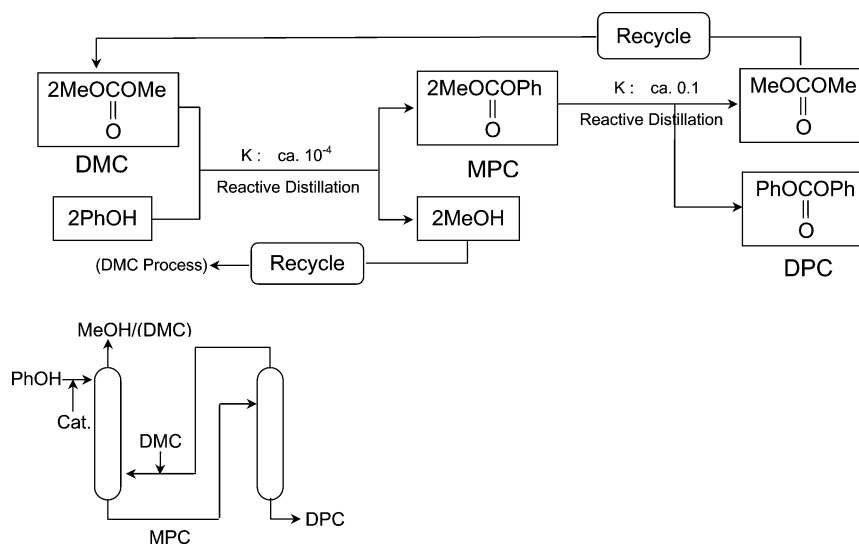
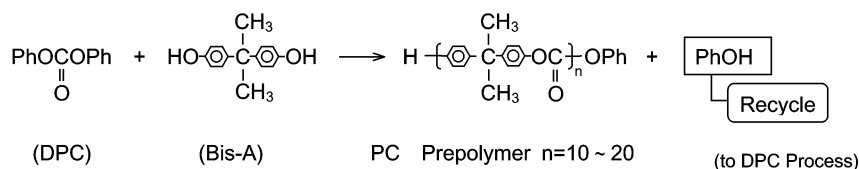


Fig. 4 Asahi Kasei's PC monomer process — DPC —.

(1) **Pre - Polymerization**



(2) **Main Polymerization**

2 New Processes Developed by AsahiKasei

Solid - State Polymn.

Gravity-Utilized Melt Polymn.

Fig. 5 Asahi Kasei's PC polymerization process

in "Green Chemistry, Designing Chemistry for the Environment" (*ACS Symposium Series 626*, Chapter 2).¹⁵ Different from amorphous polymers such as PC, for crystalline polymers such as PET and Nylon it is known that solid-state polymerization of a pellet that has sufficient molecular weight for general purposes can be carried out to get higher molecular weight polymer for special uses such as tire cord.¹⁶ However, none of the trials to get PC resins by solid-state polymerization had been published until our disclosure. This is perhaps because of the reason that PC is an amorphous polymer and becomes a molten state at the temperatures necessary to effect polymerization and, therefore, solid-state polymerization is impossible. We have found several new facts. That is, a PC prepolymer having a polymerization degree of about 10–20 can be easily crystallized by contact with a solvent such as acetone to give a porous crystalline powdery prepolymer with a melting point of 225–230 °C and a surface area of more than about 2 m² g⁻¹, and this porous crystalline prepolymer can polymerize at relatively low temperatures such as 210–220 °C with effective removal of PhOH under reduced pressure or under blowing of nitrogen gas, *etc.* These discoveries led to the new concept, and a solid-state polymerization process suitable for industrialization using this new concept has been developed. After disclosure of Asahi Kasei's technologies of the solid-state polymerization of PC,^{15,17} a lot of work from universities and companies in this field has been published.¹⁸ We are very glad to see the expansion of this technical field as a pioneer of the solid-state polymerization of amorphous PC.

2.2.2 Melt polymerization process. In order to get PC having the molecular weight required for engineering plastic (a polymerization degree of about 30–60) by melt polymerization, a lot of trials have been carried out. However, almost all of these have used horizontal reactors which have been developed for the polymerization of polymers having super high viscosity. These reactors in the further-polymerization step have twin mechanical axes of a self-cleaning type for mixing and for surface renewal of the polymer.¹⁹ However, these reactors have several problems as follows:

(1) They need to use a high power motor for rotating the twin axes and consume a large quantity of electric energy, because very high viscosity polymers must be mixed. (2) Air or small size contaminants easily leak into the reactor through the seals of rotary axes, because the operations are carried out at high temperature under high vacuum. These leaks cause deterioration of the color tone and the physical properties of PC. (3) It is difficult to produce PC grades having middle to high viscosities, which are the grades that are important for injection and extrusion products. This means that even the most effective stirring systems now available cannot produce all grades of PC for general purposes.

We have developed a new unique reactor to solve the problems experienced with these mechanical mixing type reactors. The new type reactor utilizes only the earth's gravity without using any mechanical mixing system. This is the world's first reactor for the polycondensation of PC. The new reactor can smoothly progress the further-polymerization

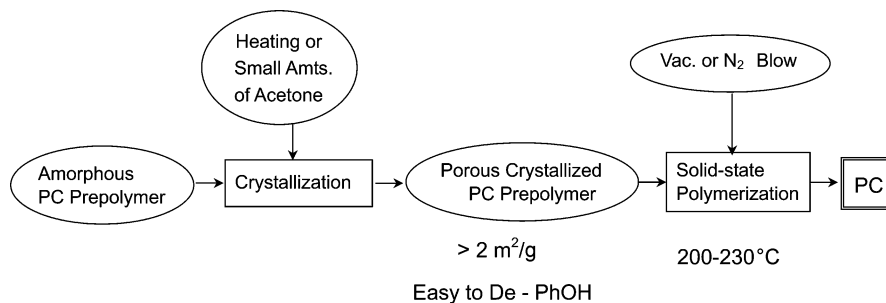


Fig. 6 Asahi Kasei's PC solid-state polymerization process

reaction of PC during which the prepolymer falls down along the guides fitted in the space of the reactor. The new reactor makes it possible to produce high-purity and high-performance PC having good physical properties with clear color tone. We have established the industrial technology for producing PC having molecular weight from the disk grade (a polymerization degree of about 30–35) to a higher viscosity than the usual high viscosity grade (a polymerization degree of about 50–60).

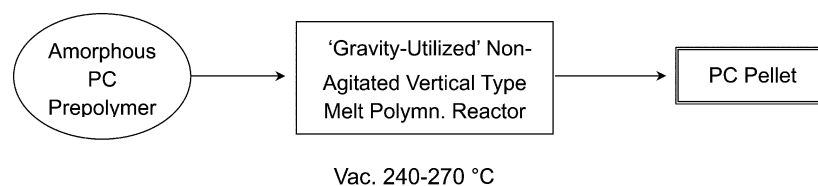
Until now, both technical and scientific approaches for production of the high viscosity polymer have been focusing on development of an effective stirring system for the horizontal twin axes reactor with self-cleaning performance, wherein the polymer is stirred mechanically and compulsorily by the rotating twin axes for the surface renewal. No one has noticed that the combination of the gravity of the earth with the adhesive force of the polymer itself makes the compulsory mixing unnecessary in the polymerization of PC.

Therefore, this is exactly based on the “reverse conception,” because Asahi Kasei's new polymerization technology utilizes inversely the troublesome high viscosity of the polymer.

Thus Asahi Kasei's new polymerization reactor just realizes the spirit of “Green Chemistry” or “Green and Sustainable Chemistry” because it simply utilizes the gravity of the earth. The world's first commercial plant based on the new melt polymerization technology developed by Asahi Kasei has been smoothly operating in the capacity of 50,000 tons year⁻¹ in Taiwan.

3 Experimental

For the following brief experimental examples it should be understood that they are only showing the principle of the new non-phosgene process for producing PC. These examples are based on the data obtained in the research and development stages of the new technology and on the description of the patent applications of Asahi Kasei. Therefore, it should be understood that they are not necessarily based on the present commercial plant because more and more improvements and development have been practiced to make the process more green in the commercial plant.



ASAHI Patents : World's First

USP 5,840,826 etc.

Fig. 7 Asahi Kasei's PC melt polymerization process.

3.1 Ethylene carbonate (EC)²⁰

26.4 g (0.6 mol) of ethylene oxide (EO) and 0.64 g of anion exchange material containing tetramethylammonium chloride groups (the water content was less than 0.03 wt%) were charged into the 200 ml autoclave. After replacing the atmosphere in the reactor with CO₂, 52.8 g of liquid CO₂ was pumped into the reactor. The reaction was conducted at 100 °C for 3 h with stirring. The yield of EC was 98% with 100% selectivity based on EO used. None of the by-products were found in the reaction mixture.

3.2 Dimethylcarbonate (DMC) and monoethylene glycol (MEG)^{7,21}

For the reaction of EC with MeOH, the preferred catalysts are alkali or alkaline earth compounds (such as hydroxides, carbonates, bicarbonates, alkoxides), tertiary amines, N-containing heteroaromatics, and alkoxy metal (Sn, Ti, Zn) compounds as homogeneous catalysts, and anion exchange resins having tertiary amino groups or quaternary ammonium groups as heterogeneous catalysts.

3.2.1 Continuous method using the tube reactor packed with the solid catalyst. A tube reactor (12.7 mm outer diameter) packed with 60 ml of an anion exchange material containing tetramethylammonium carbonate groups was used. The mixture of MeOH and EC (molar ratio of MeOH : EC = 2 : 1) was continuously fed into the reactor with the rate of LHSV = 0.33 h⁻¹. The reaction was conducted at 60 °C. Analysis of the reaction mixture at steady state showed that the conversion of EC was 39%, the selectivity for both DMC and MEG was 99%. The value of EC conversion showed that the reaction reached the equilibrium state. The reaction was continuously carried out for 8,100 hours, the results were not practically changed during the long reaction hours.

3.2.2 Continuous method using the distillation column packed with the solid catalyst. A continuous distillation apparatus was used within which a 60 cm height of an anion

exchange material containing tetramethylammonium chloride and carbonate groups was packed in the middle part of the distillation column (2 cm inner diameter, 1 m length) and 10 cm height of the Dixon packing (2 mm diameter) was packed in both the upper and the lower part of the column. The packed anion exchange material performed both as the catalyst and as the packing for distillation, and the theoretical number of stages was 18. The gaseous MeOH was fed into the column from the lower part at a rate of 81.6 g h⁻¹, and the liquid mixture of EC and MeOH (EC : MeOH = 5 : 1 in weight ratio) was heated at 70 °C and fed into the column from the upper part. The reaction and the distillation were continuously carried out to keep the temperatures at about 78 °C in the lower part of the column and about 65 °C in the upper part of the column. After reaching the steady state, the gaseous component distilled off from the top of the distillation column was continuously withdrawn as a liquid after condensation at a rate of 77.2 g h⁻¹, the liquid component was continuously withdrawn from the bottom of the column at a rate of 30.8 g h⁻¹. The condensate of the gaseous component consisted of 29 wt% DMC and 71 wt% MeOH, and the liquid component consisted of 50 wt% of MEG and 49.5 wt% of MeOH. The conversion of EC was 100%, both yield and selectivity for DMC were 99.5%. And both yield and selectivity for MEG were 99.5%. In this manner, DMC and MEG were produced for many hours; the results were not changed during 400 hours.

3.3 Diphenyl carbonate (DPC)²²

3.3.1 Batch reaction method using a tank reactor fitted with a distillation column on it. 12.6 kg of a mixture containing of 73.2 wt% DMC and 26.8 wt% PhOH, and 79.38 mmol of Pb(OPh)₂ as a catalyst were charged into an autoclave type reactor having a capacity of 15 l and provided with a distillation column of 1 m in height and 1 inch in diameter (packed with a stainless steel-made Dixon packing of about 6 mm in diameter) and reflux condenser, and stirrer. The reactor was heated, while stirring, so as to keep the temperature of the mixture at 204 °C, thereby performing the reaction. The gaseous component distilled off from the top of the column was condensed, and a portion of the condensate was recycled into the column top with a reflux ratio of 0.8, and the rest of the condensate was continuously withdrawn at a rate of 2.1 kg h⁻¹. After this operation was carried out for 2 hours, the reactor was cooled to stop the reaction. 8.4 kg of the reaction mixture contained 1.8 wt% methyl phenyl carbonate (MPC), 0.01 wt% DPC and 0.07 wt% anisole. This result shows that the conversion of PhOH was 2.94%, the yield and selectivity of MPC were 2.77% and 94%, respectively, and the yield and selectivity of DPC were 0.02% and 1%, respectively, and the yield and selectivity of anisole were 0.15% and 5%, respectively, by the batch-wise reaction for 2 hours.

Before disclosure of our patent, all efforts for producing DPC from DMC and PhOH were carried out using a similar method to that described here by batch-wise reaction.

3.3.2 Reactive distillation method using one distillation column. A mixture of DMC (73.2 wt%), PhOH (26.8 wt%) and Pb(OPh)₂ as a catalyst (6.3 mmol kg⁻¹ of the raw materials) was continuously fed in a liquid form at a rate of 6.3 kg h⁻¹ to a continuous multi-stage distillation column at a position 1 m below the top of the column through a preheater. This column comprised of a packed column of 4 m in height and 3 inches in diameter and packed with a stainless steel-made Dixon packing (about 6 mm in diameter). The thermal energy necessary for reaction and distillation was supplied by heating the liquid in the bottom of the distillation column with a reboiler. Both the

reaction and the distillation were carried out continuously in the column under conditions where the temperature at the bottom of the column was 204 °C, the pressure at the top of the column was 0.78 Mpa, and the reflux ratio was 0.8. The condensed distillate was continuously withdrawn at a rate of 2.1 kg h⁻¹, and the liquid component was continuously withdrawn from the bottom at a rate of 4.2 kg h⁻¹. The reaction liquid withdrawn from the bottom contained 3.4 wt% MPC, 0.05 wt% DPC and 0.02 wt% anisole. The average residence time (essentially equal to the average reaction time) of the feed liquid was 0.143 h. This result shows that the conversion of PhOH was 5.39%, the yield and selectivity of MPC were 5.22% and 97%, respectively, the yield and selectivity of DPC were 0.11% and 2%, respectively, and the yield and selectivity of anisole were 0.06% and 0.8%, respectively, in the reaction time of 0.143 hours.

In addition to the high selectivity of 99% (MPC + DPC), the advantage of the reactive distillation method is clear when the relative production rate (yield/reaction time) of (MPC + DPC) in this new reactive distillation method is compared with the batch method described in 3.3.1. The new method has a production rate about 26 times as high [(5.33%/0.143 h)/(2.79%/2 h) = 26] as the batch method.

It is believed that the advantages of this process over conventional processes such as that described in 3.3.1 are mainly due to the following points:

(1) A catalyst is present throughout a continuous multi-stage distillation column and, hence, it is possible to advance the reaction in a large region. And the area of the gas-liquid interface can be extremely large compared to that provided by the conventional process in which the reaction is performed using a tank reactor, and as a result, the MeOH produced in the liquid phase is easily and quickly transferred to the vapor phase. (2) The liquid phase of the reaction system in a continuous multi-stage distillation column flows down while repeatedly experiencing a gas-liquid contact with a vapor ascending from a lower portion and being subjected to reaction and, hence, despite the fact that the process is a continuous process, high productivity can be achieved in a short reaction time. (3) The vapor ascending in a continuous multi-stage distillation column ascends while repeatedly experiencing a gas-liquid contact with a liquid descending in the column and, hence, the thermal energy of the vapor is effectively utilized.

3.3.3 Reactive distillation method using two distillation columns combined each other. An apparatus comprising two distillation columns of the same type described in 3.3.2 was employed. In the first column, the reaction and the distillation were performed by continuously feeding in a liquid form a mixture of DMC, PhOH and the catalyst at a rate of 4.6 kg h⁻¹. This liquid consisted of the fresh raw materials and the recycled materials withdrawn from the top of the second distillation column as a distillate, and was fed into the first distillation column at a position 1 m below the column top through a preheater, together with the fresh gaseous DMC (3 kg h⁻¹) which was fed to the first column from the bottom part. The fresh raw materials fed from the upper portion contained 3.8 wt% DMC, 92.8 wt% PhOH and 3.4 wt% Pb(OPh)₂, and the flow rate was 0.9 kg h⁻¹. The combined raw materials contained 50.6 wt% DMC, 45.3 wt% PhOH, 3.3 wt% MPC and 0.8 wt% of the catalyst. The temperature at the bottom of the first column was 204 °C, and the pressure of the top of the first column was 0.78 MPa, and the reflux ratio was zero. The condensed distillate containing MeOH and DMC from the first column was continuously withdrawn at a rate of 3.1 kg h⁻¹. The bottom liquid of the first column containing 27.4 wt% of MPC was continuously withdrawn at a rate of 4.5 kg h⁻¹, and was continuously fed into the second distillation column at a position 1 m below the column top. The temperature of the bottom of the second column was 195 °C, and the pressure of

the top of the second column was 41 KPa, and the reflux ratio was 1.5. The condensed distillate containing DMC from the second column was continuously withdrawn at a rate of 3.7 kg h⁻¹. The bottom liquid of the second column containing 92.6 wt% DPC with selectivity of 98% was continuously withdrawn at a rate of 0.81 kg h⁻¹.

3.4 Polycarbonate (PC) by the solid-state polymerization^{15,17,23}

68.4 g of bisphenol-A and 77.0 g of DPC produced by the method described in 3.3.3 were put into a 500 ml three-necked flask provided with a stirrer, a gas inlet and a gas suction port. De-aeration by applying a vacuum and introduction of dry nitrogen were performed five to six times. Then, the flask was immersed in an oil bath kept at from 180 °C to 190 °C, thereby melting the contents of the flask. Again, de-aeration by applying a vacuum and introduction of dry nitrogen were performed. Thereafter, the temperature of the oil bath was elevated to 230 °C, and dry nitrogen was introduced into the flask at a rate of 25 l h⁻¹ (volume at normal temperature and pressure) while stirring so as to distill off the phenol formed. About 50 minutes later, the reaction system was evacuated, and the reaction mixture was stirred at from 260 to 660 Pa for about 15 minutes, thereby distilling off phenol and DPC. As a result, 7 g of a colorless, transparent prepolymer having a weight average molecular weight of 6,200 was obtained. The prepolymer had terminal-OCOOPh groups and terminal-OH groups in amounts of 72 mol% and 28 mol%, respectively, based on the total number of moles of all the terminal groups of the prepolymer. The prepolymer was taken out of the flask and pulverized. The resultant powdery prepolymer was immersed in 250 ml of acetone, thereby effecting crystallization of the prepolymer. The crystallization of the prepolymer occurred immediately after the immersion. Thirty minutes after the immersion, sufficient crystallinity was obtained, but immersion was further continued for 1 hour. The resultant white powdery crystallized prepolymer was filtered off and dried. From the powder X-ray diffraction patterns, it has been found that the crystallized prepolymer had a crystallinity of 30%. With respect to the ratio of each of the terminal groups, there was substantially no change between the prepolymer before the crystallization, *i.e.*, amorphous prepolymer, and that after crystallization, *i.e.*, crystallized prepolymer.

The powdery crystallized prepolymer, was put into the same type of flask as that used in the prepolymer preparation. While introducing a little amount of dry nitrogen into the flask which was under 260 to 660 Pa, the flask was put in a oil bath kept at 190 °C. While stirring the content of the flask, the temperature of the oil bath was elevated at a rate of 5 °C h⁻¹. After the temperature of the oil bath reached 220 °C, stirring of the contents of the flask was continued at this temperature for 8 hours under a reduced pressure of 260 to 660 Pa while introducing a little amount of dry nitrogen, thereby effecting solid-state polymerization. As a result, a white powdery crystallized polycarbonate having an average molecular weight of 28,000 ($M_w/M_n = 2.4$) was obtained. The thus obtained crystallized polycarbonate had a hydroxyl terminal group content of 0.001% by weight, based on the weight of the polymer. In contrast, with respect to commercially available polycarbonates, the content of terminal hydroxyl groups is in the range of from about 0.01 to 0.05% by weight.

Test pieces were obtained by subjecting the white crystallized polycarbonate to customary injection molding. The testing pieces were colorless, transparent and tough. The test pieces were subjected to testing for boiling water resistance by putting in an autoclave containing water and heating at 120 °C for 50 hours. As a result, although the weight average molecular

weight had been slightly reduced to 25,000, no occurrence of crazing or discoloration was observed.

3.5 Polycarbonate(PC) by melt polymerization using the new type reactor utilized gravity without mechanical agitating²⁴

The polymerization was carried out using a vertical, cylindrical reactor which has an internal volume of 0.6 m³ and is equipped with thirty column-shaped guides made of stainless steel, each having a diameter of 1 mm and a length of 8 m. The reactor is also equipped with a distributing plate at the upper position, through which prepolymer fed to the reactor can be distributed to cylindrical guides so that the distributed prepolymer can be caused to uniformly fall along and in contact with the surface of each of the cylindrical guides. Further, the reactor has an external jacket, and the inside is adapted to be heated by passing a heating medium through the jacket. The reactor has no agitating means for the prepolymer.

A prepolymer having a number average molecular weight of 6,200, which had been prepared by reacting bisphenol-A with diphenyl carbonate produced by the method described in 3.3.3 in a molar ratio of 1 : 1.05, was continuously fed to the polymerization reactor through the inlet fitted on the top part of the reactor at a flow rate of 18 kg h⁻¹. A polymerization reaction of the prepolymer was carried out under conditions where the reaction temperature was 265 °C, and the reaction pressure was 67 Pa, while continuously withdrawing the produced aromatic polycarbonate from an outlet fitted under the bottom part of the reactor. Each of the polycarbonate products obtained 25 hours and 50 hours after the start of the polymerization reaction had a number average molecular weight of 11,7000. Both of the aromatic polycarbonate products were colorless, transparent and contained no impurities and thermal decomposition products.

4 Conclusion

Asahi Kasei's new non-phosgene PC process using CO₂ as a raw material satisfies almost of all the 12 Articles for Green Chemistry proposed by Dr. Anastas and Dr. Warner.²⁵ That is, (1) no waste, no waste water to be treated, (2) material-saving due to high yields and selectivity (>99%), complete reuse by recycling of all the intermediates, (3) use of low toxic reactants: phosgene-free and CH₂Cl₂-free, (4) safer products: DPC alternates phosgene, (5) no use of sub-materials (solvent-free), (6) energy-saving due to high yields and selectivity; no use of H₂O in EG production process, (7) CO₂ as a raw material can be regenerated, (8) no chemical modification, (9) use of a small amount of catalysts and they are recycled, (10) good process control by using many instruments for analysis and control system, (11) phosgene-free which means hard for a hazardous chemical accident to occur.

Furthermore, the PC produced by Asahi Kasei's new non-phosgene process has good performances as follows:

(1) High clear transparency. (2) High-purity without any of the impurities, such as Cl-containing compounds, necessarily contained in the PC produced by the phosgene processes. No occurrence of corrosion of the metal mold, or the stumper for disk molding, or the recording layer of disks. (3) Low content of oligomers having a molecular weight of less than about 1000. This means that long time molding without interrupting is possible and material- and energy-savings can be achieved. As the oligomers cause so-called mold deposits on the surface of the mold or stumper, in order to get good molding products, the mold deposits must be removed by interrupting the molding and cleaning the mold or stumper. The early molding products after interrupting are usually wasted, because the PC residing in the

molding machine at high temperature during the interruption suffers fatal damage. Therefore, this interruption causes lowering of the productivity of molding (energy loss) and material loss.

In addition to the above performance in "Green Chemistry," or "Green and Sustainable Chemistry", the new process also has economic advantages with lower plant construction costs²⁶ and lower feedstock costs.^{27,28} It is anticipated that Asahi Kasei's new non-phosgene process will be widely adopted for PC production throughout the world, and can contribute to society in terms of sustainability.

References and notes

- (a) S. Fukuoka, Producing polycarbonate, in Green and clean innovations, *Chem. Ind.* 6 October 1997, p. 757; (b) *Eur. Chem. News*, 15–21 November 1999, p. 44.
- K. Nakadai, "6.1.7 Ethylene Oxide, Ethylene Glycol" in *Petrochemical Process (Sekiyu Kagaku Purosesu in Japanese)*, Japan Petroleum Institute, pp. 120–125, Kodansya Scientific Co., 2001.
- (a) P. P. McClellan, *US Pat.*, 2 873 282, Feb. 10, 1959, to Jefferson Chemical Co; (b) E. Yasui and T. Shibata, *Jap. Pat.*, 38-23175 B1, Oct. 10, 1963, to Toa Gosei Co; (c) A. H. Emmons, *US Pat.*, 3 535 342, Oct. 20, 1970, to Dow Chemical Co; (d) F. Ohta and S. Tobita, *Jap. Pat.*, 48-27314 B1, Aug. 21, 1973, to Nisso Yuka Co; (e) A. Kato, S. Nagasawa and T. Noro, *Jap. Pat.*, 50-14632 A1, Feb. 15, 1975, to Toa Gosei Co; (f) "Ethylene Carbonate and Propylene Carbonate" in *Encyclopedia of Chemical Processing and Design*, executive ed. J. J. McKetta and associate ed. W. A. Cunningham, **Vol. 20**, pp. 177–199, Marcel Dekker, Inc., New York, 1984; (g) M. Tojo and S. Fukuoka, *Jap. Pat.*, 3-120270 A1, May 22, 1991; 8-32700 B1, March 29, 1996, to Asahi Kasei Corp.
- (a) L. K. Frevel and J. A. Gilpin, *US Pat.*, 3,642,858, Feb. 15, 1972, to Dow Chemical Co; (b) H-J. Buysch, H. Krimm and H. Rudolph, *US Pat.*, 4,181,676, Jan. 1, 1980, to Bayer AG; (c) S. W. King and B. C. Ream, *Eur. Pat.*, 0 478 073 A2, April 1, 1992, to Union Carbide Chemicals & Plastics Co.
- U. Romano and U. Melis, *US Pat.*, 4 062 884, Dec. 13, 1977, to ANIC, S.p.A.
- (a) R. G. Duranleau, E. C. Y. Nieh and J. F. Knifton, *US Pat.*, 4 691 041, Sep. 1, 1987, to Texaco Inc; (b) J. F. Knifton and R. G. Duranleau, *J. Mol. Catal.*, 1991, **67**, 389.
- (a) S. Fukuoka, Y. Sasaki and M. Tojo, *Jap. Pat.*, 4-198141 A1, July 17, 1992 (Application: Nov. 29, 1990); P2529025, June 14, 1996, to Asahi Kasei Corp; (b) about 8 months later, an analogous US Patent was applied for. H-J. Buysch, A. Klausener and F-J. Mais, *US Pat.*, 5 231 212, July 27, 1993 (Foreign Application Priority: Sep. 3, 1991), to Bayer AG.
- M. M. Mauri, U. Romano and F. Rivetti, *Ing. Chim. Ital.*, 1985, **21**(N. 1-3, Gen-Mar), 6.
- (a) T. Matsuzaki, Novel Method for Preparation of Dimethyl Carbonate (Japanese), *Syokubai (Catalysis)*, 1999, **41**, p. 53; (b) M. Misono, *Kagaku Keizai* (Japanese), 2002, No.13, (Nov.), **49**, 38 (Published by The Chemical Daily Co., Ltd).
- P. Tundo, F. Trotta, G. Moraglio and F. Ligorati, *Ind. Eng. Chem. Res.*, 1988, **27**, 1565.
- (a) S. Fukuoka, M. Tojo and M. Kawamura, *World Pat.* WO 91/09832 A1, July 11, 1991 (Priority: Dec. 28, 1989); (b) S. Fukuoka, M. Tojo and M. Kawamura, *Jap. Pat.*, 4-224547 A1, Aug. 13, ju; 7-91234 B2, Oct. 4, ju, to Asahi Kasei Corp.
- (a) G. Illuminati, U. Romano and R. Tesei, *US Pat.*, 4 182 726, Jan. 8, 1980, to Snamprogetti, S.p.A; (b) Y. Harano and T. Mitani, *Jap. Pat.*, 61-291545A1, Dec. 22, 1986; 62-8091 B1, Feb. 20, 1987, to Daicel Chemical Co; (c) V. Mark, *US Pat.*, 4 554 110, Nov. 19, 1985, to General Electric Co; (d) V. Mark, *US Pat.*, 4 552 704, Nov. 12, 1985, to General Electric Co; (e) V. Mark, *US Pat.*, 4 609 501, Sep. 2, 1986, to General Electric Co; (f) H. Krimm, H-J. Buysch and H. Rudolph, *Eur. Pat.*, 0 000 879 A1, March 7, 1979, to Bayer AG; (g) H. Krimm, H-J. Buysch and H. Rudolph, *US Pat.*, 4 252 737, Feb. 24, 1981, to Bayer AG; (h) H-J. Buysch, N. Schon and J. Rechner, *US Pat.*, 5 284 965, Feb. 8, 1994, to Bayer AG; (i) Y. Kiso and Y. Matsunaga, *US Pat.*, 5 034 557, July 23, 1991, to Mitsui Petrochemical Ind; (j) T. Onoda, K. Tano and Y. Hara, *Jap. Pat.*, 61-5467 B1, Feb. 18, 1986, to Mitsubishi Chemical Co; (k) E. Yoshisato and T. Yoshitomi, *Jap. Pat.*, 9-59209 A1, March 4, 1997, to Teijin Co.
- J. E. Hallgren, *US Pat.*, 4 410 464, Oct. 18, 1983, to General Electric Co.
- (a) N. Schon, R. Langer and H-J. Buysch, *US Pat.*, 5 334 742, Aug 2, 1994 (Priority Application: Aug. 13, 1992), to Bayer AG; (b) N. Schon, R. Langer, H-J. Buysch, P. Wagner and R. Langer, *US Pat.*, 5 344 954, Sep. 6, 1994 (Priority Application: Aug. 13, 1992), to Bayer AG; (c) R. Paludetto, G. Paret, G. Donatti and F. Rivetti, *Ital. Pat.*, 01255746, Nov. 15, 1995 (Application April 1, 1992), to Enichem Synthesis S.p.A; (d) F. Rivetti, R. Paludetto and U. Romano, *US Pat.*, 5 705 673, Jan. 6, 1998, (Priority Application: Jan. 16, 1996) to Enichem S.p.A; (e) M. H. Oyevaar, B. W. To, M. F. Doherty and M. F. Malone, *US Pat.*, 6 093 842, July 25, 2000, to General Electric Co; (f) M. Inaba, K. Sawa and T. Tanaka, *Jap. Pat.*, 9-59225 A1, March 4, 1997, to Mitsubishi Chemical Co; (g) H. Tsuneki, Y. Onda, A. Moriya and H. Yoshida, *Eur. Pat.*, 0 684 221 A1, Nov. 29, 1995, to Nippon Syokubai Co.
- K. Komiya, S. Fukuoka, M. Aminaka, K. Hasegawa, H. Hachiya, H. Okamoto, T. Watanabe, H. Yoneda, I. Fukawa and T. Dozono, New Process for Producing Polycarbonate Without Phosgene and Methylene Chloride in *Green Chemistry Designing Chemistry for the Environment*, Ch. 2, *ACS Symp. Ser.* **626**, ed. P. Anastas and T. C. Williamson, 1996, pp. 20–32.
- (a) P. J. Flory, *US Pat.*, 2 172 374, Sep. 12, 1939, to E. I. DuPont Co; (b) H. J. Hagemeyer Jr., *US Pat.*, 3 043 808, July 10, 1962, to Eastman Kodak Co.
- S. Fukuoka, T. Watanabe and T. Dozono, *Jap. Pat.*, 1-158033 A1, June 21, 1989 (Priority Sept. 28, 1987); 7-94546 B2, Oct. 11, 1995; *World Pat* WO 89/02904, April 6, 1989; *US Pat.*, 4 948 871, Aug. 14, 1990; *Eur. Pat.*, 0 338 085 B1, June 22, 1994, to Asahi Kasei Corp.
- (a) S. Sivaram, J. C. Sehra, V. S. Iyer and K. Ravindranath, *US Pat.*, 5 266 659, Nov. 30, 1993; S. Sivaram and S. B. Halt, *Eur. Pat.*, 0 801 089 A1, Oct. 15, 1997, and *Eur. Pat.*, 0 9080 483 A1, April 14, 1999, all to Council of Scientific & Industrial Research; (b) B. B. Idage, S. Sivaram, G. S. Varadarajan and J. A. King Jr., *US Pat.*, 5 717 056, Feb. 10, 1998 and *US Pat.*, 5 905 135, May 18, 1999, *Eur. Pat.*, 0 949 288 A1, Oct. 13, 1999; S. Sivaram and S. B. Halt, *US Pat.*, 5 710 238, Jan. 20, 1998, all to General Electric Co; (c) R. Hisanishi and M. Okamura, *Jap. Pat.*, 6-228299 A1, Aug. 16, 1994; S. Kuze, K. Tanaka, A. Shishikura and R. Hisanishi, *Jap. Pat.*, 9-235368 A1, Sep. 9, 1997; S. Kuze and K. Tanaka, *Jap. Pat.*, 10-7785 A1, Jan. 13, 1998; S. Kuze, M. Ito and Y. Ishikawa, *Jap. Pat.*, 10-130384 A1, May 19, 1998; M. Ito, *Jap. Pat.*, 11-217430, Aug. 10, 1999; *Jap. Pat.*, 11-236444 A1, Aug. 31, 1999; M. Ito, *World Pat.*, WO 99/26995 A1, June 3, 1999; M. Okamoto and M. Ito, *World Pat.*, WO 99/36458 A1, July 22, 1999; M. Ito and S. Kuze, *World Pat.*, WO 99/48947 A1, Sep. 30, 1999; M. Ito, *Jap. Pat.*, 2001-247671 A1, Sep. 11, 2001, 2002-155162 A1, May 28, 2002 and 2002-220456 A1, Aug. 9, 2002; M. Ito and A. Shishikura, *Jap. Pat.*, 2002-241484 A1, Aug. 28, 2002, all to Idemitsu Petrochemical Co; (d) M. G. Ormand and S. Munjal, *US Pat.*, 5 864 006, Jan. 26, 1999, to Dow Chemical Co; (e) K. Matsumoto, *Jap. Pat.*, 6-322097 A1, Nov. 22, 1994; T. Sakurai and N. Kido, *Jap. Pat.*, 2001-247670 A1 and 2001-247672 A1, Sep. 11, 2001, all to Teijin Co; (f) V. S. Iyer, J. C. Sehra, K. Ravindranath and S. Sivaram, *Macromolecules*, 1993, **26**, 1186; (g) S. M. Gross, G. W. Roberts, D. J. Kiserow and J. M. DeSimone, *Macromolecules*, 2001, **34**, 3916.
- (a) K. Tominari, A. Kanazawa and Y. Shigeta, *Jap. Pat.*, 2-153923 A1; 2-153924 A1; 2-153925 A1; 2-193926 A1; and 2-193927 A1, all June 13, 1990, all to GE Plastics Japan Co; (b) M. Kimura, H. Nakano, M. Nakajima and K. Hayashi, *Jap. Pat.*, 2000-159879 A1 and 2000-159880 A1, all June 13, 2000, all to Mitsubishi Chemical Co. and Mitsubishi Gas Chemical Co; (c) T. Tayama, M. Kawai, K. Hayashi and T. Kawakami, *Jap. Pat.*, 2000-178354 A1, June 27, 2000, to Mitsubishi Chemical Co. and Mitsubishi Gas Chemical Co.
- M. Tojo and S. Fukuoka, *Jap. Pat.*, 3-120270 A1, 22 May 1991; 8-32700 B2, 29 March 1996, to Asahi Kasei Corp.
- (a) M. Tojo and S. Fukuoka, *Jap. Pat.*, 63-238043 A1, Oct. 4, 1988; 7-37422 B2, April 26, 1995, to Asahi Kasei Corp; (b) H. Minoura and H. Nakajima, *Jap. Pat.*, 3-109358 A1, May 9, 1991; P2955866, July 23, 1999, to Asahi Kasei Corp; (c) M. Tojo and S. Fukuoka, *Jap. Pat.*, 4-9356 A1, Jan. 14, 1992; 7-91232 B2, Oct. 4, 1995, to Asahi Kasei Corp; (d) Y. Sasaki, K. Komiya and S. Fukuoka, *Jap. Pat.*, 4-54156 A1, Feb. 21, 1992; 7-91233 B2, Oct. 4, 1995, to Asahi Kasei Corp; (e) Y. Sasaki, K. Komiya and S. Fukuoka, *Jap. Pat.*, 4-103561 A1, April 6, 1992; 7-110840 B2, P2086543, Sep. 2, 1996, to Asahi Kasei Corp; (f) S. Fukuoka, Y. Sasaki and M. Tojo, *Jap. Pat.*, 4-198141 A1, July 17, 1992; P2529025, June 14, 1996, to Asahi Kasei Corp; (g) S. Fukuoka, M. Tojo and Y. Sasaki, *Jap. Pat.*, 4-230243 A1, Aug. 19, 1992; 7-68180 B2, July 26, 1995, to Asahi Kasei Corp; (h) S. Fukuoka and K. Komiya, *Jap. Pat.*, 5-78284 A1, March 30, 1993; P3016289, Dec. 24, 1999, to Asahi Kasei Corp; (i) H. Okamoto and S.

- Fukuoka, *Jap. Pat.*, 6-16596 A1, Jan. 25, 1994; P3214576, July 27, 2001, to Asahi Kasei Corp; (j) M. Tojo, S. Fukuoka and M. Kawamura, *Jap. Pat.*, 9-183744 A1, July 15, 1997, to Asahi Kasei Corp; (k) M. Tojo, S. Fukuoka and M. Kawamura, *Jap. Pat.*, 9-194435 A1, July 29, 1997, to Asahi Kasei Corp; (l) M. Tojo, S. Fukuoka and M. Kawamura, *World Pat.*, WO 97/23445 A1, July 3, 1997; *US Pat.*, 5 847 189, Dec. 8, 1998, *Eur. Pat.*, 0889025 B1, April 3, 2002, to Asahi Kasei Corp; (m) M. Tojo, S. Fukuoka and M. Kawamura, *Jap. Pat.*, 9-176061 A1, Dec. 28, 1995, to Asahi Kasei Corp; (n) S. Kawazoe and M. Tojo, *Jap. Pat.*, 9-221436 A1, Feb. 14, 1996, to Asahi Kasei Corp; (o) M. Tojo and K. Onishi, *World Pat.*, WO 99/64382, Dec. 16, 1999; *US Pat.*, 6 346 638 B1, Feb. 12, 2002, to Asahi Kasei Corp; (p) M. Tojo, K. Onishi and K. Tomoyasu, *Jap. Pat.*, 2002-308804 A1, Oct. 23, 2002, to Asahi Kasei Corp; (q) M. Tojo and K. Onishi, *US Pat.*, 6 479 689 B1, Nov. 12, 2002, to Asahi Kasei Corp.
- 22 (a) T. Watanabe and S. Fukuoka, *Jap. Pat.*, 57-176932 A1, Dec. 30, 1981; 64-3181B2, Jan. 19, 1989, to Asahi Kasei Corp; (b) T. Watanabe and S. Fukuoka, *Jap. Pat.*, 57-183745 A1, May 6, 1981; 64-5588 B2, Jan. 31, 1989, to Asahi Kasei Corp; (c) S. Fukuoka, R. Deguchi and M. Tojo, *US Pat.*, 5 166 393, Nov. 24, 1992; *Jap. Pat.*, 1-93560 A1, April 12, 1989; 5-44938 B2, July 7, 1993, to Asahi Kasei Corp; (d) S. Fukuoka and R. Deguchi, *Jap. Pat.*, 3-200746 A1, Sep. 2, 1991; 7-91230 B2, Oct. 4, 1995, to Asahi Kasei Corp; (e) S. Fukuoka and R. Deguchi, *Jap. Pat.*, 3-236354 A1, Oct. 22, 1991; 7-91231 B2, Oct. 4, 1995, to Asahi Kasei Corp; (f) S. Fukuoka, M. Tojo and M. Kawamura, *Jap. Pat.*, 3-291257 A1, Dec. 20, 1991 (Priority Dec. 28, 1989); 7-91236 B2, Oct. 4, 1995, to Asahi Kasei Corp; (g) S. Fukuoka, M. Tojo and M. Kawamura, *Jap. Pat.*, 4-9358 A1, Jan. 14, 1992 (Priority Dec. 28, 1989); 7-91235 B2, Oct. 4, 1995, to Asahi Kasei Corp; (h) S. Fukuoka, M. Tojo and M. Kawamura, *Jap. Pat.*, 4-211038 A1, Aug. 3, 1992 (Priority Feb. 21, 1990); 7-68182 B2, July 26, 1995, to Asahi Kasei Corp; (i) S. Fukuoka, M. Tojo and M. Kawamura, *US Pat.*, 5 210 268, May 11, 1993; *Eur. Pat.*, 461274 B1, June 15, 1994, to Asahi Kasei Corp; (j) S. Fukuoka, M. Tojo and M. Kawamura, *Jap. Pat.*, 4-224547 A1, Dec. 26, 1990; 7-91234 B2, to Asahi Kasei Corp; (k) S. Fukuoka, M. Tojo and M. Kawamura, *Jap. Pat.*, 4-230242 A1, Aug. 19, 1992; 7-68179 B2, July 26, 1985, to Asahi Kasei Corp; (l) S. Fukuoka, M. Tojo and M. Kawamura, *Jap. Pat.*, 4-235951 A1, Aug. 25, 1992; 7-72158 B2, Aug. 2, 1995, to Asahi Kasei Corp; (m) K. Komiya, M. Tojo and S. Fukuoka, *World Pat.*, WO 97/11049, March 27, 1997 (Priority Sept. 22, 1995); *Eur. Pat.*, 0 855 384 A1, July 29, 1998; *US Pat.*, 5 872 275, to Asahi Kasei Corp; (n) M. Tojo, K. Onishi and K. Komiya, *Jap. Pat.*, 11-92429 A1, April 6, 1999; *World Pat.*, WO 99/14183, March 25, 1999 (Priority Sept. 16, 1997); *Eur. Pat.*, 1 016 648 A1, July 5, 2000, to Asahi Kasei Corp.
- 23 (a) I. Fukawa, S. Fukuoka, K. Komiya and Y. Sasaki, *Jap. Pat.*, 3-223330, Oct. 2, 1991 (Priority March 28, 1989); P 2546724, Aug. 8, 1996; (b) I. Fukawa, S. Fukuoka, K. Komiya and Y. Sasaki, *US Pat.*, 5 204 377, Apr. 20, 1993; *Eur. Pat.*, 0 403 657 B1, Jan. 28, 1998, to Asahi Kasei Corp; (c) I. Fukawa, S. Fukuoka, K. Komiya and Y. Sasaki, *US Pat.*, 5 214 073, May 25, 1993, to Asahi Kasei Corp; (d) K. Komiya, S. Fukuoka and A. Yamaguchi, *Jap. Pat.*, 4-72326 A1, March 6, 1995; 7-86138 B1, Sept. 20, 1995, to Asahi Kasei Corp; (e) K. Komiya, *Jap. Pat.*, 6-271659 A1, Sep. 27, 1995; P3208210, 6 July 1995, to Asahi Kasei Corp.
- 24 (a) I. Fukawa and T. Tanabe, *Jap. Pat.*, 3-252421 A1, Nov. 11, 1995; 7-98862 B2 Oct. 25, 1995, to Asahi Kasei Corp; (b) K. Komiya, M. Aminaka and Y. Kawakami, *Jap. Pat.*, 8-225641 A1, Sep. 13, 1995, to Asahi Kasei Corp; (c) H. Hachiya and K. Komiya, *Jap. Pat.*, 8-231844 A1, Sept. 10, 1996; P3393167, Jan. 24, 2003, to Asahi Kasei Corp; (d) K. Komiya, S. Fukuoka and Y. Kawakami, *Jap. Pat.*, 8-325372 A1, 8-325373 A1, Nov. 10, 1996, to Asahi Kasei Corp; (e) K. Komiya, Y. Kawakami and H. Okamoto, *Eur. Pat.*, 0 710 687 B1, Nov. 11, 2001, to Asahi Kasei Corp; (f) K. Komiya, Y. Kawakami and H. Okamoto, *US Pat.*, 5 589 564, Dec. 31, 1996, to Asahi Kasei Corp; (g) K. Komiya, Y. Kawakami and H. Okamoto, *US Pat.*, 5 596 067, Jan. 21, 1997, to Asahi Kasei Corp; (h) K. Komiya, K. Hasegawa and S. Fukuoka, *Jap. Pat.*, 6-56984 A1, March 1, 1994; P3100008, Aug. 18, 2000, to Asahi Kasei Corp; (i) K. Komiya, K. Hasegawa and M. Aminaka, *Jap. Pat.*, 10-330474 A1, Dec. 15, 1998; P2989578, Oct. 8, 1999, to Asahi Kasei Corp; (j) K. Komiya, S. Fukuoka and M. Kawamura, *US Pat.*, 5 840 826, Nov. 24, 1998, to Asahi Kasei Corp.
- 25 P. T. Anastas and J. C. Warner, *Green Chemistry: Theory and Practice*, Oxford University Press, Oxford, 1998.
- 26 The newspapers say that new construction costs of the PC production plants are as follows: (a) Phosgene process
(1) About 20 thousand million yen for 60 000 ton/year plant for "T. Co." in Singapore. *Sekiyu-Kagaku-Shinbun* (Japanese) [*The Petro-Chemical Press*] (weekly), Dec. 6, 1999.
(2) About 20 thousand million yen for 40 000 ton/year plant for "S.D. Co." in Japan. *Kagaku Kogyo Nippo* (Japanese) [*The Chemical Daily*], Oct. 7, 1993.
(b) Non-phosgene Asahi Kasei process
About 9 thousand million yen for 50 000 ton/year plant for Chimei-Asahi Corp. in Taiwan. *Kagaku Kogyo Nippo* (Japanese) [*The Chemical Daily*], Nov. 8, 1999.
- 27 In the Asahi Kasei process, all raw materials (EO, CO₂ and Bis-A) are converted to the products (PC and MEG). However, in the phosgene process, Cl₂ and NaOH (raw materials) are wasted as NaCl. At least this point shows that the Asahi Kasei Process is more economical than the phosgene process.
- 28 J. Plotkin and E. Glatzer describe our process in the article "Polycarbonate", *European Chemical News* (ECN), July 2002/Process Review pp. 32–34 as follows (the extract is shown): "Phosgene is a toxic chemical that requires rigorous process design standards to protect the health and safety of workers. Investment requirements are increased by the need for close analytical monitoring and control, equipment designs for lethal service, and treatment of vent streams by caustic scrubbing or incineration. Toughening of environmental restrictions worldwide has added impetus to the search for non-phosgene routes to polycarbonate.
In addition to phosgene concerns, the interfacial polymerization process typically uses a chlorinated solvent, methylene chloride, another material with exposure limits. A further incentive to eliminate the use of phosgene is the economic penalty incurred because the chlorine content of the phosgene is wasted and converted to sodium chloride. Caustic soda is consumed in the conversion, and the disposal of waste salt solutions presents ecological problems in itself.
In a second stage reactor, the ethylene carbonate is transesterified with methanol to give two products – dimethyl carbonate and ethylene glycol.
Since a large portion of ethylene oxide is normally converted to ethylene glycol for use in polyester production, this approach in essence converts methanol to dimethyl carbonate with virtually no addition raw material costs. And, as an extra bonus, selectivity to ethylene glycol is very high, avoiding diethylene glycol and triethylene glycol, which are by-products of conventional ethylene glycol processes via hydrolysis of ethylene oxide".



Recycling of monomers and fillers from high-temperature-vulcanized silicone rubber using tetramethylammonium hydroxide†

Yuko Ikeda,^a Wei Huang^b and Akira Oku^{*c}

^a Faculty of Engineering and Design, Kyoto Institute of Technology, Matsugasaki, Sakyo, Kyoto 606-8585, Japan

^b Venture Laboratory, Kyoto Institute of Technology, Matsugasaki, Sakyo, Kyoto 606-8585, Japan

^c Research Institute for Production Development, 15-Morimoto, Shimogamo, Sakyo, Kyoto 606-0805, Japan

Received 23rd April 2003

First published as an Advance Article on the web 21st August 2003

The effects of reaction conditions on a novel monomer recycling method for high-temperature-vulcanized silicone rubber are described. A mixture of a methanol solution of $(\text{CH}_3)_4\text{NOH}$, diethylamine and hexane was adopted to partially depolymerize and dissolve the high-temperature-vulcanized silicone rubber under reflux. Hexane was useful to completely separate the fillers from the suspension of depolymerized products. After the removal of fillers followed by treatment of the filtrate with KOH and distillation under reduced pressure, cyclosiloxane monomers were obtained in high yields ($\sim 78\%$). $(\text{CH}_3)_4\text{NOH}$ adsorbed and chemically bound to the fillers was found to be pyrolyzed to $(\text{CH}_3)_3\text{N}$ and CH_3OH . The separated fillers were thermally treated to be reused without further purifications. The yields of recovered fillers were as high as over 95%.

Introduction

The recycling of polymer materials is now one of the most important issues at both post-manufacturer and post-consumer stages for the global conservation of the environment and carbon resources particularly in conjunction with the protection of petroleum resources from depletion. In the recycling of polymer materials, there are two categories in general, *i.e.*, material recycling and chemical (monomer) recycling. The former seems easy to conduct because only physical treatments such as heat processing and pulverization are required to reuse the recovered materials. However, many polymer materials which are used in our life are composites and frequently composed of network structures. Therefore, the material recycling methods of those polymer materials are not so easy. In addition, the performance of recovered materials is often poorer than that of the virgin materials. Monomer- and chemical-recycling methods, on the other hand, have the advantage of reproducing polymers comparable to the original ones. For this purpose, efficient depolymerization methods to produce monomers *via* low-energy processes have to be established.

Up to now, the polymers that are industrially recycled *via* monomers have been limited. Poly(ethylene terephthalate) (PET), polyamide, polyurethane are the examples. One of the authors (A. O.) has been studying monomer recycling from poly(ethylene terephthalate) to terephthalic acid and ethylene glycol,^{1,2} poly(carbonate) to dimethyl carbonate and bisphenol A,³ and poly(carbonate) to bisphenol A and cyclic heterocarbonates.^{4–6} Using the same concept, we focused on the chemical recycling of organosilicon polymers in this study because the worldwide annual production of organosilicon polymers has now reached millions of tons and they have caused similar problems of waste treatment to other conven-

tional plastics.⁷ As well as being against our basic concept that plastic wastes should not be incinerated, organosilicon polymers are incombustible and therefore can't be used as a heat resource like hydrocarbon polymers. Moreover, because a large amount of manufacturing energy is required for their production from resources, we convinced ourselves that efficient methods and social systems to recover cyclosiloxane monomers from organosilicon polymer wastes have to be established.

It is well known that a thermodynamic equilibrium between cyclic monomers and linear polymers is involved in the polymerization procedure of cyclosiloxane monomers with ring-sizes ranging from six to twelve.^{8–14} Based on this fact, some recycling methods to reproduce cyclosiloxane monomers from linear poly(dimethylsiloxane)s (PDMS) and cross-linked PDMS (vulcanized silicone rubbers) have been reported.^{15–25} Recently, we have reported effective depolymerization methods for PDMS to reproduce cyclosiloxane monomers such as hexamethylcyclotrisiloxane (D_3) and octamethylcyclotetrasiloxane (D_4) by the use of tandem catalyst systems that are composed of potassium hydroxide (KOH) and buffer acids.²⁶

Green Context

The chemical recycling of used polymers not only provides a way of dealing with an increasingly large plastic waste problem but also provides useful products from that waste. Here a novel method of recycling silicone rubbers is described including the easy separation of fillers present in the original polymer. The quaternary ammonium hydroxide catalyst is needed in only very small amounts and the relatively benign solvent hexane is used to facilitate the separation of the filler. Thus a resource-efficient relatively benign system can be used to effectively turn waste into useful chemicals.

JHC

† Presented at The First International Conference on Green & Sustainable Chemistry, Tokyo, Japan, March 13–15, 2003.

Indeed, not only PDMS but also vulcanized PDMS were efficiently depolymerized to a mixture of cyclosiloxane monomers (D₃-tetradecamethylcycloheptasiloxane (D₇)) by this tandem base–acid operation. We have also reported a monomer recycling of high-temperature-vulcanized silicone rubbers containing fillers, in which the rubbers were depolymerized by the KOH catalyst in specifically designed triad solvent mixtures to a mixture of cyclosiloxane monomers in high yields together with the recovery of fillers.²⁷ The triad solvent mixture used in the study was composed of diethylamine (DEA), methanol and hexane, and it was proven effective not only for dissolving, or partially depolymerizing, the vulcanized silicone rubber to a suspension but also for separating fillers completely by filtration. In this recycling method where KOH was used from the beginning, however, the separated fillers cannot be reused for reproducing silicone rubbers unless treated with acid, because the majority of the KOH remains on the fillers as potassium silanolate and affords a poor thermal stability to the reproduced silicone rubber. Therefore, post-treatments such as the neutralization of recovered fillers and removal of the salts, which are somewhat tedious, are required. Thus, we have developed a novel recycling method to recover the monomers and fillers without contamination by alkali metal cations. For this purpose, tetramethylammonium hydroxide ((CH₃)₄NOH, TMAH) was adopted as a base catalyst in the first stage of the depolymerization of high-temperature-vulcanized silicone rubber.²⁷ In this process, TMAH was adsorbed and remained on the surface of fillers but it was easily decomposed to trimethylamine ((CH₃)₃N) and methanol (CH₃OH) at high temperatures, as shown in Fig. 1. The decomposition products were volatile

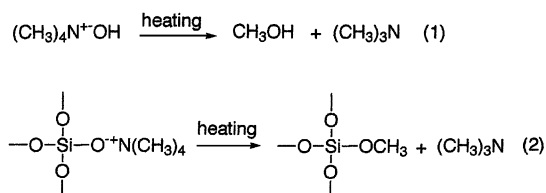


Fig. 1 Decomposition of TMAH and ammonium silanolate on the surface of silica.

and easily removed from the fillers. TMAH can also be bound chemically to silica in the form of ammonium silanolate, but it is also decomposed by heating as shown in Fig. 1. Thus, both

cyclosiloxane monomers and fillers were recovered easily by the use of TMAH. In our preceding report,²⁷ we briefly communicated the outline of this novel recycling method, and in this article, the detail of this reaction is described.

Results and discussion

Effect of solvent on the dissolution of high-temperature-vulcanized silicone rubber in the presence of (CH₃)₄NOH (TMAH)

Table 1 shows the dissolving ability of the mixed solvents (methanol solution of TMAH, DEA and hexane) for the vulcanized silicone rubber. It was found that DEA was a powerful solvent for dissolving the high-temperature-vulcanized silicone rubber in the presence of TMAH under the solvent reflux conditions. However, the use of DEA alone brought about the formation of a suspension from which it was difficult to completely separate the fillers. This is because very fine particulates of silica and alumina did not aggregate well in this DEA suspension. As reported in our previous paper,²⁷ the unseparated filler particulates hindered the depolymerization of poly(siloxane) and resulted in poor yields of recovered monomers and fillers. Therefore, the sole use of DEA was not preferable for the isolation of cyclosiloxane monomers and fillers from the depolymerization mixture of high-temperature-vulcanized silicone rubber containing fillers. This problem was solved by using a mixture of DEA and hexane as shown in Table 1. Because hexane is a non-polar solvent, the aggregation of filler particulates was promoted by its addition to the suspension mixture enabling easy separation of fillers from the mixture.

For saving energy of dissolution, the vulcanized silicone rubber was dissolved in the same solvent mixture in the presence of TMAH at rt. However, the monomers and fillers were not recovered even after agitating the reaction mixture for 24 h using a mechanical stirrer (Table 2 No. 10) and the filtration of fillers was difficult. Indeed, the formation of gel was observed on the filter paper. These results suggest that the room temperature dissolution of high-temperature-vulcanized silicone rubber in the mixture was not successful in collapsing the network structure of the high-temperature-vulcanized silicone rubber.

Table 1 Results of dissolution of the high-temperature-vulcanized silicone rubber in the presence of TMAH

Ex. no.	Rubber/g	Solvent/ml			10% CH ₃ OH solution of TMAH/g	Temp./°C	Time/h	Solubilization time/h
		Hexane	DEA					
1	6.2	0	20	0.62	Reflux	3	1	
2	7.0	20	0	0.72	Reflux	8	Insoluble	
3	7.0	20	10	0.72	Reflux	4.5	1.5	

Table 2 Effect of the amount of solvent and TMAH on the recycling of monomers and fillers ^a

Ex. no.	Solvent/ml		10% CH ₃ OH solution of TMAH/g	Temp./°C	Time/h	Second ^b treatment	Yield (%)	
	Hexane	DEA					Monomers	Filler
4	20	10	0.75	Reflux	5	No	55	98
5	20	10	1.0	Reflux	5	No	60	95
6	40	20	1.0	Reflux	5	No	69	98
7	60	30	1.0	Reflux	5	No	73	95
8	20	10	1.0	Reflux	5	Yes	68	95
9	20	10	1.5	Reflux	5	Yes	67	85
10	20	10	1.0	rt	24	No	0	0

^a Amount of filler-containing silicone rubber used in these experiments was 10.0 g. ^b Carried out under reflux for 2 h.

Effect of the amounts of solvent and TMAH on the recycling of monomers and fillers

Table 2 shows the effect of the total amount of solvents on the recycling of monomers and fillers, where the weight ratio between hexane and DEA was fixed to hexane/DEA = 2/1. Apparently, the yields of monomers increased as the total amount of solvents was increased. The reason was thought to be ascribable to the increased amount of dissolved poly(siloxane) in the increased amount of solvent. In order to remove the poly(siloxane) remaining on the fillers, the separated fillers were treated again for an additional 2 h with the same reagent and solvents. All the filtrates were combined and heated to remove the solvents, followed by distillation at 170 °C/30 mmHg for 3 h to recover the monomers. As shown in Table 2, the second treatment increased the yields of recovered monomers to a small extent and the purity of recovered fillers became higher. Thus, to increase the yields of monomers and fillers, the amount of solvents and the repetition of treatment must be taken into account.

By comparison of the amount of TMAH (Table 2, No. 4 and 5), the preferable amount of the base catalyst was found to be 0.01 wt% to the weight of vulcanized silicone rubber for the recovery of monomers and fillers. No appreciable effect of further increasing the amount of TMAH was observed (Table 2, No. 8 and 9). The yield of recycled fillers in No. 9 was low, probably due to the increase in the amount of polar solvent methanol, where the aggregation of fillers became disfavored. Thus, in the following depolymerization, a 25 wt% methanol solution of TMAH was used and the effect of solvent ratios of hexane to DEA on the yields of monomers and fillers were investigated.

Effect of solvent ratios on the recovery of monomers and fillers from silicone rubbers using a 25% methanol solution of TMAH

Table 3 summarizes the yields of monomers and fillers obtained from repeated treatment procedures using a 25% methanol solution of TMAH. In the second repetition, the primarily separated fillers were treated with a similar mixture of DEA, hexane and a methanol solution of TMAH. To attain high yields of recovered monomers and fillers, adequate solvent ratios must be chosen (e.g., Table 3, No. 13 ~ 15). For example, hexane was necessary to efficiently separate the fillers but a large amount of hexane decreased the solubility of TMAH eventually causing a decrease in the yields of monomers (No. 11 and 12). The reproducibility of the chemical treatment (e.g. No. 13) was confirmed by a large scale-treatment where the experimental scale was three times as large as that of No. 13. The yields of recovered monomers and fillers were 76 and 93%, respectively. Interestingly, the composition of cyclosiloxane monomers seems to be influenced by the solvent ratio of hexane to DEA, as shown in Table 3. It was observed that as the relative amount of hexane to DEA increases, the higher the fraction of D₃ tends

to become, albeit, the composition of obtained monomers is not so important for the recycling polymerization reaction. For example, 20 g of the recycled monomers were polymerized in toluene at rt by using concentrated H₂SO₄ (0.6 g) as the catalyst in the presence of hexamethyldisiloxane (0.35 g) and a small amount of water (0.3 g). After a proper work-up procedure of washing and drying, the yield of obtained α,ω -trimethylsilyl-terminated PDMS was 75% and the degree of polymerization was 98, which was determined by the ¹H-NMR analysis.

All the recovered fillers were heated in open air at 150 °C for 5 h and their pH values in aqueous solution were found to be neutral suggesting that the pyrolysis reactions illustrated by Fig. 1 occurred smoothly and satisfactorily. The model experiments using the vulcanized silicone rubber filled with commercial silica supported this consideration.²⁷

Although the yields of recovered fillers were satisfactory, as high as above 90% as shown in Tables 2 and 3, the yields of cyclosiloxane monomers were always lower than 80%. Although these yields were better than those reported for different methods by other authors,^{15–25} the decreased yields from a quantitative level may be ascribable to the following reasons. (1) The moiety of the carbon–carbon bonded bridging network cannot be transformed to monomer structures and remains in the distillation residue. (2) Depending on the amount of base catalyst TMAH, a fraction of the organo-silicone molecules was removed by the work-up procedure in the form of water-soluble silanolates.

Experimental

Materials

The high-temperature-vulcanized silicone rubbers containing the fillers were prepared from commercially available poly-(dimethylsiloxane-*co*-methylvinylsiloxane) gum (SH 401, Dow Corning Co.), silica and alumina. The molar ratio of the vinyl group to the silicon units of this gum was 0.02, which was measured by ¹H-NMR. The vulcanization was carried out at 170 °C for 10 min using 0.8 phr of 2,5-bis(*tert*-butylperoxy)-2,5-dimethylhexane as a cross-linking agent. The silica and alumina contents in the vulcanizates were 9 and 51 wt%, respectively. The methanol solution of TMAH, DEA, toluene, methanol, hexane and KOH were commercially available from Wako Pure Chemical Co. and used without further purification. The cyclosiloxane monomers, D₃, D₄, decamethylcyclopentasiloxane (D₅) and dodecamethylcyclohexasiloxane (D₆) were available from Shin-Etsu Co. and used without further purification. The hazardous properties of TMAH described in the MSDS²⁸ state that, as a strong alkali, it is corrosive and toxic to skins and eyes, but there is no description of carcinogenic or mutagenic properties. Therefore, ordinary caution in handling caustic chemicals was paid to TMAH.

Table 3 Effect of the solvent ratio on the recycling of monomers and fillers using a 25% methanol solution of TMAH^a

Ex. no.	Solvent/ml		Yield (%)		Composition of monomers				
	Hexane	DEA	Monomers	Fillers	D ₃	D ₄	D ₅	D ₆	D _n (n > 6)
11	27.5	2.5	33	—	—	—	—	—	—
12	20.0	10.0	67	85	10.5	78.1	9.6	1.5	0.3
13	15.0	15.0	75	93	6.6	64.5	25.9	2.6	0.4
14	10.0	20.0	78	83	6.7	71.0	20.1	2.0	0.2
15	2.5	27.5	72	94	4.2	71.5	21.9	2.2	0.2
16	0	30.0	47	82	—	—	—	—	—

^a Amount of filler-containing silicone rubber used in these experiments was 10.0 g. Amount of 25% methanol solution of TMAH was 0.6 g. First treatment was carried out under reflux for 5 h and the second treatment under reflux for 2 h.

Recovery of monomers and fillers from high-temperature-vulcanized silicone rubber containing fillers

Vulcanized silicone rubber sheets containing the fillers were cut into pieces (*ca.* $2 \times 3 \times 4$ mm³ in size) and they were mixed with the methanol solution of TMAH and solvents (DEA and/or hexane) in a 100 ml flask. The mixture was agitated by a mechanical stirrer at rt or under solvent reflux. After the vulcanized silicone rubber had dissolved, the obtained suspension was filtered using a paper filter. After the removal of fillers, the filtrate was transferred to a 100 ml flask and a small amount of KOH (0.2 wt% to the rubber) was added. Then, the solution was heated to remove the solvent first followed by distillation at 170 °C/30 mmHg for 3 h to obtain depolymerized products. The distillates were collected in a trap cooled at -78 °C. To improve the yields of monomers and fillers, the filtration residue was treated again with a mixture of methanol solution of TMAH, DEA and hexane. The fillers were recovered after filtration and heated under atmospheric pressure at 150 °C for 5 h to obtain reusable fillers. The second filtrate was combined with the first one and subjected to the monomer recovery.

Characterization

The measurement of ¹H-NMR was conducted on a Fourier-transform high resolution NMR spectrometer DRX500 (Bruker Co.) in CDCl₃ solutions using tetramethylsilane as the internal standard.

The composition of monomers was analyzed by gas chromatography on a GC-14B model chromatograph (Shimadzu Co.) using commercially available cyclosiloxanes as the standard substances. The chromatographic conditions were as follows. Solvent: acetone; concentration of the sample: *ca.* 0.05 g ml⁻¹; temperature programming: 10 °C min⁻¹ for 50~320 °C; injector and detector temperature: 320 °C.

A 0.5 g sample of recovered fillers was added to a 10 ml mixture of methanol and water (*v/v* = 1/1), the total mixture was stirred for 2 h at rt, and the pH value of the solution was measured.

Conclusion

TMAH was found to be useful for depolymerizing and dissolving high-temperature-vulcanized silicone rubber in a mixed solvent of DEA and hexane under reflux. The preferable amount of TMAH was found to be 0.01~0.015 wt% to the weight of vulcanized silicone rubber for the recycling of monomers and fillers. The addition of hexane to the solvent DEA was found to be effective for easy separation of fillers from the depolymerization suspension of vulcanized rubbers. The total amount of solvent mixture, consisting of DEA, hexane and TMAH in methanol, also influenced the yields of recovered cyclosiloxane monomers and fillers, and thus, as the total amount of solvent was increased, the yield of monomers

became higher. The repeated treatment of primarily recovered fillers with the same mixture of DEA, hexane and methanol solution of TMAH improved the yield of the cyclosiloxane monomers. TMAH and ammonium silanolate absorbed and chemically bound, respectively, on the silica surface were decomposed to (CH₃)₃N and CH₃OH or methyl silanolate by heating, and the separated amine-free fillers can be recycled for the purpose of manufacturing silicone rubbers. In conclusion, the use of TMAH as a depolymerization catalyst seems to be highly efficient for chemical recycling of silicone rubbers and, thus, will play a small part in "Green and Sustainable Chemistry".

Acknowledgement

This study was partially supported by Grant-in-Aid for Science Research on Priority Area (A) No. 413/14045247 from the Ministry of Education, Culture, Sport, Science and Technology of Japan.

References

- 1 A. Oku, L.-C. Hu and E. Yamada, *J. Appl. Polym. Sci.*, 1997, **63**, 595.
- 2 C. Hu, E. Yamada and A. Oku, *Polym. J.*, 1997, **29**, 708.
- 3 L.-C. Hu, A. Oku and E. Yamada, *Polymer*, 1998, **39**, 3841.
- 4 Hata, H. Goto, E. Yamada and A. Oku, *Polymer*, 2002, **43**, 2109.
- 5 A. Oku, S. Tanaka and S. Hata, *Polymer*, 2000, **41**, 6749.
- 6 S. Hata, H. Goto and A. Oku, *J. Appl. Polym. Sci.*, 2003, in press.
- 7 W. Noll, *Chemistry and Technology of Silicone*, Academic Press, New York, 1968.
- 8 D. T. Hurd, R. C. Osthoff and M. L. Corrin, *J. Am. Chem. Soc.*, 1954, **76**, 249.
- 9 D. T. Hurd, *J. Am. Chem. Soc.*, 1955, **77**, 2998.
- 10 J. F. Hyde, *US Pat.* 2490357, 1949.
- 11 J. F. Hyde, *US Pat.* 2634284, 1953.
- 12 S. W. Kantor, W. T. Grubb and R. C. Osthoff, *J. Am. Chem. Soc.*, 1954, **76**, 5190.
- 13 M. Mazurek and J. Chojnowski, *J. Makromol. Chem.*, 1977, **178**, 1005.
- 14 H. R. Allock, *J. Macromol. Sci. Rev., Macromol. Chem.*, 1970, **C4**(2), 149.
- 15 A. S. Shapatin, E. A. Simanenko, G. Ya. Zhigalin and A. G. Trufanov, *SU Pat.* 939445, 1982.
- 16 T. A. Koshkina, A. V. Kisina and A. S. Shapatin, *Zh. Prikl. Khim.*, 1993, **66**, 1662.
- 17 T. D. Wilford, *DE Pat.* 4300168, 1994.
- 18 C. V. Allandrieu and D. V. Cardinaud, *DE Pat.* 19619002, 1996.
- 19 J. S. Razzano, *US Pat.* 6037486, 2000.
- 20 F. H. Kreuzer and Gebauer, *EP Pat.* 126792, 1982.
- 21 W. Knies, G. Vogel and V. Frey, *DE Pat.* 4126319, 1992.
- 22 T. Bunce and A. E. Surgenor, *GB Pat.* 2331992, 1999.
- 23 P. Hron and M. Heidingsfeldova, *J. Sb. Vys. Sr. Chem. Technol. Praze [Oddil]*, 1980, **S4**, 79.
- 24 P. Hron and M. Schätz, *Plasty Kaučuk*, 1990, **27**, 33.
- 25 W. Knies, G. Vogl and W. Guske, *DE Pat.* 19502393, 1996.
- 26 W. Huang, Y. Ikeda and A. Oku, *Polymer*, 2003, **43**, 7289.
- 27 A. Oku, W. Huang and Y. Ikeda, *Polymer*, 2002, **43**, 7295.
- 28 MS Data Sheets No.33316.



Selective anodic fluorination of phthalides in ionic liquids†‡

Masaru Hasegawa, Hideki Ishii and Toshio Fuchigami*

Department of Electronic Chemistry, Tokyo Institute of Technology, Midori-ku, Yokohama 226-8502, Japan. E-mail: fuchi@echem.titech.ac.jp; Fax: +81 45 924-5406

Received 24th April 2003

First published as an Advance Article on the web 13th June 2003

Anodic fluorination of phthalide and its derivatives was carried out using $\text{Et}_4\text{NF}\cdot 4\text{HF}$, $\text{Et}_3\text{N}\cdot 5\text{HF}$ and imidazolium ionic liquids like 1-ethyl-3-methylimidazolium triflate [emim][OTf]. Despite the high oxidation potential of phthalide, the fluorination proceeded efficiently in ionic liquids (ILs) containing fluoride salts. Fluorodesulfurization of 3-phenylthiophthalide took place predominantly in [emim][OTf] and CH_2Cl_2 while the use of 1,2-dimethoxyethane (DME) resulted in selective α -fluorination without the desulfurization. It was also demonstrated that the electrochemical fluorodesulfurization could be achieved by the reuse of IL. This is the first example of selective anodic fluorination using imidazolium ionic liquids.

Introduction

Although many methods for the preparation of fluoroorganics have been developed to date, the construction of ring-fluorinated heterocyclic systems has been less explored. Recently, selective electrochemical fluorination has been shown to be a highly efficient new tool to synthesize various fluorinated heteroatom compounds including heterocycles.² The reaction can be carried out under mild conditions using relatively simple equipment to avoid hazardous or toxic reagents, which are usually necessary in chemical fluorination. However, only limited successful examples of selective anodic direct fluorination at the position α to a ring-oxygen atom of oxygen-containing heterocycles have been reported.³ It is also well recognized that incorporation of a fluorine atom into the organic molecules used for medicines can profoundly influence their biological properties. Moreover, phthalide and its derivatives are valuable as they possess significant biological activities.⁴

Recently, room temperature ionic liquids (ILs) have proved to be a new class of good media for many synthetic organic reactions.⁵ Previously, we reported successful solvent-free anodic fluorination of organooxygen compounds in ILs like alkylammonium hydrogen fluoride salts.⁶ However, there have been only a few papers dealing with electroorganic synthesis in ILs.⁷

With these facts in mind, anodic fluorination of biologically interesting phthalide **1a** and its derivatives was attempted using conventional solvents and ionic liquid media. Here, we wish to report the first example of anodic fluorination of phthalides in imidazolium ionic liquids.

At first, anodic fluorination of **1a** was carried out at a constant current using a platinum anode under various conditions. The results are summarized in Table 1.

As shown in Table 1, conventional electrolysis using organic solvents resulted in no fluorination (Run 3) or low yields of fluorinated product **2a** (Runs 1 and 2). Since the oxidation potential of phthalide **1a** is extremely high (2.86 V vs. SCE), the oxidation of solvents seemed to take place preferentially or predominantly (in DME). Even under solvent-free conditions without any solvent, the yield was also very low (Runs 4 and 5). In these cases, a large excess amount of fluoride salts were used

Table 1 Anodic fluorination of phthalide (**1a**) under various conditions

Run	Reaction media	Supporting electrolyte	Charge passed/ F mol ⁻¹	Yield (%) ^a
1	MeCN	$\text{Et}_3\text{N}\cdot 5\text{HF}$	6	16
2	CH_2Cl_2	$\text{Et}_3\text{N}\cdot 5\text{HF}$	8	23 ^b
3	DME	$\text{Et}_4\text{NF}\cdot 4\text{HF}$	8	0
4	—	$\text{Et}_3\text{N}\cdot 3\text{HF}$	4	17
5	—	$\text{Et}_3\text{N}\cdot 5\text{HF}$	8	16 ^b
6	[emim][OTf]	$\text{Et}_3\text{N}\cdot 3\text{HF}$	6	78
7	[emim][OTf]	$\text{Et}_4\text{NF}\cdot 4\text{HF}$	4.7	70
8	[emim][OTf]	$\text{Et}_3\text{N}\cdot 5\text{HF}$	4	90

^a Determined by ¹⁹F-NMR. ^b Reaction was complicated.

as a solvent, fluorine source, and supporting electrolyte. Hence, the low yields seemed to be attributable to simultaneous oxidation of the fluoride salts during the electrolysis. In sharp contrast, when imidazolium ionic liquid, [emim][OTf] was used instead of organic solvents, the yield increased markedly (Runs 6–8). Among the combination of fluoride salts and [emim][OTf], that of $\text{Et}_3\text{N}\cdot 5\text{HF}$ and [emim][OTf] afforded **2a** in the highest yield (Run 8). Such a pronounced effect of imidazolium ionic liquid on anodic fluorination has never been reported so far. The ionic liquid, [emim][OTf] may play an important role for the fluorination. In order to obtain more information to clarify the role of the imidazolium IL, we attempted anodic

Green Context

The selective fluorination of organics remains a challenge, mainly due to the high reactivity of most electrophilic fluorinating agents. Here, an electrochemical route is demonstrated, which holds promise for many systems. High yields and selectivities are obtainable when ionic liquids are used as solvents/electrolytes, especially when mixed with quaternary ammonium polyfluorides. This is in contrast to the very poor activities seen in conventional solvents. *DJM*

† Presented at The First International Conference on Green & Sustainable Chemistry, Tokyo, Japan, March 13–15, 2003.

‡ Electroorganic Reactions in Ionic Liquids. Part 4. For Part 3, see ref. 1

fluorination of **1a** similarly in various imidazolium ILs containing Et₃N·5HF. The results are summarized in Table 2.

Table 2 Anodic fluorination of **1a** in various imidazolium ionic liquids

Run	Reaction media	Supporting electrolyte	Charge passed/ F mol ⁻¹	Yield (%) ^a
1	[emim][OTf]	Et ₃ N·5HF	4	90
2	[emim][BF ₄]	Et ₃ N·5HF	4	16
3	[bmim][BF ₄]	Et ₃ N·5HF	6	23
4	[bmim][NTf ₂]	Et ₃ N·5HF	5	29
5	[bmim][OTf]	Et ₃ N·5HF	4	39
6	[EMIF][2.3HF]	—	6	31

All reaction were carried out under the same conditions in Table 1.^a Determined by ¹⁹F-NMR.

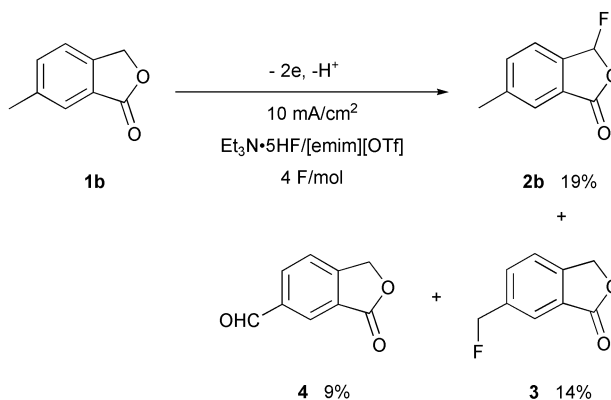
As shown in Table 2, ionic liquid, [emim][BF₄] was not effective for the fluorination (Run 2) while [emim][OTf] was highly effective (Run 1). 1-Butyl-3-methylimidazolium ionic liquids were much less effective for the fluorination compared with [emim][OTf] (Runs 3–5). Among the 1-butyl-3-methylimidazolium ionic liquids, the use of [bmim][OTf] gave the best result although the yield was moderate (Run 5). These results suggest that both cations and anions of imidazolium ILs affect the fluorination significantly. Recently, Hagiwara *et al.* developed a new class of ionic liquid, 1-ethyl-3-methylimidazolium fluoride-2.3HF, [EMIF][2.3HF].⁸ Electrochemical fluorination of **1a** was attempted in [EMIF][2.3HF] (Run 6). Although the fluorination proceeded, the yield was much lower compared with the fluorination in [emim][OTf] owing to many fluorinated products formed and the low conversion. From these results, it seems to be that the double ionic liquid system consisted of [emim][OTf] and a fluoride salt enhances not only the nucleophilicity of F⁻ but also the electrophilicity of a cationic intermediate of phthalide **1a**. However, the reason is not clear at present.

Since the double ionic liquid system was the most suitable for the fluorination of **1a**, anodic fluorination of phthalide derivatives **1b** and **1c** was carried out under the same conditions as shown in Schemes 1 and 2.

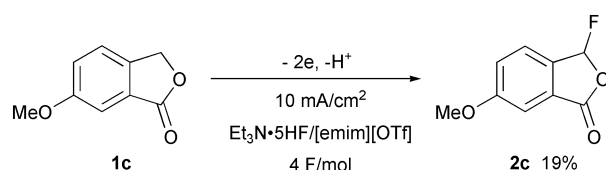
Anodic fluorination of **1b** afforded a regioisomeric mixture of monofluorophthalides **2b** and **3** along with a formyl derivative **4**. In this case, 35% of starting **1b** was recovered. Contrary to this case, **1c** selectively gave product **2c** fluorinated at the lactone moiety in reasonable yield.

Considering the formation of **3** and **4**, the initial electron transfer should take place from the benzene ring of **1** to generate the radical cation as shown in Scheme 3.

The deprotonation from the lactone ring followed by further oxidation generates cationic intermediate **A**. The nucleophilicity of fluoride ions is well-known to be extremely low, and the electrophilicity of **A** of **1b** and **1c** having an electron-



Scheme 1



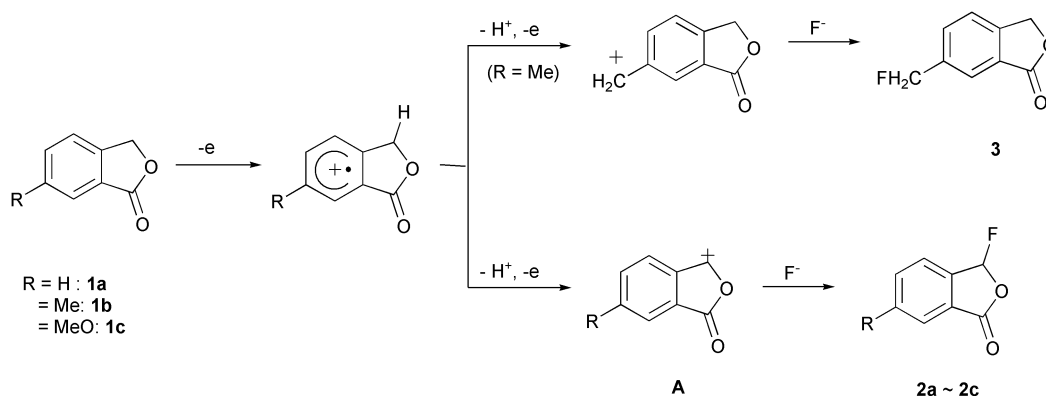
Scheme 2

donating group seems to be lower than that of **1a**. Therefore, the low yields of the fluorinated products **2b** and **2c** are reasonable. In the case of **1b**, the deprotonation from the methyl group also takes place. Therefore, the formation of **3** is understandable.

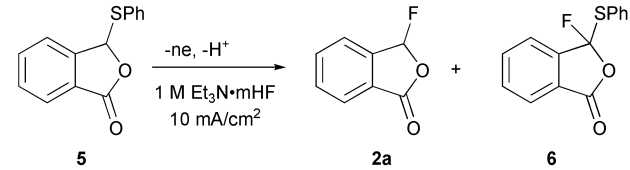
Anodic fluorination of 3-phenylthiophthalide **5** was also attempted in various solvents. The results are listed in Table 3. Interestingly, fluorodesulfurization proceeded predominantly in CH₂Cl₂ and MeCN while the use of DME and THF resulted in selective α -fluorination. A similar solvent effect was observed in the anodic fluorination of 4-arylthio-1,3-dioxolan-2-ones.^{3c} Notably, the fluorodesulfurization took place predominantly in IL, [emim][OTf] to give **2a** in high yield. This suggests that [emim][OTf] may destabilize the radical cation intermediate **B** electrogenerated from **5** similarly to CH₂Cl₂ as shown in Scheme 4.^{3c}

Finally, we examined the possibility of the reuse of ILs for anodic fluorodesulfurization (Table 4).

After the electrolysis of **5** in [emim][OTf], the product **2a** was readily separated by extraction with organic solvents such as ether. The residual organic solvents in IL were removed by evaporation *in vacuo*, and then recovered IL was reused for the fluorodesulfurization of **5**. In the second cycle, the product **2a** was obtained in moderate yield. Although the yield was decreased in the third cycle due to the consumption of HF in fluoride salt Et₃N·5HF, the yield increased markedly by addition of the fluoride salt in the fourth cycle.

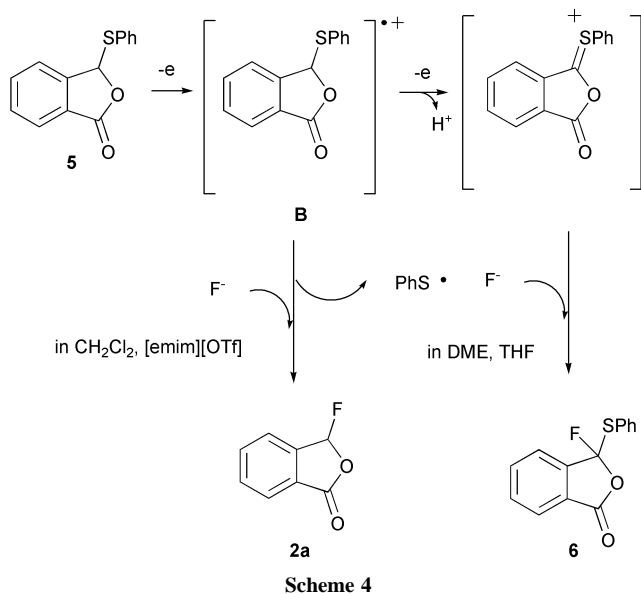
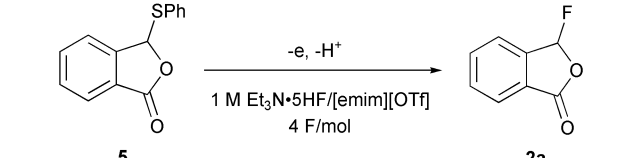


Scheme 3

Table 3 Solvent effect on anodic fluorination of 3-phenylthiophthalide (5)


Run	Reaction media	Supporting electrolyte	Charge passed/ F mol ⁻¹	Yield (%) ^a	
				2a	6
1	MeCN	Et ₃ N·3HF	4	44	—
2	CH ₂ Cl ₂	Et ₃ N·3HF	4	86	—
3	THF	Et ₃ N·3HF	4	6	22
4	DME	Et ₃ N·3HF	3	9	72
5	[emim][OTf]	Et ₃ N·5HF	4	83	trace

^a Determined by ¹⁹F-NMR.

**Table 4** Anodic fluorodesulfurization of 3-phenylthiophthalide (5)


Cycle	Yield (%) ^a
1st	83
2nd	55
3rd	30
4th	81

^a Determined by ¹⁹F-NMR.

Conclusion

Oxidative fluorinating agents, such as N-F compounds, generate equivalent amounts of residues as well as product; electrochemical fluorination, which uses “the positively charged anode as the reagent” does not suffer from this problem.

By careful selection of the IL and the anion, excellent yields can be obtained thus reducing by-products needing disposal.

Evidence is provided that the IL can be easily recycled by adding more Et₃N·5HF.

Experimental

¹H, ¹³C, ¹⁹F-NMR spectra were obtained on a JEOL JNM EX-270 in a deuteriochloroform (CDCl₃) solution using tetramethylsilane as an internal standard, unless otherwise stated. ¹⁹F-NMR spectra were given in δ ppm with CFCl₃ as an external standard (actual internal standard was monofluorobenzene). Mass spectra were obtained by the EI method with a Shimadzu GCMS-QP5050A. High-resolution mass spectra were obtained on a JEOL MStation JMS-700 mass spectrometer operating at an ionization energy of 70 eV. Melting points were determined with a Yamato model MP-21. Cyclic voltammetry was performed using ALS CH instruments Electrochemical Analyzer Model 600A. Preparative electrolysis experiments were carried out using a Hokutodenko Potentiostat/Galvanostat HA-501. Silica gel (60N particle size 63 ~ 210 μm by Kanto) was used for column chromatography. [bmim][NTf₂], [bmim][BF₄] and [bmim][OTf] were prepared according to the procedures reported in the literature.⁵

General procedure of anodic fluorination

The electrochemical cell was fabricated using polypropylene. A single compartment polypropylene cell of 2 ml capacity was used. Anodic oxidation of 1a (1 mmol) was carried out at a constant current (10 mA cm⁻²) with platinum electrodes (1 × 1 cm²) in 2 ml of anhydrous solvent or ionic liquid containing a fluoride salt (1 M) at ambient temperature. After electrolysis, the electrolytic solution was extracted repeatedly by ether and the ethereal extracts were washed with brine to remove the fluoride salt. The organic layer was dried over anhydrous Na₂SO₄, and evaporated to give a crude product, which was purified by column chromatography (EtOAc : hexane = 1 : 3).

3-Fluorophthalide (2a). White crystal; mp 52–53 °C; ¹H NMR (270 MHz, CDCl₃) δ 7.923–7.712 (m, 4H), 6.908 (d, *J* = 63 Hz, 1H); ¹³C NMR (67.8 MHz, CDCl₃) δ 166.78 (d, *J* = 3.33 Hz), 142.88 (d, *J* = 17.3 Hz), 134.96 (d, *J* = 2.24 Hz), 131.91 (d, *J* = 2.85 Hz), 125.89 (d, *J* = 1.70 Hz), 123.70 (d, *J* = 1.70 Hz), 105.65 (d, *J* = 230 Hz); ¹⁹F-NMR (CDCl₃, 254 MHz) δ -48.86 (d, *J* = 63 Hz); MS (*m/z*) 152 (M⁺), 133, 124, 104; HRMS *m/z* calcd for C₈H₅FO₂: 152.0274. Found: 152.0299.

3-Fluoro-6-methylphthalide (2b). White crystal; mp 47–48 °C; ¹H NMR (270 MHz, CDCl₃) δ 7.714–7.566 (m, 3H), 6.858 (d, *J* = 63 Hz, 1H), 2.503 (s, 3H); ¹³C NMR (67.8 MHz, CDCl₃) δ 166.98 (d, *J* = 3.35 Hz), 142.67 (d, *J* = 2.79 Hz), 140.41 (d, *J* = 17.3 Hz), 135.93 (d, *J* = 2.24 Hz), 126.18 (d, *J* = 1.02 Hz), 125.84 (d, *J* = 1.70 Hz), 123.37 (d, *J* = 1.70 Hz), 105.67 (d, *J* = 229 Hz), 21.562 (d, *J* = 1.16 Hz); ¹⁹F-NMR (CDCl₃, 254 MHz) δ -48.01 (d, *J* = 63 Hz); MS (*m/z*) 166 (M⁺), 147, 137, 118; HRMS *m/z* calcd for C₉H₇FO₂: 166.0430. Found: 166.0426.

6-Fluoromethylphthalide (3). White crystal; mp 112 °C; ¹H NMR (270 MHz, CDCl₃) δ 7.912–7.524 (m, 3H), 5.343 (s, 2H), 5.485 (d, *J* = 47 Hz, 2H); ¹³C NMR (67.8 MHz, CDCl₃) δ 170.29, 146.67 (d, *J* = 2.79 Hz), 137.75 (d, *J* = 17.9 Hz), 132.79 (d, *J* = 5.64 Hz), 126.23, 124.17 (d, *J* = 6.11 Hz), 122.38 (d, *J* = 1.70 Hz), 83.401 (d, *J* = 169 Hz), 69.554; ¹⁹F-NMR (CDCl₃, 254 MHz) δ -133.01 (d, *J* = 46 Hz); MS (*m/z*)

166 (M⁺), 147, 109; HRMS *m/z* calcd for C₉H₇FO₂: 166.0430. Found: 166.0429.

3-Fluoro-6-methoxyphthalide (2c). White crystal; mp 59 °C; ¹H NMR (270 MHz, CDCl₃) δ 7.552–7.261 (m, 3H), 6.847 (d, *J* = 64 Hz, 1H), 3.904 (s, 3H); ¹³C NMR (67.8 MHz, CDCl₃) δ 166.89 (d, *J* = 3.33 Hz), 162.60 (d, *J* = 1.70 Hz), 135.19 (d, *J* = 17.9 Hz), 127.72, 124.64 (d, *J* = 1.09 Hz), 123.96 (d, *J* = 2.79 Hz), 108.16, 105.67 (d, *J* = 230 Hz), 55.86; ¹⁹F-NMR (CDCl₃, 254 MHz) δ –47.2 (d, *J* = 65 Hz); MS (*m/z*) 182 (M⁺), 153, 135; HRMS *m/z* calcd for C₉H₇FO₂: 182.0379. Found: 182.0367.

3-Fluoro-3-phenylthiophthalide (6). White crystal; mp 51 °C; ¹H NMR (270 MHz, CDCl₃) δ 7.812–7.141 (m, 9H); ¹³C NMR (67.8 MHz, CDCl₃) δ 161.73 (d, *J* = 2.17 Hz), 144.28 (d, *J* = 21.2 Hz), 136.29, 135.04, 134.46, 131.92 (d, *J* = 1.70 Hz), 130.10, 129.12, 129.02, 125.50, 123.08, 119.65 (d, *J* = 266 Hz); ¹⁹F-NMR (CDCl₃, 254 MHz) δ –5.15 (s); MS (*m/z*) 260 (M⁺), 151; HRMS *m/z* calcd for C₁₄H₉FO₂S: 260.0307. Found: 260.0309.

Acknowledgements

We would like to express our thanks to Prof. Hagiwara of Kyoto University, Central Glass Co., Ltd. and Morita Chemical Industrials Co., Ltd. for generous gifts of [EMIF][2.3HF],

[emim][OTf] and fluoride salts (Et₄NF·4HF and Et₃N·5HF), respectively.

References and notes

- 1 K. Sekiguchi, M. Atobe and T. Fuchigami, *J. Electroanal. Chem.*, in press.
- 2 T. Tajima and T. Fuchigami, *Synthesis*, 2002, **17**, 2597.
- 3 (a) M. K. Dawood and T. Fuchigami, *Tetrahedron Lett.*, 2001, **42**, 2513; (b) Y. Hou, S. Higashiya and T. Fuchigami, *J. Org. Chem.*, 1999, **64**, 3346; (c) H. Ishii, N. Yamada and T. Fuchigami, *Chem. Commun.*, 2000, **17**, 1617.
- 4 K. A. Dekker, T. Inagaki, T. D. Gootz, K. Kaneda and E. Nomura, *J. Antibiot.*, 1997, **50**, 833.
- 5 (a) K. R. Seddon, *J. Chem. Technol. Biotechnol.*, 1997, **68**, 351; (b) T. Welton, *Chem. Rev.*, 1999, **99**, 2071; (c) J. D. Holbrey and K. R. Seddon, *Clean Prod. Processes*, 1999, **1**, 223; (d) H. Ishii and T. Fuchigami, *Electrochemistry*, 2002, **70**, 46; (e) P. Wasserscheid and W. Keim, *Angew. Chem., Int. Ed.*, 2000, **39**, 2772; (f) R. Sheldon, *Chem. Commun.*, 2001, 2399.
- 6 M. Hasegawa, H. Ishii and T. Fuchigami, *Tetrahedron Lett.*, 2002, **43**, 1503.
- 7 (a) K. Momota, M. Morita and Y. Matsuda, *Electrochim. Acta*, 1993, **38**, 1123; (b) S. Chen, T. Hatakeyama, T. Fukuhara, S. Hara and N. Yoneda, *Electrochim. Acta*, 1997, **42**, 1951; (c) K. Sekiguchi, M. Atobe and T. Fuchigami, *Electrochem. Commun.*, 2002, **4**, 881.
- 8 (a) R. Hagiwara and Y. Ito, *J. Fluorine Chem.*, 2000, **105**, 221; (b) R. Hagiwara, T. Hirashige, T. Tsuda and Y. Ito, *J. Fluorine Chem.*, 1999, **99**, 1.



Oxidative total chlorine free photochemical bleaching of cellulosic fabrics†‡

Akihiko Ouchi,*^a Hitoshi Sakai,^a Takeshi Oishi,^a Teruyuki Hayashi,^a Wataru Ando^a and Jun Ito^b

^a Research Institute for Green Technology, National Institute of Advanced Industrial Science and Technology, Tsukuba, Ibaraki 305-8565, Japan. E-mail: ouchi.akihiko@aist.go.jp

^b Textile Research & Development Center, Nisshinbo Industries, Inc., Miei, Okazaki, Aichi 444-8510, Japan

Received 30th April 2003

First published as an Advance Article on the web 1st July 2003

Water-insoluble natural colored compounds adsorbed or chemically bound on cellulosic fabrics were bleached effectively by a selective photolysis of the colored compounds using various excimer lasers (KrF, XeCl, XeF), a low-pressure mercury lamp, and a black-light fluorescent lamp in the presence of sodium peroxocarbonate or mixtures of sodium carbonate and hydrogen peroxide aqueous solutions at room temperature. The efficiency of the photochemical bleaching was found to be comparable to that of the commercial thermal bleaching processes when a XeF excimer laser or a black-light fluorescent lamp were used as light sources.

1. Introduction

Bleaching is one of the most important chemical processes for the utilization of natural cellulosic fabrics. In textile¹ and paper² industries, halogenated oxidizing reagents are widely used in large quantities for bleaching. However, such halogenated oxidizing reagents are reported to form harmful compounds known as adsorbable organically bound halogens.^{3,4} Therefore, development of total chlorine free (TCF) processes is one of the most important issues for preventing the formation of these halogenated compounds.

To avoid the use of such halogenated oxidizing reagents, hydrogen peroxide is partly used in conventional TCF bleaching processes. However, long processing times at high temperature are required in the conventional processes¹ so that considerable amounts of gasses that have negative effects on the environment are generated by the combustion of a large amount of fuels. Peracids, especially peracetic acid and performic acid, which are generated *in situ* from hydrogen peroxide and acids, are also used in the bleaching of cellulosic fabrics. Peracids can be considered as an activated form of hydrogen peroxide, which enable the temperature and processing time of the bleachings to be reduced; however, the use of peracids give some drawbacks such as the strong odor, the danger of explosion, and others.¹ Photochemical bleaching of cellulosic fabrics without the use of any reagents is reported but it was found to be much less effective than the conventional chemical processes.⁵

We report here a more environmentally friendly TCF bleaching process of cellulosic fabrics; a photochemical process in the presence of aqueous solutions of various halogen free oxidizing reagents at room temperature.⁶ Photochemical process implies the use of electricity but the electric energy required for our process was found to be smaller than the thermal energy used in the present standard processes.

2. Results

2.1 Effect of oxidative bleaching reagents

Scoured cotton fabric (SF) was subjected to the laser bleaching using aqueous solutions of six different halogen free oxidizing reagents, namely, hydrogen peroxide, sodium peroxocarbonate ($\text{Na}_2\text{CO}_3 \cdot 1.5\text{H}_2\text{O}_2$), sodium peroxide (Na_2O_2), potassium superoxide (KO_2), urea hydrogen peroxide addition compound ($\text{H}_2\text{NCONH}_2 \cdot \text{H}_2\text{O}_2$), and sodium peroxoborate (NaBO_3). During the preparation of these solutions, generation of gasses was observed when Na_2O_2 and KO_2 were dissolved in water. The pH of the solutions was 6.94 for H_2O_2 , 10.58 for $\text{Na}_2\text{CO}_3 \cdot 1.5\text{H}_2\text{O}_2$, 12.81 for Na_2O_2 , 12.83 for KO_2 , 4.86 for $\text{H}_2\text{NCONH}_2 \cdot \text{H}_2\text{O}_2$, and 10.17 for NaBO_3 .

Among the four major excimer lasers, *i.e.*, ArF (193 nm), KrF (248 nm), XeCl (308 nm), and XeF (351 nm) lasers, a KrF laser was used for the bleaching because this wavelength was found to be most effective in the case of laser bleaching using NaBH_4 aqueous solution.⁷ Fig. 1 shows the whiteness and the yellow index of laser bleached cotton fabrics (LF) as a function of laser irradiation time. The increase of the reagent concentrations [6 wt% H_2O_2 (aq), 2 wt% Na_2O_2 (aq), and 2 wt% $\text{H}_2\text{NCONH}_2 \cdot \text{H}_2\text{O}_2$ (aq)] and the use of 6 wt% TMSOOTMS

Green Context

The ability to bleach fabrics is essential to have a white matrix on which dyes can be adsorbed with true coloration. The bleaching is typically done with chlorine compounds, and non-chlorine systems rarely have the oxidizing power to destroy all the chromophores present in the untreated cloth. Here, a photochemically assisted system is used (in conjunction with non-chlorine containing oxidants) which allows bleaching to take place as efficiently as the traditional, polluting process. With the correct choice of light source, minimal fabric damage is incurred. *DJM*

† Presented at The First International Conference on Green & Sustainable Chemistry, Tokyo, Japan, March 13–15, 2003.

‡ Electronic supplementary information (ESI) available: the results on the whiteness and the yellow index of KrF laser bleached fabrics using high concentration oxidizing reagents. Emission spectra of the low-pressure mercury lamp and the black-light fluorescence lamp. See <http://www.rsc.org/suppdata/gc/b3/b304680j/>

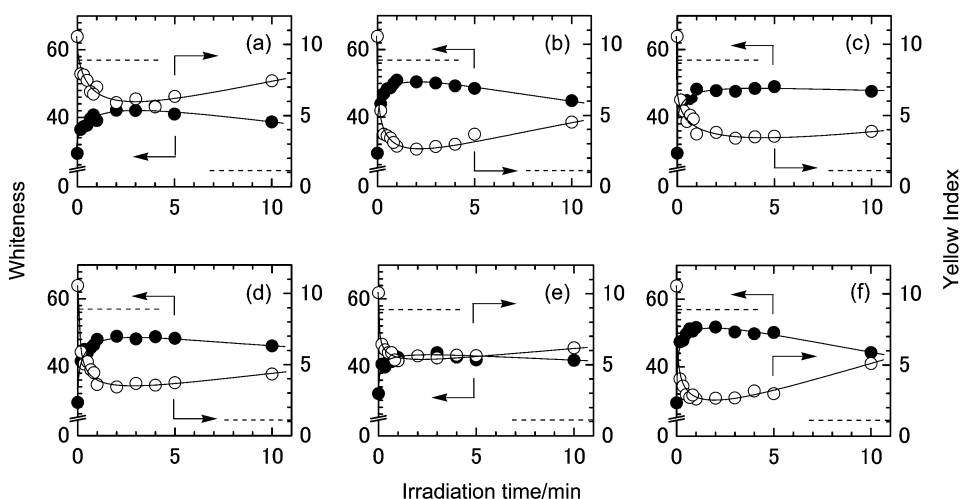


Fig. 1 Whiteness and yellow index of KrF excimer laser bleached cotton fabrics (**LF**) as a function of irradiation time. Reagents: (a) 132 mM H_2O_2 (aq), (b) 132 mM $\text{Na}_2\text{CO}_3 \cdot 1.5\text{H}_2\text{O}_2$ (aq) (the concentration is based on H_2O_2), (c) 132 mM Na_2O_2 (aq), (d) 132 mM KO_2 (aq), (e) 132 mM $\text{H}_2\text{NCONH}_2 \cdot \text{H}_2\text{O}_2$ (aq), and (f) 132 mM NaBO_3 (aq). Whiteness: black symbols, yellow index: white symbols. Laser bleaching conditions: $40 \text{ mJ cm}^{-2} \text{ pulse}^{-1}$, 5 Hz, room temperature. Number of cotton cloths: 1 sheet. Whiteness and yellow index of conventionally bleached fabric (**CF**) are shown in the figures as horizontal broken lines.

(aq) did not show considerable improvements in the whiteness and the yellow index of **LF**.⁸

The figure shows that $\text{Na}_2\text{CO}_3 \cdot 1.5\text{H}_2\text{O}_2$ and NaBO_3 gave the highest whiteness and the smallest yellow index. In all cases, back coloration was observed with prolonged laser irradiations.

Fig. 2 shows the whiteness and the yellow index of thermally bleached cotton fabrics (**TF**) using the same six oxidizing reagents without laser irradiations. The figure clearly shows that the laser irradiation is essential for efficient bleaching.

2.2 Effect of laser wavelength

For further experiments, $\text{Na}_2\text{CO}_3 \cdot 1.5\text{H}_2\text{O}_2$ was selected as a promising reagent because the efficiency of the bleaching was found to be high (*cf.* Fig. 1) and less harmful than NaBO_3 which contains the slightly toxic boron atom.⁹

Fig. 3 shows the whiteness and the yellow index of **LF** as a function of laser irradiation time. The bleaching was conducted by using 6 wt% $\text{Na}_2\text{CO}_3 \cdot 1.5\text{H}_2\text{O}_2$ aqueous solution (pH: 10.48).

In the case of KrF laser irradiation, the efficiency of the bleaching reached its maximum at 2 min, giving maximum whiteness (56) and minimum yellow index (1.2). However, back coloration proceeded with further irradiation. The maximum whiteness and the minimum yellow index were almost the same as those of conventionally bleached cotton fabric (**CF**) using NaClO_2 .

In contrast to the case of the KrF laser, XeCl and XeF laser irradiations showed no decrease of the whiteness by prolonged laser irradiations after reaching their maxima. The maximum whiteness was 57–58, which was almost the same as that of **CF**. In the case of the XeCl laser bleaching, the yellow index showed its minimum (−0.1) at 4 min with a slight back coloration with further irradiation, whereas that of the XeF laser bleaching (0–0.4) stayed constant under prolonged irradiation. The minimum yellow indexes of both XeCl and XeF laser irradiations were better than that of **CF**.

Fig. 4 shows the whiteness and the yellow index of **TF** as a function of bleaching time. As seen in the figure, the whiteness and the yellow index leveled off after 3–4 min and did not show considerable change with further treatment. However, the

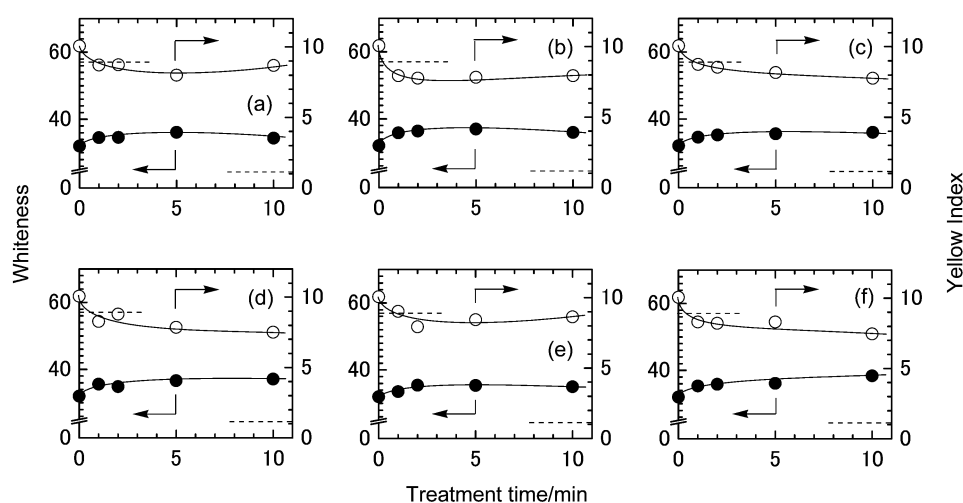


Fig. 2 Whiteness and yellow index of thermally bleached cotton fabrics (**TF**) as a function of reaction time. Reagents: (a) 132 mM H_2O_2 (aq), (b) 132 mM $\text{Na}_2\text{CO}_3 \cdot 1.5\text{H}_2\text{O}_2$ (aq) (the concentration is based on H_2O_2), (c) 132 mM Na_2O_2 (aq), (d) 132 mM KO_2 (aq), (e) 132 mM $\text{H}_2\text{NCONH}_2 \cdot \text{H}_2\text{O}_2$ (aq), and (f) 132 mM NaBO_3 (aq). Whiteness: black symbols, yellow index: white symbols. Treatment temperature: room temperature. Number of cotton cloths: 1 sheet. Whiteness and yellow index of conventionally bleached fabric (**CF**) are shown in the figures as horizontal broken lines.

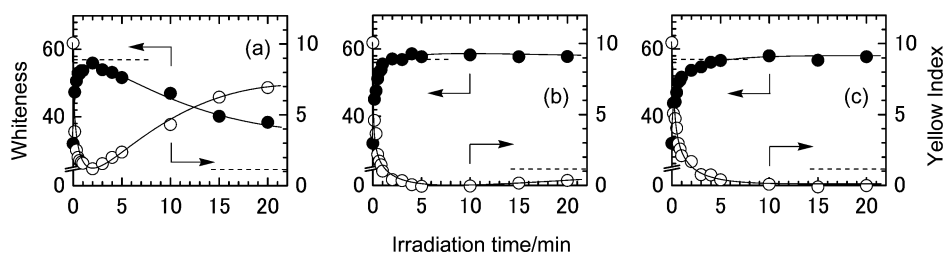


Fig. 3 Wavelength dependence on the whiteness and yellow index of excimer laser bleached cotton fabrics (**LF**) by $\text{Na}_2\text{CO}_3 \cdot 1.5\text{H}_2\text{O}_2$ as a function of irradiation time. Utilized lasers, (a) KrF (248 nm), (b) XeCl (308 nm), and (c) XeF (351 nm) excimer lasers. Whiteness: black symbols, yellow index: white symbols. Laser bleaching conditions: $40 \text{ mJ cm}^{-2} \text{ pulse}^{-1}$, 5 Hz, 6 wt% $\text{Na}_2\text{CO}_3 \cdot 1.5\text{H}_2\text{O}_2$ (aq), room temperature. Number of cotton cloths: 1 sheet. Whiteness and yellow index of conventionally bleached fabric (**CF**) are shown in the figures as horizontal broken lines.

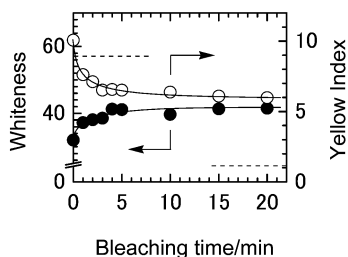


Fig. 4 Whiteness and yellow index of thermally bleached cotton fabrics (**TF**) as a function of bleaching time. Whiteness: black symbols, yellow index: white symbols. Bleaching conditions: 6 wt% $\text{Na}_2\text{CO}_3 \cdot 1.5\text{H}_2\text{O}_2$ (aq), room temperature. Number of cotton cloths: 1 sheet. Whiteness and yellow index of conventionally bleached fabric (**CF**) are shown in the figure as horizontal broken lines.

whiteness and the yellow index reached 52 and 2.5, respectively, after 8 h treatment at room temperature. This result indicates that the irradiation of the lasers is essential for fast bleachings.

Figs. 5, 6, and 7 show the whiteness and the yellow index of **LF** that were bleached by using 2 wt% H_2O_2 and 4 wt%

Na_2CO_3 aqueous solutions and water, respectively. The concentrations of H_2O_2 and Na_2CO_3 were set equal to those of the 6 wt% $\text{Na}_2\text{CO}_3 \cdot 1.5\text{H}_2\text{O}_2$ aqueous solution.

Fig. 5 shows that the whiteness and the yellow index of the KrF and XeCl laser bleaching followed the same trend as those in the 6 wt% $\text{Na}_2\text{CO}_3 \cdot 1.5\text{H}_2\text{O}_2$ aqueous solution but with less efficiency for the bleaching, especially in the case of KrF laser irradiation. However, the whiteness and the yellow index of the XeF laser bleaching exceeded the values of those of **CF** over 15 min irradiation.

Fig. 6 shows that the efficiency of the bleaching became less efficient than that with 2 wt% H_2O_2 aqueous solution. In addition to the less efficient bleaching, fast back coloration was observed in the KrF laser irradiation.

Fig. 7 shows similar features as those in Fig. 6. However, back coloration was slightly suppressed in the cases of the KrF laser irradiation and constant bleaching was observed by continuous XeCl irradiation. These results indicate that the basicity of the solution enhances back coloration but the back coloration is strongly dependent on the utilized laser wavelengths. However, a detailed mechanism on the back coloration is not clear at the moment.

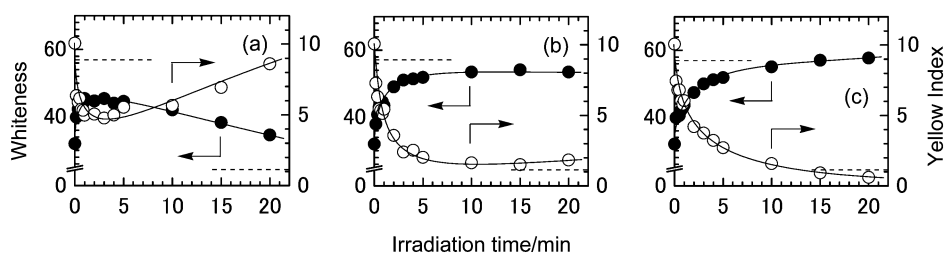


Fig. 5 Wavelength dependence of the whiteness and yellow index of excimer laser bleached cotton fabrics (**LF**) by H_2O_2 as a function of irradiation time. Utilized lasers, (a) KrF (248 nm), (b) XeCl (308 nm), and (c) XeF (351 nm) excimer lasers. Whiteness: black symbols, yellow index: white symbols. Laser bleaching conditions: $40 \text{ mJ cm}^{-2} \text{ pulse}^{-1}$, 5 Hz, 2 wt% H_2O_2 (aq), room temperature. Number of cotton cloths: 1 sheet. Whiteness and yellow index of conventionally bleached fabric (**CF**) are shown in the figures as horizontal broken lines.

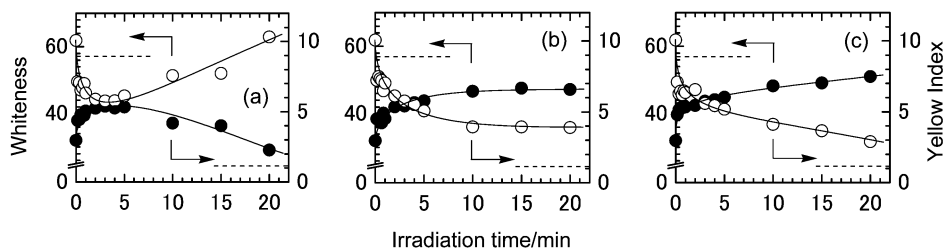


Fig. 6 Wavelength dependence of the whiteness and yellow index of excimer laser bleached cotton fabrics (**LF**) by Na_2CO_3 as a function of irradiation time. Utilized lasers, (a) KrF (248 nm), (b) XeCl (308 nm), and (c) XeF (351 nm) excimer lasers. Whiteness: black symbols, yellow index: white symbols. Laser bleaching conditions: $40 \text{ mJ cm}^{-2} \text{ pulse}^{-1}$, 5 Hz, 4 wt% Na_2CO_3 (aq), room temperature. Number of cotton cloths: 1 sheet. Whiteness and yellow index of conventionally bleached fabric (**CF**) are shown in the figures as horizontal broken lines.

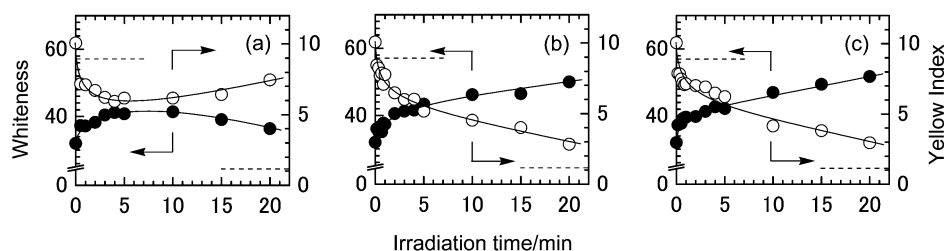


Fig. 7 Wavelength dependence of the whiteness and yellow index of excimer laser bleached cotton fabrics (LF) by H₂O as a function of irradiation time. Utilized lasers, (a) KrF (248 nm), (b) XeCl (308 nm), and (c) XeF (351 nm) excimer lasers. Whiteness: black symbols, yellow index: white symbols. Laser bleaching conditions: 40 mJ cm⁻² pulse⁻¹, 5 Hz, H₂O, room temperature. Number of cotton cloths: 1 sheet. Whiteness and yellow index of conventionally bleached fabric (CF) are shown in the figures as horizontal broken lines.

Table 1 Whiteness, yellow index, and tensile strength of the fabrics obtained by different bleaching methods

Bleaching method		Whiteness ^a	Yellow index ^a	Tensile strength/kg
KrF laser ^b	6 wt% SPC ^c (aq)	56	0.9	13.1
	2 wt% H ₂ O ₂ (aq)	45	5.1	13.1
	4 wt% Na ₂ CO ₃ (aq)	42	5.9	31.9
	H ₂ O	38	6.7	35.2
XeCl laser ^b	6 wt% SPC ^c (aq)	57	0.4	23.6
	2 wt% H ₂ O ₂ (aq)	49	3.6	25.9
	4 wt% Na ₂ CO ₃ (aq)	42	6.1	32.4
	H ₂ O	41	6.5	31.3
XeF laser ^b	6 wt% SPC ^c (aq)	54 (57 ^d)	1.7 (0.4 ^d)	33.7 (33.3 ^d)
	2 wt% H ₂ O ₂ (aq)	47	4.2	33.6
	4 wt% Na ₂ CO ₃ (aq)	42	6.7	33.6
	H ₂ O	40	7.0	34.3
Low-pressure Hg lamp ^e	6 wt% SPC ^c (aq)	56	1.1	17.6
Black-light lamp ^e	6 wt% SPC ^c (aq)	56	1.2	31.8
	NaClO ₂ (aq) ^f	57	1.1	34.4
Thermal	H ₂ O ₂ (aq) ^g	55	1.7	22.5
	None ^h	32	10.1	32.7

^a Number of cotton cloths: 1 sheet. ^b Laser bleaching conditions: 40 mJ cm⁻² pulse⁻¹, 5 Hz, 2 min, room temperature. ^c SPC: Na₂CO₃·1.5H₂O₂. ^d Irradiation time: 5 min. ^e Bleaching conditions: 0.93 mW cm⁻², 60 min, room temperature. ^f Conventionally bleached fabric (CF). ^g Bleaching conditions: 14 wt% H₂O₂ (aq), 0.33 wt% NaOH (aq), 102 °C, 30 min. ^h Scoured fabric (SF).

Table 1 shows the tensile strengths of LF obtained by the KrF, XeCl, and XeF laser bleaching under various conditions. These results indicate that the decrease of the tensile strength is observed only in the presence of peroxides (Na₂CO₃·1.5H₂O₂ and H₂O₂) and the damage of LF decreases with the increase of the laser wavelength. In the absence of peroxides (Na₂CO₃ and H₂O), the decrease of the tensile strength was not observed. It should be noted that no damage was observed in the XeF laser bleaching even in the presence of peroxides. This is a big advantage to the reported photochemical bleaching of cellulosic fabrics in the presence of aqueous H₂O₂ which showed strong degradation of the fabric despite the acceleration of the bleaching.¹⁰

Table 2 shows results on the back coloration of LF using a test of the color fastness to light. When Na₂CO₃·1.5H₂O₂ was used as an oxidizing reagent, the bleached fabrics showed no back coloration under the utilized test except for the case with KrF laser bleaching. However, in the case of the bleaching by H₂O₂ aqueous solution, a further improvement in the whiteness and the yellow index was observed using the test.

It should be noted that the laser bleaching required only 2 ~ 5 min irradiation and was operated at room temperature, in contrast to the standard thermal processes using Na₂CO₃·1.5H₂O₂ and other peroxides such as H₂O₂ that are used in production sites (ca. 1 h at 93 ~ 99 °C or 8 ~ 16 h at room temperature).¹

Table 2 Back coloration of the fabrics obtained by different bleaching methods. Test of the color fastness to light

Bleaching method	Before test ^a		After test ^a		
	Whiteness ^b	Yellow index ^b	Whiteness ^b	Yellow index ^b	
KrF laser ^c	6 wt% SPC ^d (aq)	56	1.7	50	3.7
XeCl laser ^c	6 wt% SPC ^d (aq)	58	0.6	57	1.0
	2 wt% H ₂ O ₂ (aq)	48	4.2	53	2.7
XeF laser ^e	6 wt% SPC ^d (aq)	58	0.7	58	0.7
Low-pressure Hg lamp ^f	6 wt% SPC ^d (aq)	57	1.0	57	1.1
Black-light lamp ^f	6 wt% SPC ^d (aq)	54	2.0	57	1.3
Thermal	NaClO ₂ (aq) ^g	57	1.1	58	0.7
	H ₂ O ₂ (aq) ^h	55	1.7	56	1.7
None ⁱ		33	10.1	45	5.6

^a Test method for color fastness to xenon arc lamp light. ^b Number of cotton cloths: 1 sheet. ^c Laser bleaching conditions: 40 mJ cm⁻² pulse⁻¹, 5 Hz, 2 min, room temperature. ^d SPC: Na₂CO₃·1.5H₂O₂. ^e Laser bleaching conditions: 40 mJ cm⁻² pulse⁻¹, 5 Hz, 5 min, room temperature. ^f Bleaching conditions: 0.93 mW cm⁻², 60 min, room temperature. ^g Conventionally bleached fabric (CF). ^h Bleaching conditions: 14 wt% H₂O₂ (aq), 0.33 wt% NaOH (aq), 102 °C, 30 min. ⁱ Scoured fabric (SF).

2.3 Effect of bleaching conditions

The effect of laser frequency and pulse energy was tested in order to improve the efficiency of the bleaching. The effect of Na₂CO₃·1.5H₂O₂ concentration was also studied to minimize the amount of reagent used for the bleaching.

Fig. 8 shows the whiteness and the yellow index of LF as a function of laser frequency. In the case of the KrF laser irradiation, a decrease of the whiteness and an increase of the yellow index were observed with the increase of the laser frequency. However, in the cases of the XeCl and XeF laser bleedings, the whiteness and the yellow index did not change with the increase of the laser frequencies.

Fig. 9 shows the whiteness and the yellow index of LF as a function of the laser pulse energy; in this experiment, total energy irradiated at a unit area was kept constant so that the number of laser pulses decreased with the increase of the laser pulse energy. The figure shows that the efficiency of the bleaching decreased with the increase of the KrF laser pulse energy but it remained constant in the cases of the XeCl and XeF laser irradiations.

These results indicate that the necessary time for the bleaching can be shortened by increasing the laser frequency and/or the laser pulse energy, especially in the cases of the XeCl and XeF laser irradiations.

Fig. 10 shows the whiteness and the yellow index of LF as a function of Na₂CO₃·1.5H₂O₂ concentration. Considerable im-

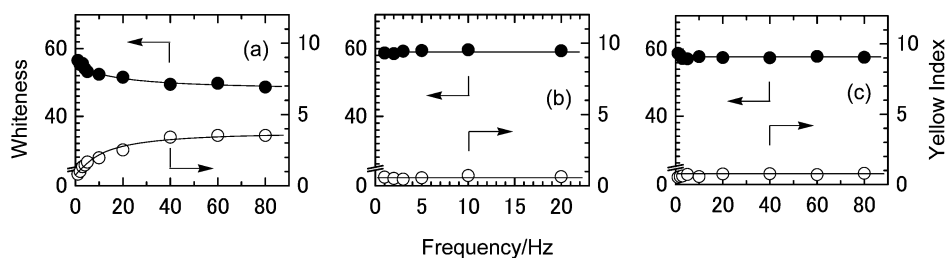


Fig. 8 Wavelength dependence of the whiteness and yellow index of excimer laser bleached cotton fabrics (LF) by $\text{Na}_2\text{CO}_3 \cdot 1.5\text{H}_2\text{O}_2$ as a function of laser frequency. Utilized lasers and irradiated number of laser pulses, (a) KrF (248 nm, 600 pulses), (b) XeCl (308 nm, 600 pulses), and (c) XeF (351 nm, 1500 pulses) excimer lasers. Whiteness: black symbols, yellow index: white symbols. Laser bleaching conditions: $40 \text{ mJ cm}^{-2} \text{ pulse}^{-1}$; 6 wt% $\text{Na}_2\text{CO}_3 \cdot 1.5\text{H}_2\text{O}_2$ (aq), room temperature. Number of cotton cloths: 1 sheet.

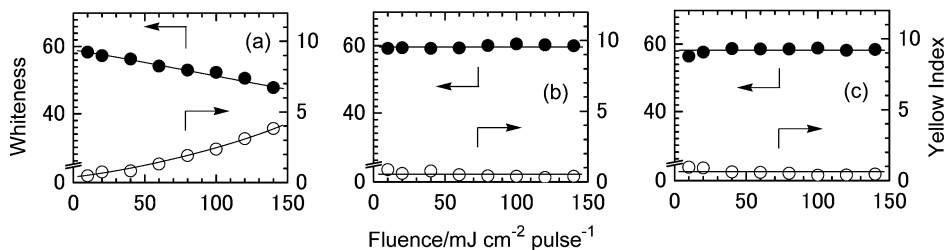


Fig. 9 Wavelength dependence of the whiteness and yellow index of excimer laser bleached cotton fabrics (LF) by $\text{Na}_2\text{CO}_3 \cdot 1.5\text{H}_2\text{O}_2$ as a function of laser pulse energy. Utilized lasers and irradiated energy, (a) KrF (248 nm, 12 J cm^{-2}), (b) XeCl (308 nm, 24 J cm^{-2}), and (c) XeF (351 nm, 60 J cm^{-2}) excimer lasers. Whiteness: black symbols, yellow index: white symbols. Laser bleaching conditions: 5 Hz, 6 wt% $\text{Na}_2\text{CO}_3 \cdot 1.5\text{H}_2\text{O}_2$ (aq), room temperature. Number of cotton cloths: 1 sheet.

provement of the whiteness and the yellow index was observed by increasing the reagent concentration but they leveled off after reaching their maximum and minimum, respectively. Fig. 10 shows that sufficient bleaching was possible with a lower amount of $\text{Na}_2\text{CO}_3 \cdot 1.5\text{H}_2\text{O}_2$ when XeCl and XeF lasers were used instead of the KrF laser. The figure also shows that some extent of bleaching was also observed in pure water (at an $\text{Na}_2\text{CO}_3 \cdot 1.5\text{H}_2\text{O}_2$ concentration of 0%). When a sheet of dry SF was irradiated with the KrF laser ($40 \text{ mJ cm}^{-2} \text{ pulse}^{-1}$, 5 Hz, 3 min), the whiteness and the yellow index of the fabric were 32 and 9.4, respectively, which were almost the same as those before irradiation. These results indicate that water plays an important role in the laser bleaching processes; however, the role of water is still not clear at the moment.

Instead of using $\text{Na}_2\text{CO}_3 \cdot 1.5\text{H}_2\text{O}_2$ the XeF laser bleaching was conducted by using 2 wt% H_2O_2 and various concentrations of Na_2CO_3 , whose results are shown in Fig. 11. As seen in the figure, the whiteness and the yellow index were constant at a Na_2CO_3 concentration of 1 to 10 wt%. The pH of the solution was 6.86 without the addition of Na_2CO_3 and gradually increased from 10.41 (1 wt% Na_2CO_3) to 10.75 (10 wt% Na_2CO_3). This result indicates that a smaller amount of Na_2CO_3 is sufficient for the effective bleaching compared with the use of 6 wt% $\text{Na}_2\text{CO}_3 \cdot 1.5\text{H}_2\text{O}_2$, which corresponds to 4 wt% Na_2CO_3 and 2 wt% H_2O_2 .

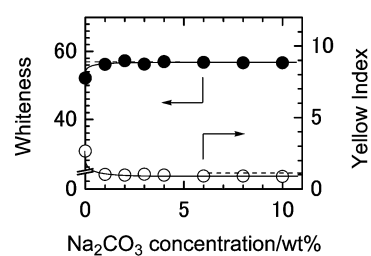


Fig. 11 Whiteness and yellow index of XeF excimer laser bleached cotton fabrics (LF) by mixtures of H_2O_2 and Na_2CO_3 as a function of Na_2CO_3 concentration. Whiteness: black symbols, yellow index: white symbols. Laser bleaching conditions: $40 \text{ mJ cm}^{-2} \text{ pulse}^{-1}$; 5 Hz, 5 min, room temperature. Number of cotton cloths: 1 sheet. Whiteness and yellow index of conventionally bleached fabric (CF) are shown in the figure as horizontal broken lines.

2.4 Bleaching with conventional light sources

Instead of using lasers, the use of more common light sources was investigated. Fig. 12 shows the whiteness and the yellow index of the photochemically bleached fabrics (PF) with a low-

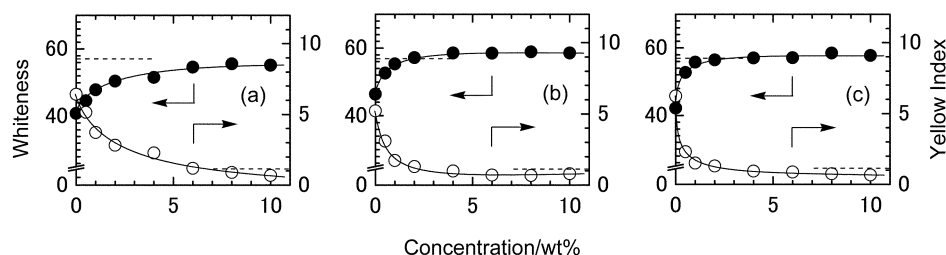


Fig. 10 Wavelength dependence of the whiteness and yellow index of excimer laser bleached cotton fabrics (LF) as a function of $\text{Na}_2\text{CO}_3 \cdot 1.5\text{H}_2\text{O}_2$ concentration. Utilized lasers and irradiation time, (a) KrF (248 nm, 2 min), (b) XeCl (308 nm, 2 min), and (c) XeF (351 nm, 5 min) excimer lasers. Whiteness: black symbols, yellow index: white symbols. Laser bleaching conditions: $40 \text{ mJ cm}^{-2} \text{ pulse}^{-1}$; 5 Hz, room temperature. Number of cotton cloths: 1 sheet. Whiteness and yellow index of conventionally bleached fabric (CF) are shown in the figures as horizontal broken lines.

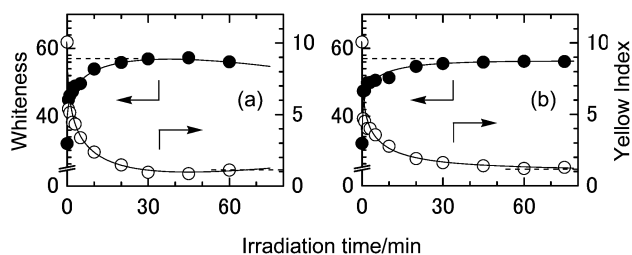


Fig. 12 Whiteness and yellow index of photochemically bleached cotton fabrics (**PF**) by $\text{Na}_2\text{CO}_3 \cdot 1.5\text{H}_2\text{O}_2$ as a function of irradiation time. Irradiation conditions: (a) Low-pressure Hg lamp (0.93 mW cm^{-2}) and (b) black-light fluorescent lamp (0.93 mW cm^{-2}). Whiteness: black symbols, yellow index: white symbols. Reaction conditions: 6 wt% $\text{Na}_2\text{CO}_3 \cdot 1.5\text{H}_2\text{O}_2$ (aq), room temperature. Number of cotton cloths: 1 sheet. Whiteness and yellow index of conventionally bleached fabric (**CF**) are shown in the figures as horizontal broken lines.

pressure mercury lamp (major emission: 254 nm) and a black-light fluorescent lamp (352 nm).⁸ In both cases, the whiteness and the yellow index reached the level of **CF**.

The tensile strength of **PF** bleached by the low-pressure mercury lamp (254 nm) decreased to 1/3 of that of **CF**, which was the same as that in the case with the KrF laser (248 nm) bleaching (*cf.* Table 1). However, a decrease of the tensile strength was not observed for **PF** bleached by the black-light fluorescent lamp (352 nm), which was the same as that in the case with the XeF laser (351 nm) (*cf.* Table 1). These results indicate that sufficient bleaching is also possible with the use of conventional light sources if the wavelength of the light is properly selected.

Back coloration of **PF** was also tested (*cf.* Table 2). The fabric bleached by the low-pressure mercury lamp did not show a change in the whiteness and the yellow index whereas a slight improvement of the whiteness and the yellow index was

observed for the fabric bleached by the black-light fluorescent lamp.

2.5 UV-vis spectra of cellulosic fabrics and oxidizing reagents

Fig. 13 shows the absorbance and absorbance difference of various cotton fabrics. Figs. 13A–C show the absorbance of **SF**, **LF**, and **LF** after the test of color fastness to light (**LFT**). Figs. 13D,E show the absorbance of **SF**, **PF**, and **PF** after the test of color fastness to light (**PFT**). The results of the conventional thermal bleaching by H_2O_2 are also shown in the figure as a comparison (Fig. 13F), where **TFT** is the cotton fabric after the test of color fastness to light. In all cases, a considerable decrease of the absorption was observed after the bleaching (*cf.* **SF** – **LF**, **SF** – **PF**, and **SF** – **TF** in Figs. 13a–f). Although the structures of the natural colored compounds remaining on the scoured cotton fabrics are still not clarified, this decrease indicates that the colored compounds have broad absorption in the UV to visible region, which is evidence for the existence of extended π -electron systems. The decrease of this absorption by the bleaching indicates the decomposition or the shortening of the extended π -electron systems of the colored compounds.

The absorbances of **LF** and **SF** were very similar in the XeCl and XeF laser bleaching (*cf.* **LF** – **CF** in Figs. 13b,c), whereas the absorption difference **LF** – **CF** of the KrF laser showed considerable absorption at 260–350 nm. A continuous increase of this absorption was observed with prolonged KrF laser irradiation after the fast decrease of the absorption at the initial stage of the bleaching (Fig. 14).

The absorbance of **PF** by the low-pressure mercury lamp showed similar features as that of the KrF laser bleaching but with smaller absorbance (*cf.* **PF** – **CF** in Fig. 13d). The absorbance of **PF** by the black-light fluorescent lamp was also the same as that of **CF** (*cf.* **PF** – **CF** in Fig. 13e).

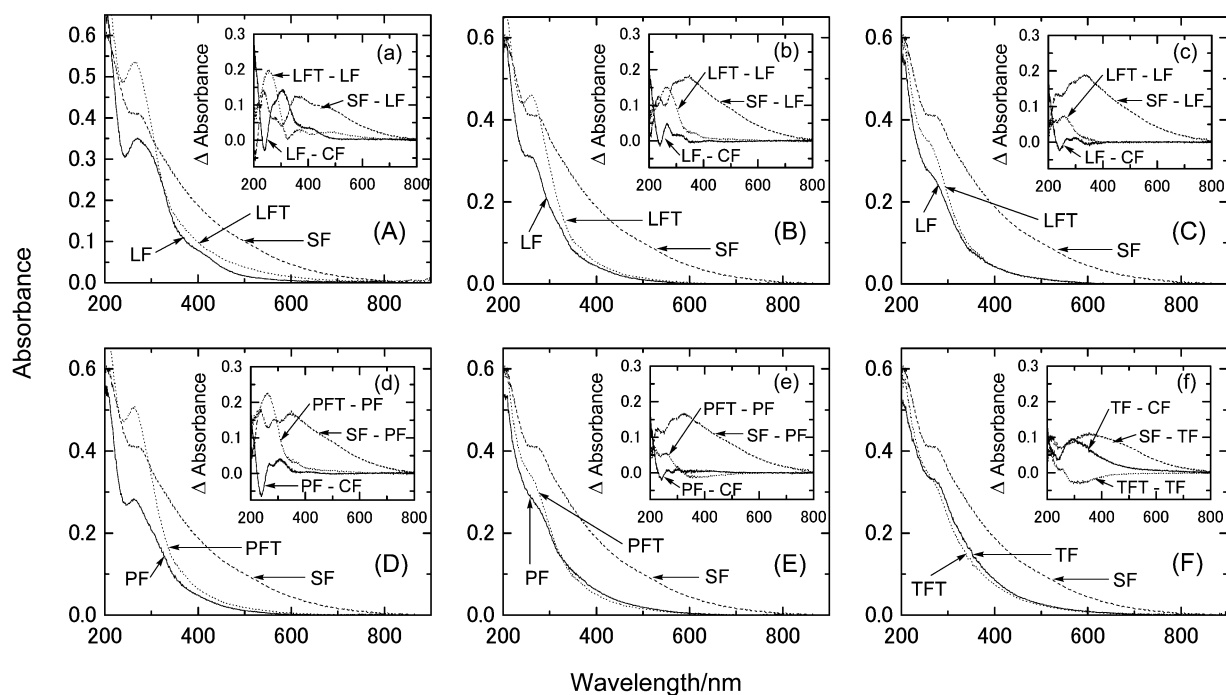


Fig. 13 Absorption (A–F) and absorption difference (a–f) spectra of cotton fabrics. Bleaching conditions: (A, a) KrF laser [$40 \text{ mJ cm}^{-2} \text{ pulse}^{-1}$, 5 Hz, 2 min, 6 wt% $\text{Na}_2\text{CO}_3 \cdot 1.5\text{H}_2\text{O}_2$ (aq), room temperature], (B, b) XeCl laser [$40 \text{ mJ cm}^{-2} \text{ pulse}^{-1}$, 5 Hz, 2 min, 6 wt% $\text{Na}_2\text{CO}_3 \cdot 1.5\text{H}_2\text{O}_2$ (aq), room temperature], (C, c) XeF laser [$40 \text{ mJ cm}^{-2} \text{ pulse}^{-1}$, 5 Hz, 5 min, 6 wt% $\text{Na}_2\text{CO}_3 \cdot 1.5\text{H}_2\text{O}_2$ (aq), room temperature], (D, d) low-pressure Hg lamp [0.93 mW cm^{-2} , 60 min, 6 wt% $\text{Na}_2\text{CO}_3 \cdot 1.5\text{H}_2\text{O}_2$ (aq), room temperature], (E, e) black-light fluorescent lamp [0.93 mW cm^{-2} , 60 min, 6 wt% $\text{Na}_2\text{CO}_3 \cdot 1.5\text{H}_2\text{O}_2$ (aq), room temperature], (F, f) Thermal [30 min, 14 wt% H_2O_2 (aq), 0.33 wt% NaOH (aq), 102 °C]. (A–F) ---: scoured fabric (**SF**), —: laser bleached fabric (**LF**) or photochemically bleached fabric (**PF**) or thermally bleached fabric (**TF**),: **LF** or **PF** or **TF** after the test of color fastness to light (**LFT**, **PFT**, **TFT**, respectively). (a–f) —: **LF** – **CF** or **PF** – **CF** or **TF** – **CF** (**CF**: conventionally bleached fabric), ---: **SF** – **LF** or **SF** – **PF** or **SF** – **TF**,: **LFT** – **LF** or **PFT** – **PF** or **TFT** – **TF**. Number of cotton cloths: 5 sheets.¹²

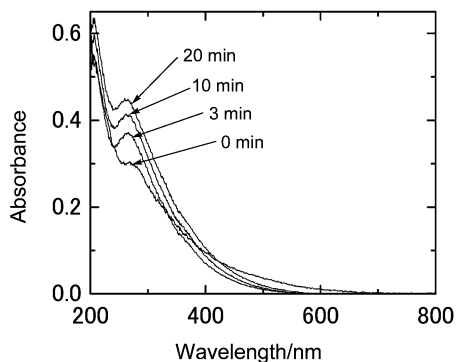


Fig. 14 Absorption spectra of KrF excimer laser bleached cotton fabrics (LF) by $\text{Na}_2\text{CO}_3 \cdot 1.5\text{H}_2\text{O}_2$. Laser bleaching conditions: $40 \text{ mJ cm}^{-2} \text{ pulse}^{-1}$, 5 Hz, 6 wt% $\text{Na}_2\text{CO}_3 \cdot 1.5\text{H}_2\text{O}_2$ (aq), room temperature. Number of cotton cloths: 1 sheet.

The increase of the absorption after the test of color fastness to light showed similar results in LF and PF [cf. LFT – LF and PFT – PF in Figs. 13a–e]. A considerable increase of the absorption at λ_{max} ca. 260 nm was observed, especially in the KrF laser and the low-pressure mercury lamp irradiations.

Fig. 15 shows the UV-vis spectra of $\text{Na}_2\text{CO}_3 \cdot 1.5\text{H}_2\text{O}_2$, H_2O_2 , and Na_2CO_3 aqueous solutions. As seen in the figure,

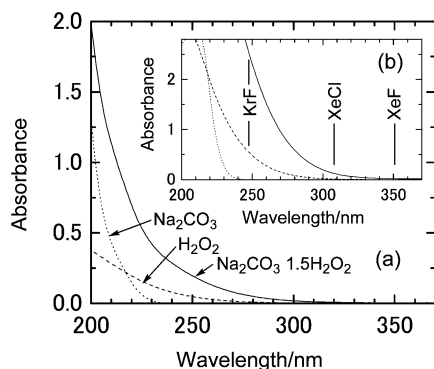


Fig. 15 Absorption spectrum of (a) 0.06 wt% $\text{Na}_2\text{CO}_3 \cdot 1.5\text{H}_2\text{O}_2$ (aq), 0.02 wt% H_2O_2 (aq), 0.04 wt% Na_2CO_3 (aq), and (b) 0.6 wt% $\text{Na}_2\text{CO}_3 \cdot 1.5\text{H}_2\text{O}_2$ (aq), 0.2 wt% H_2O_2 (aq), 0.4 wt% Na_2CO_3 (aq). —: $\text{Na}_2\text{CO}_3 \cdot 1.5\text{H}_2\text{O}_2$, ---: H_2O_2 ,: Na_2CO_3 . Optical path: 10 mm. The wavelengths of the KrF, XeCl, and XeF lasers are marked in the figure.

$\text{Na}_2\text{CO}_3 \cdot 1.5\text{H}_2\text{O}_2$ and H_2O_2 have a considerable absorption at the KrF laser (248 nm) and the low-pressure mercury lamp (254 nm) emissions and a slight absorption at the XeCl laser (308 nm) emission. It should be noted that no absorption was observed at the XeF laser (351 nm) and the black-light fluorescent lamp (352 nm) emissions.

3. Discussion

Bleaching of natural cellulosic fabrics can be interpreted as a decolorization of natural dyes adsorbed or chemically bound on the surface of cellulosic polymers. In the case of scoured cotton fabrics, these colored compounds are practically insoluble in water because most of the water-soluble compounds are removed by the treatment with hot alkaline aqueous solutions before bleaching, which is a process called scouring. The structure of the natural colored compounds remaining on the scoured cotton fabrics is still not identified. However, in analogy with the structure of known natural dyes in plants, the remaining colored compounds on the scoured cotton fabrics are expected to have extended π -electron systems mainly consist-

ing of aromatic, olefinic, carbonyl, and carboxylic moieties, and some ether linkages. The decolorization of the colored compounds can be accomplished by cleaving the extended π -electron systems.

Considering the chromophores of the cellulosic fabrics, the light used in our experiments was not absorbed by the cellulosic fabrics themselves, which can avoid direct photochemical damage of the fabrics. However, a considerable decrease of the tensile strength was observed (cf. Table 1) when the KrF laser and the low-pressure mercury lamp were used as the light sources in the presence of $\text{Na}_2\text{CO}_3 \cdot 1.5\text{H}_2\text{O}_2$ and H_2O_2 , which indicates significant damage of the cellulosic fabrics. This can be explained by the photochemical generation of hydroxyl radicals from H_2O_2 ¹¹ and their successive reactions with the fabrics. The generation of hydroxyl radicals is supported by the presence of a considerable absorption of $\text{Na}_2\text{CO}_3 \cdot 1.5\text{H}_2\text{O}_2$ and H_2O_2 at the wavelength of the emissions of the KrF laser and the low-pressure mercury lamp (cf. Fig. 15). The damage of the fabrics by the action of hydroxyl radicals has also been reported in the conventional thermal bleaching of cellulosic fabrics using H_2O_2 .¹

The damage of the fabric is expected to become larger with the increase of the hydroxyl radical concentration. The absorbance of $\text{Na}_2\text{CO}_3 \cdot 1.5\text{H}_2\text{O}_2$ and H_2O_2 at each laser and conventional light emission was in the order KrF \gg XeCl $>$ XeF \approx 0 and low-pressure mercury lamp $>$ black-light fluorescent lamp \approx 0 so that the concentration of hydroxyl radicals in the laser and the photochemical bleaching is expected to be in the order KrF $>$ XeCl $>$ XeF and low-pressure mercury lamp $>$ black-light fluorescent lamp. The wavelength dependence of the decrease of the tensile strength (KrF $>$ XeCl $>$ XeF \approx none and low-pressure mercury lamp $>$ black-light fluorescent lamp \approx none) is in good accord with the expected order of the concentration of hydroxyl radicals generated by each light source.

The structural change resulting from the damage of the cellulosic fabrics is not clear at the moment. The UV-vis absorption at λ_{max} ca. 260 nm seems to be due to such chemical change but FTIR measurements using the ATR method did not show a clear difference between SF, CF, and LF (KrF, XeCl, and XeF lasers).

For all the utilized oxidizing reagents, the bleaching was largely accelerated by the irradiation with light. For the oxidizing reagents containing hydrogen peroxide, hydroxyl radicals seem to be also responsible for the bleaching when KrF and XeCl lasers and the low-pressure mercury lamp were used as light sources. However, when the XeF laser and black-light fluorescent lamp were used, the contribution of hydroxyl radicals should be similar to that of the room temperature thermal treatments (cf. Fig. 2). Therefore, the acceleration of the bleaching by the light irradiation is only due to the excitation of the colored compounds. The effect of the excitation is an increase of the reducing power of the natural colored compounds. In thermal bleachings, the bleaching is initiated when one of the electrons in the occupied molecular orbitals is transferred from the natural colored compounds to the oxidizing reagents. However, in the excited states, an excited electron of the colored compounds that has higher energy than the HOMO electron of the ground state is transferred to the oxidizing reagents. Such electrons have larger reducing power than the electrons of the occupied molecular orbitals, which explains the facilitation of the oxidation by the irradiation of light to the colored compounds.

It is also interesting that an efficient bleaching was accomplished by our method which is a heterogeneous phase photolysis; water-insoluble organic compounds adsorbed or chemically bound on the cellulosic fibers were photolyzed by wetting the fibers with an aqueous solution of water-soluble reagents. Further basic studies are necessary to understand this efficient heterogeneous phase photochemical reaction.

4. Experimental

The sample used for the laser and photochemical bleaching was a scoured cotton fabric (**SF**) [G poplin (J6220), scoured by Awazu Rensen Kogyo]. A sheet of **SF** (ca. 5 × 5 cm²) was padded in the aqueous solutions of H₂O₂, Na₂CO₃·1.5H₂O, Na₂O₂, KO₂, H₂NCONH₂·H₂O, NaBO₃, Na₂CO₃ and water. The uptake of the solutions or water by the 1 g **SF** was 2.3–2.8 g (average of four to five independent runs). The sheet was then irradiated with a light source at room temperature, washed with water, and dried. The light sources used were a Lambda Physik LPX210i [KrF (248 nm) and XeF (351 nm)] and a Lambda Physik COMPex102 [XeCl (308 nm)] excimer lasers, a 50 W low-pressure mercury lamp (Sen Lights Corp., UVB-110 Power Supply and SUV50UL-1 lamp), and a 15 W black-light blue fluorescent lamp (National FL15BL-B). The pulse energy of the lasers was measured by a Gentec ED-500 joulemeter and a digital storage oscilloscope (Gould Classic 9500, 500 MHz, 2GS/s). The light intensities and the emission spectra of the low-pressure mercury lamp and the black-light fluorescent lamp were measured by an Ushio USR-40D Spectroradiometer.

Conventionally bleached fabric (**CF**) was obtained by bleaching the same batch of **SF** used in the photochemical bleaching experiments by using NaClO₂ [G poplin (J6220), bleached by Awazu Rensen Kogyo]. Thermal bleaching with H₂O₂ was conducted by padding a sheet of **SF** in the aqueous solution of 14 wt% H₂O₂, 0.33 wt% NaOH, and a small amount of sodium silicate, and then the sheet was treated at 102 °C for 30 min, washed with water, and dried.

Reflectance and absorption spectra, whiteness, and yellow index of the fabrics were measured by a UV-vis spectrophotometer (Shimadzu UV-2400PC) equipped with an integration sphere (Shimadzu ISR-2200) using BaSO₄ (Merck, for white standard DIN 5033) as a reference. The whiteness and the yellow index were those defined in JIS Z 8715 (CIE 1986c) and JIS K 7103, respectively (larger whiteness and smaller yellow index indicate better bleaching). The tensile strength of the fabrics was measured by “breaking strength method A (raveled strip method)” defined in JIS L 1096 A (ISO 5081) using a Schopper’s type tensile strength tester (Toyo Seiki Seisaku-sho, Ltd., No. 551 model C). The tensile strength was obtained by the average of 3 or 4 independent runs. Color fastness to light was measured by the “test method for color fastness to xenon arc lamp light” defined in JIS L 0843 (ISO 105 B-02) using a xenon long life fade meter (Suga Test Instruments

Co., Ltd., FAL-25AX). The data were obtained by the average of 5 independent runs. The pH of the aqueous solutions was measured by a Sartorius PT-15 Portable Meter equipped with a pH/ATC electrode [standardized by pH buffer solutions (DKK-TOA Corp.) at pH 4.01, 6.86, and 9.18].

Acknowledgements

We thank the Ministry of Economy, Trade and Industry, Japan for financial support. T. O. thanks the New Energy and Industrial Technology Development Organization for a fellowship.

References and Notes

- 1 M. Lewin, in *Handbook of Fiber Science and Technology, Chemical Processing of Fibers and Fabrics, Fundamentals and Preparation*, ed. M. Lewin and S. B. Sello, Marcel Dekker, Inc., New York, 1984, vol. 1, part B, ch. 2.
- 2 V. Lorås, in *Pulp and Paper*, ed. J. P. Casey, John Wiley & Sons, Inc., New York, 1980, vol. 1, ch. 5.
- 3 For textiles see, for example: G. Schulz, H. Herlinger and P. Schäfer, *Textilveredlung*, 1992, **27**, 167.
- 4 For pulps see, for example: J. Rutkowski, *Cellul. Chem. Technol.*, 1997, **31**, 485.
- 5 J. Ludwig, J. P. Fouassier, R. Freytag and P. Viallier, *Bull. Sci. Inst. Text. Fr.*, 1982, **11**, 81.
- 6 Preliminary results using sodium peroxocarbonate aqueous solutions: A. Ouchi and H. Sakai, *Green Chem.*, 2003, **5**, 329.
- 7 A. Ouchi, T. Obata, H. Sakai and M. Sakuragi, *Green Chem.*, 2001, **3**, 221.
- 8 The experimental data are shown in the supplementary material†.
- 9 (a) *The Merck Index*, ed. S. Budavari, Merck & Co., Inc., Whitehouse Station, NJ, 12th edn., 1996; (b) *Comprehensive Toxicology*, ed. I. G. Sipes, C. A. McQueen and A. J. Gandolfi, Elsevier, Oxford, UK, 1997.
- 10 I. Rusznák, I. Kovács, B. Losonczi and J. Morgós, *Textilveredlung*, 1979, **14**, 442.
- 11 J. G. Calvert and J. N. Pitts Jr., *Photochemistry*, John Wiley & Sons, Inc., New York, 1966, 3-3A-2, pp. 200–202.
- 12 The number of the sheets of **SF** was varied from one to ten; the reflectance increased with the increase in the number of sheets until four but it leveled off over five. The increase in the reflectance by increasing the number of the sheets was due to the suppression of transmitted light.



Green Baeyer–Villiger oxidation with hydrogen peroxide: $\text{Sn}[\text{N}(\text{SO}_2\text{C}_8\text{F}_{17})_2]_4$ as a highly selective Lewis acid catalyst in a fluorous biphasic system†

Xiuhua Hao, Osamu Yamazaki, Akihiro Yoshida and Joji Nishikido*

The Noguchi Institute and Japan Chemical Innovation Institute (JCII), Kaga, Itabashi-ku, Tokyo 173-0003, Japan. E-mail: nishikido@noguchi.or.jp; Fax: +81 3 5248 3597; Tel: +81 3 5248 3596

Received 24th April 2003

First published as an Advance Article on the web 27th June 2003

In a fluorous biphasic catalytic system for Baeyer–Villiger oxidation of cyclic ketones, it was shown that $\text{Sn}[\text{N}(\text{SO}_2\text{C}_8\text{F}_{17})_2]_4$ catalyst can give an excellent yield and selectivity with the green, safe and cheap 35% aqueous hydrogen peroxide as the oxidant. Furthermore, it was also found that the catalyst can be completely recovered and reused without loss of its activity in the fluorous immobilized phase.

Introduction

The Fluorous Biphasic System (FBS), first introduced by Horváth and Rábai in 1994,¹ bears some potential advantages over classical homogeneous catalytic ones, including easy and effective separation and recycling of the catalyst. From the viewpoint of the catalyst, it is designed on the principle of “like dissolves like” so that the metal complex catalyst, with one or more highly fluorinated ligands dissolved in a fluorous solvent, can be mixed with the reactants in an organic solvent. Subsequently, the catalytic reaction can be conducted under biphasic conditions. In a significant variant, the phase miscibility can increase sharply on heating, enabling it to behave as an homogeneous phase during the reaction step, while subsequent cooling finally yields two phases. As an ideal result, the catalyst will remain only in the fluorous phase for reuse, and the pure product will appear only in the organic phase for separation. This kind of fluorous technique has so far been used for some organic syntheses.²

As is well known, the Baeyer–Villiger (BV) oxidation was reported as early as 1899,³ but it still plays an important role in practical processes. With the increase in environmental concern, much research has focused on the development of a catalytic BV oxidation process using low cost oxidants. Based on recent reports, an attempt was made to replace the traditionally-used carboxylic peroxy acids with the green and cheap hydrogen peroxide.⁴ Regarding the catalytic system, several kinds of catalysts have been evaluated for the purpose of facilitating the nucleophilic attack of hydrogen peroxide on the electrophilic carbonyl carbon, including both homogeneous (*e.g.*, rhenium complexes,^{4,5} platinum complexes^{4,6}) and heterogeneous catalysts (*e.g.*, polymer-anchored platinum,⁷ acid zeolitic materials⁸ like HZSM-5, USY). However, most of the recent results showed either poor selectivity or a low turnover number (TON) for the desired lactones, indicating difficulties for their further practical application. In view of the methodology, some researchers have begun to consider an alternative reaction route consisting of an initial activation of carbonyl groups to increase the electrophilicity of the carbonyl carbon and a subsequent interaction with the non-activated hydrogen peroxide.⁹ Accordingly, we were motivated to design an

efficient catalyst to achieve such a purpose. Since Lewis acid catalysts can activate carbonyl groups,¹⁰ our interest was concentrated on metal complexes with perfluorinated ligands, whose Lewis acidity can be adjusted by the choice of different metals (*e.g.*, Sn, Hf, Sc) and its nucleophilicity by the variation of the fluorine load in different perfluorinated ligands (*e.g.*, $-\text{C}_8\text{F}_{17}$, $-\text{CF}_3$).

In our previous work, it was found that lanthanide complexes with tris(perfluorooctanesulfonyl)methide ponytails could be immobilized in the fluorous recyclable phase. There, they can act as efficient Lewis acid catalysts for alcohol acylation, Friedel–Crafts acylation and Diels–Alder reactions by virtue of the highly electron-withdrawing effect resulting from the ponytail's property of having no hydrocarbon spacer.¹¹

From both industrial and environmental standpoints, it is necessary to develop a Lewis acid-catalyzed BV oxidation process using hydrogen peroxide in a fluorous recyclable phase. In this paper, we will report our newest results on a successful approach to FBS (*i.e.*, perfluoro(methylcyclohexane)/1,2-dichloroethane and perfluoro(methylcyclohexane)/1,4-dioxane systems) for BV oxidation using 35% hydrogen peroxide catalyzed by tin(IV) bis(perfluorooctanesulfonyl)amide complex (Fig. 1).

Results and discussion

BV oxidation of adamantanone in FBS was firstly examined with various Lewis acid catalysts (Scheme 1), whose representative results are summarized in Table 1. In the absence of the catalyst (entry 11), both conversion and selectivity were

Green Context

Clean versions of the Baeyer–Villiger reaction are of clear benefit, since the reaction is an effective way of synthesising esters from ketones, and can potentially be carried out using green oxidants. This paper relates to the use of fluorous biphasic conditions, which allow the recovery and reuse of the catalyst in an extremely simple fashion. Conversions and selectivities are excellent for a range of structures. DJM

† Presented at The First International Conference on Green & Sustainable Chemistry, Tokyo, Japan, March 13–15, 2003.

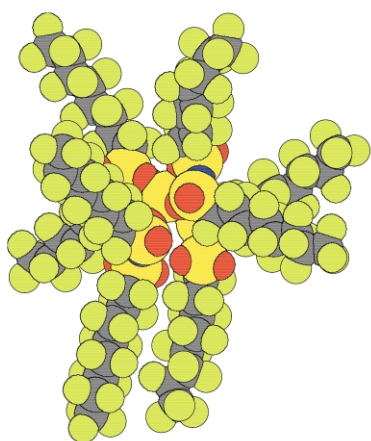
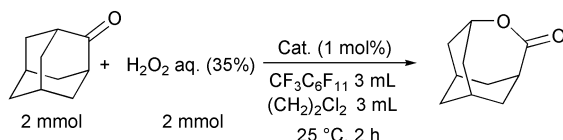


Fig. 1 MNDO/FF optimized structure of $\text{Sn}[\text{N}(\text{SO}_2\text{C}_8\text{F}_{17})_2]_4$. The $\text{Sn}[\text{N}(\text{SO}_2\text{CF}_3)_2]_4$ core part is optimized by the MNDO/AM1¹⁷ method using Gaussian-98¹⁸ and the C_8F_{17} -chain moiety is optimized by Universal Force Field¹⁹ with the fixed core geometry.



Scheme 1 Baeyer–Villiger oxidation of 2-adamantanone.

Table 1 Baeyer–Villiger oxidation of 2-adamantanone in fluorous biphase system under the conditions in Scheme 1

Entry	Catalyst	Yield ^a (%)	Selectivity (%)	TON ^b
1	$\text{Sn}[\text{N}(\text{SO}_2\text{C}_8\text{F}_{17})_2]_4$	93(91) ^c	99	94
2	$\text{Sn}[\text{N}(\text{SO}_2\text{C}_8\text{F}_{17})_2]_2$	48	83	58
3	$\text{Sn}(\text{OSO}_2\text{CF}_3)_2$	37	87	42
4	SnCl_4	41	79	52
5	$\text{Hf}[\text{N}(\text{SO}_2\text{C}_8\text{F}_{17})_2]_4$	82	92	88
6	$\text{Hf}(\text{OSO}_2\text{CF}_3)_4$	41	91	43
7	$\text{Sc}[\text{N}(\text{SO}_2\text{C}_8\text{F}_{17})_2]_3$	53	69	77
8	$\text{Sc}(\text{OSO}_2\text{CF}_3)_3$	31	66	47
9	$\text{Yb}[\text{N}(\text{SO}_2\text{C}_8\text{F}_{17})_2]_3$	31	73	41
10	$\text{Yb}(\text{OSO}_2\text{CF}_3)_3$	19	83	23
11	None	2	26	—

^a GC yields (internal standard: *n*-nonane). ^b Turnover number: mmol converted adamantanone/mmol catalyst. ^c Value in parentheses refers to the isolated yield.

poorest. All of the metal complexes (Sn^{II} , Hf^{IV} , Sc^{III} , Yb^{III}) with the $-\text{N}(\text{SO}_2\text{C}_8\text{F}_{17})_2$ ligand (entries 2, 5, 7 and 9) gave better yields and TON than those with the $-\text{OSO}_2\text{CF}_3$ ligand (entries 3, 6, 8 and 10), but with no significant difference in selectivity. These results can be attributed to the presence of the powerfully electron-withdrawing $-\text{N}(\text{SO}_2\text{C}_8\text{F}_{17})_2$ ligand bearing the higher fluorine load on the metal center: the electrophilicity of the carbonyl carbon would have been increased making it more easily attacked by the poor nucleophile H_2O_2 .¹² This ligand effect was further clearly proven by the Sn-based catalysts: yield and TON followed the order of $\text{Sn}[\text{N}(\text{SO}_2\text{C}_8\text{F}_{17})_2]_4 > \text{Sn}[\text{N}(\text{SO}_2\text{C}_8\text{F}_{17})_2]_2 > \text{Sn}(\text{OSO}_2\text{CF}_3)_2$ (entries 1–3). As for $\text{M}[\text{N}(\text{SO}_2\text{C}_8\text{F}_{17})_2]_n$ ($n = 3, 4$) complexes, yield, selectivity and TON were in the order of $\text{Sn}^{\text{IV}} > \text{Hf}^{\text{IV}} > \text{Sc}^{\text{III}} > \text{Yb}^{\text{III}}$ (entries 1, 5, 7 and 9), except that the selectivity of Yb^{III} was slightly higher than that of Sc^{III} . With

respect to $\text{Sn}[\text{N}(\text{SO}_2\text{C}_8\text{F}_{17})_2]_4$ (entry 1), a conversion of 94% was obtained which corresponded to a TON of 94 (for 2 h at 25 °C), while the selectivity towards the lactone was 99%. Such a result showed a great improvement in the reaction conditions compared with the best reported Sn–zeolite catalytic system⁹ (TON of about 116 for 6 h at 56 °C).

As our previously reported lanthanide complex catalysts,¹¹ $\text{Sn}[\text{N}(\text{SO}_2\text{C}_8\text{F}_{17})_2]_4$ was also found to be completely immobilized and could be reused in the fluorous phase,¹³ *i.e.*, completely remained in the fluorous phase and recycled without depression of its catalytic activity as shown in Fig. 2. These

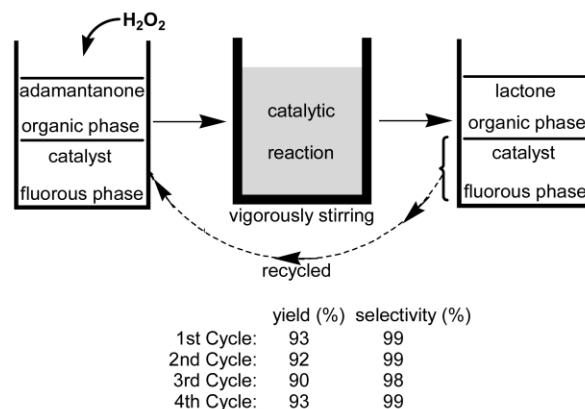
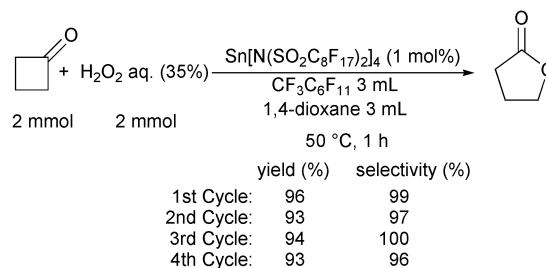


Fig. 2 Recycles of $\text{Sn}[\text{N}(\text{SO}_2\text{C}_8\text{F}_{17})_2]_4$ catalyst in Baeyer–Villiger oxidation of 2-adamantanone.

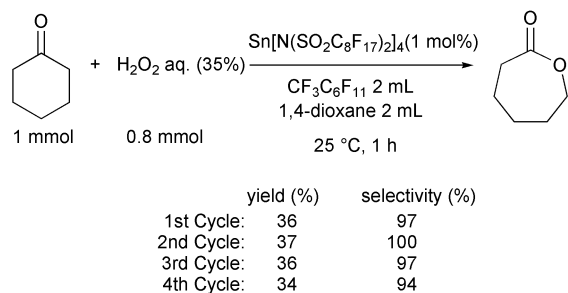
results manifested that even after the catalyst was recycled four times, the GC yield still kept higher than 90%.

The possibility of recycling $\text{Sn}[\text{N}(\text{SO}_2\text{C}_8\text{F}_{17})_2]_4$ catalyst in the BV oxidation of cyclobutanone (Scheme 2) and cyclohex-



Scheme 2 Baeyer–Villiger oxidation of cyclobutanone.

anone (Scheme 3) was also investigated. It was found that there was almost no reduction of the catalytic activity and no other by-products detected except for the desired lactone formation.



Scheme 3 Baeyer–Villiger oxidation of cyclohexanone.

In order to analyze and quantify the catalyst recovery, the reaction rates (= activity) at different cycle times were compared. In Fig. 3, the representative results obtained from cyclobutanone oxidation were shown. It can be found that there

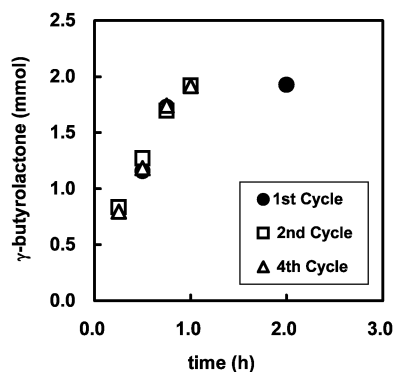


Fig. 3 Lactonization of cyclobutanone catalyzed by $\text{Sn}[\text{N}(\text{SO}_2\text{C}_8\text{F}_{17})_2]_4$ at different cycles under the conditions in Scheme 2.

was almost no difference for the formation rate of γ -butyrolactone at Cycle 1 and Cycle 4 within 1 h reaction time, which confirmed that there was not only no loss of the catalyst but also no depression of catalytic activity during the repetition. Accordingly, it can be deduced that 99% of the catalyst¹⁴ should still remain in the fluororous phase even after the 4th cycle. In fact, the product yield kept a constant level undering specific period (e.g., about 1 h for Cycle 1 in Fig. 3), which is a criteria for us to determine the reaction time.

In Table 2, a series of BV oxidations of several ketone substrates were examined to evaluate the above catalytic system

Table 2 Baeyer–Villiger oxidation of ketones

Entry	Substrate	Product	Conditions	Conversion (%)	Selectivity (%)
1 ^a			50 °C, 1 h	97	99
2 ^a			50 °C, 2 h	59	91
3 ^b			25 °C, 1 h	37	97
4 ^c			25 °C, 2 h	94	99
5 ^{e,d}			50 °C, 5 h	67	99
6 ^{e,d}			70 °C, 2 h	43	99

^a Other reaction conditions as in Scheme 2. ^b Other reaction conditions as in Scheme 3. ^c Other reaction conditions as in Scheme 1. ^d 3 mol% of catalyst was employed with respect to the ketone. ^e Regioselectivity (>99%) determined by GC and ¹H NMR.

under our obtained optimal reaction conditions. It was found that $\text{Sn}[\text{N}(\text{SO}_2\text{C}_8\text{F}_{17})_2]_4$ gave a relatively high selectivity to the desired lactone (>91%) for all of these BV reactions, which can be viewed as superior to most of the reported catalytic systems with 35% H_2O_2 where a mixture of lactone, epoxide and epoxy lactone was produced.^{5–8} It may be noticed that the conversions for cyclopentanone, cyclohexanone, menthone and camphor only reached moderate levels (entries 2, 3, 5 and 6), a little lower than the reported ones.¹⁵ This can contribute to the differences of aqueous hydrogen peroxide concentration and the

ratio of substrate/ H_2O_2 , i.e., 50% higher and excess H_2O_2 were used in their works, whereas 35% and equimolar H_2O_2 in ours. However, as an ideal catalytic synthesis, it not only takes account of the high catalytic activity, but also accounts for the atom economy, safety and easy handling.¹⁴ Since combination of higher concentration H_2O_2 (>50%) with ketones was potentially explosive, it is very significant to develop a practical system with 35% H_2O_2 for the industrial operation. On the other hand, the present turnover frequency (TOF) of the system $\text{Sn}[\text{N}(\text{SO}_2\text{C}_8\text{F}_{17})_2]_4/\text{H}_2\text{O}_2/\text{cyclohexanone}$ (Scheme 3) amounted to 37 h^{-1} , which was comparable to the reported TOF of 23 h^{-1} with the catalyst (Sn-MCM-41) for the same reaction.¹⁶ Furthermore, in our catalytic system, no significant H_2O_2 decomposition was detected.

Additionally, it was also confirmed that such a high selectivity could not be achieved when the catalyst was used in an organic monophase (Table 3), i.e., either 1,2-dichloroethane

Table 3 Comparison of $\text{Sn}[\text{N}(\text{SO}_2\text{C}_8\text{F}_{17})_2]_4$ activities in FBS and in organic monophase system

Ketone	Reaction system	Conversion (%)	Yield (%)	Selectivity (%)
	^a Fluororous biphasic (1st cycle) ($\text{CH}_2\text{Cl}_2/\text{CF}_3\text{C}_6\text{F}_{11}$)	94	93	99
	Organic monophase (CH_2Cl_2 (3 mL))	88	71	81
	^b Fluororous biphasic (1st cycle) 1,4-dioxane/ $\text{CF}_3\text{C}_6\text{F}_{11}$	97	96	99
	Organic monophase 1,4-dioxane (3 mL)	58	38	66
	^c Fluororous biphasic (1st cycle) 1,4-dioxane/ $\text{CF}_3\text{C}_6\text{F}_{11}$	37	36	97
	Organic monophase 1,4-dioxane (2 mL)	48	30	62

^a Other reaction conditions as in Scheme 1. ^b Other reaction conditions as in Scheme 2. ^c Other reaction conditions as in Scheme 3.

as a solvent for adamantanone BV oxidation or 1,4-dioxane as a solvent for cyclobutanone and cyclohexanone BV oxidations, whose respective selectivities (81%, 66%, 62%) were considerably lower than those in FBS (selectivity >97%). Another exceptional advantage in FBS is that the catalyst can be recovered and reused as described above, which is an impossible task in the organic monophase system. It is worth emphasizing that such excellent yield and selectivity benefit greatly from both the efficient Lewis acidity of $\text{Sn}[\text{N}(\text{SO}_2\text{C}_8\text{F}_{17})_2]_4$ and the unique solution property of FBS.

In conclusion, $\text{Sn}[\text{N}(\text{SO}_2\text{C}_8\text{F}_{17})_2]_4$ has proved to be a favorable catalyst for the Baeyer–Villiger oxidation of cyclic ketones in FBS not only due to the improved selectivity but also due to the environmental benignity. We believe that the following results endow the catalytic approach with great potential for synthetic application: (1) 35% aqueous hydrogen peroxide, a safe and economic oxidant for practical processes, was shown to provide satisfactory oxidizing ability; (2) the catalyst, completely immobilized in the fluororous phase, can be recovered and reused; (3) high yields and purities of lactone can be obtained under very mild conditions.

Experimental

General

¹H, ¹³C and ¹⁹F NMR spectra were recorded on a JEOL JNM-ECA600 (600 MHz) instrument using tetramethylsilane (δ

0.00), chloroform-d (δ 77.0) and α,α,α -trifluorotoluene (δ -63.20) as internal standards, respectively. GC analysis was carried out on a SHIMADZU GC-1700AF. GC-MS measurement was performed on a Hewlett-Packard G1800A GLS. Atomic emission spectra were taken on IRIS/AP (Nippon Jarrell Ash Co.). Products after isolation were qualitatively identified by GC-MS, ^1H and ^{13}C NMR, and quantitatively analyzed by GC with *n*-nonane as an internal standard, comparing their retention times with those of the authentic samples.

Typical procedure for ketone oxidation

The experiment was carried out in a 20 mL flask placed on a magnetic stirrer. During the reaction period, the mixture was vigorously stirred by a Teflon-coated stirring bar. The amount of residual H_2O_2 was determined by sampling the upper 1,2-dichloroethane phase, which was titrated with $\text{Na}_2\text{S}_2\text{O}_3$.

To a mixture of perfluoro(methylcyclohexane) (3 mL) and 1,2-dichloroethane (3 mL) were added $\text{Sn}[\text{N}(\text{SO}_2\text{C}_8\text{F}_{17})_2]_4$ (81 mg, 0.02 mmol), 2-adamantanone (300 mg, 2.00 mmol) and 35% H_2O_2 (194 mg, 2.00 mmol). The reaction mixture was stirred continuously at 25 °C for 2 h. Once the stirring was stopped, the reaction mixture settled down and turned into two liquid phases within 10 s, i.e., an upper 1,2-dichloroethane and a lower perfluoro(methylcyclohexane) phase. Pure lactone was obtained from the upper phase after silica gel chromatography and reduced pressure evaporation (302 mg, 91% isolated yield). The lower fluorine phase containing the catalyst was reused in the subsequent recycling reactions, to which 1,2-dichloroethane (3 mL), 2-adamantanone (300 mg, 2.00 mmol) and 35% H_2O_2 (194 mg, 2.00 mmol) were added. The other operations and procedure (e.g., stirring at 25 °C for 2 h, product separation) were the same as described above for the first cycle. Such a procedure was repeated a further three times. Substantially, the yields of lactone were 92%, 90%, 93% in the succeeding three times, respectively.

4-Oxatricyclo[4.3.1.1^{3,8}]undecan-5-one. ^1H NMR (600 MHz, CDCl_3): δ 1.63–2.11 (m, 12H), 3.08 (br.s, 1H), 4.49 (br.s, 1H); ^{13}C NMR (150 MHz, CDCl_3): δ 25.82, 30.94, 33.79, 35.74, 41.21, 73.12, 178.92.

γ -Butyrolactone. ^1H NMR (600 MHz, CDCl_3): δ 2.30 (quintet, $J = 7.5$ Hz, 2H), 2.50 (t, $J = 7.5$ Hz, 2H), 4.35 (t, $J = 7.5$ Hz, 2H); ^{13}C NMR (150 MHz, CDCl_3): δ 21.95, 27.57, 68.35, 177.61.

δ -Valerolactone. ^1H NMR (600 MHz, CDCl_3): δ 1.86–1.90 (m, 2H), 1.91–1.93 (m, 2H), 2.55 (t, $J = 6.9$ Hz, 2H), 4.35 (t, $J = 6.9$ Hz, 2H); ^{13}C NMR (150 MHz, CDCl_3): δ 18.50, 21.73, 29.28, 68.94, 170.95.

ϵ -Caprolactone. ^1H NMR (600 MHz, CDCl_3): δ 1.75–1.84 (m, 4H), 1.86–1.90 (m, 2H), 2.6–2.7 (m, 2H), 4.24 (t, $J = 4.5$ Hz, 2H); ^{13}C NMR (150 MHz, CDCl_3): δ 22.59, 28.52, 28.94, 34.17, 68.95, 175.92.

3,7-Dimethyl-6-octanolide. ^1H NMR (600 MHz, CDCl_3): δ 0.97 (d, $J = 7.8$ Hz, 3H), 1.04 (d, $J = 6.0$ Hz, 3H), 1.09 (d, $J = 7.2$ Hz, 3H), 1.41–2.20 (m, 7H), 2.41–2.62 (m, 1H), 4.06–4.21 (m, 1H); ^{13}C NMR (150 MHz, CDCl_3): δ 16.81, 19.65, 23.76, 26.75, 30.20, 30.75, 37.27, 57.01, 84.61, 175.01.

1,8,8-Trimethyl-2-oxabicyclo[3.2.1]octan-3-one. ^1H NMR (600 MHz, CDCl_3): δ 1.00–1.17 (m, 9H), 1.56 (ddd, $J = 4.1$, 9.8, 14.4 Hz, 1H), 1.93–1.98 (m, 2H), 2.05–2.08 (m, 1H); 2.18

(ddd, $J = 4.8$, 9.6, 14.4 Hz, 1H), 2.42 (d, $J = 19.2$ Hz, 1H), 2.80 (dm, $J = 19.2$ Hz, 1H); ^{13}C NMR (150 MHz, CDCl_3): δ 17.45, 18.28, 23.80, 27.79, 36.97, 38.51, 42.38, 43.28, 93.03, 172.02.

Acknowledgement

This work was supported by New Energy and Industrial Technology Development Organization (NEDO) through the R&D program for Process Utilizing Multi-Phase Catalytic Systems.

References

- I. T. Horváth and J. Rábai, *Science*, 1994, **266**, 72.
- (a) I. T. Horváth, *Acc. Chem. Res.*, 1998, **31**, 641; (b) D. P. Curran, *Angew. Chem. Int. Ed. Engl.*, 1998, **37**, 1175; (c) J. Nishikido, H. Nakajima, T. Saeki, A. Ishii and K. Mikami, *Synlett.*, 1998, 1347; (d) S. Kobayashii and S. Iwamoto, *Tetrahedron Lett.*, 1998, **39**, 4697; (e) D. P. Curran, *Synlett.*, 2001, 1488; (f) J. Xiang, S. Toyoshima, A. Orita and J. Otera, *Angew. Chem. Int. Ed. Engl.*, 2001, **40**, 3670; (g) S. Colonna, N. Gaggero, F. Montanari, G. Pozzi and S. Quici, *Eur. J. Org. Chem.*, 2001, **66**, 181; (h) J. A. Gladysz and D. P. Curran, *Tetrahedron*, 2002, **58**, 3823; (i) *Tetrahedron "Symposium-in-print No. 91: Fluorous Chemistry"*, ed. L. Ghosez and H. H. Wasserman, Pergamon, Oxford, 2002, vol. **58**, No. 20.
- M. Renz and B. Meunier, *Eur. J. Org. Chem.*, 1999, **64**, 737.
- G. Strukul, *Angew. Chem. Int. Ed. Engl.*, 1998, **37**, 1198.
- W. A. Herrmann, R. W. Fischer and J. D. G. Correia, *J. Mol. Catal.*, 1994, **94**, 213.
- R. Gavagnin, M. Cataldo, F. Pinna and G. Strukul, *Organometallics*, 1998, **17**, 661.
- C. Palazzi, F. Pinna and G. Strukul, *J. Mol. Catal. A*, 2000, **151**, 245.
- (a) J. Fischer and W. F. Hölderich, *Appl. Catal. A*, 1999, **180**, 435; (b) I. W. C. E. Arends, R. A. Sheldon, M. Wallau and U. Schuchardt, *Angew. Chem. Int. Ed. Engl.*, 1997, **36**, 1144; (c) A. Bhaumik, P. Kumar and R. Kumar, *Catal. Lett.*, 1996, **40**, 47.
- A. Corma, L. T. Nemeth, M. Renz and S. Valencia, *Nature*, 2001, **412**, 423.
- (a) P. J. Hayward, D. M. Blake and G. Wilkinson and C. J. Nyman, *J. Am. Chem. Soc.*, 1970, **92**, 5873; (b) R. Ugo, G. M. Zanderighi, A. Fusi and D. Carreri, *J. Am. Chem. Soc.*, 1980, **102**, 3745; (c) M. D. T. Frisone, F. Pinna and G. Strukul, *Organometallics*, 1993, **12**, 148.
- K. Mikami, Y. Mikami, Y. Matsumoto, J. Nishikido, F. Yamamoto and H. Nakajima, *Tetrahedron Lett.*, 2001, **42**, 289.
- (a) I. A. Koppel, R. W. Taft, F. Anvia, S.-Z. Zhu, L.-Q. Hu, K.-S. Sung, D. D. DesMarteau, L. M. Yagupolskii, Y. L. Yagupolskii, N. V. Ignat'ev, N. V. Kondratenko, A. Y. Volkonskii, V. M. Vlasov, R. Notario and P.-C. Maria, *J. Am. Chem. Soc.*, 1994, **116**, 3047; (b) J. Nishikido, F. Yamamoto, H. Nakajima, Y. Mikami, Y. Matsumoto and K. Mikami, *Synlett.*, 1999, 1990.
- The catalyst recovered from the fluorine phase without apparent weight loss, i.e., 80 mg modified catalyst was recovered after the original 81 mg was recycled for 4 times. The recovered $\text{Sn}[\text{N}(\text{SO}_2\text{C}_8\text{F}_{17})_2]_4$ catalyst was characterized by elemental analysis: calcd C 19.02, Sn 2.94, found C 19.50, Sn 2.90. For further supporting evidence, see Fig. 3.
- J. A. Gladysz, *Pure Appl. Chem.*, 2001, **73**, 1319.
- (a) K. Neimann and R. Neumann, *Org. Lett.*, 2000, **2**, 2861; (b) G.-J. ten Brink, J.-M. Vis, I. W. C. E. Arends and R. A. Sheldon, *J. Org. Chem.*, 2001, **66**, 2429; (c) A. Berkessel and M. R. M. Andree, *Tetrahedron Lett.*, 2001, **42**, 2293.
- A. Corma, M. T. Navarro, L. Nemeth and M. Renz, *Chem. Commun.*, 2001, 2190.
- (a) M. J. S. Dewar, E. G. Zoebisch, E. F. Healy and J. J. P. Stewart, *J. Am. Chem. Soc.*, 1985, **107**, 3902; (b) M. J. S. Dewar and C. H. Reynolds, *J. Comp. Chem.*, 1986, **2**, 140.
- M. J. Frisch, G. W. Trucks, H. B. Schlegel, G. E. Scuseria, M. A. Robb, J. R. Cheeseman, V. G. Zakrzewski, J. A. Montgomery, R. E. Stratmann, J. C. Burant, S. Dapprich, J. M. Millam, A. D. Daniels, K. N. Kudin, M. C. Strain, O. Farkas, J. Tomasi, V. Barone, M. Cossi, R. Cammi, B. Mennucci, C. Pomelli, C. Adamo, S. Clifford, J. Ochterski, G. A. Petersson, P. Y. Ayala, Q. Cui, K. Morokuma, N.

Rega, P. Salvador, J. J. Dannenberg, D. K. Malick, A. D. Rabuck, K. Raghavachari, J. B. Foresman, J. Cioslowski, J. V. Ortiz, A. G. Baboul, B. B. Stefanov, G. Liu, A. Liashenko, P. Piskorz, I. Komaromi, R. Gomperts, R. L. Martin, D. J. Fox, T. Keith, M. A. Al-Laham, C. Y. Peng, A. Nanayakkara, M. Challacombe, P. M. W. Gill, B. Johnson, W. Chen, M. W. Wong, J. L. Andres, C. Gonzalez, M.

Head-Gordon, E. S. Replogle and J. A. Pople, *Gaussian 98, Revision A.11.3*, Gaussian, Inc., Pittsburgh PA, 2002.
19 (a) A. K. Rappe, C. J. Casewit, K. S. Colwell, W. A. Goddard III and W. M. Skiff, *J. Am. Chem. Soc.*, 1992, **114**, 10024; (b) L. A. Castonguay and A. K. Rappe, *J. Am. Chem. Soc.*, 1992, **114**, 5832; (c) A. K. Rappe and K. S. Colwell, *Inorg. Chem.*, 1993, **32**, 3438.



Screening of adsorbents for removal of H₂S at room temperature†

Mei Xue,* Ramesh Chitrakar, Kohji Sakane and Kenta Ooi*

Institute for Marine Resources and the Environment, National Institute for Advanced Science and Technology, AIST-Shikoku, 2217-14 Hayashi-cho, Takamatsu 761-0395, Japan

Received 19th March 2003

First published as an Advance Article on the web 4th June 2003

The present paper describes the synthesis of H₂S selective adsorbents, which are environmentally economical for removal of H₂S at sewage plant facilities. A series of adsorbents (simple oxides of Ag, Cu, Zn, Co, Ni, Ca, Mn and Sn, mixed oxides of Zn containing Fe, Ni, Co, Mn, Cu, Al, Ti and Zr) derived from hydrous oxides and hydroxycarbonates of different metal ions were prepared. The performance of these adsorbents for the removal of H₂S was studied at room temperature by a batch method. Several adsorbents (CuO, Zn/Mn type, Zn/Ti/Zr type, Zn/Co type, and Zn/Al type) showed markedly high adsorptivity (100 ~ 280 mg g⁻¹) for H₂S gas. A detailed characterization of the adsorbents and sulfided adsorbents was carried out using X-ray diffraction, DTA-TG, SEM and TEM analysis. The H₂S adsorption progresses by the chemical reaction of sulfide formation. The mixed metal oxides containing small crystallites of ZnO with hexagonal structure showed high H₂S uptakes. Analysis of sulfided adsorbents showed that microcrystalline particles were developed after sulfidation. DTA-TG analysis suggested that two kinds of processes, metal sulfide → metal sulfate → metal oxide reaction and metal sulfide → metal oxide reaction, take place during the thermal desorption of sulfur.

Introduction

Hydrogen sulfide and other sulfur compounds are present in fossil fuels (coal and oil), natural gas and sewage treatment facilities. The sulfur compounds need to be removed to less than 1 ppm level for a clean environment, because high concentrations of sulfur compounds result in health hazards, air pollution, acid rain and corrosion of metallic materials used for different purposes. The removal of H₂S can be performed by different routes such as adsorption in liquid alkanolamine, ammonia solution and alkaline salt solution, oxidation with Fe(III) oxide and activated carbon.¹ Westmoreland and Harrison identified the oxides of Fe, Mo, Zn, Mn, Ca, Ba, Sr, Cu, W, Co and V to be the most suitable adsorbents for the removal of H₂S at high temperatures.² Much studies have also been done for desulfurization of coal gas by ZnO doped with transitional metal ions^{3,4} and zinc ferrites,⁵ zinc titanates,^{6,7} Zr-doped zinc titanate⁸ and metal ions doped manganese oxides^{9–11} at high temperatures.

Activated carbons are also used for H₂S removal from natural gas or municipal sewage treatment facilities, because of their developed high surface area and large pore volumes.^{12,13} Activated carbon was found to be a better adsorbent after extensive humidification of its surface.¹⁴

There has been little work done on the H₂S removal by metal oxides at room temperature. Stirling *et al.* investigated in detail by preparing different adsorbents such as ZnO and ZnO doped with 5% oxides of Cu, Fe and Co,¹⁵ high surface area Zn/Co/Al oxides¹⁶ and ZnCo oxides with different Co/Zn ratios for the H₂S removal at room temperature.¹⁷ Among the oxides studied, they reported the Co₃O₄ oxide to be the best one because it showed almost stoichiometric reaction with H₂S. Davidson *et al.* studied the rate of reaction of H₂S with a high surface area of undoped and doped ZnO samples at 0 °C–45 °C and they reported that the fast rates appeared to depend upon the crystallite size, morphology and coexisting water.^{18,19}

Recently, in a study by Carnes and Klabunde,²⁰ the adsorption of H₂S on microcrystalline metal oxides of Zn, Ca, Mg and Al were compared at low temperatures (25 ~ 100 °C) and higher temperatures (250 ~ 500 °C) and they concluded that at elevated temperature, CaO was the best choice for H₂S adsorption and ZnO appeared to be superior at temperatures lower than 100 °C.

We are interested in hydrous oxides and hydroxycarbonates as precursors for superior adsorbents for removal of H₂S at room temperature. We can expect several advantages from these precursors, because co-precipitation of mixed metal salts with alkaline carbonate solution at low supersaturation and constant pH provides a route to the synthesis of mixed phase metal carbonates or hydrotalcite-like materials. The calcination of these materials around 300 °C ~ 400 °C may lead to the formation of high surface area mixed oxides which usually contain the metal components finely dispersed and in close interaction, which are essential properties for the materials to function as promising adsorbents.²¹

There has been no study done on ZnMn-oxides with a Zn/Mn mole ratio of 3, although studies on ZnO doped with MnO (Zn/Mn = 9 in mole ratio)²² or MnO doped with ZnO (Mn/Zn = 9

Green Context

Sulfur compounds including hydrogen sulfide are major environmental hazards and need to be reduced to low levels in natural gas, municipal sewage treatment facilities and other areas of occurrence. Numerous methods for the removal of H₂S have been developed but little has been reported on the use of metal oxides for this purpose. This article describes the preparation and use as H₂S traps of precursors of hydrous oxides, mixed hydrous oxides and hydrotalcite compounds. Some of these are shown to have very high H₂S capacities. Regeneration studies have also been carried out.

JHC

† Presented at The First International Conference on Green & Sustainable Chemistry, Tokyo, Japan, March 13–15, 2003.

in mole ratio)¹⁰ prepared by solid state reaction have been reported for desulfurization of coal at high temperature.

The present study deals with the preparation of precursors of hydrous oxides, mixed hydrous oxides and hydrotalcite-like compounds of different metal ions by a co-precipitation method. Adsorption behaviors of H₂S with different calcined precursors were examined at room temperature. We found that some of the adsorbents showed high H₂S adsorptive capacity.

Results and discussion

Preparation

The starting precursors of different metal ions were prepared by the co-precipitation method. Hydrotalcite-like compounds of Zn/Fe, Zn/Ni, Zn/Co, Zn/Mn and Zn/Cu could not be obtained in pure phase; the phases were mainly dominated by ZnO with minor phases of layered compounds. Only the hydrotalcite-like compounds of Zn/Al, Zn/Co/Al and Zn/Al/Mo could be obtained. The dried samples were decomposed to oxides by heat treatment at 300 °C for 4 h in air. The results of the metal analysis of the adsorbents showed a good agreement between the nominal and actual mole percentages of the metals (Table 1). The chemical formulas were calculated from the metal ion contents of the samples.

XRD and DTA-TG analysis

The XRD patterns of selected adsorbents are shown in Fig. 1. The main diffraction peaks in Cu–O could be indexed to monoclinic structure of CuO (JCPDS No. 05–0661) and other additional small peaks were due to the cubic phase of CuO. The d-spacing calculated from the diffraction patterns of Zn/Mn, Zn/Al, Zn/Co and Zn/Ti/Zr showed a hexagonal close-packed ZnO type lattice of wurtzite structure (JCPDS No. 36–1451). The intensities of the XRD peaks of all the mixed oxides were weak as compared to the pure ZnO sample. The absence of peaks of Mn₃O₄, Co₃O₄, TiO₂ and Al₂O₃ in the XRD patterns of Zn/Mn, Zn/Co, Zn/Ti/Zr and Zn/Al, respectively indicates that these cations are included in the ZnO lattice, which forms significant structures of microcrystalline phase. The XRD patterns of Zn/Fe, Zn/Ni, Zn/Co/Al, Zn/Al/Mo and Zn/Cu/Zr showed mixed phases of ZnO and the corresponding metal oxide. The lattice parameters and space groups of all adsorbents are given in Table 2. The lattice parameters of the adsorbents derived from mixed oxides showed the values almost similar to pure ZnO sample. The average crystallite size (*L*) of different adsorbents were estimated from the values of the full-width at half-maximum (fwhm) by means of the Scherrer equation $L = 0.89 \lambda / \beta(\theta) \cos \theta$, where *L* is the crystallite size, λ is the wavelength of the CuK α radiation used, θ is the Bragg diffraction angle and $\beta(\theta)$ is the fwhm. The calculated crystallite sizes are 13–44 nm and 4–25 nm for single oxides and mixed oxides, respectively.

Table 1 Chemical characterization of different oxides and their maximum H₂S uptake

Sample	Zn/M ^a		Formula	Surface area/ m ² g ⁻¹	H ₂ S uptake/ mg g ⁻¹	
	Added in solution	Found in solid				
Simple oxides	Sn–O	—	—	SnO	n.d. ^b	2
	Ni–O	—	—	NiO	n.d.	2
	Co–O	—	—	Co ₃ O ₄	n.d.	6
	Ca–O	—	—	CaO	n.d.	11
	Mn–O	—	—	Mn ₃ O ₄	n.d.	16
	Ag–O	—	—	Ag ₂ O	n.d.	31
	Zn–O	—	—	ZnO	17	32
	Cu–O	—	—	CuO	37	283
	Mixed oxides	Zn/Fe	75/25	75/25	Zn _{3.1} FeO _{4.4}	58
Zn/Ni		75/25	76/24	Zn ₃ NiO ₄	37	69
Zn/Co		75/25	77/23	Zn _{3.5} CoO _{4.9}	49	134
Zn/Mn		75/25	75/25	Zn _{2.9} MnO _{4.2}	11	152
Zn/Fe/Zr		72/23/5	78/21/1	Zn _{3.7} FeZr _{0.05} O _{5.2}	16	75
Zn/Ti/Zr		68/23/9	65/24/11	Zn _{2.9} TiZr _{0.5} O ₆	64	145
Zn/Cu/Zr		71/24/5	75/24/0.5	Zn ₃ CuZr _{0.03} O ₄	23	135
Zn/Co/Al		50/25/25	50/29/21	Zn _{2.6} Co _{1.5} AlO _{6.1}	11	107
Zn/Al		75/25	75/25	Zn ₃ AlO _{4.5}	58	146
Zn/Al/Mo		(Mo-intercalated)			28	115

^a mol %, ^b n.d.—not determined

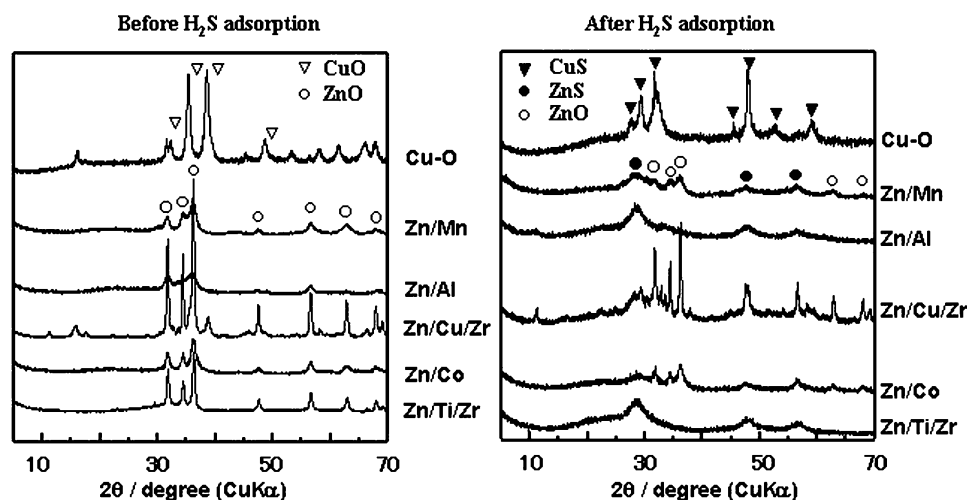


Fig. 1 XRD patterns of adsorbents.

The DTA-TG curves of two adsorbents (Cu–O and Zn/Ti/Zr) are shown in Fig. 2. Initially, there was a gradual weight loss of 3.5% with a small endothermic peak around 220 °C for Cu–O and 5% for Zn/Ti/Zr up to 300 °C. These weight losses might be due to the dissipation of water adsorbed on the surface of oxide after exposure in atmosphere. The other adsorbents also showed low weight loss up to 200 °C.

SEM and TEM photographs

SEM images of two adsorbents (Zn/Ti/Zr and Zn/Mn) are shown in Fig. 3. Stacking of layers of small crystallites could be seen with cuboidal morphology for Zn/Ti/Zr and cubic-like morphology for Zn/Mn with sizes of 20–50 μm . Similar morphology of stacking layers was also observed for Zn/Co and Zn/Al. Cu–O showed only aggregates of particles; the size of aggregates is around 2 μm . TEM observation for Cu–O adsorbent shows that it consists of crystallites having crystallite sizes of 10–15 nm (Fig. 4).

Adsorptive capacity for H₂S

The adsorptive capacities of H₂S at 10 ppm concentration level by different adsorbents were determined from a batch type breakthrough curve at room temperature. The breakthrough behaviors of H₂S by different adsorbents are shown in Fig. 5. The volume for H₂S saturation varies largely depending on the kind of adsorbent. It is interesting to note that even a small amount 25 mg of Cu–O can consume 500 L of 10 ppm H₂S gas at room temperature. The H₂S adsorptive capacities calculated from the breakthrough volume are given in Table 1. Among the adsorbents of single metal oxides, Cu–O shows a maximum H₂S uptake of 283 mg g⁻¹, while the other adsorbents have considerably lower H₂S uptakes (2 ~ 32 mg g⁻¹). Sample Co–O does not show a high adsorptive capacity for H₂S, contrary to the results in the literature.¹⁷ Adsorbents Zn/Mn, Zn/Co, Zn/Ti/Zr and Zn/Al show relatively high H₂S uptakes (135 ~ 152 mg g⁻¹), while Zn/Fe, Zn/Ni and Zn/Fe/Zr relatively low H₂S uptakes (66 ~ 75 mg g⁻¹). The reaction rate is a critical factor in any possible application of the materials. When we used adsorbents Cu–O, Zn/Mn, Zn/Co, the reaction of H₂S adsorp-

Table 2 Lattice parameters of different oxides

Sample	Crystal phase	Lattice parameter/nm	Space group	Crystal size/nm
Sn–O	SnO	$a_0 = 0.380, c_0 = 0.484$	Tetragonal(<i>P4/nmm</i>)	37
Ni–O	NiO	$a_0 = 0.295, c_0 = 0.725$	Trigonal(<i>R3m</i>)	13
Co–O	Co ₃ O ₄	$a_0 = 0.806$	Cubic(<i>Fd3m</i>)	15
Ca–O	CaO	$a_0 = 0.359, c_0 = 0.491$	Orthorhombic(<i>P3m</i>)	42
Mn–O	Mn ₃ O ₄	$a_0 = 0.575, c_0 = 0.945$	Tetragonal(<i>I4₁/amd</i>)	21
Ag–O	Ag ₂ O	$a_0 = 0.473$	Cubic(<i>Pn3m</i>)	44
Zn–O	ZnO	$a_0 = 0.325, c_0 = 0.521$	Hexagonal(<i>P6₃mc</i>)	19
Cu–O	CuO	$a_0 = 0.454, b_0 = 0.341, c_0 = 0.516, \beta = 102.6^\circ$	Monoclinic(<i>C2/c</i>)	16
Zn/Fe	ZnO + Fe ₂ O ₃	$a_0 = 0.325, c_0 = 0.521$	Hexagonal(<i>P6₃mc</i>)	25
Zn/Ni	ZnO + NiO	$a_0 = 0.33, c_0 = 0.52$	Hexagonal(<i>P6₃mc</i>)	4
Zn/Co	ZnO	$a_0 = 0.32, c_0 = 0.52$	Hexagonal(<i>P6₃mc</i>)	8
Zn/Mn	ZnO	$a_0 = 0.32, c_0 = 0.52$	Hexagonal(<i>P6₃mc</i>)	6
Zn/Ti/Zr	ZnO	$a_0 = 0.32, c_0 = 0.52$	Hexagonal(<i>P6₃mc</i>)	20
Zn/Cu/Zr	ZnO + CuO	$a_0 = 0.32, c_0 = 0.52$	Hexagonal(<i>P6₃mc</i>)	24
Zn/Al/Mo	Weak ZnO	$a_0 = 0.32, c_0 = 0.52$	Hexagonal(<i>P6₃mc</i>)	9
Zn/Al	ZnO	$a_0 = 0.32, c_0 = 0.52$	Hexagonal(<i>P6₃mc</i>)	6
Zn/Fe/Zr	Mixture of three phases (ZnO, Fe ₃ O ₄ , ZrO ₂)			25

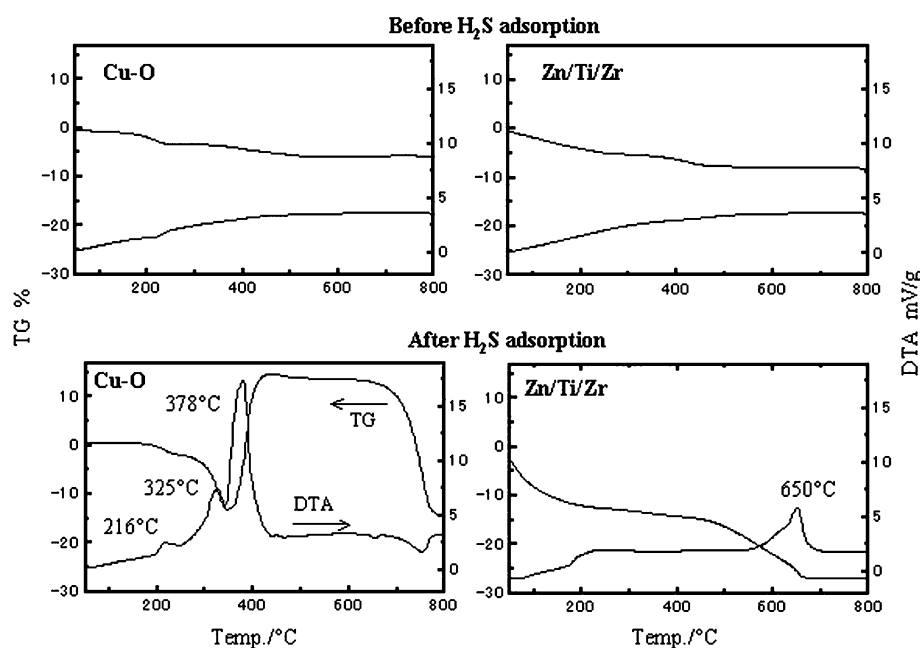


Fig. 2 DTA-TG curves of Cu–O and Zn/Ti/Zr before sulfidation (top) and after sulfidation (bottom).

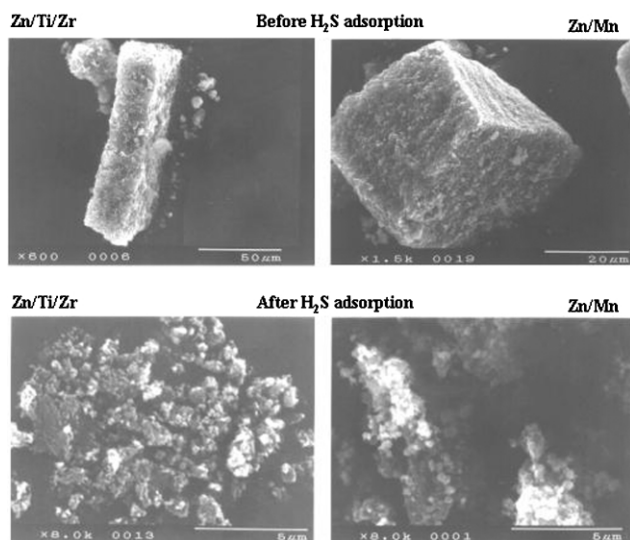


Fig. 3 SEM photographs of different adsorbents.

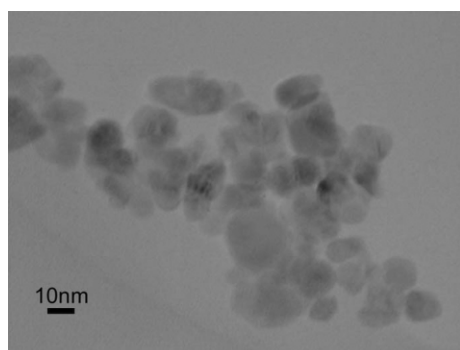


Fig. 4 TEM image of Cu-O.

tion (25 mg of adsorbent and 20 L H₂S of 10 ppm) is complete within 5 min, so the reaction rate is considerably fast. But, reaction rates of H₂S adsorption with Zn/Fe, Zn/Ni are a little slow.

The degree of reaction, calculated from the ratio of the number of moles of H₂S adsorbed to the total number of moles of metal in the adsorbent, was plotted against the surface area of different oxides, as is shown in Fig. 6. The degree of reaction is markedly high on Cu-O among the adsorbents studied although the surface area of Cu-O was low as compared to Zn/Al, Zn/Ti/Zr; it reaches up to 73% for Cu-O. The ZnO type adsorbent can be classified into two groups: those with a relatively high degree

($\approx 40\%$) of adsorption and those with a low degree ($\approx 20\%$) of adsorption. Except for samples Zn/Ti/Zr and Zn/Ni, the adsorbents with smaller crystallite sizes show a higher H₂S adsorptive capacity. This indicates that crystallite size of ZnO has an important role in the chemical reaction of H₂S adsorption. It is interesting that Zn/Ti/Zr has a high H₂S adsorptivity although the crystallite size of ZnO is relatively large. A further study is needed to clarify the reason for its high H₂S adsorptivity. Stirling *et al.*^{15–17} prepared Zn/Co, Zn/Al and Zn/Co/Al adsorbents from metal nitrate solution by a coprecipitation method and reported the degree of reaction for sulfidation to be 46, 9 and 12%, respectively. Our present results showed much higher values for Zn/Al and Zn/Co/Al, and a close value to Zn/Co as compared to the data by Stirling *et al.*

Although Zn-O and Zn/Mn have almost the same surface area, Zn/Mn showed high H₂S uptake as compared to Zn-O. This indicates that although the surface area of the oxides is important, it is not the only factor determining the degree of reaction. The effect of surface area may be limited for samples with a high surface area above 50 m² g⁻¹.

The adsorptive capacity of H₂S at 300 ppm concentration level were also determined for selected adsorbents by a batch method at room temperature. The data collected after 3 days replacing the H₂S gas each time are shown in Fig. 7. The H₂S uptakes by Zn/Mn, Zn/Co, Zn/Cu/Zr and Zn/Ti/Zr were comparable with the data obtained at the 10 ppm concentration level above, while low H₂S uptake was observed for Zn/Al, which may be due to a relatively slow rate of H₂S adsorption. The calculated H₂S removals from 300 ppm are as follows: Cu-O, 71%; Zn/Mn, 80%; Zn/Cu/Zr, 87%; Zn/Co, 83%; Zn/Ti/Zr, 76%; and Zn/Al, 38%. These values are comparable to those from the 10 ppm concentration level, except for Zn/Al, which is lower.

The reaction rate of H₂S adsorption at 300 ppm concentration level by Cu-O, Zn/Cu/Zr, Zn/Co, Zn/Ti/Zr and Zn/Mn are relatively fast as compared to Zn/Al. Cu-O showed 100% adsorption of H₂S in 1 day. It further showed 100% adsorption in 2 days. Zn/Cu/Zr, Zn/Co and Zn/Ti/Zr showed 100% adsorption in 1 day, followed by 52, 48, and 30% respectively in 3 days. Zn/Mn showed 88% adsorption in 1 day, followed by 84% in 3 days. Zn/Al showed 59% adsorption in 3 days.

XRD analysis and SEM observation for sulfided adsorbents

The structural changes occurring in sulfided adsorbents were studied by XRD analysis (Fig. 1). All the diffraction peaks could be assigned to CuS (JCPDS No. 06-0464) after sulfidation of Cu-O. Sulfidation of Cu-O occurred by phase

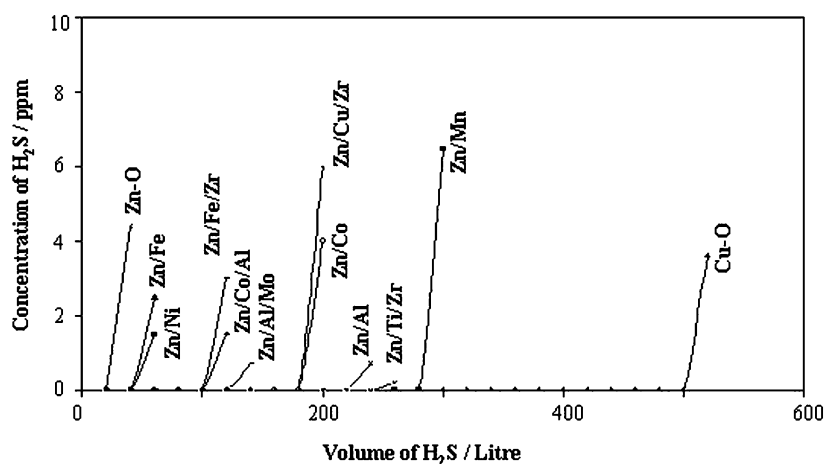


Fig. 5 Breakthrough behaviors for H₂S adsorption. Adsorbent = 25 mg, H₂S concentration = 10 ppm in nitrogen, room temperature.

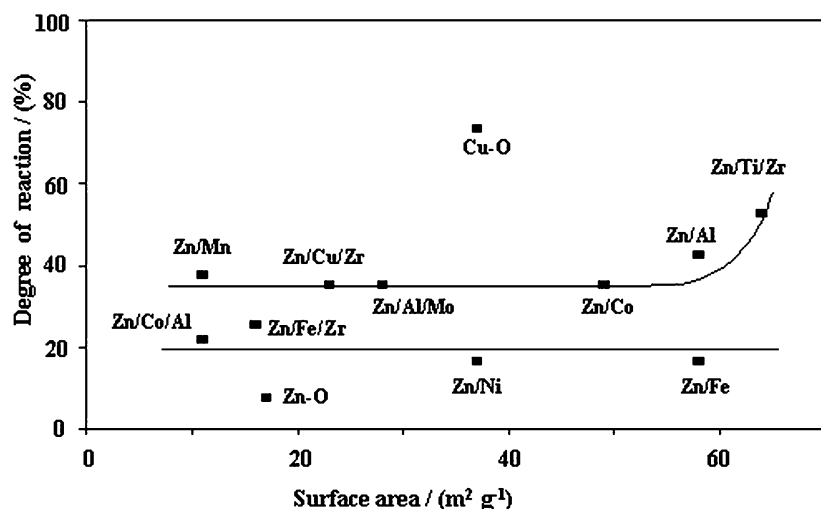


Fig. 6 Plot of degree of sulfidation reaction vs. surface area. Degree of reaction(%) = $100 \times$ number of moles of H_2S adsorbed/total number of moles of metal ions in the adsorbent.

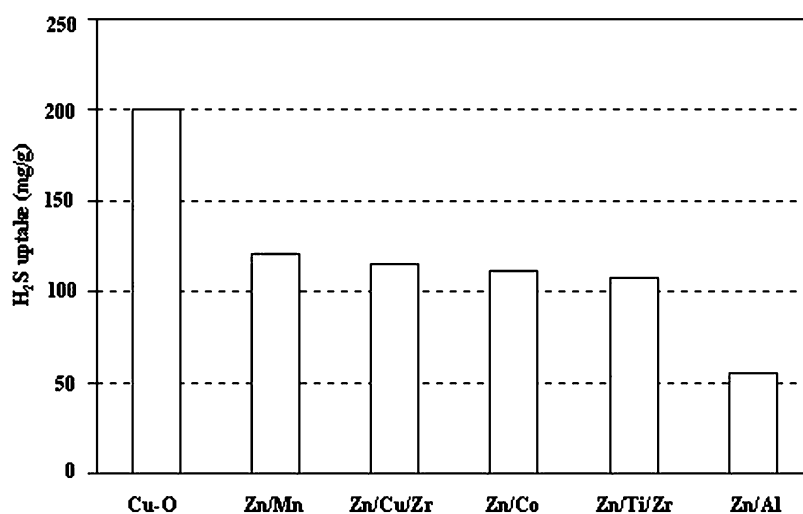


Fig. 7 H_2S uptake by selected adsorbents at room temperature from N_2 gas containing 300 ppm H_2S .

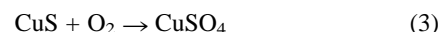
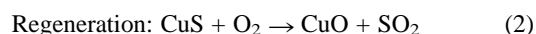
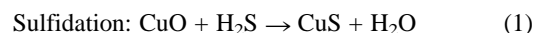
change from monoclinic CuO to hexagonal CuS . For other adsorbents, the diffraction peaks corresponding to ZnS (JCPDS No. 05–0566) were dominant after sulfidation. The peaks corresponding to unreacted ZnO could also be observed, because the degree of sulfidation was below 60%. However, the diffraction peaks corresponding to other metal sulfides could not be found in the XRD patterns of sulfided adsorbents. ZnO consisted of hexagonal close packed (HCP) lattice of oxide ions with Zn ions in the tetrahedral sites, while ZnS formed had a cubic closed packed (CCP) lattice of sulfide ions (Zn ions were still in tetrahedral sites). This requires some rearrangement of the anions.

SEM images of all sulfided adsorbents showed that the morphology due to stacking of layers was not retained after the sulfidation. The particle sizes of Zn/Ti/Zr and Zn/Mn were reduced to *ca.* $0.5 \mu\text{m}$ (Fig. 3). The breakdown of some oxide particles to small ZnS crystallites may be caused by rearrangement of the anion lattice from HCP to CCP along with the exchange of O^{2-} and S^{2-} .

DTA-TG analysis for sulfided adsorbents

The DTA-TG curves are shown in Fig. 2. The small endothermic peaks around 216°C and 325°C on the DTA curve of sulfided Cu-O is due to partial desorption of SO_2 accompanied by weight loss. A sharp exothermic peak around 378°C

accompanied by weight gain is due to sulfate formation.²³ Finally, a sudden weight loss occurred around 700°C , which could be due to the destruction of sulfate with the dissipation of SO_2 gas. The DTA-TG curves of Zn/Mn , Zn/Co , and Zn/Cu/Zr also showed two small endothermic peaks below 350°C and a broad exothermic peak around 400°C . But DTA-TG curves of Zn/Ti/Zr did not show any sulfate formation because of the absence of an exothermic peak around 400°C , similar behaviors were also observed on Zn/Al . From DTA-TG analysis of the sulfided adsorbents, which involved sulfate formation, the adsorption–desorption reactions could be written as follows:



Reaction (2) showed that sulfided CuO could be partially regenerated with air as indicated by weak endothermic peaks. Reaction (3) showed that CuSO_4 was formed after a partial stage of regeneration with an increase in weight along with an appearance of a sharp exothermic peak around 380°C . Finally it decomposed to CuO and SO_2 around 800°C . Zn/Al and Zn/Ti/Zr appeared mostly as stable phases not associated with sulfate formation during regeneration of the sulfided samples.

The reaction between ZnO and H_2S is non-catalytic gas–solid reaction. H_2S is known to be dissociated into HS^- and H^+ on a

ZnO surface. It is believed that the gas–solid reaction is controlled by either pore or lattice diffusion.¹⁷ In pore diffusion, the rate of reaction will be controlled by the rate of diffusion of HS⁻ into the pores of fresh oxide. In the lattice diffusion, HS⁻ reacts with the oxide surface and the sulfided surface is then replenished by migration of fresh oxide and water formed to the sulfided surface. At present in our present study, we could not confirm the possibility of the reaction mechanism mentioned above. We will investigate the reaction mechanism in our next study.

In conclusion, the data presented here shows that nearly stoichiometric a solid–gas reaction took place in Cu–O adsorbent at room temperature. The adsorbents exhibited a reactivity trend of Cu–O > Zn/Mn ≥ Zn/Ti/Zr, Zn/Co, Zn/Al. The H₂S adsorptive capacity of ZnO could be enhanced considerably by doping it with metal ions such as Mn, Co, Cu, Ti and Zr. The doping of such metal ions produced microcrystalline oxides, which showed considerable high H₂S uptakes as compared to pure ZnO. Adsorbed sulfide could be desorbed at 680 °C with Zn/Al and Zn/Ti/Zr, while other adsorbents (Cu–O, Zn/Mn, Zn/Co, Zn/Cu/Zr) involved partial desorption of SO₂ and accompanied by sulfate formation around 400 °C and sulfur desorption was complete around 800 °C. Some adsorbents mentioned above could be used for H₂S adsorption in sewage plant facilities.

Experimental

Preparation of precursors

Hydrous oxides of Ag, Sn, Ni, Co, Mn, Cu, Zn and Ca were prepared by addition of a 0.1 M (1 M = mol l⁻¹) NaOH solution to a 0.1 M of appropriate metal chloride solution under vigorous stirring at room temperature, the equivalent ratio of OH⁻/Mⁿ⁺ being kept at ca. 1.2. Mixed hydrous oxides and hydroxalcalite-like samples of different metals were prepared by addition of a 1 M Na₂CO₃ solution and 20 ml of mixed solution of ZnCl₂ and metal chloride (Zn/Mⁿ⁺ = 3, Mⁿ⁺ = Mn, Ni, Co, Fe, Ti, Zr; total metal concentration = 1 M) simultaneously to a 200 ml deionized water under vigorous stirring, while maintaining the pH of solution at 8.

After the addition of solution, all the precipitates were aged at room temperature for 1 day. The precipitates were then separated by centrifugation, washed with deionized water till neutral and finally dried at 50 °C for 1 day.

Preparation of adsorbents

The dried precursors were crushed to ca. 200 mesh size and then were heat-treated at 300 °C for 3 h in air and then allowed to cool to room temperature. The adsorbent was designated as M–O (M is metal) for the simple metal oxide and a Zn/M (M is Mn, Ni, etc.) for the mixed oxides.

Adsorptive capacity of H₂S

Adsorbent (25 mg) was reacted with 20 L of nitrogen gas containing 10 ppm of H₂S gas in a 30 L of TEDLAR BAG®. After equilibration for 1 day, H₂S gas concentration was analyzed with H₂S detector tube (GASTEC Co. Ltd., Japan) using No. 4LT for 0.2–2.0 ppm level, 4LK for 2–20 ppm level and 4LL for 2–60 ppm level. H₂S gas can be detected by observing color change occurred in detector tube. The fresh H₂S

gas was introduced everyday until the H₂S adsorption saturation was occurred. Similarly, some selected adsorbents (100 mg) were reacted with 20 L of nitrogen gas containing 300 ppm of H₂S.

Physical analysis

X-ray diffraction analysis was carried out using a Rigaku type RINT 1200 X-ray diffractometer with a graphite monochromator. DTA-TG curves of adsorbents were measured on a MAC Science Thermal Analyzer (System 001, 200 TG-DTA) at a heating rate of 10 °C min⁻¹ in air. SEM and TEM observations were carried out on a Hitachi-type S-2460 N scanning electron microscope and JEOL-type JEM-3010 transmission electron microscope, respectively. Nitrogen gas adsorptions were carried out with a Quantachrome-type 1-C apparatus for samples degassed at 150 °C for 4 h.

Chemical analysis

Adsorbent (50 mg) was dissolved in a HCl, HNO₃ (for Ag–O), or a HCl + H₂O₂ (for Zn/Mn) solution. Metal concentrations of the solution were determined with a Shimadzu AA-760 atomic absorption spectrophotometer or a Seiko ICP Atomic Emission Plasma Spectrometer (SPS 7800).

References

- 1 D. Stirling, *The Sulfur Problem: Cleaning up Industrial Feedstocks*, RSC Clean Technology Monograph, The Royal Society of Chemistry, Cambridge, UK, 2000.
- 2 P. R. Westmoreland and D. P. Harrison, *Environ. Sci. Technol.*, 1976, **10**, 659.
- 3 M. Pineda, J. M. Palacios, L. Alonso, E. Garcia and R. Moliner, *Fuel*, 2000, **79**, 885.
- 4 L. Alonso, J. M. Palacios and R. Moliner, *Energy Fuels*, 2001, **15**, 1396.
- 5 M. A. Ahmed, L. Alonso, J. M. Palacios, C. Cilieruelo and J. C. Abanades, *Solid State Ionics*, 2000, **138**, 51.
- 6 S. Lew, K. Jothimurugesan and M. F. Stephanopoulos, *Ind. Eng. Chem. Res.*, 1989, **28**, 535.
- 7 M. C. Woods, S. K. Gangwal, K. Jothimurugesan and D. P. Harrison, *Ind. Eng. Chem. Res.*, 1990, **29**, 1160.
- 8 E. Sasaoka, N. Sada, A. Manabe, M. A. Uddin and Y. Sakata, *Ind. Eng. Chem. Res.*, 1998, **38**, 958.
- 9 L. Alonso and J. M. Palacios, *Chem. Mater.*, 2002, **14**, 225.
- 10 L. Alonso and J. M. Palacios, *Energy Fuels*, 2002, **16**, 1550.
- 11 H. Katoh, I. Kuniyoshi, M. Hirai and M. Shoda, *Appl. Catal. B: Environ.*, 1995, **6**, 255.
- 12 T. J. Bandoz, *Carbon*, 1999, **37**, 483.
- 13 T. J. Bandoz, A. Bagreev, F. Adib and A. Turk, *Environ. Sci. Technol.*, 2000, **34**, 1069.
- 14 A. Bagreev and T. J. Bandoz, *Carbon*, 2001, **39**, 2303.
- 15 T. Baird, P. J. Denny, R. Hoyle, F. McMonagle, D. Stirling and J. Tweedy, *J. Chem. Soc. Faraday Trans.*, 1992, **88**, 3375.
- 16 T. Baird, K. C. Campbell, P. J. Holliman, R. Hoyle, D. Stirling and B. P. Williams, *J. Chem. Soc. Faraday Trans.*, 1995, **91**, 3219.
- 17 T. Baird, K. C. Campbell, P. J. Holliman, R. W. Hoyle, M. Huxam, D. Stirling, B. P. Williams and M. Morris, *J. Mater. Chem.*, 1999, **9**, 599.
- 18 J. M. Davidson, C. H. Lawrie and K. Sohail, *Ind. Eng. Chem. Res.*, 1995, **34**, 2981.
- 19 J. M. Davidson and K. Sohail, *Ind. Eng. Chem. Res.*, 1995, **34**, 23675.
- 20 C. L. Carnes and K. J. Klubunde, *Chem. Mater.*, 2002, **14**, 1806.
- 21 F. Cavani, F. Trifiro and A. Vaccari, *Catal. Today*, 1991, **11**, 173.
- 22 Y. Li, H. Guo, C. Li and S. Zhang, *Ind. Eng. Chem. Res.*, 1997, **36**, 3982.
- 23 E. M. Bollin, in *Differential Thermal Analysis*, ed. R. C. Mackenzie, Academic Press, 2000, p. 197.



Oxidative polymerization to form poly(2,6-dimethyl-1,4-phenylene oxide) in water†

Kei Saito, Toru Masuyama and Hiroyuki Nishide*

Department of Applied Chemistry, Waseda University, Tokyo 169-8555, Japan.

E-mail: nishide@waseda.jp; Fax: (+813)-3209-5522

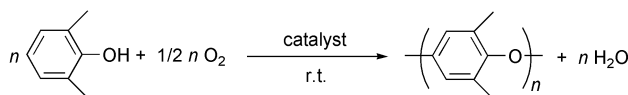
Received 19th March 2003

First published as an Advance Article on the web 10th June 2003

An engineering plastic, poly(2,6-dimethyl-1,4-phenylene oxide) (PPO), was prepared *via* oxidative polymerization in water. 4-(2',6'-Dimethylphenoxy)-2,6-dimethylphenol was stirred in an aqueous alkaline solution with a metal catalyst to yield PPO with a molecular weight of three to four thousand. The formation of diphenoquinone as the side-product was inhibited in this reaction. This reaction is slow but also proceeded under oxygen without a catalyst. The oxidative polymerization in water provides a new polymerization procedure for PPO.

Introduction

One of the critical factors in realizing a green chemical reaction process involves the choice of water as the reaction solvent.¹ Poly(2,6-dimethyl-1,4-phenylene oxide) (PPO) is widely used as a high-performance engineering plastic, since the polymer has excellent chemical and physical properties.² The oxidative polymerization of 2,6-dimethylphenol (DMP) to form PPO was established by A. S. Hay and the GE group,³ and provides a convenient method to manufacture multiple tons of PPO. The reaction proceeds with a small amount of catalyst at room temperature by eliminating an equimolar amount of water (Scheme 1). That is, this PPO formation is a typical atom



Scheme 1

economical reaction that does not require any leaving groups from the resulting polymer and one of the ideal polymerization processes that provides for green chemistry. However, in spite of its importance from the viewpoint of green chemistry, PPO preparation processes and mechanistic studies of DMP polymerization have so far been restricted to oxidative polymerization of DMP using an organic solvent such as toluene and benzene in the presence of a copper-amine catalyst under oxygen.^{4–6} Therefore, both a solvent recovery process and an explosion-proof reactor are needed for the facility in industrial PPO production. The use of water as the solvent for the oxidative polymerization to form PPO would be a challenging subject from the greening chemical approach.

There have been only a few studies which used water as the solvent for PPO preparation.^{7–11} The oxidative polymerization of 4-bromo-2,6-dimethylphenol in an aqueous–benzene mixture was reported to form PPO.^{7,9} The enzymatic polymerization of DMP and the biphasic coupling polymerization of DMP in an aqueous–organic solvent mixture were also examined.^{10,11} However, it should be noted that all of the previous studies involved reactions in aqueous–organic solvent biphasic mixtures and not the reaction that uses only water as the polymerization solvent. The unsolved problem of the oxidative polymerization of DMP in water is that 4-(3,5-dimethyl-4-oxo-

2,5-cyclohexadienyliene)-2,6-dimethyl-2,5-cyclohexadienone (diphenoquinone, DPQ) becomes the main product in the reaction (Scheme 2).⁷ DPQ is an undesired red colored product which tremendously reduces the properties of the PPO polymer, for example, upon further processing at high temperature. DPQ formation could not be avoided in previous studies using water as the solvent. The mechanism of the chain extension to form PPO also remains unsolved; the DPQ formation could be suppressed by the polymerization starting from oligo(2,6-dimethyl-1,4-phenylene oxide)s.¹²

The dimer of DMP, 4-(2',6'-dimethylphenoxy)-2,6-dimethylphenol (DPP), is the simplest oligomer, and was reported to have a lower oxidation potential and higher reactivity than those of DMP.^{4,6,13} The oxidation potential of phenol is known to decrease as the pH increases. It is expected that the reaction in alkaline water reduces the oxidation potential of phenol and facilitates PPO formation.^{14,15} In this study, we have succeeded in the oxidative polymerization of DPP to yield PPO by inhibiting the DPQ formation in water (Scheme 3).

Results and discussion

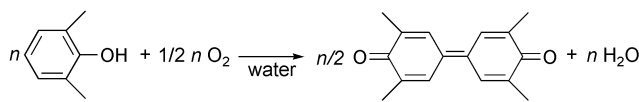
The oxidative polymerization of DPP was examined in an aqueous alkaline solution with a metal complex as the oxidative catalyst. Sodium hydroxide was used as the alkaline source, and the reaction was vigorously stirred at room temperature under oxygen. The polymerization results are summarized in Table 1. The polymerization catalyzed by the water soluble copper(II) complex with ethylenediamine-*N,N,N',N'*-tetraacetic acid (edta) yielded a polymer with the molecular weight $M_n = 2.2 \times 10^3$ ($M_w/M_n = 1.7$, determined by gel permeation chromatography with polystyrene standard) (entry 6). The amount of DPQ

Green Context

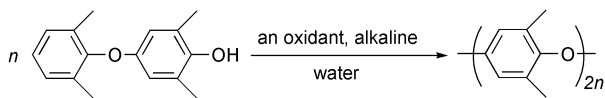
Poly(2,6-dimethyl-1,4-phenylene oxide), PPO, is an important high performance plastic. It can be manufactured by oxidative polymerization of 2,6-dimethylphenol. While the process is atom efficient it is normally carried out in a volatile organic compound as solvent and using a copper-amine catalyst. Here it is shown that PPO can be prepared in water and does not require a catalyst. Side products are minimised.

JHC

† Presented at the First International Conference on Green & Sustainable Chemistry, Tokyo, Japan, March 13–15, 2003.



Scheme 2



Scheme 3

Table 1 Oxidative polymerization of DPP in water^a

Entry	Catalyst	NaOH/ M	SDS ^b / M	Time/ h	PPO ^c (%)	M_n^d ($\times 10^3$)	M_w^e ($\times 10^3$)
1	Cu(edta)	0		3	0		
2	Cu(edta)	0.10		3	11	1.9	3.3
3	Cu(edta)	0.25		3	57	1.5	3.3
4	Cu(edta)	1.0		3	56	2.1	3.3
5	Cu(edta)	2.5		3	19	1.8	2.7
6	Cu(edta)	0.25		12	64	2.2	3.7
7	Cu(edta)	0.25	0.025	12	77	3.9	5.7
8	Mn(edta)	0.25		3	45	1.6	3.4
9	Cu(tmeda)	0.25		3	64	2.1	3.8
10	Cu(Nmiz)	0.25		3	63	1.6	3.6
11		0.25		12	19	1.7	2.1
12		0.25	0.025	12	47	2.2	3.3

^a Polymerization of DPP (0.25 M), catalyst (0.025 M) (except entry 11,12) in water at r.t. under O₂. ^b Sodium *n*-dodecyl sulfate. ^c Methanol-insoluble part. ^d Number-average molecular weight of the polymer, determined by GPC with polystyrene standard. ^e Weight-average molecular weight of the polymer, determined by GPC with polystyrene standard.

formed was carefully determined by UV-vis spectroscopy ($\lambda_{\text{max}} = 421 \text{ nm}$) of the product; the DPQ yield was 0.03% in this reaction. In comparison with the DPQ yield (3–5%) under conventional conditions (*e.g.*, catalyzed by a copper-pyridine complex in toluene at room temperature),¹² dramatic inhibition of the DPQ formation occurred even using water as the solvent.

The formed oligomer and polymer were insoluble in the aqueous alkaline solution and the reaction mixture was heterogeneous. The PPO polymer could be obtained as an off-white powder by a simple filtration after the polymerization. The polymer structure, *i.e.*, the repeating 2,6-dimethyl-1,4-oxyphenylene unit, was identified by ¹H-NMR, ¹³C-NMR, and IR spectroscopies.

The alkaline concentration of the water solvent influenced the yield and the molecular weight of the polymer in this reaction (entries 1–5) (Fig. 1). Both the yield and the molecular weight of the polymer increased with the alkaline concentration and reached their maximum values at a concentration of 0.75 M. The reductions after the maxima could be explained by the quenching or the hydrolysis of the copper complex. In addition, the reaction mixture turned gray at >5.0 M alkaline concentration.

The addition of a surfactant increased the molecular weight; the polymer ($M_n = 3.9 \times 10^3$, $M_w/M_n = 1.5$, determined by gel permeation chromatography with polystyrene standard) was formed using sodium *n*-dodecyl sulfate as the surfactant (entry 7). The polymer could also be obtained by a simple filtration after salting out. The molecular weight of the formed polymer would be improved by further studies on surfactant addition.

Manganese(II) (edta) and copper(II) complexes with *N,N,N',N'*-tetramethylethylenediamine (tmeda) and *N*-methylimidazole (Nmiz) were also effective for this reaction (entries 8–10). The oxidative polymerization of DPP in water seemed to proceed with most of the water-soluble metal complexes.

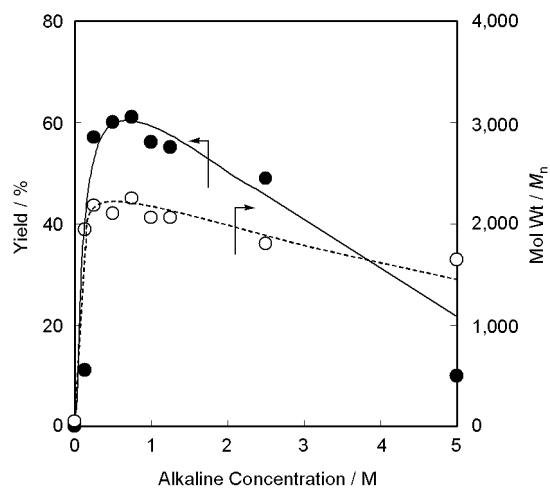


Fig. 1 Effect of the alkaline concentration of the water solvent on the polymer yield and molecular weight of the DPP polymerization. DPP: 0.25 M, Cu(edta): 0.025 M. (●) yield of the polymer, (○) molecular weight of the polymer.

Furthermore, it should be noted that the oxidative polymerization of DPP slowly proceeded under oxygen without any catalyst (entry 11). The molecular weight of the polymer increased by adding a surfactant (entry 12). These results could be explained by a significant decrease in the oxidation potential of the phenol group in an alkaline solution.^{14,15} The pH of this reaction mixture was greater than 13. A cyclic voltammogram of DPP in the alkaline water showed an irreversible oxidation

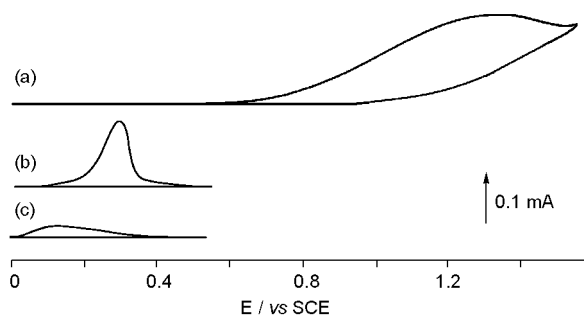


Fig. 2 Cyclic voltammograms (a) DMP in CH₂Cl₂ with pyridine (3.0 M), (b) DMP in water with sodium hydroxide (0.5 M), (c) DPP in water with sodium hydroxide (0.5 M). Phenol conc.: 0.01 M, scan rate: 25 mV s⁻¹.

peak (Fig. 2): the oxidation peak potential (*vs.* SCE) was estimated to be at 0.12 V which was much lower than that of DMP in an organic solvent such as CH₂Cl₂ with pyridine as an alkaline medium (1.31 V). In the oxidative polymerization of DPP, the reaction step of DPP from DMP is additionally required. However, the formed DPP displayed a lower oxidation potential and higher reactivity than those of DMP in the alkaline water. Because of this reduced oxidation potential, DPP could be oxidized and polymerized by the oxygen without any catalyst, which provides a new polymerization procedure for PPO from the viewpoint of a green chemical process.

The alkaline water solution could be repeatedly reused through simple filtration after the polymerization. Although one must be cautious in handling the alkaline water, the simple solvent recovery process would reduce the disadvantage of using an alkaline water.

Conclusion

We found that in alkaline water the oxidative polymerization of DPP formed PPO almost without DPQ side product formation.

This polymerization is slow but also proceeded under oxygen without any catalyst. From the viewpoint of a green chemical process, the oxidative polymerization of DPP in water provides a new polymerization procedure for PPO.

Experimental

4-(2',6'-dimethylphenoxy)-2,6-dimethylphenol (DPP)

The starting material, 4-bromo-2,6-dimethylanisole, was prepared from 2,6-dimethylphenol (DMP) according to the method described by Bruice *et al.*¹⁶ The Ullmann reaction of 4-bromo-2,6-dimethylanisole with DMP was carried out as follows. 4-Bromo-2,6-dimethylanisole (107 g, 0.5 mol) and DMP (61 g, 0.5 mol) were heated at 150 °C, in the presence of copper powder (5.0 g), cupric acetate (5.0 g), and potassium *tert*-butoxide (56 g, 0.5 mol). When the calculated amount of *tert*-butanol was removed, the reaction mixture was heated to 200 °C for 12 h. The crude product was recrystallized from hexane, yielding 51% of 4-(2',6'-dimethylphenoxy)-2,6-dimethylanisole. 4-(2',6'-Dimethylphenoxy)-2,6-dimethylanisole (25 g, 0.1 mol) was treated with hydroiodic acid (60 ml) in refluxing glacial acetic acid (120 ml) for 12 h. Recrystallization from hexane gave DPP in 97% yield. ¹H-NMR: (500 MHz, CDCl₃, TMS) δ 7.08 (2H, d, aromatic C–H), 7.03 (H, t, aromatic C–H), 6.37 (2H, s, aromatic C–H), 4.23 (H, s, –OH), 2.17 (s, 6H, –CH₃), 2.12 (s, 6H, –CH₃), ¹³C-NMR: (125 MHz, CDCl₃, TMS) δ 151.2, 146.4, 146.2, 131.6, 128.9, 124.7, 124.3, 114.2, 16.4, 16.2, IR (KBr): ν_{C–O–C} = 1195 cm^{–1}.

Oxidative polymerization of DPP in water

The following is a typical procedure for the polymerization (entry 7 in Table 1). DPP (1.21 g, 5 mmol), sodium hydroxide (0.20 g, 5 mmol), and sodium *n*-dodecyl sulfate (0.21 g, 0.5 mmol) were dissolved in water (10 ml). Sodium ethylenediamine-*N,N,N',N'*-tetraacetatocuprate(II) (0.042 g, 0.5 mmol) in water (10 ml) was added to the mixture and the reaction mixture was vigorously stirred under oxygen at room temperature for 12 h (stirring speed 3000 rpm). In this reaction, the formed oligomer and polymer precipitated out from the mixture and the reaction mixture became heterogeneous. The polymer was obtained as an off-white powder by filtration after salting out by sodium chloride. (yield: 77%) ¹H-NMR: (500 MHz, CDCl₃, TMS) δ 6.44 (2H, s, aromatic C–H), 6.36 (m, aromatic C–H head end group), 7.09 (m, aromatic tail end group), 4.22 (m, –OH), 2.09 (s, 6H, –CH₃), ¹³C-NMR: (125 MHz, CDCl₃, TMS) δ 154.7, 145.4, 132.5, 114.5, 16.8, IR (KBr): ν_{C–O–C} = 1186 cm^{–1}.

UV-vis spectral detection of DPQ

12 mg of the obtained polymer were dissolved in toluene (10 ml). The absorption maximum of DPQ was observed at 421 nm. The molar extinction coefficient ε was determined to be 54000 M^{–1} cm^{–1} in toluene using pure DPQ. The amount of DPQ formed is given as a percentage of the initial amount of DMP.

Electrochemical measurements

Cyclic voltammetry was carried out in a conventional two-compartment cell. The reference electrode was a commercial SCE electrode. The formal potential of the ferrocyanide/ferricyanide couple in water was 0.24 V vs. this reference electrode. The voltammetric investigation was carried out in

water in the presence of 0.01 M of a sample, 0.5 M of sodium hydroxide, and all potentials were quoted with respect to this SCE reference electrode at a scan rate of 25 mV s^{–1}. The voltammetric investigation of DMP (0.01 M) was also carried out in CH₂Cl₂ with 3.0 M of pyridine and 0.1 M of tetrabutylammonium tetrafluoroborate using a Ag/AgCl electrode of which potential was normalized with the SCE standard. A Nikko Keisoku DPGS-1 dual potentiogalvanostat and a Nikko Keisoku NFG-3 universal programmer were employed with a Graphtec WX2400 X–Y recorder to obtain the voltammograms.

Other measurements

¹H and ¹³C NMR spectra were recorded on a Jeol JNM-LA500 spectrometer with chemical shifts downfield from tetramethylsilane as the internal standard. All spectra were obtained in CDCl₃ at room temperature. Molecular weights of PPO were determined by gel permeation chromatography (GPC) with a Tosoh high sensitive GPC system HLC-8220GPC equipped with UV-8220, in which the calibration curves were obtained using polystyrene standards.

Acknowledgements

We thank Dr. Kenichi Oyaizu for productive discussions. This work was partially supported by Grants-in-Aid for Scientific Research (No. 13450384) and for COE Research "Practical Nano-Chemistry" from MEXT, Japan.

References

- (a) C.-J. Li and T.-H. Chan, *Organic Reactions in Aqueous Media*, John Wiley & Sons, New York, 1997; (b) J. M. Desimone, *Science*, 2002, **297**, 799–803.
- (a) D. Aycok, V. Abolins and D. M. White, *Encyclopedia of Polymer Science and Engineering*, John Wiley & Sons, New York, 2nd edn., 1986, vol. **13**, 1–30; (b) F. E. Karasz, H. E. Bair and J. M. O'Reilly, *J. Polym. Sci., Polym. Phys. Ed.*, 1968, **6**, 1141–1148.
- (a) A. S. Hay, H. S. Blanchard, G. F. Endres and J. W. Eustance, *J. Am. Chem. Soc.*, 1959, **81**, 6335–6336; (b) A. S. Hay, *Adv. Polym. Sci.*, 1967, **4**, 496–527; (c) A. S. Hay, *J. Polym. Sci., Part A: Polym. Chem.*, 1998, **36**, 505–517.
- (a) E. Tsuchida, M. Kaneko and H. Nishide, *Makromol. Chem.*, 1972, **151**, 221–234; (b) E. Tsuchida and H. Nishide, *Makromol. Chem.*, 1975, **176**, 1349–1358; (c) E. Tsuchida and H. Nishide, *Adv. Polym. Sci.*, 1977, **24**, 1–87; (d) K. Oyaizu, Y. Kumaki, K. Saito and E. Tsuchida, *Macromolecules*, 2000, **33**, 5766–5769.
- (a) G. D. Copper, H. S. Blanchard, G. F. Ender and H. L. Finkbeiner, *J. Am. Chem. Soc.*, 1965, **87**, 3996–3997; (b) D. A. Bolon, *J. Org. Chem.*, 1967, **32**, 1584–1590; (c) W. Koch, W. Risse and W. Heitz, *Makromol. Chem., Suppl.*, 1985, **12**, 105–123; (d) P. J. Baesjou, W. L. Driessen, G. Challa and J. Reedijk, *J. Am. Chem. Soc.*, 1997, **119**, 12590–12594.
- H. Higashimura, K. Fujisawa, Y. Moro-oka, M. Kubota, A. Shiga, A. Terahara, H. Uyama and S. Kobayashi, *J. Am. Chem. Soc.*, 1998, **120**, 8529–8530.
- (a) G. D. Staffin and C. C. Price, *J. Am. Chem. Soc.*, 1960, **82**, 3632–3634; (b) C. C. Price and N. S. Chu, *J. Polym. Sci.*, 1962, **61**, 135–141.
- H. Komoto and K. Ohmura, *Makromol. Chem.*, 1973, **166**, 57–68.
- (a) V. Percec and T. D. Shaffer, *J. Polym. Sci., Polym. Lett. Ed.*, 1986, **24**, 439–446; (b) K. Mühlbach and V. Percec, *J. Polym. Sci., Polym. Chem. Ed.*, 1987, **25**, 2605–2627.
- (a) R. Ikeda, J. Sugihara, H. Uyama and S. Kobayashi, *Macromolecules*, 1996, **29**, 8702–8705; (b) H. Yonami, H. Uyama and S. Kobayashi, *J. Macromol. Sci., Pure Appl. Chem.*, 1999, **A36**, 719–730.

- 11 Y. M. Chung, W. S. Ahn and P. K. Lim, *J. Mol. Catal. A: Chem.*, 1999, **148**, 117–126.
- 12 (a) F. J. Viersen and G. Challa, *Recl. Trav. Chim. Pays-Bas*, 1990, **109**, 97–102; (b) F. J. Viersen, J. Renkema, G. Challa and J. Reedijk, *J. Polym. Sci. A*, 1992, **30**, 901–911.
- 13 (a) G. F. Endres and J. Kwiatekm, *J. Polym. Sci.*, 1962, **58**, 593–609; (b) W. Risse, W. Heitz, D. Freitag and L. Botterbruch, *Makromol. Chem.*, 1985, **186**, 1835–1853; (c) D. P. Mobley, *J. Polym. Sci., Polym. Chem. Ed.*, 1984, **22**, 3203–3215.
- 14 C. G. Haynes, A. H. Turner and W. A. Waters, *J. Chem. Soc.*, 1956, 2823–2831.
- 15 W. A. Waters, *J. Chem. Soc.*, 1971, 2026–2029.
- 16 T. C. Bruice, N. Kharasch and R. J. Winzler, *J. Org. Chem.*, 1953, **18**, 83–91.



Conversions of some small organic compounds with metal oxides in supercritical water at 673 K†

Masaru Watanabe, Toru Iida, Yuichi Aizawa, Haruo Ura, Hiroshi Inomata* and Kunio Arai

Research Center of Supercritical Fluid Technology, Tohoku University, 07, Aoba, Aramaki, Aoba-ku, Sendai, 980-8579, Japan. E-mail: inomata@scf.che.tohoku.ac.jp; Fax: +81-22-217-7283; Tel: +81-22-217-7283

Received 29th April 2003

First published as an Advance Article on the web 4th July 2003

Reactions of formaldehyde (HCHO), acetic acid (CH₃COOH), 2-propanol (2-PrOH), and glucose with some metal oxides (CeO₂, MoO₃, TiO₂, and ZrO₂) were conducted in supercritical water at 673 K and 25–35 MPa, using batch reactors. For the reactions of HCHO, CeO₂ and ZrO₂ showed basicity, on the other hand, MoO₃ and TiO₂ were acid catalysts. ZrO₂ catalyst promoted bimolecular decarboxylation of CH₃COOH to form acetone, which indicates that both acid and base sites exist on the surface of ZrO₂ in supercritical water. Dehydration of 2-PrOH with formation of propylene was promoted by acid catalyst (H₂SO₄), while its dehydrogenation with formation of acetone was catalyzed by alkali (NaOH). All the metal oxides that were used in this study promoted dehydration of 2-PrOH; namely there are mainly acidic sites for 2-PrOH reactions on the surface of all the metal oxides under the conditions used. Among the metal oxides, ZrO₂ and TiO₂ (rutile) enhanced the formation of acetone in the case of 2-PrOH reaction. This means there are also basic sites for 2-PrOH on the ZrO₂ and TiO₂ (rutile). In supercritical water at 673 K and 15 min, H₂ yield from glucose in the acidic atmosphere (namely in the presence of H₂SO₄) is lower than that in the absence of additive whereas, on the other hand, the H₂ yield in the presence of NaOH is twice as much as that in the absence of the additive. With CeO₂ and ZrO₂, the H₂ yield from glucose was almost twice as high as that without catalyst. By adding MoO₃ and TiO₂, the amount of H₂ formation was suppressed. Through this study, we can show the generality of acidity and basicity of the metal oxides for organic reactions in SCW.

Introduction

Recently, supercritical water (SCW) has been recognized as a green chemical environment for some organic reactions because they can proceed without any catalyst.^{1–18} That is, in SCW, Friedel–Crafts alkylation,^{1–3} hydrolysis (ethers^{4–11} and esters^{12,13}), and dehydration^{14–18}), which require strong acid and base in ambient atmosphere, occur even in the absence of catalyst. However, some reactions, such as dehydration of small alcohols^{15–18} and decarboxylation of acetic acid,¹⁹ require addition of H₂SO₄ (acid) or NaOH (base) to increase the reaction rate even in SCW. Furthermore, even for a reaction that occurs without catalyst, increase and/or control of the reaction rate can be achieved with an acid and a base catalyst.¹¹ If one wanted to enhance and control an acidic and basic reaction in SCW, a catalyst must be added because the amounts of H⁺ and OH[–] in pure water are the same for all temperatures and pressures without additive. Although homogeneous acids (such as H₂SO₄) and bases (such as NaOH) would normally be used for controlling the pH of water, the acid and base have a negative impact for the inner wall of a reactor and the global environment.

One of the possibilities for environmental-friendly pH control is to use a solid acid and base catalyst in SCW. Up to date, there have been several reports that solid acid and base catalysts work in SCW.^{19–22} HCHO reaction can be controlled by CeO₂, MoO₃, TiO₂, and ZrO₂.²² Among the metal oxides, CeO₂ and ZrO₂ were basic whereas MoO₃ and TiO₂ were acidic catalysts for the HCHO reaction. ZrO₂ also works as a solid base for

acetic acid¹⁹ and biomass gasification.²⁰ MoO₃ is an acid catalyst for hydration of propylene.²¹ These results suggest that a metal oxide is an acid or a base catalyst for organic reactions in SCW, instead of a homogeneous acid or alkali.^{19–22}

For utilization of metal oxide instead of a homogeneous acid and base catalyst, the acidity and basicity of a metal oxide in SCW must be evaluated for a variety of organic reactions. For the evaluation, an activity test through a reaction is useful, for example, the contribution of dehydration and dehydrogenation of 2-propanol can be indicator of the acidity and basicity of a metal oxide.²³ In a previous study,²² we proposed an evaluation method of the acidity and basicity of a metal oxide in SCW using HCHO reaction as a probe reaction. If the acidity and basicity of a solid functioned in the same way as H⁺ and OH[–] in SCW, organic reactions could be controlled by solid acid and base catalyst. A common scale of the acidity and basicity of metal oxides for organic reactions in SCW is required for application of metal oxides widely as an acid–base catalyst.

Green Context

The combination of supercritical fluids and heterogeneous catalysts has proved to be a fruitful area of research (see *e.g.* *Green Chem.*, 2003, 5, 99 and *Green Chem.*, 2002, 4 507). This article gives information on the activity of a series of heterogeneous catalysts in supercritical water, and relates activity in a series of test reactions to the acidity and basicity of the catalysts, producing a useful guide to the properties of these materials in a novel solvent system. *DJM*

† Presented at The First International Conference on Green & Sustainable Chemistry, Tokyo, Japan, March 13–15, 2003.

In this study, we reviewed our previous studies (HCHO,²² CH₃COOH,¹⁹ and glucose²⁰ reactions with and without catalyst using batch reactors) briefly. Further, we conducted 2-propanol reactions with the same metal oxides as the previous studies (CeO₂, MoO₃, TiO₂, and ZrO₂) and compared them with the experimental results obtained by adding homogeneous catalysts (H₂SO₄ (acid) and NaOH (base)). Also, we added the experimental data of glucose reactions with the homogenous catalysts and the metal oxides. Through the comparison of these studies, we would like to discuss the acidity and basicity of catalysts in organic reactions in SCW.

Experimental

Paraformaldehyde (as a source of HCHO), acetic acid (CH₃COOH), 2-propanol (2-PrOH), sodium hydroxide (NaOH), potassium hydroxide (KOH) and sulfuric acid (H₂SO₄) were purchased from Wako pure chemical and used without further purification. Glucose was obtained from Aldrich. Pure water was obtained with a water distillation apparatus (Yamato Co., model WG-220). Ceria (CeO₂) was obtained from Merck. Titania (TiO₂) (both anatase form and rutile form) and MoO₃ were purchased from the Wako Chemicals. CeO₂, MoO₃, and TiO₂ (anatase and rutile) were used as received. Zirconia (ZrO₂) catalyst was prepared by calcination of zirconium hydroxide (ZrO₂·xH₂O, which was purchased from Nakarai Tesque Inc.) at 673 K for 3 h. The metal oxide catalysts that were used in the study are listed in Table 1 with information on structure and BET surface area.

Table 1 Metal catalysts used in the study

	BET surface area/m ² g ⁻¹	Structure before HCHO reaction	Structure after the reaction
CeO ₂	1.7	cubic	cubic
MoO ₃	4.9	orthorhombic	orthorhombic
TiO ₂ (a)	47	anatase	anatase
TiO ₂ (r)	6.8	rutile	rutile
ZrO ₂	68	monoclinic and tetragonal mixture	monoclinic

Except for ZrO₂, the structures of the metal oxides were not changed before and after the reaction. For ZrO₂, the monoclinic and tetragonal mixture of ZrO₂ before the reaction was changed into pure monoclinic zirconia after the reaction in all the cases.

The reactions were carried out using a SS 316 stainless steel tube bomb reactor (inner volume of 6 cm³). The loaded amounts of sample were 0.1–0.3 g and the loaded amounts of water were from 1.0 g (0.17 g cm⁻³) to 2.1 g (0.35 g cm⁻³). In the case of using homogeneous acid and alkali, the acid or alkali aqueous solution was introduced to the reactor instead of pure water. In the case of the experiments with solid catalysts (CeO₂, MoO₃, TiO₂, and ZrO₂), 0.3 g of the catalyst was loaded. After loading samples, the air in the reactor was purged with Ar gas and the reactor filled with it pressurized to 1 MPa. The reactor was submerged in a fluidized sand bath (Takabayashi Rico Co., model TK-3) whose temperature was controlled to keep the reaction temperature (673 K). After a given reaction time (15 and 60 min), the reactor was taken out of the bath and rapidly quenched in a water bath. After the reactor reached room temperature, it was connected to a syringe that was equipped with gas samplers to collect the produced gas and measure its volume. After the sampling of the produced gases, the reactor was opened and washed with pure water. Water insoluble material (including the solid catalyst or char) was separated by filtration with a 1 μm membrane filter.

The identification and quantification of produced gas was conducted by GC-TCD (Shimadzu, model GC-7A, and Hitachi, model GC163). An external standard (1-propanol) was added to the recovered water solution for GC-FID analysis (Hewlett Packard, model 6890). Some samples were analyzed using HPLC with RI and UV detectors (JASCO, model Gulliver series). The amount of organic and inorganic carbon in the water solution was evaluated using TOC (total organic carbon detector, Shimadzu, model TOC-5000A). The surface areas of the metal oxides were measured by the single point BET method (Quantachrome Instruments, model ChemBET-3000), and are listed in Table 1. The structures of the solid catalysts before and after the reaction were analyzed by X-ray diffractometer (Mac Science, model M18XHF-SRA) with Mo Kα radiation (the results are also listed in Table 1).

The product yield (mol%) of carbon compound was evaluated from the carbon base as shown below:

$$\text{Product yield [mol\%]} = \frac{\text{Amount of carbon atoms in the product}}{\text{Amount of carbon atoms in the loaded starting material}} \times 100 \quad (1)$$

Hydrogen yield (H₂ yield, mol%) was evaluated from the hydrogen base of a loaded amount of sample as follows:

$$\text{H}_2 \text{ yield [mol\%]} = \frac{\text{Amount of hydrogen atoms in the produced H}_2}{\text{Amount of hydrogen atoms in the loaded starting material}} \times 100 \quad (2)$$

Results and discussion

1 HCHO²²

Firstly, we explained the OH⁻ dependence of the HCHO reaction in SCW at 673 K (the details can be seen elsewhere^{22,24}). The yield of CH₃OH increased with increasing OH⁻ gradually whereas, on the other hand, the yield of CO increased with a decrease of OH⁻ concentration. Based on the above experimental results, we developed a simple network model for HCHO reaction in supercritical water.²² According to this network model,²² the Cannizzaro reaction is predominant at high OH⁻ concentration conditions (basic conditions) whereas, on the other hand, HCHO decomposition into CO and H₂ is dominant at low OH⁻ concentrations (acidic conditions) (see Fig. 1). Thus, the ratio of CH₃OH/CO must be related to OH⁻

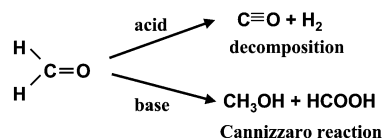


Fig. 1 Primary reaction pathways of HCHO in SCW at 673 K.

concentration. Using the network model, we correlated the CH₃OH/CO ratio at 15 min reaction time with OH⁻ concentration and obtained the following equation:²²

$$\text{CH}_3\text{OH}/\text{CO} = 63 \exp(0.26\log[\text{OH}^-]) \quad (3)$$

In the absence of a solid catalyst at 673 K and 30 MPa (0.35 g cm⁻³ water density), the CH₃OH/CO ratio is calculated to be 7.8 using the correlation shown in eqn. 3.²² In the presence of CeO₂ and ZrO₂, the CH₃OH/CO ratios were higher than 7.8 (16 for CeO₂ and 8 for ZrO₂). On the other hand, the CH₃OH/CO ratios were lower than 7.8 with MoO₃ (3.7) and TiO₂ (both anatase (1.7) and rutile (2.8)). Thus, CeO₂ and ZrO₂ are possibly basic and MoO₃ and TiO₂ (both anatase and rutile) are acidic catalysts for HCHO reaction in SCW at 673 K.

Fig. 2 shows the plot of the product yields against the OH⁻ concentration (calculated using eqn. 3) on the metal oxides. The

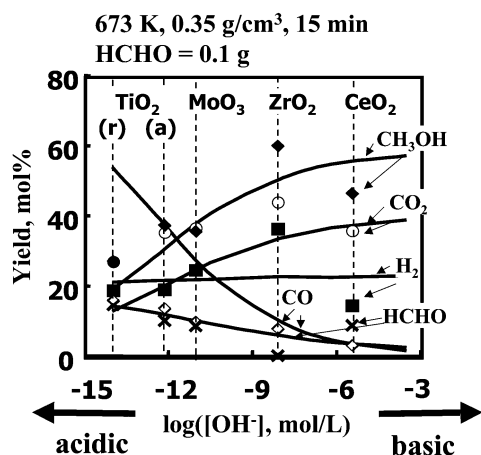


Fig. 2 Effect of metal oxides on the product distribution of HCHO reaction (673 K, 0.35 g cm⁻³ water density, 15 min reaction time, HCHO = 0.1 g).

X-axis is the calculated OH⁻ concentration (called the “effective OH⁻” on the metal oxides), which is defined as that participating in the reaction, determined from the product distribution. That is, the CH₃OH yields with CeO₂ and ZrO₂ were larger than 40% (see Fig. 2) whereas, on the other hand, the CO yields with these catalysts were less than 10%. Using TiO₂ (anatase and rutile) and MoO₃, the CO yield is more than 10% and CH₃OH is less than 40% as shown in Fig. 2. According to the definition of the “effective OH⁻”, the substance that can lead the product distribution to high CH₃OH yield and/or low CO yield must be a base for HCHO reaction in supercritical water at 673 K. On the contrary, an acid enhances CO formation and inhibits CH₃OH formation. Therefore, for the HCHO reaction under these conditions, CeO₂ and ZrO₂ are basic and TiO₂ (both anatase and rutile) and MoO₃ show acidity.

For evaluation of the effect of the acidity and basicity of the metal oxides on the HCHO reaction, we tried to express the experimental results using the simple network model. In order to compare the experimental results and the model, the “effective OH⁻” on the metal oxides must be known. Thus, using the experimental ratio of CH₃OH/CO obtained with the metal oxides, the “effective OH⁻” on the metal oxides for the HCHO reaction was evaluated using the correlation shown in eqn. 3. The results for the “effective OH⁻” values (unit is mol L⁻¹) are 10⁻⁵ for CeO₂, 10⁻⁸ for ZrO₂, 10⁻¹¹ for MoO₃, 10⁻¹² for TiO₂(r), and 10⁻¹⁴ for TiO₂(a). In Fig. 2, the calculated results obtained with the simple network model²² are also shown (solid lines). The trends of the increase of CH₃OH yield and the decrease of CO yield with increasing the “effective OH⁻” concentration are the same between the experimental results and the model.²²

2 CH₃COOH¹⁹

The CH₃COOH reactions with and without additives (KOH and ZrO₂) are shown in Fig. 3.¹⁹ For this case, we examined only the basicity of ZrO₂ for the reaction because CH₃COOH is an organic acid and CH₃COOH is possibly stable under acidic conditions. As shown in the figure, CH₃COOH was very stable after 60 min of reaction time in the absence of the additives. The same experiment was conducted using KOH aqueous solution instead of pure water; CH₄, CO₂, and acetone were obtained from acetic acid. Thus both monomolecular and bimolecular decarboxylations competitively proceeded in the KOH–SCW system. In the presence of ZrO₂, since the ratio of acetone and

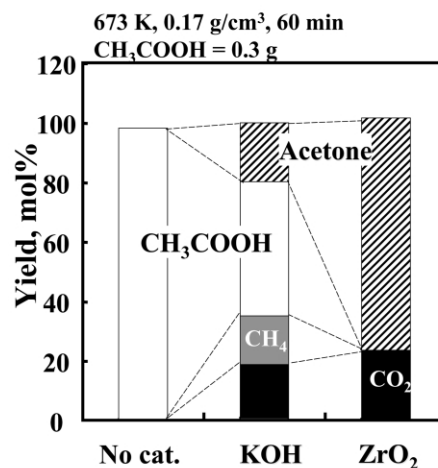


Fig. 3 Carbon compound distribution of CH₃COOH reaction with and without additives (673 K, 0.17 g cm⁻³ water density, 60 min reaction time, CH₃COOH = 0.3 g).

CO₂ was always about three, CH₃COOH was also selectively converted into acetone and CO₂. The primary reaction pathways of CH₃COOH in the presence of KOH and ZrO₂ are shown in Fig. 4. As reported by Tomishige *et al.*,²⁵ there are both acid and

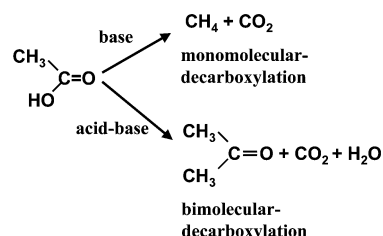


Fig. 4 Primary reaction pathways of CH₃COOH with additive in SCW at 673 K.

base sites on the surface of ZrO₂ and the amounts of acid and base sites are almost the same. The high selectivity of acetone formation from CH₃COOH is probably due to the acidity–basicity of ZrO₂. At the moment, ZrO₂ is assumed to be both an acid and a base functional catalyst, even in SCW.

3 2-propanol

The qualified and quantified products of 2-propanol (2-PrOH) reactions in SCW at 673 K, 0.35 g cm⁻³ water density, and 15 min reaction time are H₂, propylene, and acetone. Fig. 5 shows the effect of the additives on the product distribution (carbon compound). Under these conditions, 2-PrOH is stable at 15 min reaction time. As shown in this figure, acetone formation was enhanced by adding NaOH (0.01 mol L⁻¹), on the other hand, propylene formation was enhanced by adding H₂SO₄ (0.01 mol L⁻¹). Fig. 6 shows the yields of H₂ and acetone. In the presence of NaOH, the yields of H₂ and acetone were almost the same, and thus, dehydrogenation of 2-PrOH occurred under basic conditions in SCW at 673 K and 0.35 g cm⁻³ water density. In contrast, propylene formation was significantly enhanced by H₂SO₄. Although we cannot analyze the amount of water that formed through the reaction due to the reaction in water, the dehydration of 2-PrOH was promoted by acid, as reported by Antal *et al.*²⁶ Fig. 7 shows the primary reaction pathway of 2-PrOH under acidic and basic conditions in SCW at 673 K and 0.35 g cm⁻³ water density.

As shown in Fig. 5, all the metal oxides catalyzed the formation of propylene. Thus, the metal oxides have acidic sites for 2-PrOH reactions in SCW at 673 K and 0.35 g cm⁻³ water density. Haffad *et al.*²³ reported that CeO₂, ZrO₂, and TiO₂

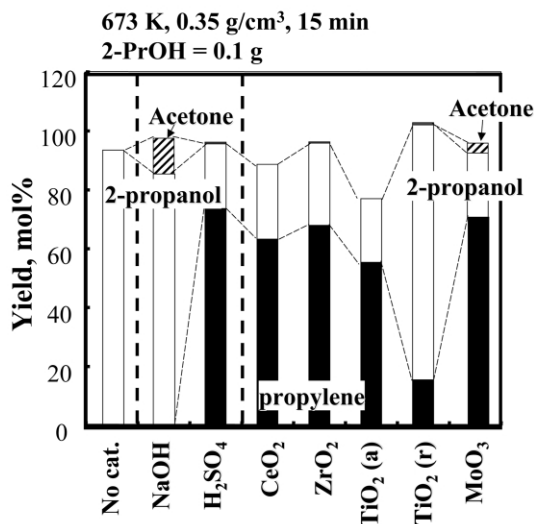


Fig. 5 Carbon compound distribution of 2-propanol reaction with and without additives (673 K, 0.35 g cm⁻³ water density, 15 min reaction time, 2-PrOH = 0.1 g).

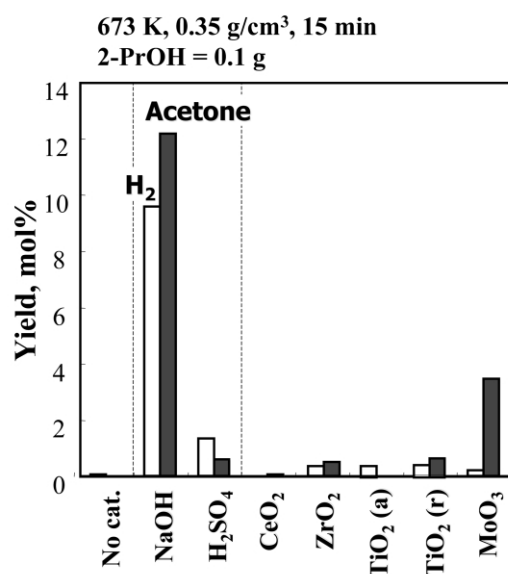


Fig. 6 Yields of H₂ and acetone from 2-propanol reaction with and without additives (673 K, 0.35 g cm⁻³ water density, 15 min reaction time, 2-PrOH = 0.1 g).

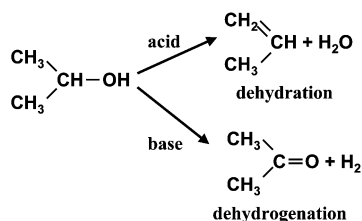


Fig. 7 Primary reaction pathways of 2-propanol with additive in SCW at 673 K.

(anatase) have both acidic and basic sites on their surface for 2-PrOH in atmospheric He conditions. The order of acidic character of the metal oxides is: TiO₂ > ZrO₂ > CeO₂ whereas the order of basicity of the metal oxides is reverse the order of acidity at 433–523 K.²³ Further, according to Haffad *et al.*,²³ the basicity of CeO₂ decreased with increasing reaction tem-

perature, while its acidity increased. For example, the yields of acetone and propylene were both 40 mol% at 523 K in He; however, those of acetone and propylene were about 10 and 70 mol% at 623 K, respectively. Our reactions were carried out at 673 K and in SCW and all the metal oxides that were used in this study show an acidity the same as the results by Haffad *et al.*²³

In the presence of ZrO₂ and TiO₂ (rutile), the formation of acetone and H₂ was enhanced, even at quite low yield. As shown in Fig. 7, the equimolar H₂ and acetone must form *via* dehydrogenation of 2-PrOH. Thus, on ZrO₂ and TiO₂ (rutile), there are basic sites for 2-PrOH reactions. Although the acetone yield with MoO₃ is the highest among that with the other metal oxides, the H₂ yield with MoO₃ is significantly lower than the acetone yield. The loss of H₂ is probably due to consumption of H₂ to form propane from propylene or acetone formation from 2-PrOH oxidation by MoO₃. This probability (redox property of MoO₃ in SCW) will be studied in future.

4 Glucose

In this study, the products, which were quantified, were H₂, CO, CO₂, C₁–C₄ hydrocarbons, and TOC (total organic carbon in the recovered water). The yields of short hydrocarbons were negligibly small for all the experimental conditions. The lack of mass balance (for example = 100 – (TOC + gaseous carbon (CO, CO₂, and hydrocarbons))) was possibly due to the water insoluble products which were not measured.

Fig. 8 and 9 show the gas and liquid carbon compounds distribution (C distribution: CO, CO₂, and TOC) and the yield

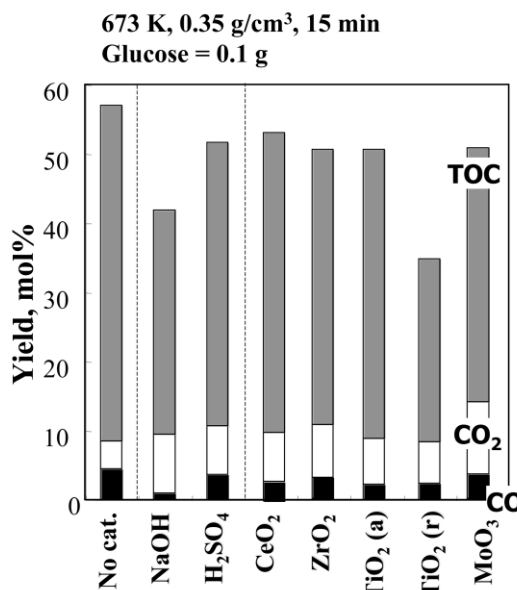


Fig. 8 Carbon compound distribution of glucose reaction with and without additives (673 K, 0.35 g cm⁻³ water density, 15 min reaction time, glucose = 0.1 g).

of H₂ from glucose decomposition at 673 K at 15 minutes with and without catalyst, respectively. Without catalyst, the yield of CO plus CO₂ was only 10% and that of H₂ was about 2%. In the presence of homogeneous acid (0.01 mol L⁻¹ of H₂SO₄) and base (0.01 mol L⁻¹ of NaOH), gasification efficiency (the yields of CO plus CO₂) was almost the same as that without catalyst, as shown in Fig. 8. On the other hand, the H₂ yield (Fig. 9) was affected by the homogeneous catalysts. The H₂ yield was enhanced in the presence of NaOH, while it was inhibited by H₂SO₄. As reported by some researchers, the mechanism of

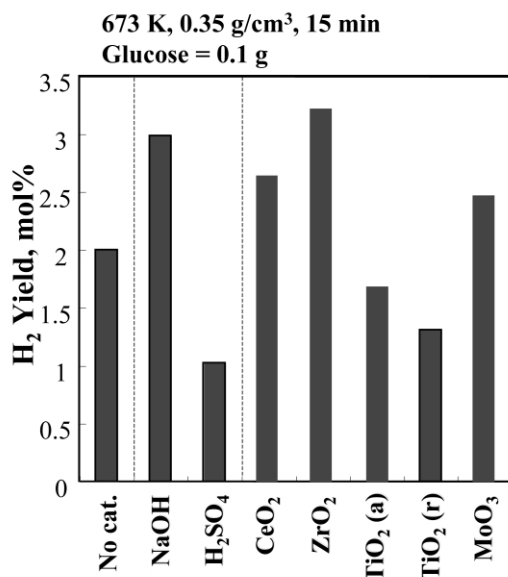


Fig. 9 H₂ yield from glucose reaction with and without additives (673 K, 0.35 g cm⁻³ water density, 15 min reaction time, glucose = 0.1 g).

glucose decomposition in SCW is quite complex including many reaction intermediates (aldehydes, alcohols, acids, furans, and so on).^{27,28} Now, we have studied the effect of reaction conditions and additives on glucose reactions, and in the near future, we will report the glucose reactions under various conditions in more detail. At the moment, through the reaction behavior observed by adding acid and alkali as described above, we briefly elucidated the acidity and basicity of the catalyst for glucose reaction from the H₂ yield under these conditions (Fig. 10).

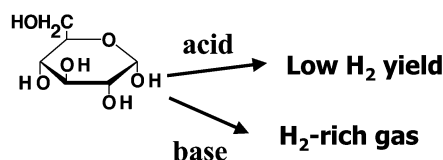


Fig. 10 Evaluation of acidity and basicity of catalyst from glucose reaction in SCW at 673 K.

The order of the gasification efficiency (= CO + CO₂) of glucose with the metal oxides was as follows: MoO₃ > ZrO₂ > CeO₂ > TiO₂ (a) > TiO₂ (r) (Fig. 8). As shown in Fig. 9, the order of H₂ yields with metal oxides was ZrO₂ > CeO₂ > MoO₃ > TiO₂ (a) > TiO₂ (r). Therefore, except for MoO₃, the orders of the gasification efficiency and H₂ yield were the same. In the presence of ZrO₂ and CeO₂, the H₂ yields were higher than that without catalyst. In contrast, the H₂ yields with TiO₂ (a) and (r) were lower than that without catalyst. For H₂ formation from glucose, there are basic sites on ZrO₂ and CeO₂ and basic sites on TiO₂ (a) and (r). In the case of MoO₃, the gasification efficiency (in particular, CO₂ yield) was the highest among all the results of the glucose reaction in this study; however, H₂ yield was not so high. This means that some portion of CO₂ from glucose was produced by oxidation. As well as the effect of MoO₃ on the 2-PrOH reactions, MoO₃ is probably a redox catalyst for some organic reactions in SCW. This will also be investigated in future.

Almost all the metal oxides have acid and base sites on their surface and the acidity and/or basicity on the surface of the metal oxides are controlled by the structure.^{25,29} Furthermore, the catalytic properties of the metal oxides were also controlled by some dopants. We will also try some solid solutions in the reaction, and we will clarify the relationship between the acid-

base properties of the metal oxide and organic reactions in SCW in more detail.

Conclusion

Organic reactions in SCW (673 K) were conducted using batch type reactors. As a result, for each metal oxide, the following results were obtained.

CeO₂: on the surface of CeO₂, there are basic sites for HCHO and glucose reaction.

MoO₃: for HCHO reaction, MoO₃ shows an acidity, based on the ratio of CH₃OH/CO yield. However, oxidations of 2-PrOH (into acetone) and glucose (into CO₂) were probably catalyzed by MoO₃. Thus, some portion of CO yield from HCHO was probably catalyzed by MoO₃.

TiO₂: for all the reactions (HCHO, 2-PrOH, and glucose) at 673 K, TiO₂ (both anatase and rutile) was an acid catalyst. In addition, the rutile phase of TiO₂ (TiO₂ (r)) has basic sites for 2-PrOH reaction.

ZrO₂: ZrO₂ has basic sites for all the reactions in this study. For 2-PrOH reactions, the acidity of the ZrO₂ was stronger than its basicity. The acidity and basicity of ZrO₂ can be controlled by pretreatment and/or dopants. Now, we are studying the relationship between the acidity and basicity of metal oxides and organic reactions in SCW.

Acknowledgements

New Energy and Industrial Technology Development Organization (NEDO) financially supported this study (Project ID: 02A44001d).

References

- 1 T. Sato, G. Sekiguchi, T. Adschiri and K. Arai, *Ind. Eng. Chem. Res.*, 2002, **41**, 3064.
- 2 K. Chandler, F. Deng, A. K. Dillow, C. L. Liotta and C. A. Eckert, *Ind. Eng. Chem. Res.*, 1997, **36**, 5175.
- 3 K. Chandler, C. L. Liotta, C. A. Eckert and D. Schiraldi, *AIChE J.*, 1998, **44**, 2080.
- 4 S. H. Townsend, M. A. Abraham, G. L. Huppert, M. T. Klein and S. C. Paspek, *Ind. Eng. Chem. Res.*, 1988, **27**, 143.
- 5 G. L. Huppert, B. C. Wu, S. H. Townsend, M. T. Klein and S. C. Paspek, *Ind. Eng. Chem. Res.*, 1989, **28**, 161.
- 6 M. T. Klein, L. A. Torry, B. C. Wu and S. H. Townsend, *J. Supercrit. Fluids*, 1990, **3**, 222.
- 7 T. Funazukuri, R. M. Serikawa and K. Yamaura, *Fuel*, 1997, **76**, 865.
- 8 J. M. L. Penninger, R. J. A. Kersten and H. C. L. Baur, *J. Supercrit. Fluids*, 1999, **16**, 119.
- 9 J. M. L. Penninger, R. J. A. Kersten and H. C. L. Baur, *J. Supercrit. Fluids*, 2000, **17**, 215.
- 10 J. D. Taylor, J. I. Steinfeld and J. W. Tester, *Ind. Eng. Chem. Res.*, 2001, **40**, 67.
- 11 J. D. Taylor, F. A. Pacheco, J. I. Steinfeld and J. W. Tester, *Ind. Eng. Chem. Res.*, 2001, **41**, 1.
- 12 P. Krammer and H. Vogel, *J. Supercrit. Fluids*, 2000, **16**, 189.
- 13 H. Oka, S. Yamago, J. Yoshida and O. Kajimoto, *Angew. Chem., Int. Ed.*, 2002, **41**, 623.
- 14 N. Akiya and P. E. Savage, *Ind. Eng. Chem. Res.*, 2001, **40**, 1822.
- 15 R. Narayan and M. J. Antal, Jr., *J. Am. Chem. Soc.*, 1990, **112**, 1927.
- 16 X. Xu, C. D. Almeida and M. J. Antal, Jr., *J. Supercrit. Fluids*, 1990, **3**, 228.
- 17 X. Xu, C. P. D. Almeida and M. J. Antal, Jr., *Ind. Eng. Chem. Res.*, 1991, **30**, 1478.

- 18 X. Xu and M. J. Antal, Jr., *AIChE J.*, 1994, **40**, 1524.
- 19 M. Watanabe, H. Inomata, R. L. Smith Jr. and K. Arai, *Appl. Catal., A*, 2001, **219**, 149.
- 20 M. Watanabe, H. Inomata and K. Arai, *Biomass Bioenergy*, 2002, **22**, 405.
- 21 K. Tomita, S. Koda and Y. Oshima, *Ind. Eng. Chem. Res.*, 2002, **41**, 3341–3344.
- 22 M. Watanabe, M. Osada, H. Inomata, K. Arai and A. Kruse, *Appl. Catal., A*, 2003, **245**, 333–341.
- 23 D. Haffad, A. Chambellan and J. C. Lavalley, *J. Mol. Catal. A: Chem.*, 2001, **168**, 153.
- 24 M. Osada, M. Watanabe, K. Sue, T. Adschiri and K. Arai, *J. Supercrit. Fluids*, 2003, in press.
- 25 K. Tomishige, T. Sakaihorii, Y. Ikeda and K. Fujimoto, *Catal. Lett.*, 1999, **58**, 225.
- 26 M. J. Antal, Jr., M. Carlsson, X. Xu and D. G. M. Anderson, *Ind. Eng. Chem. Res.*, 1998, **37**, 3820.
- 27 B. M. Kabyemela, T. Adschiri, R. M. Malaluan, K. Arai and H. Ohzeki, *Ind. Eng. Chem. Res.*, 1997, **36**, 5063.
- 28 A. Kruse and A. Gawlik, *Ind. Eng. Chem. Res.*, 2003, **42**, 267.
- 29 K. Parida and H. K. Mishra, *J. Mol. Catal. A: Chem.*, 1999, **139**, 73.



Microbial production of poly(hydroxyalkanoate)s from waste edible oils†

Ikuo Taniguchi, Kumi Kagotani and Yoshiharu Kimura*

Department of Polymer Science and Engineering, Kyoto Institute of Technology, Matsugasaki, Sakyo-ku, Kyoto 606-8585, Japan. E-mail: ykimura@ipc.kit.ac.jp; Tel: +81-75-724-7804; Fax: +81-75-712-3956

Received 29th April 2003

First published as an Advance Article on the web 22nd July 2003

The biosynthesis of poly(3-hydroxyalkanoate) (PHA) from waste edible oils and tallow by *Ralstonia eutropha* was investigated. Waste plant oils as well as waste tallow were assimilated and successfully converted to PHA with relatively high yield by the bacterial fermentation. The waste plant oils usually gave poly(3-hydroxybutyrate) (PHB) while waste tallow gave poly(3-hydroxybutyrate-co-3-hydroxyvalerate) (PHBV). The ratio of 3-hydroxyvalerate (3HV) unit in the copolyester was controlled by the addition of sodium propionate to the cultivation medium containing waste plant oils as carbon sources. The ratio of PHA accumulated was also quite high and up to 80% of the cell dry weight. The PHA accumulated was easily isolated by simply mixing the cells in aqueous sodium hypochlorite without using any organic solvents. We propose herein the biorecycling of waste oils as renewable resources for sustainable society.

Introduction

Waste edible oils exhausted from the food industry and the food service industry are recovered legally as industrial wastes and converted to animal-based feed, fatty acids, soaps, and so on. However, household waste oils are not recovered and are disposed of by incineration as inflammable waste after being adsorbed in papers or coagulation with a certain coagulant, which causes serious environmental problems, such as waste management, global warming. In addition, a part of the waste oils flows out into sewage, resulting in water pollution. Especially, in Japan, 1.4×10^5 t of waste edible oils are exhausted from the general family in a year, which corresponds to the emission of about 4.0×10^5 t of CO₂ with a heat value of 9.5×10^5 MJ.

We have investigated the reuse of waste edible oils as renewable resources and succeeded in converting them to PHAs by microbial fermentation. PHAs are carbon and energy storage materials synthesized by many microorganisms.¹ These polymers have attracted much attention because of their potential as biodegradable substitutes for fossil fuel-based thermoplastics and elastomeric materials.² For example, PHB and PHBV have been produced and marketed by Monsanto Co., Ltd. (USA). However, commercial applications of these PHAs have been limited by their high production cost.³ The use of inexpensive carbon sources may reduce the cost. Plant oils and fats are renewable and inexpensive agricultural co-products, and thus, waste oils would be one of the most suitable candidates for microbial production of PHAs. However, there have been a few reports about PHA biosynthesis from triacylglycerides. Several pseudomonades produce medium- and long-chain-length PHA from plant oils⁴ and tallow,⁵ and *Aeromonas caviae* also accumulates PHBHHx from olive oil.⁶ These PHAs are potentially useful in the formation of biodegradable adhesives and elastomers, although the productivities of them are quite low in all the cases.

In this paper, PHA production by *Ralstonia eutropha* was investigated with waste edible oils and fats as carbon sources. PHAs accumulated in the bacteria are usually extracted using an

organic solvent such as chloroform followed by reprecipitation into hexane or methanol. The use of a large amount of organic solvents is one of the difficulties for commercial production of PHAs. A low energy, low cost and environmentally friendly alternative extraction method is also studied.

Results and discussion

The *R. eutropha* H16 strain shows high PHA producing ability compared to other PHA producing microorganisms, such as pseudomonades or *A. caviae*.³ Fukui and Doi reported that the PHB production by *R. eutropha* was saturated for 72 h incubation when 1.0% olive oil was used as a sole carbon source, and 3.4 g of PHB per 1 L of culture medium was obtained. In this study, virgin and waste sesame oils (1.0%), or fructose (5.0%) as a reference experiment,¹ were supplemented as sole carbon sources in the nitrogen-limited culture medium, and *R. eutropha* precultured in a nutrient rich medium was inoculated in those culture media and incubated for 72 h. Both of the virgin and waste oils were completely assimilated and converted to PHB. The PHB biosynthesized was isolated by hot chloroform extraction with Soxhlet apparatus. The results are summarized in Table 1. The weight average molecular weight (M_w) of PHB from fructose was the highest of the three. However, the productivities of PHB from virgin and waste sesame oils (3.1 to 4.1 g L⁻¹) were higher than that from

Green Context

Waste edible oils are largely destroyed by incineration or lost into the environment – both routes being unacceptable from a green chemistry perspective. Here the useful polymers, poly(hydroxyalkanoates) are biosynthesised from these wastes using *Ralstonia eutropha*. The efficiency of this interesting process is high and the polymer can be easily extracted. Thus a waste is converted by an environmentally benign method to a valuable product. **JHC**

† Presented at The First International Conference on Green & Sustainable Chemistry, Tokyo, Japan, March 13–15, 2003.

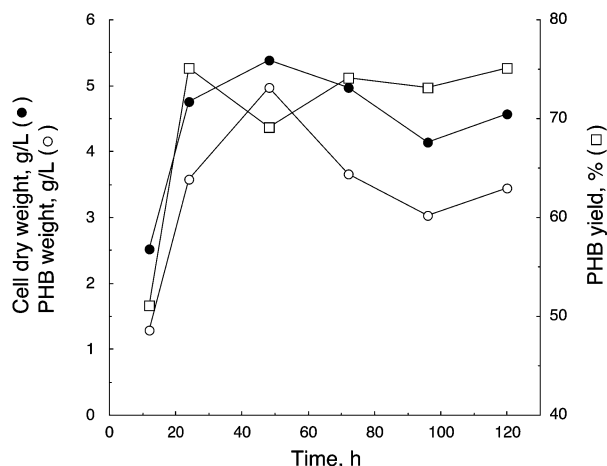
Table 1 Production of PHB by *Ralstonia eutropha* from various carbon sources, and weight average molecular weight (M_w) and polydispersity (M_w/M_n) of PHB^a

Carbon source	Concentration (%)	Cell dry weight/g L ⁻¹	PHB/g L ⁻¹	Yield (%)	$M_w \times 10^{5a}$	M_w/M_n^a
Fructose	5	4.9	2.6	54	13.2	2.0
Virgin sesame oil	1	6.1	4.1	68	5.3	1.8
Waste sesame oil	1	4.8	3.1	63	5.5	1.1

A 120 mg cell wet weight of *R. eutropha* was cultivated in 100 mL of the nitrogen-limited culture medium for 72 h at 30 °C.^a Weight average molecular weight and polydispersity were determined by GPC.

fructose (2.6 g L⁻¹) even though the carbon concentration was in 5-fold excess of the oils.

The time course of PHB production was monitored for optimization of culture conditions. A 120 mg cell wet weight of *R. eutropha* was incubated in 100 mL of the nitrogen-limited medium containing 1.0 mL waste sesame oil (1.0%). At an appropriate time, 10 mL of the bacterial suspension was collected, and the PHB produced was recovered by hot chloroform extraction with Soxhlet apparatus. As shown in Fig. 1, PHB accumulation was recognized from 12 h incubation. The

**Fig. 1** Time course of cell growth and PHB accumulation during batch culture of *Ralstonia eutropha* on 1.0% waste sesame oil at 30 °C.

yield of PHB was approx. 50% at 12 h and then increased to a level of 70%. The optimum incubation time was determined to be 48 h, but an incubation time of 72 h was employed for the following experiments because a part of the oil was observed in the supernatant for less than 72 h incubation.

To investigate the optimum oil concentration, *R. eutropha* with several cellular concentrations was incubated in the nitrogen-limited culture medium containing waste sesame oil with various concentrations. The PHB produced was also recovered by hot chloroform extraction followed by reprecipitation in methanol. As shown in Table 2, the cell growth and the PHB productivity were strongly related to the initial cellular and oil concentrations, and 3.0 g L⁻¹ of cell wet weight concentration versus 1.0% oil concentration showed the optimum PHB production. The waste sesame oil at concentrations under 2.0% was completely assimilated by the bacteria during incubation. On the other hand, at a supplemented oil concentration of 5.0%, a large part of the oil remained in the supernatant, which would cause the inhibition of cell growth at higher cellular concentration.

An environmentally friendly isolation method of PHB with aqueous media has been required since the usual PHB extraction consumes a large amount of organic solvents. An

Table 2 Production of PHB by *Ralstonia eutropha* from waste sesame oil with various concentrations

Initial cell wet weight/g L ⁻¹	Oil concentration (%)	Cell dry weight/g L ⁻¹	PHB/g L ⁻¹	Yield (%)
1.2	0.1	1.0	0.2	20
1.2	0.3	3.1	1.5	49
1.2	0.5	3.9	2.0	53
1.2	1	5.3	3.5	66
1.8	1	4.3	2.7	63
3.0	1	6.3	4.9	78
1.2	2	2.8	1.2	44
1.2	5	6.6	2.8	42
5.0	5	4.0	2.1	51
10.0	5	3.9	1.6	41

R. eutropha was cultivated for 72 h at 30 °C.

effective extraction using a suspension of chloroform and sodium hypochlorite solution was once reported.⁷ Here, we have developed that method with only aqueous sodium hypochlorite, and the extraction efficiency was compared with the usual Soxhlet extraction or just simply stirring extraction in chloroform. PHB extraction of each method was carried out with 300 mg of lyophilized cells from the same batch culture. A sodium hypochlorite concentration of 30% was employed, and the results are summarized in Table 3. The stirring extraction

Table 3 Isolation of PHB from *Ralstonia eutropha* with different extraction methods, and weight average molecular weight (M_w) and polydispersity (M_w/M_n) of PHB

Extraction method	PHB/mg	Yield (%)	$M_w \times 10^{5a}$	M_w/M_n^a
Soxhlet	201	67	3.3	2.8
Stirring	155	52	5.3	2.5
Sodium hypochlorite	183	61	2.3	4.2

A 300 mg of lyophilized cell was used in each extraction.^a Weight average molecular weight and polydispersity were determined by GPC.

had the lowest yield although the value of M_w was the highest among the three methods. Because of the oxidative nature of sodium hypochlorite, the polyester chain was cleaved during extraction, leading to an increase in polydispersity. Slight decreases in yield and M_w were found in the extraction compared with the usual Soxhlet extraction. However, it was concluded that this extraction was comparable and used hereafter as an effective alternative extraction method.

PHA production was studied with various waste edible oils and fats. A 120 mg cell wet weight of *R. eutropha* was incubated in 100 mL of the nitrogen-limited medium containing 1.0% of various waste plant oils and fats. The PHA accumulated was isolated by the aqueous sodium hypochlorite extraction. The results are summarized in Table 4. In each case, PHA

Table 4 Production of PHA by *Ralstonia eutropha* from various waste oils and fats

Waste oils and fats	Cell dry weight/g L ⁻¹	PHA/g L ⁻¹	Yield (%)	3HV (%) ^a
Soybean and rapeseed	6.1	3.5	57	0
Soybean, rapeseed, corn, and lard	6.5	5.1	79	2
Palm and lard	6.8	5.7	83	1
Tallow	7.3	5.8	80	1

A 120 mg cell wet weight of *R. eutropha* was cultivated in 100 mL of the nitrogen-limited culture medium for 72 h at 30 °C.^a The 3HV content was determined by ¹H-NMR.

production was recognized with high yield (up to 5.8 g L⁻¹). Especially, the feeding of animal triacylglycerides gave PHBV

even the incorporation ratio of 3HV was trace. Different from other liquid waste oils and fats, tallow was solid under the culture conditions but completely degraded during incubation. The obtained results demonstrate that *R. eutropha* can assimilate various waste oils and fats, and convert them to useful biodegradable polyesters with much higher efficiency than ever. By using *R. eutropha*, renewable and inexpensive agricultural fats/oils and their waste products are potentially useful feedstocks for the PHA fermentation processes.

The crystalline and brittle nature of PHB, which is developed by addition of certain nucleation additives or by incorporation of a hetero unit, such as the 3HV unit, in the polymer chain, often becomes a disadvantage in processing.⁸ PHBV is the typical example and was once commercially available as Biopol®. The incorporation ratio of the hetero unit usually determines the thermal and mechanical properties of the copolyesters. PHBV having various 3HV contents was biosynthesized by *R. eutropha* fermentation with waste sesame oil and sodium propionate salt at various mixture ratios, where the carbon source concentration of 1.0% was kept. A 300 mg cell wet weight of *R. eutropha* was incubated in 100 mL of the nitrogen-limited medium containing the mixture of waste sesame oil and sodium propionate. The results are represented in Table 5 and Fig. 2. The 3HV content in PHBV increased with

Table 5 Production of PHA by *Ralstonia eutropha* from waste sesame oil and sodium propionate (SP) at various mixture ratios and thermal properties of PHA

Oil : SP, w/w	Cell dry weight/g L ⁻¹	PHA/g L ⁻¹	Yield (%)	T _c /°C ^a	T _m /°C ^a
100 : 0	7.4	4.6	62	59.5	172
80 : 20	5.5	3.5	63	65.4	168
60 : 40	5.1	3.3	65	66.0	167
40 : 60	4.1	1.7	42	n.d.	165
20 : 80	2.7	0.8	29	n.d.	n.d.
0 : 100	2.6	0.5	21	n.d.	n.d.

Total carbon source content was 1.0 %.^a The values of T_c and T_m were determined by DSC.

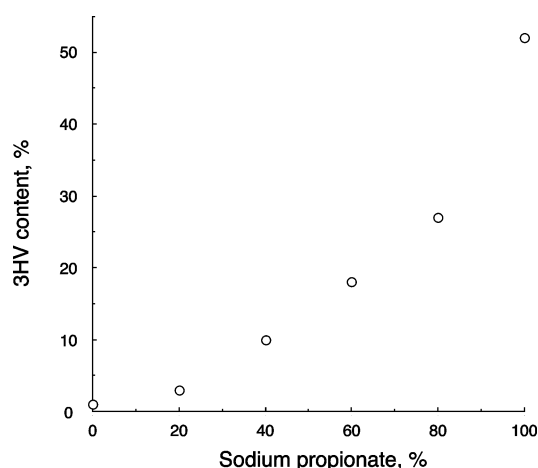


Fig. 2 3HV content of PHA from 1.0% mixture of waste sesame oil and sodium propionate as a function of sodium propionate concentration during batch culture of *Ralstonia eutropha* for 72 h at 30 °C.

the mixture ratio of sodium propionate while the cell viability decreased. When the 3HV content was below 10%, the value of the crystallization temperature (T_c) increased with the 3HV content, which indicated the inhibition of crystallization and/or spherulite growth of PHB. Thus, the melting temperature (T_m) decreased with the 3HV content. However, with an 3HV

content over 10%, the copolyester did not show an obvious T_c and T_m, being amorphous and ductile. These results suggested the potential for tailoring the biodegradable polyesters with desired physicochemical properties for their application fields.

Experimental

Abbreviations

Biodegradable polyesters and its composition units were abbreviated as follows; PHA: poly(3-hydroxyalkanoate), PHB: poly(3-hydroxybutyrate), PHBV: poly(3-hydroxybutyrate-co-3-hydroxyvalerate), PHBHHx: poly(3-hydroxybutyrate-co-3-hydroxyhexanoate), 3HB: 3-hydroxybutyrate, and 3HV: 3-hydroxyvalerate.

Strain information and preservation

R. eutropha H16 strain (ATCC 17699) was used throughout the experiments. Stock cultures were produced in 500 mL shake flasks by growing the organism in 100 mL nutrient broth medium (Difco, Detroit, MI, USA) (pH 7.0) at 30 °C on a reciprocal shaker (120 rpm). At late log phase (approx. 20 h), the culture was diluted 1 : 1 with sterile 30% glycerol and the organisms aseptically transferred to sterile cryogenic vials. The vials are stored in liquid nitrogen.

Fermentation

PHA biosynthesis was carried out by two-stage batch culture. At first, *R. eutropha* was cultivated in 100 mL nutrient broth at 30 °C and 120 rpm for 20 h. The cells were harvested by centrifugation at 20,000 × g for 2 min and washed with sterile deionized water. The weight of the cells so obtained was defined as cell wet weight. The cells were then transferred into 100 mL of the modified E* medium⁵ containing an appropriate amount of waste edible oils, tallow, or fructose as carbon sources. Tallow was first melted in a 60 °C oven before the addition. All of the oils and tallow were not sterilized. Cultures were incubated at 30 °C and 120 rpm for a predetermined time. After the incubation, the cells were centrifuged at 20,000 × g for 2 min and washed with deionized water and weighed as cell dry weight after lyophilization. The modified E* medium contains the following (per liter): NH₄Cl 0.5 g, Na₂HPO₄ 3.3 g, KH₂PO₄ 2.8 g, MgSO₄·7H₂O 0.25 g, and 1.0 mL micro-mineral solution. The micro-mineral solution consists of the following in 0.5 M HCl (g L⁻¹): FeCl₃·6H₂O 20 g, MnCl₂·4H₂O 0.05 g, CuSO₄·5H₂O 0.03 g, ZnSO₄·7H₂O 0.1 g, and CaCl₂·H₂O 10 g.

Extraction of PHA

Intracellular PHA was collected by 3 kinds of extraction method. One was solvent extraction, which was just simply mixing the lyophilized cells in chloroform at ambient temperature for 3 days. The second was solvent extraction with hot chloroform using Soxhlet apparatus for 12 h. Both of the chloroform solutions were filtered to remove any cellular debris, concentrated by rotary evaporation, and added dropwise to cold methanol (1 : 50 v/v) to precipitate PHA. The white precipitate obtained was well washed and dried *in vacuo*. In the third method, the lyophilized cells were treated with 30%

aqueous sodium hypochlorite with stirring for 90 min at 30 °C. The biomass concentration in the solution was 4 wt%. The precipitate was well washed with deionized water and ethanol, and then dried *in vacuo*. The dried PHA was weighed, and the yield was defined as a percentage of the dried polyester to the cell dry weight.

Polymer characterization

PHA was identified by ¹H-NMR using a Varian Gemini 200 FT-NMR spectrometer according to the literature.⁹ The samples were dissolved in deuterated chloroform, and tetramethylsilane was used as an internal standard. The composition of 3HB and 3HV unit was determined from the integral values of those methyl proton signals (3HB: 1.27 and 3HV: 0.90 ppm, respectively). The apparent average molecular weight and the polydispersity were determined by gel permeation chromatography (GPC). The GPC system consisted of a Shimadzu LC-10A pump (Shimadzu Co. Ltd., Kyoto, Japan), a Shodex RI SE-31 RI detector (Showa Denko K.K., Tokyo Japan), and a C-R7A Chromatopac data processor (Shimadzu). A combination of two polystyrene gel columns of TSK gel G4000H and G2500H (ϕ 7.5 × 300 mm in each column, Tosoh Ltd., Tokyo, Japan) was used. Polystyrene standards with a low polydispersity were used to generate a calibration curve, and chloroform was used as an eluent at a flow rate of 0.7 mL min⁻¹ and at 35 °C. The sample concentration and injection volume were 0.5 wt% and 50 μ L, respectively. The thermal property of PHA was examined by differential scanning calorimetry measurement using a Shimadzu DSC50. The temperature was scanned from -50 to 190 °C at a heating rate of 10 °C min⁻¹. For the precise determination of T_c and T_m values, the samples were first melted at 190 °C and immediately quenched in liquid nitrogen before the measurement.

Acknowledgements

The authors would like to thank Professors Kohei Oda and Hiroshi Oyama, and Dr. Kazumi Hiraga for their helpful discussions and suggestions. The authors are grateful to Mr. Kenji Kimura (Tenmates Inc., Osaka, Japan) for providing various virgin and waste oils and fats, and also grateful to Miss Yuko Nagahara for skilful DSC measurement.

References

- (a) O. P. Peoples and A. J. Sinskey, *J. Biol. Chem.*, 1989, **264**, 15293; (b) A. Steinbüchel and H. E. Valentin, *FEMS Microbiol. Lett.*, 1995, **128**, 219; (c) L. L. Madison and G. W. Huisman, *Microbiol. Mol. Biol. Rev.*, 1999, **63**, 21; (d) A. Steinbüchel, *Macromol. Biosci.*, 2001, **1**, 1.
- (a) A. J. Anderson and E. A. Dawes, *Microbiol. Rev.*, 1990, **54**, 450; (b) Y. Doi, *Microbial polyesters*, VCH, New York, 1990; (c) A. Steinbüchel, *PHB and other polyhydroxyalkanoic acids*, in *Biotechnology*, H. J. Rehm, G. Reed, A. Pühler and P. Stadler, Wiley-VCH Verlag GmbH, Weinheim, Germany, 2nd edn., 1996, vol. 6, pp. 403–464.
- T. Fukui and Y. Doi, *Appl. Microbiol. Biotechnol.*, 1998, **49**, 333.
- (a) G. Eggink, P. deWaard and G. N. M. Huijberts, *Can. J. Microbiol.*, 1995, **41**, 14; (b) M. Kato, T. Fukui and Y. Doi, *Bull. Chem. Soc. Jpn.*, 1996, **69**, 515; (c) B. Fuchtenbusch, D. Wullbrandt and A. Steinbüchel, *Appl. Microbiol. Biotechnol.*, 2000, **53**, 167.
- A. M. Cromwick, T. Foglia and R. W. Lenz, *Appl. Microbiol. Biotechnol.*, 1996, **46**, 464.
- (a) E. Shimamura, K. Kasuya, G. Kobayashi, T. Shiotani, Y. Shima and Y. Doi, *Macromolecules*, 1994, **27**, 878; (b) Y. Doi, S. Kitamura and H. Abe, *Macromolecules*, 1995, **28**, 4822.
- S. K. Hahn, Y. K. Chang, B. S. Kim and H. N. Chang, *Biotechnol. Bioeng.*, 1994, **44**, 256.
- R. H. Marchessault, *Trends Polym. Sci.*, 1996, **4**, 163.
- Y. Doi, M. Kunioka, Y. Nakamura and K. Soga, *Macromolecules*, 1986, **19**, 2860.



Solid-phase intramolecular oxyselenenylation and deselenenylation reactions using polymer-supported selenoreagents and their application to aqueous media organic synthesis†

Ken-ichi Fujita,^{*a} Shigeru Hashimoto,^a Mitsuhiro Kanakubo,^b Akihiro Oishi^a and Yoichi Taguchi^a

^a National Institute of Advanced Industrial Science and Technology (AIST), Tsukuba Central 5, 1-1-1, Higashi, Tsukuba, Ibaraki, 305-8565, Japan. E-mail: k.fujita@aist.go.jp

^b National Institute of Advanced Industrial Science and Technology (AIST), 4-2-1, Nigatake, Miyagino-ku, Sendai, Miyagi, 983-8551, Japan

Received 8th April 2003

First published as an Advance Article on the web 21st August 2003

Polymer-supported organoselenium reagents with amide linker were readily prepared from substituted-polystyrene resins. Through the use of polymer-supported arylselenenyl bromides, the oxyselenenylation reaction of olefins was carried out even in water. An amphiphilic polymer-supported arylselenenyl bromide was employed, and the intramolecular oxyselenenylation and the subsequent deselenenylation reactions proceeded smoothly in water with fair chemical yields (up to an 83% total yield).

Introduction

Organoselenium compounds are frequently used as convenient reagents for introducing various functional groups into the carbon–carbon double bond¹ and for constructing a heterocyclic skeleton *via* an intramolecular ring-closure process.² These transformations are otherwise difficult to achieve.

Solid-phase organic synthesis is a powerful and rapid method for the preparation of large numbers of structurally distinct molecules.³ In this technique, the purification of products has been greatly simplified through the use of polymer-resins, and the eliminated auxiliary that is bound to polymer-resins can be easily recovered entirely by filtration after sequential solid-phase conversion. The use of polymer-supported organoselenium reagents is urgently desired because the toxicity and strong odor of unsupported organoselenium reagents are often problematic in the laboratory. Recently, several polymer-supported selenoreagents were prepared, and their applications to solid-phase organic synthesis and the combinatorial approach were then reported by us^{4–6} and by other groups.^{7,8}

Furthermore, owing to today's environmental concerns about harmful and volatile organic solvents, the use of organic transformations in water is presently undergoing very rapid growth so that green and sustainable chemistry can be realized.^{6,9} However, in selenium chemistry, most organoselenium reagents are insoluble or decomposed in water. For example, phenylselenenyl bromide, which is a representative electrophilic selenoreagent, is easily decomposed in water.¹⁰ Herein, we wish to report the very simple preparation of polymer-supported arylselenenyl bromides from substituted-polystyrene resins, their application as reagents to solid-phase oxyselenenylation and deselenenylation reactions, and the first example of the oxyselenenylation and the deselenenylation reactions in water, conducted by employing polymer-supported arylselenenyl bromide.

Results and discussion

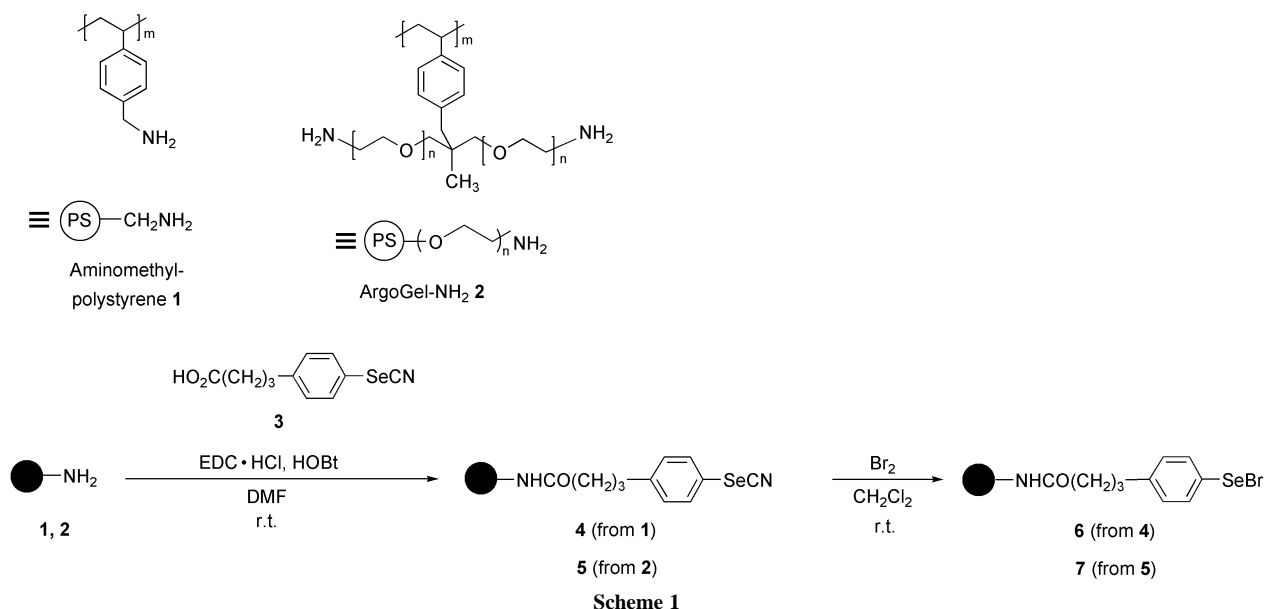
Polymer-supported selenenyl bromides **6** and **7** were synthesized according to the method outlined in Scheme 1. We have prepared polymer-supported arylselenocyanates **4**⁴ and **5** by the condensation of aminomethyl-polystyrene resin **1** and poly(ethylene glycol)–polystyrene graft copolymer resins (ArgoGel@-NH₂) **2**, respectively, with **3**. Thus obtained **4** and **5** were converted to polymer-supported selenenyl bromides **6** and **7** with an addition of bromine in dichloromethane. Recently, Nicolaou *et al.* have reported the preparation of polystyrene-bound selenenyl bromide **8**,⁷ which is shown in Table 1. On the other hand, **7** is the first example of selenenyl bromide immobilized on amphiphilic polymer-resin.

The utility of polymer-supported selenenyl bromides **6** and **7** as electrophilic reagents was then demonstrated by the intramolecular oxyselenenylation (namely, selenolactonization) and the subsequent deselenenylation reactions in dichloromethane as shown in Scheme 2.⁴ After stirring polymer-supported selenenyl bromides and (*E*)-styrylacetic acid in dichloromethane at room temperature, the corresponding polymer-supported selenolactone **9** was then obtained. Subsequently, through the oxidation of **9**, which was collected by filtration, with hydrogen peroxide in dichloromethane at room temperature, the deselenenylation product **10** was obtained. The yields of **10** are shown in Table 1. Both polymer-supported

Green Context

Selenium-based reagents offer some very mild and selective transformations, but require volatile organic solvents to function well. This paper shows that such reagents perform poorly in water when used directly, but when attached to a polymer support, actually perform better in water than in organic solvents. This inversion of activity is an important observation, since it may be possible to extend it to other systems where water is not effective. *DJM*

† Presented at The First International Conference on Green & Sustainable Chemistry, Tokyo, Japan, March 13–15, 2003.



selenenyl bromides **6** and **7** afforded the deselenenylation product **10** in a decent yield (Entries 2 and 3), similar to the commercially available polystyrene-bound selenenyl bromide **8** (Entry 1).

We next examined this two-step transformation in water, conducted by employing these polymer-supported arylselenenyl bromides **6–8**. Phenylselenenyl bromide is easily decomposed in water to afford diphenyl diselenide by intermolecular Se–Se bond formation.¹⁰ Therefore, because polymer-supported arylselenenyl bromide was employed, we expected the decomposition of the bromoselenenyl group in water to be suppressed because of the inhibition of Se–Se bond formation due to the immobilization of the selenogroup on the polymer-backbone. First, when commercially available **8** was employed, the yield of **10** obtained in water was low, contrary to our expectation (29% yield; Entry 1). However, by the bromine elemental analysis of **9**, it was found that the bromoselenenyl group was probably not decomposed even in water due to its immobilization on the polymer-backbone.

On the other hand, when **6**, which had an amide linker, was used, the corresponding selenolactonization and the subsequent deselenenylation reactions proceeded in water to afford **10** in a fair chemical yield (59% yield; Entry 2). In this case in particular, the yield of **10** obtained in water exceeded the yield obtained in dichloromethane¹¹ using **6** (46% yield). Although

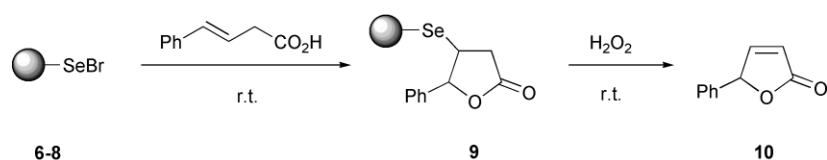
we have no definitive explanation at the moment for the high yield obtained in water, the hydrophobic effect¹² due to the cohesion of organic substrates in water could be responsible. This is the first example of oxydeselenenylation and deselenenylation reactions performed in water. In these aqueous transformations, organic solvents are not needed even in the washing process of the obtained **9** by filtration. Furthermore, in this method, it should be noted that the selenocompound could be easily recovered entirely by filtration after the deselenenylation process. We subsequently proceeded to use amphiphilic polymer-supported **7**. In this case, this two-step transformation proceeded more smoothly in water, with rapid resin decolorization, than that using **6**, due to its amphiphilic property (62% yield; Entry 3).

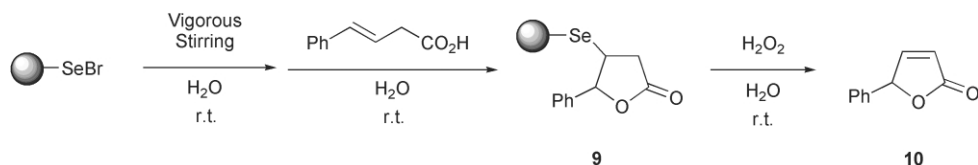
We then examined the stabilities of phenylselenenyl bromide and polymer-supported **7** in water (Scheme 3, Table 2). After stirring phenylselenenyl bromide or **7** in water vigorously for the time shown in Table 2, the selenolactonization reaction was performed by the addition of (*E*)-styrylacetic acid. When **7** was used, only the total yields of **10** are shown in Table 2 because of the solid-phase sequential conversion. Under the usual conditions, the selenolactonization reaction using phenylselenenyl bromide afforded the corresponding selenolactone **9**, which was not bound to polymer resin in this case, and diphenyl diselenide in 49 and 36% yields, respectively (Entry 1). However, by

Table 1 Selenolactonization and deselenenylation reactions of (*E*)-styrylacetic acid

Entry	SeBr	Solvent:	Total yield of 10 (%) ^a	
			CH ₂ Cl ₂	H ₂ O
1	(PS)-SeBr	8	50	29
2	(PS)-CH ₂ NHCO(CH ₂) ₃ -C ₆ H ₄ -SeBr	6	46	59
3	(PS)-(O-CH ₂) _n NHCO(CH ₂) ₃ -C ₆ H ₄ -SeBr	7	44	62

^a Isolated yield.





Scheme 3

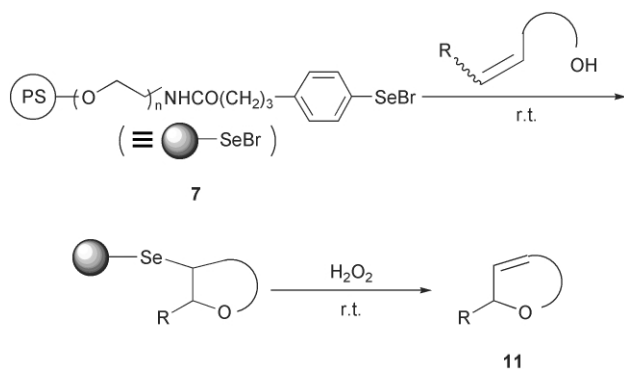
Table 2 Stabilities of phenylselenenyl bromide and polymer-supported arylselenenyl bromide **7** in water

Entry	SeBr	Stirring time	Yield of 9 (%) ^a	Total yield of 10 (%) ^a
1	PhSeBr	0	49 (36% (PhSe) ₂)	38 ^b
2	PhSeBr	1 min	9 (54% (PhSe) ₂)	7 ^b
3	PhSeBr	5 min	1 (83% (PhSe) ₂)	1 ^b
4	 7	0	—	62
5		1 h	—	58
6		24 h	—	36

^a Isolated yield. ^b The yield of **10** from **9**: 77%.

stirring phenylselenenyl bromide in water before the addition of (*E*)-styrylacetic acid, the yields of **9** were decreased significantly, probably due to the rapid decomposition of phenylselenenyl bromide in water (Entries 2 and 3). On the other hand, in the case of polymer-supported **7**, in spite of the stirring of **7** in water for 1 h, the total yield of **10** was decreased only slightly as compared with the yield under the usual procedure (Entries 4 versus 5). This is probably because the bromoselenenyl group immobilized on the polymer-backbone is very stable in water due to the inhibition of the Se–Se bond formation of the immobilized selenogroup. Therefore, it is presumed that polymer-supported selenenyl bromide acts as an electrophilic selenoreagent, even in water.

By employing **7**, we subsequently performed various intramolecular oxyselenenylation and deselenenylation reactions in dichloromethane and in water (Scheme 4, Table 3). Selenolacto-



Scheme 4

nization and deselenenylation reactions proceeded smoothly to afford the corresponding allylic lactones **11** in decent yields both in dichloromethane and in water in all cases (Entries 1–4). However, employing alkenic alcohol in water, the corresponding allylic ether **11** was not obtained entirely, probably due to the interruption of the intramolecular nucleophilic attack by water in the oxyselenenylation step (Entry 5). On the other hand, in the case in which *o*-allyl phenol derivatives were used, the intramolecular selenoetherification and deselenenylation reactions proceeded smoothly to afford the corresponding benzopyrans even in water (up to an 83% yield; Entry 6).

Conclusion

We have prepared polymer-supported arylselenenyl bromides of a new type from substituted-polystyrene resins. By employ-

Table 3 Various intramolecular oxyselenenylation and deselenenylation reactions using **7**

Entry	Olefin	11	Total yield of 11 (%) ^a	
			CH ₂ Cl ₂	H ₂ O
1	Ph-CH=CH-CO ₂ H		44	62
2	C ₂ H ₅ -CH=CH-CO ₂ H		62	61
3			45	47
4			56	41
5			40	0
6			65	83
7			66	82
8			39	43

^a Isolated yield.

ing these polymer-supported arylselenenyl bromides, the corresponding intramolecular oxyselenenylation and the subsequent deselenenylation reactions proceeded in dichloromethane and even in water. This is the first example of oxyselenenylation and deselenenylation reactions performed in water. In this method, the selenocompound can be easily recovered entirely by filtration after the deselenenylation process. This methodology of realizing aqueous media reactions by the immobilization of reagents, which are easily decomposed in water, is a very effective approach to green chemistry and may greatly expand the range of organic syntheses that can be carried out in water.

Experimental

Infrared (IR) spectra were recorded on a Nicolet Nexus 470 FT-IR spectrometer. 500 MHz ¹H-NMR and ¹³C-NMR were measured on a JEOL LA-500 instrument in chloroform-*d*₁

containing tetramethylsilane (TMS) as an internal standard. ^{77}Se -NMR was measured on a Varian Inova 500 instrument in chloroform- d_1 . Chemical shifts are shown by the lower field shifts from dimethylselenide as an external standard for ^{77}Se -NMR. The melting point is uncorrected. Column chromatography was carried out with silica gel (Wakogel C-300, Wako Pure Chemical Industries, Ltd.). High performance liquid chromatography (HPLC) was done with JAI LC-908 instruments using JAIGEL-IH, 2H. The agitation of the reaction mixture was performed on a solid-phase organic synthesizer (Tokyo Rikakikai Co. Ltd.). 4-(4'-aminophenyl)butanoic acid was purchased from Aldrich. Aminomethyl-polystyrene **1** and ArgoGel@-NH₂ **2** were purchased from Fluka and Argonaut Technologies, respectively. Dry *N,N*-dimethylformamide was purchased from Aldrich.

4-(4'-Selenocyanatophenyl)butanoic acid (**3**)

According to the reported procedure,¹³ a 3 M sodium nitrite solution (15 ml, 45 mmol) was added dropwise to a 6 M hydrochloric acid suspension (24 ml) of 4-(4'-aminophenyl)butanoic acid (6.229 g, 34.8 mmol) with stirring at 0 °C. A saturated urea solution was added after 20 min, and the reaction was checked with starch-iodide paper. After the addition of a saturated aqueous solution of sodium acetate to give a pH of 5 on pH paper, an aqueous solution of potassium selenocyanate (6.84 g, 47.5 mmol) was added slowly, and the reaction mixture was stirred overnight at room temperature. The obtained dark brown precipitates were extracted with dichloromethane. The organic layer was washed with a saturated aqueous solution of sodium chloride, dried over magnesium sulfate, and evaporated under reduced pressure. After purification of the crude products by column chromatography on silica gel (hexane–ethyl acetate as eluent), pure **3** (4.604 g, 17.2 mmol) was obtained as a pale yellow powder (49.4% yield). m.p. 94.3–95.3 °C; IR (KBr): 2950, 2156, 1692, 1278, 1012 cm⁻¹; ^1H -NMR: δ (ppm) 7.62–7.48 (m, 2H), 7.41–7.20 (m, 2H), 2.70 (2H, t, $J = 7.3$ Hz), 2.39 (2H, t, $J = 7.4$ Hz), 2.04–1.90 (2H, m); ^{13}C -NMR: δ 179.2, 143.6, 133.3, 130.6, 118.9, 101.6, 34.6, 33.1, 25.9 ppm; ^{77}Se -NMR: δ 318.2 ppm; Anal. Calcd. for C₁₁H₁₁O₂NSe: C, 49.29; H, 4.13; N, 5.22. Found: C, 49.68; H, 4.01; N, 5.18%.

Preparation of **5**

A mixture of ArgoGel@-NH₂ **2** (0.35 mmol g⁻¹; 481.3 mg, 0.17 mmol), which was washed with acetonitrile and with dichloromethane before use, **3** (96.0 mg, 0.358 mmol), 3-ethyl-1-[3-(dimethylamino)propyl]carbodiimide hydrochloride (EDC·HCl; 95.0 mg, 0.496 mmol) and 1-hydroxybenzotriazole (HOBT; 89.0 mg, 0.659 mmol) in dry *N,N*-dimethylformamide (DMF; 4 ml) was agitated with shaking for 24 h at room temperature under a nitrogen atmosphere. After the filtration of the reaction mixture, the resin was washed with DMF, water, tetrahydrofuran, dichloromethane and with methanol, and then dried under reduced pressure. A Kaiser test¹⁴ indicated that the condensation was completed to form polymer-supported arylselenocyanate **5** quantitatively (523 mg, pale yellow beads). IR (KBr): 2864, 1655, 1453, 1350, 1111, 700 cm⁻¹; ^{13}C -NMR (gel-phase): δ 173.2, 102.3, 39.5, 35.8, 27.2 ppm; ^{77}Se -NMR (gel-phase): δ 317.6 ppm; Anal. Calcd.: N, 1.08; Se, 3.10. Found: N, 0.84; Se, 3.10%.

4 was prepared from **1** (2.0 mmol g⁻¹, crosslinked with 3% divinylbenzene) and **3** according to the above procedure (**4**: pale yellow beads). IR (KBr): 3025, 2922, 2149, 1605, 1510, 1248, 1175, 1017, 758 cm⁻¹; Anal. Calcd.: N, 3.73; Se, 10.52. Found: N, 3.32; Se, 9.05%.

Polymer-supported arylselenenyl bromides **6** and **7** were prepared from **4** and **5**, respectively, by the addition of 5 equiv.

bromine in dichloromethane at room temperature under a nitrogen atmosphere followed by the removal of the solvent and the excess amount of bromine before the oxyselenenylation reactions.

General procedure for the intramolecular oxyselenenylation and deselenenylation reactions

We stirred **7** (517 mg, 0.163 mmol) and (*E*)-styrylacetic acid (134 mg, 0.826 mmol) in water (3 ml) at room temperature for 15 hours, and the corresponding polymer-supported seleno-lactone **9** was then obtained. Subsequently, **9**, which was collected by filtration, and 30% hydrogen peroxide (0.11 ml, 0.97 mmol) were stirred in water (3 ml) at room temperature for 15 hours. After the reduction of the excess amount of hydrogen peroxide by the addition of sodium hydrogen sulfite solution, the reaction mixture was filtered off and the filtrate was extracted with dichloromethane. The organic layer was washed with a saturated sodium hydrogen carbonate solution and with a saturated sodium chloride solution, dried over magnesium sulfate, and evaporated under reduced pressure. After purification by HPLC (chloroform as eluent), the deselenenylation product **10** (16.2 mg, 0.101 mmol) was obtained as a colorless oil (62% yield).

The intramolecular oxyselenenylation reaction performed in dichloromethane was carried out under a nitrogen atmosphere.

References

- (a) *Organoselenium Chemistry*, ed. D. Liotta, Wiley, London, 1987; (b) *Selenium Reagents and Intermediates in Organic Synthesis*, ed. C. Paulmier, Pergamon Press, Oxford, 1986; (c) *Organoselenium Chemistry*, ed. T. G. Back, Oxford University Press, New York, 1999; (d) *Organoselenium Chemistry*, ed. T. Wirth, Springer-Verlag, Berlin, 2000; (e) H. J. Reich, *J. Org. Chem.*, 1974, **39**, 428; (f) K. C. Nicolaou, S. P. Seitz, W. J. Sipio and J. F. Blount, *J. Am. Chem. Soc.*, 1979, **101**, 3884; (g) T. Hayama, S. Tomoda, Y. Takeuchi and Y. Nomura, *Tetrahedron Lett.*, 1982, **23**, 4733; (h) S. Tomoda, Y. Usuki, K. Fujita and M. Iwaoka, *Rev. Heteroat. Chem.*, 1995, **6**, 247; (i) K. Fujita, *J. Synth. Org. Chem. Jpn.*, 1996, **54**, 166; (j) K. Fujita, *Rev. Heteroat. Chem.*, 1997, **16**, 101; (k) T. Wirth, *Tetrahedron*, 1999, **55**, 1.
- (a) D. J. Clive, G. Chittattu, N. J. Curtis, W. A. Kiel and C. K. Wong, *J. Chem. Soc., Chem. Commun.*, 1977, 725; (b) D. Goldsmith, D. Liotta, C. Lee and G. Zima, *Tetrahedron Lett.*, 1979, **50**, 4801; (c) K. C. Nicolaou, S. P. Seitz, W. J. Sipio and J. F. Blount, *J. Am. Chem. Soc.*, 1979, **101**, 3884; (d) K. C. Nicolaou, R. L. Magolda, W. J. Sipio, W. E. Barnette, Z. Lysenko and M. M. Joullie, *J. Am. Chem. Soc.*, 1980, **102**, 3784.
- (a) *Organic Synthesis on Solid Phase, 2nd Ed.*, ed. F. Z. Dorwald, Wiley-VCH Verlag, Weinheim, 2002; (b) *Combinatorial Chemistry*, ed. W. Bannwarth, Wiley-VCH Verlag, Weinheim, 2000; (c) D. Obrecht and A. M. Villalgorido, *Solid-Supported Combinatorial and Parallel Synthesis of Small-Molecular Weight Compound Libraries*, Pergamon Press, Oxford, 1998; (d) S. Booth, P. H. H. Hermkens, H. C. J. Ottenheijm and D. C. Rees, *Tetrahedron*, 1998, **54**, 15385; (e) L. A. Thompson and J. A. Ellman, *Chem. Rev.*, 1996, **96**, 555; (f) J. S. Fruchtel and G. Jung, *Angew. Chem., Int. Ed. Engl.*, 1996, **35**, 17.
- K. Fujita, K. Watanabe, A. Oishi, Y. Ikeda and Y. Taguchi, *Synlett*, 1999, 1760.
- K. Fujita, H. Taka, A. Oishi, Y. Ikeda, Y. Taguchi, K. Fujie, T. Saeki and M. Sakuma, *Synlett*, 2000, 1509.
- K. Fujita, S. Hashimoto, A. Oishi and Y. Taguchi, *Tetrahedron Lett.*, 2003, **44**, 3793.
- K. C. Nicolaou, J. Pastor, S. Barluenga and N. Winssinger, *Chem. Commun.*, 1998, 1947.
- (a) R. Michels, M. Kato and W. Heitz, *Makromol. Chem.*, 1976, **177**, 2311; (b) R. T. Taylor and L. A. Flood, *J. Org. Chem.*, 1983, **48**, 5160; (c) T. Ruhland, K. Andersen and H. Pedersen, *J. Org. Chem.*, 1998, **63**, 9204; (d) K. C. Nicolaou, J. A. Pfefferkorn and G.-Q. Cao, *Angew. Chem., Int. Ed.*, 2000, **39**, 734; (e) K. C. Nicolaou, G.-Q. Cao and J. A. Pfefferkorn, *Angew. Chem., Int. Ed.*, 2000, **39**, 739; (f) K. C. Nicolaou, J. A. Pfefferkorn, G.-Q. Roecker, C. S. Barluenga and H. J.

- Mitchell, *J. Am. Chem. Soc.*, 2000, **122**, 9939; (g) K. C. Nicolaou, J. A. Pfefferkorn, H. J. Mitchell, A. J. Roecker, S. Barluenga, G.-Q. Cao, R. L. Affleck and J. E. Lillig, *J. Am. Chem. Soc.*, 2000, **122**, 9954; (h) K. C. Nicolaou, J. A. Pfefferkorn, S. Barluenga, H. J. Mitchell, A. J. Roecker and G.-Q. Cao, *J. Am. Chem. Soc.*, 2000, **122**, 9968; (i) L. Uehlin and T. Wirth, *Org. Lett.*, 2001, **3**, 2931; (j) H. Qian, L.-X. Shao and X. Huang, *Synlett*, 2001, 1571; (k) H. Qian and X. Huang, *Tetrahedron Lett.*, 2002, **43**, 1059; (l) X. Huang and W. Xu, *Tetrahedron Lett.*, 2002, **43**, 5495.
- 9 (a) U. M. Lindstrom, *Chem. Rev.*, 2002, **102**, 2751; (b) *Modern Solvent in Organic Synthesis*, ed. P. Knochel, Springer-Verlag, Berlin, 1999; (c) *Organic Synthesis in Water*, ed. P. A. Grieco, Blacky Academic and Professional, London, 1998; (d) C.-J. Li and T.-H. Chan, *Organic Reactions in Aqueous Media*, Wiley, New York, 1997; (e) A. Lubineau, J. Auge and Y. Queneau, *Synthesis*, 1994, 741; (f) C.-J. Li, *Chem. Rev.*, 1993, **93**, 2023.
- 10 (a) Behaghel and Seibert, *Chem. Ber.*, 1932, **65**, 812; (b) Behaghel and Seibert, *Chem. Ber.*, 1933, **66**, 708; (c) D. G. Foster, *Recl. Trav. Chim. Pays-Bas*, 1934, **53**, 405.
- 11 Among various organic solvents, dichloromethane gave the highest yield of **10** from **6**; tetrahydrofuran: 34% yield, acetonitrile 11% yield (in this case, the deselenylation process was carried out in dichloromethane).
- 12 (a) R. Breslow, *Acc. Chem. Res.*, 1991, **24**, 159; (b) W. Blokzijl and J. B. F. N. Engberts, *Angew. Chem., Int. Ed. Engl.*, 1993, **32**, 1545.
- 13 K. B. Sharpless and M. W. Young, *J. Org. Chem.*, 1975, **40**, 947.
- 14 E. Kaiser, R. L. Colescott, C. D. Bossinger and P. I. Cook, *Anal. Biochem.*, 1970, **34**, 595.



Development of the continuous-flow reaction system based on the Lewis acid-catalysed reactions in a fluorous biphasic system†

Akihiro Yoshida, Xiuhua Hao and Joji Nishikido*

The Noguchi Institute and Japan Chemical Innovation Institute (JCII), Kaga, Itabashi-ku, Tokyo 173-0003, Japan. E-mail: nishikido@noguchi.or.jp; Fax: +81 3 5248 3597; Tel: +81 3 5248 3596

Received 25th April 2003

First published as an Advance Article on the web 6th August 2003

Lanthanide(III) bis(perfluoroalkanesulfonyl)amide-catalysed reactions such as esterification and Baeyer–Villiger reactions in organic-fluorous biphasic systems were performed to yield products with high TONs using the continuous-flow system of the small- and bench-scale apparatus which consisted of a reactor with a mechanical stirrer and a decanter. In the novel continuous-flow system, the Lewis acid catalyst is immobilised in a fluorous solvent while the substrates and the products obtained are dissolved in the mobile organic phase.

Introduction

Fluorous solvents such as perfluoroalkanes are emerging as valuable and environmentally benign media for catalytic transformation.¹ Recently, the concept of “fluorous biphasic catalysis” has been introduced as a novel phase separation and immobilisation technique which is applicable to recycling of a fluorous catalyst.^{1–6} Using a catalyst attached to fluorous ligands that have sufficient fluorine content to immobilise in the fluorous phase, the organic phase containing products is readily separated from the fluorous catalytic phase after the reactions in the organic-fluorous biphasic system.

We have already found that lanthanide(III) bis(perfluoroalkanesulfonyl)amides and tris(perfluoroalkanesulfonyl)methides would be highly active and readily recyclable catalysts of Lewis acid-promoted reactions such as esterification, Diels–Alder and Friedel–Crafts reactions in an organic-fluorous biphasic system.^{7,8} For example, catalytic esterification of cyclohexanol with acetic anhydride in a fluorous biphasic system is shown in Fig. 1.

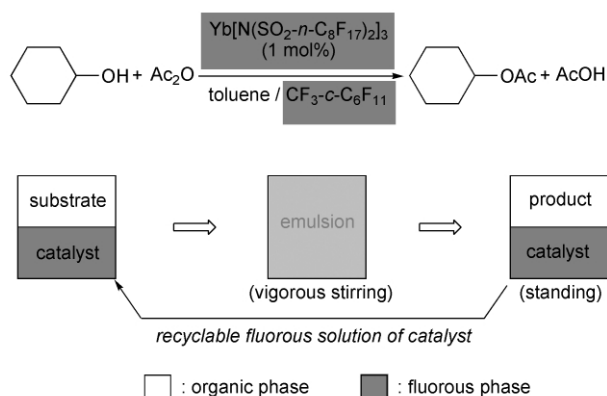


Fig. 1 Recyclable fluorous biphasic catalysis of $\text{Yb}[\text{N}(\text{SO}_2\text{-}n\text{-C}_8\text{F}_{17})_2]_3$.

Before the reaction, cyclohexanol and acetic anhydride are dissolved in the organic toluene phase, while the Yb(III) amide catalyst is dissolved in the fluorous perfluoro(methylcyclohex-

ane) phase. After the heterogeneous reaction with vigorous stirring, the resultant emulsion easily separates into an organic-fluorous biphasic system. The products, cyclohexyl acetate and acetic acid, are dissolved in the organic phase, whereas the Yb(III) catalyst still remains unchanged in the fluorous phase. Thus, the fluorous catalytic phase can be readily reused after removal of the upper organic phase. As an experimental result of this reaction for 20 min at 30 °C, the yield of cyclohexyl acetate was maintained at 98–99% even up to the 5th cycle.⁷

Our approach to the continuous-flow reaction was based on the above fluorous biphasic catalysis: a fluorous catalytic solution would be used as a stationary phase and an organic solution as a mobile phase. Development of the continuous-flow reaction system has been regarded as an important task for application to industrial processes since the continuous-flow system is much more productive than the corresponding batch system.⁹ Moreover, it is not necessary to use a large quantity of the fluorous solvent, which is relatively expensive. We report herein the first continuous-flow reactions based on the fluorous biphasic catalysis, by which the products were obtained with high turnover number (TON) using ytterbium(III) bis(perfluorooctanesulfonyl)amide in a novel continuous-flow apparatus consisted of a reactor with a mechanical stirrer and a decanter.

Green Context

While green chemistry research offers many exciting ideas for carrying out chemical processes in a more environmentally benign way, in many cases the cleaner chemistry can be frustrated by the chemists' mind set towards simple, stirred tank reactors. Here we see how a combination of known green chemistry methods — lanthanide catalysis and fluorous phase reactions, can be transformed from clever but essentially impractical chemistry processing to methodology with real application value through the use of more imaginative chemical engineering — the use of continuous flow reaction systems. In this way the expensive fluorous solvent–catalyst system can be repeatedly and easily recycled.

JHC

† Presented at The First International Conference on Green & Sustainable Chemistry, Tokyo, Japan, March 13–15, 2003.

Results and discussion

Our continuous-flow reaction system is as follows (Fig. 2). The fluorosolvent is poured into the reactor followed by adding a catalyst such as ytterbium(III) bis(perfluorooctanesulfonyl)amide, which is immobilised in the fluorosolvent because of its insolubility in general organic solvents (before reaction in Fig. 2). Next, the organic solution containing organic substrates

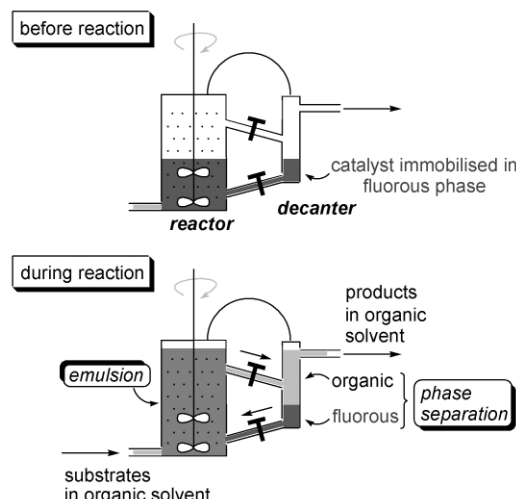


Fig. 2 Continuous-flow reaction model based on the fluorosolvent biphasic system.

and reagents as the mobile organic phase continuously flows into the stationary fluorosolvent phase in the reactor with vigorous stirring. The reaction proceeds in the resultant emulsion. After the reaction, the emulsion mixture is automatically introduced to the decanter where the organic-fluorosolvent phases are separated. Then, the upper organic phase overflows and the lower fluorosolvent phase is recycled (during reaction in Fig. 2). Thus, the substrates can be readily converted to the products through this continuous-flow system.

We performed acetylation of cyclohexanol with acetic anhydride in a biphasic system of toluene and GALDEN® SV135 (purchased from Solvay Solexis K.K.) catalysed by ytterbium(III) bis(perfluorooctanesulfonyl)amide using a small (60 mL) apparatus for the continuous-flow system. GALDEN® SV135 is a suitable fluorosolvent for fluorosolvent biphasic continuous-flow reactions due to its low solubility in toluene (<0.1 vol%). As a toluene solution of cyclohexanol and acetic anhydride was introduced to the fluorosolvent catalytic phase (30 mL) in the reactor at a rate of 0.103 mL min⁻¹ by a feed pump, the reaction proceeded successively for more than 250 h to give cyclohexyl acetate. During the reaction, chemical yield of the ester in the overflowing organic solution was maintained at >95% analysed by GC (Fig. 3), and ≤2 ppm of Yb was detected in an

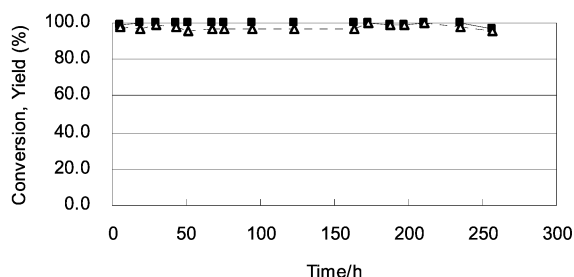


Fig. 3 Small-scale continuous-flow reaction (■-conversion of cyclohexanol, Δ-yield of cyclohexyl acetate).

overflowing organic solution by atomic emission spectrometry. This continuous-flow reaction achieved high TON of 5735 evaluated by the molar ratio of the product/catalyst.

We also carried out a bench-scale reaction, to apply to industrial processes using the novel continuous-flow system based on the design as shown in Fig. 4. A photo of our bench-scale system manufactured is shown in Fig. 5.

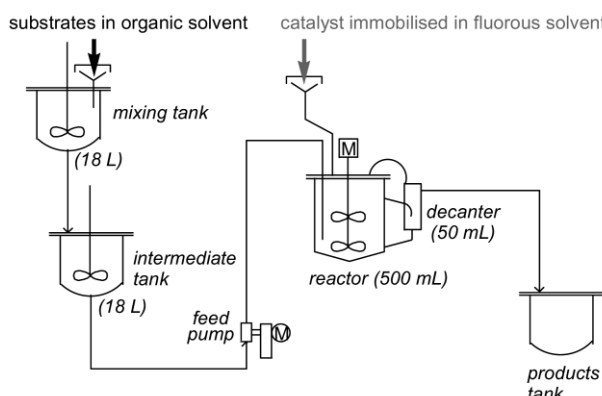


Fig. 4 Bench-scale continuous-flow reaction system.



Fig. 5 Photo of bench-scale continuous-flow reaction system (1: reactor, 2: decanter, 3: mixing tank, 4: intermediate tank, 5: products tank, 6: feed pump).

A toluene solution of cyclohexanol and acetic anhydride was poured into a mixing tank. GALDEN® SV135 (250 mL) and ytterbium(III) bis(perfluorooctanesulfonyl)amide, a catalyst, was added to the 500-mL reactor. As a toluene solution was introduced to the reactor through an intermediate tank at a rate of 0.967 mL min⁻¹, the reaction proceeded successively for more than 500 h. Chemical yield of cyclohexyl acetate was maintained at >90% during most of the reaction time, and ≤2 ppm of Yb was detected in an overflowing organic solution. Much higher TON of 9812 was attained for Lewis acid catalysis (Fig. 6).

This continuous-flow reaction system based on the organic-fluorosolvent biphasic system is superior to that based on the organic-aqueous biphasic system, which is represented by aqueous HRh(CO)(tppts)₃-catalysed hydroformylation known as the Ruhrchemie/Rhone-Poulenc process,⁹ when (1) unstable re-

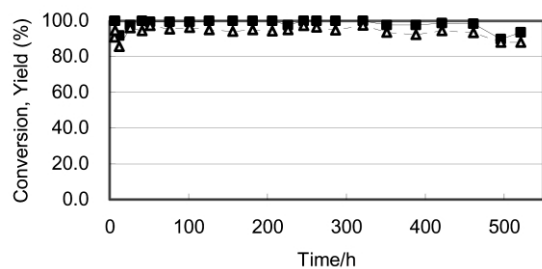
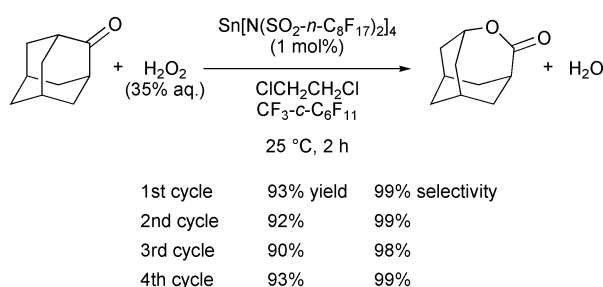


Fig. 6 Bench-scale continuous-flow reaction (■-conversion of cyclohexanol, Δ-yield of cyclohexyl acetate).

agents to water such as acetic anhydride are used, (2) aqueous reagents are used, or (3) water is formed as a by-product after the reactions. To confirm whether our continuous-flow system can be applied to the water-forming reaction using an aqueous reagent we attempted Baeyer–Villiger reaction of 2-adamantanone with 35 wt% aqueous solution of hydrogen peroxide, which we have recently reported in the batch system^{10,11} (Scheme 1).



Scheme 1 Baeyer–Villiger reaction in the fluorous biphasic batch system.

As a result of continuous-flow Baeyer–Villiger reaction of 2-adamantanone (0.1000 mL min⁻¹) with an equimolar amount of 34.6 wt% aqueous hydrogen peroxide (0.0028 mL min⁻¹) in 1,2-dichloroethane/GALDEN[®] SV135 biphasic catalysed by tin(IV) bis(perfluorooctanesulfonyl)amide, high selectivity and moderate to relatively high conversion were maintained for more than 200 h (Fig. 7) and TON attained 2191. A small

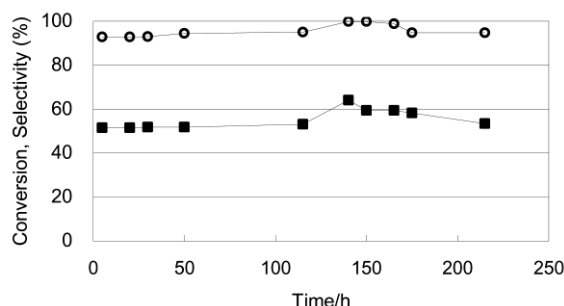


Fig. 7 Continuous-flow Baeyer–Villiger reaction using small-scale apparatus (■-conversion of adamantanone, ○-selectivity to lactone).

amount of water, derived from the aqueous solution of hydrogen peroxide and as a by-product of the reaction, could be successively removed from the reaction system by overflowing along with the organic phase. From the point of view of green chemistry and energy-saving, it is noteworthy that water can be removed from the reactor by simple phase separation-overflowing technique instead of azeotropic distillation.

In summary, we have developed a novel continuous-flow system based on the fluorous biphasic catalysis, *i.e.* immobilisation of our Lewis acid with fluorinated bisulfonamide ligands in the fluorous phase and effective phase separation to an organic-fluorous biphasic. The present continuous-flow system provided an efficient synthetic method, which could be a key technology of fluorous chemistry for industrial processes.

Experimental

General

¹H and ¹³C NMR spectra were measured on a JEOL JNM-ECA600 (600 MHz) spectrometer. Chemical shifts of ¹H NMR were expressed in parts per million relative to tetramethylsilane (δ 0.00) as an internal standard in chloroform-*d*. Chemical shifts of ¹³C NMR were expressed in parts per million relative to chloroform-*d* (δ 77.0). GC analysis was carried out on SHIMADZU GC-18A and GC-MS analysis was taken by Hewlett-Packard G1800A GLS. Atomic emission spectrometer is of IRIS/AP Nippon Jarrell Ash Co.

Typical procedure for continuous-flow reactions based on the fluorous biphasic system: acetylation of cyclohexanol using bench-scale (500 mL) apparatus.

To a solution of cyclohexanol (200.32 g, 2 mol) in dry toluene (6 L) was added acetic anhydride (245.02 g, 2.4 mol) and the solution was poured into a mixing tank for the mobile organic phase. Ytterbium(III) bis(perfluorooctanesulfonyl)amide (2.584 g, 0.83 mmol) and GALDEN[®] SV135 (250 mL; Solvay Solexis K.K.) were added to the reactor part kept at 40 °C. The mobile toluene phase was continuously introduced to the reactor through an intermediate tank at a rate of 0.967 mL min⁻¹ on vigorous stirring. After the reactor part was filled with the reaction mixture, the mixture flowed out to the decanter part kept at 25 °C. After 6.1 h, the upper organic phase automatically overflowed to the product tank. The overflowing toluene solution was analysed by GC using nonane as an external standard (Fig. 6). Before the mixing tank got empty, the toluene solution was provided.

Cyclohexyl acetate. ¹H NMR (600 MHz, CDCl₃) δ 1.2–1.4 (m, 5H), 1.5–1.6 (m, 1H), 1.7–1.8 (m, 2H), 1.8–1.9 (m, 2H), 2.03 (s, 3H), 4.7–4.8 (m, 1H); ¹³C NMR (150 MHz, CDCl₃) δ 21.5, 23.8, 25.4, 31.7, 72.6, 170.4; MS (EI, 70 eV): *m/z* 127 (C₆H₁₁CO₂⁺), 99 (C₆H₁₁O⁺), 82 (C₆H₁₀⁺), 67, 43 (CH₃CO⁺); Elemental analysis (%) calcd for C₈H₁₄O₂: C 67.57, H 9.92, found: C 67.41, H 9.96.

Continuous-flow reactions based on the fluorous biphasic system: Baeyer–Villiger reaction of 2-adamantanone using small-scale (60 mL) apparatus

A solution of 2-adamantanone (15.02 g, 100 mmol) in 1,2-dichloroethane (300 mL) and 34.6 wt% aqueous hydrogen peroxide were continuously and independently introduced to a reactor, which contained tin(IV) bis(perfluorooctanesulfonyl)amide (404 mg, 0.1 mmol) in GALDEN[®] SV135 (30 mL) and was kept at 30 °C, at a flow rate of 0.1000 mL min⁻¹ and 0.0028 mL min⁻¹, respectively, on vigorous stirring. After 5 h, the upper organic phase including a small amount of water automatically overflowed, which was analysed by GC using nonane as an external standard.

4-Oxatricyclo[4.3.1.1^{3,8}]undecan-5-one. ¹H NMR (600 MHz, CDCl₃): δ 1.63–2.11 (m, 12H), 3.08 (br s, 1H), 4.49 (br s, 1H); ¹³C NMR (150 MHz, CDCl₃): δ 25.82, 30.94, 33.79, 35.74, 41.21, 73.12, 178.92.

Acknowledgements

This work was supported by New Energy and Industrial Technology Development Organization (NEDO) through the

R&D program for Process Utilizing Multi-Phase Catalytic Systems.

References

- 1 I. T. Horváth and J. Rábai, *Science*, 1994, **266**, 72.
- 2 I. T. Horváth, *Acc. Chem. Res.*, 1998, **31**, 641.
- 3 D. P. Curran, *Angew. Chem., Int. Ed. Engl.*, 1998, **37**, 1175.
- 4 B. Cornils, *Angew. Chem., Int. Ed. Engl.*, 1997, **36**, 2057.
- 5 L. P. Barthel-Rosa and J. A. Gladysz, *Coord. Chem. Rev.*, 1999, **192**, 587.
- 6 J. A. Gladysz and D. P. Curran, *Tetrahedron*, 2002, **58**, 3823.
- 7 K. Mikami, Y. Mikami, H. Matsuzawa, Y. Matsumoto, J. Nishikido, F. Yamamoto and H. Nakajima, *Tetrahedron*, 2002, **58**, 4015.
- 8 K. Mikami, Y. Mikami, Y. Matsumoto, J. Nishikido, F. Yamamoto and H. Nakajima, *Tetrahedron Lett.*, 2001, **42**, 289.
- 9 B. Cornils and E. G. Kuntz, *J. Organometal. Chem.*, 1995, **502**, 177.
- 10 X. Hao, O. Yamazaki, A. Yoshida and J. Nishikido, *Tetrahedron Lett.*, 2003, **44**, 4977.
- 11 X. Hao, O. Yamazaki, A. Yoshida and J. Nishikido, *Green Chem.*, **5**, DOI: 10.1039/b304439d, this issue.



Synthesis of dimethyl carbonate by vapor phase oxidative carbonylation of methanol†

Hirofumi Itoh,^{*a} Yoshiyuki Watanabe,^b Kenji Mori^c and Hiroshi Umino^b

^a JGC Corporation, 2205, Narita-cho, Oarai-machi, Ibaraki, 311-1313, Japan.

E-mail: ito.hirofumi@jgc.co.jp

^b JGC Corporation, 2-3-1, Minato Mirai, Nishi-ku, Yokohama, Kanagawa, 220-6001, Japan

^c Nikki Chemical Co., LTD, 1-26, Takiya-cho, Niitsu, Niigata, 956-0855, Japan

Received 25th April 2003

First published as an Advance Article on the web 19th August 2003

To develop a vapor phase dimethyl carbonate synthesis process, the effects of reaction conditions and contaminants in feed materials on reaction performance have been investigated for CuCl₂/NaOH/activated carbon catalysts. A small spherical activated carbon particle with an average diameter of 60 μm was newly prepared. Optimal conditions for reaction temperature, pressure, contact time and reactant molar ratio were determined as follows: 393–423 K, 0.7–1.0 MPa, 0.1–0.3 kg-cat h m⁻³ and CH₃OH : CO : O₂ = 1 : 3–4 : 0.07–0.12, respectively. Among contaminants introduced, N₂, H₂, and CO₂ did not affect the catalyst performance. However, H₂O in the feed decreased the conversion of methanol and the selectivity of carbon monoxide to dimethyl carbonate. A fluidized bed reactor is preferable for the vapor phase reaction, considering the required temperature control and continual catalyst regeneration.

Introduction

Dimethyl carbonate (DMC) has been attracting wide attention as an environmentally benign chemical raw material.^{1–4} DMC is used as a safe alternative to phosgene in carbonylation, such as for production of polycarbonate, and to methyl halide or dimethyl sulfate in methylation. Besides these applications as a chemical intermediate, DMC is also drawing attention as a safe solvent and a fuel additive. DMC, as a solvent,⁵ has a good solvating ability, optimum volatility, easy biodegradability, very low photochemical ozone creating potential (POCP) and obvious benignity towards living beings and the environment. DMC, as a fuel additive,⁶ has an oxygen content about 3 times that of methyl *tert*-butyl ether (MTBE), and it does not cause phase separation of water.

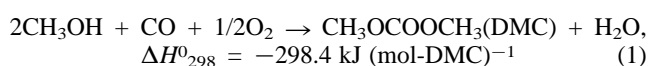
There are several synthetic methods for producing DMC, such as oxidative carbonylation of methanol, carbonylation of methyl nitrite and an ester exchange between methanol and an alkylene carbonate. EniChem first commercialized a DMC production process based on a liquid phase oxidative carbonylation of methanol in the presence of copper(I) chloride as a catalyst. This process, however, has some difficulties such as the separation of products from the catalyst, and corrosion of equipment and rapid deactivation of the catalyst due to the accumulation of water in the liquid phase.

To overcome these problems vapor phase oxidative carbonylation processes have been proposed. For example, Dow Chemical reported^{7,8} a process for producing DMC by a vapor phase oxidative carbonylation in the presence of a catalyst comprising a metal halide or a mixed metal halide impregnated on a carrier, especially, copper(II) chloride and copper(II) chloride/potassium chloride impregnated on activated carbon (AC). However, conversion of methanol and selectivity for DMC was not satisfactory and a large amount of by-products are generated. In the report, it is observed that non-catalytic thermal oxidation of CO to CO₂ is significant above 403 K.

Furthermore, catalyst systems such as CuNaX,⁹ PdCl₂–CuCl₂–CH₃COOK/AC¹⁰ and CuCl₂/AC¹¹ were reported.

JGC Corporation claimed several patents^{12–14} on vapor phase oxidative carbonylation in the presence of a supported catalyst. The catalyst, consisting of a copper halide and at least one hydroxide compound selected from the group consisting of alkali metal hydroxides and alkali earth metal hydroxides supported on activated carbon, proved to have good performance. Recently Lee *et al.*¹⁵ and Genhui *et al.*¹⁶ reported synthesis of DMC by vapor phase oxidative carbonylation using a supported copper catalyst which is the same as that used by JGC.

Because oxidative carbonylation of methanol is highly exothermic, as shown in the following eqn. (1),



and as the optimal temperature range is relatively narrow, a fluidized bed reactor is preferable for vapor phase DMC production.

Here, we report optimal reaction conditions, a procedure for regenerating a catalyst and a preparation of granular spherical activated carbon for good fluidization to develop a vapor phase DMC synthesis process using a fluidized bed reactor.

Green Context

Dimethyl carbonate (DMC) is a good example of a “greener” chemical. It can be used as a phosgene alternative in carbonylations, as a fuel additive and as a solvent. Most reported synthetic routes to DMC including a commercial process are liquid phase and suffer from separation difficulties and catalyst deactivation. Here a vapour phase route based on the oxidative carbonylation of methanol is described. A regenerable solid catalyst is used. The effects of potential catalyst poisons are described.

JHC

† Presented at The First International Conference on Green & Sustainable Chemistry, Tokyo, Japan, March 13–15, 2003.

Experimental

Catalyst preparation

In this study, two different sizes of spherical activated carbon (SAC) were used as catalyst supports. The large SAC, denoted by AC(380) with an average diameter of 380 μm , was obtained from Kureha Chemical Industry Co. The SAC with a smaller diameter, denoted by AC(60), was newly prepared by a process comprising carbonization of a spherical granular phenolic resin by heating to about 773–973 K and activation of the carbonized resin by heating in air to about 1173 K while preventing blocking of the resin.¹⁷ As shown in Fig. 1, the AC(60) diameter

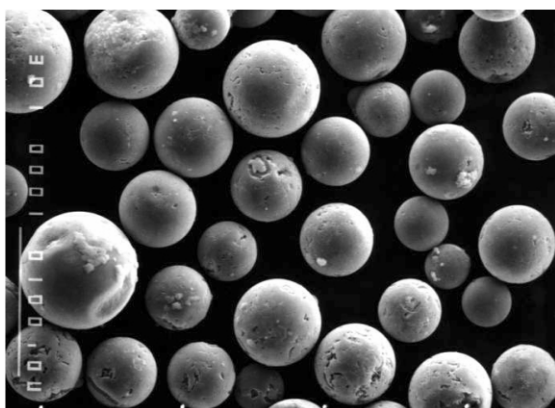


Fig. 1 Scanning electron micrograph of $\text{CuCl}_2/\text{NaOH}/\text{AC}(60)$ with an average diameter of 60 μm .

was less than 100 μm (average diameter = 60 μm) and the attrition rate of this SAC measured by a fluidization test was less than or equal to that of the catalyst for fluidized catalytic cracking (FCC). This newly developed granular spherical activated carbon is classified as an A' particle in the Geldart particle classification,¹⁸ which shows the excellent fluidity of this SAC.¹⁹ The BET surface areas of AC(380) and AC(60) were 1172 and 1008 $\text{m}^2 \text{g}^{-1}$, respectively. Based on our patent, $\text{CuCl}_2/\text{NaOH}/\text{AC}(380)$ containing 7.8 wt% Cu and $\text{CuCl}_2/\text{NaOH}/\text{AC}(60)$ containing 6.2 wt% Cu were prepared by the following procedure. First, an aqueous solution of $\text{CuCl}_2 \cdot 2\text{H}_2\text{O}$ was impregnated on SAC by a pore-filling method, followed by drying at 393 K for 8 h. Second, CuCl_2 supported on SAC was partially neutralized by $\text{NaOH}(\text{aq})$ with a ratio of Na/Cu of 1.3, followed by drying at 393 K for 8 h. Both catalysts supported on AC(380) and AC(60) showed essentially the same performance for the oxidative carbonylation of methanol.

Oxidative carbonylation

In this report, all experiments were carried out in a fixed bed reactor equipped with a backpressure regulator. A stainless steel tube reactor which had a diameter of 6 mm (outer) \times 4 mm (inner) was used and set up with a sand-bath heater to create an isothermal condition. Methanol was fed in by a micro pump and then heated sufficiently to vaporize. Carbon monoxide and oxygen were fed in, regulated by a mass-flow controller. These reactants and nitrogen as an internal standard were mixed and preheated. Liquid and gas products were analyzed by three TCD (thermal conductivity detector) gas chromatographs using the following columns, respectively: WG-100 (GL Sciences Inc.) for inorganic gases, N_2 , O_2 , CO and CO_2 ; two Gaskuropack54 (GL Sciences Inc.) for gas and liquid organic compounds: methanol, dimethyl carbonate (DMC), methyl formate (MF) and dimethoxymethane (DMM).

The effects of reaction conditions were evaluated by changing each condition in the following range: temperature =

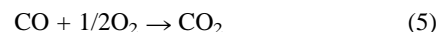
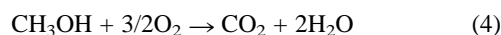
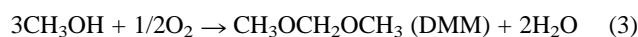
393–433 K, pressure = 0.5–1.0 MPa, W/F (catalyst weight/flow rate) = 0.03–1.6 kg h m^{-3} , and feed molar ratio of $\text{CH}_3\text{OH} : \text{CO} : \text{O}_2 = 1 : 1-4 : 0.05-0.2$. Conversion and selectivity were calculated according to the following equations: conversion of CH_3OH (C_{MeOH} , %) = $(1 - \text{CH}_3\text{OH unreacted}/\text{CH}_3\text{OH fed}) \times 100$. Selectivity for DMC from CH_3OH or CO (S_{MeOH} or S_{CO} , %) = $(\text{DMC produced}/(\text{CH}_3\text{OH reacted}/2) \text{ or } \text{CO reacted}) \times 100$.

For catalyst regeneration, a deactivated catalyst was treated with a nitrogen stream containing 5 vol% HCl at 413 K under atmospheric pressure until HCl broke through.

Results and discussion

Reaction conditions

In the vapor phase oxidative carbonylation on $\text{CuCl}_2/\text{NaOH}/\text{AC}$ catalysts, DMC was synthesized with good selectivity. MF, DMM and CO_2 were produced as by-products. A trace amount of methyl chloride was also observed. These by-products are assumed to be formed by the following reactions:



In this study, the effects of various reaction conditions have been investigated from the viewpoint of process development.

C_{MeOH} , S_{MeOH} , and S_{CO} were affected by these operating parameters.

Concerning the reaction temperature, it has been reported that on CuCl_2/AC catalyst non-catalytic thermal oxidation of CO occurred significantly above 403 K,⁷ and a large amount of CO_2 was produced above 423 K and optimal temperature is in the range of 393–413 K.¹⁵ On $\text{CuCl}_2/\text{NaOH}/\text{AC}$ catalysts, although the production of CO_2 increased above 423 K in agreement with the above-mentioned results, for C_{MeOH} and S_{CO} the suitable temperature was at around 413 K, which was higher than that on CuCl_2/AC catalyst. It shows that a $\text{CuCl}_2/\text{NaOH}/\text{AC}$ catalyst suppresses the CO_2 formation up to a higher temperature than a CuCl_2/AC catalyst.

C_{MeOH} increased significantly when increasing the reaction pressure up to about 0.5 MPa on $\text{CuCl}_2/\text{NaOH}/\text{active carbon}$ type catalysts, presumably because of the increase of actual contact time and concentrations of reactants which are adsorbed to react on the catalyst. The effect of a reaction pressure above 0.6 MPa is shown in Fig. 2. It may be considered that the

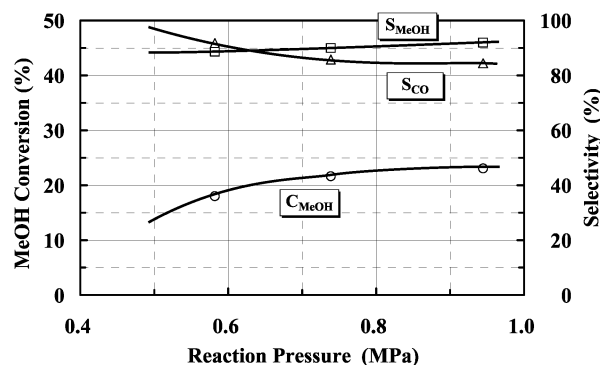


Fig. 2 Effect of reaction pressure on catalyst performance. Reaction conditions: catalyst = $\text{CuCl}_2/\text{NaOH}/\text{AC}(60)$; temp. = 413 K; W/F = 0.12 kg-cat h m^{-3} , reactant molar ratio ($\text{CH}_3\text{OH} : \text{CO} : \text{O}_2$) = 1 : 3 : 0.1.

reactive species on the catalyst surface are saturated at this pressure. Concerning the selectivities for DMC, when increas-

ing the reaction pressure, S_{MeOH} increased slightly, but S_{CO} decreased up to 0.6 MPa and then remained almost constant. As shown in Fig. 2, at the pressure range of 0.8 to 1.0 MPa, the catalyst performance was very stable and this pressure range is suitable for operation.

The W/F was varied to evaluate the effect of the contact time on a $\text{CuCl}_2/\text{NaOH}/\text{AC}(60)$ catalyst and the results are plotted in Fig. 3. Here, using an apparent bulk density of 0.65 kg m^{-3} for

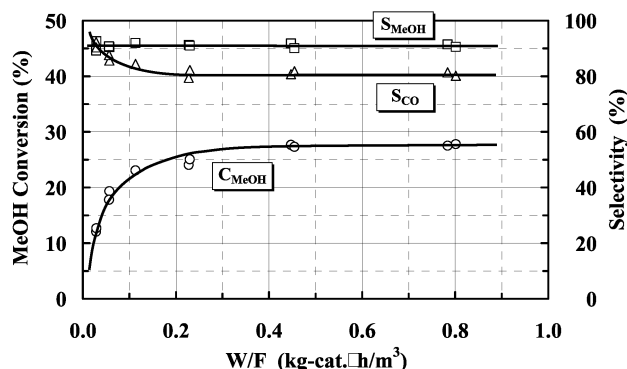


Fig. 3 Effect of contact time (W/F). Reaction conditions: catalyst = $\text{CuCl}_2/\text{NaOH}/\text{AC}(60)$; temp. = 413 K; press. = 0.94 MPa, reactant molar ratio ($\text{CH}_3\text{OH} : \text{CO} : \text{O}_2$) = 1 : 3 : 0.1.

this catalyst, a W/F of $1 \text{ kg-cat h m}^{-3}$ corresponds to a contact time of 5.54 s and conversely the contact time of 1 s corresponds to a W/F of $0.18 \text{ kg-cat h m}^{-3}$. As shown in Fig. 3, C_{MeOH} increased significantly up to around $0.1 \text{ kg-cat h m}^{-3}$ and in the same range, S_{CO} decreased from higher than 90 to 80%. Above this range, the increasing or decreasing rate of C_{MeOH} or S_{CO} , respectively, declined. On the other hand, S_{MeOH} remained constant over the whole range. Under this condition, the performance was stable above $0.5 \text{ kg-cat h m}^{-3}$, because of 100% O_2 conversion. When the ratio of $\text{O}_2/\text{CH}_3\text{OH}$ was increased to 0.15 at a W/F of $0.8 \text{ kg-cat h m}^{-3}$, C_{MeOH} rose to 35%. From the viewpoint of DMC yield on unit volume of catalyst, it is considered that the range from 0.1 to $0.3 \text{ kg-cat h m}^{-3}$ is the optimal condition for the oxidative carbonylation in a vapor phase.

According to eqn. (1), the stoichiometric ratio of reactants are 2 : 1 : 0.5 for CH_3OH , CO and O_2 , respectively.

The reactant feed ratios, which have significant effects on C_{MeOH} , S_{MeOH} and S_{CO} and affect the process operation conditions, were examined on a $\text{CuCl}_2/\text{NaOH}/\text{AC}(60)$ catalyst.

At first, under constant feed rates of CH_3OH and O_2 , the molar ratio of CO to CH_3OH was changed from 1 to 4. As shown in Fig. 4, C_{MeOH} and S_{MeOH} rose in the same manner as

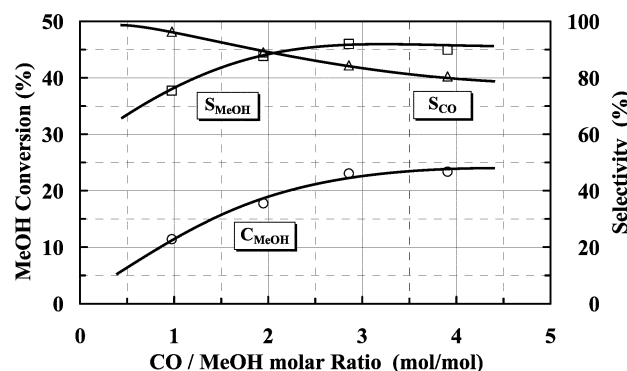


Fig. 4 Effect of the molar ratio of $\text{CO}/\text{CH}_3\text{OH}$. Reaction conditions: catalyst = $\text{CuCl}_2/\text{NaOH}/\text{AC}(60)$; temp. = 413 K; press. = 0.94 MPa, W/F = $0.11 \text{ kg-cat h m}^{-3}$ at molar ratio of $\text{CO}/\text{CH}_3\text{OH}$ = 2.9.

increasing the molar ratio of $\text{CO}/\text{CH}_3\text{OH}$. S_{CO} , however, decreased linearly between the ratio of 1 to 3, and then the

decrease became moderate. From this result, the preferred molar ratio of $\text{CO}/\text{CH}_3\text{OH}$ is considered to be 3 through 4 for the catalyst performance.

Consequently the effect of the O_2/MeOH molar ratio was examined by the same method as above for CO. The results were plotted in Fig. 5. C_{MeOH} had a maximal point at around 0.1

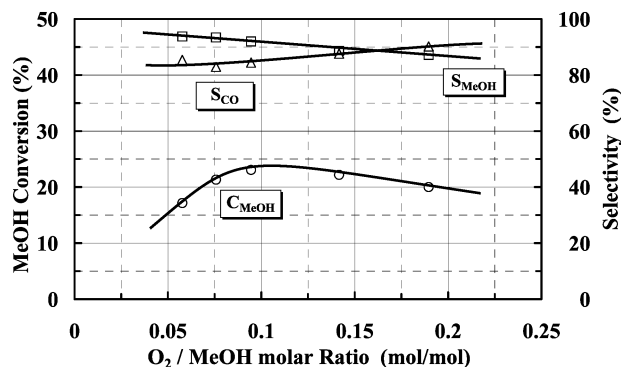


Fig. 5 Effect of the molar ratio of $\text{O}_2/\text{CH}_3\text{OH}$. Reaction conditions: catalyst = $\text{CuCl}_2/\text{NaOH}/\text{AC}(60)$; temp. = 413 K; press. = 0.94 MPa, W/F = $0.11 \text{ kg-cat h m}^{-3}$ at molar ratio of $\text{O}_2/\text{CH}_3\text{OH}$ = 0.10.

for the change in the molar ratio of $\text{O}_2/\text{CH}_3\text{OH}$, and S_{MeOH} decreased, while S_{CO} increased significantly. From this result on a $\text{CuCl}_2/\text{NaOH}/\text{AC}(60)$ catalyst under these conditions, it is considered that the adsorbed CH_3OH is easily oxidized by oxygen compared with CO, although the detailed mechanisms and the actual reaction species are not clarified. The optimal molar ratio of $\text{O}_2/\text{CH}_3\text{OH}$ is considered to be around 0.1.

Catalyst life and regeneration

Although a series of $\text{CuCl}_2/\text{NaOH}/\text{AC}$ catalysts show high performance in the vapor phase oxidative carbonylation of methanol, the activities of these catalysts decreased with time on stream. The deactivation rate depended on the reaction conditions, the Cu content and the preparation method of the catalysts. Curnett *et al.*⁷ and Lee *et al.*¹⁵ have reported that $\text{Cu}_2(\text{OH})_3\text{Cl}$ was related to the catalytic activity. Furthermore, we have considered that a copper oxychloride such as Cu_2OCl_2 is an active species, the same as in the case of CuNaX catalyst.²⁰ Though the exact structure of the active sites is unclear, it is certain that they are strongly related to the bonding structure between copper and chlorine atoms. A relationship between the copper content and the activity has also been reported.^{7,15} Curnett *et al.*, moreover, showed that the chlorine content of the 90 h-used CuCl_2/AC catalyst decreased compared with that of the fresh catalyst and was regenerated by treating with HCl-containing gas.⁷

In Fig. 6, the change in the performance of the fresh and the regenerated $\text{CuCl}_2/\text{NaOH}/\text{AC}(60)$ catalyst is shown. The catalyst activity, C_{MeOH} , decreased with time on stream. After 50 h, the deactivated catalyst was treated with 5 vol% HCl containing nitrogen gas, so that the catalyst performance recovered to the fresh level. As for the regenerated catalyst, C_{MeOH} was first decreased gradually and then quickly deactivated. As shown in Fig. 6, the deactivated rate of the fresh catalyst was larger than that of the regenerated catalyst. This seemed to be the reason why the chlorine content of the fresh catalyst is low due to evaporation of HCl formed by hydration during the preparation of the catalyst. In the oxidative carbonylation on $\text{CuCl}_2/\text{NaOH}/\text{AC}$, methyl chloride was also detected as a by-product at about 10–50 ppm in the reactor effluent on the fresh catalyst. The formation of methyl chloride is considered to be one of the reasons for the deactivation. On the other hand, S_{MeOH} was almost constant during the reaction. S_{CO} decreased from 80 to 70% on the second and the third-time regenerated catalysts.

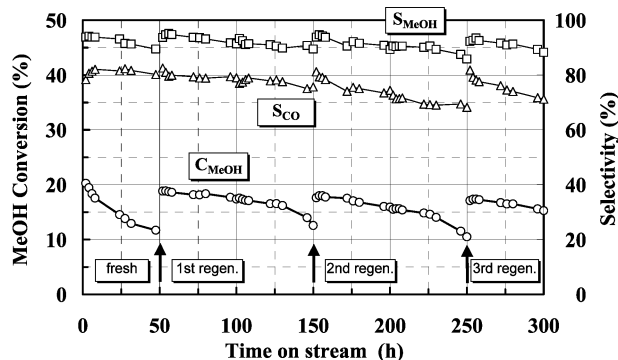


Fig. 6 Change of catalyst performance with time on stream and regeneration by treating with HCl-containing gas. Reaction conditions: catalyst = CuCl₂/NaOH/AC(60); temp. = 413 K; press. = 0.94 MPa, W/F = 0.22 kg-cat h m⁻³, reactant molar ratio (CH₃OH : CO : O₂) = 1 : 3 : 0.06. At the time shown with arrows, regenerated operations were carried out three times.

Thus, Fig. 6 shows that deactivated catalyst can be regenerated by treatment with HCl-containing gas. The ratios of Cl/Cu of the deactivated catalysts were 1.5 to 1.7, and those of the regenerated catalysts were about 2.0.

Contaminants in raw and recycled materials

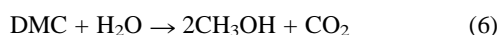
For the design of a process for DMC synthesis by oxidative carbonylation, the effect of contaminants in raw and recycled materials was evaluated. In this reaction on CuCl₂/NaOH/AC catalysts, as one-pass conversions of CH₃OH and CO are about 15–25 and 3–5%, respectively, these reactants need to be recycled after separation of reactor effluent gas. The effect of CO₂ and H₂O as by-products, and N₂ and H₂, as contaminants of raw CO were investigated and are summarized in Table 1

Table 1 The effect of contaminants in raw and recycled materials

Contaminants	C _{MeOH} (%)	S _{MeOH} (%)	S _{CO} (%)
Base condition ^a	17.2	93.2	77.9
N ₂ (34% in CO) ^b	17.0	92.6	80.2
H ₂ (15% in CO) ^b	17.1	91.7	79.5
CO ₂ (10% in CO) ^b	17.0	93.7	78.0
H ₂ O (1 wt% in CH ₃ OH) ^b	16.0	93.9	77.3

^a Reaction conditions: catalyst = CuCl₂/NaOH/AC(380); temp. = 413 K; press. = 0.89 MPa, W/F = 0.23 kg-cat h m⁻³, reactant molar ratio (CH₃OH/CO/O₂) = 1 : 3 : 0.1. ^b Percentage means concentration in CO or CH₃OH.

compared with the results of the base condition without contaminants. For all the contaminants except for H₂O, essentially the same performance of the catalyst was obtained. It can be concluded that contaminants except for H₂O did not affect reaction performance. However, H₂O slightly decreased C_{MeOH}. DMC can be hydrolyzed by H₂O in accordance with eqn. (6).



When this reaction proceeds during the oxidative carbonylation on CuCl₂/NaOH/AC catalysts, as a result of the total reaction (eqn. (1) and (6)), the oxidation of CO to CO₂ appears to occur. For this reason, S_{CO} decreases when H₂O is added to the feed methanol. In Fig. 7, the effect of the H₂O content on the catalyst performance is shown. C_{MeOH} decreased significantly with increasing the H₂O content in CH₃OH. It was also observed that S_{CO} decreased at a high content of H₂O, showing the hydration of DMC according to eqn. (6).

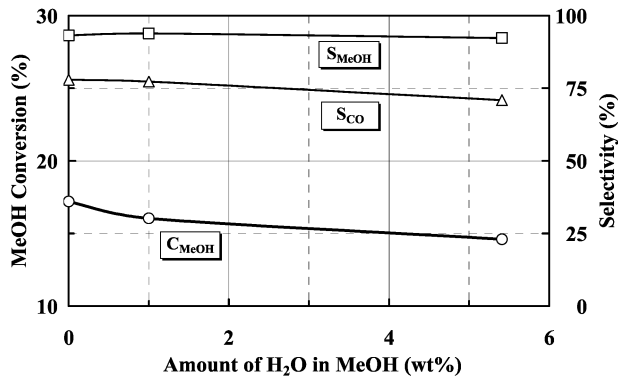


Fig. 7 Effect of H₂O in CH₃OH on catalyst performance. Reaction conditions: catalyst = CuCl₂/NaOH/AC(380); temp. = 413 K; press. = 0.89 MPa, W/F = 0.11 kg-cat h m⁻³, reactant molar ratio (CH₃OH : CO : O₂) = 1 : 3 : 0.1.

Conclusion

The optimal reaction conditions using a fixed bed reactor on CuCl₂/NaOH/AC(60) and (380) catalysts, are summarized as follows:

- Temperature: 393–423 K,
- Pressure: 0.7–1.0 MPa,
- Contact time (W/F): 0.1–0.3 kg-cat h m⁻³,
- Reactant molar ratio: CH₃OH : CO : O₂ = 1 : 3–4 : 0.07–0.12.

CuCl₂/NaOH/AC catalyst deactivates with time on stream and can be regenerated by treatment with a HCl-containing gas.

For the design of a DMC production process, the effect of contaminants such as N₂, H₂, CO₂ and H₂O in the raw and recycled streams were investigated. Contaminants, except for H₂O, do not affect the reaction performance. However, H₂O slightly decreases the conversion of CH₃OH and selectivity of CO for DMC.

From a simulation based on the above-mentioned results, such as a narrow appropriate temperature range, a catalyst regeneration cycle and a highly exothermic reaction, a fluidized bed reactor has been selected for this reaction.

In this study, a granular spherical activated carbon with average diameter of 60 μm is newly prepared for a fluidized bed reactor. Reaction results using a fluidized bed reactor and the results of fluidization experiments with large diameter cold model equipment will be further reported elsewhere.

References

- 1 D. Delledonne, F. Rivetti and U. Romano, *Appl. Catal. A*, 2001, **221**, 241.
- 2 F. Rivetti, in *Green Chemistry: Challenging Perspectives*, ed. P. Tundo and P. Anastas, Oxford University Press, New York, 2001.
- 3 Y. Ono, *Catal. Today*, 1997, **35**, 15.
- 4 Y. Ono, *Pure Appl. Chem.*, 1996, **68**, 367.
- 5 F. Mizia, M. Notani, F. Rivetti, U. Romano and C. Zecchini, *Chim. Ind. (Milan)*, 2001, **83**, 47.
- 6 M. A. Pacheco and C. L. Marshall, *Energy Fuel*, 1997, **11**, 2.
- 7 G. L. Curnutt and A. D. Harley, *Oxygen Complexes Oxygen Act. Transition Met. Proc. Annu. IUCCP Symp., 5th Meeting*, ed. A. E. Martell and D. T. Sawyer, Plenum, New York, 1987, pp. 215–32.
- 8 G. L. Curnutt, WO 87/07601, 1987.
- 9 S. T. King, *J. Catal.*, 1996, **161**, 530.
- 10 W. Yanji, Z. Xingiang, Y. Baoguo, Z. Bingchang and C. Jinsheng, *Appl. Catal.*, 1998, **171**, 255.
- 11 K. Tomishige, T. Sakai, S. Sakai and K. Fujimoto, *Appl. Catal. A*, 1999, **181**, 95.
- 12 T. Koyama, M. Tonosaki, N. Yamada and K. Mori, US Pat. 5347031, 1994.
- 13 T. Koyama, M. Tonosaki, N. Yamada and K. Mori, US Pat. 5512528, 1996.
- 14 T. Koyama, M. Tonosaki, N. Yamada and K. Mori, US Pat. 5650369, 1997.

- 15 M. S. Han, B. G. Lee, I. Suh, H. S. Kim, B. S. Ahn and S. I. Hong, *J. Mol. Catal. A*, 2001, **170**, 225.
- 16 M. Xinbin, Z. Renzhe, X. Genhui, H. Fei and C. Hong Fang, *Catal. Today*, 1996, **30**, 201.
- 17 S. Fujii, S. Inada, T. Kosaka and H. Ito, Jpn. Pat. 2000233916, 2000.
- 18 D. Gerdart, *Powder Technol.*, 1973, **7**, 285.
- 19 D. Knii and O. Levenspiel, *Fluidization Engineering*, 2nd edn., Butterworth-Heinemann, Boston, 1991.
- 20 M.-Y. Lee and D.-C. Park, *Stud. Surf. Sci. Catal.*, **66** (*Dioxygen Activation and Homogeneous Catalytic Oxidation*), 1991, pp. 631–640.



An environmentally benign process for aromatic polycarbonate synthesis by efficient oxidative carbonylation catalyzed by Pd-carbene complexes†

Ken-ichi Okuyama,^{ab} Jun-ichi Sugiyama,^{*a} Ritsuko Nagahata,^a Michihiko Asai,^a Mitsuru Ueda^{ab} and Kazuhiko Takeuchi^a

^a National Institute of Advanced Industrial Science and Technology (AIST), Tsukuba Central 5, 1-1-1 Higashi, Tsukuba, Ibaraki 305-8565, Japan. E-mail: sugiyama-j@aist.go.jp; Fax: +81-29-861-6327; Tel: +81-29-861-6300

^b Tokyo Institute of Technology, 2-12-1 Ookayama, Meguro-ku, Tokyo 152-8552, Japan

Received 30th April 2003

First published as an Advance Article on the web 24th July 2003

The direct synthesis of diphenyl carbonate (DPC) and polycarbonate (PC) by oxidative carbonylation was investigated. A palladium catalyst anchored to a resin *via* a heterocyclic carbene ligand exhibited high performance in DPC synthesis, and the total turnover number (TON) achieved 5100 (mol-DPC/mol-Pd). Bisphenol A was also effectively converted to high molecular weight PC (M_w 22,400) at 95% yield.

Introduction

Aromatic polycarbonate (PCs) are one of the most useful engineering plastics due to their good heat resistance, mechanical properties, and transparency.¹ PCs are commonly prepared by interfacial polycondensation of bisphenol A with phosgene. The transesterification method is gaining popularity in response to current demands that the chemical industry adopt a safer and more environmentally benign process for PC synthesis. The transesterification method has the advantages of involving no solvent and no salt formation. Generally, diphenyl carbonate (DPC) is used as a carbonyl source in the transesterification method. As an industrial method, although DPC can be prepared without phosgene, it involves a long process. In one typical method, DPC can be made from ethylene converted through ethylene oxide, ethylene carbonate, dimethyl carbonate, methyl phenyl carbonate, and diphenyl carbonate in turn. The direct preparation of DPC or PC from phenols with carbon monoxide would clearly be a simple and environmentally more benign process² (Scheme 1). Previous reports on oxidative

In particular, catalyst systems based on palladium-carbene complexes can produce high molecular weight PC ($M_n = 24,000$) at good yields.⁵ These catalyst systems work under homogeneous conditions, however, impeding effective recovery of the palladium. Here we report the preparation and reaction of a palladium catalyst that is anchored to a resin *via* a heterocyclic carbene ligand.

Results and discussion

The homogeneous Pd-carbene complex (**PdCl₂(c1-R)**) and heterogeneous Pd-carbene complex (**PSt-Pd(R)**) are illustrated in Fig. 1. The **PSt-Pd(R)** version was synthesized as follows.

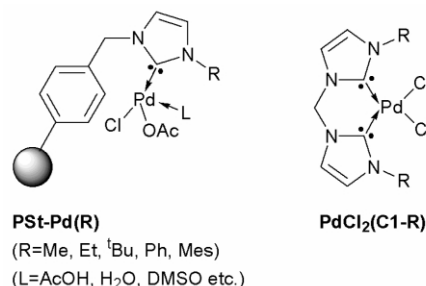
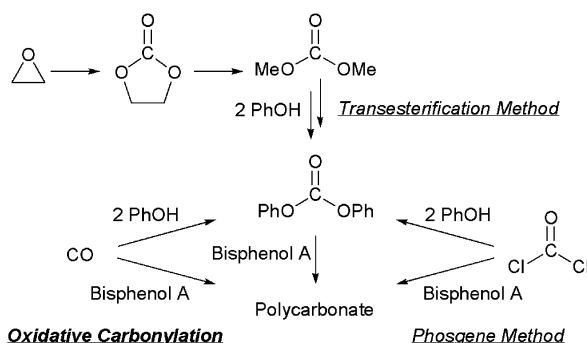


Fig. 1 Structure of Pd-carbene complexes.

Polymeric ligands were synthesized by mixing commercially available polystyrene resin containing a chloromethyl group



Scheme 1 Synthetic routes for carbonate.

carbonylation have described the synthesis of low molecular weight PC (number-averaged molecular weight $M_n < 2800$).³ On the other hand, we have recently developed an effective catalytic system for the direct synthesis of aromatic carbonates.⁴

† Presented at The First International Conference on Green & Sustainable Chemistry, Tokyo, Japan, March 13–15, 2003.

Green Context

This paper introduces a clever direct route for the preparation of polycarbonate, which avoids the use of phosgene. The trick here is to carry out the oxidative carbonylation of phenol (to generate the phosgene replacement) *in situ* and to directly carry out the polymerization without isolation. The catalyst used is a heterogeneous Pd species, which can be readily recovered.

DJM

(0.90 or 1.74 wt%) and N-substituted imidazole in toluene at 130 °C for 1 day. All the **PSt-Pd(R)** was synthesized by mixing the resulting polymeric ligand and palladium acetate (Pd(OAc)₂) in dimethyl sulfoxide (DMSO) for 1 h *in vacuo* at 50 °C. **PSt-Pd(R)** was yielded as a dark brown powder. The palladium atom content of **PSt-Pd(R)** was determined by inductively coupled plasma atomic emission spectrometry (ICP-AES) and quantitative analysis of non-combustible residue after ashing.

Initially, DPC synthesis from phenol took place.⁶ The overall catalyst system consists of palladium complex, inorganic redox agent, organic redox agent, organic onium salts, and dehydration agents. From our previous experience, suitable co-catalysts were chosen: cerium(IV) tetrakis(tetramethylheptandionato)- (Ce(TMHD)₄), benzoquinone or hydroquinone, tetra-*n*-butylammonium bromide (TBAB), and 3A molecular sieve, respectively. Carbon monoxide and oxygen were used, respectively, as a carbonyl carbon source and an oxidizer. The ratio of oxygen to carbon monoxide was limited to below 6% to avoid explosion. The effect of the substituent R group on the palladium ligand is shown in Table 1. All **PSt-Pd(R)** complexes

Table 1 Substituent effect of the ligand on Pd complexes^a

Entry	Pd complex	Pd content/ mmol g ⁻¹	DPC		PS ^{bd} (%)
			Yield ^b (%)	TOF ^c (mol/ mol-Pd h)	
1	PdCl ₂ (c1-Me)	—	8.1	183	0.00
2	PSt-Pd(Me)	0.74	19.9	442	0.13
3	PSt-Pd(Me)	1.14	15.7	348	0.00
4	PSt-Pd(Et)	0.68	18.8	417	0.12
5	PSt-Pd(^t Bu)	0.66	18.2	403	0.10
6	PSt-Pd(Ph)	0.68	18.2	404	0.11
7	PSt-Pd(Mes) ^e	0.56	18.0	402	0.11

^a Reaction conditions: phenol 40.0 mmol, Pd complex 3.0 μmol, Ce(TMHD)₄ 18 μmol, ⁿBu₄NBr 375 μmol, benzoquinone 180 μmol, 3A M.S. 1 g, CO 6.0 MPa, O₂ 0.3 MPa, 100 °C, 3 h. ^b Estimated by GC. ^c Turnover frequency of palladium for initial 3 h. ^d Phenyl salicylate. ^e Mes: 2,4,6-trimethylphenyl.

exhibited high efficiency and selectivity comparable to the results of the homogeneous Pd-carbene complex **PdCl₂(c1-Me)**. Although the tendency of the homogeneous Pd-carbene complex **PdX₂(c1-R)** (X = Cl, Br) was for the larger R group to afford a better yield of DPC,^{4c} differences in the R group on **PSt-Pd(R)** complexes had no effect. This can be explained by the fact that the resin moiety had very large steric hindrance; thus the difference of the R group was negligible. The best result was obtained from **PSt-Pd(Me)** with the turnover frequency (TOF) reaching 442 (mol-DPC/mol-Pd h). Under the present reaction conditions, oxidative carbonylation of phenol produced several by-products along with DPC. The major side product was phenyl salicylate (PS) which was identified by GC mass spectroscopy. The restraint of side reactions is important, because the salicylic acid structure is believed to be a cause of gelation during polymerization.^{4b} The selectivity of this catalyst system is also better than that of previous catalyst systems.^{4a}

Table 2 shows the result due to the change in the amount of **PSt-Pd(Me)** when amounts of phenol and co-catalyst were constant. For 40 mmol of phenol, 1.00 mmol of palladium was better than 0.50 mmol, reaching a TOF of 805. A greater quantity of palladium increased the yield of DPC but TOF was decreased, since the regeneration of Pd²⁺ by the co-catalyst becomes the rate-determining step.

The time–turnover number (TON) correlation curve for the **PSt-Pd(Me)** complex is shown in Fig. 2. The lack of an induction period indicates that the catalytic system works smoothly from the initial stage. The TON increased with increased reaction time for the initial 6 h at 100 °C, but

Table 2 Effect of the amount of palladium in DPC synthesis^a

Entry	Pd content/ mmol g ⁻¹	DPC		
		Yield ^b (%)	TOF ^c (mol/ mol-Pd h)	PS ^{bd} (%)
1	0.5	4.8	645	0.00
2	1.0	12.1	805	0.00
3	2.0	15.2	509	0.00
4	3.0	19.9	442	0.13
5	6.0	22.3	247	0.13

^a Reaction conditions: phenol 40.0 mmol, PSt-Pd(Me) (0.74 mmol g⁻¹), Ce(TMHD)₄ 18 μmol, ⁿBu₄NBr 375 μmol, benzoquinone 180 μmol, 3A M.S. 1 g, CO 6.0 MPa, O₂ 0.3 MPa, 100 °C, 3 h. ^b Estimated by GC. ^c Turnover frequency of palladium for initial 3 h. ^d Phenyl salicylate.

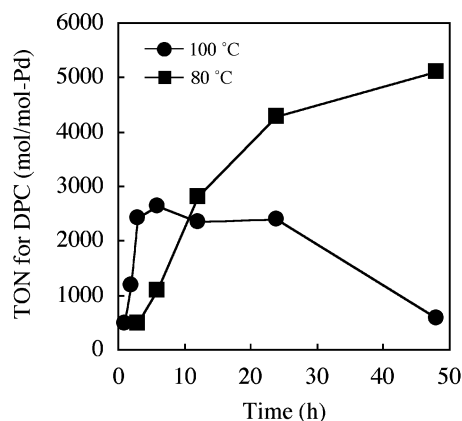


Fig. 2 Oxidative carbonylation of phenol catalyzed using the **PSt-Pd(Me)** catalyst system. Reaction conditions: phenol 40.0 mmol, **PSt-Pd(Me)** (0.74 mmol g⁻¹) 1.0 μmol, Ce(TMHD)₄ 18 μmol, ⁿBu₄NBr 375 μmol, benzoquinone 180 μmol, 3A M.S. 1 g, CO 6.0 MPa, O₂ 0.3 MPa.

decreased beyond 6 h. This is probably due to degradation of the DPC produced. On the other hand, no decrease in TON was found at 80 °C. This is because high temperature accelerates the hydrolysis of the DPC, since water was not trapped adequately. After 48 h, ICP-AES suggested that the amount of Pd in the solution was less than 3% of the initial amount. The total TON reached 5100 (mol-DPC/mol-Pd) at 80 °C. The selectivity of DPC was greater than 99% and no by-products, such as phenyl salicylate or *o*-phenylene carbonate, were observed.

Finally, direct PC synthesis from bisphenols was examined. The polymerization of bisphenol A and CO was also catalyzed by **PSt-Pd(Me)** with inorganic redox agent, organic redox agent, organic onium salts, and dehydration agents. Results of the effect of various inorganic redox agents are shown in Table 3. The molecular weight and yield were significantly affected

Table 3 Oxidative carbonylation of bisphenol A catalyzed by the **PSt-Pd(Me)** complex^a

Entry	Inorganic redox cocatalyst	$M_w^{b/10^3}$ g mol ⁻¹	$M_n^{b/10^3}$ g mol ⁻¹	Yield ^c (%)
1	Ce(TMHD) ₄	18.4	7.4	93
2	Ce(OAc) ₃ ·xH ₂ O	6.0	2.9	86
3	Mn(TMHD) ₃	6.7	3.7	22
4	Mn(OAc) ₂ ·4H ₂ O	9.5	4.8	34

^a Reaction conditions: bisphenol A 2.08 mmol, PSt-Pd(Me) 12.5 μmol, inorganic redox cocatalyst 75 μmol, ⁿBu₄NBr 188 μmol, hydroquinone 375 μmol, 3A M.S. 1 g, CH₂Cl₂ 5 mL, CO 6.0 MPa, O₂ 0.3 MPa, 100 °C, 24 h. ^b Molecular weights were determined by GPC using polystyrene standards. ^c Insoluble in methanol.

by central metals and ligands. The highest molecular weight and yield were obtained from Ce(TMHD)₄, with $M_w = 18400$, M_n

= 7400, and 93% yield. Although the organic onium salt TBAB does not act as a redox agent, its presence is found to be essential to the progress of the reaction. One probable role is its activation of phenol to onium phenoxide.^{2f} The effect of the TBAB/Pd molar ratio on the molecular weight is summarized in Fig. 3.

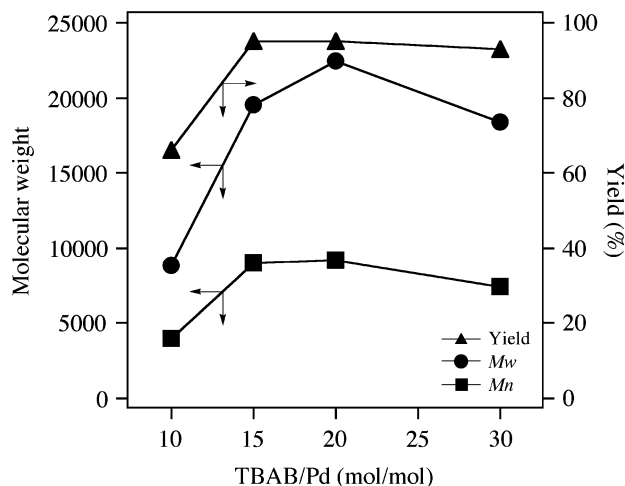


Fig. 3 Effect of the TBAB : Pd ratio on the molecular weight and yield of polymer. Reaction conditions: bisphenol A 2.08 mmol, **PSt-Pd(Me)** 12.5 μ mol, Ce(TMHD)₄ 75 μ mol, ⁿBu₄NBr 375 μ mol, hydroquinone 375 μ mol, 3A M.S. 1 g, CH₂Cl₂ 5 ml, CO 6.0 MPa, O₂ 0.3 MPa, 100 °C, 24 h.

The molecular weight reached its maximum value (M_w : 22,400 M_n : 9,200) with a good yield (95%) when the ratio TBAB : Pd was 20 : 1. This high M_w value is as good as the result for the previous homogeneous Pd-carbene complex.

The structure of the PCs obtained was confirmed by IR, ¹H NMR and ¹³C NMR analyses. The IR spectrum of PC (Entry 1 in Table 3) exhibited strong absorption at 1776 cm⁻¹ due to the presence of carbonate groups (Fig. 4). An additional small peak

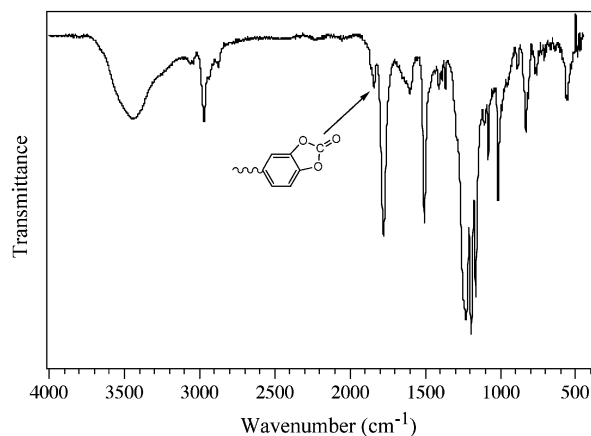


Fig. 4 IR spectrum of the polycarbonate produced by oxidative carbonylation.

at 1839 cm⁻¹ is attributable to the *o*-phenylene carbonate terminal. Fig. 5 shows the ¹H NMR spectrum of PC. The terminal aromatic protons located in the *ortho*-position of the hydroxyl group can be seen at 6.69 ppm in addition to normal repeating PC units, but the carbon of the *o*-phenylene carbonate terminal is too small to be observed. In the ¹³C-NMR spectrum, peaks for the terminal aromatic methyne carbon atoms at 114.8 ppm are minimal because the molecular weight of the product is very large. These findings clearly indicate that the formation of normal repeating polycarbonate has taken place.

In conclusion, polystyrene resin-supported Pd-carbene complexes **PSt-Pd(R)** successfully achieved selective DPC synthe-

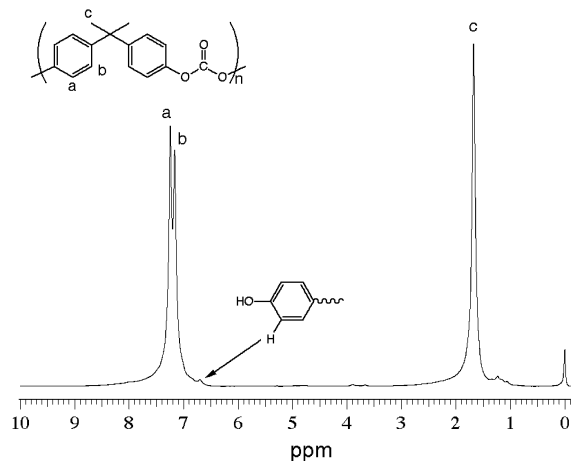


Fig. 5 ¹H NMR spectrum of the polycarbonate produced by oxidative carbonylation.

sis by oxidative carbonylation of phenol. The highest TOF of 805 (mol-DPC/mol-Pd h) was exhibited by **PSt-Pd(Me)**. Total TON reached about 5100 (mol-DPC/mol-Pd) with a high selectivity (>99%). This catalyst also yielded polycarbonate with a high molecular weight of M_w 22,400 at a good yield of 95%. Moreover, the Pd catalyst was easily removed by filtration from the reaction mixture. Normally, the benefits of using a supported catalyst have to be set against their low activity. It is noteworthy that the **PSt-Pd(R)** catalysts maintain high activity in the selective synthesis of aromatic carbonates. Direct synthesis of aromatic carbonate from phenols can thus simplify the synthetic process and reduce energy consumption.

Experimental

Materials

Phenol was purified by vacuum distillation prior to use. Dichloromethane was distilled and stored over molecular sieve 3A. 4-Chloromethyl polystyrene resin (cross-linked with 1% DVB, 0.90 or 1.74 mmol Cl g⁻¹) was purchased from Tokyo Kasei Kogyo Co., Ltd. All other reagents were obtained from commercial sources and used as received. Molecular sieve 3A was activated *in vacuo* at 250 °C for 12 h before use. 1-Substituted-imidazoles (R = ^tBu, mesityl) were prepared according to the method of Gridnev and Mihaltseva.⁶

Synthesis of polystyrene resin-supported Pd-carbene complexes

A typical procedure was as follows (for PSt-Pd(Me), Pd content 0.74 mmol g⁻¹). The polymeric ligands were synthesized by mixing the 4-chloromethyl polystyrene resin (cross-linked with 1% DVB, 0.90 mmol Cl g⁻¹) (3 g) and *N*-methylimidazole (4.3 ml, 54 mmol) in toluene (50 ml) at 130 °C for 1 day to yield a pale yellow slurry of the product, which was collected, washed with THF, and dried *in vacuo*. Palladium acetate (0.74 g, 3.3 mmol) was dissolved in 50 ml of DMSO. To the reddish brown solution was added the polymeric ligand (2.5 g). The mixture was heated for 1 h *in vacuo* at 50 °C. The obtained slurry was filtered, washed 3 times with dichloromethane, and dried overnight at 70 °C, yielding the PSt-Pd(R) as a dark brown powder. The Pd content of PSt-Pd(R) were determined by ICP-AES (inductively coupled plasma atomic emission spectrometry) and quantitative analysis of non-combustible residue after ashing.

Synthesis of DPC

A typical procedure was as follows (Entry 2 in Table 2). PSt-Pd(Me) (1.4 mg, Pd: 1.0 μmol), Ce(TMHD)₄ (15.7 mg, 18.0 μmol), benzoquinone (19.5 mg, 180.0 μmol), tetrabutylammonium bromide (124.6 mg, 375.0 μmol), and activated 3A molecular sieve (1 g), phenol (3.76 g, 40.0 mmol) were charged into a 50 ml stainless steel autoclave, followed by charging with 6.0 MPa CO and 0.3 MPa O₂. The reactor was placed in an oil bath and kept at 100 °C for 3 h. After the specified time, the reaction was quenched by cooling the autoclave in a water bath.

Analysis of reaction products

Reaction products were identified and quantified by gas chromatography using a Hewlett-Packard HP6890 series GC system with a TC-1 column.

Polymerization

A typical procedure was as follows (Entry 1 in Table 3). PSt-Pd(Me) (17.0 mg, Pd: 12.5 μmol), Ce(TMHD)₄ (65.5 mg, 75 μmol), hydroquinone (41.3 mg, 375 μmol), tetrabutylammonium bromide (83.1 mg, 25 μmol), activated 3A molecular sieve (1.0 g), bisphenol A (0.475 g, 2.08 mmol), and anhydrous dichloromethane (5 ml) were charged into a 50 ml stainless steel autoclave, followed by charging with 6.0 MPa CO and 0.3 MPa O₂. The reactor was heated at 100 °C for 24 h, after which the reaction was quenched by cooling the autoclave in a water bath and degassing. After filtering the reaction mixture, the product was isolated by precipitation from the condensed reaction mixture (5 ml) by adding excess methanol to give PC at 93% yield (0.49 g).

Polymer characterization

Molecular weight was determined using a JASCO Gulliver gel permeation chromatograph (GPC) using a SHODEX K-804L column, polystyrene standards, and chloroform as solvent. IR spectrometric analysis was carried out using a Perkin-Elmer Paragon 1000 FT-IR spectrometer. ¹H and ¹³C NMR spectra

were obtained on a JEOL LA600 spectrometer using CDCl₃ solvent containing 1% TMS as an internal reference.

Acknowledgments

This research for the Nanostructure Polymer Project was financially supported by the New Energy and Industrial Technology Development Organization (NEDO).

References

- 1 D. Freitag, U. Grigo, P. R. Muller and W. Nouvertne, in *Encyclopedia of Polymer Science and Engineering*, vol. 11, Wiley, New York, 1988.
- 2 (a) M. Takagi, H. Miyagi, T. Yoneyama and Y. Ohgomori, *J. Mol. Catal. A: Chem.*, 1998, **129**, L1; (b) A. Vavasori and L. Toniolo, *J. Mol. Catal. A: Chem.*, 1999, **139**, 109; (c) M. Goyal, R. Nagahata, J. Sugiyama, M. Asai, M. Ueda and K. Takeuchi, *Catal. Lett.*, 1998, **54**, 29; (d) M. Goyal, R. Nagahata, J. Sugiyama, M. Asai, M. Ueda and K. Takeuchi, *J. Mol. Catal. A: Chem.*, 1999, **137**, 147; (e) M. Goyal, J. Novosad, M. Necas, H. Ishii, R. Nagahata, J. Sugiyama, M. Asai, M. Ueda and K. Takeuchi, *Appl. Organomet. Chem.*, 2000, **14**, 629; (f) H. Ishii, M. Ueda, K. Takeuchi and M. Asai, *J. Mol. Catal. A: Chem.*, 1999, **138**, 311; (g) H. Ishii, M. Ueda, K. Takeuchi and M. Asai, *J. Mol. Catal. A: Chem.*, 1999, **144**, 369; (h) H. Ishii, M. Ueda, K. Takeuchi and M. Asai, *J. Mol. Catal. A: Chem.*, 1999, **144**, 477; (i) H. Ishii, M. Ueda, K. Takeuchi and M. Asai, *J. Mol. Catal. A: Chem.*, 1999, **148**, 289; (j) H. Ishii, M. Goyal, M. Ueda, K. Takeuchi and M. Asai, *Catal. Lett.*, 2000, **65**, 57; (k) G. Yin, C. Jia, T. Kimura, T. Yamaji and Y. Fujiwara, *J. Organomet. Chem.*, 2001, **630**, 11; (l) K. J. L. Linsen, J. Libens and P. A. Jacobs, *Chem. Commun.*, 2002, 2728.
- 3 (a) J. E. Hallgren and G. M. Lucas, *J. Organomet. Chem.*, 1981, **212**, 135; (b) M. Goyal, R. Nagahata, J. Sugiyama, M. Asai, M. Ueda and K. Takeuchi, *Polymer*, 1999, **40**, 3237; (c) M. Goyal, R. Nagahata, J. Sugiyama, M. Asai, M. Ueda and K. Takeuchi, *Polymer*, 2000, **41**, 2289; (d) W. B. Kim and J. S. Lee, *Chem. Lett.*, 2001, **10**, 1044.
- 4 (a) H. Ishii, M. Goyal, M. Ueda, K. Takeuchi and M. Asai, *Appl. Catal. A: Gen.*, 2000, **201**, 101; (b) H. Ishii, M. Goyal, M. Ueda, K. Takeuchi and M. Asai, *Macromol. Rapid Commun.*, 2001, **22**, 376; (c) K. Okuyama, J. Sugiyama, R. Nagahata, M. Asai, M. Ueda and K. Takeuchi, *J. Mol. Catal. A: Chem.*, in press.
- 5 (a) K. Okuyama, J. Sugiyama, R. Nagahata, M. Asai, M. Ueda and K. Takeuchi, *Polym. Prepr., Jpn.*, 2002, **51**, 1249; (b) K. Okuyama, J. Sugiyama, R. Nagahata, M. Asai, M. Ueda and K. Takeuchi, *Proc. GSC TOKYO 2003*, 2003, p. 134.
- 6 A. A. Gridnev and I. M. Mihaltseva, *Synth. Commun.*, 1994, **24**(11), 1547.



Enzymatic degradation of poly(*R,S*-3-hydroxybutanoate) to cyclic oligomers under continuous flow†

Yasushi Osanai, Kazunobu Toshima and Shuichi Matsumura*

Faculty of Science and Technology, Keio University, 3-14-1, Hiyoshi, Kohoku-ku, Yokohama 223-8522, Japan. E-mail: matsumura@applc.keio.ac.jp; Fax: +81-45-566-1582

Received 29th April 2003

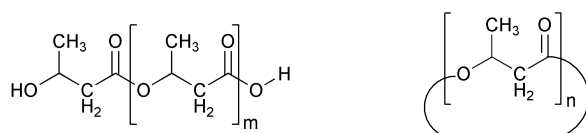
First published as an Advance Article on the web 19th August 2003

The enzymatic degradation of chemically synthesized poly(*R,S*-3-hydroxybutanoate) (PHB) to a reactive cyclic oligomer under continuous flow using an enzyme column was studied and directed towards green chemical recycling. It was confirmed that atactic and syndiotactic PHBs were quantitatively transformed into the corresponding cyclic oligomer by passing through a column packed with immobilized lipase from *Candida antarctica* (Novozym 435) at 40 °C using toluene solution. The degradability of the polymer depended on the reaction conditions, such as flow rate and the polymer concentration. A higher flow rate and higher polymer concentration caused incomplete degradation of the polymer. The 40 °C-degradation was suitable for both rapid degradation of PHB and enzyme stability. The degradation activity of the enzyme column was maintained for at least two months at 40 °C.

Introduction

The biodegradable polymer is one of the most important subjects in the field of green chemistry. Extensive studies on biodegradable polymers have been made with respect to the degradation mechanisms in the environment and the related enzymes,^{1–7} along with novel enzymatic synthetic methods in addition to the mechanical properties.^{8–19} However, there are only a few reports on the chemical recycling of such biodegradable polymers.

Chemically synthesized poly(*R,S*-3-hydroxybutanoate) (PHB) has attracted attention as a biodegradable plastic due to its characteristic mechanical properties and biodegradability, which may not be attained using conventional bacterial poly(*R*-3-hydroxybutanoate).^{20–26} However, it is produced by the polymerization of petroleum-derived monomers. From the standpoint of green chemistry, even biodegradable polymers should be recycled as much as possible with minimal energy consumption in order to save carbon resources, thus reducing carbon dioxide evolution. We previously reported the polymer production and chemical recycling of some biodegradable polyesters using an enzyme as the catalyst.^{27–33} Biodegradable polyesters, such as the unnatural type PHB and poly(ϵ -caprolactone) could be transformed into the corresponding repolymerizable cyclic oligomers in organic media or in supercritical carbon dioxide by immobilized lipase (Scheme 1).



Scheme 1 Oligomer structures from PHB degradation.

Also, the cyclic oligomers were found to be repolymerized by lipase and acted as the intermediates for the production of novel functional molecules.^{27–36} Therefore, this procedure may become an effective process for the chemical recycling of biodegradable polymers. It is pointed out that this procedure

requires a large amount of enzyme for rapid and complete degradation, and a more efficient process is now needed. In order to decrease the enzyme amount necessary for efficient polymer degradation, a continuous degradation procedure may become one possible method. However, the continuous enzymatic degradation of a polymer has not been reported yet.

In this report, the enzymatic degradation of chemically synthesized atactic and syndiotactic PHBs to the corresponding reactive cyclic oligomers under continuous flow using a column packed with immobilized lipase was studied and directed towards the chemical recycling of biodegradable polymers (Fig. 1).

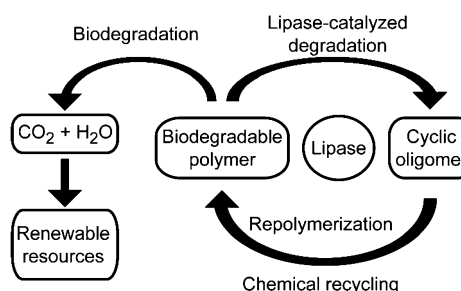


Fig. 1 The concept of the chemical recycling of biodegradable polymer.

Green Context

The recycling of waste polymers is of vital importance to a sustainable technological society. While biodegradability of polymers is an important goal in itself, it would be even more environmentally and economically attractive to enable recycling of biodegradable polymers so that those that can be recovered can provide useful products. Here a continuous conversion of polyhydroxybutanoate to a useful cyclic oligomer using an environmentally acceptable enzyme column is described.

JHC

† Presented at The First International Conference on Green & Sustainable Chemistry, Tokyo, Japan, March 13–15, 2003.

Experimental

Materials and measurements

Atactic poly(*R,S*-3-hydroxybutanoate) (aPHB) (isotactic diad fraction $[i] = 0.50$, $M_n = 110\,000$, $M_w/M_n = 1.2$) was synthesized through anionic polymerization in bulk with potassium oleate/18-Crown-6 ether complex as an initiator.³¹ Syndiotactic poly(*R,S*-3-hydroxybutanoate) (sPHB) (syndiotactic diad fraction $[s] = 0.6$, $M_n = 55\,000$, $M_w/M_n = 1.9$) was synthesized in bulk with 1,3-dichlorotetrabutyl-distannoxane as an initiator.³¹ (*R,S*)- β -Butyrolactone (β -BL) was purchased from Tokyo Kasei Kogyo Co., Ltd. (Tokyo, Japan), and used after distillation over calcium hydride under reduced pressure (bp. 75 °C/41 mmHg). Potassium oleate was purchased from Tokyo Kasei Kogyo Co., Ltd. (Tokyo, Japan). 18-Crown-6 was purchased from Aldrich Chemical Co. (Milwaukee, WI, USA), and used after recrystallization from acetonitrile. 1,3-Dichlorotetrabutyl-distannoxane was prepared from dibutyltin dichloride according to the literature^{37,38} and used after recrystallization from *n*-hexane (mp = 113–116 °C, lit. 114 °C³⁷). Dibutyltin dichloride was purchased from Aldrich Chemical Co. (Milwaukee, WI, USA), *Candida antarctica* lipase immobilized on acrylic resin [CA, Novozym 435 (triacylglycerol hydrolase + carboxyesterase) having 10000 PLU g⁻¹ (propyl laurate units: lipase activity based on ester synthesis) according to the supplier] was kindly supplied by Novozymes Japan Ltd. (Chiba, Japan).

The weight-average (M_w) and number-average (M_n) molecular weights as well as molecular weight dispersion (M_w/M_n) of the polymer and the produced oligomers were determined by size exclusion chromatography (SEC) using SEC columns (GPC K-G + GPC K-804, Showa Denko Co., Ltd., Tokyo, Japan) with a refractive index detector (RI). Chloroform was used as the eluent. The SEC system was calibrated with polystyrene standards of a narrow molecular weight distribution. ¹H-NMR spectra were recorded with a JEOL Model JNM-LA300 (300 MHz) spectrometer (JEOL Ltd., Tokyo, Japan) and Varian NMR 300 (Varian, Inc., CA, USA) in CDCl₃ with tetramethylsilane as an internal standard. The matrix-assisted laser desorption ionization time-of-flight mass spectrometry (MALDI-TOF MS) was measured with a Bruker Proflex mass spectrometer (Bruker Daltonics, Billerica, MA, USA). The spectrometer was equipped with a nitrogen laser. The detection was in the reflectron mode. 2,5-Dihydroxybenzoic acid (DHBA) was used as the matrix and positive ionization was used.

Enzymatic degradation procedure under continuous flow

A continuous degradation system consisting of an enzyme-packed column, an HPLC pump and a refractive index detector (RI) was used for the transformation of PHB into the cyclic oligomer as shown in Fig. 2. The degradation was performed using a 7.8 mm i.d. \times 300 mm column packed with 6.8 g of immobilized lipase CA. The enzyme column was equilibrated with toluene at 40 °C prior to use. The degradation of PHB was carried out using 0.025–10% toluene solution. The flow rate was 0.1–0.5 mL min⁻¹. A typical degradation was carried out as follows. A 0.25% PHB toluene solution was injected into the enzyme column at a flow rate of 0.2 mL min⁻¹. The temperature of the enzyme column was kept at 40 °C. Degradation was monitored using an RI detector. The toluene eluents containing degradation products were collected and evaporated under slightly reduced pressure to quantitatively obtain waxy products. The composition of the products was analyzed by ¹H and ¹³C NMR, SEC and MALDI-TOF MS. The spectral data of the products are shown as below; aPHB and sPHB: ¹H NMR (300 MHz; CDCl₃): $\delta = 1.3$ (–O–CH–CH₃–CH₂–CO–O–, 3H, m),

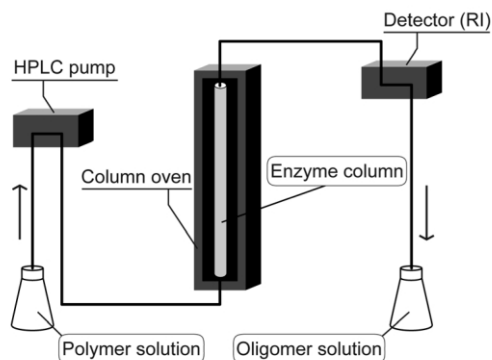


Fig. 2 Schematic diagram of the continuous degradation system.

2.6 (–O–CH–CH₃–CH₂–CO–O–, 2H, m), 5.3 (–O–CH–CH₃–CH₂–CO–O–, 1H, br)]. The ratios of the cyclic oligomer and linear oligomer were determined by using the ratios of $\sum a_i$ cyclic/ $\sum a_i$ linear (a_i = peak area) for the MALDI-TOF MS spectrum according to the methods of Cordova *et al.*³⁹

Results and discussion

Enzymatic degradation under continuous flow

The continuous degradation was performed by the direct injection of the toluene solution containing the polymer into the enzyme column using an HPLC pump. Fig. 3 shows the SEC

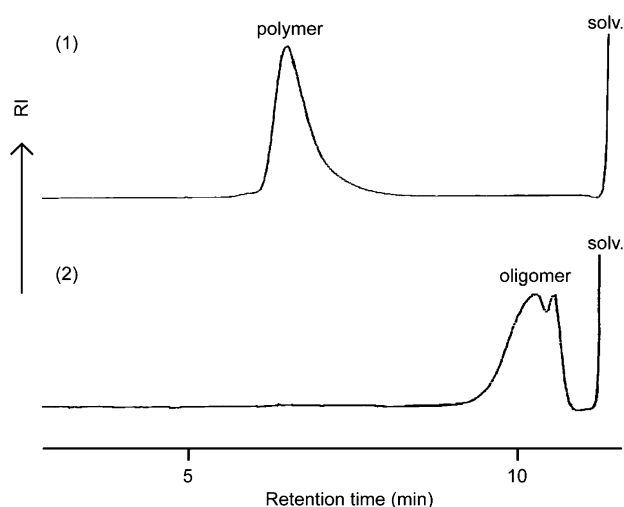


Fig. 3 SEC profiles of aPHB before (1) and after (2) passage through the enzyme column at 40 °C.

profiles of aPHB before and after passage through the enzyme column using 0.025% aPHB toluene solution at a flow rate of 0.2 mL min⁻¹ and 40 °C. As shown in Fig. 3, it was confirmed that aPHB was transformed into the corresponding oligomers by lipase, and the original polymer peak completely disappeared in the resulting oligomer after passage through the enzyme column. The same results were obtained when sPHB was used as the original polymer. Also, these results were consistent with those obtained by the batch process.³¹ The degradability depended on the reaction conditions, such as the flow rate and polymer concentration in toluene. Under the best reaction conditions using a 0.25% aPHB toluene solution at a flow rate of 0.2 mL min⁻¹ and 40 °C, the original aPHB, which had an M_n of 110 000, was quantitatively transformed into the corresponding oligomer with an M_n of ca. 500. In order to evaluate the continuous degradation behavior in this equipment, the time course of the RI intensity changes of the eluents by the

degradation of PHB after passage through the enzyme column, was studied. That is, 40 mL of the 0.025% aPHB toluene solution was injected into the enzyme column at a flow rate of 0.2 mL min⁻¹ at 40 °C. It was found that the RI intensity increased after 2 hours by the elution of the degradation products. The constant intensities of the RI of the eluents during the elution of the products indicated the homogeneous degradation and the constant concentration of the products during the degradation in the enzyme column. That is, the degradation continuously occurred in the enzyme column by producing the same oligomeric products with the same composition and concentration. An increase in the RI intensities that appeared after a 2 hour-elution suggested that the transformation of aPHB into the oligomer was completed within 2 hours. The degradation rate of aPHB might be considerably faster than that by a batch process, because the enzyme over polymer ratio of the continuous flow method became significantly higher than that by the batch process.

Molecular structure of the degradation products

The molecular structure of the produced oligomer was analyzed based on the MALDI-TOF MS and ¹H-NMR spectra with reference to our previous report.³¹ From the ¹H-NMR, it was confirmed that oligomers possessing an unsaturated terminal group (crotonate type) were not detected in the produced oligomers. Therefore, it was confirmed that the produced oligomer mainly consisted of a cyclic structure, indicated as C in Fig. 4. The composition of the cyclic oligomer mixture was

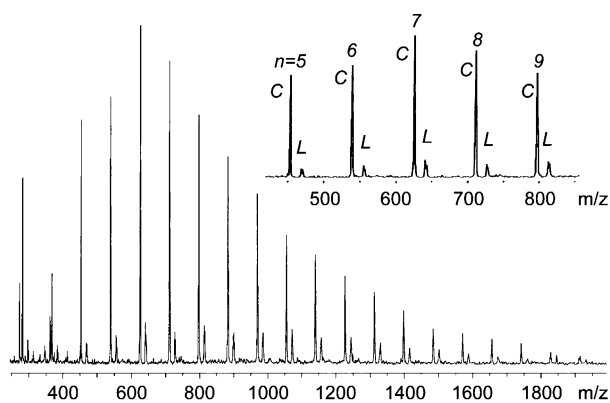


Fig. 4 MALDI-TOF MS spectrum of the degradation products of aPHB after passage through the enzyme column. (0.025% PHB was injected into the enzyme column at a flow rate of 0.2 mL min⁻¹ at 40 °C).

almost the same as that obtained by the batch method as previously reported.³¹ That is, by the batch process, the cyclic oligomer content was *ca.* 95% when aPHB was degraded by 500 wt% lipase CA in 0.25% dried toluene solution at 40 °C for 72 h. On the other hand, by the continuous flow of 0.25% PHB toluene solution using the enzyme column at 40 °C, the cyclic content was *ca.* 90%. Based on these results, it is suggested that this continuous flow system was a more efficient process for the transformation of PHB into cyclic oligomers than the batch method with respect to reducing the amount of enzyme and organic solvent. The same results were obtained when sPHB was used instead of aPHB.

The effects of reaction conditions on degradability

In the continuous flow system, the flow rate, the column temperature and the polymer concentration determined the degradation of PHB. As described above, the flow rate corresponded to the degradation time. The column temperature

was responsible for both the degradation rate and enzyme lifetime. We previously reported that PHB was transformed into cyclic oligomers in toluene at 40–60 °C within 12 hours by a batch process.³¹ Table 1 shows the effects of the column

Table 1 Effects of temperature on the continuous degradation of aPHB^a

Entry	Temp./°C	Oligomer yield (%)	M_n	$M_w \cdot M_n^{-1}$
1	40	> 99.9	500	1.5
2	50	98.9	400	1.7
3	60	96.9	500	1.6
4	70	97.2	300	1.7

^a Degradation was carried out using 1 mL of 1% aPHB toluene solution under continuous flow of toluene at a flow rate of 0.1 mL min⁻¹.

temperature under continuous flow on the degradation results. As shown in Table 1, aPHB was almost quantitatively transformed into the corresponding cyclic oligomers and molecular weight and molecular weight dispersion of oligomer were almost the same between 40 and 70 °C. However, the oligomer yield decreased slightly with increasing column temperature. Furthermore, at 70 °C, the activity of the enzyme decreased after one month. On the other hand, at 40 °C, the activity of the enzyme as estimated by the degradation profile of PHB was unchanged for at least two months in toluene. From these results, it is indicated that the 40 °C-degradation was suitable for both rapid degradation of PHB and enzyme stability.

The flow rate also influenced the degradation results. Table 2 summarizes the effects of the flow rate on the degradation

Table 2 Effects of flow rate on the continuous degradation of aPHB^a

Entry	Flow rate/ mL min ⁻¹	Oligomer yield (%)	M_n^b	$M_w \cdot M_n^{-1b}$
1	0.1	86.9	500	1.7
2	0.2	59.7	500	1.7
3	0.4	40.6	500	1.7
4	0.8	26.3	600	2.1

^a Degradation was carried out using 1 mL of 3% aPHB toluene solution at 70 °C. ^b M_n and $M_w \cdot M_n^{-1}$ of oligomer fraction of the degradation products as measured by SEC profiles.

results. It was found that the SEC profiles showed two peaks when the flow rate was fast or the polymer concentration was high. It was observed that the molecular weight and molecular weight dispersion of the oligomer were almost the same when the flow rate was increased. However, the oligomer yield significantly decreased with increasing flow rate.

The degradation rate of the polymer decreased with the increasing polymer concentration and flow rate. In such a case, unreacted polymer was contained in the degradation products. However, the unreacted polymer was readily transformed into the corresponding cyclic oligomers by passage through the enzyme column again. Fig. 5 shows the repeated degradation of the partial degradation products containing about 45% of the original unreacted PHB. That is, a 5% aPHB toluene solution was injected into the enzyme column at a flow rate 0.2 mL min⁻¹ at 40 °C to obtain the degradation products as the eluents. The degradation products contained about 45% unreacted aPHB and 55% oligomer as shown in Fig. 5 (1). These degradation products (1% toluene solution) were again injected into the enzyme column at a flow rate of 0.2 mL min⁻¹ at 40 °C to obtain the oligomer as shown in Fig. 5 (2). From Fig. 5, it was found that the residual unreacted PHB polymer in the first degradation mixture completely disappeared and transformed into the corresponding oligomers. It was also found that the second passage through the enzyme column caused no significant molecular weight change in the produced oligomer and molecular structure. These results indicated that even the

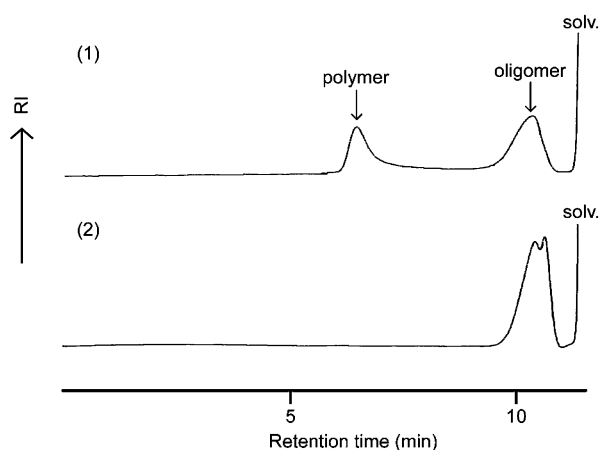


Fig. 5 SEC profiles of the partially degraded PHB oligomer (1) and of the second degradation products (2) by passage through the enzyme column at 40 °C.

original unreacted polymer contained in the produced oligomer mixture after passage through the enzyme column was readily transformed in the enzyme column by recycling to complete the degradation of the unreacted polymer.

Conclusion

Chemically synthesized PHB was enzymatically degraded to the corresponding reactive cyclic oligomers by passage through an enzyme column packed with immobilized lipase from *Candida antarctica* at 40 °C under continuous flow of toluene solution. The reaction conditions, such as flow rate, polymer concentration in the toluene solution and column temperature influenced the transformation of the original polymer into the oligomers. The degradation profiles of both atactic and syndiotactic PHBs were almost the same using the enzyme column.

Acknowledgements

Immobilized lipase from *Candida antarctica* (CA, Novozym 435) was kindly supplied by *Novozymes Japan Ltd.* (Chiba, Japan). This work was supported by a Grant-in-Aid for scientific research No. 15350095 and by a Grant-in-Aid for the 21st Century COE program "KEIO Life Conjugate Chemistry" from the Ministry of Education, Culture, Sports, Science, and Technology, Japan.

References

- B. M. Bachmann and D. Seebach, *Macromolecules*, 1999, **32**, 1777.
- T. Hiraishi, T. Ohura, S. Ito, K. Kasuya and Y. Doi, *Biomacromolecules*, 2000, **1**, 320.
- Y. He, X. Shuai, A. Cao, K. Kasuya, Y. Doi and Y. Inoue, *Macromol. Rapid Commun.*, 2000, **21**, 1277.
- Y. He, X. Shuai, K. Kasuya, Y. Doi and Y. Inoue, *Biomacromolecules*, 2001, **2**, 1045.
- Y. Wang, Y. Inagawa, Y. Osanai, K. Kasuya, T. Saito, S. Matsumura, Y. Doi and Y. Inoue, *Biomacromolecules*, 2002, **3**, 894.
- H. Abe and Y. Doi, *Biomacromolecules*, 2002, **3**, 133.
- Y. Na, Y. He, T. Nishiwaki, Y. Inagawa, Y. Osanai, S. Matsumura, T. Saito, Y. Doi and Y. Inoue, *Polym. Degrad. Stab.*, 2003, **79**, 535.
- S. Matsumura, Y. Suzuki, K. Tsukada, K. Toshima, Y. Doi and K. Kasuya, *Macromolecules*, 1998, **31**, 6444.
- S. Namekawa, H. Uyama and S. Kobayashi, *Biomacromolecules*, 2000, **1**, 335.
- J. J. Song, S. Zhang, R. W. Lenz and S. Goodwin, *Biomacromolecules*, 2000, **1**, 433.
- T. F. Al-Azemi, J. P. Harmon and K. S. Bisht, *Biomacromolecules*, 2000, **1**, 493.
- H. Nishida, M. Yamasita, M. Nagashima, T. Endo and Y. Tokiwa, *J. Polym. Sci., Part A: Polym. Chem.*, 2000, **38**, 1560.
- H. Kikuchi, H. Uyama and S. Kobayashi, *Macromolecules*, 2000, **33**, 8971.
- A. Kumar and R. A. Gross, *J. Am. Chem. Soc.*, 2000, **122**, 11767.
- Y. Osanai, K. Toshima and S. Matsumura, *Chem. Lett.*, 2000, 576.
- A. Kumar, K. Garg and R. A. Gross, *Macromolecules*, 2001, **34**, 3527.
- H. Uyama, S. Kobayashi, M. Morita, S. Habaue and Y. Okamoto, *Macromolecules*, 2001, **34**, 6554.
- H. Uyama, K. Inada and S. Kobayashi, *Macromol. Biosci.*, 2001, **1**, 40.
- Y. Osanai, K. Toshima and S. Matsumura, *Macromol. Biosci.*, 2001, **1**, 171.
- Y. Hori, Y. Takahashi, A. Yamaguchi and T. Nishishita, *Macromolecules*, 1993, **26**, 4388.
- Y. Hori, M. Suzuki, A. Yamaguchi and T. Nishishita, *Macromolecules*, 1993, **26**, 5533.
- H. Abe, I. Matsubara, Y. Doi, Y. Hori and A. Yamaguchi, *Macromolecules*, 1994, **27**, 6018.
- H. Abe and Y. Doi, *Macromolecules*, 1996, **29**, 8683.
- P. Kurcok, P. Dubois, W. Sikorska, Z. Jedlinski and R. Jerome, *Macromolecules*, 1997, **30**, 5591.
- Y. Hori and T. Hagiwara, *Biol. Macromol.*, 1999, **25**, 237.
- S. Hiki, M. Miyamoto and Y. Kimura, *Polymer*, 2000, **41**, 7369.
- S. Matsumura, H. Ebata and K. Toshima, *Macromol. Rapid Commun.*, 2000, **21**, 860.
- H. Ebata, K. Toshima and S. Matsumura, *Biomacromolecules*, 2000, **2**, 511.
- S. Matsumura, H. Ebata, R. Kondo and K. Toshima, *Macromol. Rapid Commun.*, 2000, **2**, 1329.
- S. Matsumura, S. Harai and K. Toshima, *Macromol. Rapid Commun.*, 2001, **22**, 215.
- Y. Osanai, K. Toshima, N. Yoshie, Y. Inoue and S. Matsumura, *Macromol. Biosci.*, 2002, **2**, 88.
- R. Kondo, K. Toshima and S. Matsumura, *Macromol. Biosci.*, 2002, **2**, 267.
- S. Matsumura, *Macromol. Biosci.*, 2002, **2**, 105.
- S. Kobayashi, H. Uyama and T. Takamoto, *Biomacromolecules*, 2000, **1**, 3.
- T. Takamoto, H. Uyama and S. Kobayashi, *e-Polymers*, 2001, no. 4.
- T. Takamoto, H. Uyama and S. Kobayashi, *Macromol. Biosci.*, 2001, **1**, 215.
- R. Okawara and M. Wada, *J. Organomet. Chem.*, 1963, **1**, 81.
- J. Otera, N. Dan-oh and H. Nozaki, *J. Org. Chem.*, 1991, **56**, 5307.
- A. Cordova, T. Iversen, K. Hult and M. Martinelle, *Polymer*, 1998, **39**, 6519.



Ring-opening polymerization of ϵ -caprolactone with yttrium triflate†

Yi Wang, Shun-ya Onozawa and Masao Kunioka*

National Institute of Advanced Industrial Science and Technology, Higashi 1-1-1, Tsukuba, Ibaraki 305-8565, Japan. E-mail: m.kunioka@aist.go.jp; Fax: +81-29-8614584; Tel: +81-29-8614511

Received 28th April 2003

First published as an Advance Article on the web 19th August 2003

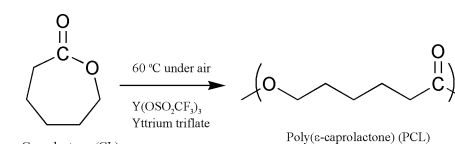
A simple and green procedure for bulk polymerization of ϵ -caprolactone (CL) has been developed using yttrium triflate (trifluoromethanesulfonate) as a catalyst under air in a simple glass vial. The efficiencies of various initiators such as diol or triol with acid or base were discussed. Little water was found to be necessary in this polymerization system. The biodegradation of direct molded poly(ϵ -caprolactone) (PCL) film during polymerization in aqueous solution with commercial compost was also studied by measuring the biochemical oxygen demand (BOD).

Introduction

Poly(ϵ -caprolactone) (PCL) is one of the most attractive aliphatic polyesters, because of its widely recognized biodegradability and unique compatibility with a large range of polymers.¹ PCL can be easily ring-opening polymerized from ϵ -caprolactone (CL) by heating or using a suitable catalyst. Alkoxides such as aluminium isopropoxide, provide a method of preparing polylactone with a controlled molecular weight and narrow molecular weight distribution (living polymerization) and specific block copolymers such as ABA type are obtained using living systems.² In addition, it was found that the CL polymerization could occur in supercritical carbon dioxide.³ Recently, the enzymatic ring-opening polymerizations of lactones by lipase, which is the hydrolysis enzyme of esters, have been studied.^{4,5} Moreover, CL could be polymerized to PCL with high molecular weight (over 50 000) under high pressure (over 800 MPa).⁶ Many reported polymerization systems of CL by a catalyst require complete desiccation involving equipment and chemicals using many steps such as flame-drying, distillation, and purging with dry nitrogen gas. In addition, the chemical impurities need to be removed, because the presence of a little water or impurity dramatically deactivates the catalyst for polymerization. These complicated steps prevent mass production and application using the polymerization system of CL.

Recently, the ring-opening polymerization of CL and other lactones has been successfully initiated by rare earth alkoxides.^{7–9} These systems were found to be a very fast polymerization, with a 100% conversion of the monomer to polymer (M_n , 10,000) being observed for the very short reaction time of 2 min. We focused on these polymerization systems because it was found that triflate compounds with rare earth metals such as Y, Ln or Sm were stable and active as Lewis acids in water.^{10,11} In addition, living ring-opening metathesis polymerization catalyzed by a ruthenium complex was carried out in aqueous media to give polymers with controlled molecular weights and distributions, where the propagating species and the catalyst are stable in water.¹² It has been found recently that the biodegradable PCL polymer could

be bulk polymerized by yttrium triflate catalyst which is stable in water and air (Scheme 1).¹³



Scheme 1

However, there were technical problems such as low molecular weight ($M_n = ca.$ 6 000 by GPC) with this method. Herein, continuing the preceding studies, we investigate the efficiencies of various initiators, such as diol or triol under acidic or basic conditions.

Experimental

Materials

Pure ϵ -caprolactone (CL, 2-oxepanone, Tokyo Kasei, Japan) was dried over CaH_2 at room temperature for 48 hours and distilled under reduced pressure (< 10 mmHg) at 110 °C. Dry yttrium triflate (trifluoromethanesulfonate) (Aldrich, 98%) was dried at 150 °C for 8 hours under reduced pressure. Lyophilized yttrium triflate was lyophilized from the aqueous yttrium triflate then exposed to air for *ca.* 24 hours. Unpurified CL, yttrium triflate and alcohols were used as received.

Green Context

The use of ϵ -caprolactone as a polymerization monomer offers the potential to produce biodegradable polymers in a reaction that proceeds under mild, catalytic conditions. The absence of a need for purification and desiccation steps for the monomers and catalyst is a great benefit in terms of reducing the process energy required for this catalytic system. *SJT*

† Presented at The First International Conference on Green & Sustainable Chemistry, Tokyo, Japan, March 13–15, 2003.

Polymerization procedure

The CL (10 mmol, 1.14 g), yttrium triflate (20 μmol , 10.7 mg) and alcohol were transferred to a glass vial (10 mL) with a plastic cap in air. The glass vial was capped, mixed well by a touch mixer and placed in an incubator at 60 °C without stirring for a specified period. At the end of the reaction period, the solid polymer was obtained in the vial after cooling to room temperature. For determination of yield and molecular weight, the contents of the vial were dissolved in chloroform (10 mL). The chloroform solution was added to methanol (300 mL) to reprecipitate the polymer, the precipitate was washed with several portions of methanol and then the volatiles were removed in a vacuum oven (<3 mmHg, R.T., 12 hours). The obtained dry polymer was weighed and characterized.

Characterization by gel permeation chromatography (GPC)

The molecular weight and molecular weight distribution were determined by GPC using a Tosoh 8000 GPC system with a refractive index detector. A combination of two TSK GMHXL columns (Tosoh, Japan, 7.8 mm \times 30 cm) with molecular weight ranges of 1 000– 1×10^7 g mol⁻¹ was used. The columns were eluted by chloroform (flow rate of 1 mL min⁻¹ at 40 °C) and calibrated with polystyrene standards.

Measurement of thermogravimetric analysis (TGA)

Thermogravimetric curves were obtained from a SEIKO TG/DTA220 assembled with a SSC/5200 thermal controller equipped with a EXSTAR6000 PC data station with 100–150 mL min⁻¹ flow of dry nitrogen. Experiments were carried out with approximately 10 mg of samples and a heating rate of 10 °C min⁻¹ with temperature ranges of ambient to 500 °C.

Biodegradation test by measuring biochemical oxygen demand (BOD)

Measurements of aerobic environmental biodegradation in aqueous medium with commercial compost were performed on a BOD tester assembled with a OM3100A coulometer (OH-KURA Co., Japan) at 25 °C while stirring. A sample with an

initial weight of about 100 mg was inserted into the BOD reactor containing 300 mL of mineral water (KH₂PO₄ 85 mg, K₂HPO₄ 217.5 mg, Na₂HPO₄·2H₂O 334 mg, NH₄Cl 5 mg, MgSO₄·7H₂O 22.5 mg, CaCl₂·2H₂O 36.4 mg, and FeCl₃·6H₂O 0.25 mg per liter deionized water) with inoculum taken from 2 g commercial compost purified by using a filter paper (based on ISO14851 and JIS K 6950). The biodegradability of the samples was evaluated in triplicate.

Results and discussion

Ring-opening polymerization of CL by yttrium triflate

Table 1 lists the results of the polymerization of CL by yttrium triflate at 60 °C for 48 hours in bulk. In all the entries, unpurified CL and as-received alcohol and yttrium triflate were used. From entry 1 to 9, alcohol with one hydroxyl (0.20 mmol, entries 1–3), two hydroxyl (diol, 0.10 mmol, entries 4, 7–9), three hydroxyl (glycerol, 0.07 mmol, entry 5), and four hydroxyl (pentaerythritol, 0.05 mmol, entry 6) initiated the polymerizations, respectively. To draw comparisons, the same mol of hydroxyl (0.20 mmol) of each alcohol initiator was used. In the following part of the table (entry 11–17), the polymerization of CL initiated from water under acidic or basic conditions were listed. The results could be summarized as follows: (a) the polymer yield ([PCL]/[CL], wt%) increased a little with carbon number in the case where alcohol with one hydroxyl was used as initiator (entries 1–3); (b) both polymer yield and molecular weight were not influenced by the carbon number of the diol (entries 4, 7–9); (c) the molecular weight distribution (M_w/M_n) broadened with the increase in the number of hydroxyl of the alcohol (entries 3–6); the weight average molecular weight (M_w) of PCL polymerized from glycerol (entry 5) and pentaerythritol (entry 6) reached 20 000, which may be due to the polymerization being initiated from more than one hydroxyl of the alcohol; (d) the existence of acid would not influence the polymerization of CL, while a relatively higher basic concentration would lower the yield and molecular weight of the received PCL (entry 15). From these results, it is clarified that yttrium triflate can catalyze the ring-opening polymerization of CL under very simple and mild conditions without purifying the reagents. Using glycerol or pentaerythritol as initiator, the molecular weight of the received PCL is relatively high.

Table 2 shows the effect of the initiator (glycerol) amount on the polymerization of CL by yttrium triflate at 60 °C for 48

Table 1 Polymerization of unpurified CL by yttrium triflate catalyst.^a

Entry	Initiator	Initiator amount/mmol	Yield ^b (wt%)	Molecular weight ^c	
				10 ⁻³ M _n	M _w /M _n
1	CH ₃ OH	0.20	48.8	6.56	1.20
2	CH ₃ CH ₂ OH	0.20	55.4	8.40	1.59
3	CH ₃ CH ₂ CH ₂ OH	0.20	70.9	7.14	1.25
4	CH ₂ OHCH ₂ CH ₂ OH	0.10	70.0	9.97	1.56
5	CH ₂ OHCHOHCH ₂ OH	0.07	54.4	12.32	1.77
6	C(CH ₂ OH) ₄	0.05	70.2	10.98	1.91
7	CH ₂ OHCH ₂ OH	0.10	65.7	8.40	1.59
8	CH ₂ OH(CH ₂) ₂ CH ₂ OH	0.10	66.8	10.20	1.50
9	CH ₂ OH(CH ₂) ₅ CH ₂ OH	0.10	74.7	11.91	1.53
10	None	—	— ^d	—	—
11	1 M HCl	10 μL	53.5	7.19	1.67
12	0.1 M HCl	10 μL	58.3	7.54	1.54
13	0.01 M HCl	10 μL	62.2	6.66	1.56
14	H ₂ O	10 μL	62.5	6.86	1.55
15	1 M NaOH	10 μL	43.0	5.08	1.38
16	0.1 M NaOH	10 μL	58.7	6.98	1.67
17	0.01 M NaOH	10 μL	63.5	8.32	1.57

^a Polymerization conditions: 10 mmol CL monomer (1.14 g), 20 μmol catalyst (10.7 mg), in 10 mL glass vial with a plastic cap in air without stirring at 60 °C for 48 hours. ^b Determined using the weight of monomer and isolated dry polymer. ^c Determined by GPC. ^d Unable to be detected.

Table 2 Effect of initiator amount on polymerization of CL by yttrium triflate catalyst using glycerol as initiator for 48 hours at 60 °C^a

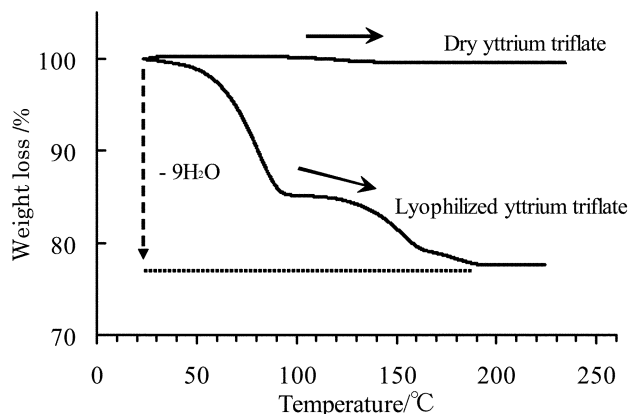
Entry	Initiator amount/ mmol	Yield ^b (wt%)	Molecular weight	
			10 ⁻³ Mn	Mw/Mn
18	0.05	38.9	11.55	1.35
19	0.07	53.7	13.28	1.45
20	0.10	71.4	15.35	1.50
21	0.15	73.8	12.43	1.58
22	0.20	68.4	10.42	1.43
23	0.40	60.3	9.09	1.31

^a Polymerization conditions: 10 mmol CL monomer (1.14 g), 20 μmol catalyst (10.7 mg), in 10 mL glass vial with a plastic cap in air without stirring, all of the reagent was used as received. ^b Determined using the weight of monomer and isolated dry polymer.

hours in bulk without purifying the reagents. It is clear that the yield increased as the amount of glycerol increased from 0.05 to 0.15 mmol. On the other hand, the molecular weight increased as the amount of initiator was increased from 0.05 to 0.10 mmol and then decreased as the initiator amount was increased from 0.10 to 0.40 mmol. Usually, in a polymerization reaction, if there is only one kind of initiator, the molecular weight of the received polymer will increase linearly with [monomer]/[initiator] ratio.¹⁴ In these experiments, water and impurities were not removed before the reactions; this might influence the molecular weight of the resulting polymer.

The role of water coordinated to the yttrium triflate in the polymerization of CL

From the results shown in Table 2, it was considered that water plays some role in the polymerization reactions. In order to study the effect of water, dry and lyophilized yttrium triflate, dehydrated 2-propanol (water less than 50 ppm, Wako) and pure CL were used in the polymerization reactions. The coordinated water numbers of the two kinds of yttrium triflate were determined by TGA as shown in Fig. 1.

**Fig. 1** Thermogravimetric analysis (TGA, the increasing temperature rate was 10 °C min⁻¹) of dry and lyophilized yttrium triflate.

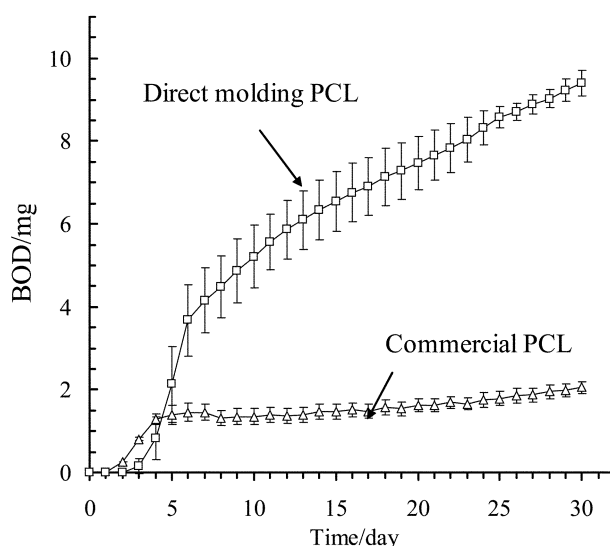
It is clear that yttrium triflate dried under 150 °C for 8 hours (dry yttrium triflate) was completely dehydrated (zero coordinated water to yttrium triflate), while one molecule of lyophilized yttrium triflate was coordinated by nine water molecules. The polymerization results showed that dry yttrium triflate had no catalytic activity in the pure polymerization system. On the other hand, lyophilized yttrium triflate catalyzed the polymerization (the molar ratio of monomer : catalysis : initiator was 10 : 0.02 : 0.6) to produce PCL with a yield of 38.0 wt% and the Mn reached 3.84×10^3 . The yield and molecular weight were a little lower than those produced under air without

purification using 2-propanol as initiator, which could reach ca. 50 wt% and 5 000, respectively.¹³ From this experiment, it is clarified that water is necessary in the polymerization system. This might be due to the different structures of hydrated and dehydrated yttrium triflate.¹¹ It has been reported recently that in the hydrated yttrium triflate coordinated with nine water molecules, the water molecules surrounding yttrium were assembled in a tricapped trigonal prism; the mean distances between the yttrium ion and water (Y–O bond distance) were six at 2.344 Å in the prism and three at 2.525 Å in the capping position.¹⁵ On the other hand, the conversion of CL during the reaction at 60 °C using 2-propanol as initiator in bulk under air condition was studied by GPC. The results showed that the conversions were 18.3, 46.0, 63.1 and 90.0% at reaction times of 18, 24, 30, and 48 hours, respectively. The rise in molecular weight was rapid at early conversions, and then slowed down, the molecular weight distributions were around 1.35 and unimodal. If the polymerization at high conversions was not quenched and was allowed to sit for longer periods of time, an increase in Mn and a corresponding increase in Mw/Mn were observed. Thus, chain transfer reaction during polymerization of CL occurs under these conditions.

Properties of direct molded PCL film

As the polymerization could occur in bulk under air, homogeneously dispersed composite materials of PCL and a filler, e.g. cellulose fiber, could be easily prepared by the direct molding method during polymerization from CL monomer. The mechanical properties such as elastic modulus and strength of this composite material were found to be better than those of direct molded PCL samples without cellulose fiber.¹⁶

On the other hand, in the previous study, we have reported that the direct molded PCL polymerized at 40 °C was degraded in aqueous medium with a lipase produced by *Rhizopus arrhizus*.¹³ Herein, we compared the biodegradability of direct molded PCL (Mn = 4 000 Mw/Mn = 2.63) and a commercial one (Aldrich, Mn = 42 500 Mw/Mn = 1.53) by a standard biodegradation test method measuring biochemical oxygen demand (BOD) in aerobic medium (Fig. 2). The direct molded

**Fig. 2** Biodegradation test measuring biochemical oxygen demand (BOD) of direct molded PCL and commercial PCL. □ Direct molded PCL (polymerized at 60 °C for 48 hours Mn = 4 000 Mw/Mn = 2.63); △ Commercial PCL (Mn = 42 500 Mw/Mn = 1.53).

PCL film was produced in a glass plate at 60 °C for 48 hours catalyzed by yttrium triflate using glycerol as initiator with a thickness of about 2 mm. The commercial PCL was molded in

a glass plate at 120 °C from the received one with a thickness of about 1.5 mm. From Fig. 2, it can be seen that the direct molded PCL film could be biodegraded by environmental bacteria in compost four times faster than the commercial PCL. This may be due to the much lower molecular weight of the direct molded PCL relative to that of the commercial one. On the other hand, the total theoretical BOD would be 210 mg when the sample was degraded completely, that is, only about 5% of the sample was degraded in one month in the compost water. This may be due to the small surface area and short evaluation time.

Conclusion

The biodegradable PCL polymer could be polymerized by yttrium triflate catalyst which is a stable Lewis acid in water and air. Furthermore, it is clarified that only the hydrated yttrium triflate has catalyst activity in the polymerization. Using this yttrium catalyst, PCL could be prepared at 60 °C under air in a simple glass vial initiated by alcohols containing one or several hydroxyl under acidic or basic conditions. The molecular weight (M_w) of the PCL polymerized from glycerol or pentaerythritol could reach 20 000. The direct molded PCL could be biodegraded by the bacteria in commercial compost very well. Since the ring-opening polymerization of CL can be performed under such simple and mild conditions, as reported in this paper, the application of the polymerization method is anticipated in many fields, especially the incorporation of drugs or enzymes, which are unstable at high temperature and in organic solvents, into biocompatible polymer materials. The polymerization conditions of other biodegradable polymers

using a similar catalyst are being studied; the results will be reported in the very near future.

References

- 1 C. G. Pitt, F. I. Chasalow, Y. M. Hibionada, D. M. Klimas and A. Schindler, *J. Appl. Polym. Sci.*, 1981, **26**, 3779.
- 2 C. Jacobs, P. Dubois, R. Jerome and P. Teyssie, *Macromolecules*, 1991, **24**, 3027.
- 3 F. Stassin, O. Halleux and R. Jerome, *Macromolecules*, 2001, **34**, 775.
- 4 H. Uyama and S. Kobayashi, *Chem. Lett.*, 1993, 1149.
- 5 R. MacDonald, S. Pulapura, Y. Svirkin, R. Gross, D. Kaplan, J. Akkara, G. Swift and S. Wolk, *Macromolecules*, 1995, **28**, 73.
- 6 A. Oishi, Y. Taguchi, K. Fujita, Y. Ikeda and T. Masuda, *Proc. AIRAPT-17*, Universities Press, Hyderabad, 2000, p. 965.
- 7 Y. Shen, Z. Shen, Y. Zhang and K. Yao, *Macromolecules*, 1996, **29**, 8289.
- 8 W. M. Stevels, M. J. K. Ankone, P. J. Dijkstra and J. Feijen, *Macromolecules*, 1996, **29**, 8296.
- 9 E. Martin, P. Dubois and R. Jerome, *Macromolecules*, 2000, **33**, 1530.
- 10 K. Satoh, M. Kamigaito and M. Sawamoto, *Macromolecules*, 1999, **32**, 3827.
- 11 K. Satoh, M. Kamigaito and M. Sawamoto, *Macromolecules*, 2000, **33**, 5836.
- 12 D. M. Lynn, S. Kanaoka and R. H. Grubbs, *J. Am. Chem. Soc.*, 1996, **118**, 784.
- 13 M. Kunioka, Y. Wang and S. Onozawa, *Polym. J.*, 2003, **35**, 422.
- 14 M. Nishiura, Z. Hou, T. Koizumi, T. Imamoto and Y. Wakatsuki, *Macromolecules*, 1999, **32**, 8245.
- 15 P. Lindqvist-Reis, K. Lamble, S. Pattanaik, I. Persson and M. Sandström, *J. Phys. Chem. B*, 2000, **104**, 402.
- 16 M. Funabashi and M. Kunioka, *Green Chem.*, **5**, DOI: 10.1039/b304759h, this issue.



Control of racemization for feedstock recycling of PLLA†

Yujiang Fan,^{ab} Haruo Nishida,^{*a} Yoshihito Shirai^b and Takeshi Endo^{ac}

^a Molecular Engineering Institute, Kinki University, 11-6 Kayanomori, Iizuka, Fukuoka 820-8555, Japan. E-mail: hnishida@mol-eng.fuk.kindai.ac.jp.

E-mail: yjfan@mol-eng.fuk.kindai.ac.jp; Fax: +81 948 22 5706; Tel: +81 948 22 5706

^b Graduate School of Life Science and Systems Engineering, Kyushu Institute of Technology, 1-1 Hibikino, Kitakyushu, Fukuoka 808-0196, Japan. E-mail: shirai@life.kyutech.ac.jp; Fax: +81 93 695 6005; Tel: +81 93 695 6070

^c Faculty of Engineering, Yamagata University, 4-3-16 Jonan, Yonezawa, Yamagata 992-8150, Japan. E-mail: tendo@yz.yamagata-u.ac.jp; Fax: +81 238 26 3092; Tel: +81-238-26-3090

Received 29th April 2003

First published as an Advance Article on the web 30th July 2003

Poly(L-lactide) (PLLA) is considered to be a possible candidate for feedstock recycling because thermal degradation of PLLA can result in the recovery of its monomer, L,L-lactide. One of the serious problems concerning the feedstock recycling of PLLA has been the racemization of lactide. To control the racemization in the pyrolysis of PLLA, various calcium compounds, which are relatively safe chemicals, were added to the PLLA. Consequently, the calcium compounds, especially calcium oxide, effectively decreased the pyrolysis temperature of PLLA and led to predominant L,L-lactide formation in the specific range of 250–300 °C. For PLLA containing calcium oxide, at temperatures above 250 °C, L,L-lactide formation was predominant. This demonstrates the possibility of a practical way of recycling PLLA feedstock to optically pure L,L-lactide.

Introduction

Poly(L-lactide), or poly(L-lactic acid) (PLLA) is mostly derived from renewable sources, such as corn, potato and other agriculture products. It can be also composted after use due to its biodegradability.¹ Therefore, it is considered to belong to a family of green and sustainable materials.² It has also traditionally received much interest because of its medical, pharmaceutical, and environmental applications. Nowadays, it is attracting much attention as a promising alternative to the normal petroleum based commodity resins, because it has many good properties that are comparable with normal plastics, such as mechanical strength and transparency.³

However, the microbial degradation of PLLA is limited to very few species of microorganisms, such as *Amycolatopsis* and *Streptomyces* strains.⁴ If it were employed in normal domestic life and if an industry was set up to manufacture common products out of it, which were then consumed and disposed of on a large scale, it would be rather difficult to biodegrade either in composting plants or in the natural environment.

One possible solution to this problem is the development of a sustainable system that converts the waste plastic products to monomers using feedstock recycling. Since thermal degradation of PLLA can result in the recovery of L,L-lactide,⁵ which is a cyclic monomer, PLLA is considered to be just such a possible candidate for feedstock recycling. But when high molecular weight PLLA is thermally degraded, high temperatures and long times are needed for the pyrolysis, causing the racemization of the lactide recovered.⁶ This diminishes the crystallizability and other useful properties of polylactide.⁷ Therefore, effective catalysts will need to be found for the feedstock recycling of PLLA.

In our previous study, it was found that the pyrolysis of PLLA with calcium salt end structure proceeds through a first order unzipping depolymerization that produces principally lactides.⁸ Further, it became evident that the racemization occurred through specific mechanisms dependent on the particular temperature ranges.⁹ Intensive racemization has been found to occur at temperatures under 250 °C, with relatively frequent racemization occurring above 320 °C. The possibility of pure L,L-lactide recovery is achievable within the temperature range of 250–320 °C, because in this temperature range, the unzipping depolymerization mechanism dominates and no racemization occurs. However, it is difficult to totally avoid pyrolysis at temperatures lower than 250 °C.

In this study, with a view to practical applications, calcium compounds including oxide, hydroxide, and carbonate were added to PLLA to form PLLA/Ca composites. The thermal degradation of these composites was studied to clarify the effect of these compounds on the degradation temperature, kinetics, and racemization during the thermal degradation process. A

Green Context

Recycling of plastics by conversion to monomers is an important area of research, which maximises the options available for the purification and processing of spent plastics. However, many problems can exist, sometimes due to additives, sometimes to the decomposition mode of the polymer, and sometimes to the stability of the monomer. The latter is the problem with poly(L-lactide) where racemisation is a difficulty. Lowering the decomposition temperature reduces the tendency to racemisation, and this paper describes some calcium oxide based systems which are effective in this area.

DJM

† Presented at The First International Conference on Green & Sustainable Chemistry, Tokyo, Japan, March 13–15, 2003.

possible approach that could be used to control the racemization was demonstrated, resulting in the recovery of optically pure L,L-lactide.

Results and discussion

Effect of calcium compounds on the pyrolysis behavior of PLLA

PLLA was synthesized through the ring-opening polymerization catalyzed by Sn 2-ethylhexanoate {Sn(Oct)₂}. After the polymerization, possible metal compounds in the PLLA were eliminated by a liquid–liquid extraction method using 1 M HCl aqueous solution. The purified PLLA was found to contain 14 ppm of Sn, which was of the order of the lower limit of detection under the experimental conditions. This indicates that most of the metals in the polymer were removed. The pure PLLA was mixed with various calcium compounds through a solution method with chloroform to prepare film samples. This method of preparation did not affect the molecular weight of the PLLA, as shown in Table 1.

Table 1 PLLA samples with various calcium compounds

Sample	M_n	M_w/M_n
PLLA	152400	1.82
CaCO ₃ ^a	158600	1.82
CaCl ₂ ^a	156200	1.87
CaAc ₂ ^a	153000	1.83
Ca(OH) ₂ ^a	160000	1.82
CaO ^a	157600	1.81

^a Calcium compound added to PLLA, containing 5% w/w of calcium.

To analyze the effect of the calcium compounds on the pyrolysis behavior, thermal degradation of the film samples was carried out with TG/DTA in a nitrogen atmosphere. The TG curves of the pure PLLA and the composites (Ca content 1% w/w to the pure PLLA) are shown in Fig. 1. It was found that the

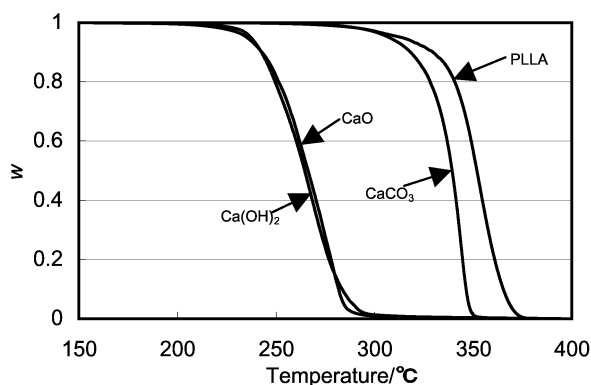


Fig. 1 TG curves of PLLA/Ca composites (calcium content: 1%). Heating rate: 5 °C min⁻¹ in N₂.

addition of calcium compounds made the degradation temperature of PLLA greatly decrease. The weight loss of the pure PLLA started at about 280 °C and then smoothly decreased to reach almost complete degradation at about 370 °C. On the other hand, the composites containing calcium compounds had a much lower degradation temperature. For the PLLA containing CaCO₃, the divergence of its degradation temperatures from that of the pure PLLA at the early stage was less than at the later stages, suggesting that the CaCO₃ has a definitive effect on the later stages of pyrolysis. When CaO and Ca(OH)₂ with higher alkalinity were included, the degradation temperature of the

composites dropped to an even greater degree and showed a similar degradation behavior. Compared with the pure PLLA, their degradation temperatures had decreased by about 80 °C. The gaps in the TG curves between these composites and pure PLLA were nearly constant, suggesting that these calcium compounds participated the degradation reaction from the beginning of the pyrolysis and continued to act until the degradation process was completed.

The pyrolysis products of the pure PLLA and composites were analyzed in detail using Py-GC/MS. In Fig. 2, Py-GC/MS

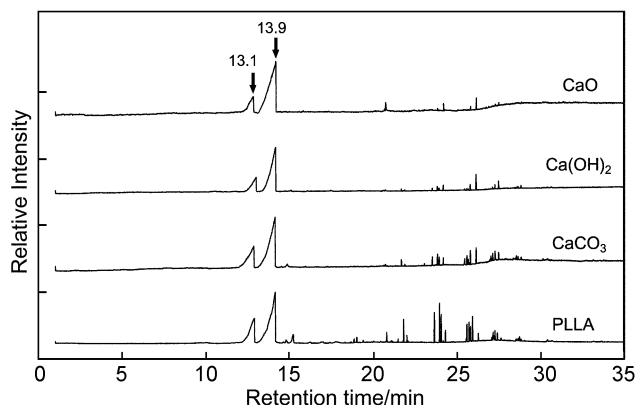


Fig. 2 Py-GC/MS (TIC) chromatograms of pyrolysis products of PLLA/Ca composites (calcium content: 5%) in the heating process from 60 °C to 400 °C (heating rate: 10 °C, min⁻¹).

chromatograms of the pyrolysis products for the pure PLLA and composites in the temperature range of 60–400 °C are shown. As discussed in our previous report,⁹ the peaks at 13.1 and 13.9 min in these chromatograms were identified as representing *meso*-lactide and D,D-/L,L-lactides, respectively, by comparison with the standard chemicals. The groups of peaks appearing periodically after 20 min were assigned to higher cyclic oligomers than lactide by comparing with a similar pattern in EI mass spectra, in which each oligomer peak showed two series of signals with $m/z = 72n - 16$ and $m/z = 72n \pm 1$ (n : number of ring members) as previously reported.^{5,6,8,9} It can be seen that the pyrolyzates of the pure PLLA consist of not only *meso*- and D,D-/L,L-lactides, but a significant number of cyclic oligomers, from trimer to nonamer ($n = 3-9$). The values of 67.8% for the content of lactides and 29.7% for that of cyclic oligomers were calculated by integrating these peak intensities. The pyrolyzates of the composites were found to contain much more lactide, being 14.4, 7.8, and 4.8% for PLLA/CaCO₃, /Ca(OH)₂, and /CaO, respectively. Compared with the PLLA having a calcium salt end structure (PLLA-Ca) in the previous report,^{8,9} it was observed that the pyrolysis products of the composite with the neutral CaCO₃ were somewhat nearer to that of pure PLLA, while the products from PLLA/Ca(OH)₂ and /CaO were similar to the pyrolysis products of PLLA-Ca. These results suggest that the alkalinity of the calcium compounds was an important factor in the pyrolysis of PLLA.

Activation energy of the thermal degradation

In the TG/DTA measurement, the temperature, T (K), for obtaining a certain fractional weight ratio value, w , should have the following relationship as a function of the heating rate ϕ :^{8,10}

$$\frac{d \log \phi}{d(1/T)} = -\frac{bE_a}{R} \quad (1)$$

where E_a and R are the apparent activation energy of the thermal degradation and the molar gas constant, respectively, and b is a constant from the Doyle's thermal degradation function approx-

imation. At a certain fractional weight ratio w , the apparent activation energy E_a is determined from the slope of the $\log(\phi)$ vs. $1/T$ plot. The results analyzed by this approach for the pure PLLA and composites are illustrated in Fig. 3. Interestingly, at

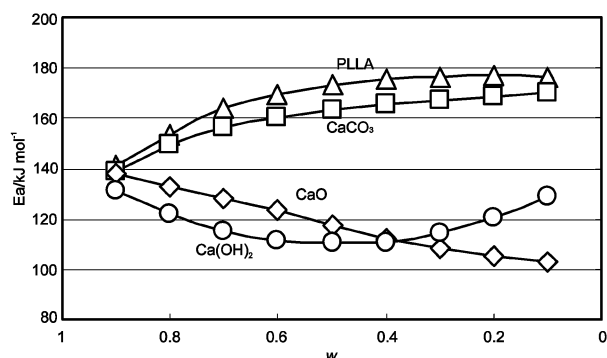


Fig. 3 Activation energy, E_a , of the pyrolysis of PLLA/Ca composites (Calcium content 1%).

the early degradation stage, the E_a values all centralized at about 140 kJ mol^{-1} . This indicates that in the initial stage the pyrolysis starts by following a similar pathway to that of the pure PLLA, suggesting any Ca compound had not yet reacted with PLLA at this stage. With the rise in temperature, the formation of each specific PLLA/Ca structure leads to each following a different degradation route.

The composite that included neutral CaCO_3 merely lowered the E_a value a little and showed a similar tendency in E_a change to that of the pure PLLA, in which the E_a value increased gradually up to about 170 kJ mol^{-1} as the degradation progressed. In contrast, the E_a value of PLLA/CaO decreased with the progress of degradation to about 100 kJ mol^{-1} , which is very close to that of the PLLA-Ca. Thus, it can be assumed that the pyrolysis of PLLA/CaO was started by a similar reaction to that of pure PLLA and gradually approximated to the reaction of PLLA-Ca.

PLLA/Ca(OH)₂ showed a rapid decrease in E_a value in the early stages to about 110 kJ mol^{-1} , and then rose again to 130 kJ mol^{-1} . Thus, the pyrolysis of PLLA/Ca(OH)₂ is considered to easily follow a reaction similar to PLLA-Ca and then shift to a different pyrolysis reaction with PLLA/CaO at a later stage.

The calculated E_a values for thermal degradation of PLLA/Ca compounds are apparent values, which may have some contribution from multiple reactions occurring at each temperature. However, the generation of similar pyrolysis products to those of pure PLLA and PLLA-Ca suggest that the main reaction is same as for the corresponding range in E_a value.

Effect of the amount of calcium compounds

The TG curves of PLLA/CaO composites with various calcium contents (Ca 0.5–5% w/w to PLLA) are illustrated in Fig. 4. The degradation temperature was found to drop with increase in Ca content. The TG curve of the composite with 0.5% of CaO shifted to the lower temperature by about $50 \text{ }^\circ\text{C}$ compared to that of pure PLLA. Another $40 \text{ }^\circ\text{C}$ drop was observed when the Ca content was increased to 1%. Further increases in calcium content had a diminishing effect on pyrolysis temperature reduction with a $10 \text{ }^\circ\text{C}$ drop for 1–2% and $15 \text{ }^\circ\text{C}$ drop for 2 to 5% suggesting saturation. The PLLA/CaO(5%) showed a decrease of more than $100 \text{ }^\circ\text{C}$ in the initial pyrolysis temperature compared with that of pure PLLA. This is very important for the recycling of PLLA, because a lower degradation temperature implies less consumption of energy and possibly a higher efficiency of monomer recovery.

In Fig. 5, the Py-GC/MS chromatograms of PLLA/CaO with various CaO contents are illustrated. It was found that the

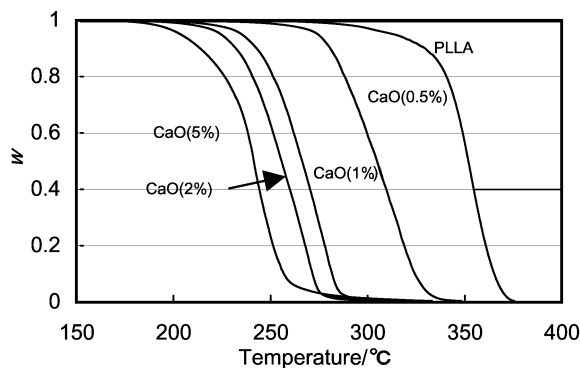


Fig. 4 TG curves of PLLA/CaO composites. Heating rate: $5 \text{ }^\circ\text{C min}^{-1}$ in N_2 .

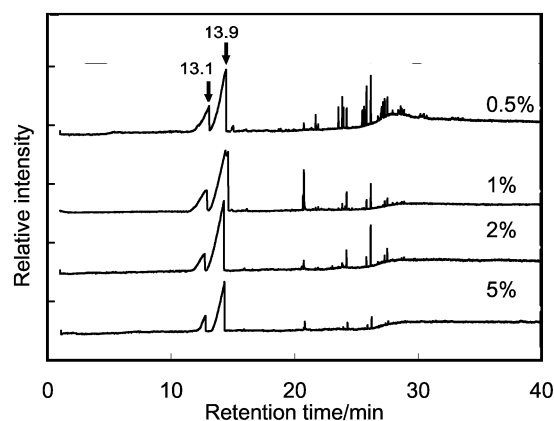


Fig. 5 Py-GC/MS (TIC) chromatograms of pyrolysis products of PLLA/CaO composites in the heating process from $60 \text{ }^\circ\text{C}$ to $400 \text{ }^\circ\text{C}$ (heating rate: $10 \text{ }^\circ\text{C min}^{-1}$)

pyrolyzates from PLLA/CaO(0.5%) contained many oligomers. Integration of the peak intensities showed that the oligomers consisted of about 20% of the pyrolyzates. When the Ca content rose to a level of 1%, the oligomer content decreased abruptly to about 8%. A further increase of Ca content to 2% and 5% made the oligomer content decrease to 6.7% and 4.8%, respectively. Thus, a Ca content of about 5% is considered to be very near the saturation point of the calcium oxide in its ability to reduce both the degradation temperature and the oligomer content.

Temperature dependence of racemization

Even when the original PLLA was composed of almost 100% of L-lactate unit, the pyrolyzates consisted of not only L,L-lactide, but a great deal of *meso*-lactide, a cyclic dimer composed of L- and D-lactate units. This indicates that racemization occurred during thermal degradation. The formation of *meso*-lactide during the pyrolysis of PLLA/CaO(5%) at different temperature ranges is illustrated in Fig. 6, in which the *meso*-lactide content was calculated by considering both the peak intensity in the Py-GC/MS chromatogram and the total weight loss in the TG data within the same temperature range. At temperatures below $200 \text{ }^\circ\text{C}$, the degradation was at a very low level, thus no formation of *meso*-lactide was observed. The racemization started at about $210 \text{ }^\circ\text{C}$, and the amount of *meso*-lactide increased gradually till the temperature reached $250 \text{ }^\circ\text{C}$. The ratio of *meso*-lactide in the total gas evaporated reached a peak of about 20% in the temperature range $230\text{--}240 \text{ }^\circ\text{C}$, and then decreased to a very low level of less than 2% in the temperature range of $250\text{--}300 \text{ }^\circ\text{C}$. The degradation of PLLA/CaO(5%) finished at about $290 \text{ }^\circ\text{C}$ and thus no further formation of *meso*-lactide at higher temperatures was observed. This result indicates that, though

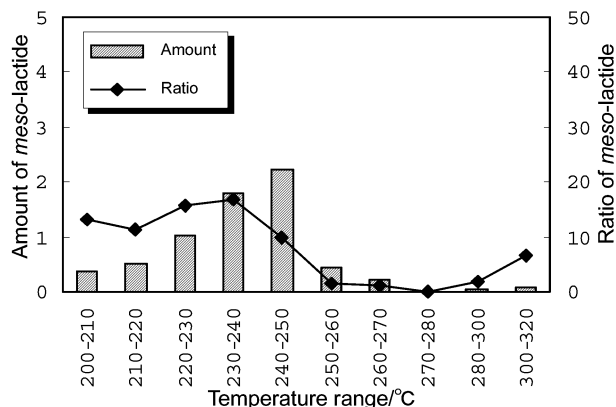


Fig. 6 Racemization on pyrolysis of PLLA/CaO composite (calcium content: 5%) at different temperature ranges.

the racemization was vigorous at temperatures lower than 250 °C, almost no racemization occurred in the temperature range of 250–300 °C. This is in accordance with our previous results investigating PLLA-Ca.⁹

These results imply that the racemization occurs only at temperatures lower than 250 °C in the pyrolysis of PLLA/CaO(5%). To prevent the formation of *meso*-lactide at this lower temperature range, the same sample was momentarily heated in a pyrolyzer preheated at 250 °C under a helium flow. This process stopped the sample experiencing the heating process below 250 °C and forced it to quickly reach the particular degradation temperature. Fig. 7 illustrates the Py-GC/

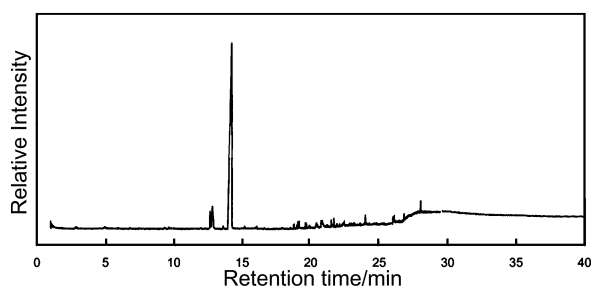


Fig. 7 Py-GC/MS (TIC) chromatograms of pyrolysis products of PLLA/CaO (Ca content: 5% w/w) in an isothermal degradation process at 250 °C for 10 min.

MS chromatogram of the evolved gases degraded at 250 °C for 10 min. Though a small amount (about 5%) of *meso*-lactide was still formed, the instantaneous heating process in the pyrolyzer

caused a considerable decrease in the *meso*-lactide content. This suggests a possible way of recovering high optically pure *L,L*-lactide from the pyrolysis of PLLA by adding CaO as the catalyst.

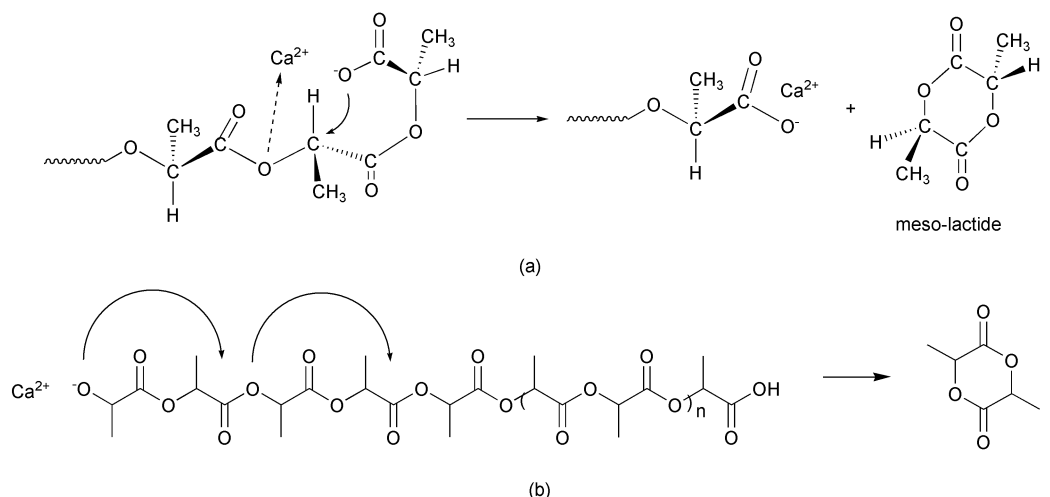
Racemization mechanism of PLLA–calcium compound composites

In our previous study, we reported on the racemization mechanism of PLLA-Ca.⁹ The racemization at lower temperature (<250 °C) follows the S_N2 reaction mechanism on the asymmetrical methyne carbon (Scheme 1a). This means that the asymmetrical carbon atom in the penultimate unit is attacked by the carboxylate anion in an end unit, followed by scission of the bond between the methyne carbon and ester oxygen. This results in an inversion of the configuration and *meso*-lactide formation.

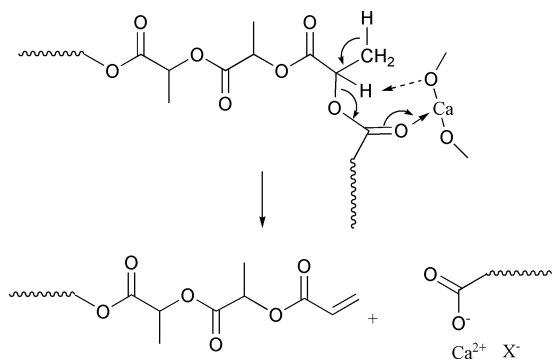
Obviously, the pyrolysis of PLLA/CaO would proceed through a similar reaction route. At the initial stage the pyrolysis of PLLA/CaO begins in a similar way to that of pure PLLA. With the increase in temperature, melted PLLA reacts with CaO particles to form a similar salt structure to PLLA-Ca, as illustrated in Scheme 2. Then the composite degrades through a similar pathway to that of the PLLA-Ca. That is, the S_N2 reaction occurs at the lower temperature range, leading to the formation of *meso*-lactide, and then it shifts to the unzipping depolymerization at the point when the temperature rises above 250 °C, leading to the dominant formation of *L,L*-lactide.

Conclusion

In conclusion, when the thermal degradation and racemization of PLLA/Ca composites, including calcium compounds, was analyzed in detail with TG/DTA and Py-GC/MS, it was found that the pyrolysis of PLLA/Ca composites proceeded through particular pathways. In the case of PLLA/CaO, a similar structure to PLLA-Ca is formed on a melt reaction and then degrades through the expected degradation route for the PLLA-Ca. In the temperature range of 250–300 °C, *L,L*-lactide formation was predominant. This is a significant result for the feedstock recycling of PLLA, because by employing a proper process, the pyrolysis of PLLA containing CaO might become an effective approach to recover *L,L*-lactide with high purity from wasted PLLA products.



Scheme 1 Pyrolysis mechanism of calcium salt end-capped PLLA. (a) *meso*-Lactide formation by S_N2 reaction on the asymmetrical methyne carbon (<250 °C). (b) Unzipping depolymerization of PLLA with calcium oxide end structure (250 °C < T < 300 °C)



Scheme 2 Possible random scission in the initial period of the pyrolysis of PLLA-CaO composite.

Experimental

Materials

Monomer, L,L-lactide, obtained from Shimadzu Co. Ltd. was purified by recrystallizing three times from dry toluene and one time from dry ethyl acetate. The vacuum dried L,L-lactide was stored in a N₂ atmosphere. After purification, *meso*-lactide was not detectable by gas chromatography (GC). Polymerization catalyst, Sn(II) 2-ethylhexanoate, obtained from Wako Pure Chemical Industries, Ltd. was distilled under reduced pressure before use. Solvents, chloroform and methanol, were purchased from Wako Pure Chemical Industries, Ltd. and used without further purification. Calcium compounds, calcium carbonate, calcium acetate, calcium oxide, and calcium hydroxide were purchased from Kanto Chemical Co., Inc. and used as received.

Measurements

Molecular weight was measured by gel permeation chromatography (GPC) on a TOSOH HLC-8220 GPC system at 40 °C using TOSOH TSKgel Super HM-H column and a chloroform eluent (0.6 mL min⁻¹). Low polydispersity polystyrene standards with M_n from 5.0×10^2 to 1.11×10^6 were used for calibration. The residual metal content in the PLLA samples was measured with a Shimadzu AA-6500F atomic absorption flame emission spectrophotometer (AA). The samples were degraded by a 25% ammonia solution, dissolved in 1 M HCl aqueous solution, and then measured by AA. Thermogravimetric analysis was conducted on a SEIKO EXSTAR 6200 TG/DTA 6200 system in an aluminium pan under a constant nitrogen flow (100 mL min⁻¹) using about 5 mg of the PLLA film sample.

Pyrolysis-gas chromatograph/mass spectra (Py-GC/MS) were measured on a Frontier Lab PY-2020D double-shot pyrolyzer connected to a Shimadzu GCMS-QP5050 chromatograph/mass spectrometer, which was equipped with an Ultra

Alloy⁺-5 capillary column. High purity helium at 50 mL min⁻¹ was used as carrier gas.

Preparation of the PLLA/Ca composites

PLLA was synthesized by the ring-opening polymerization of L,L-lactide catalyzed by Sn(II) 2-ethylhexanoate, Sn(Oct)₂, as described in the previous report.^{8,9} The obtained raw PLLA was purified in a three stage process; firstly extracting the catalyst and residues from the PLLA-chloroform solution with a 1 M HCl aqueous solution, then washing with distilled water until the aqueous phase became totally neutral, and finally precipitating the polymer with methanol and then vacuum drying. The purified PLLA was mixed with corresponding calcium compounds in chloroform solution and vigorously stirred for 1 h to disperse the inorganic particles uniformly. Then the mixtures were cast on glass Petri dishes.

Acknowledgements

This study was financially supported by Special Coordination Funds of the Ministry of Education, Culture, Sports, Science and Technology, the Japanese Government.

References

- 1 J. M. Anderson and M. S. Shive, *Adv. Drug. Delivery Rev.*, 1997, **28**, 5.
- 2 Y. Ikada and H. Tsuji, *Macromol. Rapid Commun.*, 2000, **21**, 117–32; W. Amass and A. Amass, *Polym. Int.*, 1998, **47**, 89.
- 3 M. Ajioka, K. Enomoto, K. Suzuki and A. Yamaguchi, *J. Environ. Polym. Degrad.*, 1995, **3**, 225; J. Lunt, *Polym. Degrad. Stab.*, 1998, **59**, 145.
- 4 H. Pranamuda, Y. Tokiwa and H. Tanaka, *Appl. Environ. Microbiol.*, 1997, **63**, 1637.
- 5 F. D. Kopinke and K. Mackenzie, *J. Anal. Appl. Pyrolysis*, 1997, **40–41**, 43; I. C. McNeill and H. A. Leiper, *Polym. Degrad. Stab.*, 1985, **11**, 267; H. A. Leiper and I. C. McNeill, *Polym. Degrad. Stab.*, 1985, **11**, 309; Y. Aoyagi, K. Yamashita and Y. Doi, *Polym. Degrad. Stab.*, 2002, **76**, 53.
- 6 F. D. Kopinke, M. Remmler, K. Mackenzie, M. Moder and O. Wachsen, *Polym. Degrad. Stab.*, 1996, **53**, 329; F. Khabbaz, S. Karlsson and A. C. Albertsson, *J. Appl. Polym. Sci.*, 2000, **78**, 2369; C. Westphal, C. Perrot and S. Karlsson, *Polym. Degrad. Stab.*, 2001, **73**, 281.
- 7 S. Brochu, R. E. Prud'homme, I. Barakat and R. Jerome, *Macromolecules*, 1885, **28**, 5230; H. Tsuji and Y. Ikada, *Macromolecules*, 1992, **25**, 5719.
- 8 Y. Fan, H. Nishida, S. Hoshihara, Y. Shirai, Y. Tokiwa and T. Endo, *Polym. Degrad. Stab.*, 2003, **79**, 547.
- 9 Y. Fan, H. Nishida, Y. Shirai and T. Endo, *Polym. Degrad. Stab.*, 2003, **80**, 503.
- 10 T. Ozawa, *Bull. Chem. Soc. Japan*, 1965, **38**, 1181; C. D. Doyle, *J. Appl. Polym. Sci.*, 1961, **5**, 285.



Thermal and infrared spectroscopic studies on hydrogen-bonding interaction of biodegradable poly(3-hydroxybutyrate)s with natural polyphenol catechin†

Bo Zhu,^a Jianchun Li,^a Yong He,^a Yasushi Osanai,^b Shuichi Matsumura^b and Yoshio Inoue^{*a}

^a Department of Biomolecular Engineering, Tokyo Institute of Technology, Nagatsuta 4259, Midori-ku, Yokohama 226-8501, Japan. E-mail: yinoue@bio.titech.ac.jp; Fax: +81-45-924-5827; Tel: +81-45-924-5794

^b Faculty of Science and Technology, Keio University, 3-14-1, Hiyoshi, Kohoku-ku, Yokohama 223-8522, Japan

Received 29th April 2003

First published as an Advance Article on the web 4th August 2003

Thermal and infrared spectroscopic studies were performed on the hydrogen-bonding interaction in the blends of biodegradable atactic, highly syndiotactic and isotactic poly(3-hydroxybutyrate)s with catechin. From the analysis of Fourier-transform infrared spectra, it was found that the crystalline phase could greatly restrain the formation of inter-associated hydrogen-bonds. Moreover, the effect of the steric configuration on the formation of hydrogen-bonds was testified, and the results suggested that the higher tacticity benefited the formation of hydrogen-bonds, although its effect on the strength of hydrogen-bonds was small. The strong hydrogen-bonds between the two components in the blends promised their miscibility, which could be testified by differential scanning calorimetry measurements. All the poly(3-hydroxybutyrate)–catechin blends showed one glass transition temperature over the whole range of blend compositions and it increased rapidly with catechin content, indicating that poly(3-hydroxybutyrate)s and catechin are miscible in the amorphous phase.

Introduction

Biodegradable polyesters attract much attention from industry and researchers,^{1–6} because of their good biodegradability and biocompatibility. When these materials are used, they enter the waste stream, being biodegraded by enzymes or secretion products of living organisms into carbon dioxide and water. Recently, some biodegradable polymers have been used as biomedical materials that contribute to the medical care of patients or as ecological materials that keep the earth environment clean. In addition to producing ‘green’ materials with unique physical and functional properties, the processes used to create bio-based materials lead to new manufacturing opportunities that minimize energy consumption and waste generation.

Biosynthesized isotactic poly[(*R*)-3-hydroxybutyrate] (iPHB) is one of the most representative biodegradable polyesters. Although iPHB has excellent biodegradability and biocompatibility, it has not been applied widely yet. It is believed that the reason is its poor processability and performance as compared to the engineering plastics, which arises from its big spherulites and high extent of secondary crystallization, poor thermal stability at the processing temperature and low glass transition temperature below room temperature. To overcome these undesirable properties of iPHB, blending iPHB with other materials to modify its properties seems a faster and less expensive method than exploring a new synthetic route for new polymer materials. Usually, the formation of strong hydrogen-bonds between the blend components can promise miscibility because of its negative enthalpic contribution to the free energy of mixing. For this reason, a significant amount of

work was devoted to introducing hydrogen-bonding interactions into biodegradable polyesters.^{7–11} Normally, almost all biodegradable polyesters have the ability to interact with phenols *via* hydrogen-bonds. The main reason for this is that polyesters contain carbonyl groups in their backbone, which can form hydrogen-bonds with the hydroxyl groups of phenols. However, not all polyesters can form equally strong or numerous hydrogen-bonds with such phenols, as the strength and the extent of hydrogen-bonds may depend on the chemical as well as stereo-chemical structures of polyesters. There are many reports on proton-accepting polyester–proton-donating phenol blends, such as iPHB–poly(vinyl phenol) (PVPh),¹² poly(lactic acid)–PVPh,¹³ poly(ϵ -caprolactone)–PVPh^{14,15} and so on. However, few reports have been found about the effects of the stereotactic structure of polyesters on the formation of hydrogen-bonds with phenolic components.

In this research, in order to elucidate the relationships between the formation of poly(3-hydroxybutyrate) (PHB)–phenol hydrogen-bonds and the tacticity of PHBs, and the relationships between the miscibility of PHB–phenol blends

Green Context

Polyesters account for a huge market share, and there is momentum to move from petroleum-derived polyesters to biosynthetically produced materials such as iPHB, as described here. However, physical properties such as processing temperature and glass-transition temperature are not as high as required. This paper discusses the reasons for this, proposing viable methods for a better control of the physical properties by rationalising the role of modifiers.

DJM

† Presented at The First International Conference on Green & Sustainable Chemistry, Tokyo, Japan, March 13–15, 2003.

and the strength of hydrogen-bonds, the phase behavior and intermolecular interaction will be investigated for blends of PHBs with a natural low molecular weight polyphenol. Catechin (the chemical structure of catechin is shown in Chart 1)^{16,17} is used as a modifying agent of PHBs. Catechin is one of

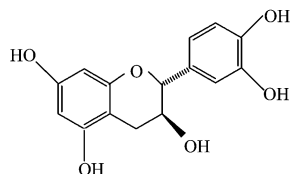


Chart 1

the naturally produced biocompatible phenolic compounds originated from green tea and the introduction of catechin into PHBs will not damage its biodegradability and biocompatibility. Amorphous chemosynthesized atactic poly[(*R,S*)-3-hydroxybutyrate] (aPHB) will be used here to prepare the hydrogen-bonding blends with catechin. As described above, it is scientifically interesting and practically important to investigate the dependence of the formation and the strength of polyester–polyphenol hydrogen-bonds on the tacticity of PHBs. Thus, chemosynthesized highly-syndiotactic poly[(*R,S*)-3-hydroxybutyrate] (sPHB) and biosynthesized iPHB are also used for comparison. aPHB is a random copolymer of *R*- and *S*-stereoisomers of hydroxybutyrate. The *R*- and *S*-repeating units break the stereoregularity of the backbone; that is, aPHB is amorphous while sPHB and iPHB are, respectively, a little and highly crystalline. By comparing the extent of hydrogen-bond formation among the three kinds of PHB–catechin blends, the effects of crystalline phase and the tacticity on the hydrogen-bonding interaction could be elucidated. Part of the experimental results for iPHB and sPHB blends with catechin has been reported elsewhere.¹⁸

Experimental

Materials

Chemosynthesized atactic poly[(*R,S*)-3-hydroxybutyrate] (aPHB, isotactic diad fraction determined by ¹H NMR was 0.50) was synthesized through anionic polymerization of racemic β-butyrolactone in bulk with potassium oleate/18-crown-6 ether complex as an initiator.¹⁹ The reagents β-butyrolactone and 18-crown-6 ether (from Tokyo Kasei Industry Co., Japan) were purified as reported in the literature. The resultant polymer was precipitated twice into methanol from the chloroform solution and dried under vacuum for a week before use. Chemosynthesized highly-syndiotactic poly[(*R,S*)-3-hydroxybutyrate] (sPHB, diad syndiotacticity is 0.6) was supplied by courtesy of Takasago International Corporation, Japan. Biosynthesized isotactic poly[(*R*)-3-hydroxybutyrate] was supplied courtesy of Mitsubishi Gas Co. Ltd., Japan. iPHB and sPHB were purified from chloroform solution by precipitation in *n*-heptane. The molecular characteristics of aPHB, sPHB and iPHB samples are tabulated in Table 1. Catechin (Lot No. 120k1194) was purchased from Sigma-Aldrich Co., USA.

Table 1 Characteristics of poly(3-hydroxybutyrate) samples

Sample	$M_w (\times 10^5)$	M_w/M_n
iPHB	5.59	2.23
sPHB	0.92	1.64
aPHB	0.53	1.17

Preparation of blend samples

A series of blend samples of polyesters with catechin were prepared by solvent-casting techniques on Teflon petri dishes by mixing chloroform–dioxane solutions of the polyesters and catechin in appropriate concentration, 10 mg ml⁻¹. The solvent was allowed to evaporate slowly at room temperature, and then the samples were dried under vacuum at 30 °C for three weeks to remove the residual solvent prior to the physical analysis. A sample film with a thickness suitable for the measurement of FT-IR spectra was prepared by casting the solution of the sample directly on the surface of the silicon wafer, which was transparent for the IR incident beam and used as the substrate. It should be emphasized here that the solvents in all the samples were removed before tests so that the repeatability of experiments could be validated. In order to indicate the catechin content in the blend samples, the following codes were used, aPHBc25, sPHBc25, iPHBc25 and so on. The numbers referred to the molar ratio of catechin to polyesters' monomeric repeating units in the blend sample, and aPHBc, sPHBc and iPHBc referred to the aPHB–catechin, sPHB–catechin and iPHB–catechin blend systems, respectively.

Analytical procedures

FT-IR measurements were carried out on a Spectra 2000 (Perkin Elmer Japan Co., Tokyo), a single-beam IR spectrometer with a digital temperature controller. All the spectra were recorded under a given temperature at a resolution of 4 cm⁻¹ and with an accumulation of 64 scans. A curve-fitting program, based on the Gauss–Newton iteration procedure, was applied here for the line-shape analysis of the FT-IR carbonyl-vibration spectra. With the least-squares parameter-adjustment criterion, the bands of carbonyl-vibration could be quantitatively resolved into three parts: the amorphous, the crystalline (if a crystalline phase existed), and the hydrogen-bonded components. This fitting adjusted the peak position, the line shape, the peak width and the height in such a way that the best fit between experimental and calculated spectra was obtained.

DSC thermograms were recorded on a SEIKO DSC 220 system connecting with a SSC5300 workstation. About 5 mg sample was encapsulated into an aluminium pan. In the first heating run, the samples were heated from –50 to 200 °C at a scanning rate of 20 °C min⁻¹. Then, they were quenched with liquid nitrogen to –50 °C, and again the samples were reheated to 200 °C at the same scanning rate (the second heating run). The glass transition temperature, T_g , was taken as what was indicated by the DDSC (differential of DSC) peak recorded in the second heating run.

Results and discussion

Hydrogen-bonding interaction between aPHB and catechin

aPHB is an amorphous random copolymer of *R*- and *S*-hydroxybutyrate. In studying the hydrogen-bonds between the hydroxybutyrate repeating units and catechin, it is interesting and also convenient to use amorphous aPHB as one component in the blends with catechin since no crystalline phase disturbs the formation of hydrogen-bonds.

As is well known, FT-IR is used extensively in the study of polymer complexes to determine the presence of specific interactions between various chemical groups due to the high sensitivity of the force constants to intermolecular and intramolecular interaction. FT-IR is also able to provide both qualitative and quantitative positive information on the specific interactions between polymers and low molecular weight

compounds. For a polyester–catechin blend combination, there are two main absorption ranges in the infrared spectra that are sensitive to the hydrogen-bond formation. One is the hydroxyl-stretching region located within 3000–3600 cm^{-1} , and the other is the carbonyl-stretching region within 1650–1800 cm^{-1} . The carbonyl-stretching mode of polyesters appears around 1740 cm^{-1} , while catechin shows no absorption in this region. Therefore, any changes observed in this region should be directly attributed to changes in the carbonyl-group environment of polyesters, such as the formation of hydrogen-bonds.

Fig. 1a and 1b show the carbonyl-stretching and hydroxyl-stretching spectra of aPHB, catechin and their blends with different compositions. When aPHB is blended with catechin, a new band appears at about 1718.5 cm^{-1} , lower than that of pure aPHB at about 1740.8 cm^{-1} . This new band should be assigned to the hydrogen-bonded carbonyl groups. The band at about 1740.8 cm^{-1} is assigned to the hydrogen-bond-free carbonyl groups. With an increase of catechin content in the blends, the relative absorbance of the hydrogen-bonded carbonyl increases. In the hydroxyl-stretching region, one main band, centering at 3324 cm^{-1} , should be assigned to the self-associated hydroxyl group of catechin, because of its position with low wavenumber. For pure aPHB, only a very weak band centering at 3448 cm^{-1} is observed in this region, which should be attributed to the stretching of the chain-end hydroxyl groups of aPHB. Because of its low intensity compared with that of catechin in this stretching region, the contribution of this band to the total spectrum can be neglected when the content of catechin is high enough. By blending aPHB and catechin, a new band centering at about 3426 cm^{-1} appears, which should be induced by the formation of the ‘polyester-catechin intermolecular’ hydrogen-bonds. The relative intensity of this new band increases with an increase of the catechin content. Compared with the wavenumber of self-associated pure catechin, this band lies in the higher wavenumber region, indicating that the strength of these polyester–catechin intermolecular hydrogen-bonds is weaker than that of the catechin–catechin ones.

Effects of crystalline phase on hydrogen-bonds

By comparing the FT-IR spectra among aPHB–catechin, sPHB–catechin and iPHB–catechin blend samples, it is interesting to detect the effects of a crystalline phase on the number and the strength of hydrogen-bonds. Fig. 2a and Fig. 2b

illustrate the carbonyl-stretching spectra of aPHB, sPHB and their blends with catechin measured at 30 °C. When sPHB is blended with catechin, it is clear that a new band appears at a lower wavenumber of about 1718.5 cm^{-1} , compared with that of pure sPHB at about 1740.8 cm^{-1} . Similarly to aPHB–catechin blends, this new band should be assigned to the hydrogen-bonded carbonyl groups. However, in iPHB–catechin blends, as shown in Fig. 2c, it can be noted that neither the position nor the shape of the carbonyl-stretching band changes, suggesting fewer or no hydrogen-bonds can be formed in the iPHB–catechin blends. Therefore it can be concluded that strong hydrogen-bonds can be formed in aPHB–catechin and sPHB–catechin blends, while few or no hydrogen-bonds can be formed in iPHB–catechin blends.

Although the chemical structures of three PHBs are the same, the stereo structures are very different among aPHB, sPHB and iPHB, that is, iPHB is completely isotactic, sPHB is highly syndiotactic, and aPHB is atactic. The alternation between *R*- and *S*- repeating units destroys the stereo regularity of backbone in aPHB and partly destroys that of sPHB; thus aPHB is amorphous, and sPHB is lowly crystalline while iPHB is highly crystalline. As shown in Fig. 2c, iPHB in the iPHBc0.25 blend sample shows a strong absorption at 1724 cm^{-1} , which is very similar to that of pure iPHB. It means that iPHB in iPHBc0.25 is still highly crystalline. Consequently, it can be suggested that the existence of a crystalline phase in iPHB blends with catechin restrains the formation of hydrogen-bonds by freezing the molecular chain and reducing the extent of amorphous phase. In order to confirm this assumption, especially to detect the formation of hydrogen-bonds in iPHB–catechin blends, an appropriate condition to avoid the crystallization in the blends should be applied. The melting point of highly crystalline iPHB is about 180 °C, so if the temperature for FT-IR measurements rises above 180 °C, the crystalline phase of iPHB would disappear and revert to the amorphous state. On the base of this assumption, the fusion of the crystalline phase should lead to the enhancement of hydrogen-bond formation.

Ahead of detecting the effects of the fusion of crystalline phase on the formation of hydrogen-bonds in these blends, it is necessary to understand the FT-IR behavior of pure PHBs at higher temperature. In Fig. 3 is the comparison of carbonyl-stretching spectra of PHBs measured at 30 °C with those at 190 °C. IR spectra are sensitive to the conformation and packing of molecular chains.²⁰ A unique phase would show a Gaussian line-shape peak in the carbonyl-stretching region. In Fig. 3a and

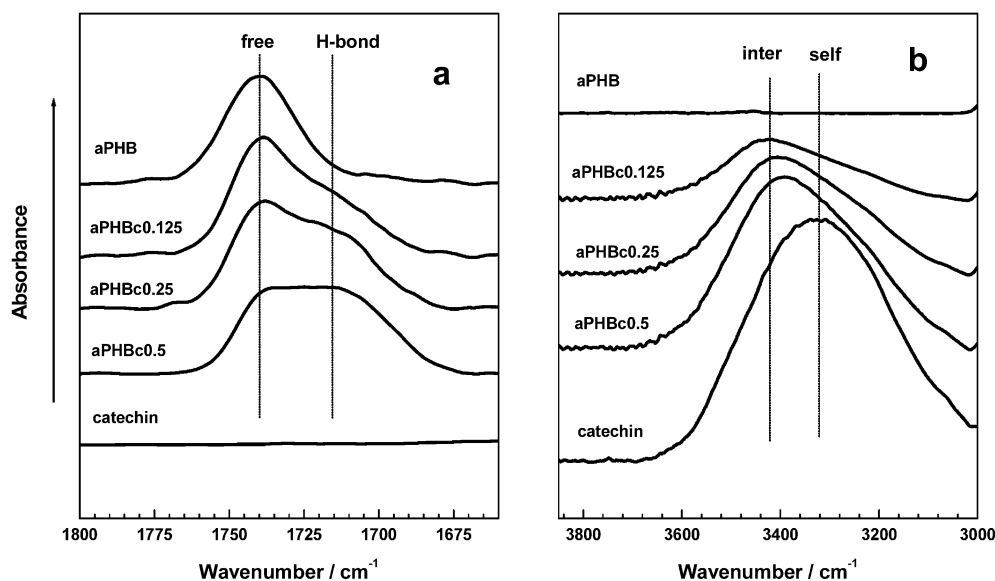


Fig. 1 FT-IR spectra of aPHB, catechin and their blends with different compositions. Free, H-bond, inter and self denote the hydrogen-bond free carbonyls, hydrogen-bonded carbonyls, inter-associated hydroxyls and self-associated hydroxyls, respectively.

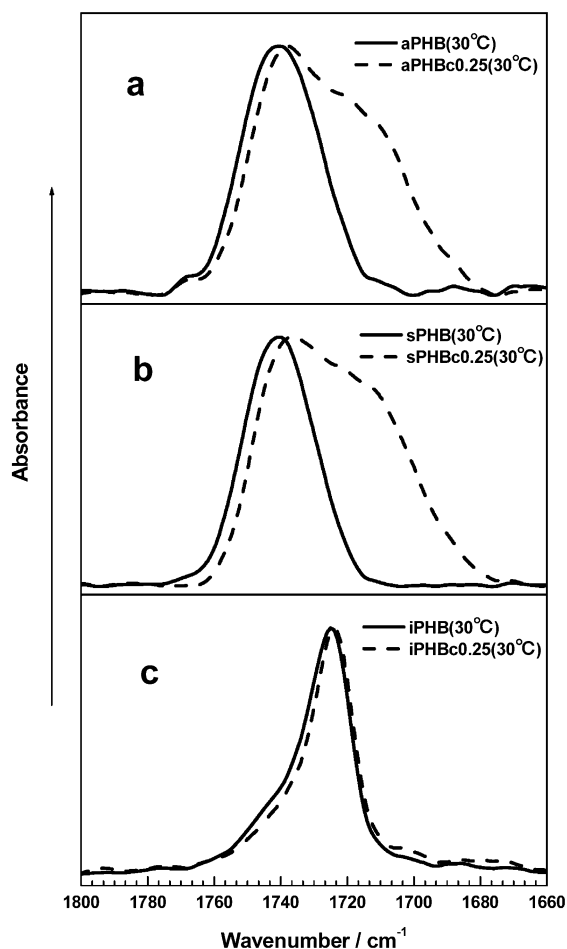


Fig. 2 Carbonyl-stretching bands, measured at 30 °C, of aPHB, sPHB, iPHB and their blends with catechin.

3b, a single Gaussian line-shape peak is observed for amorphous aPHB and lower crystalline sPHB at 30 °C, while for highly crystalline iPHB, as shown in Fig. 3c, a more complicated line-shape is observed in the carbonyl-stretching region. The complex-shape peak can be curve-resolved into two peaks, as shown in Fig. 3c. The lower wavenumber peak at 1725.2 cm^{-1} denotes the crystalline carbonyl groups, and the higher one at 1740.8 cm^{-1} denotes the amorphous carbonyl groups. Certainly, similar to aPHB and sPHB, iPHB shows a single Gaussian line-shape peak in the carbonyl-stretching region at 190 °C because of melting of the crystalline phase.

In Fig. 4 is the comparison of carbonyl-stretching spectra of pure PHBs with those of their blends measured at 190 °C. It is very clear that all PHBs in the blends show a strong absorption at a lower wavenumber position than pure PHBs, indicating the formation of strong hydrogen-bonds with catechin. The occurrence of the hydrogen-bond formation at 190 °C in iPHB–catechin blends has supported the suggestion that the crystallization of iPHB is one of the important factors preventing the formation of the hydrogen-bonds in the iPHB–catechin blends.

Effects of steric structure on hydrogen-bonds

The steric configuration of PHBs is also one of the possible factors affecting their abilities to form hydrogen-bonds with catechin at 30 °C. In order to examine the effect of steric configuration, three PHBc0.25 blend samples without the crystalline phase have been prepared by quenching the blends from 190 to 30 °C. As described in the later section of this article, the T_g values of these blends are higher than 30 °C. The crystallization of iPHB and sPHB in PHBc0.25 blends is much

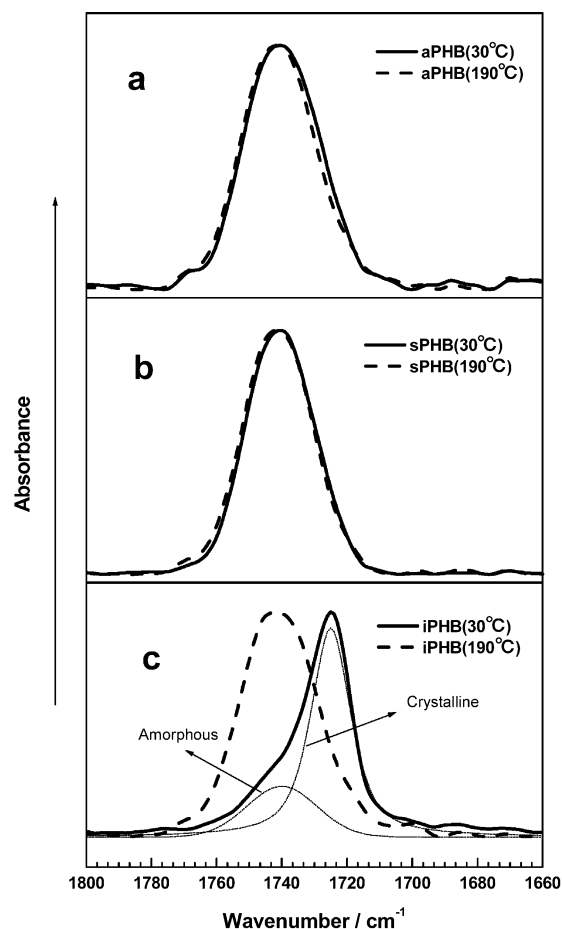


Fig. 3 Comparison of carbonyl-stretching bands of aPHB, sPHB and iPHB measured at 30 °C with those measured at 190 °C.

restrained when the blend samples are quenched to 30 °C. In fact, these quenched blends were almost amorphous during the FT-IR measurements (no melting peak could be detected by DSC). Fig. 5a shows FT-IR spectra in the carbonyl-stretching region for the quenched aPHBc0.25, sPHBc0.25, iPHBc0.25 and catechin samples. Catechin shows no absorption in this region. In addition to the hydrogen-bond-free carbonyl band at about 1740 cm^{-1} , all the quenched samples show a strong absorption at about 1718.5 cm^{-1} , indicating the formation of strong hydrogen-bonds with catechin irrespective of the steric configuration of PHBs. Any effect of the steric configuration on the hydrogen-bond formation has not been found in the hydroxyl-stretching absorption, as shown in Fig. 5b. The hydroxyl-stretching bands are sensitive to the strength of hydrogen-bonds. The hydroxyl-stretching bands with the lower wavenumber should correspond to a stronger hydrogen-bonding interaction.²¹ However, both the position and the line-shape of the hydroxyl-stretching bands are very similar for the three quenched blend samples. Thus, it is safe to conclude that the strength of hydrogen-bonds among them is almost the same.

As shown above, FT-IR spectra confirmed the existence of intermolecular hydrogen-bonds between the carbonyl groups of three kinds of PHBs and the hydroxyl groups of catechin. A curve-fitting technique is used here to quantitatively analyze the carbonyl-stretching bands. It is expected that with employing this technique, the quantitative difference in hydrogen-bonds among the three kinds of PHB–catechin blends can be distinguished. By applying the curve-fitting procedure^{12–14} based on the Beer–Lambert law, the integrated intensity of the PHB carbonyl stretching band can be resolved into three components, that is, the amorphous, $A_{(a, CO)}$, the crystalline, $A_{(c, CO)}$, and the hydrogen-bonded, $A_{(b, CO)}$. Since the quenched sample is amorphous, the carbonyl-stretching bands of these

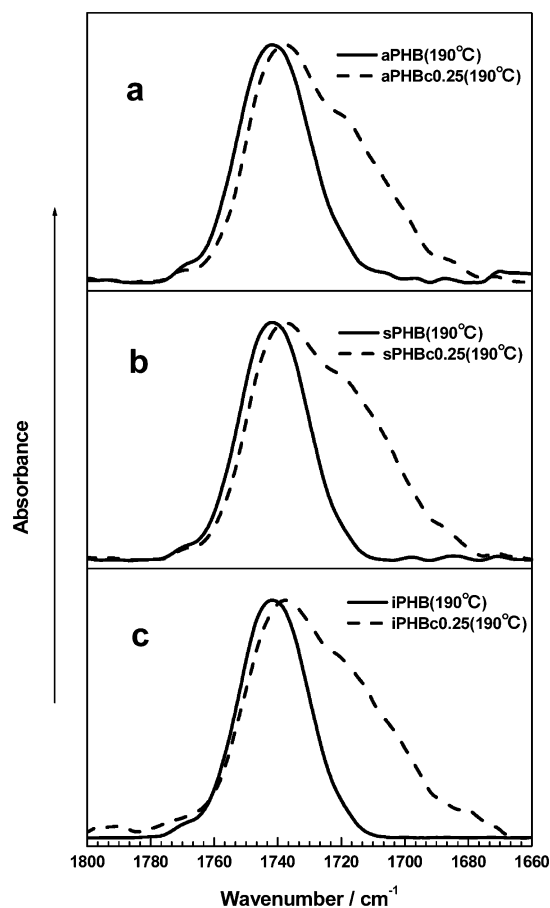


Fig. 4 Comparison of carbonyl-stretching spectra of aPHB, sPHB and iPHB with those of their blends with catechin at 190 °C.

samples were resolved into the amorphous and the hydrogen-bonded bands. The fraction of hydrogen-bonded carbonyl groups of PHB–catechin blends, F_b , can be expressed as

$$F_b = A_{(b, CO)} / (A_{(b, CO)} + \gamma_{b/a} A_{(a, CO)}) \quad (1)$$

where $\gamma_{b/a}$ is the absorption coefficient, which takes into account the difference of the absorptivities between the amorphous and the hydrogen-bonded carbonyl groups. Compared with the absorption coefficients of the similar polyester systems,^{12,22,23} the ratio $\gamma_{b/a}$ was reasonably assumed to be 1.5. Fig. 6 shows the curve-fitting results for the carbonyl-stretching

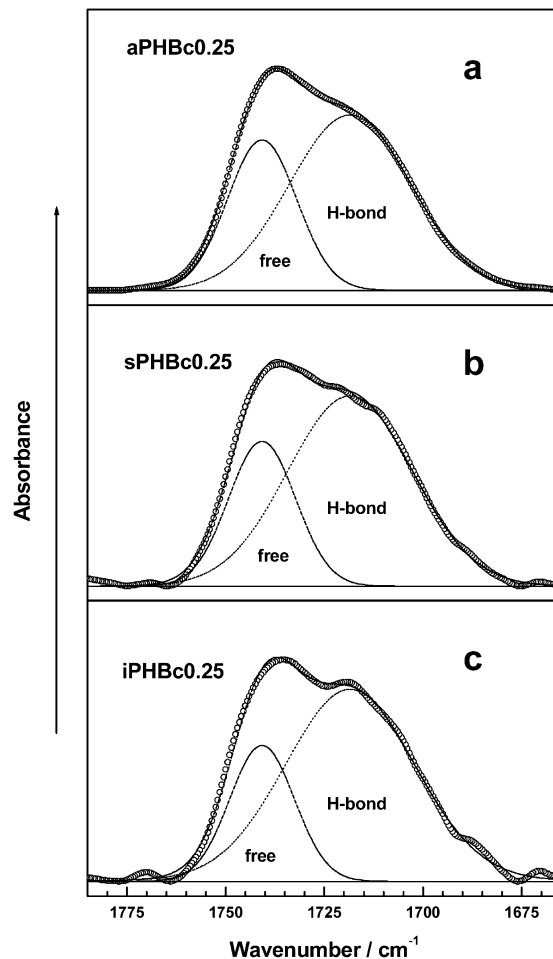


Fig. 6 Experimental and fitted spectra for the quenched aPHBc0.25, sPHBc0.25 and iPHBc0.25 in the carbonyl-stretching region. 'free' and H-bond denote the hydrogen-bond free carbonyls and hydrogen-bonding carbonyls, respectively.

band of the quenched aPHBc0.25, sPHBc0.25 and iPHBc0.25. It is obvious that the curve-fitting results agree well with the experimental data. Based on eqn. 1, the fraction of hydrogen-bonding carbonyls was calculated.

Table 2 lists the results of curve-fitting, including absorption intensity A_i and peak width at half height $W_{1/2}$. By comparing the fraction of hydrogen-bonding carbonyls among three quenched PHBc0.25 samples, it is interesting to note that the

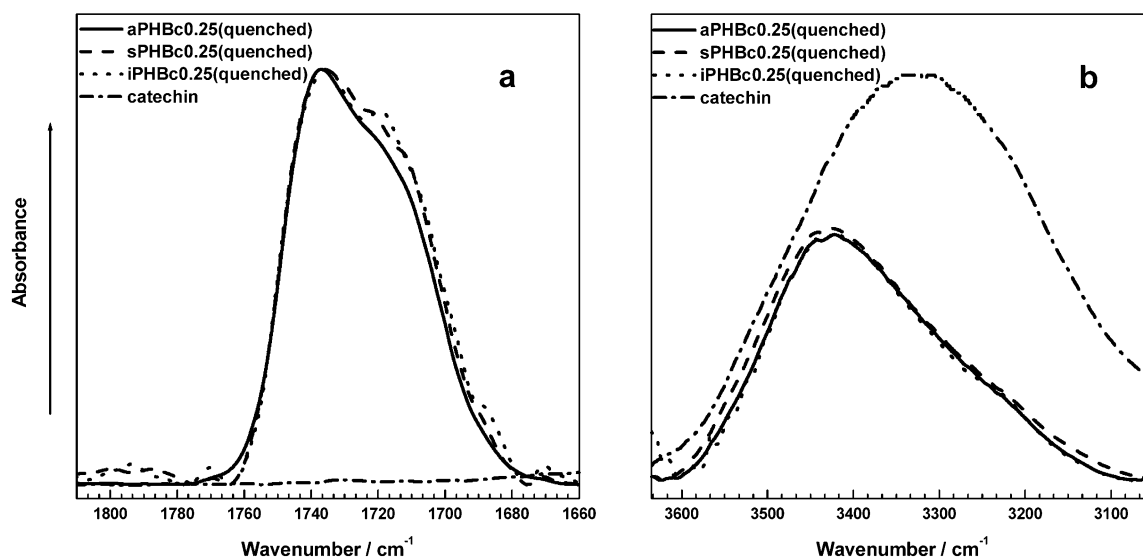


Fig. 5 Comparison of carbonyl and hydroxyl-stretching spectra among quenched aPHBc0.25, sPHBc0.25, iPHBc0.25 and catechin.

Table 2 The relative intensities and the fractions of hydrogen-bonded carbonyl groups for quenched PHB–catechin blends

Sample	'Free' carbonyl			Hydrogen-bonding carbonyl			F_b (%)
	ν/cm^{-1}	$W_{1/2}/\text{cm}^{-1}$	$A_{(a,CO)}$ (%)	ν/cm^{-1}	$W_{1/2}/\text{cm}^{-1}$	$A_{(b,CO)}$ (%)	
aPHBc0.25	1740.8	20.7	33.1	1718.5	36.2	66.9	57.4
sPHBc0.25	1740.8	20.0	29.1	1718.5	37.1	70.9	61.9
iPHBc0.25	1740.8	19.3	25.8	1718.5	38.7	74.2	65.8

quenched iPHBc0.25 contains the most hydrogen-bonding carbonyls, the sPHBc0.25 the second, and the aPHBc0.25 the least, although the difference is small. Compared with aPHB, both iPHB and sPHB seem more likely to be involved in hydrogen-bonds. There is no difference in the chemical structure of the monomeric unit among the three PHBs. Hence, other structural characteristics such as chain flexibility, steric factors and chain connectivity can be expected to influence the formation and the strength of the hydrogen-bonds.²³ Considering that the steric configuration has a pronounced effect on these characteristics, the difference in the steric tacticity among aPHB, iPHB and sPHB may be related to the observed difference in the carbonyl-stretching bands.

Phase behavior

It is well known that when an amorphous polymer in viscous state is cooled from higher temperature, it passes through the glass transition temperature, T_g , and its mechanical properties change from those of a rubber (elastic) to those of a glass (brittle). In general, below the glass transition temperature, the polymer segmental motions are limited, but above the glass transition, a larger extent of polymer segmental motion becomes possible. Besides polymers, some low molecular weight compounds also show the glass transition. Catechin, a low molecular weight polyphenol, has a glass transition because of its strong self-association.²⁴ Usually, DSC is employed to measure the glass transition temperature. Fig. 7 shows the DSC

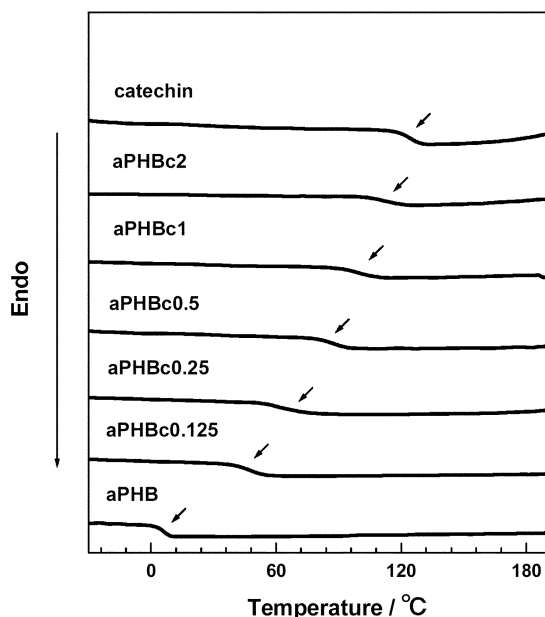


Fig. 7 DSC traces of the aPHB–catechin binary system with various compositions in the second heating scans.

traces of the aPHB–catechin binary blend system with various compositions in the second heating scans. All samples show a single glass transition temperatures, T_g , which lies between the T_g values of pure aPHB and catechin. The T_g values of catechin

and pure aPHB are 123.5 and 6.4 °C, respectively. The T_g value of the blend increased to 110.9 °C as the molar ratio of catechin to aPHB increased to 2. Thermal properties have also been investigated for sPHB–catechin and iPHB–catechin binary blends.¹⁸ The DSC traces for these blend systems are very similar to those of aPHB–catechin blend (the thermograms are not shown here). The T_g values observed by DSC are plotted against the catechin weight content (not the molar ratio) in Fig. 8 for the three binary blend systems. It is clear that all the PHB–

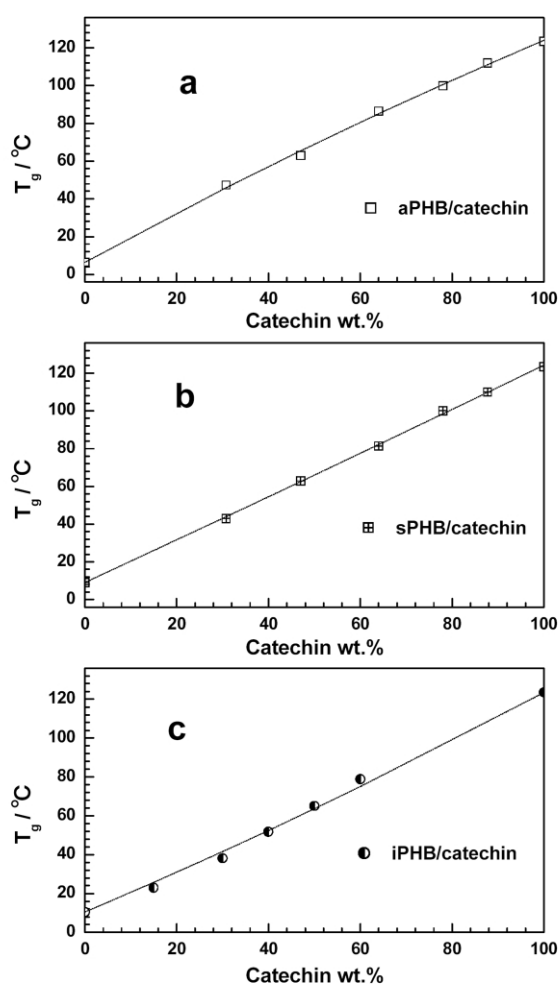


Fig. 8 T_g values observed in blends plotted against the catechin weight content.

catechin systems show only one T_g and it increases rapidly with catechin content. An observation of single glass transition is generally accepted as a qualitative criterion for the miscibility of a binary blend system. For PHB–catechin blends, it also indicates the existence of a strong intermolecular interaction between two components. Therefore, by combination with the FT-IR results, it can be suggested that the strong specific interaction with catechin leads to miscibility of the two components in the amorphous phase of the three kinds of PHB–catechin blend systems.

Conclusion

From FT-IR measurements at 30 °C, it was found that quite strong hydrogen-bonds are formed in aPHB–catechin and sPHB–catechin blends, while no evidence was found to confirm the existence of hydrogen-bonds in iPHB–catechin blends. However, strong hydrogen-bonds was found in melt-state iPHB–catechin blends at 190 °C, indicating the crystalline phase restrains the formation of hydrogen-bonds in the blends. Also the effect of the steric configuration on the hydrogen-bonds has been testified. Higher tacticity benefits the formation of hydrogen-bonds, but it was found that the steric configuration has little effect on the strength of hydrogen-bonds. The formation of strong hydrogen-bonds between PHB and catechin results in their miscibility in the amorphous phase, as testified by DSC measurements. All the PHB–catechin blends showed only one glass transition over the whole range of blend compositions, and the T_g value increased rapidly with the catechin content.

In summary, the formation of strong hydrogen-bonds between the proton-accepting PHB and proton-donating catechin has promised miscibility between them. Consequently, by introducing hydrogen-bonds into poly(3-hydroxyalkanoate)s, the modification of their physical properties could be expected without damaging their desirable biodegradability and biocompatibility.

References

- 1 Y. Doi, *Microbial Polyesters*, VCH Publishers, New York, 1990.
- 2 Y. Inoue and N. Yoshie, *Prog. Polym. Sci.*, 1992, **17**, 571.

- 3 N. Yoshie and Y. Inoue, *Biopolymers*, vol. 3, *Polyesters I*, ed. Steinbüchel, A. and Y. Doi, Wiley-VCH, Weinheim, 2001, ch. VI.
- 4 M. R. Brophy and P. B. Deasy, *Int. J. Pharm.*, 1986, **29**, 223.
- 5 K. Juni, M. Nakano and M. Kubota, *J. Controlled Release*, 1986, **4**, 25.
- 6 S. Akhtar, C. W. Pouton and L. J. Notarianni, *Polymer*, 1992, **33**, 117.
- 7 L. Fineli, B. Sarti and M. Scandola, *J. Macromol. Sci. A*, 1997, **34**, 13.
- 8 Y. Kumagai and Y. Doi, *Polym. Degrad. Stab.*, 1992, **36**, 241.
- 9 G. Geccoruli, M. Pizzoli and M. Scandola, *Macromolecules*, 1993, **26**, 6722.
- 10 Y. He, N. Asakawa and Y. Inoue, *Macromol. Chem. Phys.*, 2001, **202**, 1035.
- 11 J. Li, Y. He and Y. Inoue, *J. Polym. Sci., Polym. Phys. Ed.*, 2001, **39**, 2108.
- 12 P. Iriando, J. J. Iruin and M. J. Fernandez-berridi, *Polymer*, 1995, **36**, 3235.
- 13 L. Zhang, S. H. Goh and S. Y. Lee, *Polymer*, 1998, **39**, 4841.
- 14 J. Wang, M. K. Cheung and Y. Mi, *Polymer*, 2001, **43**, 1357.
- 15 S. Kuo, C. Huang and F. Chang, *J. Polym. Sci., Polym. Phys. Ed.*, 2001, **39**, 1348.
- 16 J. Ueda, N. Saito, Y. Shimazu and T. Ozawa, *Arch. Biochem. Biophys.*, 1996, **333**, 377.
- 17 S. B. Lotito and C. G. Fraga, *Free Radical Biol. Med.*, 1998, **24**, 4351.
- 18 J. Li, B. Zhu, Y. He and Y. Inoue, *Polym. J.*, 2003, **35**, 384.
- 19 Z. Jedlinski, A. Stolarzewicz, Z. Grobelny and M. Szwarc, *J. Phys. Chem.*, 1984, **88**, 6094.
- 20 H. Hagemann, P. G. Synder, A. J. Peacock and L. Mandelkern, *Macromolecules*, 1989, **22**, 3600.
- 21 E. J. Moskala, D. F. Varnell and M. M. Coleman, *Polymer*, 1985, **26**, 228.
- 22 D. Li and J. Brisson, *Polymer*, 1998, **39**, 801.
- 23 M. M. Coleman, J. F. Graf and P. C. Painter, *Prog. Polym. Sci.*, 1995, **20**, 1.
- 24 B. Zhu, J. Li, Y. He and Y. Inoue, *Macromol. Biosci.*, 2003, **3**, 258.



Utilization of carbon dioxide as soft oxidant in the dehydrogenation of ethylbenzene over supported vanadium–antimony oxide catalysts†

Jong-San Chang,* Vladislav P. Vislovskiy, Min-Seok Park, Do Young Hong, Jin S. Yoo and Sang-Eon Park*

Catalysis Center for Molecular Engineering (CCME), Korea Research Institute of Chemical Technology (KRICT), P.O. Box 107, Yusong, Taejeon 305-600, South Korea.
E-mail: separk@kRICT.re.kr and jschang@kRICT.re.kr

Received 29th April 2003

First published as an Advance Article on the web 1st August 2003

This work shows that carbon dioxide, which is a main contributor to the global warming effect, could be utilized as a selective oxidant in the oxidative dehydrogenation of ethylbenzene over alumina-supported vanadium oxide catalysts. The modification of the catalytically active vanadium oxide component with appropriate amounts of antimony oxide led to more stable catalytic performance along with a higher styrene yield (76%) at high styrene selectivity (> 95%). The improved catalytic behavior was attributable to the enhanced redox properties of the active V-sites.

1 Introduction

The utilization of carbon dioxide, which is known to be a main contributor to the greenhouse effect, has been of global interest from both fundamental and practical viewpoints in green chemistry.¹ The application of supercritical CO₂ is one of the most exciting ideas to replace volatile organic solvents in a green chemistry approach² as well as the usage of carbon dioxide as a carbon source through catalytic reduction processes.¹ As another way of utilization, it is worthwhile to note that carbon dioxide could be used as an oxygen source or oxidant and can be considered as a nontraditional mild oxidant and oxygen transfer agent.^{3,4} It has been proposed that carbon dioxide plays a role as a soft oxidant to abstract hydrogen from simple or functionalized hydrocarbons through the catalytic activation of carbon dioxide to form CO and oxygen species.^{5,6} Possible reactions are the oxidative conversions of alkanes, alkenes, alcohols^{5,7} and alkylaromatics, especially ethylbenzene.^{6,8–22} The role of CO₂ in catalytic reactions can give several merits in catalysis such as acceleration of the reaction rate, enhancement of product selectivity, alleviation of chemical equilibrium, suppression of the total oxidation, and prevention of hot spots on the catalyst surface.^{6,8,11,23} Taking into account its unique characteristics, it is anticipated that this concept might lead to emerging new chemistry of carbon dioxide as the oxidant.

Vapor-phase dehydrogenation of ethylbenzene (EBDH) is a representative process to produce styrene, an important monomer for synthetic polymers. This is one of the ten most important industrial processes. However, EBDH is thermodynamically limited and, moreover, it is a very energy-consuming process because of the required excess of superheated steam (steam/EB = 7–12 mol/mol). As an alternative method, the oxidative dehydrogenation of EB has been proposed to be free from thermodynamic limitations regarding conversion, operating at lower temperatures with an exothermic reaction.²⁴ However, this process with use of a strong oxidant, oxygen, suffers from loss of selectivity for styrene due to the production of carbon oxides and oxygenates.

Recently, the utilization of carbon dioxide as an oxidant for the EBDH has been attempted to explore new technology for producing styrene selectively.^{6,9–22} Several catalytic systems were found to be efficient for the CO₂-EBDH reaction. Among them, V-containing catalysts exhibited good performance in the reaction.^{14–16,20–22} These catalysts were actually known to be active and selective in partial oxidation, oxidative dehydrogenation, and ammoxidation of hydrocarbons.^{23–34} Suzuki and co-workers reported that active carbon-supported vanadium catalysts afforded high catalytic activity in the EBDH to give styrene in the presence of carbon dioxide.^{14–16} However, it suffered from severe catalyst deactivation due to coke deposition. Recently we reported high activity and selectivity of VO_x/Al₂O₃ and V–M–O/Al₂O₃ (M = Mg, P, Cr, Mo, Sb) systems in the CO₂-EBDH.²² Here we present the catalytic and redox properties of an alumina-supported vanadium–antimony oxide system as a highly active, selective and stable catalyst for the CO₂-EBDH reaction.

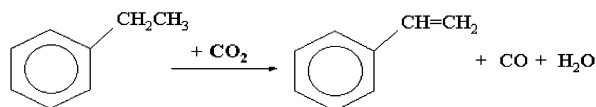
2 Experimental

Al₂O₃-supported vanadium oxide (V/Al) and vanadium–antimony binary oxide (VSb/Al) catalysts were prepared by impregnation of activated alumina (Aldrich, S_{BET} = 121 m² g⁻¹) with aqueous solutions of ammonium metavanadate and antimony(III) chloride along with tartaric acid. Numbers in the formulae of alumina-supported V–Sb oxides denote the relative atomic percentage of the element in this binary system. The impregnated samples were dried at 100 °C and then calcined in air at 600 °C for 4 h. The total amount of supported metal oxides was about 20 wt%

Green Context

The use of CO₂ as an oxidant has received little attention, despite its great abundance. Here it is shown that CO₂ can be activated over a V–Sb catalyst and dissociates to give an active oxygen. This oxygen then is capable of dehydrogenating ethylbenzene to styrene in good yield. *DJM*

† Presented at The First International Conference on Green & Sustainable Chemistry, Tokyo, Japan, March 13–15, 2003.



Calcined samples were characterized by means of XRD, XPS, H_2 -TPR, and CO_2 pulse methods. X-Ray diffraction patterns were recorded on a Rigaku D/MAX-3B diffractometer using monochromatic CuK_α radiation. The X-ray photoelectron spectra were obtained using an ESCALAB MK II spectrometer provided with a hemispherical electron analyzer and Al anode X-ray exciting source ($\text{AlK}_\alpha = 1486.6$ eV). The binding energies (BE) were referred to the adventitious C 1s peak at 284.6 eV. Temperature-programmed reduction of the catalysts with hydrogen (H_2 -TPR) was performed from 100 to 800 °C at a heating rate of 10 °C min^{-1} with a 5% H_2 in helium flow in a conventional flow system equipped with a thermal conductivity detector for monitoring of H_2 -consumption. The samples (100 mg) were previously calcined in a flow of air at 500 °C for 1 h and then cooled down to 100 °C. In order to estimate the re-oxidizability with carbon dioxide of the catalysts previously partially reduced at 600 °C in H_2 -He flow for 30 min, CO_2 pulse experiments were conducted at 600 °C in the 1/4-inch outer diameter quartz reactor with 200 mg of the catalyst. Pulses of carbon dioxide (250 μl CO_2) were injected into an inert helium flow (30 ml min^{-1}) using a gas sampling valve incorporated between the sample inlet and the GC column.

The CO_2 -EBDH reaction was carried out at 595 °C in a micro-activity test unit (Zeton, MAT 2000) with a fixed bed isothermal reactor under atmospheric pressure. A catalyst sample of 1 g was placed into the reactor on a quartz wool support. Ethylbenzene was introduced with a feed rate of 8.2 mmol h^{-1} by a syringe pump and supplied into the reactor together with a carrier gas mixture of CO_2 and N_2 (total flow rate 45 ml min^{-1}). Nitrogen was used as a diluent as well as an internal standard for gas analysis. Gas components of the reaction mixture (H_2 , N_2 , CO , CH_4 , and CO_2) were analyzed by the TCD of the on-line gas chromatograph (GC). Liquid products such as benzene, toluene, ethylbenzene, and styrene were collected each 30 min and analyzed by the FID of the GC. Catalytic performances were characterized by EB conversion, X(EB), selectivity to styrene, S(ST), yield of styrene, Y(ST), and a loss of styrene yield after 4 h on stream relative to that after 1 h on stream, $\text{RLSY}(4) = (\text{Y}_1 - \text{Y}_4)/\text{Y}_1$; Y_1 and Y_4 are the yields of styrene after 1 and 4 h on stream, respectively.

3 Results and discussion

The catalytic properties of V/Al and VSb/Al for the CO_2 -EBDH to styrene are summarized in Table 1. In the reaction, styrene and water are predominantly observed together with the unreacted EB in the condensate and CO, hydrogen and carbon dioxide in the gas phase. Only small amounts of benzene and toluene along with methane are obtained as by-products. The V/Al and VSb/Al catalysts studied here exhibit very high conversion (74–80%) and high selectivity (>95%) at an initial stage, while Sb/Al shows only 19.4% conversion for EB. This result indicates that a vanadium species, probably containing V^{5+} , is a main active component for the reaction. V/Al displays initially high styrene yield ($\text{Y}_1 = 70.7\%$), but its catalytic activity decreases significantly. It was clear from previous work that the type of additives has a stronger influence on the catalyst stability than on the initial catalytic activity or selectivity.²² Addition of MgO, P_2O_5 and MoO_3 practically did not influence initial styrene yield, but deteriorated the on-stream catalytic activity of V/Al.²² The main reason for deactivation of the

supported vanadium oxide catalysts was ascribed to coke formation as well as deep reduction of V^{5+} into V^{3+} . However, a much improved result is achieved with an antimony promoter, as illustrated in Table 1 and Fig. 1. Thus, addition of antimony oxide to V/Al leads to a profound effect on its activity and catalyst stability. EB conversions over the VSb/Al catalysts, except $\text{V}_{0.25}\text{Sb}_{0.75}/\text{Al}$, are 5% higher than that of V/Al after 1 h on stream. The CO_2 -EBDH reaction over VSb/Al catalysts is not sensitive to the vanadium content. Thus a decrease in vanadium content does not diminish the initial EB conversion. It is worth noting that the stability of VSb/Al catalysts is much better than that of the unmodified one. The effect of antimony addition on the catalyst stability is maximized at V/Sb = 0.75. The $\text{V}_{0.43}\text{Sb}_{0.57}/\text{Al}$ catalyst exhibits the highest activity and stability. This stability is also confirmed by the unchanged specific surface area after reaction. Re-oxidation of the used VSb/Al catalysts is accompanied by much less CO_x evolution than the used V/Al catalyst, implying that less coke is formed during the reaction. The catalyst activity could be easily reactivated without a loss of styrene yield by means of short-term treatment in an air stream.

Crystalline vanadium phases of the V/Al and VSb/Al catalysts obtained from XRD analysis are listed in Table 1. The XRD patterns of V/Al before and after reaction show the presence of vanadium oxide crystallites such as V_2O_5 in the fresh sample and V_2O_3 in the used one (not presented here). However, the XRD patterns of the VSb/Al catalysts do not reveal crystalline vanadium oxides. Instead, an intermediate phase of mixed vanadium–antimony oxide, $\text{V}_{1.1}\text{Sb}_{0.9}\text{O}_4$, is newly appeared in the XRD pattern of $\text{V}_{0.43}\text{Sb}_{0.57}/\text{Al}$. These results imply that vanadium oxides are well dispersed in the Sb-promoted catalysts and the mixed phase of V–Sb oxide can be formed at an optimal ratio of V/Sb. The $\text{V}_{1.1}\text{Sb}_{0.9}\text{O}_4$ phase has been reported to be the main component in the crystalline VSbO_x bulk oxide with the atomic ratio V/Sb = 1.²⁹

The H_2 -TPR profiles of the V/Al and VSb/Al catalysts are displayed in Fig. 2. The TPR profile of the V/Al catalyst is very different from those of the VSb/Al catalysts. The H_2 -TPR of the V/Al catalyst reveals two strong high-temperature peaks centered at 663 and 783 °C with a weak peak at 500 °C. However, in the reduction patterns of the VSb/Al catalysts the high-temperature reduction peaks above 600 °C are very weak, while the low-temperature reduction peak at 500 °C becomes dominant. These results strongly indicate that the addition of antimony to the V/Al catalyst increases the reducibility of vanadium oxide.

The cumulative amounts of CO produced according to repetitive injections of CO_2 pulses at 600 °C over the pre-reduced V/Al and $\text{V}_{0.43}\text{Sb}_{0.57}/\text{Al}$ catalysts are plotted in Fig. 3. It is confirmed from these pulse experiments that the dissociative adsorption of CO_2 on the reduced vanadium oxide of the catalysts produces CO and surface oxygen. One can see that the formation of CO over $\text{V}_{0.43}\text{Sb}_{0.57}/\text{Al}$ is much more intensive than over V/Al. For $\text{V}_{0.43}\text{Sb}_{0.57}/\text{Al}$, the total amount of CO formed after injections of 40 CO_2 pulses corresponds to 0.268 mol-CO/mol- V_2O_5 whereas over V/Al it is only 0.041 mol-CO/mol- V_2O_5 . This result strongly suggests that re-oxidizability of the $\text{V}_{0.43}\text{Sb}_{0.57}/\text{Al}$ catalyst with oxygen species originated from CO_2 is much higher than that of the V/Al catalyst.

Table 2 summarizes binding energies and peak widths of V and Sb components taken from XPS of V/Al and $\text{V}_{0.43}\text{Sb}_{0.57}/\text{Al}$ catalysts before and after reaction. For fresh V/Al and $\text{V}_{0.43}\text{Sb}_{0.57}/\text{Al}$ catalysts, their BEs for V 2p_{3/2} (517.2–517.6 eV) and Sb 3d_{3/2} (540.2 eV) correspond to V^{5+} and Sb^{5+} , respectively, implying that the fresh catalysts possess the highest oxidation states of V and Sb. The parameters both of Sb 3d_{3/2} and V 2p_{3/2} peaks for the $\text{V}_{0.43}\text{Sb}_{0.57}/\text{Al}$ catalyst remain almost unchanged after catalytic reaction, but peak width of the V 2p_{3/2} for the used V/Al significantly increases relative to that for the fresh one, *i.e.*, from 1.90 to 3.16 eV, pointing to the

Table 1 Catalytic behavior of V/Al, VSb/Al and Sb/Al catalysts in the CO₂-EBDH reaction

Catalyst	V ₂ O ₅ (wt.%)	S _{BET} /m ² g ⁻¹		After 1 h on-stream			RLSY(4) (%)	XRD phase (fresh)
		fresh	used	X(EB) (%)	Y(ST) (%)	S(ST) (%)		
V/Al	20.0	78	65	74.8	70.7	94.5	21.3	V ₂ O ₅
V _{0.87} Sb _{0.13} /Al	16.8	74	62	79.8	75.8	95.0	11.6	amorphous
V _{0.43} Sb _{0.57} /Al	7.4	87	88	79.9	76.0	95.1	3.3	V _{1.1} Sb _{0.9} O ₄
V _{0.25} Sb _{0.75} /Al	3.4	104	109	73.9	71.2	96.3	6.7	amorphous
Sb/Al	0	109	115	19.4	18.3	94.3	22.2	amorphous

Reaction conditions: 595 °C, EB/CO₂ = 1 (molar ratio). Notation: X(EB), EB conversion; Y(ST), Styrene yield; S(ST), Styrene selectivity; RLSY (4), Loss of styrene yield after 4 h on stream relative to that after 1 h on stream, (Y₁ - Y₄)/Y₁.

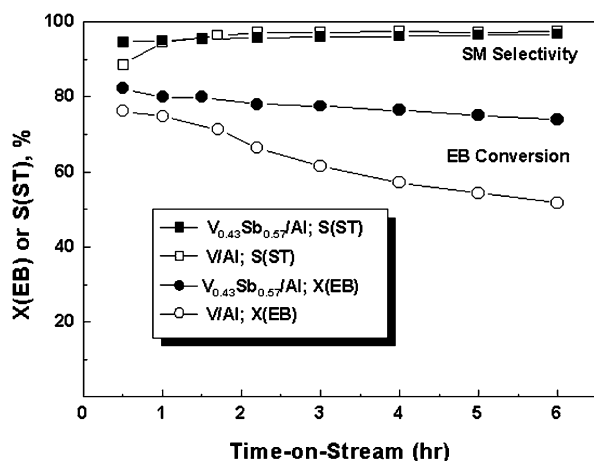


Fig. 1 Catalytic stability of V/Al and V_{0.43}Sb_{0.57}/Al catalysts in the CO₂-EBDH reaction. Reaction conditions: $T = 595$ °C, EB/CO₂ = 1 (molar ratio).

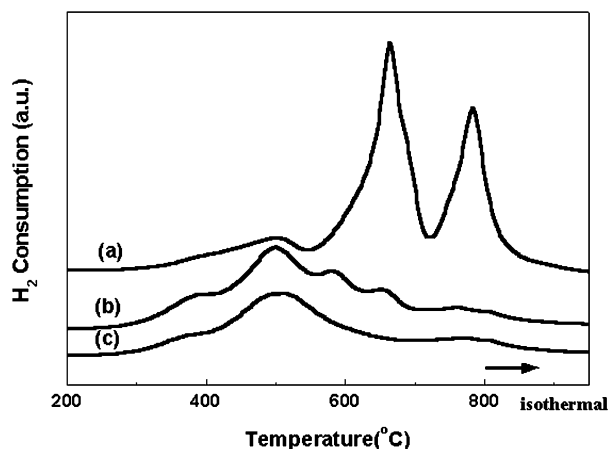


Fig. 2 H₂-TPR profiles of (a) V/Al, (b) V_{0.43}Sb_{0.57}/Al, and (c) V_{0.25}Sb_{0.75}/Al catalysts.

significant reduction of surface V-component during the reaction.

Among the factors determining the catalytic properties of vanadium oxide-based catalysts, the redox behavior of vanadium oxide is known to play a key role in oxidative dehydrogenation, oxidation, and ammoxidation of hydrocarbons in accordance with the Mars-van-Krevelen mechanism.^{23,25–30,34,35} It can be proposed that the facile redox cycle between fully oxidized and reduced vanadium species yields the more effective catalyst.²⁵ Likewise, the CO₂-EBDH is expected to follow the same mechanism. Actually, the studied catalysts, especially Sb-containing ones, easily undergo reduction (H₂-TPR data) and re-oxidation by carbon dioxide. As seen from CO₂ pulse results, in the CO₂-EBDH, carbon dioxide may act as an oxidant to provide oxygen species on the reduced catalyst

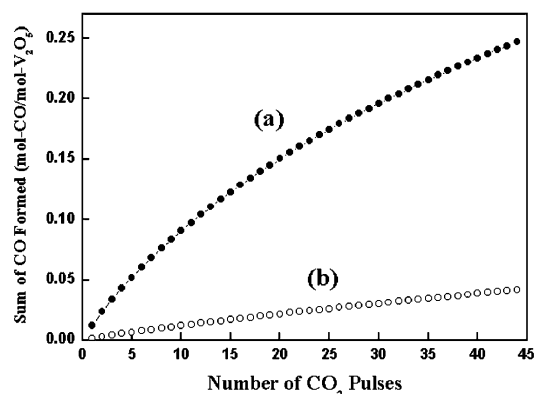


Fig. 3 Cumulative amounts of CO formed during pulse injections of CO₂ on pre-reduced (a) V_{0.43}Sb_{0.57}/Al and (b) V/Al catalysts at 600 °C. Test conditions: see text.

Table 2 XPS peaks of V/Al and VSb/Al catalysts used in the CO₂-EBDH reaction

Catalyst		V 2p _{3/2} /eV		Sb 3d _{3/2} /eV	
		BE	FWHM	BE	FWHM
V/Al	fresh	517.2	1.90	—	—
	used	517.1	3.16	—	—
V _{0.43} Sb _{0.57} /Al	fresh	517.6	2.18	540.2	2.34
	used	517.7	2.34	540.2	2.07

Notation: BE, binding energies; FWHM, full widths at half maximum.

surface and, consequently, re-oxidize the reduced vanadium species into an active (high) oxidation state. Adsorption of ethylbenzene, a strong reductant, on non-properly regenerated active sites may lead to strongly adsorbed organic intermediates similar to coke precursors and, consequently, to catalyst deactivation. The introduction of antimony oxide into the V/Al catalyst facilitated the redox cycle, resulting in enhancement of the catalyst stability as well as the catalytic activity. The most efficient catalyst, V_{0.43}Sb_{0.57}/Al contains a new V_{1.1}Sb_{0.9}O₄ phase. Centi *et al.* claimed that a non-stoichiometric rutile-type vanadium antimonate phase facilitates the redox transformation of vanadium.²⁸ Therefore, the presence of a mixed vanadium–antimony oxide phase in V_{0.43}Sb_{0.57}/Al could promote catalyst stability for the CO₂-EBDH reaction *via* the easier redox transformation of the vanadium ion. Additionally, the better dispersion of the active vanadium oxide component due to modification with antimony could be one of the reasons for the better stability of the VSb/Al catalysts in the CO₂-EBDH reaction.

The EBDH reaction in the presence of CO₂ over the supported vanadium oxide catalysts would be carried out *via* two possible pathways: (i) oxidative dehydrogenation of EB with carbon dioxide as an oxidant that produces styrene and carbon monoxide along with water in one step and (ii) non-oxidative dehydrogenation of EB that produces styrene and hydrogen (in this case CO₂ is inert). It is not easy to distinguish

the above mentioned type of oxidative CO₂-EBDH from the reverse water–gas shift reaction (CO₂ + H₂ = CO + H₂O, ΔH° = 41.6 kJ mol⁻¹ at 25 °C), in which CO₂ as an oxidant reacts with hydrogen dissociated from EB under the non-oxidative EBDH. Stoichiometric amounts of hydrogen and styrene are detected in the non-oxidative EBDH reaction without CO₂ over the V/Al and VSb/Al catalysts. However, carbon monoxide (with the stoichiometric amount of water) and hydrogen are simultaneously observed the CO₂-EBDH reaction. These observations imply that the non-oxidative and oxidative pathways coexist under the conditions of the CO₂-EBDH reaction. However, it is evident that V/Al and VSb/Al activities are increased by 10–18% upon the addition of carbon dioxide to the reaction mixture. For V_{0.43}Sb_{0.57}/Al, the molar ratio of H₂O/H₂ in the product stream is estimated to be 1.4 and conversion of CO₂ into CO is 41.8%. The formation of water along with carbon monoxide in the CO₂-EBDH reaction and formation of CO in the course of CO₂-pulse interaction with the pre-reduced catalysts (Fig. 3) strongly support that the CO₂ molecule dissociates into CO and active surface oxygen, which can abstract hydrogen atoms from EB, and then results in the generation of water. Judging from these results, it is concluded that high activity and stability of the alumina-supported vanadium–antimony oxide catalysts under CO₂ atmosphere would be mainly ascribed to the one-step oxidative route with participation of CO₂ as an oxidant.

4 Conclusion

Alumina-supported vanadium–antimony oxide catalysts have been found to be very active, selective and relatively stable catalysts for the CO₂-EBDH reaction to styrene. The most efficient V_{0.43}Sb_{0.57}/Al catalyst contains a new mixed vanadium–antimony oxide phase, V_{1.1}Sb_{0.9}O₄, and reveals an enhanced redox property. The improved catalyst activity and stability is likely to arise from the presence of the latter V–Sb phase, which induces a facile redox transformation of vanadium ions.

Acknowledgements

This work was performed for the Greenhouse Gas Research Center, one of the Critical Technology-21 Programs, funded by the Ministry of Science and Technology of Korea (MOST). V. P. V. thanks the MOST for the visiting scientist fellowship. We thank Daeho Industries Co (Korea) for financial support.

References

- 1 *Advances in Chemical Conversions for Mitigating Carbon Dioxide*, ed. T. Inui, M. Anpo, K. Izui, S. Yanagida and T. Yamaguchi, *Studies*

- in *Surface Science and Catalysis*, Vol. 114, Elsevier, Amsterdam, 1998, **114**.
- 2 J. M. DeSimone, *Science*, 2002, **297**, 799.
- 3 B. Denise and R. P. A. Sneed, *Chem. Technol.*, 1982 (Feb.), 108.
- 4 M. Aresta, C. Fragale, E. Quaranta and I. J. Tommasi, *J. Chem. Soc., Chem. Commun.*, 1992, 315.
- 5 O. V. Krylov and A. Kh. Mamedov, *Ind. Eng. Chem. Res.*, 1995, **34**, 474.
- 6 S.-E. Park, J.-S. Chang and J. S. Yoo, in *Environmental Challenges and Greenhouse Gas Control for Fossil Fuel Utilization in the 21st Century*, ed. M. M. Maroto-Valer, Y. Soong and C. Song, Kluwer Academic/Plenum Publishers, New York, 2001, pp. 359–369.
- 7 T. Nishiyama and K. Aika, *J. Catal.*, 1990, **122**, 346.
- 8 J. S. Yoo, *Catal. Today*, 1998, **41**, 409.
- 9 S.-E. Park, J.-S. Chang and M. S. Park, *Prepr. Am. Chem. Soc., Div. Fuel Chem.*, 1996, **41**, 1387.
- 10 M. Sugino, H. Shimada, T. Turuda, H. Miura, N. Ikenaga and T. Suzuki, *Appl. Catal. A*, 1995, **121**, 125.
- 11 N. Mimura and M. Saito, *Catal. Today*, 2000, **55**, 173.
- 12 N. Mimura, I. Takahara, M. Saito, Y. Sasaki and K. Murata, *Catal. Lett.*, 2002, **78**, 125.
- 13 T. Badstube, H. Papp, R. Dziembaj and P. Kustrowski, *Appl. Catal. A*, 2000, **204**, 153.
- 14 Y. Sakurai, T. Suzuki, N. Ikenaga and T. Suzuki, *Appl. Catal. A*, 2000, **192**, 281.
- 15 N. Ikenaga, T. Tsuruda, K. Senma, T. Yamaguchi, Y. Sakurai and T. Suzuki, *Ind. Eng. Chem. Res.*, 2000, **39**, 1228.
- 16 Y. Sakurai, T. Suzuki, K. Nakagawa, N. Ikenaga, H. Aota and T. Suzuki, *J. Catal.*, 2002, **209**, 16.
- 17 J.-S. Chang, S.-E. Park and M. S. Park, *Chem. Lett.*, 1997, 1123.
- 18 J. Noh, J.-S. Chang, J.-N. Park, K. Y. Lee and S.-E. Park, *Appl. Organomet. Chem.*, 2000, **14**, 815.
- 19 J.-N. Park, J. Noh, J.-S. Chang and S.-E. Park, *Catal. Lett.*, 2000, **65**, 75.
- 20 S.-E. Park, J.-S. Chang, V. P. Vislovskiy, M. S. Park, K. Y. Lee and J. S. Yoo, *6th Intern. Conference on Carbon Dioxide Utilization*, Breckenridge, CO, USA, 2001, Preprinted Abstracts, p. 60.
- 21 J.-S. Chang, M. S. Park, V. P. Vislovskiy, S.-E. Park and J. S. Yoo, *Prepr. Am. Chem. Soc., Div. Fuel Chem.*, 2002, **47**, 309.
- 22 V. P. Vislovskiy, J.-S. Chang, M.-S. Park and S.-E. Park, *Catal. Commun.*, 2002, **3**, 227.
- 23 E. Xue, J. R. H. Ross, R. Mallada, M. Menendez, J. Santamaria, J. Perregard and P. E. H. Nielsen, *Appl. Catal. A*, 2001, **210**, 271.
- 24 F. Cavani and F. Trifiro, *Appl. Catal. A*, 1995, **133**, 219.
- 25 E. A. Mamedov and V. Cortes Corberan, *Appl. Catal. A*, 1995, **127**, 1.
- 26 R. G. Rizayev, E. A. Mamedov, V. P. Vislovskii and V. E. Sheinin, *Appl. Catal. A*, 1992, **83**, 103.
- 27 B. Grzybowska-Swierkosz, *Appl. Catal. A*, 1997, **157**, 409.
- 28 G. Centi, S. Perathoner and F. Trifiro, *Appl. Catal. A*, 1997, **157**, 143.
- 29 V. P. Vislovskiy, V. Yu. Bychkov, M. Yu. Sinev, N. T. Shamilov, P. Ruiz and Z. Schay, *Catal. Today*, 2000, **61**, 325.
- 30 V. P. Vislovskiy, N. T. Shamilov, A. M. Sardarly, V. Yu. Bychkov, M. Yu. Sinev, P. Ruiz, R. X. Valenzuela and V. Cortes Corberan, *Chem. Eng. J.*, 2003, in press.
- 31 I. P. Belomestnykh, E. A. Skrigan, N. N. Rozhdestvenskaya and G. V. Isagulians, *Stud. Surf. Sci. Catal.*, 1992, **72**, 453.
- 32 J. Hanuza, B. Jezowska-Trzebiatowska and W. Oganowski, *J. Mol. Catal.*, 1985, **29**, 109.
- 33 W. S. Chang, Y. Z. Chen and B. L. Yang, *Appl. Catal. A*, 1995, **124**, 221.
- 34 E. A. Mamedov, R. M. Talyshinskii, R. G. Rizayev, J. L. G. Fierro and V. Cortes Corberan, *Catal. Today*, 1996, **32**, 177.
- 35 V. Yu. Bychkov, M. Yu. Sinev and V. P. Vislovskiy, *Kinet. Catal. (Engl. Transl.)*, 2001, **42**, 574.



Composites consisting of poly(ϵ -caprolactone) and cellulose fibers directly molded during polymerization by yttrium triflate†

Masahiro Funabashi* and Masao Kunioka

National Institute of Advanced Industrial Science and Technology, Institute for Materials & Chemical Process, Ecological Polymer Group, AIST Tsukuba Central 5, 1-1-1 Higashi, Tsukuba, Ibaraki 305-8565, Japan. E-mail: m.funabashi@aist.go.jp; Fax: +81-(0)29-861-6250; Tel: +81-(0)29-861-4584

Received 29th April 2003

First published as an Advance Article on the web 18th August 2003

Composite samples consisting of poly(ϵ -caprolactone) (PCL) and cellulose fibers (CF) were prepared by the direct molding method during polymerization from ϵ -caprolactone (CL) monomers. CL liquid was mixed with yttrium triflate as a catalyst and 2-propanol as an initiator. CF was easily added to CL liquid and was homogeneously mixed with CL liquid by this method. The mixture was put into a plastic tube. Heating temperature varied from 60 to 120 °C and heating time varied from 6 to 48 h. CF content varied from 0 to 30 wt%. After cooling, the sample was removed from the tube and cut into a column shaped specimen. PCL composites with CF dispersed homogeneously were obtained. The mechanical properties such as elastic modulus and strength of these PCL composites with CF were measured by compression test using the above specimen. The maximum values of modulus and strength of composite samples are the maximum values 654 and 13 MPa, when fiber content was 34% and these values are greater than those of PCL samples without CF. The biodegradability of PCL composites in an aqueous medium with commercial compost was evaluated measuring the biochemical oxygen demand (BOD). The biodegradability of composite samples was not affected by the presence of CF.

Introduction

Polymer composites consisting of polymer matrix and fillers are used in various industrial fields, such as car manufacturing, construction, aerospace industry, sports equipment, *etc.*, since they are easy to process, lightweight and corrosion resistant. Polymer composites are usually produced in the liquid state of matrices, such as melting polymer and polymerization by chemically reacting monomers. During the above manufacturing process, the decrease of viscosity of the matrices in the liquid state results in the increase of filler content. The polymerization process is effective for the higher filler content composites, since the viscosity of monomers is less than that of melting polymers. Biodegradable polymer composites consisting of the biodegradable polymers and the biodegradable fillers are developed in order to dispose of easily after use. The mechanical properties of biodegradable polymers should be comparable with those of standard polymers. Poly(ϵ -caprolactone) (PCL) has recently become a well-known biodegradable polymer.¹ PCL can be used as a matrix for biodegradable composites with biodegradable fillers, which are useful materials for the agricultural and medical fields. PCL can be easily polymerized by ring-opening polymerization from ϵ -caprolactone (CL) by heating or using a suitable catalyst such as Sn(OTf)₂,² Al(O⁻Pr)₃³ or Sm(OAr)₂(THF)₃⁴ with high productivity. These catalysts are unstable in both air and water.

To produce a homogeneous PCL composite, high temperature and strong stirring are required for melting PCL having high viscosity.⁵ It is reported that nano-composites of PCL with chitin whiskers could be produced.⁶ This chitin whiskers network shows the thermal stabilization at a temperature higher than the melting point of PCL. Recently, we found that yttrium

triflate which is a stable Lewis acid in water could bulk-polymerize CL to PCL under air at near room temperature.^{7,8} This method can produce PCL composites having homogeneous dispersion of fillers and is a green process.

In this study, the composite samples consisting of PCL and cellulose fibers (CF) dispersed homogeneously were prepared by a direct molding method during polymerization from CL monomer liquid at from 60 to 120 °C. The effects of conditions of sample preparation on the mechanical properties of the samples were investigated. The biodegradability of samples in an aqueous medium with commercial compost was evaluated by the biochemical oxygen demand (BOD).

Experimental

Sample preparation

PCL composites were prepared by the following procedure as shown in Fig. 1. CL monomer liquid was mixed with yttrium triflate as a catalyst and 2-propanol as an initiator at room

Green Context

Biodegradable polymers are beginning to make an impact on the plastics sector, and polycaprolactone is one of the leading examples. This paper describes the formation of composites with cellulose fibres, designed to improve the mechanical properties of the polymer. Modulus and strength can both be improved by addition of the cellulose component, without any negative impact on biodegradability. These improvements in mechanical properties will extend the utility of the polymer

DJM

† Presented at The First International Conference on Green & Sustainable Chemistry, Tokyo, Japan, March 13–15, 2003.

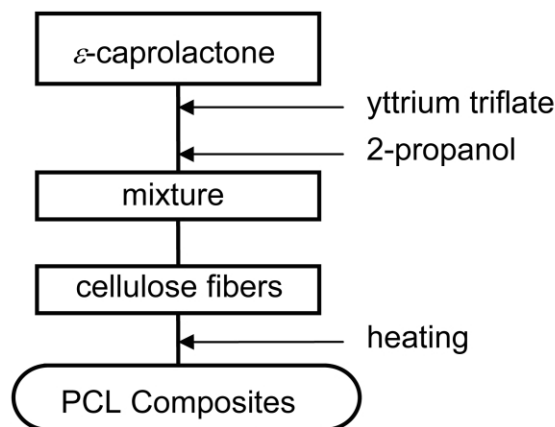


Fig. 1 Sample preparation.

temperature. Cellulose fibers (CF) from filter paper (Ashless pulp, Toyo Roshi Kaisha, Ltd.) were used as fillers for composite samples in this study. CF was added to the above mixture. CL and CF were used without drying. After mixing well, the sample was poured into a plastic tube. The tube was heated at heating temperature T_h °C for heating time t_h hours. T_h was varied in a range of 60, 80, 100 and 120 °C, and t_h was varied in a range of 6, 10, 24, 48 hours. The fiber content of CF, f_c (wt%) was defined as the ratio of CF weight to the weight of PCL. Estimated content was varied in a range of 0, 2, 5, 10, 15, 20, 34 wt%, where 0 wt% means a sample without CF. After cooling the tube to room temperature, the sample was removed. Mixing ratios of PCL, catalyst, initiator and CF, heating conditions and sample codes are shown in Table 1. The sample was cut into the column shape. Diameter and height of specimens were *ca.* 10 and 10 mm, respectively. These specimens were used for measurements of density and mechanical properties.

Mechanical tests

Mechanical properties such as elastic modulus and strength were measured by the compression test using column-shaped specimens. Compression tests were carried out using a Shimadzu Autograph AG-10TB. Test speed was 0.1 mm min⁻¹. Elastic modulus, E_c (MPa) was determined as a gradient of initial linear part of stress–strain curves. Compression strength, σ_c (MPa) was determined as the maximum stress of stress–strain curves.

Table 1 Sample codes, mixing ratio and heating conditions

Sample code	Mixing ratio				Heating conditions	
	Caprolactone/g	Yttrium triflate/g	2-Propanol/mL	Cellulose/g	Temperature/°C	Time/h
A	10	0.2	0.2	0.0	80	48
B1	10	0.2	0.2	0.5	60	48
B2	10	0.2	0.2	0.5	80	48
B3	10	0.2	0.2	0.5	100	48
B4	10	0.2	0.2	0.5	120	48
C1	10	0.2	0.2	0.5	80	6
C2	10	0.2	0.2	0.5	80	10
C3	10	0.2	0.2	0.5	80	28
C4	10	0.2	0.2	0.5	80	48
D1	10	0.2	0.2	0.2	80	48
D2	10	0.2	0.2	0.5	80	48
D3	10	0.2	0.2	1.0	80	48
D4	10	0.2	0.2	1.5	80	48
D5	10	0.2	0.2	2.0	80	48
D6	10	0.2	0.2	3.3	80	48

Samples of B2, C4 and D2 are the same.

Biodegradation evaluation

Biodegradation of samples (100 mg) was evaluated by the measuring system from consumed O₂ (biochemical oxygen demand, BOD) in aerobic water systems with commercial compost using Okura Electric Coulometer OM3100A according to ISO14851-JISK6950.

DSC measurements

In order to confirm the bond between PCL and CF, the differential scanning calorimetry (DSC) measurements of samples were carried out using SEIKO DSC5200 (EX-STAR6000 PC). PCL samples with and without CF and residual CF derived from composite samples washing by hot chloroform using a Soxhlet extraction apparatus to remove unbonded PCL to CF. The sample weight is *ca.* 10 mg and heating rate is 20 °C min⁻¹.

Results and discussion

The densities of column-shaped specimens calculated from their weights and volumes were almost 1.13 g cm⁻³ and independent of the conditions of sample preparation. This value is almost the same as that of commercial PCL, 1.145 g cm⁻³.

Mechanical properties, such as elastic modulus and strength, of samples prepared by various conditions were measured by compression tests using column-shaped specimens. The effect of heating temperature, T_h (°C), on the mechanical properties such as elastic modulus, E_c (MPa) and compression strength, σ_c (MPa) for samples B1 to B4 is shown in Fig. 2. The ▲ symbols and the continuous line correspond to values of E_c , and the ● symbols and the broken line to those of σ_c . Mechanical properties, E_c and σ_c show a maximum at heating temperature $T_h = 80$ °C. Molecular weights of the above samples measured by gel permeation chromatography (GPC) were investigated. There is no significant difference between the values of molecular weights of these samples B1–B4. 100 and 120 °C are much higher than room temperature and the crystallization process of PCL during the cooling of the samples heated at 100 and 120 °C is different from that of sample heated at 80 °C. However, further investigation of the crystallization mechanism will be necessary for the samples prepared at different heating temperatures. For the samples heated at 80 °C, the effect of the heating time, t_h (in hours) on the mechanical properties, E_c and σ_c , is shown in Fig. 3, where samples are C1 to C4. The ▲ symbols and the continuous line show results of E_c , and the ● symbols and the broken line show those of σ_c . The values of E_c

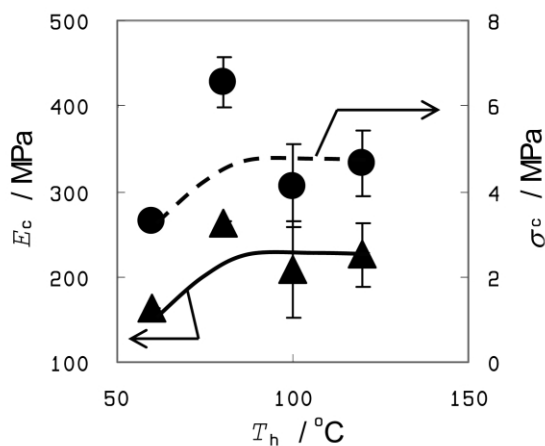


Fig. 2 Effect of heating temperature, T_h , on the mechanical properties of elastic modulus, E_c , \blacktriangle and strength, σ_c , \bullet ; samples D1–D6, these poly(ϵ -caprolactone) (PCL) composites (column shape; 10 mm height and 10 mm diameter) with cellulose fibers (CF) were prepared from 10 g caprolactone, 0.2 g yttrium triflate, 0.2 mL 2-propanol, and 0.5 g CF for 48 h at T_h °C.

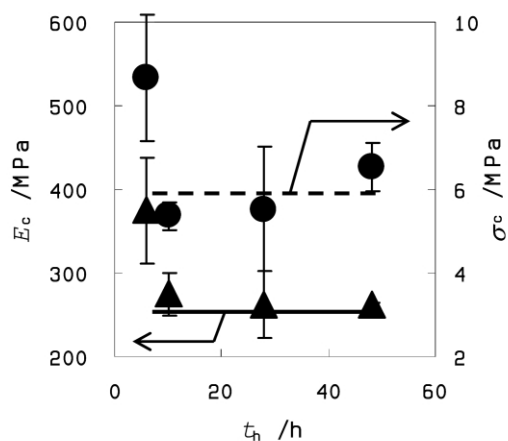


Fig. 3 Effect of heating time, t_h , on the mechanical properties of elastic modulus, E_c , \blacktriangle and strength, σ_c , \bullet ; samples C1–C4.

and σ_c are almost constant. For the samples heated at 80 °C for 48 h, the effect of the cellulose fiber content, f_c (wt%), on the mechanical properties, E_c and σ_c , is shown in Fig. 4, where

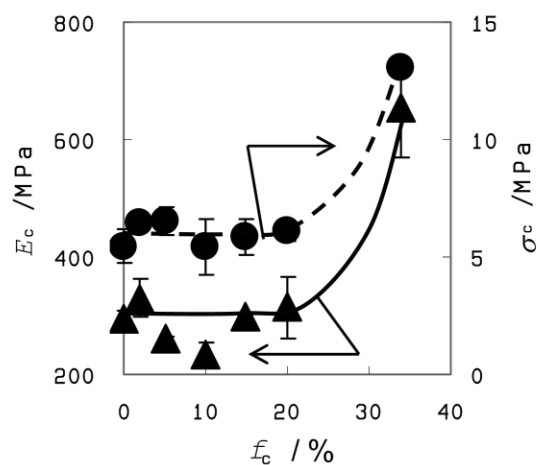


Fig. 4 Effect of cellulose fiber content, f_c , on the mechanical properties of elastic modulus, E_c , \blacktriangle and strength, σ_c , \bullet ; samples D1–D6.

samples are D1 to D6. The \blacktriangle symbols and the continuous line are E_c values and the \bullet symbols and the broken line σ_c values. The values of E_c and σ_c are almost constant in the range of fiber content from 0 to 20%. E_c and σ_c suddenly increase at fiber

content 34%, sample D6. For the composite samples in this study, the maximum fiber content seems to be 34% without pressure during the reaction process. In the range of fiber content 0 to 20%, the mechanical properties of samples were almost the same as those of sample without cellulose, A. It is thought that the effect of the cellulose fiber on the mechanical properties of these samples is not clear and the mechanical properties are determined as those of PCL. The effect of the reinforcement of the cellulose fibers on the mechanical properties is clear at the maximum fiber content, sample D6. From the above results shown in Figs. 2, 3 and 4, the following preparation conditions are sufficient: heating temperature 80 °C, heating time 48 h. The maximum values of E_c and σ_c observed for sample D6 are 654 and 13.0 MPa, respectively.

In order to confirm the bond between PCL and CF, DSC measurements were carried out for PCL samples with and without CF, sample A and B2, CF and residual CF derived from B2 samples washing by hot chloroform using a Soxhlet extraction apparatus to remove unbonded PCL to CF. The peak temperatures of DSC curves for PCL samples with and without CF are *ca.* 60 °C and are almost the same. DSC curve of CF from PCL composites after washing by hot chloroform has no peak related to PCL melting, which is the same as DSC curve of CF itself. The above results of DSC mean that there is no chemical bonding between PCL and CF. This fact might be one of the reasons why the reinforcement effect of CF is not clear in the range of f_c 0 to 20 wt%.

For specimens of commercial PCL (Aldrich, the number averaged molecular weight (M_n) 42 500), E_c and σ_c were measured under the same conditions as this study. The values of E_c and σ_c are 315 and 27.3 MPa, respectively. In comparison with these results, the modulus of sample D6 is twice that of commercial PCL sample, and the strength half. The molecular weight was investigated for the samples prepared at heating temperature 80 °C for heating time 48 h. The number averaged molecular weight (M_n) and the molecular weight distribution (M_w/M_n) of sample without cellulose fiber 4 200 and 1.77, and those of sample with 5 wt% cellulose fiber, 4 900 and 1.94. The molecular weight was not affected by the presence of cellulose fibers. It is thought that the sample D6 is more fragile than the commercial PCL, since M_n of D6 sample is much lower than that of commercial PCL.

The biodegradability of PCL composite samples was investigated by the biochemical oxygen demand (BOD) tests. BOD test results for the samples of PCL with and without CF, samples A and B2 are shown in Fig. 5. Both values of BOD for

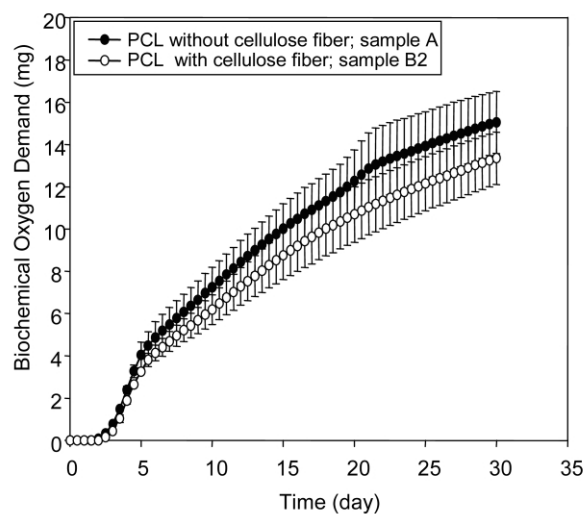


Fig. 5 Changes of biochemical oxygen demand (BOD) with time; samples A and B2.

the samples with and without cellulose fibers show almost the same behavior. When the sample is biodegraded completely,

theoretical total BOD reaches 210 mg. After 30 days, the values of BOD reach *ca.* 15 mg. This result means that 7 wt% of samples degraded after 30 days. The biodegradability of samples is independent of the presence of cellulose fibers.

Conclusion

Composites consisting of polycaprolactone (PCL) and cellulose fibers (CF) were directly molded during the polymerization reaction after mixing caprolactone (CL) monomer with catalyst of yttrium triflate and CF. The homogeneous distribution of CF in PCL matrix can be easily obtained by a new direct molding method, which is produced during the polymerization reaction after mixing caprolactone monomer and fibers. Maximum values of the mechanical properties such as elastic modulus and strength of PCL composite samples are comparable with those of commercial PCL samples. It is thought that the mechanical properties of composite samples higher than those of commercial PCL samples can be obtained by the more detailed

investigation of sample preparation conditions, such as types of catalyst and initiator, mixing ratio of catalyst, initiator and fibers. These composite materials are expected to be utilized for actual use in the agricultural or medical fields.

References

- 1 C. G. Pitt, F. I. Chasalow, Y. M. Hibionada, D. M. Klimas and A. Schindler, *J. Appl. Polym. Sci.*, 1981, **26**, 3779.
- 2 M. Möller, F. Nederberg, L. Lim, R. Kånge, C. Hawker, J. Hedrick, Y. Gu, R. Shah and N. Abbott, *J. Polymer Sci. A*, 2001, **39**, 3529.
- 3 C. Jacobs, P. Dubois, R. Jerome and P. Teyssie, *Macromolecules*, 1991, **24**, 3027.
- 4 M. Nishiura, Z. Hou, T. Koizumi, T. Imamoto and Y. Wakatsuki, *Macromolecules*, 1999, **32**, 8245.
- 5 H. Pranamuda, Y. Tokiwa and H. Tanaka, *J. Environ. Polym. Degrad.*, 1996, **4**, 1.
- 6 A. Morin and A. Dufresne, *Macromolecules*, 2002, **35**, 2190.
- 7 M. Kunioka, Y. Wang and S. Onozawa, *Polym. J.*, 2003, **35**, 422.
- 8 Y. Wang, S. Onozawa and M. Kunioka, *Green Chem.*, 2003, (DOI: 10.1039/b304678h).



Design of recyclable matrixes from lignin-based polymers†

Yukiko Nagamatsu and Masamitsu Funaoka

1515 Kamihama Tsu, Mie 514-8507, Japan. E-mail: funaoka@bio.mie-u.ac.jp;
Fax: +81-59-231-9521; Tel: +81-59-231-9521

Received 29th April 2003

First published as an Advance Article on the web 28th August 2003

1,1-Bis(aryl) propane-2-O-aryl ether-type lignin-based polymers, lignophenols (LPs) were synthesized through a phase-separation system composed of phenols and concentrated acid. LP with C1-*p*-cresol (LP-P) and LP-24X containing C1-2,4-xyleneol had a similar phase-transition point, average molecular weight, frequency of phenols in the molecule and switching functionality (nucleophilic attack of C1-phenols to C2). LP-P, however, was hydroxymethylated (HM) at its reactive cresolic and terminal phenolic nuclei to give network-type structures on heating. On the other hand, LP-24X without a reactive point on the grafted nuclei resulted in the formation of linear-type structures. The structures of polymerized LPs were controlled by the grafting ratio of *p*-cresol and 2,4-xyleneol in LPs. The resulting polymer chains were cleaved at the C2-aryl ether linkages to give low molecular weight subunits by the switching function of the C1-grafted unit. In order to use LPs as matrixes for various composites, HM-LP-P, HM-LP-24X, and HM-LP-P/24X, containing an equivalent amount of C1-*p*-cresol and C1-2,4-xyleneol, were hybridized with powdery materials such as cellulose, glass, iron or talc by applying heat and pressure. The resulting HM-LP composites had a glossy surface and high dimensional stability because the polymerized HM-LPs' matrixes tightly bound fillers. Furthermore, using the switching functionality of LPs, the composites were re-separated into LP fractions and fillers. The physical and recycling properties of the composites were controlled by the structure of the LPs matrixes and/or the density, the morphology and the accessibility for reagents of the powdery materials.

Introduction

With industrial developments and human activities growing rapidly, the energy requirement in the world is steadily increasing. On the other hand, it will not be very long before fossil fuel materials such as petroleum and coal are depleted. There is a need for sustainable energy sources. The photo-synthetic products, lignocellulosics are potential resources that can be used in place of fossil fuel resources. In recent years, there has been considerable interest in the utilization of lignocellulosics for renewable energy, such as bioethanol (ethanol from biomass)¹⁻⁵ and biogas.^{6,7} However, the source of these applications, lignocellulosics undergo only a little modification in the molecular level even after the use as woody products, having the potential for providing valuable organic chemicals. In order to achieve a prolonged cascade flow of carbon resources, these wastes of lignocellulose should not be subjected to direct gasification but be utilized as a wide range of organic materials through molecular level conversion.

The phase-separation system was originally designed by Funaoka and co-workers⁸⁻¹⁰ as a successive total utilization system of lignocellulosics leading to sustainable development. Through the system, hydrophobic lignin and hydrophilic carbohydrates, the components of the cell wall, are subjected to selective structural conversion individually in the different phases and separated quantitatively at room temperature within one hour. In the organic phase, the lignin is phenolated selectively at the C1-position of phenylpropane to give phenolic linear-type polymers, lignophenols (LPs) with 1,1-bis(aryl) propane units. On the other hand, carbohydrates are hydrolyzed into water soluble poly-, oligo- and mono- saccharides.¹¹

The resulting LPs, 1,1-bis(aryl) propane-type polymers can be applied as functional materials in extensive fields,¹²⁻¹⁵ they have high phenolic property, no conjugated system, an obvious

phase transition point (hardwood; 130 °C, softwood; 170 °C) and a high affinity for biopolymers such as proteins, enzymes¹⁶ and biopolyesters.¹⁷ Moreover, under mild alkaline conditions, C1-phenols grafted to LP at the *ortho* position to their hydroxyl group can nucleophilically attack the adjacent C2 followed by the cleavage of aryl ether interunit linkages with the exchange of phenolic functionality from C1-phenols to lignin nuclei (switching function) (Fig. 1).^{18,19}

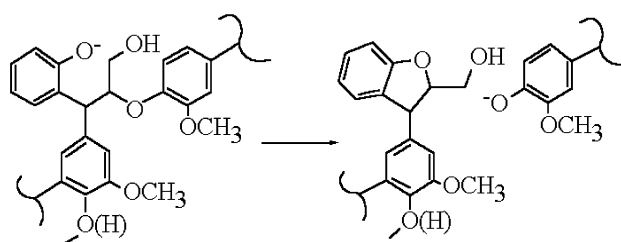


Fig. 1 Intramolecular switching function of LPs.

In the present work, successive functionality control of LPs using their phenolic reactivity and switching function was discussed: the C1-phenolic structures of LPs were controlled through the phase-separation system, and the macrostructure of LPs were designed by hydroxymethylation (HM) and heating. Furthermore, the LPs were used as recyclable matrixes for

Green Context

Polymers from biomass can help reduce our dependency on fossil fuels. This article describes how lignin can be modified so as to produce new polymers which can readily be blended with other materials such as cellulose to produce composite materials with excellent mechanical properties. DJM

† Presented at The First International Conference on Green & Sustainable Chemistry, Tokyo, Japan, March 13–15, 2003.

various materials to design the lignin-based recyclable composites.

Experimental

Synthesis of LPs

Preparation of lignocellulose. Hinoki (*Chamaecyparis obtusa*) wood meals (passed through about 20 mesh) were extracted with acetone for 72 hours to remove phenolic extractives which could cause undesirable side reactions during the phase-separation reaction. The lignin content was determined by Tappi Standard (T222,UM250).

The phase-separation system (2 step process II). The extractive-free hinoki wood meals were completely soaked in *p*-cresol, 2,4-xyleneol (3 mol equivalent/C₉) or a mixture of *p*-cresol and 2,4-xyleneol (1.5 mol equivalent/C₉ each) in acetone. After 24 hours, the acetone was evaporated with continuous stirring. To the phenol-sorpted wood meals, 72% sulfuric acid was added and the mixture was stirred vigorously for 1 hour at room temperature. The reaction mixture was poured into excess water with vigorous stirring. The precipitates were subjected to repetitive washing and centrifugation to remove acid. After drying, the precipitates were extracted with acetone. The extractives were added dropwise to an excess amount of cooled ethyl ether with vigorous stirring. The precipitates (LPs) were collected by centrifugation and dried over P₂O₅ after evaporating the solvent. The resulting LPs, ligno-*p*-cresol, ligno-2,4-xyleneol and ligno-(*p*-cresol/2,4-xyleneol), were referred to as LP-P, LP-24X and LP-P/24X, respectively.

Structural control of LPs

Hydroxymethylation (HM) and polymerization. After being dissolved in 0.5 M NaOH completely, LPs were diluted 5 fold with deionized water. To the solution, 37% formaldehyde solution (20 mol/aromatic nuclei) was added. The mixtures were heated at 60 °C for 3 hours with constant stirring and bubbling of N₂. After the reaction, they were cooled to room temperature and acidified with 1.0 M HCl to pH 2. The precipitates were purified by dialysis, and dried over P₂O₅. The resulting HM-LPs were stored at -80 °C.

The HM-LPs were polymerized by programmed heating (initial temp.; 70 °C, final temp.; 150 °C, rate; 2.0 °C min⁻¹, holding time; 60 min).

Switching functionality. LPs or HM-LPs were placed into a stainless steel bomb, to which 0.5 M NaOH was added. The mixture was heated for 1 hour in an oil bath (140 or 170 °C). After cooling to room temperature, the reaction mixtures were acidified to pH 2 with 1.0 M HCl. LPs precipitated from the solution were collected by centrifugation and dried over P₂O₅.

Structural analyses of LPs. LPs were acetylated with pyridine-acetic anhydride (1 : 1 v/v) at room temperature for 48 hours.

The amounts of grafted phenols in LPs and hydroxymethyl groups in HM-LPs were determined by ¹H-NMR spectra on a JEOL JMN-A500 fourier transform NMR using *p*-nitrobenzaldehyde (PNB) as an internal standard. CDCl₃ and C₅D₅N-CDCl₃ (1 : 3 v/v) were used as solvents for acetylated HM-LPs and original LPs, respectively.

The average molecular weights were measured by gel permeation chromatography (GPC) on a SHIMADZU CLASS LC-10 system, LC-10AD, SPD-10A with four shodex columns

(KF804, KF803, KF802 and KF801) in series. Tetrahydrofuran (THF) was used as an eluent after removing a stabilizer.

FT-IR spectra of LPs were obtained by the KBr method on a PerkinElmer Spectrum GX spectrometer (spectral resolution; 4 cm⁻¹, signal accumulation; 32 scans).

Thermomechanical analysis (TMA) was carried out with a RIGAKU TAS-200 system equipped with a RIGAKU Thermo-plus TMA8310. Under the 5 g loading, the phase-transition (Ts) of LP was measured by programmed heating from room temperature to 300 °C (rate; 2.0 °C min⁻¹).

Distribution and combination modes of phenols grafted to LPs were analyzed by a combination of phenyl nucleus exchange and the periodate oxidation technique.²⁰

Application to LPs as recyclable matrixes of composites

Preparation of HM-LP composites. Hinoki HM-LPs dissolved in THF were added to 900 mg powdery filling materials (cellulose [fine fiber], talc [amorphous], iron [amorphous] and glass for fillers of fiber-reinforced plastics (FRPs) provided by Nippon Sheet Glass Co., Ltd. [1: amorphous, 2: short fiber, 3: flake, 4: porous flake]). The mixtures were stirred continuously until the THF had evaporated. LPs-sorpted materials were molded (initial temp.; 70 °C, rate; 1.5 °C min⁻¹, final temp.; 180 °C, load; 100 kgf). The size and the apparent density of the resulting cylindrical composites were measured. The surfaces of fillers and composites were observed with a HITACHI S-3000N scanning electron microscope (SEM).

Mechanical properties of HM-LP composites. HM-LP composites were soaked in water to a depth of 3 cm for 60 min at room temperature followed by drying at 60 °C to evaluate their dimensional stabilities. The percentages of water absorption and the volumetric swelling were calculated based on the original moisture content and the volume. The Brinell hardness of HM-LP composites was measured according to JIS Z2117.

Recycling of HM-LP composites using the switching function. In the same way as in LPs and HM-LPs, ground HM-LP composites were placed into a stainless steel bomb, to which 0.5 M NaOH was added. The mixtures were heated for 1 hour at 140 or 170 °C. The reaction mixtures were filtrated. The amounts of LPs separated from the composites (filtrates) were determined quantitatively by colorimetry (absorbance at 293 nm). The precipitates (fillers) were dried at 60 °C.

Results and discussion

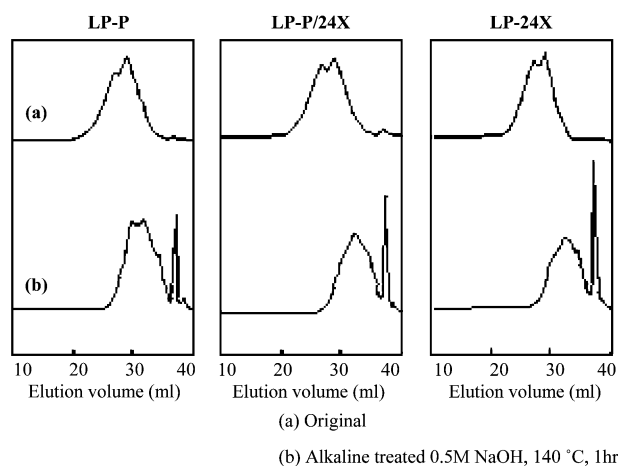
Properties of LPs

Structural characteristics of LPs. The structural characteristics of LPs synthesized from hinoki wood meal by the phase-separation system are shown in Table 1. The yields of LPs were 70–87% of klason lignin. Considering the loss of ether soluble parts of LPs during purification (about 30%), the conversion from native lignin to LPs through the phase-separation system was distinctly quantitative. The frequencies of grafted phenols were about 0.70 mol/C₉, 70% of them were confirmed to be mainly at the C1-position in LPs on their *ortho* position to the hydroxyl group by a combination of phenyl nucleus exchange and the periodate oxidation technique.²⁰ These results indicate that LPs possess a high frequency of 1,1-bis(aryl) propane units in their molecules. The average molecular weight (\bar{M}_w and \bar{M}_n) and the dispersion index (\bar{M}_w/\bar{M}_n) were around 27 000–28 000, 3 000–6 000 and 4.5–8.0, respectively. LPs with a higher polydispersity had a lower phase-transition point, indicating the plasticization effect of low molecular weight subunits in the LPs.

Table 1 Structural properties of LPs

Samples	\bar{M}_w	\bar{M}_n	\bar{M}_w/\bar{M}_n	$T_g/^\circ\text{C}$	Amount of grafted phenol (mol/C ₉)	
					Total	C1-linked
LP-P	26580	3070	7.90	146	0.68	0.46
LP-P/24X	27770	4620	6.00	141	0.76 ^a	0.52 P : 24X (0.27 : 0.25)
LP-24X	28350	6330	4.50	156	0.73	0.49

^a Estimated by a combination of ¹H-NMR and nucleus exchange analysis.

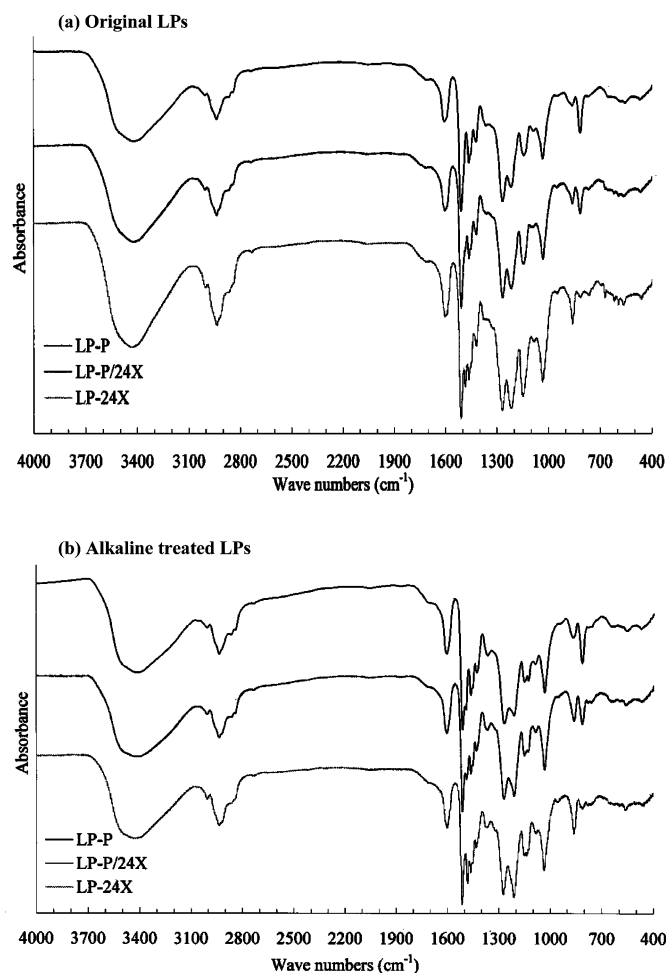
**Fig. 2** GPC profiles of LPs and alkaline treated LPs.

Functionality control of LPs. GPC profiles of original and alkaline treated LPs are shown in Fig. 2. Original LPs having similar bimodal molecular distributions were all dramatically depolymerized after alkaline treatment for 1 hour at 140 °C to give fragments with low molecular dispersion. This is due to the neighboring group participation of C1-phenols in LPs to C2 (switching function). A noticeable peak detected at around 37 minutes in alkaline treated LPs corresponds to LP fractions with 300 of the average molecular weight (\bar{M}_w), which is assumed to be 1,1-bis(aryl) propane-type dimeric units resulting from cleavage of C2-aryl ether linkages (they account for the majority of interunit linkages) by the switching function.

From GPC profiles, the switching functionalities of C1-phenols in LP-P, LP-24X and LP-P/24X were similar.

In the FT-IR spectra of the original LPs (Fig. 3(a)), no significant difference was observed except in the region of 800–855 cm^{-1} . These bands are assigned to the C–H out-of-plane deformations of aromatic nuclei. Bands at 817 cm^{-1} (two adjacent H of grafted *p*-cresol) decreased with decreasing amount of grafted *p*-cresol in the LP molecules. These results indicate that LPs have essentially the same lignin backbone structures. On the other hand, the absorption bands in alkaline treated LPs were similar to those of the original LPs (Fig. 3(b)). These results are consistent with the exchange of phenolic functionality from C1-phenolic nuclei to lignin nuclei through the switching function and no side reactions such as homolysis, condensations, rearrangement and so on.

¹H-NMR spectra of hydroxymethylated (HM) LP (HM-LP-P, HM-LP-24X and HM-LP-P/24X) acetates are given in Fig. 4. Aromatic proton signals are at 7.80 to 6.30 ppm. Methoxyl and side chains proton signals are at 4.50 to 3.10 ppm. In the 2.40 to 1.60 ppm region, the methyl proton signals of grafted phenols are overlapped with their aromatic and aliphatic acetoxy proton signals (2.40–2.01 and 2.01–1.60 ppm, respectively). The intensity of the signals at 4.70–5.30 ppm, which are assigned to methylene protons of acetylated hydroxymethyl groups,²¹ increased with increasing amount of grafted *p*-cresol. LP-P,

**Fig. 3** FT-IR spectra of LPs (a) and alkaline treated LPs (b).

which was hydroxymethylated to the largest extent, has reactive sites on the cresol nuclei as well as lignin phenolic nuclei, while the reactive sites of LP-24X are mainly on the terminal lignin units. The frequencies of hydroxymethyl groups in HM-LP-P, HM-LP-P/24X and HM-LP-24X calculated by the internal standard method were 0.54, 0.31 and 0.13 mol/C₉, respectively.

TMA profiles of HM-LPs are shown in Fig. 5. Although the original LPs were plasticized rapidly at about 150 °C, HM-LP-P had no phase-transition point. On the other hand, HM-LP-P/24X and HM-LP-24X underwent gradual plasticization at about 220 and 200 °C, respectively. The higher the ratio of 2,4-xyleneol to *p*-cresol presented in HM-LPs, the lower the phase-transition point of HM-LPs. The solubility in organic solvents of the polymerized LPs was much lower than that of the original LPs and HM-LPs; especially, the polymerized HM-LP-P was insoluble in THF. These results indicate that HM-LP-P and HM-LP-24X were polymerized by heating to the network-type and linear-type polymers, respectively, and that the structures of the LP-polymers could be controlled from linear-

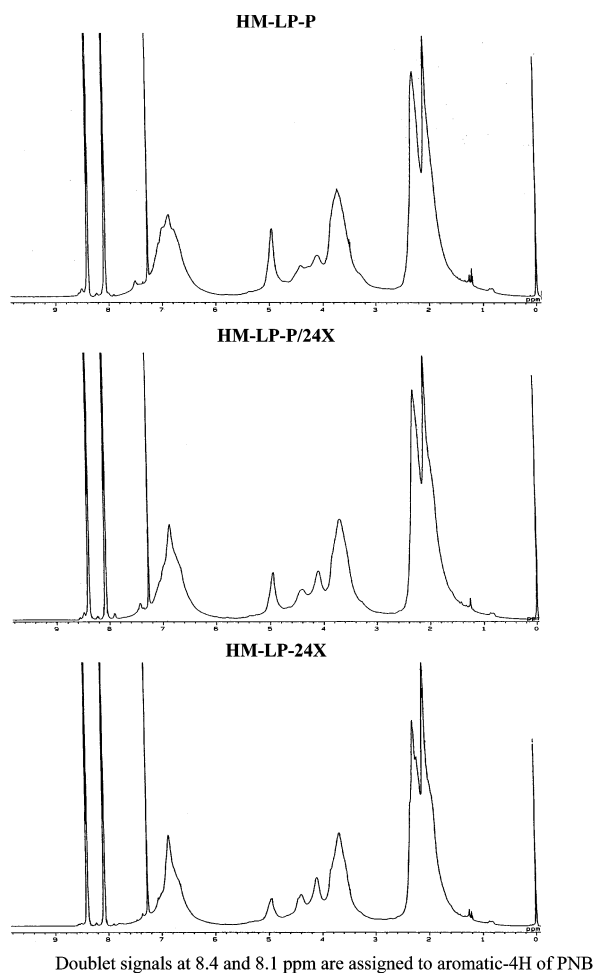


Fig. 4 $^1\text{H-NMR}$ spectra of HM-LPs (acetate).

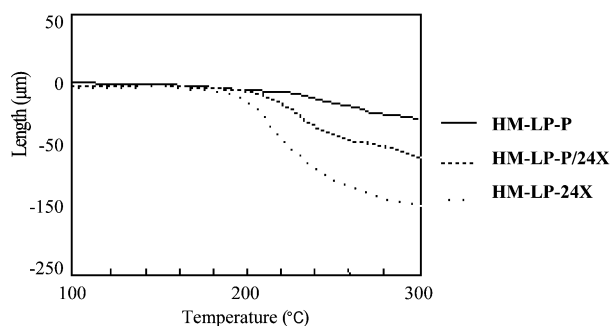


Fig. 5 Thermomechanical analysis (TMA) profiles of HM-LPs.

types to network-types by the frequencies of grafted *p*-cresol and 2,4-xyleneol in the LPs followed by hydroxymethylation.

Fig. 6 shows GPC profiles of polymerized HM-LPs after alkaline treatment at 140 or 170 °C. Although polymerized HM-LPs were slightly soluble in organic solvents, they could dissolve in alkaline solution after using the switching function. The switching functionality of the HM-LP-24X polymer was comparable to the original one (see Fig. 3) to give low molecular subunits by the mild alkaline treatment. On the other hand, the HM-LP-P polymer, which had an even greater molecular weight after being treated at 140 °C, was effectively depolymerized at 170 °C. The molecular weight distributions of fragments from the LP-polymers got more uniform with the increased ratio of 2,4-xyleneol in the polymers, indicating that C1-2,4-xyleneol nuclei had an effective switching function due to their high mobility compared with linked *p*-cresolic nuclei. These results indicate that controlling the ratio of *p*-cresol-

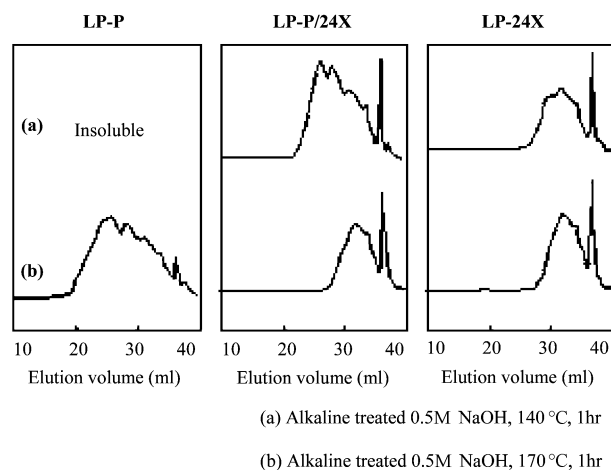


Fig. 6 GPC profiles of alkaline treated HM-LPs.

2,4-xyleneol-units within HM-LP enables design of LP-based materials with various reactivities and recycling properties. On the other hand, our previous work found that HM-LP-P and HM-LP-24X could blend in any proportions, and the control of the mixing ratio of HM-LP-P and HM-LP-24X allowed to control structures of the resulting polymer from network- to linear-type structures.²²

Application of LPs as recyclable matrixes of composites

Properties of HM-LP composites. HM-LP composites with smooth surfaces could be shaven and cut like wood although the control molds (prepared from only cellulose) with a glossy white surface were difficult to be shaven because they were readily peeled off. As shown in Table 2, the density and the appearance of cellulose-, talc- and Fe-HM-LP composites were almost the same, independent of the structure of their LP matrixes.

Table 2 Density and appearance of HM-LP composites and control molds

Fillers	HM-LPs	Properties of composites		
		Density/ g cm ⁻³	Color	Surface
Cellulose Fiber	—	0.99	White	Smooth
	P	1.08	Beige	Smooth
	P/24X	1.16	Beige	Smooth
	24X	1.09	Beige	Smooth
Fe	Amorphous P	2.97	Black	Smooth
	P/24X	3.03	Black	Smooth
	24X	3.04	Black	Smooth
Talc	Amorphous P	1.83	Beige	Smooth
	P/24X	1.83	Beige	Smooth
	24X	1.83	Beige	Smooth
Glass 1	Amorphous P	1.46	Beige	Smooth
Glass 2	Short fiber P	1.43	Beige	Smooth
Glass 3	Flake P	1.50	Dark beige	Smooth
Glass 4	Porous flake P	0.91	Light beige	Smooth

P: *p*-cresol, P/24X: the grafting ratio of *p*-cresol : 2,4-xyleneol is 1 : 1, 24X: 2,4-xyleneol.

From the surface observations of HM-LP-P composites with scanning electron microscopy (SEM) (Fig. 7 (a–h)), there were discontinuous matrixes that coated and combined fillers in the composites (b–h). On the other hand, control molds formed from compressed cellulose were entangled with each other (a).

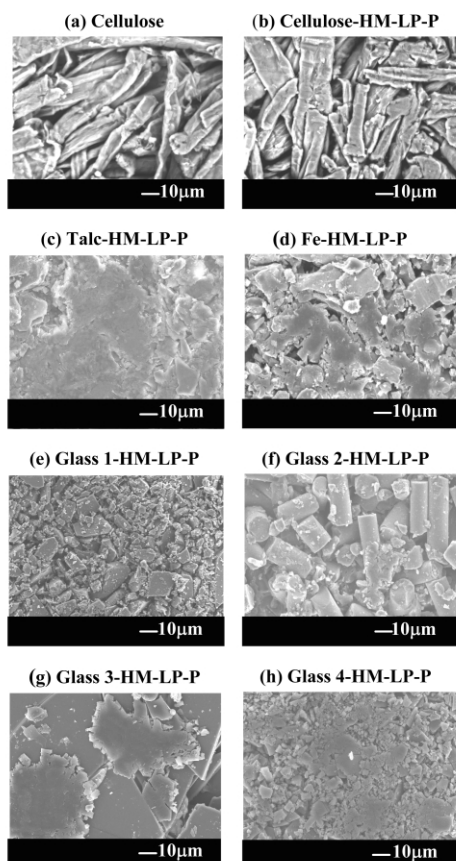


Fig. 7 SEM images of HM-LP-P composites and cellulose control molds.

Mechanical properties of HM-LP composites

Dimensional stability and water absorption. Fig. 8 and 9 show the volumetric swelling and the water absorption of composites prepared from HM-LPs and cellulose-, talc-, Fe-

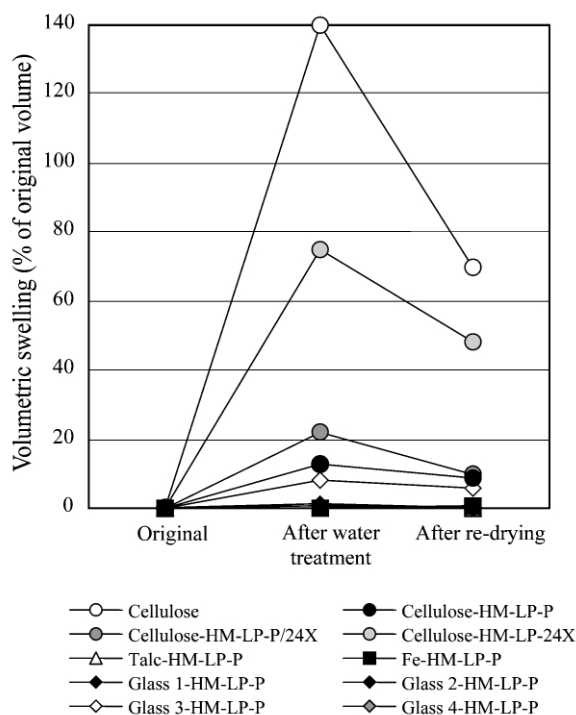


Fig. 8 Dimensional stabilities of HM-LP composites and cellulose control molds.

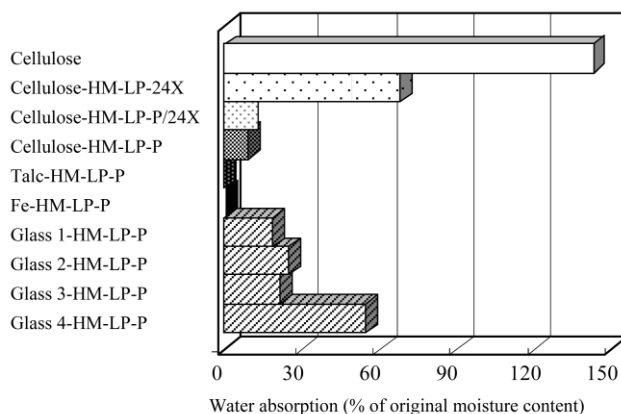


Fig. 9 Water absorption of HM-LP composites and cellulose control molds.

and glass-fillers. The volumetric swelling and the water absorption of cellulose-HM-LP composites were greatly lower as compared to cellulose control molds, and decreased in the order HM-LP-24X, HM-LP-P/24X and HM-LP-P composites. Especially, these properties of the cellulose-HM-LP-P composites were much lower, indicating that the HM-LP-P in the composite was polymerized to form highly network-type structures and kept the cellulose from swelling. Using HM-LP-P and HM-LP-P/24X as matrixes for the composites, the dimensions of cellulose-HM-LP composites treated by water were recovered to approximately the original ones by re-drying. The low dimensional stability and high water absorption of the cellulose-HM-LP-24X composite were due to a small amount (10% of the composite weight) and a linear-type structure of charged matrix, leading to uptake of excess water into the composites. On the other hand, the volumetric swelling and the water absorption of talc- and Fe-HM-LP composites were less than about 1.0% regardless of the matrix (data is not shown) because these fillers are hydrophobic and not swollen by water. The dimensional stability of glass-HM-LP-P composites was similar to that of the composites prepared from other inorganic fillers. But using glass 3 as a filler (its average particle diameter is about 200 μm), the resulting composites had higher swelling. This is due to a restricted binding effect of the HM-LP-P matrix to such large size materials. Glass (1–3)- and 4 [porous flake]-HM-LP-P composites had about 20 and 50% water absorption, respectively. These results suggest that glass materials are slightly hydrophilic in comparison with the other inorganic fillers.

Brinell hardness. As shown in Table 3, the Brinell hardness of cellulose- and talc-HM-LP composites were higher than that of the control molds. However there was no significant difference in the Brinell hardness of the composites. From this result it can be concluded that all HM-LP matrixes could hold powdery materials tightly.

Table 3 Brinell hardness of HM-LP composites and control molds

Molds	Fillers	HM-LPs	Brinell hardness/MPa
Cellulose	—	—	17.3
	P	—	30.8
	P/24X	—	26.8
	24X	—	28.6
Talc	—	—	0.7
	P	—	9.1
	P/24X	—	8.7
	24X	—	9.2

P: *p*-cresol, P/24X: the grafting ratio of *p*-cresol : 2,4-xyleneol is 1 : 1, 24X: 2,4-xyleneol.

Resistance to THF. When talc-HM-LP composites were soaked in THF at 25 °C for 24 hours, HM-LP-24X composites disintegrated immediately with elution of LP-24X moieties, while HM-LP-P composites were stable. The ratios of LP moieties eluted out from the HM-LP-P, HM-LP-P/24X and HM-LP-24X composites were 0, 1.2 and 28.4%, respectively. These results indicate that the chemical stability of composites can be controlled by choosing LP matrixes.

Recycling of HM-LP composites using the switching functionality of LP matrixes

Using C1-cresol and C1-2,4-xyleneol units within LP molecules as switching devices, the composites were recycled to the constituents, fillers and LPs (Table 4). Under mild alkaline

Table 4 Yields of LPs re-separated from the composites using the switching function

HM-LP composites		Alkaline treatment (0.5 M NaOH, 1 h)	
Fillers	HM-LPs	140 °C	170 °C
Cellulose	P	25.9 ^{ab}	138.9 ^{ab}
	P/24X	122.0 ^{ab}	109.9 ^{ab}
	24X	105.1 ^{ab}	116.3 ^{ab}
Talc	P	19.2	72.3
	P/24X	104.2	114.0
	24X	108.8	108.6
Cellulose 10%/Talc 80%	P	35.0	111.5
Glass 1	P	59.3	98.9
Glass 2	P	73.5	116.2
Glass 3	P	60.7	101.0
Glass 4	P	46.9	— ^c

^a Determination by gravimetry. ^b Including hydrolyzed cellulose. ^c LP remained on the insoluble part. P: *p*-cresol, P/24X: the grafting ratio of *p*-cresol : 2,4-xyleneol is 1 : 1, 24X: 2,4-xyleneol.

conditions (0.5 M NaOH, 140 °C, 1 hour), both HM-LP-P/24X and HM-LP-24X composites were almost quantitatively re-separated into insoluble parts (fillers) and soluble parts (low molecular weight fragments of LPs). The cellulose-HM-LP-P composites required more drastic conditions (0.5 M NaOH, 170 °C, 1 hour) to be re-separated completely due to the highly penetrated network-type structure of cellulose and polymerized HM-LP-P, and the restricted mobility of linked *p*-cresol nuclei. When using inorganic fillers, however, the recycling efficiency of HM-LP-P composites depended on the accessibility of inorganic materials to alkaline reagents. Thus, the recycling of talc-HM-LP-P composites was incomplete due to their hydrophobicity. Glass-HM-LP-P composites could be re-separated through the switching functionality of the LP-P matrix at 170 °C because glass is partly soluble in alkaline reagents. However, by adding cellulose powder to talc, which encourages composites to swell in alkaline media, the recovery ratio of LP-P moieties from the composites increased from 72 to 100% at 170 °C. On the other hand, applying glass 4, which is nanoporous, to the matrix of HM-LP-P composites, the recovery of LP-P moieties was decreased because the LP-P within the porous structures had low accessibility to alkaline reagents. These results indicate that the chemical and/or physical properties of fillers will lead to the detailed control of the mechanical and the recycling properties of the composites.

Conclusions

Through the phase-separation system, 1,1-bis(aryl) propane-type linear polymers, LPs were synthesized directly from native

lignins. C1-phenols in LPs could be designed through the system. When C1-aryl groups in LP were *p*-substituted phenols, they nucleophilically attacked adjacent C2, followed by the cleavage of aryl ether linkages under mild alkaline conditions (switching function).

LP-P, LP-P/24X and LP-24X had almost the same switching functionality and structural properties. LP-24X was hydroxymethylated preferentially on the terminal phenolic units to give a linear-type polymer, while LP-P with reactive sites on the cresolic nuclei and terminal phenolic nuclei was hydroxymethylated, giving a network-type polymer. Through the control of reactive sites in the LP molecules, the polymerization modes of the LPs could be controlled from linear-types to network-types. Furthermore, the resulting polymer chains were cleaved at the switching points to give low molecular weight subunits by the switching function.

In order to use HM-LPs as matrixes of various composites, they were hybridized with powdery materials such as cellulose, glass, iron or talc by applying heat and pressure. The resulting composites with glossy surfaces could be shaven and cut like wood. Their dimensional stability increased with increasing frequency of *p*-cresol units in the HM-LP when using water-absorbing materials like cellulose as filler. This result indicated that *p*-cresol units are responsible for forming network-type moieties in HM-LP to combine cellulose tightly. Talc-HM-LP-P composites had the highest resistance to THF. On the other hand, the mechanical properties of inorganic-HM-LP-P composites strongly depended on the morphology and the structural properties of the inorganic materials.

Using the switching functionality of LPs, the composites were re-separated into LP fractions and fillers. The physical and the recycling properties of composites were controlled by the structure of LP matrixes and/or the density, the morphology and the accessibility of fillers to reagents.

These results indicated that 1,1-bis(aryl) propane-type lignin-based polymers (LPs) could be utilized as functional materials in various fields, leading to promotion of a recycling society.

Acknowledgement

This research was supported by Core Research for Evolutional Science and Technology (CREST) of Japan Science and Technology (JST).

References

- J. Soderstrom, L. Pilcher, M. Galbe and G. Zacchi, *Biomass Bioenergy*, 2003, **24**, 475.
- M. J. Taherzadeh, M. Fox, H. Hjorth and L. Edebo, *Bioresour. Technol.*, 2003, **88**, 17.
- Z. Yu and H. Zhang, *Biomass Bioenergy*, 2003, **24**, 257.
- T. Chmielniak and M. Sciazko, *Appl. Energy*, 2003, **74**, 393.
- C. Franco, F. Pinto, I. Gulyurtlr and I. Cabrita, *Fuel*, 2003, **82**, 835.
- A. V. Bridgwater, *Chem. Eng. J.*, 2003, **91**, 87.
- G. Chen, J. Andries, Z. Luo and H. Spliethoff, *Energy Convers. Manage.*, 2003, **44**, 1875.
- M. Funaoka and I. Abe, *Tappi J.*, 1989, **72**, 145.
- M. Funaoka, M. Matsubara, N. Seki and S. Fukatsu, *Biotechnol. Bioeng.*, 1995, **46**, 545.
- M. Funaoka and S. Fukatsu, *Holzforchung*, 1996, **50**, 245.
- K. Mikame and M. Funaoka, *Polym. Prepr., Jpn.*, 2001, **50**, 917(in Japanese).
- XS. Wang, T. Suzuki and M. Funaoka, *Mater. Sci. Res. Int.*, 2002, **8**, 249.
- H. Kita, K. Nanbu, T. Hamano, M. Yoshino, K. Okamoto and M. Funaoka, *J. Polym. Environ.*, 2002, **10**, 69.

- 14 M. Uehara and M. Funaoka, *Trans. Mater. Res. Soc. Jpn.*, 2001, **26**, 825.
- 15 ZY. Xia, T. Yoshida and M. Funaoka, *Eur. Polym. J.*, 2003, **39**, 909.
- 16 H. Ioka, N. Seki and M. Funaoka, *10th Int. Symp. Wood Pulping Chem. (ISWPC)*, 1999, **III**, 418.
- 17 E. Ohmae and M. Funaoka, *Trans. Mater. Res. Soc. Jpn.*, 2001, **26**, 829.
- 18 M. Funaoka, H. Ioka, T. Hosho and Y. Tanaka, *J. Network Polym., Jpn.*, 1996, **17**, 121(in Japanese).
- 19 Y. Nagamatsu and M. Funaoka, *Sen'i Gakkaishi*, 2001, **57**, 54 (in Japanese).
- 20 M. Funaoka and Y. Z. Lai, *Bull. Fac. Bioresour., Mie Univ.*, 1993, **10**, 105.
- 21 P. R. Steiner, *J. Appl. Polym. Sci.*, 1968, **14**, 40.
- 22 Y. Nagamatsu and M. Funaoka, *Mater. Sci. Res. Int.*, 2003, **9**, 108.



Promoter effects in the polymerisation of a mixed hydrocarbon feed with silica-supported BF_3 †

C. R. Quinn, J. H. Clark,* S. J. Tavener and K. Wilson*

Clean Technology Centre, Chemistry Dept., University of York, UK YO10 5DD.

E-mail: jhc1@york.ac.uk; kw13@york.ac.uk

Received 13th May 2003

First published as an Advance Article on the web 22nd September 2003

The activity of a silica-supported BF_3 –methanol solid acid catalyst in the cationic polymerisation of an industrial aromatic C9 feedstock has been investigated. Reuse has been achieved under continuous conditions. Titration of the catalyst acid sites with triethylphosphine oxide (TEPO) in conjunction with ^{31}P MAS NMR shows the catalyst to have two types of acid sites. Further analysis with 2,6 di-*tert*-butyl-4-methylpyridine (DBMP) has revealed the majority of these acid sites to be Brønsted in nature. The role of α -methylstyrene in promoting resin polymerisation *via* chain transfer is proposed.

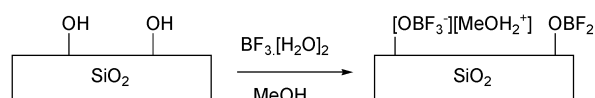
Introduction

Hydrocarbon resins are produced from the acid-catalysed (typically AlCl_3 or BF_3) cationic polymerisation of a complex mix of monomers derived from petroleum plant cracking fractions.¹ Mixtures or pure monomers may produce resins that are particularly resistant to high shear conditions and have found applications in adhesives, rubbers, tackifying resins, fixing agents, water repellents and paints.² However, the necessity to quench the polymer mixture after reaction to remove the catalyst generates vast quantities of acidic aqueous waste that is of major concern for the industry. The use of supported catalytic systems has been proposed as a way of eliminating this waste whilst also allowing for easier handling and catalyst recovery.³ Recently we have reported on the preparation and characterisation of a silica-supported BF_3 methanol complex that was found to be active in the polymerisation of hydrocarbon monomers.⁴ We now wish to report the first use of this catalyst in the polymerisation of a commercial feedstock containing a mixture of C9 aromatics including indene (20%), ring-substituted styrene monomers (20%) and α -methylstyrene (4%).⁵ The nature of the acid sites and the role of α -methylstyrene on resin properties has also been investigated.

Experimental

Catalyst preparation

A three-necked round bottom flask was purged with a flow of N_2 . $\text{BF}_3 \cdot 2\text{H}_2\text{O}$ (4.2 g, 40 mmol) was added to a slurry of silica (10 g, pre-dried at 600 °C for 8 h) and methanol (35 ml). The slurry was stirred at room temperature for 2 h. Reaction of the BF_3 with silanol groups produces two types of acid sites, shown in Scheme 1.⁶ Solvent was removed by rotary evaporation (50 °C, 2 h). Finally the catalyst was stored in a desiccator.



Scheme 1 Preparation of supported BF_3 –methanol complex.

Resin synthesis

A jacketed flask was fitted with a condenser, an argon inlet, a dropping funnel and a computer-interfaced thermocouple to accurately measure the reaction exotherm. The flask was purged with argon; solvent (heptane, 20 ml, toluene, 20 ml) and catalyst (2 g) were added and stirred at room temperature before the feed (100 ml, supplied by Exxon Chemicals) was introduced from the dropping funnel over the course of 1 hour. The reaction mixture was stirred for a further 30 minutes before the catalyst was filtered off and the filtrate passed through a column packed with silica to remove colour. The viscous material from the column was dried on a vacuum stripping line (1 mbar) at 200 °C. A single use experiment produces *ca.* 30 g of polymer. Yield is recorded as grams of polymer obtained from 100 ml of feed. Approximately 60% of the C9 feed is comprised of polymerisable monomers, the remaining 40% is solvent. The products are glassy orange yellow solids. The resins were characterised by yield, ^1H NMR, ^{13}C NMR, and differential scanning calorimetry.⁷

Results and discussion

For the supported catalyst to be a viable alternative to homogeneous BF_3 it is important to demonstrate reusability. Following an initial reaction, methods for subsequent catalyst reuse were investigated. Simple recovery of the catalyst from the polymerised feed *via* filtration in the presence of air was found to result in deactivation. Consequently it was necessary to

Green Context

The use of supported boron trifluoride in the polymerisation of alkenes is discussed. Heterogeneous catalysts for such reactions are useful since they can be easily recovered and they are less likely to leave residues of hydrolysis products in the final product, making it more acceptable and less hazardous. The work here demonstrates that the system works well, is truly heterogeneous, and physicochemical characterisation of the catalyst highlights some of the complexities of the system.

DJM

† Presented at The First International Conference on Green & Sustainable Chemistry, Tokyo, Japan, March 13–15, 2003

recover the catalyst by allowing the solid to settle and then siphoning the supernatant under argon. Fig. 1 shows the yield of

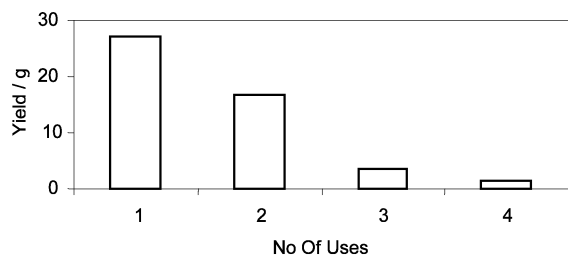


Fig. 1 Resin yield from batch reuse.

resin obtained following 4 separate additions of feed. Polymer yield decreases by *ca.* 40% after the second use, which we believe is largely due to coking and polymer build up which limits the diffusion of unreacted monomer into the catalyst pores. This hypothesis is supported by measurements of the surface area of the catalyst which decreases after one use from 244 to 14.1 m² g⁻¹ with a corresponding reduction in pore volume from 0.952 to 0.061 cm³ g⁻¹. Thermal gravimetric analysis (TGA) of the recovered catalyst shows a 35% weight loss between 325 and 425 °C consistent with pore blockage by polymer. Removal of the polymer from the pore would appear to be crucial to allow effective reuse.

The results from a continuous reuse experiment, in which 100 ml feed was simply added to the catalyst every 90 minutes, are shown in Fig. 2. Yield increases for each addition of feed and

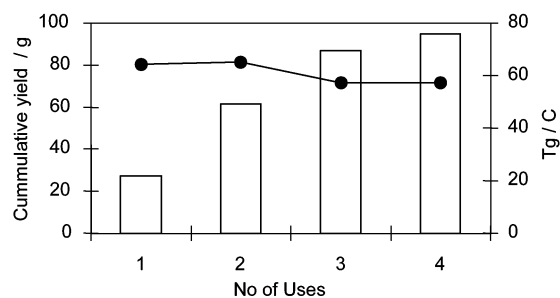


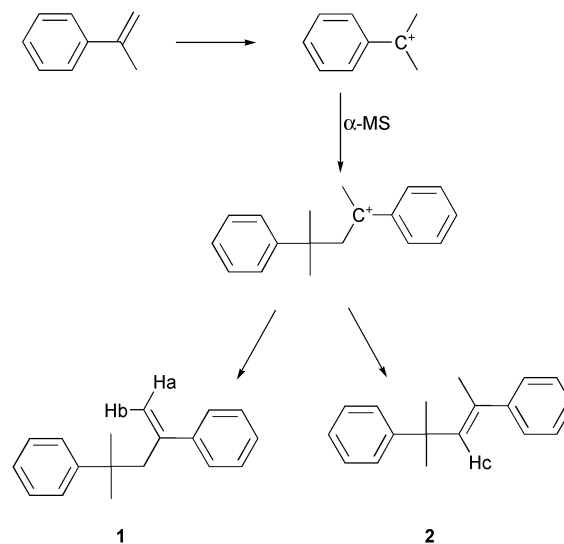
Fig. 2 Yield (columns) and T_g (●) from continuous reuse.

the glass transition temperature (T_g) of the resultant polymer remains relatively constant. An increase in T_g can be achieved by reaction of the catalyst with larger volumes of feed in one batch. This can be explained by the increased amounts of solvent serving as a heat sink, reducing the reaction exotherm. During chain propagation, high temperatures favour chain transfer. A reduction in temperature therefore limits chain transfer reactions and increases T_g . The resultant polymer from such a batch reaction has a higher T_g than a polymer produced from a continuous addition scenario (76 vs. 57 °C). However, yield is seen to decrease by *ca.* 20%, presumably due to the diffusional difficulties inherent in larger volume reactions.

The heterogeneous nature of the reaction was also investigated with removal of the catalyst by filtration at an early stage of the reaction found to result in no further polymerisation. NMR analysis detected no boron or fluorine in the filtrate. Also, XPS analysis of the polymers obtained from reuse reactions showed that the polymers did not contain B or F, indicating that there was no significant leaching of BF₃ from the supported catalyst.

We believe that the differences in yield between batch and continuous reuse can be explained if living polymerisation is occurring. In the batch reuse scenario, by removing the feed from the catalyst a source of polymerisation initiation is removed. Approximately 4% of the C9 feed is α -methylstyrene

(α -MS). We have previously reported that the addition of α -MS will increase the rate of reaction when copolymerised with indene.⁴ α -MS will typically react very quickly to produce a low molecular weight polymer with a T_g of -27 °C. Chaudhuri has demonstrated that α -MS will dimerise under homogeneous conditions to produce 2,4-diphenyl-4-methyl-1-pentene (**1**), a chain transfer agent, and 2,4-diphenyl-4-methyl-2-pentene (**2**) (see Scheme 2), which are easily detected by ¹H NMR.^{8,9} The



Scheme 2 α -MS dimerisation.

promotion of feed polymerisation by α -MS was thus investigated to verify whether such effects could be observed with the supported catalyst and what influence the dimers may have on resin properties.

Varying amounts of α -MS were added to the feed and changes in yield and T_g were recorded (Fig. 3.) As the amount

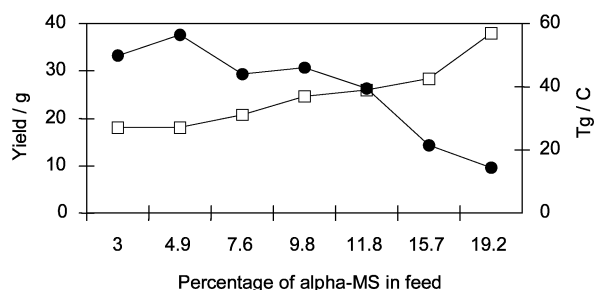


Fig. 3 Effect on yield (□) and T_g (●) of adding α -MS to the feed.

of α -MS added to the feed is increased, yield is seen to rise due to the presence of extra polymerisable monomer; also T_g decreases due to the influence of the chain transfer agent. It should be noted that a single glass transition for the new mixture is observed, indicating that a true copolymer is formed. Thus it can be assumed that as the amount of chain transfer agent increases, more initiation sites are available which results in the production of short chain polymers. α -MS may therefore be used to control the molecular weight distribution and T_g of hydrocarbon resins.

Acid site characterisation

Catalyst acidity has been investigated using 2,6 di-*tert*-butyl-4-methylpyridine (DBMP) and triethylphosphine oxide (TEPO).

The BF₃ catalyst is known to contain both Lewis and Brønsted acid sites.⁶ DBMP is a well-known sterically hindered

proton scavenger that can be used to distinguish between the relative amounts of Brønsted and Lewis acid initiation sites.¹⁰ Fig. 4 shows the effect on yield of increasing the amount of

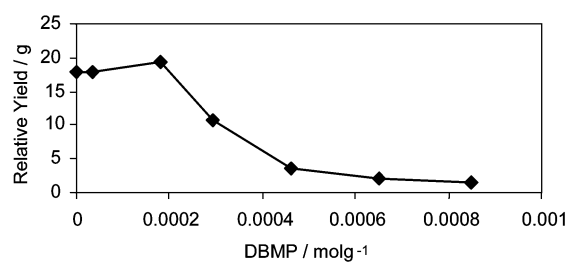


Fig. 4 Effect of DBMP.

DBMP to the reaction. The graph is split into 3 sections. In the first section, a small increase in yield is observed, possibly as DBMP consumes water and other protonic impurities that could terminate the propagating cationic chain.¹¹ This is followed by a decrease in yield as the protons from the catalyst are consumed. This occurs with 0.46 mmol g⁻¹ of DBMP. If one mole of DBMP consumes one mole of protons, this indicates that the catalyst possesses 0.46 mmol of protons. The theoretical loading should be 4 mmol g⁻¹. We can see that this titration accounts for only *ca.* 10% of the potential active sites. Finally in the third section, the graph levels off indicating that all the protons have been consumed and reaction is proceeding *via* Lewis acid catalysis. The contribution to the reaction rate from the Lewis acid sites is approximately 10%. The low contribution from the Lewis acid sites is reflected in the polymer produced by this material, which shows a unimodal molecular weight distribution by GPC analysis suggesting the existence of only one type of initiation site. Proton sources from supported reagents such as supported aluminium chloride have been shown to come from silanol groups polarised by neighbouring (Si-OAlCl₂) Lewis acid sites;¹² however, DRIFT analysis of the supported BF₃ catalyst reveals that all silanol groups are consumed during catalyst preparation. It is likely that the formation of Lewis acid Si-OBF₂ sites is hindered due to the lack of stabilisation by interaction with surface OH, thus explaining the low number of Lewis acid sites detected by DBMP.

The DRIFT spectrum of DBMP adsorbed on 600 °C calcined silica shows bands at 1565 and 1600 cm⁻¹ due to the ring vibrations of DBMP (Fig. 5). Also, the silanol peak (at 3745

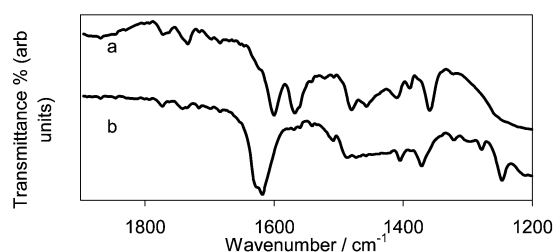


Fig. 5 DRIFT spectra of DBMP on 600 °C silica (a) and the supported catalyst (b).

cm⁻¹) on silica is attenuated indicating the silanol groups are coordinated to DBMP. The DRIFT spectrum of DBMP adsorbed onto the catalyst shows a new peak at 1618 cm⁻¹, which is assigned to the N⁺-H deformation from DBMPH⁺. To test if the protons truly originated from the catalyst surface, the catalyst/DBMP material was washed in toluene and heptane and the filtrate analysed by ¹H NMR. No DBMP or DBMPH⁺ was detected, indicating that the protons originate from the catalyst surface, and the initiation step in the polymerisation reaction is heterogeneous.

The 600 °C calcined silica support and catalyst at different loadings were investigated using triethylphosphine oxide (TEPO), a well-known solid acid probe¹³ and ³¹P MAS NMR: spectra are shown in Fig. 6. Coordination of the lone pair of

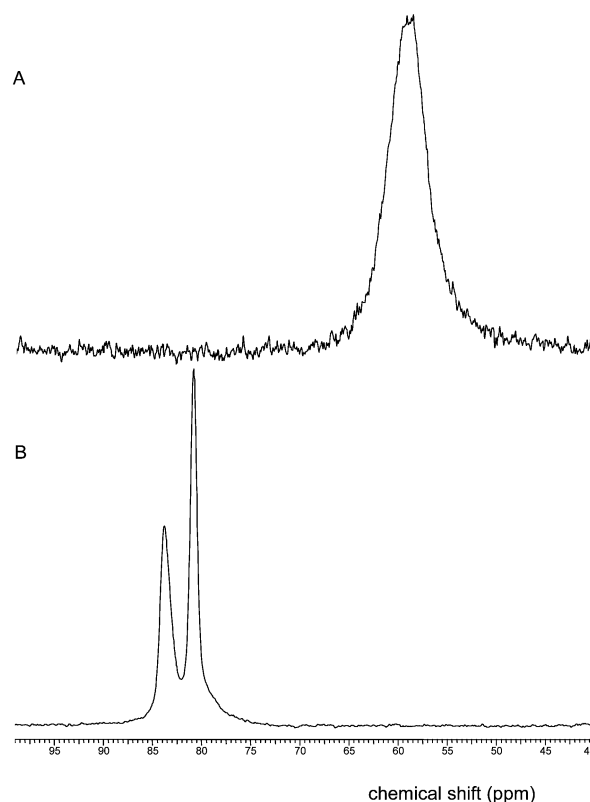
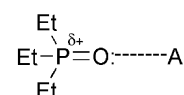


Fig. 6 ³¹P MAS NMR spectra of TEPO on 600 °C calcined silica (A) and TEPO on 4 mmol g⁻¹ supported BF₃ (B).

electrons on the oxygen atom from the TEPO probe molecule to an acid site on the catalyst will pull electron density away from the phosphorus atom (Scheme 3). The deshielding of the



Scheme 3 TEPO coordination to an acid site (A).

phosphorus atom is relative to the strength of the acid site. This change in the ³¹P chemical shift can be readily measured by ³¹P MAS NMR spectroscopy, and provides a simple method of assessing the acid strength of the catalyst.¹⁴

A single peak from the coordination of TEPO to silanol groups is observed at 58 ppm in the ³¹P MAS NMR for the 600 °C dried silica. No differentiation between geminal and vicinal silanols was observed. The peak at 58 ppm is absent in the supported catalyst, consistent with the consumption of the silanol peak evident in DRIFT data. Two new peaks are observed for the supported catalyst at 84 and 81 ppm, indicating the catalyst possesses two acid sites of differing strength.

Characterisation of the catalyst shows mainly Brønsted acidity which is reflected in a unimodal distribution from GPC analysis.

Conclusions

1. Supported BF₃ is active in the polymerisation of a C9 aromatic feed.

2. No leached components are identifiable in resin or reaction media on separation of catalyst.

3. Reuse is possible using continuous addition under an inert atmosphere. α -MS is believed to be an active promoter for the polymerisation reaction *via* a chain transfer mechanism.

4. Catalyst characterisation using TEPO probe molecule has shown two types of acid sites exist. Reaction with DBMP has indicated that the acidic sites of the catalyst are mostly of Brønsted type.

Acknowledgements

We are grateful to Exxon-Mobil Chemicals and the EPSRC, through a CASE award to C. R. Q. and JREI grant to purchase the MAS NMR, for support of this work.

References

- 1 A. V. Topchiev, S. V. Zavgorodnii and Ya. M. Paushkin, *Boron fluoride and its compounds as catalysts in organic chemistry*, Pergamon Press, London, 1958.
- 2 A. Gandini and Y. H. Yang, *ACS Symp. Ser.*, 1997, 113.
- 3 L. Babcock and D. Morrell, *Int. Pat.*, WO9830519, 1998.
- 4 J. H. Clark, K. Shorrocks, V. Budarin and K. Wilson, *J. Chem. Soc., Dalton Trans.*, 2002, **3**, 423.
- 5 R. Mildenberg, M. Zander and G. Collin, *Hydrocarbon Resins*, VCH, Weinheim, Germany, 1997.
- 6 K. Wilson and J. H. Clark, *Chem. Commun.*, 2135, **19**, 1998.
- 7 DSC spectra were measured on a Seiko exstar 6000 station with a DSC 6200 module. A heating rate of 20 °C per minute was used.
- 8 B. Chaudhuri, *Org. Process Res. Dev.*, 1999, **3**, 220.
- 9 Alkene protons H_a and H_b can be seen at 1H NMR δ 5.2 (s) and 4.9 (s). The CH alkene proton H_c can be seen at 6.2 (s). 1H NMR spectra were measured on a JEOL EX 270 instrument at 270.05 MHz. Cyclic dimers, inactive in chain transfer reactions, were also observed, the CH_2 protons of 1,1,3-trimethyl-3-phenylindane appearing at δ 2.51 (d) and 2.34 (d).
- 10 J. M. Moulis, J. Collomb, A. Gandini and H. Cheradame, *Polym. Bull.*, 1980, **3**, 197.
- 11 The reaction vessel was charged with solvent, catalyst and DBMP (0.0146–0.2732 g). The contents were stirred under argon for 30 minutes prior to the addition of the C9 feed to allow for the DBMP to consume the catalyst protons.
- 12 S. Spange, *Prog. Polym. Sci.*, 2000, **25**, 781.
- 13 J. P. Osegovic and R. S. Drago, *J. Phys. Chem. B*, 2000, **104**, 147.
- 14 100 μ l of a 1.0 M TEPO solution was pipetted onto 200 mg of the solid acid. Approximately 2 ml of n-pentane was also added to the sample to facilitate mixing. The slurries were allowed 20–30 minutes for equilibration. The samples were then dried on a rotary evaporator. Sodium dihydrogen phosphate was used as reference. NMR experiments were carried out at 162 MHz with a spinning rate of 10 kHz on a Bruker Avance 400 instrument.



Clean destruction of waste ammonia with consummate production of electrical power within a solid oxide fuel cell system

John Staniforth and R. Mark Ormerod*

Birchall Centre for Inorganic Chemistry and Materials Science, School of Chemistry and Physics, Keele University, Staffordshire, UK ST5 5BG

Received 27th June 2003

First published as an Advance Article on the web 24th July 2003

The response of a solid oxide fuel cell towards waste ammonia has been studied using a small tubular solid oxide fuel cell system, since ammonia is present in certain biogas in large quantities as a breakdown product of biological waste. SOFCs are not only tolerant to ammonia, but can actually utilise the ammonia present in biogas to produce electrical power, at the same time acting as an environmental clean-up device breaking down the ammonia pollutant to nitrogen and water. Ammonia is catalytically decomposed over the nickel cermet anode to N_2 and H_2 , and the H_2 is then electrochemically oxidised to water. Direct electrochemical oxidation of the ammonia does not occur, and no undesirable nitrogen oxides are formed.

1 Introduction

Fuel cells are currently attracting tremendous interest because of their great potential as a more efficient and cleaner alternative method of power generation than conventional methods, combining significantly higher efficiency with very much lower emissions of SO_x , NO_x and residual hydrocarbons and reduced CO_2 emissions.^{1–5} Solid oxide fuel cells (SOFCs) offer potential advantages in terms of efficiency, flexibility and cost over other fuel cell types because of their tolerance to carbon monoxide and other poisons and impurities in the fuel, and because the high operating temperatures allow the possibility of running the fuel cell directly on practical hydrocarbon fuel sources, internally reforming the fuel within the fuel cell.^{4–7} It is generally accepted that for SOFCs to be cost effective, direct or indirect reforming of the hydrocarbon fuel within the fuel cell is essential.^{6,7} Although natural gas is the most commonly used practical fuel for SOFCs, other hydrocarbon fuels such as propane and butane are particularly suitable for certain applications.

Biogas is a cheap, renewable and readily available energy reserve. However it is very under-exploited, largely because of its variable composition and often low level of methane, which prevents its use in conventional power systems.⁸ Because of this situation large quantities of biogas are presently vented to the atmosphere wasting a potentially clean, renewable energy resource, whilst at the same time making a significant contribution to greenhouse gas emissions. We have recently shown that solid oxide fuel cells offer genuine potential for converting the methane present in biogas into electrical power and useful energy,^{9,10} even when there are only very low levels of methane, with a very significant reduction in greenhouse gas emissions, thus offering a valuable and environmentally friendly use of poor quality biogas that is currently wasted. At methane contents below 50%, the methane in the biogas is internally reformed by the CO_2 present, to H_2 and CO , which are then electrochemically oxidised to CO_2 and water, with production of electrical power and heat.¹⁰

The high nitrogen content of waste bio-organic matter from which biogas is derived frequently results in the production of ammonia as a major breakdown product.¹¹ This ammonia production is so intense in certain biological waste, such as pig

and chicken slurry, that European legislation actually limits the amount of ammonia which can be discharged into the atmosphere through breakdown on biological waste.¹² This high ammonia content of biogas could potentially present a major barrier to using biogas as a fuel source for solid oxide fuel cells, since poisoning of active materials within the SOFC could occur, leading to cell deactivation and poor durability, or nitrogen oxides could be produced, which would somewhat offset the environmental benefit of converting the methane into CO_2 and water and electrical power.

In this paper we have used a small diameter thin-walled extruded tubular solid oxide fuel cell system developed in this laboratory^{13–15} to study the behaviour of an SOFC to an ammonia gas feed and the reactivity of a nickel based SOFC anode towards ammonia under SOFC operating conditions. Nickel has previously been shown to be active for the catalytic decomposition of ammonia,¹⁶ and it is interesting to note that the decomposition of ammonia over nickel catalysts has recently been considered as a possible source of H_2 for Proton Exchange Membrane (PEM) fuel cells,¹⁷ which require a source of pure (CO_x -free) H_2 as fuel. This is therefore very distinct from the objectives of the research in this paper, where the SOFC anode is exposed directly to a practical hydrocarbon fuel, which contains ammonia, and where there is no separate external catalytic unit. This paper demonstrates that SOFCs are not only tolerant to the ammonia present in biogas, but can actually utilise the ammonia to produce electrical power, at the same time acting as an environmental clean-up device by breaking down the ammonia pollutant to nitrogen and water.

Green Context

Solid oxide fuel cells are well known for their potential to extract electricity from hydrocarbons. What has always been less certain is whether they could be used with biogas, which often contains considerable amounts of ammonia. This paper demonstrates that fuel cells can not only function in the presence of ammonia, but they can convert it to nitrogen, water and electrical power, making this a potentially very clean and attractive option. *DJM*

2 Experimental

All the experiments described in this paper were carried out using the SOFC test system, which we have developed,^{13–15} based on a small diameter, thin-walled extruded yttria-stabilised zirconia tubular reactor. Briefly, the apparatus consists of a custom built furnace which houses the tubular SOFC. The furnace allows linear temperature control to 1000 °C. The test cell inlet was linked to a stainless steel gas manifold which allowed complete flexibility in gas handling and control of gas composition, enabling evaluation over a full range of operating conditions and fuel compositions. The exit and inlet gas was analysed by an on-line mass spectrometer (MKS-Spectra Minilab). The system enables both conventional catalytic measurements and temperature programmed reaction measurements to be carried out. A particular advantage of the tubular SOFC design is that it can be housed in the furnace in the same way as a conventional catalytic reactor.^{13,14} Thus the test system allows both the performance and durability of the fuel cell and the fuel reforming catalysis and surface reaction pathways to be evaluated within the actual SOFC;^{13–15,18} we have previously demonstrated the value of such *in situ* catalytic measurements on working SOFCs.^{13–15,18,19} As zirconia is a good thermal insulator the ends of the electrolyte tube which project beyond the walls of the furnace remain sufficiently cool for a gas tight seal to be maintained under operating conditions.

The SOFC anode was constructed in two layers. Both layers were prepared by milling nickel oxide (Alfa Chemicals) and 8 mol% yttria-stabilised zirconia (YSZ) (Unitec-FYT11). 10.5 g NiO and 5.0 g YSZ were mixed for the inner anode layer and 9.5 g NiO and 0.9 g YSZ for the outer layer. 0.5 g of cerium(IV) oxide (Avocado) was also added to the outer layer mixture. A mixture of methanol, 1,1,1-trichloroethane and glycerol was added to each as a solvent and the resultant slurry was milled for 3 hours. A small quantity of poly-vinyl butyrol (~0.15 g) was added at the end of the milling period as a binding agent. The anode ink was then applied to the inside of the electrolyte tubes and dried in air at 150 °C before being fired at 1300 °C for one hour, using a specific firing procedure.

Strontium-doped lanthanum manganite (Seattle Speciality Chemicals) was used as the cathode and again applied in two layers. The inner layer was a 50:50 wt% mixture of $\text{La}_{0.5}\text{Sr}_{0.5}\text{MnO}_3$ and yttria-stabilised zirconia, with a methanol, 1,1,1-trichloroethane, glyceroltrioleate mixture used as the solvent. The outer layer was $\text{La}_{0.82}\text{Sr}_{0.18}\text{MnO}_3$ mixed with acetone using KDI as a dispersant. After applying the inks to the outside of the tubular electrolyte the tubes were dried in air at room temperature before firing to 1573 K using the same procedure that was used for the anode. Nickel wire was used to collect current from the anode and silver wire was used for current collection from the cathode. Current/voltage measurements were carried out using a passive potentiostat. Before each reading was taken the cells were operated for at least 20 minutes in order to reach a steady power output.

Following firing the anode was reduced *in situ* in the test system at 900 °C in a 15% H_2/He mixture for one hour prior to testing. Ammonia was introduced by bubbling helium carrier gas through a stainless-steel saturator containing ammonia solution (s.g. 0.88) linked to the gas manifold by a four-way sampling valve. Temperature programmed measurements were carried out using a heating rate of 5 °C min^{-1} .

3 Results

Fig. 1 shows the effect of increasing temperature on the open circuit voltage of a tubular SOFC operating on ammonia in a helium carrier gas of 30 ml min^{-1} . It can be seen that the open circuit voltage falls essentially linearly with increasing temperature.

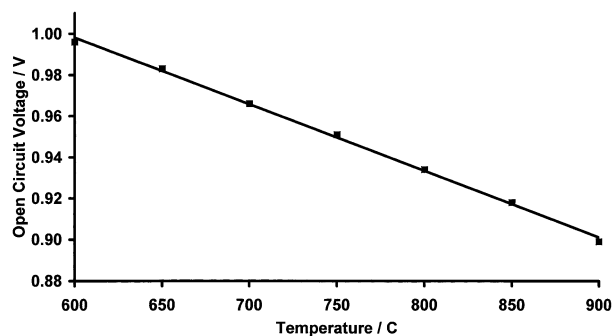


Fig. 1 The effect of operating temperature on the open circuit voltage of an SOFC operating on ammonia in a helium carrier gas.

The reactions occurring when ammonia is passed over the SOFC anode were followed using temperature programmed

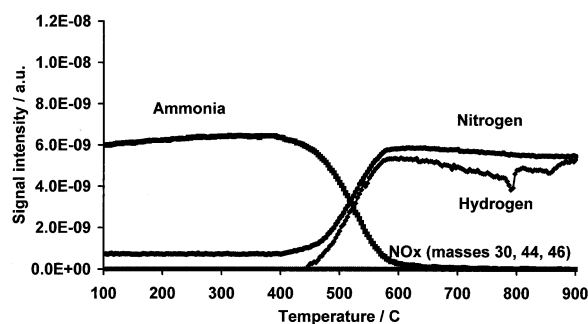


Fig. 2 Temperature programmed reaction of ammonia over a nickel/zirconia cermet anode in a tubular SOFC.

reaction measurements. Fig. 2 shows the results of temperature programmed reaction of ammonia over the SOFC anode. The onset of ammonia conversion occurs at 405 °C, with concomitant evolution of nitrogen and hydrogen. 50% conversion occurs at 516 °C, and all the ammonia is converted into N_2 and H_2 by 590 °C. No other nitrogen containing products were detected.

Such temperature programmed and continuous isothermal measurements were carried out under open circuit conditions. When current is drawn from the cell, there is a flux of oxygen ions across the zirconia electrolyte to the anode, such that the conditions at the anode become increasingly more oxidising as more current is drawn. Fig. 3 shows the composition of the exit

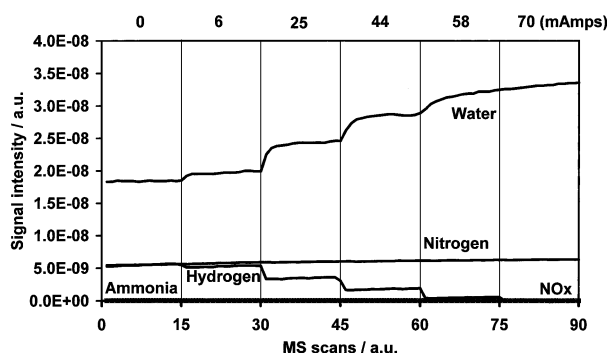


Fig. 3 The effect of drawing increasing amounts of current on the exhaust gas composition of an SOFC powered by ammonia.

gas from the SOFC anode when the SOFC is operated on ammonia at 850 °C and progressively increasing amounts of currents are drawn from the cell. As the potential across the cell is decreased and the current drawn increased, stepwise consumption of H_2 is observed, with a corresponding parallel stepwise increase in water evolution, until all the H_2 is consumed. The level of N_2 production is unaffected by the

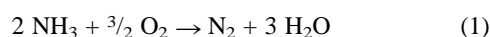
amount of current drawn, and even at the highest current drawn no NO, NO₂ or N₂O are formed.

4 Discussion

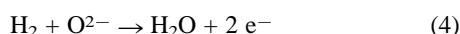
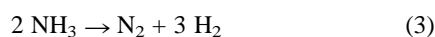
Table 1 compares ΔG° and E° for the oxidation of ammonia (1) with the oxidation of hydrogen (2).

Table 1 Comparison of thermodynamic data for the oxidation of ammonia and the oxidation of hydrogen

Reaction	$\Delta G^\circ_{(298\text{K})}/\text{kJ mol}^{-1}$	$\Delta G^\circ_{(1123\text{K})}/\text{kJ mol}^{-1}$	$E^\circ_{(298\text{K})}/\text{V}$	$E^\circ_{(1123\text{K})}/\text{V}$
$2 \text{NH}_3 + 3/2 \text{O}_2 \rightarrow \text{N}_2 + 3 \text{H}_2\text{O}$	-652.8	-772	1.13	1.33
$\text{H}_2 + 1/2 \text{O}_2 \rightarrow \text{H}_2\text{O}$	-228.6	-179	1.19	0.93



It can be seen from Table 1 that the amount of energy potentially available from electrochemically oxidising ammonia in a solid oxide fuel cell is effectively twice that from oxidising hydrogen. The thermodynamics of ammonia oxidation *via* eqn. (1) suggests that the open circuit voltage of the SOFC should increase with operating temperature when ammonia is passed over the anode. However, Fig. 1 shows clearly that as the SOFC temperature is increased from 600 °C to 900 °C there is an essentially linear decrease in the open circuit voltage. This is not what is expected from the thermodynamics of the oxidation of ammonia (1), but is consistent with the thermodynamics of hydrogen oxidation (2). This suggests that the oxidation of ammonia within an SOFC is a two stage process, with decomposition of ammonia to nitrogen and hydrogen (3) occurring initially, followed by oxidation of hydrogen to water (4).



Thus the two reactions are effectively uncoupled. This means that although there should be twice as much free energy available from oxidising a mole of ammonia as opposed to a mole of H₂, due to uncoupling of the reactions, only one and a half times as much energy will actually be available, *i.e.* 3/2 moles of H₂ are produced from every mole of ammonia.

Fig. 2 shows clearly that the nickel cermet anode is active for ammonia decomposition, with decomposition starting at 405 °C, and complete conversion of the ammonia to N₂ and H₂ has occurred by 590 °C, well below the operating temperature of SOFCs. McCabe has previously showed that nickel wire is active for ammonia decomposition over the temperature range 480 °C to 1080 °C.¹⁶ At temperatures below 730 °C the decomposition of ammonia is highly activated and the rate is independent of NH₃ pressure. Thus at the operating temperature of SOFCs all the ammonia has been converted over the anode into N₂ and H₂, and it is the hydrogen which is then the fuel for the SOFC, with there being no direct oxidation of the ammonia.

When current is drawn from the cell, there is a flux of oxygen ions across the zirconia electrolyte to the anode, such that the conditions become progressively more oxidising as more current is drawn. As the conditions become increasingly more oxidising it is more likely that nitrogen oxides, such as N₂O and NO, will be formed by direct oxidation of the ammonia (eqns. (5) and (6)). It would clearly be undesirable for an SOFC running on biogas, with the concomitant environmental benefits this brings, including the significant reduction in greenhouse gas emissions, to emit N₂O or NO.

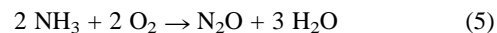


Fig. 3 shows that when the SOFC was operated on ammonia at 850 °C, and progressively increasing current is drawn from the cell, corresponding to an increased oxygen flux across the cell, no nitrogen oxides are formed, even at the highest currents drawn. Instead as the current drawn from the cell is increased, stepwise consumption of the H₂ formed from ammonia decomposition is observed, with a corresponding parallel stepwise increase in water evolution until all the H₂ is consumed. Drawing current from the cell has no effect at all on the N₂ evolution.

It is also worth noting that all the products associated with the reaction of ammonia in an SOFC are gaseous, and so there are none of the problems that can potentially occur with hydrocarbon fuels, due to carbon deposition from hydrocarbon pyrolysis,^{7,15,18,20,21} and sulfur poisoning from sulfur-containing hydrocarbons, which are for example added to natural gas as odorants.^{7,22,23}

5 Conclusions

Having previously demonstrated that solid oxide fuel cells can be run directly on biogas,^{9,10} converting the methane in the biogas in the fuel cell into CO₂ and water, and generating electrical power and useful heat, even at very low levels of methane, whilst at the same time resulting in a very significant reduction in greenhouse gas emissions, we have now shown that the high ammonia content of biogas does not present a problem in using biogas as a fuel source for SOFCs. Thus SOFCs do indeed offer a valuable and environmentally friendly use of poor quality biogas that is currently disposed of by simply venting wastefully and detrimentally to the atmosphere.

We have demonstrated that SOFCs are not only tolerant to the ammonia that is present in biogas, but can actually utilise the ammonia to produce electrical power. Direct electrochemical oxidation of the ammonia does not occur. Instead the ammonia is catalytically decomposed over the nickel cermet anode to nitrogen and hydrogen, and the H₂ is then electrochemically oxidised to water. No N₂O, NO or NO₂ are formed.

Thus in addition to producing useful electrical power from the electrochemical oxidation of the ammonia, the SOFC at the same time acts as an environmental clean-up device by breaking down the ammonia pollutant to N₂ and water, with no emission of any undesirable nitrogen oxides.

Acknowledgements

The UK Engineering and Physical Sciences Research Council is gratefully acknowledged for the award of an Advanced Research Fellowship to RMO.

References

- 1 R. Kingston, *Chem. Brit.*, June 2000, 24.
- 2 G. Hoogers and D. Thompson, *Chem. Ind.*, 1999, 796.
- 3 C. K. Dyer, *Sci. Am.*, 1999, **281**, 70.
- 4 D. Hart, *Chem. Ind.*, 1998, 344.
- 5 A. C. Lloyd, *Sci. Am.*, 1999, **281**, 64.
- 6 B. C. H. Steele and A. Heinzel, *Nature*, 2001, **414**, 345.
- 7 R. M. Ormerod, *Chem. Soc. Rev.*, 2003, 17.

- 8 J. Huang and R. J. Crookes, *Fuel*, 1998, **77**, 1793.
- 9 J. Staniforth and R. M. Ormerod, *Green Chem.*, 2001, **3**, G61.
- 10 J. Staniforth and R. M. Ormerod, *Catal. Lett.*, 2002, **81**, 19.
- 11 J. R. Fischer, D. M. Sievers and C. D. Fulhaye, in *Energy, Agriculture and Waste Management*, ed. W. J. Jewell, Chpt. 5, Ann Arbor Science, New York, USA, 1975.
- 12 S. G. Sommer and N. J. Hutchings, *Eur. J. Agron.*, 2001, **15**, 1.
- 13 C. M. Finnerty, R. H. Cunningham, K. Kendall and R. M. Ormerod, *Chem. Commun.*, 1998, 915.
- 14 C. M. Finnerty, R. H. Cunningham and R. M. Ormerod, *Catal. Lett.*, 2000, **66**, 221.
- 15 R. M. Ormerod, *Stud. Surf. Sci. Catal.*, 1999, **122**, 35.
- 16 R. W. McCabe, *J. Catal.*, 1983, **79**, 445.
- 17 T. V. Choudhary, C. Sivadinarayana and D. W. Goodman, *Chem. Eng. J.*, 2003, **93**, 69.
- 18 C. M. Finnerty, N. J. Coe, R. H. Cunningham and R. M. Ormerod, *Catal. Today*, 1998, **46**, 137.
- 19 C. M. Finnerty and R. M. Ormerod, *J. Power Sources*, 2000, **86**, 390.
- 20 J. R. Rostrup-Nielson and L. J. Christiansen, *Appl. Catal. A: General*, 1995, **126**, 381.
- 21 J. R. Rostrup-Nielson, *Catal. Today*, 1993, **18**, 305.
- 22 A. L. Dicks, *J. Power Sources*, 1996, **61**, 113.
- 23 R. M. Ormerod, Fuels and Fuel Processing in SOFCs, in *Solid Oxide Fuel Cells: Fundamentals and Applications*, ed. S. C. Singhal and K. Kendall, Elsevier, London, 2003, p. 350, in press.



Chemoenzymatic synthesis of glycoconjugate polymers: greening the synthesis of biomaterials

Yoshiko Miura,* Takayasu Ikeda, Natsuko Wada, Hajime Sato and Kazukiyo Kobayashi

Department of Molecular Design and Engineering, Graduate School of Engineering, Nagoya University, Furo-cho, Chikusa-ku, Nagoya 464-8603, Japan.

E-mail: miuray@mol.nagoya-u.ac.jp; Fax: +81-52-789-2528; Tel: +81-52-789-2538

Received 12th May 2003

First published as an Advance Article on the web 4th August 2003

Glycoconjugate polymers with biodegradable poly(vinyl alcohol) (PVA) were synthesized *via* lipase-catalyzed transesterification of sugar alcohols (maltitol and lactitol) with divinyl dicarboxylates and subsequent radical polymerization. The conversion and chemoselectivity in transesterification were dependent on the lipases, the sugar alcohols, and the alkyl chain length of the dicarboxylates. Chemoselective esterification was attained in the presence of lipase from *Candida antarctica* (lipase CA) to give maltitol 6-vinyl sebacate, lactitol 6-vinyl sebacate, and lactitol 6-vinyl adipate in high yields. Polymerization of these vinyl esters with hydrogen peroxide/ascorbic acid as initiator gave glycoconjugate polymers. These polymers were suggested to take micellar conformations in water and to bind strongly to specific lectins (concanavalin A or RCA₁₂₀). The biodegradabilities of these polymers were modest but higher than PVA. This simple synthesis will be useful to develop various glycoconjugate polymers with high biological activities due to the multivalent glyco-cluster effect and biodegradability due to their PVA backbone and ester linkage.

Introduction

Carbohydrates are the most abundant renewable resources on earth and hence the most promising substances in green and sustainable chemistry to develop high-performance materials with biodegradability.¹ Chemical modifications of carbohydrates, however, are usually troublesome because modifications require multi-step reactions including protection–deprotection steps of multiple hydroxyl groups. In these respects, enzymes are advantageous as catalysts to perform conversions and modifications of carbohydrates with high efficiency and high selectivity. In addition to carbohydrate-specific enzymes such as glycosyltransferases, glycosidases, and glycosylphosphorylases, a variety of esterases such as lipases and proteases have been reported to be effective in the biotransformation of carbohydrates.^{2,3} Carbohydrate-based polyesters as well as poly(vinyl esters) carrying pendant carbohydrates have been synthesized *via* enzymatic esterification of carbohydrates.^{4,5}

In addition to their renewable resources, carbohydrates in living systems also play key roles as biological recognition signals and as functional biomolecules.⁶ Interest has been devoted to the recognition activities of carbohydrates to develop specialty materials with highly qualified functionality. We have reported the synthesis of various types of glycoconjugate polymers and their biological activities such as hepatocyte culture substrates, virus adsorption materials, and toxin neutralization reagents.^{7,8}

This paper attempts the simple synthesis of artificial glycoconjugate polymers exhibiting both biodegradation abilities and biological recognition abilities (Fig. 1). As shown in Scheme 1, disaccharide alcohols (maltitol and lactitol) were employed as target carbohydrates, and divinyl sebacate and divinyl adipate as target acyl donors. This paper describes the screening of lipases of various origins to catalyze efficient transesterification giving vinyl derivatives of selectively esterified maltitol and lactitol. The glycoconjugate polymers exhibited high biological activities due to the multivalent glyco-

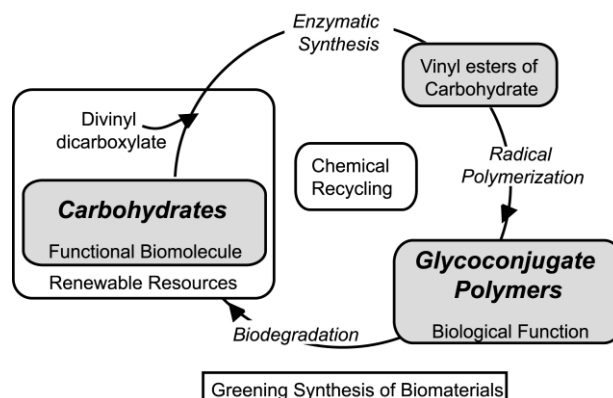
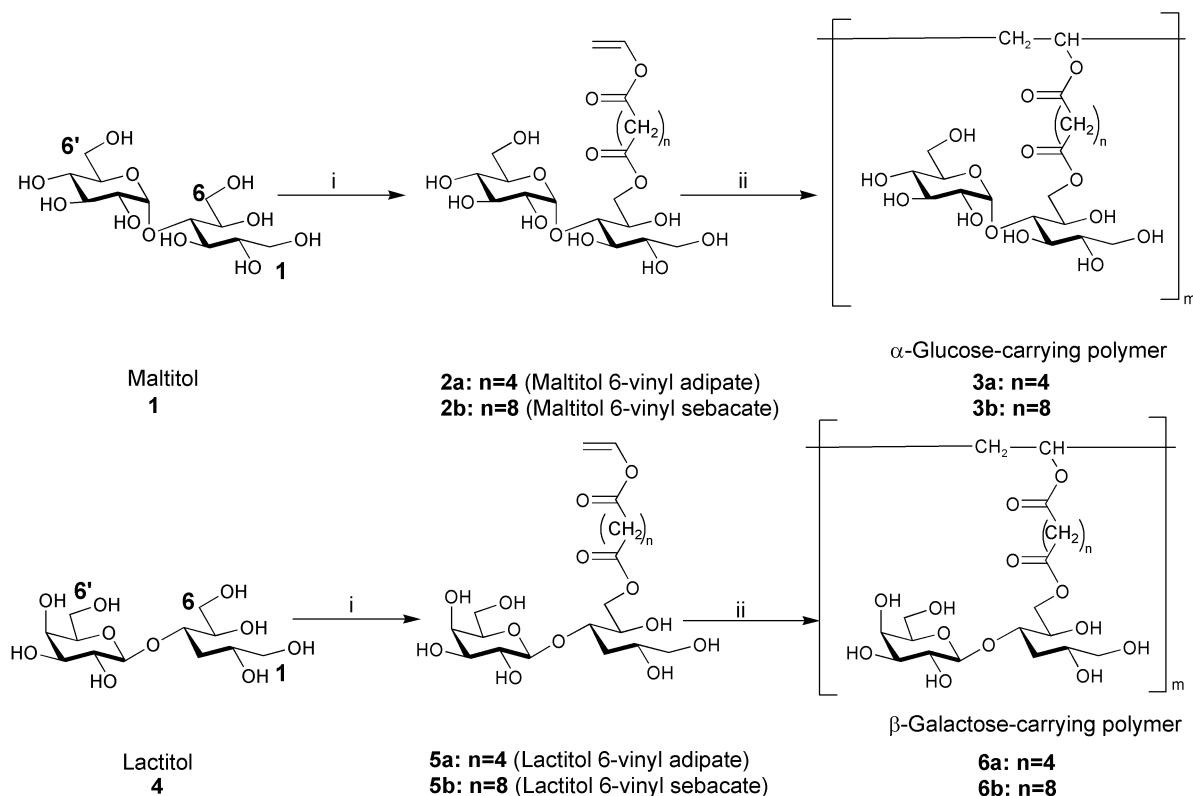


Fig. 1 Schematic illustration of biomaterials *via* chemoenzymatic syntheses.

Green Context

Glycoconjugate polymers are useful biomaterials derived from naturally occurring and renewable carbohydrates. Some of these materials show good biological activities as hepatocyte cultures and for virus adsorption. Unfortunately, the 'green credentials' of these materials are normally reduced by inefficient and complex chemical modification procedures. Here a chemoenzymatic procedure is described with much improved green chemistry characteristics. Sugar esters are prepared *via* enzymatic reactions and these are polymerised using quite benign chemical initiators.

JHC



Scheme 1 Synthesis of glycoconjugate polymers *via* enzymatic esterification of sugar alcohols and subsequent radical polymerization. *Conditions:* (i) divinyl sebacate or divinyl adipate, pyridine, 50 °C, 72 h, lipase; (ii) radical initiator (H₂O₂ and L-ascorbic acid), H₂O–DMSO.

cluster effect⁹ and biodegradability due to their poly(vinyl alcohol) backbone and ester linkages.

Experimental

Chemicals

The solvent for enzymatic esterification was dried with molecular sieves (4 Å) for at least 24 h. The lipase from *Candida antarctica* (CA) was kindly donated by Novo Nordisk Bioindustry Ltd. (Bagsvaerd, Denmark). Lipases from *Pseudomonas fluorescens* (AK) and *Pseudomonas cepacia* (PS) were gifts from Amano Enzyme Inc. (Nagoya). The lipase from Porcine pancreas (PP) and *Rhizomucor miehei* (RM) were purchased from Sigma-Aldrich (Louisiana, MO) and Fluka (Buch, Switzerland), respectively.

Characterizations

¹H (500 MHz) and ¹³C (125 MHz) NMR spectra were recorded on a Varian Inova 500 equipped with a Sun workstation. The spectra were measured in a mixture of DMSO-d₆ and D₂O (100/1, v/v). Fluorescence spectroscopy was carried out using a JASCO FP-777 spectrometer at 25 °C. Size exclusion chromatography (SEC) analyses were performed with a JASCO L800 on Shodex B804+B805 columns equipped with BOWIN chromatography software. PBS was used as the eluent at a flow-rate of 0.5 ml min⁻¹ at an oven temperature of 40 °C. The molecular masses and polydispersities were estimated using a pullulan standard.

Preparation of sugar vinyl esters

Enzyme screening was carried out with a mixture of 52 mg of maltitol or 54 mg of lactitol monohydrate (0.15 mmol), 0.15 g

of divinyl sebacate or 0.12 g of divinyl adipate (0.60 mmol) and 50 mg of enzyme in 1 ml of pyridine at 50 °C for 72 h. The conversion of sugar alcohols and the chemoselectivities of the sugar alcohol esters were estimated by high performance liquid chromatography (HPLC) on an Amide 80 column (Tosoh Co. Ltd., Kawasaki, Japan) eluting with a mixture of acetonitrile : water : methanol (3 : 1 : 1 for conversion of sugar alcohols and 4 : 1 : 1 for chemoselectivities), and by thin-layer chromatography (TLC). The larger-scale reaction was carried out with 0.52 g of maltitol or 0.54 g of lactitol (1.5 mmol) and 1.5 g of divinyl sebacate or 1.2 g of divinyl adipate (6.0 mmol) in 10 ml of pyridine at 50 °C for 72 h. The esters of sugar alcohols were purified by column chromatography (reversed phase SiO₂: MeOH–water gradient from 2/1 to 1/1 (v/v)) to confirm the chemical structures by ¹³C NMR.

Dynamic light scattering (DLS)

DLS measurements were performed at 25 °C on a DLS-6600HK (Otsuka Electronics, Osaka, Japan) equipped with a 5 mW He–Ne laser. The mean diameter of the polymer micelles was calculated by cumulant analysis.

Lectin recognition assay

The binding constants of the glycoconjugates with FITC-labeled lectins were evaluated by Scatchard plots of the fluorescence spectroscopy.

Biochemical oxygen demand (BOD) test

BOD was determined with a BOD tester (Model 200F; TAITEC, Koshigaya) by the oxygen consumption method, basically according to the JIS standard guidelines (JIS K 6950) at 25 °C using an activated sludge obtained from the Nagoya municipal sewage treatment plant in Nagoya City.

Results and discussion

Enzymatic esterification of sugar alcohols

A total of five lipases (lipase AK, CA, PP, PS, and RM) were examined for their ability to catalyze the esterification of sugar alcohols in pyridine. The results of conversion and chemoselectivity are summarized in Table 1. From the point of view of conversion, divinyl sebacate was a better acyl reagent than divinyl adipate, reflecting that lipases prefer hydrophobic substrates.¹⁰ The conversion of lactitol was much higher than that of maltitol, suggestive of the contribution of the hydrophobicity of the α -anomeric surface in the galactose and the hydration of lactitol (lactitol monohydrate is used).¹¹

The esterified products were analyzed by HPLC and ¹³C NMR (Fig. 2). For an example, the esterification of lactitol with divinyl adipate using lipase CA gave only one elution peak in the HPLC trace (Amide 80, acetonitrile : water : methanol = 4 : 1 : 1). The ¹³C NMR spectrum of the product was simple. Among the three primary hydroxyl methylene (1, 6, and 6') carbons of the starting lactitol, only one signal at the 6 position (63.7 ppm) of the glucitol moiety was shifted downfield (66.4 ppm).¹² The product esterified chemoselectively at position 6 is termed lactitol 6-vinyl adipate (**5a**) in this paper. On the other hand, the esterification using lipase PS gave another product in addition to **5a** in the HPLC trace. The product was identified as lactitol 6'-vinyl adipate as judged from the downfield shift of the 6'-galactosyl moiety in the ¹³C NMR spectrum.

Esterification in other solvents was also investigated with maltitol and divinyl sebacate using lipase CA (Table 2). The conversion and chemoselectivity of maltitol were decreased in DMF, and completely lost in pyridine with a small amount of water. These results indicated that lipases were inactive in the polar solvents which stripped the essential water of lipases resulting in denaturation.¹¹ The addition of water also caused ester hydrolysis and an unfavorable thermodynamic equilibrium in the esterification.¹¹

The hydroxyl group of position 6 in the open-chain D-glucitol moiety of both maltitol and lactitol was the most reactive in terms of esterification. Lipase CA in pyridine was the best catalyst in terms of conversion and chemoselectivity to synthesize maltitol 6-vinyl sebacate, lactitol 6-vinyl adipate, and lactitol 6-vinyl sebacate, while even lipase CA gave a mixture of maltitol 6-vinyl adipate and maltitol 6'-vinyl adipate. With this achievement, maltitol 6-vinyl sebacate, lactitol 6-vinyl adipate, and lactitol 6-vinyl sebacate could be useful as starting monomers for green and sustainable synthesis of artificial glycoconjugate polymers.

Polymerization of sugar alcohol esters

The resultant vinyl esters of sugar alcohols were polymerized with free radical initiators to yield glycoconjugate polymers (Table 3). The polymerization must be carried out using low monomer concentrations owing to the poor solubilities of these amphiphilic vinyl esters. Maltitol 6-vinyl sebacate (**2b**) was soluble in water, DMSO, and a mixture of water and DMSO, and was polymerized with 2,2'-azobis(2-amidinopropane) dihy-

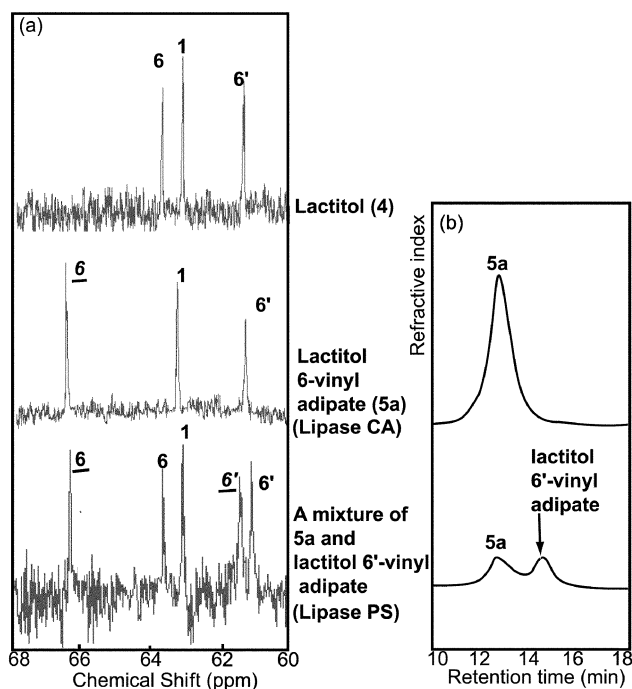


Fig. 2 Expanded (a) ¹³C NMR and (b) HPLC diagrams: lactitol (top), lactitol 6-vinyl adipate (middle), and the mixture of lactitol 6-vinyl adipate and lactitol 6'-vinyl adipate (bottom).

Table 2 Enzyme-catalyzed esterification of maltitol with divinyl sebacate with various solvent systems^a

Solvent	Conversion (%) (Chemoselectivity) ^b	
	Lipase CA	
Pyridine	44 (>99 : 0 : 0)	
DMF	28 (39 : 33 : 28)	
Pyridine (0.95)/water (0.05)	0	

^a HPLC (Amide 80). ^b Ratio (%) of 6-acylated : 6'-acylated : 1-acylated compounds in the vinyl esters of maltitol by HPLC (Amide 80; acetonitrile/water/methanol, 4/1/1).

drochloride or hydrogen peroxide with L-ascorbic acid (As-A) in aqueous solution.¹³ Vinyl esters of lactitol (**5a** and **5b**) were insoluble in water, and the polymerization with hydrogen peroxide didn't proceed in pure DMSO solution due to the unreactivity of the redox initiator in DMSO. The resulting polymers were purified by dialysis and used for further investigation (Run nos. 1, 5 and 8).

Despite the poor solubility of the monomers, the resulting polymers were readily soluble in water, suggesting that these polymers consisting of amphiphilic units underwent micelle formation in water. The self-assembling structures (**6a** and **6b**) were monitored by DLS (Fig. 3). Both polymers showed micelle formation, and the diameter of **6b** (average 402 nm) was larger than that of **6a** (average 55 nm).

Table 1 Enzyme screening for esterification of sugar alcohols in pyridine

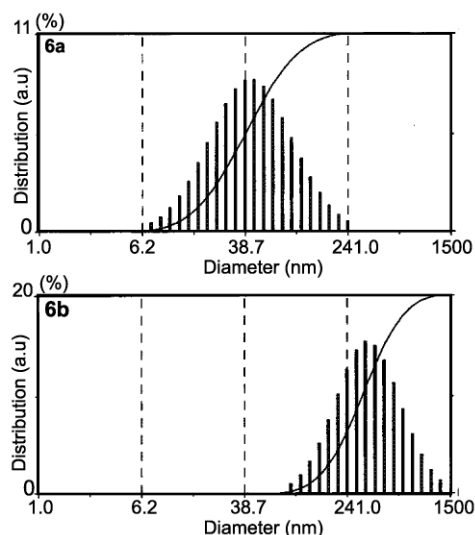
Enzyme	Conversion (%) ^a (Chemoselectivity) ^b			
	Maltitol		Lactitol	
	Divinyl adipate	Divinyl sebacate	Divinyl adipate	Divinyl sebacate
Lipase AK	0	1 ^c	21 (>99 : 0 : 0)	93 (>99 : 0 : 0)
Lipase CA	7 (78 : 21 : 0) ^b	44 (>99 : 0 : 0) ^c	70 (>99 : 0 : 0)	99 (>99 : 0 : 0)
Lipase PP	5 ^c	5 ^c	3 ^c	4 ^c
Lipase PS	0	0	10 (47 : 53 : 0)	13 (81 : 19 : 0)
Lipase RM	0	21 (57 : 29 : 14)	0	15 (64 : 25 : 11)

^a HPLC (Amide 80) (acetonitrile/water/methanol, 3/1/1). ^b Ratio (%) of 6-acylated : 6'-acylated : 1-acylated compounds in the vinyl esters of sugar alcohols by HPLC (Amide 80; acetonitrile/water/methanol, 4/1/1). ^c The chemoselectivity was not detectable.

Table 3 Polymerization of maltitol 6-vinyl sebacate (**2b**), lactitol 6-vinyl adipate (**5a**), and lactitol 6-vinyl sebacate (**5b**)^a

Run no.	Monomer	Solvent (ml) H ₂ O/DMSO	Yield (%)	$M_n (\times 10^{-4})^b /$ g mol ⁻¹	M_w/M_n
1	2b ^c	0.20/0	35	2.8	2.6
3	2b ^d	0.11/0	>99	1.5	3.1
4	5a ^{c,e}	0.25/0.25	55	0.80	3.4
5	5a ^{c,e}	0.15/0.10	75	1.20	1.7
7	5b ^{c,e}	0.20/0.0	49	2.0	1.9
8	5b ^{c,e}	0.10/0.10	82	1.3	1.7

^a 10 mg of monomer. ^b SEC using pullulan standard. ^c 0.032% H₂O₂ and 10 mM As-A, temperature: 35 °C, time: 2.5 h. ^d 0.18 μM 2,2'-azobis(2-amidinopropane) dihydrochloride, temperature: 60 °C, time: 20 h. ^e Suspension polymerization.

**Fig. 3** Diameters of the glycoconjugate polymers **6a** (top), and **6b** (bottom) at a sugar unit concentration of 100 μM.

Biological ability of the polymers

The affinities for lectins were investigated by fluorescence spectrometry using FITC-labeled lectins, and the association constants (Table 4) were estimated by means of Scatchard

Table 4 Estimation of lectin recognition abilities

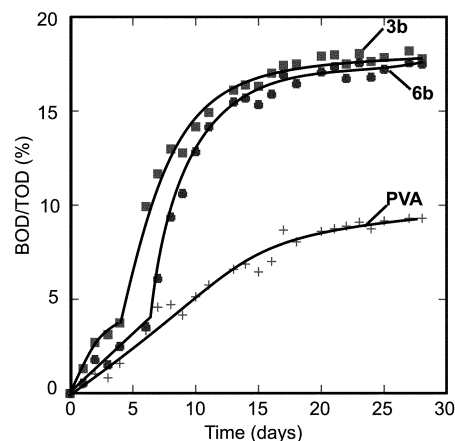
	Affinity constant/M ⁻¹ ^a	
	ConA	RCA120
1	2.1 × 10 ³	nd ^b
3b	7.0 × 10 ⁴	nd
4	nd	1.4 × 10 ³
6a	nd	2.6 × 10 ⁴
6b	nd	6.1 × 10 ⁴

^a The affinity constants are based on the molarity of the glycosyl unit, ^b nd: not detectable.

plots. **3b**, **6a**, and **6b** showed specific affinities for ConA and RCA₁₂₀, respectively. Since sugar units in the polymers were assembled along the polymer backbone, the affinities of the polymers based on the glyco-cluster effect were much higher than those for the sugar alcohols.⁹ The affinity constant of **6b** was larger than that of **6a**, which suggests that the amphiphilic structure affects the glyco-cluster formation.

Biodegradability

Biodegradation was followed by the biochemical oxygen demand (BOD)/theoretical oxygen demand (TOD) value using the oxygen consumption method (Fig. 4). Degradation of both

**Fig. 4** Biodegradability of the glycoconjugate polymers (**3b** and **6b**) with a PVA backbone.

3b and **6b** was enhanced rather than the continuous slow degradation of PVA ($M_n = 2.2 \times 10^4$ (g mol⁻¹), 87–89 mol% hydrolyzed).¹⁴ The degradation was gradual for the first 5 days, increased sharply over days 5–15, and then slowed down again. Since these polymers consist of a poly(vinyl alcohol) main chain and dicarboxylic esters of carbohydrates, dicarboxylic esters in the branches could be degraded preferentially.¹⁵ The biodegradabilities of **3b** and **6b** imply that these glycoconjugate polymers are useful not only as biomaterials but also as green materials which can be regarded as a chemical recycling system for biomaterials.

Conclusion

Maltitol and lactitol were esterified with divinyl carboxylate using lipase catalysts. The esterification of sugar alcohols depended on the kinds of sugar alcohols, the alkyl chain length of divinyl carboxylate and the polarity of the solvents. Lipase from *Candida antarctica* showed the best chemoselectivities to synthesize maltitol and lactitol 6-vinyl esters, which were subjected to radical polymerization. The glycoconjugate polymers formed micelles because of the amphiphilicity of the polymer in water. The glycoconjugate polymers showed strong and specific interactions with lectins based on the glyco-cluster effects. The biodegradabilities of the glycoconjugate polymers were modest, but higher than that of PVA. We believe that this chemoenzymatic synthesis is a new green method for bio-material fabrication.

Abbreviations

As-A	L-ascorbic acid
ConA	concanavalin A
BOD	biochemical oxygen demand
DLS	dynamic light scattering
DMSO	dimethyl sulfoxide
HPLC	high-performance liquid chromatography
Gal	galactose
Glc	glucose
PVA	poly(vinyl alcohol)
RCA ₁₂₀	<i>Ricinus communis</i> agglutinin 120
SEC	size exclusion chromatography
TLC	thin-layer chromatography
TOD	theoretical oxygen demand

Acknowledgements

This work was supported by a Grant-in Aid for Young Scientists (B), Shoei Science Foundation, Sekisui Chemical Foundation,

Eno Science Foundation, and the 21st Century COE Program “Nature-Guided Materials Processing”.

References

- 1 Q. Wang, J. S. Dordick and R. J. Linhardt, *Chem. Mater.*, 2002, **14**, 3232.
- 2 B. G. Davis, *J. Chem. Soc., Perkin Trans. 1*, 2000, 2137.
- 3 (a) M. Therisod and A. M. Klivanov, *J. Am. Chem. Soc.*, 1987, **109**, 3977; (b) R. Sergio, J. Chopineau, A. P. G. Kieboom and A. M. Klivanov, *J. Am. Chem. Soc.*, 1988, **110**, 584.
- 4 H. Uyama, E. Klegraf, S. Wada and S. Kobayashi, *Chem. Lett.*, 2000, 800.
- 5 (a) S. Shibatani, M. Kitagawa and Y. Tokiwa, *Biotechnol. Lett.*, 1997, **19**, 511; (b) M. Kitagawa and Y. Tokiwa, *Carbohydr. Lett.*, 1997, **2**, 343.
- 6 A. Variki, *Glycobiology*, 1993, **3**, 97.
- 7 (a) A. Kobayashi, T. Akaike, K. Kobayashi and H. Sumitomo, *Makromol. Chem. Rapid. Commun.*, 1986, **7**, 645; (b) A. Tsuichida, K. Kobayashi, N. Matsubara, T. Muramatsu, T. Suzuki and Y. Suzuki, *Glycoconjugate J.*, 1998, **15**, 1047; (c) H. Dohi, Y. Nishida, Y. Furuta, H. Uzawa, S.-I. Yokoyama, S. Ito, H. Mori and K. Kobayashi, *Org. Lett.*, 2002, **4**, 355.
- 8 Y. Miura, T. Ikeda and K. Kobayashi, *Biomacromolecules*, 2003, **4**, 410.
- 9 Y. C. Lee and R. T. Lee, *Acc. Chem. Res.*, 1985, **28**, 321.
- 10 G. Lin, C.-T. Shieh, H.-C. Ho, J.-Y. Chouhwang, W.-Y. Lin and C.-P. Lu, *Biochemistry*, 1999, **38**, 9971.
- 11 A. M. Klivanov, *Chemtech*, 1986, **16**, 354.
- 12 K. Yoshimoto, Y. Itatani and Y. Tsuda, *Chem. Pharm. Bull.*, 1980, **28**, 2065.
- 13 C. Larpent and T. F. Tadros, *Colloid Polym. Sci.*, 1991, **269**, 1171.
- 14 Y. Tokiwa, H. Fan, Y. Hiraguri, R. Kurane, M. Kitagawa, S. Shibatani and Y. Maekawa, *Macromolecules*, 2000, **33**, 1636.
- 15 In the FTIR spectra of the glycoconjugate polymers, the strong adsorptions of the alkyl chain and ester bond around 2950 and 1730 cm^{-1} decreased after biodegradation.



Rapid microwave-promoted Suzuki cross coupling reaction in water

Lin Bai,^a Jin-Xian Wang^{*ab} and Yumei Zhang^a

^a Institute of Chemistry, Department of Chemistry, Northwest Normal University, 95 An Ning Road (E.), Lanzhou 730070, P. R. China. E-mail: Wangjx@nwnu.edu.cn; Fax: +86(931)-7768159

^b State Key Laboratory of Applied Organic Chemistry, Lanzhou University, Lanzhou 730000, P. R. China

Received 8th May 2003

First published as an Advance Article on the web 4th August 2003

Water is an inexpensive and nontoxic reaction medium for the microwave-promoted Suzuki cross coupling of arylboronic acids with aryl halides. This environmentally friendly microwave protocol offers convenient operation and synthesis of a variety of substituted biaryls in good yield very rapidly employing PdCl₂(PPh₃)₂ as catalyst and potassium carbonate as the base.

Introduction

The palladium-catalyzed cross coupling reaction of aryl boronic acids with aryl halides in the presence of base, a Suzuki type reaction, provides a very convenient method for forming carbon–carbon bonds, in particular for the formation of biaryls.¹ In recent years, various modifications have been developed that involve the catalyst, solvents, bases, reaction conditions and synthetic technique, which permit the use of organoboron compounds that are thermally stable and inert to water and oxygen. The low toxicity, stability and ease of handling of boronic acids have made them among the most popular intermediates for cross coupling reaction with a variety of substrates. One area of research interest has been in the use of water², poly(ethylene glycol) (PEG)³ or ionic liquids⁴ as solvent for the Suzuki reaction. Usually, such reactions are carried out in conventional solvents such as benzene, toluene, acetone, dioxane, dimethoxyethane, dimethyl-formamide, tetrahydrofuran, or they tolerate water as a cosolvent, which can limit their attractiveness from the environmental point of view. Water, being cheap, readily available and nontoxic, results in a safer process and has clear advantages as an environmentally friendly solvent alternative in organic synthesis. The use of water facilitates the catalyst–product separation.

The use of microwave ovens in organic synthesis is well acknowledged, which is another alternative green technology in heating. The heating effect utilized in microwave-assisted organic transformations is due to the dielectric constant of the solvent. It is particularly convenient that, qualitatively, the larger the dielectric constant of the reaction medium, the greater the coupling with microwaves.⁵ With its high dielectric constant, water is also potentially a very useful solvent for microwave-assisted organic synthesis. Microwave heating has been used to promote Suzuki reaction in water with poly(ethylene glycol) as soluble support and phase transfer catalyst. The poly(ethylene glycol) ester of bromo, iodo, and triflated *para*-substituted benzoates is smoothly coupled with aryl boronic acids.⁶ The commercially available and nontoxic sodium tetraphenylborate has been used as a phenylation reagent for microwave-assisted aqueous-phase biaryl synthesis.⁷ Very recently, Leadbeater and Marco⁸ reported the efficiency of Suzuki coupling in neat water using a pressure microwave oven and monitoring temperature. The reaction was performed in a sealed tube. When using aryl iodides and bromides, the best

yields of biaryl are formed at 150 °C. For aryl chlorides, it is necessary to increase the temperature to 175 °C to obtain reasonable yields of biaryl product. However, at temperatures above 150–175 °C significant deactivation of the catalyst and the onset of decomposition of the organic substrates and products are observed.

Recently, we have reported a method which enables the Heck reaction⁹, synthesis of unsymmetrical diaryl ketones¹⁰ to be efficiently carried out in water and acetone separately using simple commercially available reagents. We are interested in a simple, straightforward, and reliable method for cross coupling reactions. We herein report a palladium-catalyzed heterogeneous Suzuki cross coupling reaction in water using microwave technology. Microwave irradiation is carried out with an improved reflux commercial microwave oven. A 50 mL round-bottomed flask was placed inside the microwave cavity and a double-surface reflux condenser and a nitrogen protecting tube attached to this. The reaction process is safe and smooth compared to a sealed tube. This results in a relatively large energy saving, as well as making it possible to carry out reactions in a relatively simple reflux system. The results for a variety of biaryl compounds are summarized in Table 1.

Results and discussion

Using the reaction [eqn. 1] of 2-bromonaphthalene with phenylboronic acid as an example, we investigated the effect of the power and time of microwave irradiation on the reaction.

Green Context

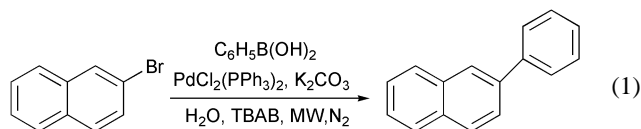
The Suzuki reaction is one of the most frequently studied of synthetic transformations, especially in terms of green chemistry. Here, the use of microwaves and an aqueous solvent has been used to good effect, giving high yields of products in very short times. What is interesting is the low extent of protodeborylation which takes place – a reaction which often takes place as a side reaction, and which can be quite severe in aqueous systems. *DJM*

Table 1 Synthesis of biaryls

Entry ^a	Ar-Br	Product ^b	Yield (%) ^c
1			90
2			91
3			92
4			93
5			88
6			91
7			93
8			92
9			92
10			94

^a Reagents and conditions: aryl bromide (1 mmol), phenylboronic acid (1.1 mmol), K₂CO₃ (5 mmol), PdCl₂(PPh₃)₂ (0.02 mmol), TBAB (0.3 mmol), and water (10 mL). Microwave irradiation at 750 W for 10 min under N₂. ^b All products gave satisfactory ¹HNMR and IR. ^c Yield of isolated product.

The highest yield can be obtained at 750 W power with 10 min reaction time. The results are summarized in Table 2.



The effect of base on the reaction [eqn. (1)] was also important, because the desired cross coupling products were not obtained in any noticeable amounts in the absence of base. A comparative reactivity study of base in the reaction showed the following sequence: K₂CO₃ > KF > KF/Al₂O₃ > KOH > Na₂CO₃. The quantity of K₂CO₃ is also found to be important. 5 mmol of K₂CO₃ works most efficiently in 10 mL water. These levels of base are higher than those normally utilized in organic solvent reactions. The results are shown in Table 3.

Despite the broad synthetic utility of Pd(PPh₃)₄ in cross coupling reactions, it is air and light sensitive and often forms a number of byproducts in these reactions. Thus, a wide range of Pd catalysts has been employed for the synthesis of biaryls including Pd(OAc)₂, Pd(OAc)₂ plus PPh₃, PdCl₂, PdCl₂(PPh₃)₂, Pd(acac)₂ and PdCl₂(dppf). Herein we chose PdCl₂(PPh₃)₂ as catalyst, which is stable to air and inexpensive. In addition, since the PdCl₂(PPh₃)₂ catalyst is reduced easily to Pd black, simple filtration affords isolation of the desired products and enables recycling of the Pd.

Taking the coupling of 2-bromonaphthalene and phenylboronic acid as a starting point, we performed the reaction using conventional heating (oil bath). We kept the quantities of catalyst, base, TBAB, and water exactly the same as in the microwave-promoted reaction and performed the reaction in a 50 mL three-necked flask with a reflux condenser, a thermometer and a nitrogen protecting tube. The mixture was refluxed at

Table 2 Coupling of 2-bromonaphthalene with phenylboronic acid under different power and time microwave irradiation conditions

Entry ^a	Power/W	Time/min	Yield (%) ^b
1	600	10	83
2	675	10	86
3	675	11	90
4	675	12	93
5	750	8	84
6	750	9	90
7	750	10	94
8	750	11	92
9	750	12	89

^a Reagents and conditions: aryl bromide (1 mmol), phenylboronic acid (1.1 mmol), K₂CO₃ (5 mmol), PdCl₂(PPh₃)₂ (0.02 mmol), TBAB (0.3 mmol), and water (10 mL). Microwave irradiation under N₂. ^b Yield of isolated product.

Table 3 Effect of the quantity of K₂CO₃ on the reaction [eqn. (1)]

Entry ^a	K ₂ CO ₃ /mmol	Yield (%) ^b
1	3.5	74
2	4.0	82
3	4.5	91
4	5.0	94
5	5.5	93
6	6.0	88

^a Reagents and conditions: aryl bromide (1 mmol), phenylboronic acid (1.1 mmol), K₂CO₃ (5 mmol), PdCl₂(PPh₃)₂ (0.02 mmol), TBAB (0.3 mmol), and water (10 mL). Microwave irradiation at 750 W for 10 min under N₂. ^b Yield of isolated product.

100 °C and the reaction held for 6 h under vigorous stirring. An isolated yield of 2-phenylnaphthalene of 92% was obtained. This compares to an isolated yield of 94% when using microwave heating. This also shows that the same temperature (100 °C) was reached under the microwave irradiation conditions. Compared to the conventional heating, clearly, the microwave irradiation shortened the reaction time from 6 h to 10 min.

Conclusion

A reliable, rapid and efficient method for synthesis of biaryls has been developed which involves the use of water as solvent under microwave irradiation. This methodology is superior from the point of view of yield, short reaction time and is more environmentally friendly than the reported methods.

Experimental

The melting points were determined on a WRS-1A digital melting point apparatus. IR spectra were measured for KBr discs using an Alpha Centauri FT-IR spectrophotometer. ¹HNMR spectra (80 MHz) were recorded in CDCl₃ using a FT-80 spectrometer. *J* values are given in Hz. Microwave irradiation was carried out with an improved reflux Galanz WP 750B commercial microwave oven (2450 MHz, 750 W). All solvents were used without further purification. PdCl₂(PPh₃)₂ was prepared according to reference 11. The remaining chemicals were obtained from commercial sources. All reactions were conducted under nitrogen atmosphere.

Typical procedure

General procedure for the synthesis of biaryls: the aryl bromide (1.0 mmol), phenylboronic acid (1.1 mmol), K₂CO₃ (5 mmol),

$\text{PdCl}_2(\text{PPh}_3)_2$ (0.02 mmol), tetrabutyl-amine bromide (0.3 mmol), H_2O (10 mL) were added in a bottle (50 mL), and irradiated at 750 W for 10 min in a microwave oven under nitrogen. After cooling to room temperature, the reaction mixture was extracted with ethyl acetate–acetone (5 : 1 v/v, 20 mL \times 2). The organic phase was dried over anhydrous MgSO_4 . The solvent was removed by evaporation under reduced pressure to afford the biaryls. The product was recrystallized from 95% ethanol or purified by column chromatography on silica gel using petroleum–ethyl acetate (30 : 1 v/v) as the eluent to give the analytically pure product.

Acknowledgement

This work was supported by the National Natural Science Foundation of China (NO. 20272047) and the Northwest Normal University Science and Technology Development Foundation of China.

References

- (a) J. Hassan, M. Sévignon, C. Gozzi, E. Schulz and M. Lemaire, *Chem. Rev.*, 2002, **102**, 1359; (b) A. F. Litke and G. C. Fu, *Angew. Chem., Int. Ed.*, 2002, **41**, 4176; (c) G. Cheng, Q. Tao, Q. Yang and Y. Wang, *Chin. Org. Chem.*, 2000, **20**, 874; (d) N. Miyaura and A. Suzuki, *Chem. Rev.*, 1995, **95**, 2457.
- (a) N. A. Bumagine and V. V. Bykov, *Tetrahedron*, 1997, **53**, 14437; (b) D. Badone, M. Baroni, R. Cardamone, A. Ielmini and U. Guzzi, *J. Org. Chem.*, 1997, **62**, 7170; (c) J. C. Bussolari and D. C. Rehborn, *Org. Lett.*, 1999, **1**, 965.
- V. V. Namboodiri and R. S. Varma, *Green Chem.*, 2001, **3**, 146.
- (a) C. J. Mathews, P. T. Smith and T. Welton, *Chem. Commun.*, 2000, 1249; (b) T. Welton, *Chem. Rev.*, 1999, **99**, 2071.
- (a) *Microwaves in Organic Synthesis*, ed. A. Loupy, Wiley-VCH, Weinheim, 2002; (b) P. Lidstrom, J. Tierney, B. Wathey and T. Westman, *Tetrahedron*, 2001, **57**, 9225; (c) N. Elander, J. R. Jones, S. Y. Lu and S. Stone-Elander, *Chem. Soc. Rev.*, 2000, **29**, 239; (d) R. S. Varma, *Green Chem.*, 1999, **1**, 43; (e) R. S. Varma and K. P. Naicker, *Green Chem.*, 1999, **1**, 247; (f) C. Gabriel, S. Gabriel, E. H. Grant, B. S. J. Halstead and D. M. P. Mingos, *Chem. Soc. Rev.*, 1998, **27**, 213; (g) S. Caddick, *Tetrahedron*, 1995, **51**, 10403; (h) C. R. Strauss and R. W. Trainor, *Aust. J. Chem.*, 1995, **48**, 1665.
- C. G. Blettner, W. A. König, W. Stenzel and T. Schotten, *J. Org. Chem.*, 1999, **64**, 3885.
- D. Villemin, M. J. Gomez-Escalonilla and J.-F. Saint-Clair, *Tetrahedron Lett.*, 2001, **42**, 635.
- (a) N. E. Leadbeater and M. Marco, *Org. Lett.*, 2002, **4**, 2973; (b) N. E. Leadbeater and M. Marco, *J. Org. Chem.*, 2003, **68**, 888.
- (a) J.-X. Wang, Z. Liu, Y. Hu, B. Wei and L. Bai, *J. Chem. Res. (S)*, 2000, 484; (b) J.-X. Wang, Z. Liu, Y. Hu, B. Wei and L. Bai, *Synth. Commun.*, 2002, **32**, 1607; . For a review see: (c) D. Macquarrie, *Green Chem.*, 2001, **3**, G8; (d) M. Larhed, C. Moberg and A. Hallberg, *Acc. Chem. Res.*, 2002, **35**, 717.
- (a) J.-X. Wang, Y. Yang, B. Wei, Y. Hu and Y. Fu, *Bull. Chem. Soc. Jpn.*, 2002, **75**, 1381; . For a review see: (b) D. Macquarrie, *Green Chem.*, 2001, **3**, G48.
- H. Itatani and J. C. Baibar, *J. Am. Oil Chem. Soc.*, 1967, **44**, 147.



A volumetric and viscosity study for the mixtures of 1-n-butyl-3-methylimidazolium tetrafluoroborate ionic liquid with acetonitrile, dichloromethane, 2-butanone and N, N – dimethylformamide

Jianji Wang,* Yong Tian, Yang Zhao and Kelei Zhuo

Department of Chemistry, Henan Normal University, Xinxiang, Henan 453002, P. R. China

Received 3rd April 2003

First published as an Advance Article on the web 4th August 2003

The densities and viscosities for mixtures of 1-n-butyl-3-methylimidazolium tetrafluoroborate ionic liquid with acetonitrile, dichloromethane, 2-butanone and N,N-dimethylformamide have been determined at 298.15 K. From these measurements, it was found that viscosities of the mixtures can generally be described by an exponential equation. Their densities are linear functions of the mass fraction of the ionic liquid in the mixtures. These physical properties can be predicted as a function of the concentration of ionic liquid provided that the properties for pure components are known. The excess molar volume V_m^E and the excess logarithm viscosities $(\ln \eta)^E$ were calculated and fitted to the Redlich–Kister polynomials. It is shown that the values of V_m^E are negative but those of $(\ln \eta)^E$ are positive. Surprisingly, the minimum in V_m^E and the maximum in $(\ln \eta)^E$ are observed at about the same mole fraction of the ionic liquid, $x \approx 0.3$. The results are discussed in terms of the ion–dipole interactions between the cations of the ionic liquid and the organic solutes.

Introduction

Room temperature ionic liquids (ILs) are a class of organic salts that are liquids at or near room temperature in their pure state. They exhibit many interesting properties such as negligible vapor pressure, low melting point, a large liquid range and favorable solvation behavior. Due to their non-volatile nature and favorable solvation properties, ILs have been suggested as green and benign replacements for traditional volatile organic solvents.

Air and moisture stable ILs have been the subject of an increasing number of scientific investigations.^{1,2} Most of these ILs are based on N,N'-dialkylmethylimidazolium, N-alkylpyridinium, tetraalkylammonium or tetraalkylphosphonium cations with typical anions, including $[\text{BF}_4]^-$, $[\text{PF}_6]^-$, $[\text{CF}_3\text{SO}_3]^-$ and $[(\text{CF}_3\text{SO}_3)_2\text{N}]^-$. These ionic liquids have been recently used as solvents in chemical reactions,^{1–3} multiphase bioprocess operation,⁴ liquid–liquid separations,^{5,6} batteries and fuel cells investigations.⁷ In spite of their importance and interest, detailed knowledge on the behavior of the mixtures of ionic liquids with organic molecular solutes, which is paramount for the design of any technological processes, is very limited.⁸ Seddon *et al.*⁹ studied the effect of chloride, water and organic solvents on the physical properties of various ionic liquids. Heintz and co-workers^{10–12} determined activity coefficients in infinite dilution of various organic solvents in 4-methyl-N-butylpyridinium tetrafluoroborate ($[\text{4MBP}][\text{BF}_4]$), and the excess molar volumes and viscosities for mixtures of methanol with $[\text{4MBP}][\text{BF}_4]$ at different temperatures. In addition, studies on the solid–liquid and liquid–liquid equilibria of 1-ethyl-3-methylimidazolium hexafluorophosphate $[\text{Emim}][\text{PF}_6]$ + water, the vapor–liquid and liquid–liquid equilibria of imidazolium-based ionic liquids + water, the high-pressure phase behavior of CO_2 with six ionic liquids, the liquid–liquid equilibria of 1-butyl-3-methylimidazolium hexafluorophosphate $[\text{Bmim}][\text{PF}_6]$ + water, $[\text{Bmim}][\text{PF}_6]$ + (water + ethanol), 1-ethyl-3-methylimidazolium triiodide $[\text{Emim}][\text{I}_3]$ + toluene + heptane, $[\text{Bmim}][\text{I}_3]$ + toluene + heptane have also been carried out.^{13–17}

In the present work, we report the volumetric and viscosity properties for mixtures of some small molecules including acetonitrile, dichloromethane, 2-butanone and N,N-dimethylformamide with 1-n-butyl-3-methylimidazolium tetrafluoroborate ($[\text{Bmim}][\text{BF}_4]$) ionic liquid (whose chemical structure is shown in Fig. 1) over the entire composition range at 298.15 K.

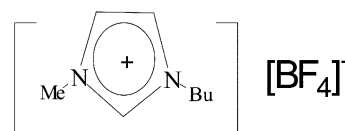


Fig. 1 Molecular structure of the ionic liquid $[\text{Bmim}][\text{BF}_4]$.

The excess molar volumes V_m^E and the excess logarithm viscosities $(\ln \eta)^E$ were determined. Results have been discussed in terms of the ion–dipole interactions between the cations of the ionic liquid and the organic solutes. Both a useful set of data for chemical engineering purposes and an insight into the interactions in the mixtures were provided.

Results and discussion

A comparison is made for the pure components in Table 1 between the experimental density and viscosity determined in

Green Context

The development of a detailed knowledge of a solvent's properties is of the utmost importance, both in terms of its physical parameters and how they change in the presence of solutes, and in terms of the fundamental chemistry of the solvent–solute interactions which take place and which can influence the chemistry of the systems. This paper provides details on some of these parameters for a series of solutes in $[\text{Bmim}][\text{BF}_4]$.

DJM

Table 1 Comparison of experimental density (ρ) and absolute viscosity (η) with literature values for [Bmim][BF₄] and the organic solutes investigated at 298.15 K

IL/solute	$\rho/\text{g cm}^{-3}$		$\eta/\text{mPa s}$	
	Expt.	Lit.	Expt.	Lit.
[Bmim][BF ₄]	1.21105	1.15 ^a	110.308	154 ^b 201 ^c
Acetonitrile	0.77667	0.7768 ^d	0.341	0.341 ^d
Dichloromethane	1.31825	1.3165 ^e	0.401	0.406 ^e
2-Butanone	0.79985	0.79971 ^f	0.373	0.374 ^g
N,N-Dimethylformamide	0.94545	0.94560 ^h	0.802	0.8012 ⁱ

^a Ref. (1), at 303.15 K. ^b Ref. (9), [Cl⁻]/mol kg⁻¹ = 0.01 at 293.15 K. ^c Ref. (9), [Cl⁻]/mol kg⁻¹ = 0.5 at 293.15 K. ^d Ref. (18). ^e Ref. (19). ^f Ref. (20). ^g Ref. (21). ^h Ref. (22). ⁱ Ref. (23).

this work and those reported in the literature. It can be seen that the values for organic solutes agree well with those reported in the literature. However, great discrepancy was observed for the density and viscosity of [Bmim][BF₄]. Besides the effect of temperature, trace amounts of impurities such as water, chloride and sodium ions in ILs can have a dramatic effect on density and viscosity values. From the studies of Seddon and co-workers,⁹ the density of 1.15 g cm⁻³ at 303.15 K suggests that the molar concentration of impurities (say Cl⁻) in [Bmim][BF₄] is greater than 1.5 mol kg⁻¹. In addition, extrapolation of the viscosity data of [Bmim][BF₄] at 298.15, 308.15, 318.15 and 328.15 K²⁴ gives a value of 136 mPa s at 293.15 K. This value is smaller than the value (201 mPa s) determined at the impurity [Cl⁻] = 0.5 mol kg⁻¹, but is in good agreement with the result (154 mPa s) reported at the impurity [Cl⁻] = 0.01 mol kg⁻¹. Therefore, it is believed that the density and viscosity data determined in this work are more acceptable.

Experimental values of density and absolute viscosity at 298.15 K are collected in Table 2 for [Bmim][BF₄], acetonitrile, dichloromethane, 2-butanone, N,N-dimethylformamide and their mixtures over the whole composition range. In general, ionic liquids are miscible with medium- to high-dielectric liquids and immiscible with low dielectric liquids.²⁵ In the present work, [Bmim][BF₄] is completely miscible with acetonitrile ($\epsilon = 36.01$), N,N-dimethylformamide ($\epsilon = 36.7$), 2-butanone ($\epsilon = 18.51$) and dichloromethane ($\epsilon = 8.93$) at 298.15 K. The effect of the organic solutes on the densities and viscosities of the ionic liquid has been examined. It is found that the densities of the mixtures decrease or increase linearly with increasing mass fraction of the ionic liquid, as shown in Fig. 2. These linear relations can be represented by

$$\rho = \rho_{\text{I}} + (\rho_{\text{I}} - \rho_{\text{s}})w \quad (1)$$

with correlation coefficients greater than 0.99, where ρ , ρ_{I} and ρ_{s} are, respectively, densities of the mixtures, the ionic liquid and the organic solutes, w is the mass fraction of [Bmim][BF₄] in the mixtures. Therefore, the slopes for these straight lines are positive or negative depending on the relative density value of the ionic liquid and the organic solute. This equation is very useful in predicting densities of the mixtures in practice as the densities for pure components are known at given temperatures.

As far as the viscosity of the mixtures is plotted against mole fraction of the organic solutes, it is found that all the organic solutes studied in this work appear to have a surprisingly similar effect on the viscosity of the ionic liquids (see Fig. 3). In fact, a single exponential equation

$$\eta = \eta_{\text{I}} \exp(-x_{\text{s}}/a) \quad (2)$$

can be fitted to these data with a correlation coefficient of 0.98. In this equation, η_{I} is the viscosity of the pure ionic liquid, x_{s} is the mole fraction of the organic solutes and a is a constant with a value of 0.216 ± 0.004 . This confirmed the findings of Seddon and co-workers.⁹ Therefore, the viscosity of a reaction mixture

Table 2 Experimental density, absolute viscosity, excess molar volume and excess logarithm viscosities for the mixtures of x [Bmim][BF₄] + (1 - x) organic solutes at 298.15 K

x	w	$\rho/\text{g cm}^{-3}$	$\eta/\text{mPa s}$	$V_{\text{m}}^{\text{E}}/\text{cm}^3 \text{mol}^{-1}$	$(\ln \eta)^{\text{E}}/\text{mPa s}$
[Bmim][BF ₄] + acetonitrile					
0.00	0.00	0.77667	0.341	0.00	0.00
0.0487	0.2199	0.85159	0.593	-0.587	0.272
0.1012	0.3827	0.91243	0.887	-0.887	0.371
0.2012	0.5810	0.99481	1.792	-1.096	0.496
0.3027	0.7050	1.05220	3.344	-1.122	0.533
0.3559	0.7526	1.07437	4.576	-0.983	0.540
0.3995	0.7855	1.09012	6.069	-0.856	0.570
0.4531	0.8202	1.10735	8.248	-0.713	0.567
0.4941	0.8432	1.11932	10.215	-0.629	0.544
0.5446	0.8681	1.13248	13.191	-0.511	0.508
0.6001	0.8920	1.14534	17.585	-0.380	0.475
0.6953	0.9263	1.16432	27.711	-0.154	0.379
0.7735	0.9495	1.17890	40.270	-0.107	0.301
0.9018	0.9806	1.19833	70.913	-0.041	0.126
1.00	1.00	1.21105	110.308	0.00	0.00
[Bmim][BF ₄] + dichloromethane					
0.00	0.00	1.31825	0.401	0.00	0.00
0.0523	0.1282	1.30911	0.715	-0.305	0.285
0.0985	0.2255	1.30386	1.118	-0.668	0.472
0.1981	0.3970	1.28828	2.592	-1.106	0.753
0.3042	0.5381	1.27241	4.600	-1.125	0.731
0.3529	0.5924	1.26520	5.918	-1.073	0.710
0.4042	0.6439	1.25823	7.695	-1.000	0.684
0.4548	0.6897	1.25101	10.052	-0.826	0.667
0.5493	0.7646	1.24052	14.263	-0.619	0.486
0.6015	0.8009	1.23546	17.010	-0.500	0.369
0.7146	0.8697	1.22657	26.322	-0.316	0.170
0.8010	0.9147	1.22134	37.223	-0.244	0.031
0.9007	0.9602	1.21570	67.855	-0.105	0.000
1.00	1.00	1.21105	110.308	0.00	0.00
[Bmim][BF ₄] + 2-butanone					
0.00	0.00	0.79985	0.373	0.00	0.00
0.0498	0.1411	0.84651	0.564	-0.719	0.130
0.1026	0.2638	0.88860	0.847	-1.133	0.236
0.1863	0.4178	0.94511	1.548	-1.492	0.363
0.3005	0.5738	1.00711	3.170	-1.622	0.430
0.3455	0.6233	1.02785	4.104	-1.596	0.432
0.3938	0.6706	1.04810	5.379	-1.518	0.428
0.4479	0.7177	1.06877	7.133	-1.397	0.402
0.5000	0.7581	1.08681	9.315	-1.235	0.373
0.5505	0.7933	1.10277	11.975	-1.045	0.337
0.6031	0.8265	1.11822	15.223	-0.844	0.278
0.6893	0.8743	1.14005	22.692	-0.348	0.186
0.7996	0.9260	1.16850	42.246	-0.266	0.180
0.8995	0.9656	1.19101	67.855	-0.152	0.086
1.00	1.00	1.21105	110.308	0.00	0.00
[Bmim][BF ₄] + N,N-dimethylformamide					
0.00	0.00	0.94545	0.802	0.00	0.00
0.0530	0.1476	0.98239	1.191	-0.451	0.134
0.0995	0.2546	1.00921	1.603	-0.683	0.203
0.1992	0.4347	1.05498	2.910	-0.928	0.308
0.2990	0.5687	1.08998	5.041	-0.988	0.366
0.3350	0.6090	1.10068	6.371	-0.982	0.423
0.3986	0.6721	1.11758	7.783	-0.940	0.310
0.4541	0.7200	1.13069	11.032	-0.892	0.385
0.4948	0.7518	1.13956	12.738	-0.860	0.328
0.5592	0.7968	1.15194	17.633	-0.754	0.337
0.5939	0.8189	1.15810	20.808	-0.698	0.332
0.6976	0.8770	1.17464	32.908	-0.562	0.279
0.7959	0.9234	1.18767	52.208	-0.245	0.257
0.8976	0.9644	1.20002	78.408	-0.141	0.163
1.00	1.00	1.21105	110.307	0.00	0.00

can be predicted as a function of the concentration of the dissolved reactants and/or products, independent of their polarity.

An excess property of a solution is defined as the difference between the actual mixture property and that which would be obtained for an ideal solution at the same temperature, pressure, and composition. So the excess molar properties represent the deviation from ideal behavior of the mixtures, and provide an

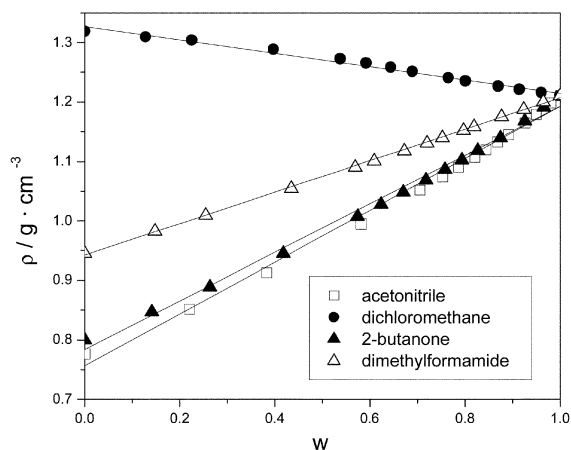


Fig. 2 Densities for the mixtures of organic solutes + [Bmim][BF₄] vs. mass fraction of [Bmim][BF₄]; the solid line represents the theoretical fit of these data to eqn. (1).

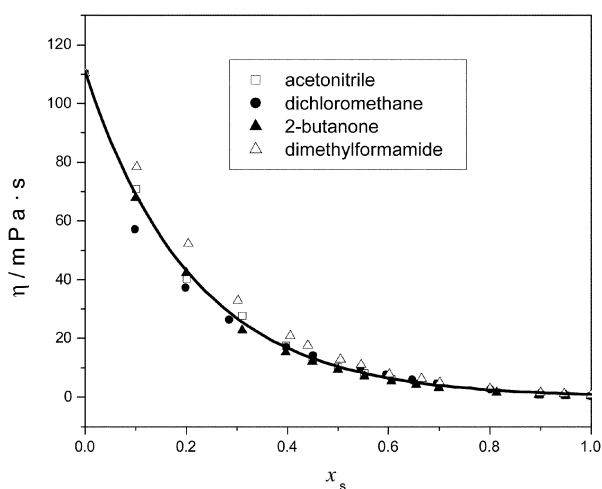


Fig. 3 Viscosities for the binaries vs. mole fraction of organic solutes; the solid line represents the theoretical fit of these data to eqn. (2).

indication of the interactions between the ionic liquid and the molecular solutes. The excess molar volumes V_m^E and the excess logarithm viscosities $(\ln \eta)^E$ have been calculated using the following equations:¹²

$$V_m^E = [xM_I + (1-x)M_S]/\rho - [xM_I/\rho_I + (1-x)M_S/\rho_S] \quad (3)$$

$$(\ln \eta)^E = \ln \eta_{\text{mix}} - [x \ln \eta_I + (1-x) \ln \eta_S] \quad (4)$$

where ρ_I , ρ_S and ρ in eqn. (3) and η_I , η_S and η in eqn. (4) are the densities and viscosities of [Bmim][BF₄], organic solutes and their mixtures at 298.15 K, respectively. M_I and M_S are the molar mass of [Bmim][BF₄] and the solutes, and x is the mole fraction of [Bmim][BF₄] in the mixtures. Values of V_m^E and $(\ln \eta)^E$ for the binary mixtures at 298.15 K are also listed in Table 2. These properties were mathematically represented by the Redlich–Kister polynomials:

$$Y^E = x(x-1) \sum_{j \geq 1} B_j (1-2x)^j \quad (5)$$

where Y^E refers to V_m^E or $(\ln \eta)^E$, B_j are adjustable parameters and can be obtained by least-squares analysis. Values of the fitted parameters are presented in Table 3 along with the standard deviations of the fit.

Fig. 4 shows the variation V_m^E of as a function of mole fraction of the ionic liquid. It can be seen that the values of V_m^E are negative in all the ranges of composition, indicating negative deviations from ideal behavior. It is more interesting that all the V_m^E in every [Bmim][BF₄] + organic solute systems have

Table 3 Derived parameters and the standard deviations of the fit for the excess molar volumes and the excess logarithm viscosities at 298.15 K

Y^E	B_0	B_1	B_2	B_3	S_R^a
[Bmim][BF ₄] + acetonitrile					
$V_m^E/\text{cm}^3 \text{ mol}^{-1}$	-2.4061	5.1555	-4.0647	1.2718	0.034
$(\ln \eta)^E/\text{mPa s}$	2.1157	-0.6326	0.8908	-1.8725	0.023
[Bmim][BF ₄] + dichloromethane					
$V_m^E/\text{cm}^3 \text{ mol}^{-1}$	-3.0220	5.2707	-2.5160	-2.5906	0.043
$(\ln \eta)^E/\text{mPa s}$	2.2471	-3.1561	0.1883	-1.0801	0.025
[Bmim][BF ₄] + 2-butanone					
$V_m^E/\text{cm}^3 \text{ mol}^{-1}$	-4.7119	7.1294	-2.8046	-0.3450	0.074
$(\ln \eta)^E/\text{mPa s}$	1.4539	-1.4836	0.5604	0.8541	0.014
[Bmim][BF ₄] + N,N-dimethylformamide					
$V_m^E/\text{cm}^3 \text{ mol}^{-1}$	-3.3549	2.3982	-1.4920	2.6469	0.028
$(\ln \eta)^E/\text{mPa s}$	1.3880	-0.5191	1.0769	0.3390	0.027

^a Standard deviation of the fit.

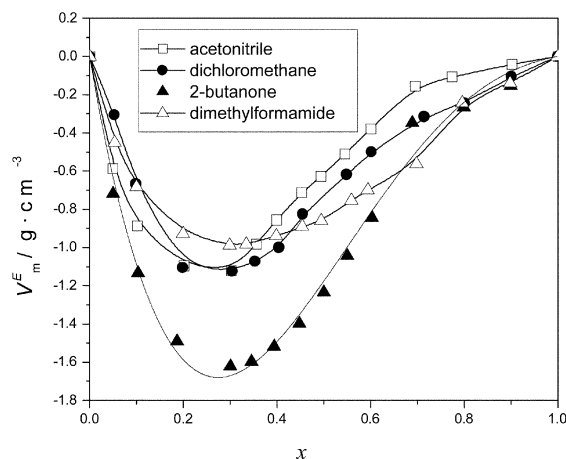


Fig. 4 Excess molar volumes V_m^E for the mixtures of x [Bmim][BF₄] + $(1-x)$ organic solutes at 298.15 K.

minimum values at about $x \approx 0.3$. In interpreting V_m^E in terms of molecular interactions, positive values are explained by the breaking of chemical or non-chemical interactions among molecules in the pure components during the mixing process, whereas a more efficient packing and attractive interaction in the mixtures than in the pure liquids is considered to be the major contribution to the negative V_m^E .

NMR studies²⁶ of the 1-ethyl-3-methylimidazolium tetrafluoroborate [EMIM][BF₄] ionic liquid revealed that ‘discrete ion-pairs’ were formed between [EMIM]⁺ and [BF₄]⁻ ions by formation of a hydrogen bond between the hydrogen on the C₂ carbon (C₂H) of the imidazolium ring and fluorine of the anion [BF₄]⁻. From molecular dynamic simulations of some small molecules dissolved in dimethylimidazolium chloride,²⁷ it is found that the hydrogen bonding solutes are strongly solvated, principally by forming hydrogen bonds with the chloride anion (Cl⁻), while the non-hydrogen bonding solutes interact more strongly with the cation. According to these investigations, when acetonitrile, dichloromethane, 2-butanone or N,N-dimethylformamide is mixed with [Bmim][BF₄], ion–dipole interactions will occur between the solute molecules and the imidazolium ring of the ionic liquid. This will reduce the hydrogen bonding between cation and anion in the ionic liquid, leading to the negative V_m^E , the higher mobility of the ions and the decreased viscosity of the mixtures.

The excess logarithm viscosities $(\ln \eta)^E$ for the mixtures in Fig. 5 show a clear trend: all values are positive in the studied ranges of composition for every binary mixture. It is noticeable that the maximum values are also observed at about $x \approx 0.3$, this is just the mole fraction where the excess molar volumes have the minimum values for the systems investigated. From these

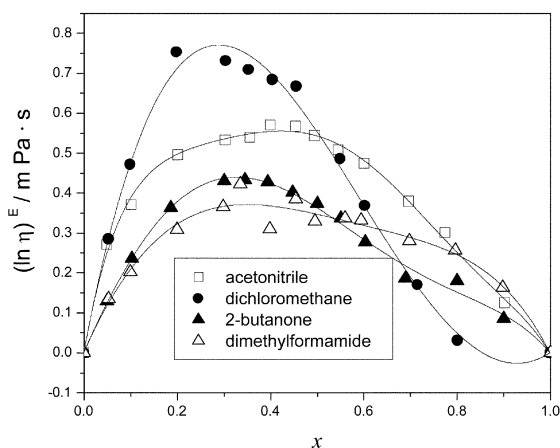


Fig. 5 The excess logarithm viscosities for the mixtures of $x[\text{Bmim}][\text{BF}_4] + (1 - x)$ organic solutes at 298.15 K.

observations, it seems possible to suggest that an unusual structure occurs in the vicinity of this particular composition of the mixtures.

Conclusions

From the above discussions, it can be concluded tentatively that viscosities and densities for the binary mixtures of $[\text{Bmim}][\text{BF}_4] +$ organic solutes were dependent mainly on the composition of the added molecular solutes and only to a lesser extent upon their identity. Therefore, viscosities and densities for these mixtures can be predicted as a function of concentration of the dissolved reactants and/or products from the corresponding properties of pure liquids, independent of their polarity. Ion–dipole interactions between the solute molecules and the imidazolium ring of the ionic liquid are suggested to be mainly responsible for the negative V_m^E and the decreased viscosity of the mixtures.

Experimental

Chemicals and reagents

$[\text{Bmim}][\text{BF}_4]$ was prepared and purified by using the procedures described by Seddon and Holbrey.²⁸ Because trace amounts of water in ILs can have a dramatic effect on physical properties and phase behavior, the ILs were dried under vacuum at 343 K for 2–3 days before use. Karl–Fisher analysis of the samples subjected to this treatment indicated that the water content was reduced to 0.16 mass%. Another impurity that can affect the physical properties is the residual sodium and chloride ions. A chloride content of $0.018 \text{ mol kg}^{-1}$ was determined in the ionic liquid by a chloride-selective electrode. A sodium content of $0.034 \text{ mol kg}^{-1}$ was detected with a Z-5000 polarized Zeeman atomic absorption spectrophotometer.

Acetonitrile (Beijing Chem. Co., A. R.) was distilled after being stored over activated 3A molecular sieves for several days. Dichloromethane (Tianjin Fudi Chemical Factory, A. R.) was stored over CaCl_2 and then twice distilled. 2-Butanone (Shanghai Chemical Factory, A. R.) was distilled twice after being dried over NaSO_4 for several days. N,N-Dimethylformamide (Tianjin Chemical Factory, A.R.) was mixed with 10% (by volume) benzene (Beijing Chemical Factory, A.R.), and the azeotrope was distilled off under atmospheric pressure at about 353 K. The product was dried over silica gel and distilled at reduced pressure. The middle fraction of the distillate was collected. All the purified solvents were stored over P_2O_5 in a

desiccator before use. Water content for the four solvents analyzed by Karl–Fisher titration was less than 100 ppm.

Methods

Mixtures were prepared by mass on the molality concentration scale. Every precaution was taken to minimize contamination by water. Solution densities were determined to $\pm 1.5 \times 10^{-5} \text{ g cm}^{-3}$ with an Anton Paar DMA 60/602 vibrating-tube digital densimeter. The temperature around the density meter cell was controlled to $298.15 \pm 0.01 \text{ K}$ using a CT-1450 temperature controller and a CK-100 ultracryostat. The densimeter was calibrated with known densities of pure water and dry air every day. The other details have been described previously.²⁹

Solution viscosities were measured with a suspended level Ubbelohde viscometer, which was placed in a water thermostat (Schott, Germany) and has a flow time of about 200 s for water at 298.15 K. The temperature of the water thermostat was controlled to be as precise as the density measurements. The viscometer was calibrated using the efflux time of water at 298.15 and 308.15 K. Flow time measurements are performed by a Schott AVS 310 photoelectric time unit with a resolution of 0.01 s. The estimated error of experimental viscosity is $\pm 0.3\%$ mPa s. Solution viscosity, η , is given by the following equation:

$$\rho/\eta = ct - k/t \quad (6)$$

where c and k are the viscometer constants. Since the viscosity values are greatly different for the ionic liquid and the organic solutes, two Ubbelohde viscometers were used in the experiments according to the varied viscosity values for the mixtures. The viscometer constants are $c_1 = 0.03104 \times 10^{-3} \text{ cm}^2 \text{ s}^{-2}$, $k_1 = 2.5637 \text{ cm}^2$; $c_2 = 0.3129 \times 10^{-3} \text{ cm}^2 \text{ s}^{-2}$, $k_2 = 0.1529 \text{ cm}^2$ individually. The estimated error of experimental viscosity is $\pm 0.3\%$. The details of the experimental procedure are given elsewhere.³⁰

Acknowledgments

We wish to acknowledge the financial support from the National Natural Science Foundation of China (Grant No. 20273019).

References

- 1 J. Dupont, R. F. de Souza and P. A. Z. Suarez, *Chem. Rev.*, 2002, **102**, 3667.
- 2 P. Wasserscheid and W. Keim, *Angew. Chem., Int. Ed.*, 2000, **39**, 3772.
- 3 M. J. Earle and K. R. Seddon, *Pure Appl. Chem.*, 2000, **72**, 1391.
- 4 S. G. Cull, J. D. Holbrey, V. Vargas-Mora, K. R. Seddon and G. J. Lye, *Biotechnol. Bioeng.*, 2000, **69**, 227.
- 5 J. G. Huddleston, H. D. Willauer, R. P. Swatloski, A. E. Visser and R. D. Rogers, *Chem. Commun.*, 1998, 1765.
- 6 A. G. Fadeev and M. M. Meagher, *Chem. Commun.*, 2001, 295.
- 7 J. F. Brennecke and E. J. Maginn, *AIChE J.*, 2001, **47**, 2384.
- 8 A. E. Visser, R. P. Swatloski and R. D. Rogers, *Green Chem.*, 2000, **2**, 1.
- 9 K. R. Seddon, A. Stark and M. J. Torres, *Pure Appl. Chem.*, 2000, **72**, 2275.
- 10 A. Heintz, D. V. Kulikov and S. P. Verevkin, *J. Chem. Eng. Data*, 2001, **46**, 1526.
- 11 A. Heintz, D. V. Kulikov and S. P. Verevkin, *J. Chem. Eng. Data*, 2002, **47**, 894.
- 12 A. Heintz, D. Klasen and J. K. Lehmann, *J. Solution Chem.*, 2002, **31**, 467.

- 13 D. S. H. Wong, J. P. Chen, J. M. Chang and C. H. Chou, *Fluid Phase Equilib.*, 2002, **194–197**, 1089.
- 14 J. L. Anthony, E. J. Maginn and J. F. Brennecke, *J. Phys. Chem.*, 2001, **105**, 10942.
- 15 L. A. Blanchard, Z. Gu and J. F. Brennecke, *J. Phys. Chem.*, 2001, **105**, 2437.
- 16 V. Najdanovic-Visak, J. M. S. S. Esperanca, L. P. N. Rebelo, M. N. da Ponte, H. J. R. Guedes, K. R. Seddon and J. Szydlowski, *Phys. Chem. Chem. Phys.*, 2002, **4**, 1701.
- 17 M. S. Selvan, M. D. Mckinley, R. H. Dubois and J. L. Atwood, *J. Chem. Eng. Data*, 2000, **45**, 841.
- 18 M. Salomon, *J. Power Sources*, 1989, **26**, 9.
- 19 A. Pal and G. Dass, *Can. J. Chem.*, 2000, **78**, 327.
- 20 F. Commelli and R. Francesconi, *J. Chem. Eng. Data*, 1994, **39**, 108.
- 21 P. J. Petrino, Y. H. J. Gaston-Bonhomme and J. L. E. Chevalier, *J. Chem. Eng. Data*, 1995, **40**, 136.
- 22 A. Marchetti, C. Preti, M. Tagliazucchi, L. Tassi and G. Tosi, *J. Chem. Eng. Data*, 1991, **36**, 360.
- 23 G. Chittleborough, C. James and B. Steel, *J. Solution Chem.*, 1988, **17**, 1043.
- 24 Y. Tian, *MSc Thesis*, Henan Normal University, P. R. China, 2003.
- 25 P. Bonhote, A. P. Dias, N. Papageorgiou, K. Kalyanasundaram and M. Gratzel, *Inorg. Chem.*, 1996, **35**, 1168.
- 26 J. F. Huang, P. Y. Chen, I. W. Sun and S. P. Wang, *Inorg. Chim. Acta*, 2001, **320**, 7.
- 27 C. G. Hanke, N. A. Atamas and R. M. Lynden-Bell, *Green Chem.*, 2002, **4**, 107.
- 28 J. D. Holbrey and K. R. Seddon, *J. Chem. Soc., Dalton Trans.*, 1999, 2133.
- 29 J. Wang, Y. Zhao, K. Zhuo and R. Lin, *Can. J. Chem.*, 2002, **80**, 753.
- 30 J. Wang, Y. Zhao, K. Zhuo and R. Lin, *Z. Phys. Chem.*, 2003, **217**, 637.



Solvent-free reactions as green chemistry procedures for the synthesis of cosmetic fatty esters

C. Villa,^a E. Mariani,^{*a} A. Loupy,^b C. Grippo,^a G. C. Grossi^a and A. Bargagna^a

^a Dipartimento di Scienze Farmaceutiche dell'Università, Viale Benedetto XV, 3 - 16132 Genova, Italy. E-mail: e.mariani@unige.it; Fax: 0103538358

^b Laboratoire des Réactions Sélectives sur Supports, ICMMO, Université Paris-Sud CNRS, UMR 8615, bâtiment 410, 91405 Orsay Cédex, France

Received 18th June 2003

First published as an Advance Article on the web 5th August 2003

Solid–liquid solvent-free phase transfer catalysis (PTC) and acidic catalysis in dry media were applied, as green chemistry procedures, to the synthesis under mild conditions of long chain aliphatic esters of interest in the cosmetic field. The reactions were performed under conventional heating and microwave activation, analysing the profiles of the temperature increases during the reactions and studying the yields at different reaction times. The selected esters were obtained with very good yields within short reaction times.

Using Aliquat 336 as phase transfer agent, the results showed lower yields under classical heating for very short reaction times (5 min), but usually comparable to the yields obtained under microwave heating extending the reaction time up to 15 min.

The simple heterogeneous mixture of reagents with catalytic amount of neat *p*-toluenesulfonic acid (PTSA) under classical heating leads to good results, similar to those obtained under microwave activation with regards to yields and reaction times (10 min for microwave activation/15 min for oil bath).

Introduction

Long chain aliphatic esters are important cosmetic ingredients applied as emollients, solubilizers, conditioning agents, spreading agents *etc.* They often have been used to replace naturally occurring oils and waxes for ecological and above all economical reasons being based on rather low cost raw materials. Esters are classically prepared either by esterification of carboxylic acids with alcohols using acidic catalysis, transesterification of methyl or ethyl esters, or alkylation of carboxylate anions. Several reports refer to the use of *p*-toluenesulfonic acid (PTSA), sulfonated resins, zeolites, zirconium oxide or supported acids and polymers, as useful catalysts in non-conventional techniques for esterification reactions^{1–4} Taking into account that the most common procedures require large amounts of organic solvents, the presence of strong acidic reagents, long reaction times and complex work-up, the aim of this work was to study more ecological and economic conditions, as green chemistry procedures, for the synthesis of these widespread ingredients with special interest focused on solvent-free methodologies.^{5–8} It is well known that, in organic synthesis, avoiding the solvent leads to enhanced yields, milder conditions, increased safety and cost reduction.⁹

In previous works, we reported the synthesis in dry media of some compounds interesting as potential cosmetic ingredients.^{10–11} In pursuing our research, in this study a number of long chain aliphatic esters derived from three monocarboxylic acids (pivalic, myristic and palmitic acid) and a dicarboxylic one (sebacic acid) have been synthesised. The reactions were performed under both classical heating and microwave activation, using solvent-free solid–liquid PTC and heterogeneous mixtures of reagents in the presence of neat PTSA without any support (Table 1). The profiles of the temperature increases during the processes and the yields at different reaction times have been studied.

Results and discussion

The fatty esters **1–10** (Table 1) were synthesized under dry conditions with two kinds of reactions:

Esterification of carboxylic acids with alcohols by acidic catalysis (Scheme 1)

PTC alkylation of carboxylate anions (generated *in situ*) with alkyl bromides (Scheme 2)

In order to evaluate the most efficient catalytic conditions, a number of experiments were performed under microwave activation and classical heating using:

solid–liquid PTC with Aliquat 336 (methyltri-*n*-octylammonium chloride) or TBAB (tetra-*n*-butylammonium bromide) as transfer agents and different bases;

heterogeneous mixtures of reagents and neat PTSA as the acidic catalyst, without any support;

montmorillonite KSF as acidic mineral solid support.

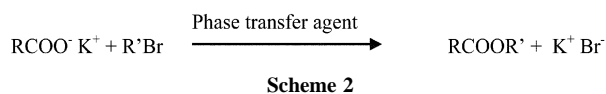
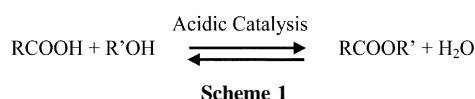
Green Context

Green chemistry as applied to chemical processes can be considered as a series of reductions (energy, auxiliaries, waste, etc.) and should always lead to the simplification of the process in terms of the number of chemicals and steps involved. Removing the solvent from a chemical process is likely to often be the greatest reduction and simplification (in the work-up as well as the reaction) that can be achieved. Here solvent-free procedures are described for the synthesis of compounds of commercial value. The use of different catalysts and both classical and microwave heating are compared.

JHC

Table 1 Long chain aliphatic esters, compounds 1–10

Compound	R	R'	Name	Formula	
RCOOR'	1	(CH ₃) ₃ C	CH ₃ CH(C ₂ H ₅)(CH ₂) ₄	2-Ethylhexyl pivalate	C ₁₃ H ₂₆ O ₂
	2	CH ₃ (CH ₂) ₁₂	(CH ₃) ₂ CH	Isopropyl myristate	C ₁₇ H ₃₄ O ₂
	3	CH ₃ (CH ₂) ₁₄	(CH ₃) ₂ CH	Isopropyl palmitate	C ₁₉ H ₃₈ O ₂
	4	CH ₃ (CH ₂) ₁₄	(CH ₃) ₂ CH–CH ₂	Isobutyl palmitate	C ₂₀ H ₄₀ O ₂
	5	CH ₃ (CH ₂) ₁₄	CH ₃ –(CH ₂) ₃	Butyl palmitate	C ₂₀ H ₄₀ O ₂
	6	CH ₃ (CH ₂) ₁₄	CH ₃ CH(C ₂ H ₅)(CH ₂) ₄	2-Ethylhexyl palmitate	C ₂₄ H ₄₈ O ₂
	7	CH ₃ (CH ₂) ₁₄	CH ₃ –(CH ₂) ₇	Octyl palmitate	C ₂₄ H ₄₈ O ₂
R'OOC(CH ₂) ₈ COOR'	8		(CH ₃) ₂ CH	Diisopropyl sebacate	C ₁₆ H ₃₀ O ₄
	9		CH ₃ –(CH ₂) ₃	Dibutyl sebacate	C ₁₈ H ₃₄ O ₄
	10		CH ₃ CH(C ₂ H ₅)(CH ₂) ₄	Bis(2-ethylhexyl) sebacate	C ₂₆ H ₅₀ O ₄



The most favourable conditions (Tables 2 and 3) involved the use of:

Aliquat 336 as transfer agent and K₂CO₃ as the base, at 140 °C as final temperature;
neat PTSA at 160 °C as final temperature.

Table 2 Synthesis of compounds 1, 2, 5 and 9 at different reaction times using PTSA or PTC (Aliquat 336)

Compound	Method ^a	Activation mode ^a	Yield% ^b			
			5 min	10 min	15 min	
1	2-Ethylhexyl pivalate	PTSA	Δ	85	86	90
			MW	87	91	
		PTC	Δ	11	90	91
			MW	93	93	
2	Isopropyl myristate	PTSA	Δ	53	65	72
			MW	84	87	
		PTC	Δ	23	60	91
			MW	90	91	
5	Butyl palmitate	PTSA	Δ	90	91	94
			MW	93	93	
		PTC	Δ	28	88	96
			MW	97	97	
9	Dibutyl sebacate	PTSA	Δ	60	80	87
			MW	86	91	
		PTC	Δ	22	83	85
			MW	91	91	

^a Δ = Thermostated oil bath; MW = Microwave activation; PTSA: 160 °C as final temperature; PTC: 140 °C as final temperature. ^b Yield refers to pure isolated product.

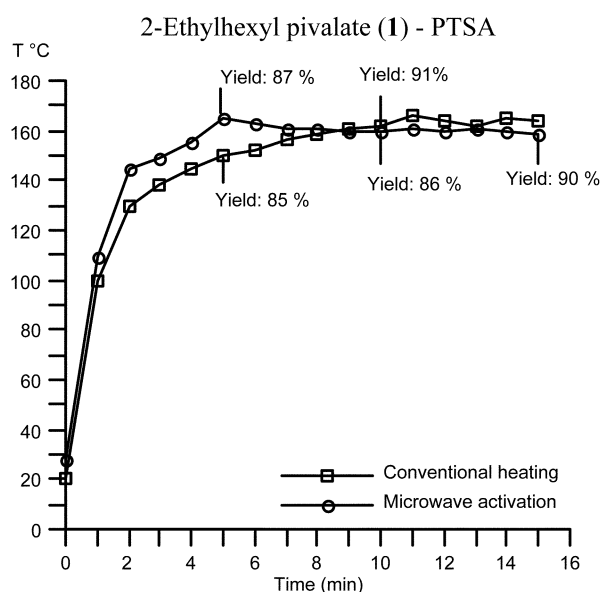
The experiments carried out with the above methodologies under both conventional heating and microwave activation were performed recording the thermal evolution of the reaction medium as a function of time and evaluating yields obtained at different reaction times.

The profiles in temperature rises were studied and showed that, under conventional heating, a slower rise in temperature occurred. With PTC in oil bath, the final temperature (140 °C) was reached in 8–10 min against 1–2 min under MW. Using PTSA in oil bath, the final temperature (160 °C) was reached in 5–7 min against 2–4 min under MW. To evaluate the differences of rise in temperature, as examples, the thermal profiles for compounds 1 and 9 (with PTSA as the catalyst) are reported in Fig. 1–2 and for compounds 2 and 5 the profiles obtained with Aliquat and K₂CO₃ are reported in Fig. 3–4.

Table 3 Best results obtained for the synthesis of compounds 1–10

Compound	Activation mode ^a	Yield% ^b	
		PTSA ^c	Aliquat 336 ^d
1	Δ	90	91
	MW	91	93
2	Δ	72	91
	MW	87	90
3	Δ	76	88
	MW	88	93
4	Δ	81	88
	MW	94	94
5	Δ	94	96
	MW	93	97
6	Δ	95	91
	MW	94	94
7	Δ	92	90
	MW	92	92
8	Δ	65	61
	MW	73	63
9	Δ	87	85
	MW	91	91
10	Δ	91	86
	MW	94	94

^a Δ = Thermostated oil bath, reaction time = 15 min; MW = Microwave activation; reaction time = 5 min for Aliquat 336, 10 min for PTSA. ^b Yields refer to pure isolated products. ^c Final temperature = 160 °C. ^d Final temperature = 140 °C.

**Fig. 1** Temperature rise profiles under microwave activation and conventional heating during PTSA reaction for the synthesis of compound 1

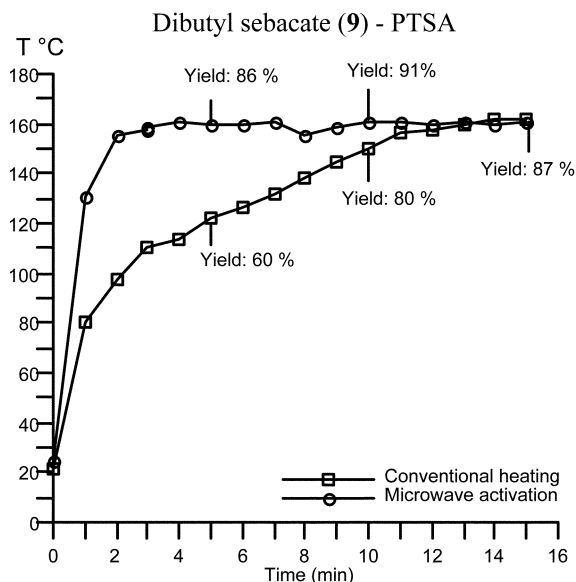


Fig. 2 Temperature rise profiles under microwave activation and conventional heating during PTSA reaction for the synthesis of compound **9**.

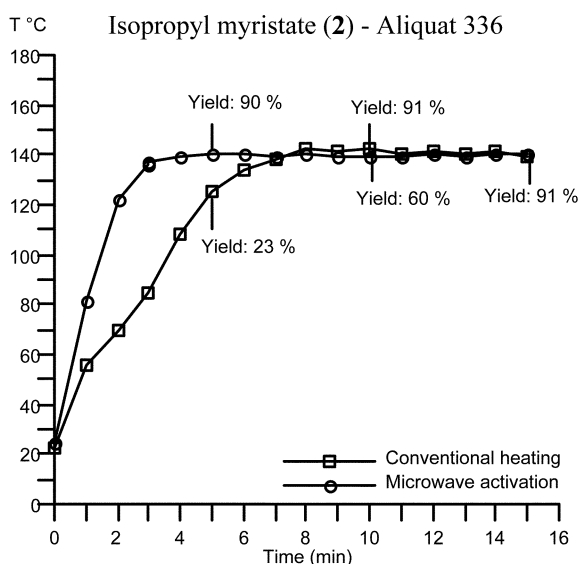


Fig. 3 Temperature rise profiles under microwave activation and conventional heating during PTC reaction for the synthesis of compound **2**.

The yields obtained with PTSA under conventional and microwave heating were quite similar. In Table 2, as examples, the yields obtained for the synthesis of compounds **1**, **2**, **5** and **9** at different reaction times (5, 10 and 15 min in oil bath, 5, 10 min under microwaves) are reported.

The comparison of the results obtained applying the PTC technique shows that for short reaction times (5 min) under conventional heating yields were dramatically lower than those obtained under microwave activation. Yields became comparable extending the reaction time up to 15 min.

Whereas no specific non-purely thermal MW effects appear in the case of PTSA promoted esterifications, a very important one is additionally revealed under the PTC procedure for very short reaction times (Table 2, 5 min: Δ 11–28%, MW 86–93%). This effect disappears by extending reaction times up to 15 min.

An interpretation of this phenomenon is as follows.¹² In the mechanism of alkylation, there is a charge delocalization in the anion in the transition state (TS) due to charge repartition between the nucleophile and the electrophile (Scheme 3). The ion pair with M^+ in TS could be therefore looser than in the

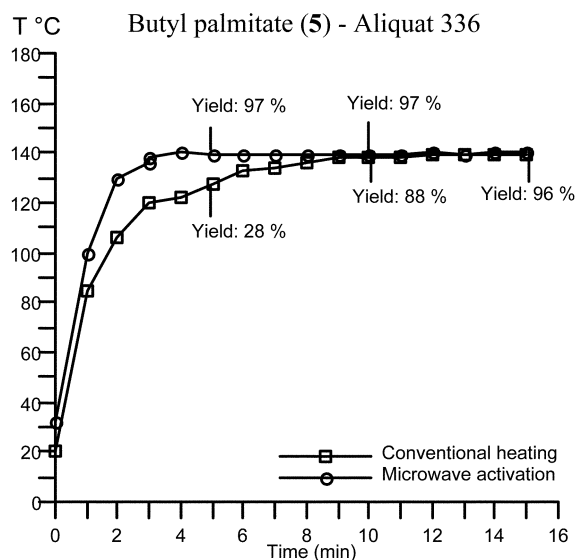
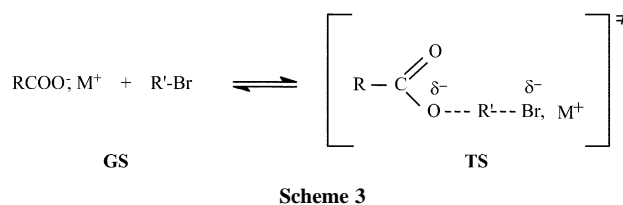


Fig. 4 Temperature rise profiles under microwave activation and conventional heating during PTC reaction for the synthesis of compound **5**.



ground state (GS) (tighter ion pairs) and consequently more polar.

As polarity is increased during the progress of the reaction from GS to TS, it results an enhancement in electrostatic stabilization with the electric field in TS *versus* GS. As a consequence, the activation energy ΔG^\ddagger is decreased and a specific MW effect can be expected.

In Table 3 the best results obtained for all compounds are reported.

The use of montmorillonite KSF as acidic mineral support gave negative results. Some experiments were also carried out at 120° and 140° as final temperatures with Aliquat and with PTSA respectively. The yields achieved were lower in comparison to the ones obtained under the most favourable conditions (Table 3).

To evaluate the advantages of the solvent-free procedures on the rate of esterification, the reactions were also carried out using two classical methods:

H_2SO_4 , the carboxylic acid and the appropriate alcohol in excess, under reflux;

anhydrous pyridine *via* acyl chloride and the corresponding alcohol at 100 °C.

The results (yield% – reaction time) obtained for the synthesis of compounds **3**, **5**, **9** were the following:

H_2SO_4 : isopropyl palmitate (**3**) 61% – 2 h;

butyl palmitate (**5**) 73% – 2 h;

dibutyl sebacate (**9**) 69% – 2 h

pyridine: isopropyl palmitate (**3**) 60% – 6 h;

butyl palmitate (**5**) 87% – 3 h;

dibutyl sebacate (**9**) 76% – 18 h

Conclusion

All compounds studied were obtained in high yields, by simple experimental conditions under either microwave or conventional heating.

Concerning PTC, microwave methods lead to a reduction in reaction times when compared to the oil bath ones (Δ /MW: 15 min/5 min) as a consequence of thermal effects consisting in a faster and more homogeneous rise in temperature, but also specific effects probably connected to mechanistic considerations.

The solvent-free procedures under both microwave activation and classical heating can be considered efficient, fast, economical and eco-friendly methods to synthesize long chain aliphatic esters. In fact, the chemical transformations occur with higher efficiency, purity and easier work-up when compared to the classical methods, with evident economic and ecological advantages, also resulting from stoichiometric use of reagents.

Experimental

Apparatus

Microwave irradiation was carried out using a monomode reactor Synthwave™ S402 (temperature control and monitoring by IR detection, optimal emitted power 300 W) from Prolabo – Fontenay-Sous-Bois, France. IR spectra were recorded with a Perkin-Elmer 398 spectrophotometer. ¹H-NMR spectra were recorded on a Varian-Gemini 200 instrument (200 MHz) with TMS as an internal standard; chemical shifts are reported as δ (ppm) relative to TMS. GC-MS spectra were recorded on an Agilent GC 6890-MS597 instrument (Column: HP5 5% diphenylmethylsiloxane; carrier He). Elemental analyses for C and H were performed on CE Instruments – EA 1110 CHNS–O. Melting points were determined on a Büchi 510 apparatus and were uncorrected. Oil bath temperature measurements were carried out using a digital thermometer Comark C9007.

Materials

Diethyl ether and dichloromethane were supplied by Merck (Darmstadt, Germany); Florisil 100–200 mesh, KSF montmorillonite, *p*-toluenesulfonic acid, H₂SO₄, pivalic acid, myristic acid, palmitic acid, sebacic acid, TBAB, Aliquat 336, KOH, K₂CO₃, all the alkyl bromides and alcohols were supplied by Sigma-Aldrich (Milan, Italy).

General procedure for the synthesis of compounds 1–10 with neat PTSA

Microwave activation. The carboxylic acid (10 mmol), the appropriate alcohol in stoichiometric amounts and PTSA (10% or 20% by weight of mono or dicarboxylic acids respectively) were mixed together into a 40 mL Pyrex tube, introduced into the microwave reactor and irradiated under mechanical stirring for 10 min at 140 °C, maintaining this temperature by power modulation between 15 and 300 W. After cooling to room temperature, 20 mL of diethyl ether were added. The solution was washed twice with NaOH 2 M, then with H₂O, dried over

MgSO₄ and filtered. The solvent was evaporated under reduced pressure and the crude product obtained was purified by bulb-to-bulb distillation under vacuum.

Conventional heating. The syntheses were carried out with the procedure above described but inside a thermostated oil bath for 15 minutes.

General procedure for the synthesis of compounds 1–10 with Aliquat 336/K₂CO₃

Microwave activation. In a 40 mL Pyrex tube, the appropriate mono or dicarboxylic acid (10 mmol) was mixed together with anhydrous K₂CO₃ (10 mmol for monocarboxylic acid and 20 mmol for the dicarboxylic one), Aliquat 336 (1.5–3 mmol) and a stoichiometric amount of the corresponding alkyl bromide. The reaction mixture was introduced into the microwave reactor and irradiated under stirring for 5 min at 140 °C, maintaining this temperature by power modulation from 15 to 300 W. After cooling to room temperature, the organic product was recovered by elution with dichloromethane (50 mL) and subsequent filtration on Florisil (100–200 mesh). The solution was evaporated under reduced pressure and the crude product was purified by bulb-to-bulb distillation under vacuum.

Conventional heating. The syntheses were carried out with the procedure above described but inside a thermostated oil bath for 15 minutes.

Microanalyses for C and H of all the synthesized compounds were within \pm 0.3% of the theoretical values. The ¹H-NMR spectral data were in agreement with the proposed structures and the GC-MS data confirmed compound purity.

References

- 1 F. Chemat, M. Poux and S. A. Galema, *J. Chem. Soc., Perkin Trans. 2*, 1997, 2371.
- 2 K. Okuyama, X. Chen, K. Takata, D. Odawara, T. Suzuki, S. Nakata and T. Okuhara, *Appl. Catal. A: Gen.*, 2000, **190**, 253.
- 3 R. Ballini, G. Bosica, S. Carloni, L. Ciaralli, R. Maggi and G. Sartori, *Tetrahedron Lett.*, 1998, **39**, 6049.
- 4 A. Loupy, A. Petit, M. Ramdani, C. Yvanaeff, M. Majdoub, B. Labiad and D. Villemin, *Can. J. Chem.*, 1993, **71**, 90.
- 5 S. Deshayes, M. Liagre, A. Loupy, J. L. Luche and A. Petit, *Tetrahedron*, 1999, **55**, 10870.
- 6 *Microwaves in Organic Synthesis*, ed. A. Loupy, Wiley-VCH, Weinheim, Germany, 2002.
- 7 E. Perez, N. C. Carnevalli, P. J. Cordeiro, U. P. Rodrigues-Filho and D. W. Franco, *Org. Prep. Proced. Int.*, 2001, **33**, 395.
- 8 R. S. Varma, *Green Chem.*, 1999, **1**, 43.
- 9 A. Loupy, *Top. Curr. Chem.*, 1999, **206**, 153.
- 10 M. T. Genta, C. Villa, E. Mariani, M. Longobardi and A. Loupy, *Int. J. Cosmet. Sci.*, 2002, **24**, 257.
- 11 C. Villa, M. T. Genta, A. Bargagna, E. Mariani and A. Loupy, *Green Chem.*, 2001, **3**, 196.
- 12 L. Perreux and A. Loupy, *Tetrahedron*, 2001, **57**, 9199.



Domino reaction of anilines with 3,4-dihydro-2H-pyran catalyzed by cation-exchange resin in water: an efficient synthesis of 1,2,3,4-tetrahydroquinoline derivatives

Liang Chen and Chao-Jun Li*

Tulane University, Department of Chemistry, New Orleans, Louisiana, USA.
E-mail: cjli@tulane.edu; Fax: 504-865-5596; Tel: 504-865-5573

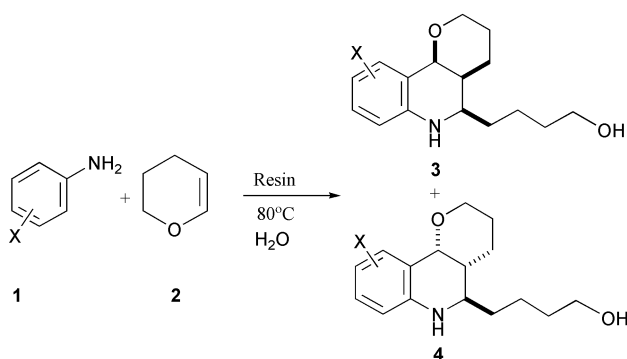
Received 23rd April 2003

First published as an Advance Article on the web 7th August 2003

A highly efficient method for the synthesis of 1,2,3,4-tetrahydroquinoline derivatives by using a domino reaction of aromatic amines with 3,4-dihydro-2H-pyran over cation-exchange resin (H form) catalysts in water is described.

Tetrahydroquinoline derivatives exist in various natural products and pharmaceutical agents that show broad biological activities.¹ Various new synthesis methods for the tetrahydroquinoline derivatives have been reported.² The aza-Diels–Alder reaction of N-arylimines with dienophiles in the presence of Lewis acid catalysts has been shown to be a very powerful method for synthesis of the tetrahydroquinoline derivatives.³ Recently the Lewis acid catalyzed three-component-reaction of a substituted aniline, an aryl aldehyde, and an electron-rich olefin has also been reported.⁴ More recently, we reported a synthesis of such compounds through an indium(III) chloride-catalyzed domino reaction of aromatic amines with cyclic enol ethers in water.⁵ We also reported a synthesis of those compounds by using aromatic nitro compounds with cyclic enol ethers in aqueous media.⁶ However, all of the previous methods would bring metals or other undesired chemical species into the “environment” from the catalysts being used. The concept of green chemistry⁷ encouraged us to develop a new synthetic method using an even safer and non-waste-producing alternative catalyst. Solid acid catalysts are not only environmentally friendly but also have many economic advantages.⁸ Acidic cation-exchange resins have been used as solid acid catalysts commercially in many fields.⁹ Herein we wish to report a simple and general method for the synthesis of tetrahydroquinoline derivatives *via* a domino reaction of aromatic amine compounds and cyclic enol ethers (3,4-dihydro-2H-pyran) catalyzed by an acidic cation-exchange resin in water (Scheme 1).

aqueous media. Among them, the AG[®] 50W-X2 resin achieved the best conversion with 77% isolated yield of a pair of diastereomers, **3a** and **4a**. The reactivity difference may be due to the size of the commercial resin particles which had a significant influence on the yields of the desired products. A higher reactivity was observed with resins of smaller particle size, possibly due to the increased surface area. The results are listed in Table 1. For instance, in Table 1 the resin catalysts AG[®]50W-X2, DOWEX[®]50WX4-200R and Nafion[®]H with almost the same exchange capacities (0.9 meq/wet g, 1.0 meq/wet g, and 0.8 meq/wet g, respectively) but different sizes (the smallest size 200–400 mesh, the medium size 100–200 mesh and the largest 7–9 mesh, respectively) achieved significantly different conversions together with different isolated yields 77%, 38% and trace, respectively. Hence, the smallest particle size achieved the highest yield. The resin catalyst Amberlite[®]IR-120 has a higher exchange capacity (1.9 meq/wet g) than the AG[®]50W-X2 (0.9 meq/wet g), but still provided a lower yield of the desired product (48%) than the AG[®]50W-X2 (77%), most possibly because the AG[®]50W-X2 has a much smaller size (200–400 mesh) than the Amberlite[®]IR-120 (16–50 mesh). Using the AG[®] 50W-X2 as catalyst, various conditions were examined for the reaction of aniline with 3,4-dihydro-2H-pyran. Either lowering (50 °C) or increasing (100 °C, reflux) the reaction temperature did not improve the yields. Microwave¹⁰ (CEM[®], 300 W, 1 min, 5 min, 10 min, 20 min) or ultrasonic¹¹ (BRANSON[®], 100 W, overnight) radiations were also effective as the heat sources, but they provided lower yields. With these preliminary results, the scope of the reaction was examined with a variety of aromatic amine derivatives and 3,4-dihydro-2H-pyran in the presence of



Scheme 1

To begin our study, different resins (hydrogen form) were used as solid acid catalysts in the reaction of aniline (**1a**, 0.5 mmol) with 3,4-dihydro-2H-pyran (**2a**, 1.5 mmol) at 80 °C in

Green Context

Tetrahydroquinolines have various applications including pharmaceuticals. Several synthetic routes are available including, most recently, the domino reaction of aromatic amines with cyclic enol ethers using an aqueous solution of a metal catalyst. Such a process presents obvious problems in separation and work-up with release to the environment of heavy metals being difficult to avoid. Here a method to overcome this problem is described whereby a recoverable solid catalyst is used while maintaining the advantages of a water solvent.

JHC

Table 1 The reaction of aniline with 3,4-dihydro-2 *H*-pyran using different resin catalysts

	AG®50W-X2	Amberlite® IR-120	DOWEX®50WX4-200R	Nafion® H
Yield (%)	77	48	38	trace
<i>cis</i> : <i>trans</i>	42 : 58	54 : 46		
Conditions	80 °C/2h	80 °C/6h	80 °C/2h	80 °C/12h
Size	200–400 mesh	16–50 mesh	100–200 mesh	7–9 mesh
Exchange capacity	0.9 meq/wet g	1.9 meq/wet.g	1.0 meq/wet g	0.8 meq/wet g

AG®50W-X2 resin and Amberlite® IR-120 resin, respectively. The results are listed in Table 2.

As shown in Table 2, the AG®50W-X2 resin catalyst (with the smaller particle size) achieved significantly higher yields than the Amberlite® IR-120 resin. The reactions catalyzed by Amberlite® IR-120 resin showed slower reaction rates but provided a slightly higher *cis/trans* selectivity. The substituent had a significant effect on the reactions. The presence of a CN[−] or NO₂[−] group decreased the rate of the reaction and enhanced the *trans* selectivity considerably (Table 2, entries 13–15). A proposed mechanism for the product formation is illustrated in Scheme 2.

In all the cases the products were obtained as a mixture of *cis*- and *trans*-isomers and could not be completely separated by column chromatography. The ratio of *cis* : *trans* was determined by ¹H NMR. Unlike the reactions using Lewis acid catalysts or In/HCl, which produce heavy metal or acid pollution, the use of the solid AG®50W-X2 resin catalyst offers a cleaner process in that the resin can be reused and will not bring additional pollutants into the “environment”. For recycling studies, the catalyst solution of InCl₃ and AG®50W-X2 resin were recovered, washed with ethyl ether, and reused in subsequent reactions. The reaction of aniline (**1a**, 0.5 mmol) with 3,4-dihydro-2H-pyran (**2a**, 1.5 mmol) was also performed in

Table 2 Synthesis of tetrahydroquinolines *via* the reaction of anilines with 3,4-dihydro-2H-pyran entry

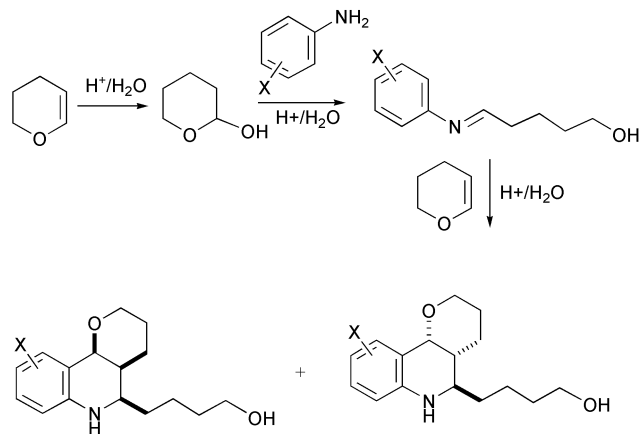
Entry	Anilines	Conditions/time	Product (3+4)	<i>cis</i> : <i>trans</i> overall yield (%)
1		A. 80 °C/2 h		47 : 53 77
2		B. 80 °C/6 h		42 : 58 48
3		A. 80 °C/4 h		47 : 53 69
4		B. 80 °C/10 h		53 : 47 29
5		A. 80 °C/1.5 h H3C		55 : 45 79
6		B. 80 °C/6 h		45 : 55 50
7		A. 80 °C/h		51 : 49 72
8		B. 80 °C/7 h		42 : 58 44
9		A. 80 °C/2 h		44 : 56 59
10		B. 80 °C/7 h		36 : 64 41
11		A. 80 °C/1.5 h		58 : 42 68
12		B. 80 °C/4 h		58 : 42 44
13		A. 80 °C/7 h		34 : 66 69
14		A. 80 °C/7 h		36 : 64 71
15		B. 80 °C/17 h		26 : 74 22

Conditions: A. AG®50W-X2 hydrogen form cation-exchange resin as catalyst (0.9 meq/wet g, 200–400 mesh) B. Amberlite® IR-120 plus ion-exchange acidic resin as catalyst (1.9 meq/wet g, 16–50 mesh).

Table 3 Comparison of the AG[®]50W-X2-H₂O method with other conditions

Method	InCl ₃ -H ₂ O ^a	AG [®] 50W-X2-H ₂ O ^b	AG [®] 50W-X2-CH ₃ CN	AG [®] 50W-X2-THF
Yield	76%	77%	48%	26%
<i>cis</i> : <i>trans</i>	51 : 49	47 : 53	54 : 46	55 : 45
Conditions	80 °C/2 h	80 °C/2 h	80 °C/2 h	80 °C/2 h
Yield (2nd run)	31%	41%		
Yield (3rd run)	27%	31%		

^a 5 mol% InCl₃ used. ^b 5 mol% AG[®]50W-X2 used.

**Scheme 2** Mechanism for the synthesis.

THF and acetonitrile (two common organic solvents). The results are shown in Table 3. Compared to the traditional methods that use metal-based catalysts or use organic solvent, the AG[®]50W-X2-H₂O method is clearly more efficient; at the same time, it is readily recyclable and does not leave metal ions in the water.

In summary, an efficient and simple method for the synthesis of tetrahydroquinoline derivatives was developed *via* a solid acidic resin-catalyzed domino reaction of anilines and dihydropyrans in water. No organic solvent was required and no metal-based catalyst was used. The solid resin and the aqueous solvent can be recycled readily. The products have various pharmaceutical applications. The scope and synthetic applications of the method are currently under investigation.

Experimental

Analytical Grade Cation-Exchange Resin, AG[®]50W-X2 (hydrogen form, 200 ~ 400 mesh), was purchased from BIO-RAD Laboratories. Amberlite[®] IR-120 (plus) ion-exchange resin (strongly acidic gel-type resin, 16 ~ 50 mesh) was purchased from Aldrich Chemical Company. 400 M NMR was performed at the Department of Chemistry of Tulane University.

General procedure for the resin-catalyzed domino reaction in water

A mixture of cation-exchange resin (30 mg), aromatic amines (0.5 mmol) and 3,4-dihydro-2H-pyran (**2a**, 1.5 mmol) was stirred at 80 °C in water (2 mL). The reaction progress was monitored by TLC. When the reaction was completed, the reaction mixture was extracted with ethyl ether or methylene chloride. The combined organic phases were dried and concentrated. Subsequently, the crude mixture was purified by column chromatography on silica gel using a mixture of hexane and ethyl acetate as eluent to give the tetrahydroquinoline derivatives.

Acknowledgement

This work was supported by the NSF and NSF-EPA Joint Program for a Sustainable Environment.

Notes and references

- (a) M. Ramesh, P. S. Moham and P. Shanmugam, *Tetrahedron*, 1984, **40**, 4041; (b) K. M. Witherup, R. W. Ransom, S. L. Varga, S. M. Pitzengerger, V. J. Lotti and W. J. Lumma, *U. S. Pat.*, 1994, US 5288725; (c) N. B. Perry, J. W. Blunt, J. D. McCombs and M. H. G. Munro, *J. Org. Chem.*, 1986, **51**, 5476; (d) N. M. Williamson, P. R. March and A. D. Ward, *Tetrahedron Lett.*, 1995, **36**, 7721; (e) J. V. Johnson, S. Rauckman, P. D. Baccanari and B. Roth, *J. Med. Chem.*, 1989, **32**, 1942; (f) S. A. Biller and R. N. Misra, *U. S. Pat.*, 1989, US 4843082; (g) E. A. Mohamed, *Chem. Pap.*, 1994, **48**, 261; *Chem. Abstr.*, 1995, **123**, p. 9315; (h) R. W. Caling, P. D. Leeson, A. M. Moseley, R. Baker, A. C. Foster, S. Grimwood, J. A. Kemp and G. R. Marshall, *J. Med. Chem.*, 1992, **35**, 1942; (i) R. W. Carling, P. D. Leeson, A. M. Moseley, J. D. Smith, K. Saywell, M. D. Tricklebank, J. A. Kemp, G. R. Marshall, A. C. Foster and S. Grimwood, *Bioorg. Med. Chem. Lett.*, 1993, **3**, 65; (j) G. D. Cuny, J. D. Hauske, M. Z. Hoemann, R. F. Rossi and R. L. Xie, *PCT Int. Appl.*, 1999, WO 9967238; *Chem. Abstr.*, 1999, **132**, p. 64182; (k) K. Hanada, K. Furuya, K. Inoguchi, M. Miyakawa and N. Nagata, *PCT Int. Appl.* 2001, WO 0127086.
- A. R. Katritzky, S. Rachwal and B. Rachwal, *Tetrahedron*, 1996, **52**, 15031.
- (a) L. S. Povarov, *Russ. Chem. Rev., Engl. Transl.*, 1967, **36**, 656; (b) D. L. Boger and S. M. Weinreb, *Hetero Diels-Alder Methodology in Organic Synthesis*, Academic, San Diego, 1987, ch. 2 and 9; (c) B. Crousse, J. Begue and D. Bonnet-Delpon, *J. Org. Chem.*, 2000, **65**, 5009; (d) J. S. Mendoza, *PCT Int. Appl.*, 1998, WO 9827093; *Chem. Abstr.*, 1998, **129**, p. 95393; (e) Y. Makioka, T. Shindo, Y. Taniguchi, K. Takaki and Y. Fujiwara, *Synthesis*, 1995, 801; (f) V. Lucchini, M. Prato, G. Scorrano, M. Stivanello and G. Valle, *J. Chem. Soc., Perkin Trans. 2*, 1992, 259; (g) T. Kametani, H. Furuyama, Y. Fukuoka, H. Takeda, Y. Suzuki and T. Honda, *J. Heterocycl. Chem.*, 1986, **23**, 185; (h) G. Babu and P. T. Perumal, *Tetrahedron Lett.*, 1998, **39**, 3225; (i) G. Sundarajan, N. Prabakaran and B. Varghese, *Org. Lett.*, 2001, **3**, 1973.
- (a) Y. Ma, C. Qian, M. Xie and J. Sun, *J. Org. Chem.*, 1999, **64**, 6462; (b) S. Kobayashi, S. Komiyama and H. Ishitani, *Biotechnol. Bioeng.*, 1998, **61**, 23; (c) S. Kobayashi and S. Nagayama, *J. Am. Chem. Soc.*, 1996, **118**, 8977; (d) R. A. Batey, D. A. Powell, A. Acton and A. J. Lough, *Tetrahedron Lett.*, 2001, **42**, 7935.
- (a) J. Zhang and C. J. Li, *J. Org. Chem.*, 2002, **67**, 3969; (b) Z. Li, J. Zhang and C. J. Li, *Tetrahedron Lett.*, 2003, **44**, 153.
- L. Chen, Z. Li and C. J. Li, *Synlett*, 2003, 732.
- P. Anastas and J. C. Warner, *Green Chemistry, Theory and Practice*, Oxford University Press, New York, 1998.
- M. A. Harmer and Q. Sun, *Appl. Catal. A: Gen.*, 2001, **221**, 45. For an excellent review on the usage of solid acids in green chemistry, see: J. H. Clark, *Acc. Chem. Res.*, 2002, **35**, 791. See also: T. Okuhara, *Chem. Rev.*, 2002, **102**, 3641.
- A. Heidekum, M. A. Harmer and W. F. Hoeldrich, *J. Catal.*, 1999, **181**, 217; P. K. Paakkonen and I. Krause, *React. Funct. Polym.*, 2003, **55**, 139.
- N. Tsumori, Q. Xu, Y. Souma and H. Mori, *J. Mol. Catal. A: Chem.*, 2002, **179**, 271; S. D. Kim and K. H. Lee, *J. Mol. Catal.*, 1993, **78**, 237; T. Baba and Y. Ono, *Appl. Catal.*, 1986, **22**, 321; R. S. Varma *Advances in Green Chemistry: Chemical Syntheses Using Microwave Irradiation*, Astra Zeneca Research Foundation, Kavitha Printers, Bangalore, India, 2002.
- Synthetic Organic Sonochemistry*, ed. J. L. Luche, Plenum, New York, 1998.



Reduction of aqueous CO₂ at ambient temperature using zero-valent iron-based composites

Guoqing Guan,^{*a} Tetsuya Kida,^b Tingli Ma,^a Kunio Kimura,^a Eiichi Abe^a and Akira Yoshida^c

^a Clarification Composite Materials Group, National Institute of Advanced Industrial Science and Technology, AIST Kyushu, Shuku-machi, Tosu, Saga 841-0052, Japan.

E-mail: guoqing-guan@aist.go.jp; Fax: +81-942-81-3690; Tel: +81-942-81-3641

^b Department of Chemistry and Applied Chemistry, Faculty of Science and Engineering, Saga University, Honjo 1, Saga, 840-8502, Japan

^c Department of Materials Science and Chemical Engineering, Kitakyushu National College of Technology, Shii 5-20-1, Kokuraminami-ku, Kitakyushu, Fukuoka, 802-0985, Japan

Received 22nd April 2003

First published as an Advance Article on the web 11th August 2003

The reduction of CO₂ was investigated over zero-valent Fe⁰ and Fe⁰-based composites in an aqueous solution at room temperature. It was found that H₂ and a small amount of CH₄ were formed from the CO₂-H₂O-Fe⁰ system, while no H₂ was formed without CO₂. When potassium-promoted Fe⁰-based composites, Fe⁰-K-Al and Fe⁰-Cu-K-Al, were used, the CO₂ reduction rates were increased and CH₄, C₃H₈, CH₃OH, and C₂H₅OH were produced together with H₂. The fresh and used Fe⁰ powders after the reaction were analyzed by XPS, XRD, and photoemission yield measurements. The obtained results suggest that in the presence of CO₂ as a proton source zero-valent Fe⁰ is readily oxidized to produce H₂ stoichiometrically and that CO₂ is reduced catalytically over the Fe⁰-based composites with the resulting H₂ to produce hydrocarbons and alcohols.

1 Introduction

Iron is one of the most prevalent metals on the earth, thus being used as low-cost catalysts for various reactions. In recent years, zero-valent iron has been successfully used to dechlorinate chlorinated hydrocarbons such as trichloroethylene and perchloroethylene in groundwater.¹⁻⁴ It is considered that, in this system, the corrosion of iron yields ferrous iron and provides electrons for reducing the chlorinated compounds. Agrawal and Tratnyek⁵ made use of this property in order to degrade other contaminants such as nitro aromatic compounds, and found that the nitro reduction by Fe⁰ is significantly faster than the dechlorination. Fe⁰ has also been used as a strong agent for reducing heavy metal contaminants such as Cr(vi), Pb(II) and TcO₄⁻.⁶ On the other hand, Getty *et al.*⁷ invented a method for the continuous production of hydrogen using Fe⁰ as the catalyst with a degassed aqueous organic acid solution. They proposed a reaction mechanism in which Fe⁰ reacts with water to generate hydrogen and to oxidize itself into Fe₃O₄, while the organic acid reduces the resulting Fe₃O₄ to regenerate the Fe⁰ and to produce water, thus permitting continuous hydrogen production to occur. Hardy and Gillham⁸ investigated the reduction of CO₂ in a simulated groundwater by zero-valent Fe⁰. Ten hydrocarbons up to C₅ were identified as products of the reduction process and the products were shown to have an Anderson-Schulz-Flory product distribution. Moreover, the pretreatment of the catalyst with H₂ was found to increase the total mass of the hydrocarbons detected in the solution. However, the yields of the hydrocarbons were very low even for a long reaction time, and they did not investigate the H₂ production from their system.

Under these circumstances, we have separately found that hydrogen and hydrocarbons were simultaneously formed from water over zero-valent Fe⁰ in the presence of gaseous CO₂ in a closed reactor under anaerobic conditions at ambient tem-

perature. Here, we present the results obtained on this newly developed CO₂ reduction method. Furthermore, in order to improve the CO₂ reduction rate, potassium-promoted Fe⁰-based composites were also developed.

2 Experimental

The chemicals used in the present study were of reagent grade, purchased from Wako Pure Chemical Industry, and used without further purification. The iron powders were prepared by a precipitation method using Fe(NO₃)₃·9H₂O and an ammonium hydroxide solution. The resulting precipitate was subjected to a multiple filtration and a washing treatment, and then dried in air at 373 K for 24 h, followed by calcination at 723 K for 5 h, and reduction at 723 K for 20 h. The potassium-promoted Fe⁰-based composites, Fe⁰-Cu-K-Al and Fe⁰-K-Al, were prepared by coprecipitation and subsequent incipient wetness methods. The precipitates containing the Fe, Cu, and Al components were first prepared by mixing an aqueous solution containing the corresponding metal nitrates with an ammonium

Green Context

The enormous quantities of carbon dioxide produced by modern civilisation are a cause of increasing concern both in terms of global warming and the consequential irreversible consumption of declining carbon resources. Fixation of CO₂ is a subject of increasing interest and importance. Here a novel approach to this is proposed which involves reduction to hydrocarbons and alcohols using zero-valent iron-based composites.

JHC

hydroxide solution. The resulting precipitates were subjected to multiple filtrations and washing treatments, then dried in air at 373 K for 24 h. The obtained precursors were impregnated in an aqueous solution containing K_2CO_3 , followed by drying at 373 K for 24 h and then calcinations at 723 K for 5 h. They were also reduced under hydrogen flow at 723 K for 20 h. The prepared Fe^0 -Cu-K-Al and Fe^0 -K-Al composites have molar ratios of 1.0 Fe : 0.03 Cu : 0.7 K : 2.0 Al and 1.0 Fe : 0.7 K : 2.0 Al, respectively.

The reduction of CO_2 over the prepared samples in water was carried out in a closed reactor (173 mL) at room temperature with no stirring or shaking. The reactor was connected to a closed-gas circulation system and an on-line gas chromatograph. A 0.3 g sample of the prepared powder was dispersed in 5.0 mL of distilled water. After degassing using a vacuum system, 95 kPa of highly purified CO_2 was introduced into the reactor. The H_2 and CH_4 produced in the gas phase were determined using a gas chromatograph (GC) (Shimadzu, GC-14B) equipped with a molecular sieve 5A column and detected by a thermal conductivity detector (TCD) and a flame ionization detector (FID), respectively. Argon was used as the carrier gas in this case. CH_3OH and C_2H_5OH were determined using a GC (Shimadzu, GC-17A) equipped with a capillary column and an FID. Helium was used as a carrier gas for the analysis of products in the liquid phase. The amount of samples taken from the liquid phase for the analysis was 0.005 mL.

The prepared composites were analyzed using an X-ray diffractometer (Rigaku, RINT-1400) with Cu-K α radiation. The BET surface area of the sample powders was measured by the nitrogen adsorption method. Surface characterization of the fresh and used (20 h-reaction) powders was carried out using an X-ray photoelectron spectrometer (ESCA-3400, Shimadzu) as well as a photoemission spectrometer (AC-I, Riken Keiki Inc.). Samples were kept in ampoules under vacuum conditions before being subjected to the measurements. The ferrous iron contents in the solution after the reactions were determined by a spectrometric analysis, which is composed of three steps, *i.e.*, reduction of Fe^{3+} into Fe^{2+} by hydroxylamine hydrochloride, formation of a red-colored complex by 1,10-phenanthroline, and spectrometric determination of the complex using a spectrophotometer (U-2000, Hitachi).

3 Results and discussion

Fig. 1 shows the XRD diffraction patterns of the synthesized Fe^0 , Fe^0 -K-Al, and Fe^0 -Cu-K-Al. The formation of the zero-valent iron phase is confirmed for Fe^0 . The peaks corresponding to the Fe^0 phase are also clearly seen for the Fe^0 -K-Al and Fe^0 -Cu-K-Al composites but are hardly seen for the Fe^0 -Al composite. The obtained results show that the Fe^0 phase is difficult to form when only Al is combined with Fe, although the Al addition improves the Fe dispersion on the catalyst. It is reported that the addition of Cu aids Fe^0 formation in the Fe^0 -Cu-K-Al composites.^{9–12} The BET specific surface areas of the prepared powders are shown in Table 1. The combination of Fe^0 with the K, Cu, and Al components leads to the increased surface area.

Fig. 2 shows the amount of H_2 evolved as a function of the reaction time over the Fe^0 . Every 24 h during the reaction period, the reactor was degassed and highly purified CO_2 was re-introduced into the reactor. It can be seen that the activity was slowly degraded as the reaction proceeded. However, the total amount of evolved H_2 reached 4529 μmol for the 72 h-reaction. Fig. 2 also compares the above results with those obtained for purchased Fe powders (initial 24 h). The amount of H_2 evolved over the purchased Fe powders is lower than that for the synthesized Fe^0 . This may be due to the smaller surface area of the purchased Fe powders (particle size: *ca.* 0.045 mm, surface

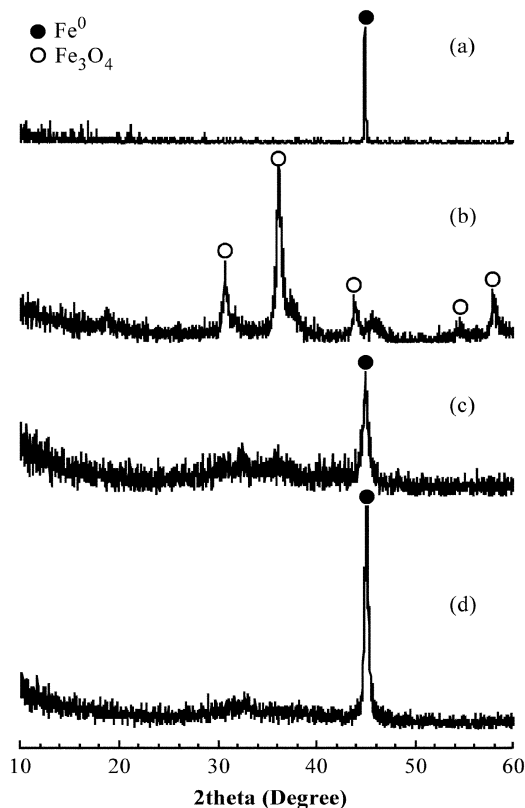


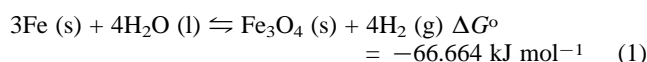
Fig. 1 XRD patterns for the prepared samples reduced at 450 °C for 20 h. (a) Fe^0 ; (b) Fe^0 -Al; (c) Fe^0 -K-Al; (d) Fe^0 -Cu-K-Al

Table 1 Reaction products from the reduction of H_2O and CO_2 over the Fe^0 -based composites^a

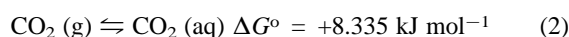
Catalyst	Surface area/ $m^2 g^{-1}$	Yields of products/ $\mu\text{mol (g catalyst)}^{-1}$				
		H_2	CH_4	C_3H_8	CH_3OH	C_2H_5OH
Fe^0	25.3	5808.1	0.63	0	0	0
Fe^0 -Al	94.6	0	0	0	0	0
Fe^0 -K-Al	104.4	3541.7	24.37	44.70	28.23	32.70
Fe^0 -Cu-K-Al	126.5	4776.3	29.73	57.34	61.63	78.68

^a Each experiment was carried out using 0.3 g of powders with 95 kPa of CO_2 and 5 mL of H_2O for 20 h.

area: 2.42 $m^2 g^{-1}$) compared to that of the prepared Fe^0 . Since the reaction of Fe^0 with H_2O basically occurs over the surface, it can readily be anticipated that the surface area of the Fe^0 influences the kinetics of the reaction. Fig. 3 shows the amount of H_2 evolved over the prepared Fe^0 for a more prolonged time (*ca.* 100 h). The rate of H_2 evolution almost remained constant during the initial period, but decreased to some extent after 50 h. The amount of H_2 evolved reached 5012 μmol after 90 h, although the H_2 evolution would continue for a longer period. It should be noted that no H_2 evolution was observed when the reaction was performed without CO_2 , although the reaction of Fe with H_2O is thermodynamically favorable as shown below.



Thus, this observation seems to indicate that the formation of carbonic acid has a key role in the H_2 evolution; the dissolution of CO_2 produces protons that can catalyze the oxidation of Fe to produce H_2 according to the following reactions:



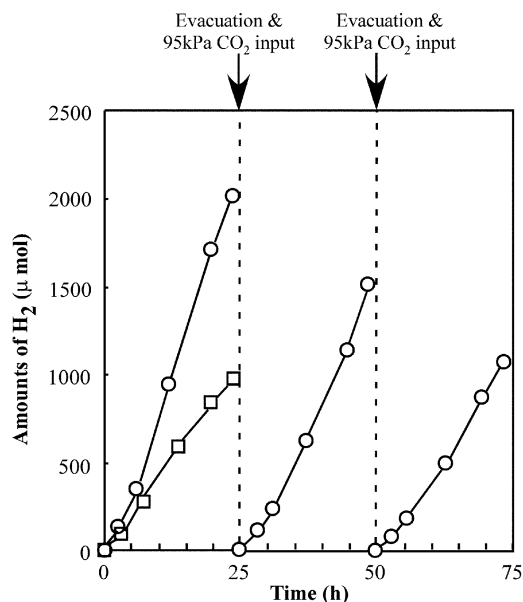


Fig. 2 H₂ evolution from the CO₂–H₂O system over 0.3 g of the prepared zero-valent Fe⁰ (○) and purchased Fe⁰ (□).

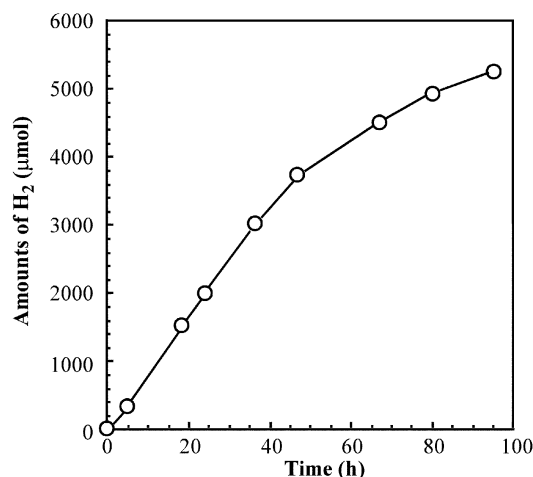
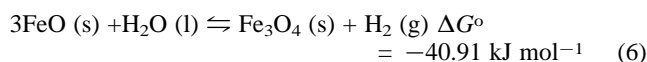
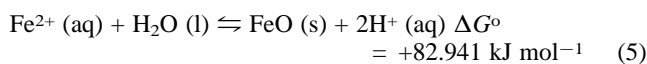
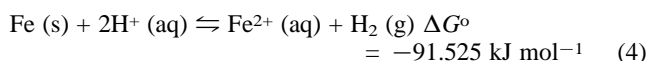
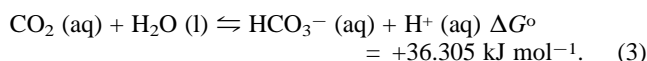


Fig. 3 H₂ evolution from the CO₂–H₂O system over 0.3 g of the zero-valent Fe⁰ (initial CO₂ pressure = 95 kPa; H₂O = 5 mL).



The equilibrium of reactions (2) and (3) is forced to the left, but once even a small amount of protons are formed Fe is readily oxidized to produce H₂.

Table 1 shows the amounts of hydrocarbons resulting from the reduction of aqueous CO₂ over the prepared Fe⁰. In this case, 0.63 μmol (g Fe⁰)⁻¹ of CH₄ and a trace amount of CH₃OH were formed after the 20 h-reaction. From the pe–pH diagram for the Fe–H₂O–CO₂ system, Hardy and Gillham⁸ suggested that the formation of CH₄ and other hydrocarbons such as C₂H₆ and C₂H₄ is thermodynamically possible, although the reactions are extremely slow without a suitable catalyst due to the required multiple electron transfer. On the other hand, Kudo *et al.*¹³ suggested that, during the electroreduction of CO₂ in water

using iron as the electrode, the zero-valent iron could act not only as a reactant for supplying electrons by corrosion but also as a catalyst for promoting the formation of hydrocarbons. As is also known, Fe can be used as an active catalyst for CO₂ hydrogenation.^{9–12} Thus, it is possible that the H₂ evolved resulting from reaction (1) could act as a reactant for the catalytic reduction of CO₂ over the Fe⁰. In addition, as shown in Table 2, only a slight amount of H₂ and no CO₂ reduction

Table 2 The yields of H₂ from the reduction of H₂O and CO₂ over purchased metal powders^a

Catalyst	Average particle size/μm	Surface area/m ² g ⁻¹	H ₂ /μmol g ⁻¹
Fe	45	0.224	2980.3
Co	45	0.119	80.7
Ni	6	2.732	93.3
Cu	75	0.089	0
Zn	75	0.104	381.7

^a Each experiment was carried out using 0.3 g of powders with 95 kPa of CO₂ and 5 mL of H₂O for 20 h in the reactor.

products were formed when purchased Co, Ni, Cu, and Zn powders (Wako Pure Chemical Industry) were used, suggesting that Fe has more superior properties than other metals for producing H₂ from water in the presence of CO₂ and for reducing CO₂ under anaerobic conditions.

The XPS measurements were carried out using AlKα radiation at an acceleration voltage of 15 kV to examine the oxidation state of each atom on the surface of the fresh and used Fe⁰ powders. The Au 4f_{7/2} peak (84.0 eV) is taken as the energy reference to calibrate the binding energy (BE) scale. Fig. 4

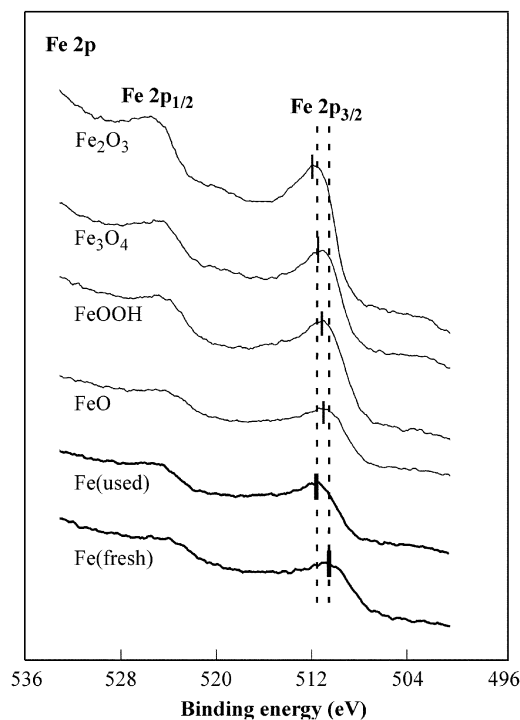


Fig. 4 Fe 2p spectra of the fresh and used Fe⁰ and standard FeO, FeOOH, Fe₃O₄, and Fe₂O₃.

shows the Fe 2p spectra observed on the fresh and used Fe⁰ powders, and is compared with the results of those for the FeO, FeOOH, Fe₃O₄ and Fe₂O₃ reagents. It is obvious that the BE value of Fe 2p_{3/2} (which is more intense than Fe 2p_{1/2}) for the Fe⁰ shifts to the higher value after the reaction, indicating a change in the Fe⁰ surface to an oxidation state which may lead to the deactivation of the Fe⁰. Fig. 5 shows the O 1s spectra

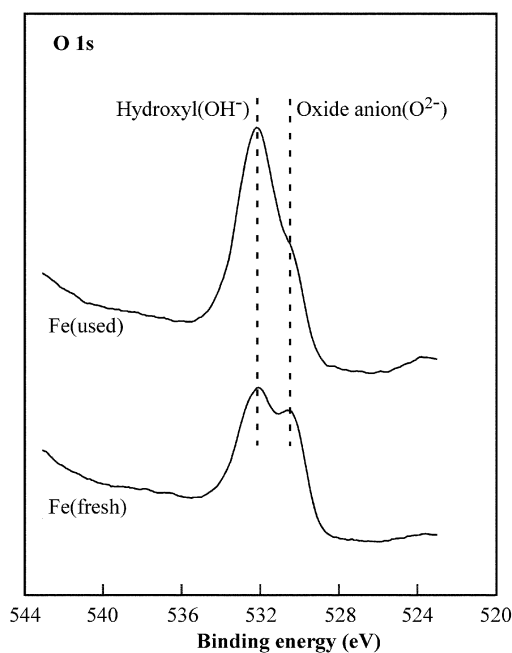


Fig. 5 O 1s spectra of the fresh and used Fe⁰.

recorded on the fresh and used Fe⁰. Two peaks are observed in the spectra at a BE of 530.5 and 532.1 eV. The former is attributable to the oxide anion, O²⁻, and the latter to the hydroxyl anion, OH⁻;^{14,15} the intensity of OH⁻ increased after the reaction, suggesting the possible formation of FeOOH on the surface.

The photoemission yield measurements on the fresh and used Fe⁰ were carried out at room temperature under atmospheric conditions in the incident light energy range of 3.4 to 6.8 eV using a photoelectron spectrometer equipped with a 150 W xenon lamp as the light source and an air-filled electron counter.¹⁶ Fig. 6 shows the photoemission yields of the fresh

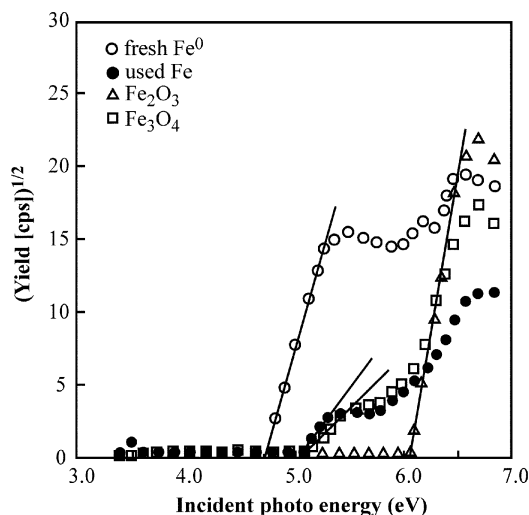


Fig. 6 Photoemission yield curves of the fresh and used Fe⁰, Fe₃O₄ and Fe₂O₃ vs. incident photon energy.

and used Fe⁰ as a function of incident light energy, and those for Fe₂O₃ and Fe₃O₄ reagents for comparison. In theory, the threshold energy of photoemission corresponds to the work function of a metal. For the fresh Fe⁰, the work function can be determined to be 4.7 eV; this value is in good agreement with that of Fe metal. However, for the used Fe⁰, the threshold energy increased to 5.0 eV, which is almost the same value as that obtained for Fe₃O₄. This suggests the formation of Fe₃O₄ on the Fe⁰ surface after the reaction.

The XRD patterns of the fresh and used Fe⁰ are shown in Fig. 7. Although it is difficult to distinguish Fe₃O₄ from Fe₂O₃ by

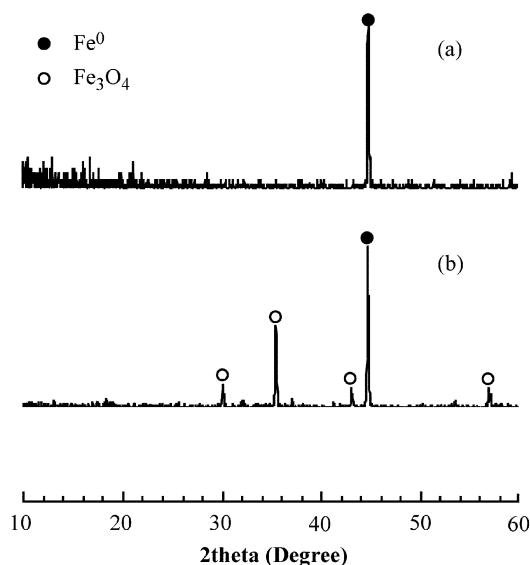


Fig. 7 XRD patterns for the Fe⁰ before (a) and after (b) the reaction.

XRD, particularly for small particles, the XRD results indicate that the Fe⁰ bulk was oxidized to Fe₃O₄ after the reaction in the present study. This does not exclude the possible formation of other oxide phases that are either amorphous or composed of particles too small to be detected through XRD analysis.

The above analytical results show that the Fe⁰ surface as well as the bulk were mainly oxidized to Fe₃O₄ and FeOOH, and to Fe₃O₄, respectively, after the reaction. As is known, when iron starts to be oxidized, it will puff up because iron oxide is a larger molecule than iron. Thus, it is considered that the puffing causes cracks and voids, which make the growing oxide layer porous and let protons diffuse through it, so that the residual iron bulk could be oxidized continuously. Such bulk oxidation is important because if the reaction did stop on the surface only a small amount of H₂ would be produced. Indeed, as shown in Fig. 3, the amount of H₂ formed after the 90 h-reaction was 5012 μmol, which is not so much lower than the 7162 μmol (0.3 g Fe⁰) of the stoichiometric amount of H₂ formed from reaction (1). Thus, the proton diffusion into the Fe⁰ bulk through a growing porous oxide layer may sustain the continuous H₂ production in this system.

We also measured the amount of ferrous ion in the reaction solution after the measurements by spectrometric analysis. However, it was found that the ferrous ion content was negligibly small, *i.e.*, under the detection limit (0.02 ppm). The ferrous ion content was also determined in the system developed by Getty *et al.*,⁷ in which 3 mmol of gluconic acid was added to 5.0 mL of water containing iron powders. In this case, ferrous ion was analyzed to be 86.2 ppm and the reaction solution was acidic (pH = 4.5) for the 20 h-reaction, although a large amount of H₂, 5210 μmol, was formed. In addition, when another organic compound such as formic acid was used (pH = 4), a comparable amount of H₂ and ferrous ion were detected. An acidic solution is known to accelerate the corrosion of iron and produce H₂, but the Fe⁰ is solubilized and cannot be recycled in that case. In contrast, in the present study, the pH of the reaction solution after the measurements was around 6, which resulted from the dissolution of CO₂. Such a moderate pH prevents the complete dissolution of Fe⁰ and is beneficial for re-use.

As is the case reported by Hardy and Gillham,⁸ the hydrocarbon yields over the zero-valent Fe⁰ were very low in spite of the longer reaction time. On the other hand, the Fischer-Tropsch (FT) synthesis of hydrocarbons in the CO₂-H₂ system

using iron-based catalysts has shown that the addition of K to the catalysts is beneficial for the FT conversion of CO₂, and that the further additions of Cu and Al promote the Fe⁰ formation and Fe⁰ dispersion in the catalysts, respectively.^{9–12} In this study, in order to improve the CO₂ reduction rate, the potassium-promoted Fe⁰ composites, *i.e.*, Fe⁰–K–Al and Fe⁰–Cu–K–Al, were used. As a result, the yields of CH₄ and CH₃OH increased to a great extent as compared to those for the pure zero-valent Fe⁰ (Table 1). Moreover, C₃H₈, C₂H₅OH and other unidentified gaseous compounds were also formed. In addition, a wax-like compound was observed in a significant amount. The results obtained suggest that the combination of Fe⁰ with the Cu, K and Al components promotes the reduction of CO₂ to organic compounds. Inui *et al.*¹⁰ reported that an Fe–Cu–K–Al catalyst with a ratio of 1.0Fe : 0.03Cu : 0.7K : 2.0Al had C–C formation activity and that CH₃OH and C₂H₅OH were formed over the catalyst in the presence of CO₂ and H₂ under reaction conditions of 80 atm and 350 °C. However, in the above report, the main phase of iron was Fe₃O₄ and H₂ was externally provided to the reaction system. In contrast, in the present study, zero-valent Fe⁰ is the dominant phase and H₂ is evolved through the anaerobic corrosion of Fe⁰ in water; the resulting H₂ serves as a reactant for the CO₂ hydrogenation over the Fe⁰-based composites. For the CO₂ hydrogenation, it can be assumed that the carbene groups such as –CH₂– and –CH₂–CH₂– are formed on the active site of Fe⁰ in the presence of the promoter K and are transformed to hydrocarbons such as CH₄ and C₃H₈, as in the case reported in the literature.^{9–13} The formation of alcohols can be considered as the result of the reaction of the carbene group with the hydroxyls (–OH) on the composite surface. Furthermore, it is reported that potassium addition to iron-based catalysts can lead to an increase in the amount of adsorbed CO₂ and H₂ on the catalysts, which could assist in the CO₂ hydrogenation.¹²

The obtained results suggest that the zero-valent Fe⁰-based composite is a promising candidate for H₂ production and CO₂ fixation. It should be noted, however, that the present reaction system is unfortunately a semi-catalytic process, *i.e.*, the reaction comes to an end when Fe⁰ has completely been oxidized although the regeneration of Fe⁰ is possible because the dissolution of Fe⁰ is almost negligible. The conversion of the present system into a truly catalytic one is desired but a challenging goal.

4 Conclusions

We have performed the reduction of CO₂ over zero-valent Fe⁰-based composites in water under anaerobic conditions at room temperature. It is found that H₂ can be effectively evolved from water over zero-valent Fe⁰ in the presence of gaseous CO₂ together with a small amount of hydrocarbons. When the Fe⁰

was combined with Cu, K, and Al components, hydrocarbons such as CH₄ and C₃H₈ and alcohols such as CH₃OH and C₂H₅OH were also effectively produced. The XPS, XRD, and photoemission yield measurements revealed that the Fe⁰ surface as well as the bulk was oxidized to Fe₃O₄ and other possible oxides during the reaction. This corrosion process is promoted by the dissolution of CO₂ in water and the resultant protons oxidize Fe⁰ to evolve H₂. Moreover, the evolved H₂ serves as the reactant for the CO₂ hydrogenation on the active site of Fe⁰, especially for the Fe⁰–K–Al and Fe⁰–Cu–K–Al composites.

Acknowledgments

The financial support provided for this work from Japan Science and Technology Corporation (JST) is gratefully acknowledged.

References

- 1 G. W. Reynolds, J. T. Hoff and R. W. Gillham, *Environ. Sci. Technol.*, 1990, **24**, 135.
- 2 L. J. Matheson and P. G. Tratnyek, *Environ. Sci. Technol.*, 1994, **28**, 2045.
- 3 T. L. Johnson, M. M. Scherer and P. G. Tratnyek, *Environ. Sci. Technol.*, 1996, **30**, 2634.
- 4 M. M. Scherer, B. A. Balko, D. A. Gallagher and P. G. Tratnyek, *Environ. Sci. Technol.*, 1998, **32**, 3026.
- 5 A. Agrawal and P. G. Tratnyek, *Environ. Sci. Technol.*, 1996, **30**, 153.
- 6 S. M. Ponder, J. G. Darab, J. Bucher, D. Caulder, I. Craig, L. Davis, N. Edelstein, W. Lukens, H. Nitsche, L. Rao, D. K. Shuh and T. E. Mallouk, *Chem. Mater.*, 2001, **13**, 479.
- 7 J. P. Getty, M. T. Orr and J. Woodward, U.S. patent 6,395,252 B1, May 28, 2002.
- 8 L. I. Hardy and R. W. Gillham, *Environ. Sci. Technol.*, 1996, **30**, 57.
- 9 T. Inui and T. Yamamoto, *Catal. Today*, 1998, **45**, 209.
- 10 T. Inui, T. Yamamoto, M. Inoue, H. Hara, T. Takeguchi and J. B. Kim, *Appl. Catal., A: Gen.*, 1999, **186**, 395.
- 11 J. S. Hong, J. S. Hwang, K. W. Jun, J. C. Sur and K. W. Lee, *Appl. Catal., A: Gen.*, 2001, **218**, 53.
- 12 T. Riedel, M. Claeys, H. Schulz, G. Schaub, S. S. Nam, K. W. Jun, M. J. Choi, G. Kishan and K. W. Lee, *Appl. Catal., A: Gen.*, 1999, **186**, 201.
- 13 A. Kudo, S. Nakagawa, A. Tsuneto and T. Sakata, *J. Electrochem. Soc.*, 1993, **140**, 1541.
- 14 M. Muhler, R. Schlögl and G. Ertl, *J. Catal.*, 1992, **138**, 413.
- 15 A. Miyakoshi, A. Ueno and M. Ichikawa, *Appl. Catal. A: Gen.*, 2001, **219**, 249.
- 16 K. Yanagida, O. Okada and K. Oka, *Jpn. J. Appl. Phys.*, 1993, **32**, 5603.



A highly active and reusable heterogeneous catalyst for the Suzuki reaction: synthesis of biaryls and polyaryls

Satya Paul† and James H. Clark*

Clean Technology Centre, Department of Chemistry, University of York, Heslington, York, UK YO10 5DD. E-mail: jhc1@york.ac.uk; Fax: +44 1904 434550

Received 29th May 2003

First published as an Advance Article on the web 12th August 2003

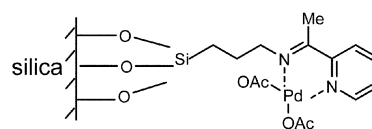
A novel silica supported palladium catalyst has been prepared and investigated for the Suzuki cross-coupling reaction between aryl bromides and benzenboronic acid in the presence of K_2CO_3 as base and *o*-xylene as solvent. The key features of the catalyst include rapid reactions with 100% conversion of aryl bromides, excellent catalyst recyclability and total stability under the reaction conditions (passes hot filtration test successfully). No change in the catalyst structure has been observed on the basis of surface analysis and simultaneous thermal analysis even after the 7th use. The catalyst can be used for consecutive Suzuki reactions in a single step and hence successfully applied to the synthesis of polyaryls.

Introduction

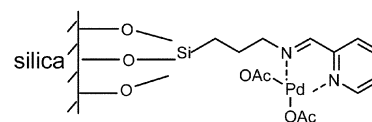
The importance of biaryl¹ units as components of many kinds of compounds, mainly pharmaceuticals, herbicides, and natural products, as well as in the field of engineering materials, such as conducting polymers, molecular wires, and liquid crystals, has attracted enormous interest from the chemistry community. Palladium- and nickel-catalysed Suzuki–Miyaura cross-coupling² is the most important and efficient strategy for the construction of unsymmetrical biaryl compounds as it is attractive compared to other methods using organometallics because organoboranes are air- and moisture-stable with relatively low toxicity. For Suzuki reactions, soluble complex palladium catalysts are normally employed alongside bases such as soluble amines; these are rarely recoverable without elaborate and wasteful procedures that are commercially unacceptable. In recent years there has been an increasing interest in developing greener processes. In this context, heterogeneous catalysis³ is emerging as an alternative to homogeneous processes so that catalysts can be recovered after the reaction and re-used several times to achieve very high turnover numbers. One strategy to transform a homogeneous into a heterogeneous process is to anchor the active site onto a large surface solid carrier provided that the anchoring methodology maintains the intrinsic activity and selectivity of the catalytic centre.⁴ Recently, palladium immobilised on the surface of silica was used as a heterogeneous catalyst for the Suzuki cross-coupling reaction.⁵

In our earlier communication,⁶ we have reported a heterogeneous catalyst for the Suzuki cross-coupling reaction prepared by the anchoring of palladium on the surface of modified silica with N–N ligand interaction. Recently, we have studied the structure–activity relationship between various silica supported palladium catalysts formed by the interaction of N–N, N–O and N–S ligands in the Suzuki cross-coupling reaction. The results are reported elsewhere.⁷ From our study we discovered that the most active catalyst studied is one which is formed by the interaction of the N–N ligands containing methyl group on the carbon of C=N bond (Cat 1). There is a significant difference in the rate of the model reaction between bromobenzene and benzenboronic acid using potassium carbonate as base and *o*-

xylene as solvent using new catalyst (Cat 1, rate constant = 0.0364) and the catalyst⁶ (Cat 2, rate constant = 0.00198) reported earlier.



Cat 1



Cat 2

In this paper we report the results of the Suzuki reaction between aryl bromides and benzenboronic acid in the presence of K_2CO_3 as base and *o*-xylene as solvent using our new catalyst Cat 1.

Multinuclear aromatics develop the concept of aromaticity and supramolecular benzene chemistry,⁸ and lead to wide applications in material and biological sciences.⁹ For example, terphenyls (*o*, *m*, *p*-isomers) are used industrially as heat storage and transfer agents and as textile dye carriers whilst the *p*-isomer has found application as a laser dye. The transition metal catalysed cross-coupling of Grignard reagents with dihalobenzenes^{10,11} and other methods¹² produce the desired terphenyls in poor yields. Recently, the synthesis of polyaryls has been

Green Context

Easily recoverable catalysts are important, especially where the catalyst is an expensive transition metal, and where traces of the metal in the final product can be extremely problematic. The synthesis of biaryls using Pd complexes is one such case, and this contribution describes a novel catalytic system which allows for very good reaction rates, along with excellent recovery and reusability. The increase in rate with minor ligand modification is interesting. DJM

† Present address: Department of Chemistry, University of Jammu, Jammu-180006, India. E-mail: paul17@rediffmail.com

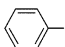
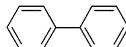
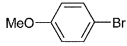
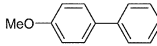
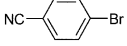

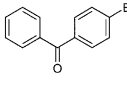
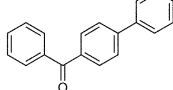
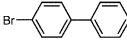
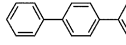
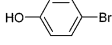
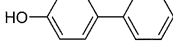
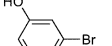
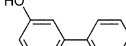
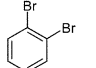
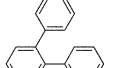
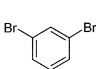
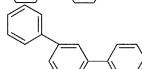
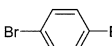
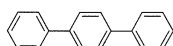
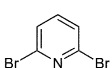
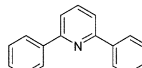
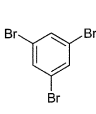
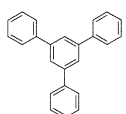
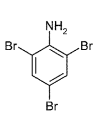
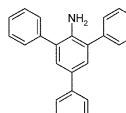
reported¹³ using palladium acetate in a domestic microwave oven. Although the authors have reported good yields of polyaryls this process is commercially unacceptable as it leads to non-recoverable palladium acetate. To the best of our knowledge, heterogeneous catalysis has not been employed for consecutive Suzuki reactions in a single step. Here we extend the use of Cat 1 to consecutive Suzuki reactions leading to the synthesis of polyaryls in a single step in high yields.

Results and discussion

The preparation procedure followed to obtain the catalyst (Cat 1) is indicated in Scheme 1. It consists of building up a suitable ligand structure on the surface of a commercial silica gel (K100) followed by complexation of palladium(II). The characterisation of Cat 1 was done on the basis of simultaneous thermal analysis (STA), diffuse reflectance infrared fourier transform spectroscopy (DRIFTS), X-ray photoelectron spectroscopy (XPS) and atomic absorption spectroscopy (AAS). Simultaneous thermal analysis shows a loss of residual solvent at 80 °C followed by a gradual weight loss between 198 and 405 °C. The weight loss between these temperatures indicates that 3-aminopropyl is chemically bound on the surface of silica. The DRIFTS of 3-aminopropyl-silica displays the characteristic C–H₂ stretching bands at 2936 and 2865 cm⁻¹ and aliphatic deformation bands at 1469 and 1445 cm⁻¹. The DRIFTS of chemically modified silica (imine) shows a sharp peak at 1639 cm⁻¹ due to the C=N bond, which on complexation with Pd disappears and appears as a band at 1599 cm⁻¹. The lowering in frequency of the C=N peak is indicative of the formation of a metal–ligand bond. The binding energy of the palladium in Cat 1 was found to be 333.45 eV on the basis of X-ray photoelectron spectroscopy. This is comparable to the binding energy of palladium in palladium acetate, 336.25 eV, determined under the same conditions. Surface analysis of Cat 1 shows the BET surface area to be 249.40 sq.m g⁻¹ and total pore volume as 0.7130 cm³ g⁻¹. The catalyst was thoroughly conditioned for 30 h at reflux temperature in toluene (3 × 3 h), ethanol (3 × 3 h), acetonitrile (3 × 3 h) and xylene (1 × 3 h at 130 °C). The conditioning of the catalyst was done with polar as well as non-polar solvents so as to remove any physisorbed palladium acetate on the surface of the silica gel and hence helping to make the process completely heterogeneous. Conditioning with xylene at 130 °C was so as to expose the catalyst to reaction conditions prior to actual use. The amount of palladium loaded on the surface of the silica was found to be 0.1 mmol g⁻¹ (corresponding to ca. 10% of the ligands available) on the basis of atomic absorption spectroscopy of a solution of palladium in dilute nitric acid (four standards containing 2, 4, 6 and 8 ppm of palladium in dilute nitric acid were used). The activity of the catalyst was tested in the Suzuki reaction between aryl bromides and phenylboronic acid

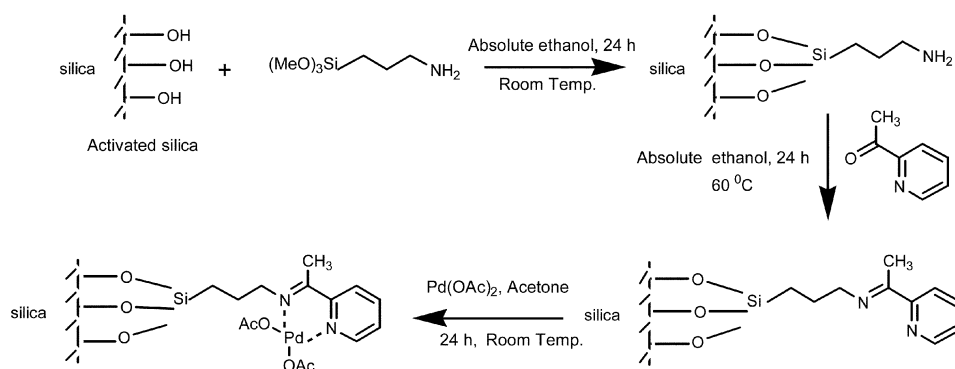
using potassium carbonate as base and *o*-xylene as solvent in an N₂ atmosphere. The results are presented in Table 1.

Table 1 Silica-supported palladium catalysed synthesis of biaryls and polyaryls

Entry	Substrate	Product ^a	Time	Yield (%) ^b
1			90 min	100
2			120 min	92
3			60 min	97
4			90 min	95
5			60 min	93
6			90 min	85
7			105 min	76
8			10 h	72 (65)
9			20 h	78 (71)
10			20 h	75 (65)
11			20 h	60 (52)
12			20 h	80 (72)
13			20 h	79 (71)

^a The products were characterised by GC/GC-MS, NMR and comparison with authentic samples. ^b In brackets, isolated yields are given.

Initially we focussed our attention on the cross-coupling of bromobenzene with phenylboronic acid under the same conditions (95 °C, *o*-xylene as solvent, K₂CO₃ as base) in order to compare our new catalyst Cat 1 with Cat 2 reported earlier.⁶ It has been found that Cat 1 (equivalent to 0.02 mmol of Pd) is much more active than Cat 2 (equivalent to 0.06 mmol of Pd)



Scheme 1

i.e. Cat 1: 90 min, 100% yield of biphenyl; Cat 2: 180 min, 98% of biphenyl. Since Cat 1 with very low loading of palladium is much more active than Cat 2, we extended its use for the Suzuki cross-coupling to other substituted bromobenzenes containing both electron withdrawing and electron releasing groups at 110 °C using K_2CO_3 as base and *o*-xylene as solvent. In all cases 100% conversion of bromobenzenes was observed in short reaction times. Cat 1 works equally well for phenols (entry 6 and 7). For the previous catalyst Cat 2, electron withdrawing and electron releasing substituents have little effect on the rate of the reaction, but with our new catalyst Cat 1, electron withdrawing and electron releasing substituents on bromobenzene have significant effects on the rate of the reaction (entry 2 and 3).

To the best of our knowledge, heterogeneous catalysis has not been applied to consecutive Suzuki reactions *i.e.* synthesis of polyaryls in a single step. The results from using our new catalyst are shown in Table 1, entries 8–13. High yields have been obtained with Cat 1 at 120 °C. In 1 h, complete conversion of di- (entries 8–11) or tribromobenzenes (entries 12 & 13) were observed by GC. The reaction was continued for 20 h in order that complete conversion of intermediate bromobenzene also took place. Complete conversion of bromoarenes was found in 20 h except for entry 11, where a little 2-bromo-6-phenylpyridine also seen by GC.

When using a supported metal catalyst a critical crucial issue is the possibility that some active metal migrates from the solid to the liquid phase and that this leached palladium would become responsible for a significant part of the catalytic activity. To rule out the contribution of homogeneous catalysis in the results shown in Table 1, one reaction was carried out in the presence of the solid until the conversion was 46% and at that point the solid was filtered off at the reaction temperature. The liquid phase was then transferred to another flask containing K_2CO_3 and then again allowed to react, but no further significant conversion was observed (Fig. 1, 48% after

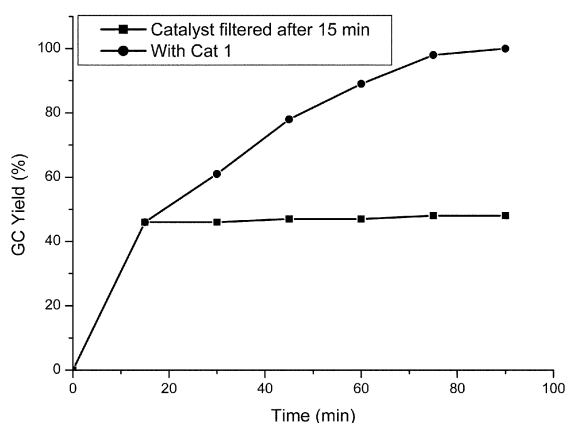


Fig. 1 Time conversion plot for the Suzuki reaction of bromobenzene and phenylboronic acid using K_2CO_3 as base and *o*-xylene as solvent in the presence of Cat 1 (●) and after removal of the catalyst (■) by filtration at the reaction temperature.

90 minutes). This indicates that no active species was present in the supernatant. The second point was the deactivation and reusability of the catalyst. To test this, a series of seven consecutive runs were carried out with the same sample (1st use: 100% after 90 min; 4th use: 95% after 150 min; 7th use: 97% after 180 min). This reusability demonstrates the high stability of the heterogeneous catalyst. Although no significant change in the activity of the catalyst was observed, we have performed surface analysis and simultaneous thermal analysis of Cat 1 after the 7th use in order to determine any change in the catalyst structure. Surface analysis shows that there is no significant change in the surface area (from 249.40 to 246.28 $m^2 g^{-1}$) and a slight increase in the total pore volume from 0.7130 to 0.7385

$cm^3 g^{-1}$. Simultaneous thermal analysis also shows the same weight loss after the 7th use as for the fresh catalyst. Clearly no significant restructuring of the catalyst has taken place on multiple use. There is a very little change from 0.1 to 0.098 $mmol g^{-1}$ of palladium loaded on the surface of the silica gel after 7 uses as measured by AAS.

Conclusion

In conclusion, we have reported a new silica supported palladium catalyst, which is more active than previously reported solid palladium catalysts. The catalyst which has a very low loading of palladium is completely heterogeneous and is highly stable under the reaction conditions. We describe the first use of a heterogeneous catalysis for consecutive Suzuki reactions *i.e.* synthesis of polyaryls in a single step.

Experimental

General

All reagents were purchased from Aldrich Chemical Company and Lancaster chemicals and used as received. The amount of palladium loaded on the surface of silica was determined by atomic absorption spectroscopy. The thermal analysis was performed using a Netzsch 409 STA with a temperature range of 10 °C min^{-1} . The presence of C–H and C=N bonds was confirmed by DRIFTS using a Bruker Equinox 55 FTIR spectrometer. The binding energy of palladium in the catalysts was determined by XPS using a Kratos AXIS HIS instrument equipped with a charge neutraliser and Mg K_{α} X-ray source. The pore size distribution and BET surface area were determined by using a Beckman Coulter SA 3100 porosimeter with dinitrogen as an adsorbate. Product yields were calculated by GC, using internal standards, using a Varian 3800 gas chromatograph fitted with a Varian 8200 autosampler and a CP-SIL8CB capillary column. The structure of the products was analysed by GC/GC-MS, NMR and comparison with authentic samples.

Catalyst preparation

Grafting of ligand structure on the surface of silica gel.

Activated silica (K100) (10 g) was added to a solution of aminopropyl(trimethoxy) silane (6.64 g, 3 mmol) in absolute ethanol (200 cm^3) and stirred at room temperature for 24 h. The aminopropyl silica (AMPS) was filtered, washed with ethanol and dried in air at 95 °C overnight. The oven dried aminopropyl silica (5 g) was added to absolute ethanol (100 cm^3) in a 250 cm^3 round bottomed flask followed by 2-acetylpyridine (0.605 g, 5 mmol). The reaction mixture was stirred at 60 °C for 24 h. The ligand-grafted silica was filtered at the reaction temperature and washed with ethanol thoroughly to remove unreacted 2-acetylpyridine. It was dried in air at 95 °C overnight.

Preparation of silica supported palladium catalyst (Cat 1).

The catalyst was prepared by stirring a mixture of modified silica (4 g) and palladium acetate (0.112 g, 0.5 mmol) in acetone (100 cm^3) at room temperature for 24 h. After stirring, the catalyst was filtered, washed with acetone till washings were colourless. It was dried in air at 95 °C overnight and then conditioned for a total of 30 h (3 × 3 h each refluxing in toluene, ethanol, acetonitrile and 1 × 3 h in xylene at 130 °C). The

catalyst was dried at 70 °C in a vacuum oven for 4 h before its use in the Suzuki reaction.

Catalyst testing

General procedure for the synthesis of biaryls. Aryl bromide (5 mmol), phenylboronic acid (8 mmol), potassium carbonate (10 mmol), dodecane (1 cm³, internal standard; for entry 2, tetradecane was used as internal standard) and the Cat 1 (0.2 g at 0.1 mmol Pd per gram) were stirred together in *o*-xylene (14 cm³) at 110 °C in an N₂ atmosphere for the appropriate time (Table 1). The samples were withdrawn periodically and analysed by GC/GC-MS. The isolated products were analysed by GC/GC-MS, NMR and compared with authentic samples.

General procedure for the synthesis of polyaryls. Dibromoarene or tribromoarene (2 mmol), phenylboronic acid (6 mmol for dibromo and 9 mmol for tribromoarene), tetradecane (1 cm³, internal standard), potassium carbonate (5 mmol for dibromo and 6.5 mmol for tribromoarene) and Cat 1 (0.2 g at 0.1 mmol of palladium per gram) were stirred together in *o*-xylene (12 cm³ for dibromo and 15 cm³ for tribromoarene) at 120 °C in an N₂ atmosphere for the appropriate time (Table 1). The samples were withdrawn periodically and analysed by GC/GC-MS. The solvent was removed on a rotary evaporator and, to the residue, hexane was added and kept in a refrigerator overnight. The products in the form of crystals were obtained by filtration and washing with hexane. In the case of entry 8, the product was obtained by passing the residue through a column of silica and elution with hexane–EtOAc: 9 : 1. The isolated products were analysed by GC/GC-MS, NMR and compared with authentic samples.

Acknowledgement

The authors thank the department of Science & Technology, Govt. of India for awarding a BOYSCAST fellowship to S. P.

The constant support and advice of the York Green Chemistry group is warmly acknowledged.

References

- 1 For a review, see: S. P. Stanforth, *Tetrahedron*, 1998, **54**, 263.
- 2 (a) A. Suzuki, *J. Organomet. Chem.*, 1999, **576**, 147; (b) A. Suzuki, in *Metal Catalyzed Cross-coupling Reactions*, ed. F. Diederich and P. J. Stang, Wiley-VCH, Weinheim, 1998; (c) H. Geissler in *Transition Metals for Organic Synthesis*, vol. 1, ed. M. Beller and C. Bolm, Wiley-VCH, Weinheim, 1998; (d) N. Miyaura and A. Suzuki, *Chem. Rev.*, 1995, **95**, 2457; (e) N. Miyaura, T. Yanagi and A. Suzuki, *Synth. Commun.*, 1981, **11**, 513.
- 3 (a) J. K. Shorrocks, J. H. Clark, K. Wilson and J. Chisem, *Org. Proc. Res. Dev.*, 2001, **5**, 249; (b) K. Okubo, M. Shirai and C. Yokoyama, *Tetrahedron Lett.*, 2002, **43**, 7115; (c) M. Lagasi and P. Moggi, *J. Mol. Catal. A: Chem.*, 2002, **182–183**, 61; (d) K. Wilson, A. F. Lee, D. J. Macquarrie and J. H. Clark, *Appl. Catal. A: Gen.*, 2002, **228**, 127; (e) K. A. Utting and D. J. Macquarrie, *Appl. Catal. A: Gen.*, 2002, **232**, 7; (f) S. Tanaka, F. Mizukami, S. Niwa, M. Toba, K. Maeda, H. Shimada and K. Kunimori, *Appl. Catal. A: Gen.*, 2002, **229**, 165.
- 4 A. Corma and H. Garcia, *Chem. Rev.*, 2002, **102**, 3879.
- 5 C. Baleizao, A. Corma, H. Garcia and A. Leyva, *Chem. Commun.*, 2003, 606.
- 6 E. B. Moberg, J. H. Clark and D. J. Macquarrie, *Green Chem.*, 2001, **3**, 23.
- 7 S. Paul and J. H. Clark, submitted for publication.
- 8 M. D. Watson, A. Fechtenkotter and K. Mullen, *Chem. Rev.*, 2001, **101**, 1267 and references cited therein.
- 9 (a) G. W. Gary and P. A. Winsor, *Liquid Crystals and Plastic Crystals*, John Wiley and Sons: New York, 1974, vol. 1.; (b) D. J. Schneider, D. A. Landis, P. A. Fleitz, C. J. Seliskar, J. M. Kaufman and R. N. Steppel, *Laser Chem.*, 1991, **11**, 49; (c) A. J. Heeger, *J. Phys. Chem. B*, 2001, **105**, 8475; (d) S.-M. Yang, J.-J. Shie, J.-M. Fang, S. K. Nandy, H.-Y. Chang, S.-H. Lu and G. Wang, *J. Org. Chem.*, 2002, **67**, 5208 and references cited therein.
- 10 S. Li, B. Wei, P. M. N. Low, H. K. Lee, T. S. A. Hor, F. Xue and T. C. W. Mak, *J. Chem. Soc., Dalton Trans.*, 1997, 1289.
- 11 A. Minato, K. Tamao, T. Hayashi, K. Suzuki and M. Kumada, *Tetrahedron Lett.*, 1980, **21**, 845.
- 12 M. Nakada, C. Miura, H. Nishiyama, F. Higashi and T. Mori, *Bull. Chem. Soc. Jpn.*, 1989, **62**, 3122.
- 13 B. Basu, P. Das, M. M. H. Bhuiyan and S. Jha, *Tetrahedron Lett.*, 2003, **44**, 3817.



One-pot desulfurization of light oils by chemical oxidation and solvent extraction with room temperature ionic liquids

Wen-Hen Lo,^{ab} Hsiao-Yen Yang^a and Guor-Tzo Wei^{*a}

^a Department of Chemistry and Biochemistry, National Chung Cheng University, Ming-Hsiung, Chia-Yi, 621 Taiwan. E-mail: chegtw@ccu.edu.tw; Fax: 886-5-2721040; Tel: 886-5-2428121

^b CPC Refining & Manufacturing Research Center, Chia-Yi, 600, Taiwan. E-mail: lowh@rmrc.gov.tw; Fax: 886-5-2294282; Tel: 886-5-2224171

Received 27th May 2003

First published as an Advance Article on the web 14th August 2003

We have investigated removing sulfur-containing compounds from light oils by a combination of both chemical oxidation and solvent extraction using the room temperature ionic liquids (RTILs), 1-butyl-3-methylimidazolium hexafluorophosphate (BMIM⁺PF₆⁻) and 1-butyl-3-methylimidazolium tetrafluoroborate (BMIM⁺BF₄⁻). In a one-pot operation, the sulfur-containing compounds in the light oils were extracted into RTILs and then S-oxidized (H₂O₂-acetic acid) to form the corresponding sulfones. The advantage of performing both extraction and oxidation of sulfur compounds from light oil simultaneously in RTILs is that this process increases the desulfurization yield by about an order of magnitude relative to that of merely extracting with RTILs. The room temperature ionic liquids can be recycled after workup and reused without any loss of activity.

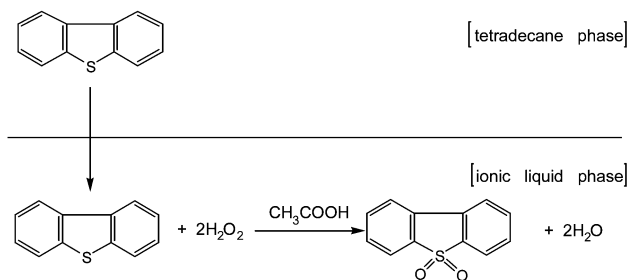
Introduction

The desulfurization of light oils attracts wide interest because sulfur compounds in these oils are converted by combustion to SO_x, which is a major source of acid rain and air pollution. To protect the environment against SO_x pollution, the European Union currently limits the sulfur level in light oil to 350 ppm and soon will restrict it further to 50 ppm.¹ The production of light oil having very low levels of sulfur is, therefore, an important challenge for oil refineries to meet strict regulatory requirements. The removal of sulfur compounds is carried out industrially by a catalytic hydrodesulfurization (HDS) method. It requires both high temperatures and high pressures of hydrogen gas to produce light oil having low levels of sulfur compounds. The efficiency of HDS is limited, however, to treat benzothiophenes (BTs) and dibenzothiophenes (DBTs), especially DBTs having alkyl substituents on their 4 and/or 6 positions.^{2,3}

Alternative desulfurization processes that operate under moderate conditions without requiring H₂ and catalysts have been extensively investigated, among which oxidative desulfurization (ODS) has drawn wide attention.^{4–17} ODS processes involve oxidizing sulfur compounds in a first step to transform them into sulfones,¹⁵ which are then removed by selective extraction with polar solvents, such as dimethyl sulfoxide (DMSO), in a second step.¹² Although these ODS processes are effective, one of the prime concerns is that a large amount of flammable and volatile organic compounds (VOCs) is required. The use of VOCs raises further environmental and safety concerns, such as emission losses and fire hazards.

RTILs have recently gained recognition as environmentally benign alternative solvents for separations, chemical synthesis, electrochemistry and catalysis.^{18–35} Generally, they are non-volatile, non-explosive, recyclable, easy to handle, and thermally robust. Therefore, RTILs are regarded as “green solvents”.^{36,37} The extractions of fuels using RTILs to remove sulfur compounds have been reported recently.^{13,38} The efficiencies of sulfur removal, however, are rather low and in the range 10–30%.³⁸ In this paper, we describe that a combination

of ODS and extraction with RTILs is an efficient method for the desulfurization of light oils. Tetradecane doped with DBT was used as a model light oil for the investigation of sulfur removal. The RTILs BMIM⁺PF₆⁻ and BMIM⁺BF₄⁻, which are immiscible with light oils, were selected as solvents for the liquid–liquid extraction systems. DBT was extracted from the model light oils and oxidized in the ionic-liquid phase, as is shown in Scheme 1.^{15,39,40} The effectiveness of this method for the



Scheme 1 Representative oxidation reaction of DBT using H₂O₂ and AcOH as the oxidizing agent in an oil–ionic liquid system.

desulfurization of light oils was studied and then the feasibility of regenerating the ionic liquid was examined.

Green Context

The versatility of ionic liquids is remarkable. We have become used to reading of their use as alternative reaction media but other applications are frequently being reported. Here they are used to facilitate the desulfurization of light oils. The ILs act as both extraction media for the organo-sulfur compounds and as oxidation environments for the conversion of those sulfur compounds to sulfones using the benign oxidant H₂O₂.

JHC

Results and discussion

Effect of RTILs on desulfurization of DBT in tetradecane

Desulfurization of model light oil was examined first. Fig. 1 displays the concentration of DBT remaining in tetradecane

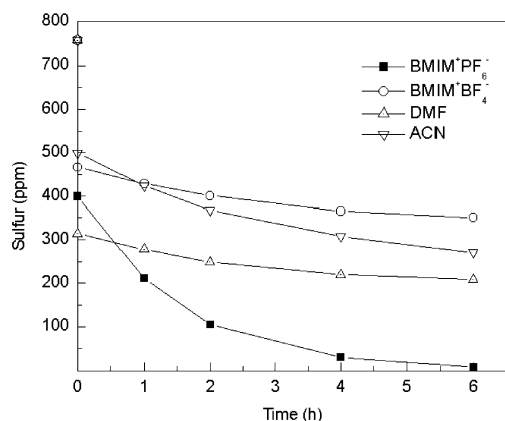


Fig. 1 Sulfur content remaining in model light oil as a function of time with different solvents in the ODS/extraction system.

during the ODS of the model light oil with various solvents as a function of reaction time. The data at time zero reflected the abilities of each solvent to extract DBT from tetradecane. The sulfur content of the model light oil decreased from its original value of 758 ppm to 314, 400, 466, and 499 ppm in DMF, BMIM+PF₆⁻, BMIM+BF₄⁻, and ACN, respectively. Thus, the amount of DBT in the model light oil that was extracted by BMIM+PF₆⁻ and BMIM+BF₄⁻ is 47 and 39%, respectively. In a combination of extraction and oxidation, DBT was oxidized in the solvent phase as it was extracted from tetradecane, and so a continuous decrease in the concentration of DBT in tetradecane was observed for each solvent during the oxidation process, as shown in Fig. 1. The concentration of DBT in tetradecane decreased rapidly when the oxidation was carried out in BMIM+PF₆⁻. In contrast, the concentration of DBT in tetradecane hardly decreased at all for the oxidation in the water-soluble polar solvents DMF, ACN and BMIM+BF₄⁻.

With DMF, ACN, and BMIM+BF₄⁻ as the solvents for ODS of the model light oil, biphasic systems were formed in which the oil layer was the upper phase and the solvent layer, along with oxidizing agents, was the lower phase. We attribute the lower desulfurization efficiency when using these solvents to the low rate of oxidation of DBT. The S-oxidation of DBT in hydrocarbon solvent has been studied in detail by Heimlich and Wallace, who found that the rate of DBT oxidation was first order with respect to acetic acid, second order with respect to hydrogen peroxide, and inversely proportional to the water concentration.⁴⁰ The high water content in BMIM+BF₄⁻ and polar solvents—a result of using aqueous H₂O₂ as oxidant—led to a low oxidation rate of DBT when it was extracted from the tetradecane phase. In contrast, when BMIM+PF₆⁻ was used as the solvent, a triphasic system was formed with the oil layer as the top phase, BMIM+PF₆⁻ as the bottom phase, and an aqueous layer in between. This state was formed because of the immiscibility of BMIM+PF₆⁻ with both the aqueous and tetradecane phases.⁴¹ The water content in BMIM+PF₆⁻ was relatively low and results in a higher rate of oxidation of DBT. This argument is further confirmed from direct oxidation of DBT in ionic liquids, as shown in Fig. 2. In this experiment, the same amount of DBT was dissolved in BMIM+PF₆⁻ and BMIM+BF₄⁻ and then oxidized with H₂O₂ and AcOH. The oxidation rate constants of DBT in BMIM+PF₆⁻ and BMIM+BF₄⁻ are 1.83 and 0.15 h⁻¹, respectively, by assuming it to be a first-order reaction because excesses of H₂O₂ and AcOH were employed.¹⁵

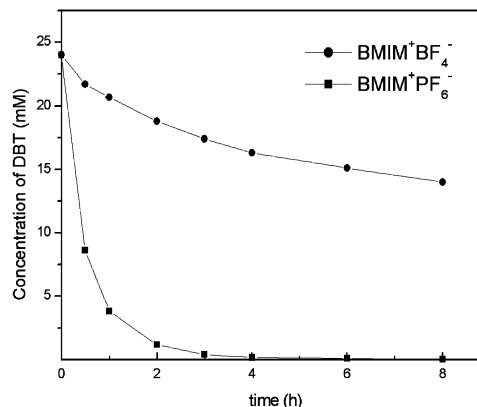


Fig. 2 Time course variation in concentration of DBT dissolved in various ionic liquids, during oxidation reaction.

Once DBT was oxidized chemically, the remaining DBT in the tetradecane phase was further extracted into the BMIM+PF₆⁻ phase because of the extractability of DBT by BMIM+PF₆⁻. Therefore, the concentration of DBT in the model light oil continued to decrease rapidly with increasing oxidation time (Fig. 1). In fact, after 6 h of oxidation the DBT content had decreased from 758 to 7.8 ppm, which means that *ca.* 99% of DBT was extracted from the model light oil. This experiment clearly indicates that a combination of chemical oxidation and solvent extraction in a water-immiscible ionic liquid has the potential to completely remove sulfur compounds from light oil. The results also demonstrate the advantage of this process over the desulfurization of light oil by mere solvent extraction with ionic liquids.^{13,38}

Desulfurization of light oil with room temperature ionic liquids

Next, we applied this oxidation/extraction system to an actual light oil containing a sulfur content of 8040 ppm. The light oil contains a large number of different DBTs and several other types of sulfur compound. Fig. 3 displays the sulfur content

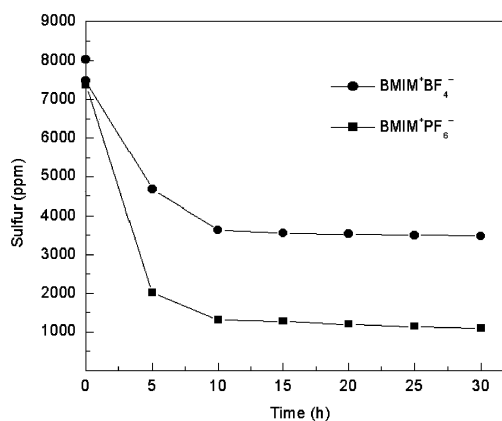


Fig. 3 The variation of sulfur content in light oil over time when combining oxidation and extraction with the room temperature ionic liquids system.

remaining in light oil as a function of time in the ODS/extraction system. The data at time zero indicate the equilibrium concentrations of sulfur compounds distributed between the two phases. We found that the RTILs display a rather low extractability (7–8%) of sulfur compounds from actual light oil when compared with model light oil (39–47%). Using the BMIM+BF₄⁻ extraction/oxidation system, however, resulted in the sulfur content decreasing from 8040 to 3640 ppm after 10 h. In the BMIM+PF₆⁻ extraction/oxidation system, an even larger

decrease of sulfur content was observed (from 8040 to 1300 ppm). After 5 h oxidation, the amounts of sulfur compounds that were removed from light oil were about 73 and 40% for BMIM⁺PF₆⁻ and BMIM⁺BF₄⁻, respectively. Therefore, the water-immiscible ionic liquid BMIM⁺PF₆⁻ not only offers a better desulfurization yield, but also a higher oxidation rate, when compared with BMIM⁺BF₄⁻. In both cases, the desulfurization rate of feed oil leveled off after 10 h of oxidation. The enhanced desulfurization obtained using BMIM⁺PF₆⁻ rather than BMIM⁺BF₄⁻ mirrors the findings when using the model light oil.

Light oil also contains a large quantity of aromatic hydrocarbons. To examine the effect of the oxidation/extraction process on the content of sulfur and aromatic compounds in light oil, Table 1 displays an analysis of the unoxidized and oxidized light oils that had been treated with different ionic liquids. The sulfur content of unoxidized light oil was 7370 and 7480 ppm in the presence of BMIM⁺PF₆⁻ and BMIM⁺BF₄⁻, respectively; after 10 h of oxidation and extraction, the sulfur content was reduced to 1300 and 3640 ppm, respectively. Thus, for a combination of oxidation and extraction with RTILs, the use of BMIM⁺BF₄⁻ and BMIM⁺PF₆⁻ increased the desulfurization yields from 7 to 55% and 8 to 84%, respectively. Each case represents an increase of roughly one order of magnitude in the yield of desulfurization of light oil when a combination of ODS and extraction with ionic liquid is used, when compared with merely extracting using the ionic liquid. Unfortunately, the desulfurization yield of light oil is lower than that of model light oil.

Besides the effect on the content of sulfur compounds, there was also a decrease in the concentration of aromatic compounds in the light oil after desulfurization of the feed light oils. This result was because the aromatic hydrocarbons are extracted to some extent into ionic liquid phases. During the oxidation process, some of the aromatic compounds in the light oils were oxidized.¹⁵ The extraction of aromatic hydrocarbons from the oxidized oil was more significant than that of the unoxidized light oil. This process leads to a larger reduction in the content of aromatic hydrocarbons, especially for two-ring aromatic compounds, in the light oil during the removal of sulfur compounds.

Regeneration/recycling of the ionic liquids

We examined the possibility of recycling the ionic liquids. At the end of each run the oxidation product and extracted substrates in the ionic liquids were washed out with water, then the ionic-liquid phase was filtered, the volatiles were evaporated, and the residue extracted with diethyl ether. ¹H NMR spectroscopy confirmed that the purity of BMIM⁺PF₆⁻ and BMIM⁺BF₄⁻ was retained. The system was charged again with the oxidizing agent (H₂O₂ and AcOH) and the desulfurization yields of 85 and 55% for BMIM⁺PF₆⁻ and BMIM⁺BF₄⁻, respectively, were maintained after four cycles of operation.

Conclusions

We have employed a combination of chemical oxidation and solvent extraction in a one-pot operation using RTILs for the effective desulfurization of light oil. In this process, both an environmentally benign oxidation system (H₂O₂ and AcOH) and extraction solvent (RTILs) are employed. RTILs have several advantages over polar organic solvents, such as that they can be used over a wider temperature range and are compatible with oxidizing agents. More general advantages are that ionic liquids have no measurable vapor pressure, they are thermally stable, and they tolerate moisture. Chemical oxidation in conjunction with ionic liquid extraction improves the yield of desulfurization of light oil. The water-immiscible ionic liquid BMIM⁺PF₆⁻ was found to be a more-effective solvent than the water-soluble BMIM⁺BF₄⁻ for providing an environment that results in a higher rate of chemical oxidation. A further advantage of this approach is that the ionic liquids can be recycled after workup.

Experimental

Preparation of ionic liquids

Preparation of BMIM⁺BF₄⁻ and BMIM⁺PF₆⁻. The ionic liquids were prepared by a literature procedure.³⁰ 1-Butyl-3-methylimidazolium chloride was prepared by adding equimolar amounts of 1-methylimidazole and chlorobutane to a round-bottom flask fitted with a reflux condenser and then reacting them at 70 °C for 48–72 h. The resulting viscous liquid was cooled to room temperature and then washed three times with ethyl acetate. The remaining ethyl acetate was removed by rotary evaporation. The residue was added to acetone (200 mL), an equimolar amount of the appropriate salt (NaBF₄ or KPF₆) was added, and the mixture was stirred at room temperature for 24 h. The resulting precipitate of NaCl or KCl was then filtered off, and the solvent was removed by rotary evaporation to leave a yellowish liquid.

The desulfurization procedure

Desulfurization of the model light oil was carried out as follows: dibenzothiophene (0.044 g) was dissolved in tetradecane (10 mL) and then an extracting solvent (10 mL) was added. The mixture was stirred and heated to 70 °C. H₂O₂ (30%, 2.72 mL) and AcOH (0.72 mL) were added carefully to the mixture, which was then stirred vigorously. The upper phase (tetradecane) was periodically withdrawn and analyzed for sulfur content. The content of all sulfur compounds present in the oil was determined with an Antek pyroreactor 771, which was equipped with an Antek UV fluorescence detector 714.

Oxidation of DBT in ionic liquids was carried out as follows: each ionic liquid (5 mL) containing dibenzothiophenes (0.022 g) was mixed carefully with H₂O₂ (30%, 1.36 mL) and AcOH

Table 1 Content of aromatic and sulfur compounds in light oil before and after contact with ionic liquids

Sample		Saturated hydrocarbon (vol%)	One-ring aromatics (vol%)	Two-ring aromatics (vol%)	Sulfur content (ppm)	Desulfurization yield (%)
Feed (light oil)	Before contact	78.8	15.5	5.7	8040	
Unoxidized feed ^a	With BMIM ⁺ BF ₄ ⁻	78.9	15.5	5.6	7480	7
Oxidized feed ^b	With BMIM ⁺ BF ₄ ⁻	80.1	15.3	4.6	3640	55
Unoxidized feed ^a	With BMIM ⁺ PF ₆ ⁻	80.1	15.2	4.7	7370	8
Oxidized feed ^b	With BMIM ⁺ PF ₆ ⁻	83.8	14.4	1.8	1300	85

^a No oxidation reagents. ^b With oxidation reagents added to the extraction system.

(0.36 mL). The resulting mixture was then stirred vigorously and heated at 70 °C. The solution was removed and analyzed by reversed-phase HPLC (Shimadzu LC-6A equipped with a spectrophotometric detector SPD-6A) with detection at 241 nm.

Desulfurization of light oil was carried out as follows: light oil (10 mL) was mixed with an ionic liquid (10 mL), and then 30% H₂O₂ (7 mL) and AcOH (2.5 mL) were added. The mixture was stirred at 70 °C. After settling, the concentration of sulfur compounds in the light oil was measured. The total contents of saturated hydrocarbon and one- and two-ring aromatic hydrocarbons in the light oil were analyzed by reversed-phase HPLC (Shimadzu LC-6A equipped with a refractive-index detector RID-6A).

Recovery/regeneration of used ionic liquids

The light oil was separated by decantation from the solution of the ionic liquid. An equal volume of water was added to the solution of the ionic liquid and some precipitate was removed either by filtration or by centrifuge. The water and oxidizing agent were then evaporated from the ionic liquid phase at 100 °C for 3 h by rotary evaporation. The residue was then extracted three times with an equal volume of diethyl ether to recover the ionic liquid for reuse. Analysis of the ionic liquid by ¹H NMR spectroscopy (Varian Inova 500-MHz NMR spectrometer) indicated that its purity was retained.

Acknowledgments

We thank National Chung Cheng University and the National Science Council, Taiwan, for supporting this research financially (grant NSC91-2113-M-194-021), and Professor I. W. Sun, Department of Chemistry, National Cheng Kung University, for his help in the preparation of the ionic liquids.

References

- 1 <http://w3.epa.gov.tw/epalaw/index.htm>.
- 2 X. Ma, K. Sakanishi and I. Mochida, *Ind. Eng. Chem. Res.*, 1994, **33**, 218.
- 3 T. Kabe, A. Ishihara and H. Tajima, *Ind. Eng. Chem. Res.*, 1992, **31**, 1577.
- 4 T. Aida, *EP Pat.*, 565,324, 1993.
- 5 W. Gore, S. Bonde, G. E. Dolbear and E. R. Skov, *US Pat.*, 0,035,306, 2002.
- 6 A. S. Rappas, V. P. Vincent and S. J. DeCanio, *US Pat.*, 0,029,997, 2002.
- 7 R. C. Schucker, *US Pat.*, 6,338,788, 2002.
- 8 A. Attar and W. H. Corcoran, *Ind. Eng. Chem. Proc. Res. Dev.*, 1978, **17**, 102.
- 9 P. S. Tam, J. R. Kettrel and J. W. Eldridge, *Ind. Eng. Chem. Res.*, 1990, **29**, 321.
- 10 F. Zannikos, E. Lois and S. Stournas, *Fuel Process. Technol.*, 1995, **42**, 35.
- 11 F. M. Collins, A. R. Lucy and C. Sharp, *J. Mol. Catal. A: Chem.*, 1997, **117**, 397.
- 12 S. Otsuki, T. Nonaka, N. Takashima, W. Qian, A. Ishihara, T. Imai and T. Kabe, *Energy Fuels*, 2000, **14**, 1232.
- 13 A. Bösmann, L. Datsevich, A. Jess, A. Lauter, C. Schmitz and P. Wasserscheid, *Chem. Commun.*, 2001, 2495.
- 14 V. Hulea, F. Fajula and J. Bousquet, *J. Catal.*, 2001, **198**, 179.
- 15 Y. Shiraishi, K. Tachibana, T. Hirai and I. Komasa, *Ind. Eng. Chem. Res.*, 2002, **41**, 4362.
- 16 I. V. Babich and J. A. Moulijn, *Fuel*, 2003, **82**, 607.
- 17 H. Mei, B. W. Mei and T. F. Yeh, *Fuel*, 2003, **82**, 4015.
- 18 J. S. Wilkes and M. J. Zaworotko, *J. Chem. Soc., Chem. Commun.*, 1992, 965.
- 19 P. A. Z. Suarez, J. E. L. Dullius, S. Einloft, R. F. de Souza and J. Dupont, *Polyhedron*, 1996, **15**, 1217.
- 20 C. J. Adams, M. J. Earle, G. Roberts and K. R. Seddon, *Chem. Commun.*, 1998, 2097.
- 21 P. J. Dyson, D. J. Ellis, D. G. Parker and T. Welton, *Chem. Commun.*, 1999, 25.
- 22 S. Toma, B. Gotov, I. Kmentova and E. Solcaniova, *Green Chem.*, 2000, **2**, 149.
- 23 C. E. Song and E. J. Roh, *Chem. Commun.*, 2000, 837.
- 24 J. N. Rosa, C. A. M. Afonso and A. G. Santos, *Tetrahedron*, 2001, **57**, 4189.
- 25 D. J. Bauer, K. W. Kottsieper, C. Liek, O. Stelzer, H. Waffenschmidt and P. Wasserscheid, *J. Organomet. Chem.*, 2001, **630**, 177.
- 26 S. T. Handy and X. Zhang, *Org. Lett.*, 2001, **3**, 233.
- 27 F. Favre, H. Olivierbourbigou, D. Commereuc and L. Saussine, *Chem. Commun.*, 2001, 1360.
- 28 J. G. Huddleston, H. D. Willauer, R. P. Swatloski, A. E. Visser and R. D. Rogers, *Chem. Commun.*, 1998, 1765.
- 29 L. A. Blanchard, D. Hancut, E. J. Beckman and J. F. Brennecke, *Nature*, 1999, **399**, 28.
- 30 D. W. Armstrong, L. He and Y.-S. Liu, *Anal. Chem.*, 1999, **71**, 3873.
- 31 S. Dai, Y. H. Ju and C. E. Barnes, *J. Chem. Soc., Dalton Trans.*, 1999, 1201.
- 32 E. G. Yanes, S. R. Gratz, M. J. Baldwin, S. E. Robison and A. M. Stalcup, *Anal. Chem.*, 2001, **73**, 3838.
- 33 A. E. Visser, R. P. Swatloski, S. T. Griffin, D. H. Hartman and R. D. Rogers, *Sep. Sci. Technol.*, 2001, **36**, 785.
- 34 G.-T. Wei, Z. Yang and C.-J. Chen, *Anal. Chim. Acta*, 2003, **488**, 183.
- 35 I. W. Sun and C. L. Hussey, *Inorg. Chem.*, 1989, **28**, 2731.
- 36 K. P. Stephen, *Chem. Eng. News*, 2001 (July 16), **79**, 27.
- 37 P. Wasserscheid, R. V. Hal and A. Bösmann, *Green Chem.*, 2002, **4**, 400.
- 38 S. Zhang and Z. C. Zhang, *Green Chem.*, 2002, **4**, 376.
- 39 K. Yazu, Y. Yamamoto, T. Furuya, K. Miki and K. Ukegawa, *Energy Fuels*, 2001, **15**, 1535.
- 40 B. N. Heimlich and T. J. Wallace, *Tetrahedron*, 1966, **22**, 3571.
- 41 J. G. Huddleston, A. E. Visser, W. M. Reichert, H. D. Willauer, G. A. Broker and R. D. Rogers, *Green Chem.*, 2001, **3**, 156.



Palladium-catalysed aminocarbonylation of steroidal 17-iodo-androst-16-ene derivatives in *N,N'*-dialkyl-imidazolium-type ionic liquids

Rita Skoda-Földes,^{*a} Eszter Takács,^a Judit Horváth,^b Zoltán Tuba^b and László Kollár^c

^a University of Veszprém, Department of Organic Chemistry and Research Group for Petrochemistry of the Hungarian Academy of Sciences, Wartha V. u. 1. (P.O.Box 158), H-8200 Veszprém, Hungary. E-mail: skodane@almos.vein.hu; Fax: 36-88-427492; Tel: 36-88-422022

^b Chemical Works of Gedeon Richter Ltd., Budapest, Hungary

^c University of Pécs, Department of Inorganic Chemistry and Research Group for Chemical Sensors of the Hungarian Academy of Sciences, Ifjúság u. 6. (P.O.Box 266), H-7624 Pécs, Hungary

Received 29th May 2003

First published as an Advance Article on the web 19th August 2003

The use of [bmim][BF₄]⁻, [bmim][PF₆]⁻ and [emim][PF₆]⁻ ionic liquids as solvents in homogeneous catalytic aminocarbonylation of 17-iodo-5 α -androst-16-ene at atmospheric carbon monoxide pressure has been investigated. It has been proved that after the extraction of the product with toluene, the ionic liquid–catalyst mixture could be recycled several times. Although there was a loss of catalytic activity in the further cycles, even 94% conversion can be achieved after the fifth run by using [bmim][BF₄]⁻ ionic liquid. The conversion depended strongly both on the properties of the ionic liquid and those of the catalyst. The activities of the *in situ* palladium(0) catalysts prepared from Pd(OAc)₂ and various phosphine ligands (PPh₃, TPPTS, DPPBA) have been compared. The method can be effectively used for the aminocarbonylation of other steroids with 17-iodo-16-ene functionality.

Introduction

Homogeneous catalysis may serve as an attractive tool in organic synthesis due to the mild reaction conditions, high activity and selectivity of the catalysts. The main drawback is in the difficulty of product separation and catalyst recovery.

Several methods have been developed in order to overcome this problem: the use of various two-phase systems,¹ supported catalysts,² aqueous/organic media,³ and alternative solvents like supercritical fluids,⁴ fluorosolvents⁵ and ionic liquids.⁶ Homogeneous catalysis carried out in ionic liquids drew particular attention in the last few years and several examples for various palladium catalysed reactions carried out in ionic liquids have been published: *e.g.* Heck-, Sonogashira-, Suzuki-coupling, allylic alkylation, oxidation, polymerisation, amidocarbonylation, hydroesterification, alkoxy carbonylation.⁶ At the same time, to the best of our knowledge there is only one example for the palladium catalysed aminocarbonylation of organic halides in ionic liquids.⁷ Mizushima and his coworkers carried out the aminocarbonylation of iodobenzene in [bmim][PF₆]⁻ ionic liquid at 5–40 bar CO pressure. A mixture of the mono- and the double carbonylated products has been obtained. The Pd(OAc)₂ + PPh₃ *in situ* catalyst could be reused twice, with a combined yield of the two products of 57% in the third run.

In recent years we examined various carbonylation reactions of steroidal alkenyl iodides.⁸ These reactions raised several problems. Because of the relatively low reactivity of steroidal substrates a high catalyst/substrate ratio should be used. Recycling of the catalyst is also problematic: water/organic solvent systems cannot be used because of the side reaction with water leading to the corresponding steroidal carboxylic acid and anhydride.⁹ Products cannot be separated by distillation, several repetitive chromatographic separations are needed for the

complete removal of the catalyst, which is essential for compounds of pharmaceutical interest.

We found recently, that homogeneous catalytic aminocarbonylation of steroidal substrates can be effectively carried out in ionic liquids as solvents even at atmospheric CO pressure using various palladium–phosphine catalytic systems. In this paper the applicability and the possible recycling of the palladium catalyst/ionic liquid system will be discussed.

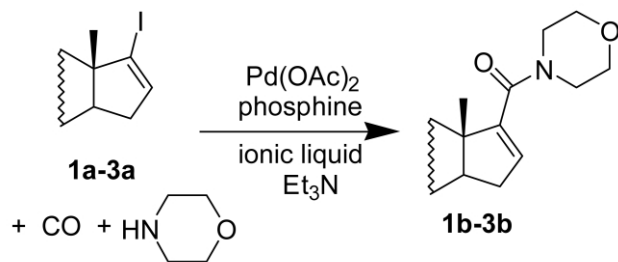
Results and discussion

Carbonylation of 17-iodo-5 α -androst-16-ene (**1a**) in the presence of morpholine as the nucleophile has been chosen as the model reaction (Scheme 1). It should be mentioned that the reaction was completely selective in all cases, besides amide **1b** no other products were detected.

Green Context

The use of Pd catalysts to effect a number of transformations cleanly. Recovery of the catalyst, particularly where high quantities are required, is a pressing problem, which is approached here by the use of ionic liquids. Steroidal iodides are here smoothly converted to the corresponding amides *via* carbonylation reactions in ionic liquids. The product is then separated from the solvent/catalyst mix, which can be successfully recycled. It is important to use non-coordinating anions in the ionic liquid – simple halides destroy the catalytic activity rapidly.

DJM



Scheme 1 Carbonylation of 17-iodo-androst-16-ene derivatives **1a–3a**.

The first experiments were carried out in the presence of the *in situ* Pd(OAc)₂ + 2 PPh₃ catalytic system, that had been successfully employed in various carbonylation reactions of this steroidal substrate before.⁸

As a molten salt, Bu₄NBr has been reported to be a suitable solvent for palladium-catalysed butoxycarbonylation of aryl halides even at atmospheric pressure,¹⁰ this medium was our first choice. Although the reaction was complete within 2 h, the relatively good solubility of Bu₄NBr in those organic solvents that solve the product, made product separation impossible.

No reaction was observed in ionic liquids with halide anions like [emim]⁺I[−], [bmim]⁺Cl[−] (emim: 1-ethyl-3-methylimidazolium, bmim: 1-butyl-3-methylimidazolium). This phenomenon might be explained by the formation of palladium–carbene complexes by the reaction of Pd(OAc)₂ and the ionic liquid, as it has been shown by Xiao *et al.*¹¹ Even more likely, since these complexes have found active catalysts *e.g.* for Heck reactions, the anion effect has to be considered. That is, the halide (iodide, chloride) coordination might deactivate the catalyst.

At the same time carbonylation could be carried out smoothly in ionic liquids containing noncoordinating anions like [emim]⁺[PF₆][−], [bmim]⁺[PF₆][−] and [bmim]⁺[BF₄][−] (Table 1.).

A high loss of activity was observed in the case of the Pd(OAc)₂ + 2 PPh₃ — [bmim]⁺[PF₆][−] system after the first run (Entry 1). The ¹H-NMR investigation of the toluene extract showed the presence of a considerable amount of PPh₃ and OPPh₃, which was highly dependent on the bulk of toluene used. The phosphine loss could be minimised at 25% of the phosphine supplied at the beginning of the reaction. Upon

addition of a further 2 equivalents of PPh₃ per palladium in each run, the activity was increased considerably (Entry 2). The PPh₃ and OPPh₃ content of the extracts was in the same range as in the first experiment. Reaction times were not optimised, but their considerable decrease led to smaller conversions after the first run.

Among the three ionic liquids, the use of [bmim]⁺[BF₄][−] was found to be the most effective: a 76% conversion was obtained even in the fifth run (Entry 4).

Although the activity of the Pd(OAc)₂ + 2 TPPTS catalytic system (TPPTS: triphenylphosphine-3,3',3''-trisulfonic acid trisodium salt) was much lower (Entry 5) than that containing PPh₃, according to the ¹H-NMR investigations no leaching of the phosphine into the extract was observed. Here also, the ionic liquid [bmim]⁺[BF₄][−] was found to be superior to the other two (Entry 7). A catalyst with higher activity and with no phosphine-leaching was obtained using 4-(diphenylphosphino)-benzoic acid (DPPBA) as ligand, but conversion dropped again to 57% in the third run (Entry 8). In the case of these polar ligands, a further supply of ligand in subsequent runs led only to minor improvement.

Comparing the results obtained with phosphine ligands of different polarity, no correlation was found between phosphine-leaching and the loss of activity in the subsequent runs. Besides, the palladium-content of the toluene extracts obtained in the first run was usually higher (10–12% of the original supply) than that of the second (3–6% of the original supply). As the role of the phosphine is twofold: it reduces Pd(OAc)₂ into the catalytically active Pd(0) complex¹² while the remainder serves as a ligand, it was possible that the relatively low ligand/palladium ratio led to the formation of inactive palladium–carbonyl complexes.¹³ In order to avoid this, phosphine/palladium ratio was increased in the first run without supplying any loss in the further runs. As a result, a high increase in the conversion was observed using a sixfold excess of ligand compared to palladium in the case of all the three ligands (Entries 12, 14, 15). At the same time, the palladium-content of the toluene extracts decreased to some extent, but it was higher again in the first run (6–7% of the original supply, compared to 3–4% in the second run). A further increase in the phosphine/palladium ratio did not alter the results considerably using TPPTS or DPPBA ligands, and even led to a loss of activity in

Table 1 Carbonylation of steroids in ionic liquids using Pd(OAc)₂ + phosphine *in situ* catalysts^a

Entry	Substrate	Ionic liquid	Phosphine	P/Pd	Conversion (%)				
					Run 1	Run 2	Run 3	Run 4	Run 5
1	1a	[bmim] ⁺ [PF ₆] [−]	PPh ₃	2	100	47	—	—	—
2 ^b	1a	[bmim] ⁺ [PF ₆] [−]	PPh ₃	2	100	79	67	51	—
3 ^b	1a	[emim] ⁺ [PF ₆] [−]	PPh ₃	2	100	64	54	—	—
4 ^b	1a	[bmim] ⁺ [BF ₄] [−]	PPh ₃	2	100	98	95	91	76
5	1a	[bmim] ⁺ [PF ₆] [−]	TPPTS	2	67	58	42	—	—
6	1a	[emim] ⁺ [PF ₆] [−]	TPPTS	2	52	40	—	—	—
7	1a	[bmim] ⁺ [BF ₄] [−]	TPPTS	2	94	71	49	—	—
8	1a	[bmim] ⁺ [PF ₆] [−]	DPPBA	2	100	87	57	—	—
9	1a	[bmim] ⁺ [PF ₆] [−]	PPh ₃	4	100	81	57	—	—
10	1a	[bmim] ⁺ [PF ₆] [−]	TPPTS	4	67	57	—	—	—
11	1a	[bmim] ⁺ [PF ₆] [−]	DPPBA	4	100	90	59	—	—
12	1a	[bmim] ⁺ [PF ₆] [−]	PPh ₃	6	100	100	95	93	82
13	1a	[bmim] ⁺ [BF ₄] [−]	PPh ₃	6	100	100	99	98	94
14	1a	[bmim] ⁺ [PF ₆] [−]	TPPTS	6	97	92	82	72	—
15	1a	[bmim] ⁺ [PF ₆] [−]	DPPBA	6	100	96	94	91	70
16	1a	[bmim] ⁺ [PF ₆] [−]	PPh ₃	10	94	65	57	—	—
17	1a	[bmim] ⁺ [PF ₆] [−]	TPPTS	10	99	91	76	71	—
18	1a	[bmim] ⁺ [PF ₆] [−]	DPPBA	10	100	97	96	95	73
19	1a	[bmim] ⁺ [BF ₄] [−]	DPPBA	10	100	100	100	99	87
20	2a	[bmim] ⁺ [BF ₄] [−]	DPPBA	10	100	100	100	—	—
21	3a	[bmim] ⁺ [BF ₄] [−]	DPPBA	10	98	95	85	—	—

^a Reaction conditions: ionic liquid (600 mg), **1** (0.2 mmol), Pd(OAc)₂ (0.01 mmol), the phosphine (as indicated), Et₃N (0.1 ml) and morpholine (0.1 ml) were heated in CO atmosphere for 8 h at 100 °C. ^b 2 eq PPh₃ was added in each run.

case of PPh_3 (Entries 16–18). The use of $[\text{bmim}]^+[\text{BF}_4]^-$ as solvent was again more advantageous (compare entries 12–13 or 18–19).

Other steroidal substrates (**2a** and **3a**) could also be converted into the corresponding amides in ionic liquids (entries 20,21). In the successive runs no loss of activity was observed in the reaction of **2a**. The use of **3a** gave poorer results.

In conclusion, we have shown that aminocarbonylation of steroidal alkenyl iodide **1a** can be carried out in ionic liquids even at atmospheric carbon monoxide pressure. The optimisation of the phosphine–ionic liquid system and the ligand/palladium ratio makes it possible to recycle the ionic liquid–catalyst mixture with a small loss of activity. The extraction of the steroidal components leads to a crude product with only traces of phosphine impurities when phosphine ligands with polar groups are used.

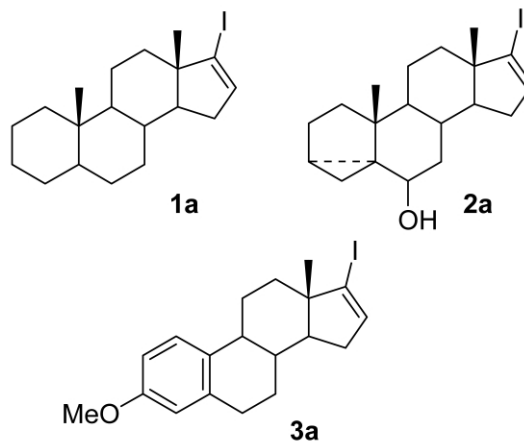


Fig. 1 17-iodo-androst-16-ene derivatives used as substrates.

Experimental

In a typical procedure, the steroidal alkenyl iodide (0.2 mmol), $\text{Pd}(\text{OAc})_2$ (0.01 mmol), PPh_3 (0.02 mmol) and 600 mg $[\text{bmim}]^+[\text{PF}_6]^-$ were placed in a Schlenk-tube equipped with a magnetic stirrer, a septum inlet and a reflux condenser with a balloon on the top. It was placed under carbon monoxide, and Et_3N (0.1 ml) and morpholine (0.1 ml) was added. The reaction mixture was heated at 100°C for 8 h. The mixture was extracted twice with 400 μl toluene. Any volatiles were removed from the ionic liquid *in vacuo* and new load of starting materials (steroid, Et_3N and morpholine) for the next catalytic run were added to the ionic liquid/catalyst mixture and the atmosphere was changed to carbon monoxide. The consecutive runs were conducted for the same reaction time.

Spectroscopic data for **1b**: $^1\text{H-NMR}$ δ : 5.65(s, 1H); 3.58 (m, 8H); 2.22–0.72 (m, 22H, ring protons); 1.00 (s, 3H); 0.80 (s, 3H). $^{13}\text{C-NMR}$ δ : 168.2; 148.5; 131.0; 67.1; 56.9; 55.3; 48.8; 47.3; 38.5; 36.5; 34.4; 33.9; 32.2; 32.1; 29.0; 28.9; 26.8; 22.1; 20.6; 16.8; 12.2. MS m/z 371 (M^+)/70; 356/100; 285/28; 257/30; 114/48; 105/43; 91/58; 67/58; 55/47. Analysis calculated for $\text{C}_{24}\text{H}_{37}\text{NO}_2$ (371.56): C, 77.58; H, 10.04; N, 3.77; Found: C, 77.42; H, 10.11; N, 3.69.

Spectroscopic data for **2b**: $^1\text{H-NMR}$ δ : 5.72(s, 1H); 3.62 (m, 8H); 3.25(m, 1H); 2.30–0.70 (m, 17H, ring protons); 1.07 (s, 3H); 1.06 (s, 3H); 0.52 (m, 1H); 0.29 (m, 1H). MS m/z 367 ($\text{M}^+ - \text{H}_2\text{O}$)/69; 352/55; 281/20; 114/61; 105/84; 91/100. Analysis calculated for $\text{C}_{24}\text{H}_{35}\text{NO}_3$ (385.55): C, 74.77; H, 9.15; N, 3.63; Found: C, 74.95; H, 9.37; N, 3.77.

Spectroscopic data for **3b**: $^1\text{H-NMR}$ δ : 7.19(d, 7.2 Hz, 1H); 6.71(dd, 7.2 Hz, 1.5 Hz, 1H); 6.62(d, 1.5 Hz, 1H); 5.77(s, 1H); 3.75(s, 3H); 3.65 (m, 8H); 3.0–1.20 (m, 13H, ring protons); 1.05 (s, 3H). MS m/z 381 (M^+)/74; 366/36; 295/22; 173/89; 147/92; 121/100; 91/78; 56/59. Analysis calculated for $\text{C}_{24}\text{H}_{31}\text{NO}_3$ (381.52): C, 75.56; H, 8.19; N, 3.67; Found: C, 75.22; H, 8.36; N, 3.51.

Acknowledgements

The authors thank the Hungarian National Science Foundation (OTKA T-035047, T-032111, TS-044800, TS 044742) for the financial support.

References

- 1 F. Joó, Biphase Catalysis—Homogeneous, in *Encyclopedia of Catalysis*, ed. I. T. Horváth, J. Wiley & Sons, Inc., 2002, vol. 1, pp. 737–805.
- 2 P. Panster and S. Wieland, *Applied Homogeneous Catalysis with Organometallic Compounds*, ed. B. Cornils and W. A. Herrmann, Wiley-VCH, Weinheim, 1996, pp. 605–623.
- 3 *Aqueous-Phase Organometallic Catalysis. Concepts and Applications*, ed. B. Cornils and W. A. Herrmann, Wiley-VCH, Weinheim, 1998.
- 4 P. G. Jessop, T. Ikariya and R. Noyori, *Chem. Rev.*, 1999, **99**, 475.
- 5 I. T. Horváth, *Acc. Chem. Res.*, 1998, **31**, 641; L. P. Barthel-Rosa and J. A. Gladysz, *Coord. Chem. Rev.*, 1999, **190–192**, 587.
- 6 T. Welton, *Chem. Rev.*, 1999, **99**, 2071; C. M. Gordon, *Appl. Catal. A: General*, 2001, **222**, 101; H. Olivier-Bourbigou and L. Magna, *J. Mol. Catal. A*, 2002, **182–183**, 419; D. Zhao, M. Wu, Y. Kou and E. Min, *Catal Today*, 2002, **74**, 157; W. Keim, *Green Chem.*, 2003, **5**, 105.
- 7 E. Mizushima, T. Hayashi and M. Tanaka, *Green Chem.*, 2001, **3**, 76.
- 8 R. Skoda-Földes, Zs. Szarka, L. Kollár, Z. Dinya, J. Horváth and Z. Tuba, *J. Org. Chem.*, 1999, **64**, 2134; Zs. Szarka, R. Skoda-Földes, L. Kollár, J. Horváth and Z. Tuba, *Synth. Commun.*, 2000, **30**, 1945; Zs. Szarka, R. Skoda-Földes, L. Kollár, Z. Berente, J. Horváth and Z. Tuba, *Tetrahedron*, 2000, **56**, 5253; R. Skoda-Földes, Z. Székely, L. Kollár, Z. Berente, J. Horváth and Z. Tuba, *Tetrahedron*, 2000, **56**, 3415.
- 9 R. Skoda-Földes, Z. Csákai, L. Kollár, G. Szalontai, J. Horváth and Z. Tuba, *Steroids*, 1995, **60**, 786.
- 10 V. Calò, P. Giannocaro, A. Nacci and A. Monopoli, *J. Organomet. Chem.*, 2002, **645**, 152.
- 11 L. Xu, W. Chen and J. Xiao, *Organometallics*, 2000, **19**, 1123.
- 12 C. Amatore, A. Jutand and M. A. M'Barki, *Organometallics*, 1992, **11**, 3009.
- 13 M. Beller, W. Mägerlein, A. F. Indolese and C. Fischer, *Synthesis*, 2001, 1098.



An efficient and green procedure for the preparation of acylals from aldehydes catalyzed by $\text{Fe}_2(\text{SO}_4)_3 \cdot x\text{H}_2\text{O}$

Xinying Zhang,* Lingjun Li and Guisheng Zhang

School of Chemical and Environmental Sciences, Key Laboratory of Environmental Science and Engineering for Colleges and Universities of Henan Province, Henan Normal University, Xixiang, Henan 453002, P. R. China. E-mail: xyzh518@sohu.com

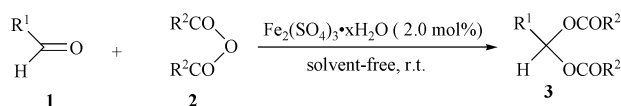
Received 22nd May 2003

First published as an Advance Article on the web 21st August 2003

The utilization of $\text{Fe}_2(\text{SO}_4)_3 \cdot x\text{H}_2\text{O}$ as a heterogeneous catalyst, at ambient temperature, under solvent-free conditions is described for the efficient preparation of *gem*-dicarboxylates (acylals). The preparation procedure presented is operationally simple, environmentally benign and has the advantage of enhanced atom utilization. Furthermore, the catalyst can be recovered simply and reused efficiently without any activation.

Introduction

Conversion of aldehydes into their corresponding *gem*-dicarboxylates is gaining importance in organic synthesis. This is partly due to the stability of *gem*-dicarboxylates in neutral as well as in moderate acidic media,¹ which makes acylals complementary to acetals as carbonyl protecting groups.² In addition, *gem*-dicarboxylates are also important starting materials in organic synthesis, especially for the preparation of acyloxydienes and vinyl acetates in Diels–Alder reactions.³ As a result, many methods have been examined for this transformation and they usually necessitate the use of strong protic acids, such as H_2SO_4 ,^{4a} $\text{CH}_3\text{SO}_3\text{H}$ ^{4b} and H_3PO_4 ,^{4c} or Lewis acids, such as ZnCl_2 ^{5a} and PCl_3 ^{5b} as catalysts. Recently, $\text{Sc}(\text{OTf})_3$,^{6a} I_2 ,^{6b} NBS ,^{6c} LiBF_4 ^{6d} and WCl_5 ^{6e} have also been employed for this purpose. However, these methods have not been entirely satisfactory because the use of conventional Brønsted or Lewis acid catalysts as well as excess organic solvents usually entails the problems of corrosiveness, tedious work-up and effluent pollution. Therefore, there are still genuine needs for the development of efficient and environmentally benign catalytic methods for this transformation by using inexpensive and non-polluting reagents. As a continuation of our research work in using $\text{Fe}_2(\text{SO}_4)_3 \cdot x\text{H}_2\text{O}$ as a mild, efficient and heterogeneous Lewis acid in organic synthesis,^{7a,b} herein we wish to report an efficient and green procedure for the conversion of aldehydes into *gem*-diacetates catalyzed by hydrated ferric sulfate (shown in Scheme 1).



R^1 = aromatic or aliphatic group

R^2 = CH_3 , CH_3CH_2

Scheme 1

Results and discussion

When a mixture of benzaldehyde (**1a**, 10 mmol), acetic anhydride (12 mmol) and a catalytic amount of $\text{Fe}_2(\text{SO}_4)_3 \cdot x\text{H}_2\text{O}$ (0.10 g, 0.2 mmol⁸) was stirred in a flask at ambient

temperature, an exothermic reaction took place immediately. Several minutes later, the temperature of the reaction mixture went down to r.t. and the mixture solidified. At this stage, TLC analysis showed that benzaldehyde had been completely consumed and the corresponding benzal diacetate was formed. Thus, 1 mL CH_2Cl_2 was added to the mixture to dissolve the product. The catalyst remained as a solid due to its low solubility in CH_2Cl_2 . Then, after separation of the catalyst through filtration and subsequent removal of the solvent under reduced pressure, the corresponding benzal diacetate was obtained in 97% yield. In a similar manner, other substrates with various substitution types also reacted smoothly with acetic anhydride and afforded the corresponding acylals in fairly good yields (Table 1).

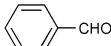
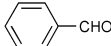
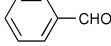
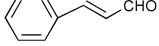
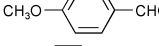
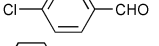
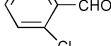
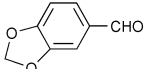

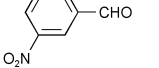
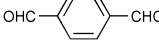
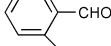
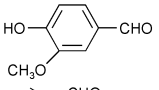
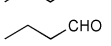
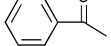
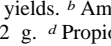
The results listed in Table 1 show that both aromatic and aliphatic aldehydes react smoothly with acetic anhydride to afford the corresponding geminal diacetates in good to excellent yields. Deactivated aldehydes such as *p*-nitrobenzaldehyde and *m*-nitrobenzaldehyde can also produce good yields but need a little longer time (Table 1, entry 9–10). Moreover, it should be noted that steric hindrance seems to have no significant effects on the efficiency of this transformation considering that *o*-chlorobenzaldehyde afforded the corresponding acylals in 92% yield within a short reaction time (Table 1, entry 7). The tolerance of various functional groups under the present reaction conditions is also worthy of mention in that acid sensitive or oxidizable groups such as methoxy, methylenedioxy, nitro, chloro, and double bonds do survive under such conditions. As for the amount of catalyst used, for 10 mmol of substrate, 0.20 mmol of catalyst is enough to push the reaction to completion in a rather short reaction time. In fact, with a catalyst concentration of less than 0.20 mmol, a very good yield

Green Context

The protection of aldehydes is a very common procedure in synthetic chemistry. Dicarboxylates are becoming important as protected aldehydes since they have a convenient range of stability. This paper describes a solvent-free and simple method for the protection of aldehydes, which is rapid and allows for simple and efficient catalyst recovery.

DJM

Table 1 Preparation of acylals catalyzed by $\text{Fe}_2(\text{SO}_4)_3 \cdot x\text{H}_2\text{O}$

Entry	Substrates	Mole ratio		Time/ min	Yield ^{ab} (%)
		Substrate/an- hydride	Product		
1		1 : 1.2	3a	3	97
2		1 : 1.2 ^c	3a	15	97
3		1 : 1.2 ^d	3b	10	90
4		1 : 1.2	3c	20	93
5		1 : 1.2	3d	10	94
6		1 : 3.0 ^e	3e	8	98
7		1 : 3.0 ^e	3f	20	97
8		1 : 2.0 ^e	3g	8	92
9		1 : 2.0 ^e	3h	90	85
10		1 : 3.0 ^e	3i	90	90
11		1 : 2.4	3j	5	98 ^f
12		1 : 2.0	3k	8	94 ^g
13		1 : 2.0	3l	30	92 ^g
14		1 : 1.2	3m	25	90
15		1 : 1.2	3n	30	85
16		1 : 1.2	3o	120	— ^h

^a Isolated yields. ^b Amount of catalyst used: 0.10 g. ^c Amount of catalyst used: 0.02 g. ^d Propionic anhydride was used. ^e Excessive amount of anhydride used as solvents. ^f Yield of tetraacetate. ^g Yields of triacetate. ^h No reaction took place.

of the product could also be achieved, but a longer reaction time was needed.

On the other hand, acetophenone did not give any acylal under the present conditions (Table 1, entry 16). Thus, when a 1 : 1 mixture of benzaldehyde and acetophenone was allowed to react with acetic anhydride in the presence of a catalytic amount of $\text{Fe}_2(\text{SO}_4)_3 \cdot x\text{H}_2\text{O}$ for 20 minutes, TLC and GC-MS analysis of the reaction mixture indicated complete disappearance of benzaldehyde, while acetophenone was still intact due to the electron-donating and steric effects of the methyl group in acetophenone. Therefore, chemo-selective protection of an aldehyde in the presence of a ketone could be achieved by the present method.

$\text{Fe}(\text{III})$ compounds have been found to be very useful in various organic transformations, such as Friedel–Crafts reactions, Biginell reactions,⁹ translation of protective groups¹⁰ and preparation of *gem*-dicarboxylates.¹¹ In most of these cases, $\text{Fe}(\text{III})$ compounds were used in a homogeneous way, such as FeCl_3 being a soluble catalyst in the preparation of *gem*-dicarboxylates.¹¹ While $\text{Fe}(\text{III})$ catalysts showed high efficiency in these processes, they also necessitated tedious work-ups such as extraction, washing, drying and distillation in getting the desired products. Moreover, $\text{Fe}(\text{III})$ catalysts homogeneously used could not be recovered as conveniently as in the

heterogeneous cases. On the other hand, several heterogeneous Fe^{3+} -type catalysts including PVC- FeCl_3 ,^{12a} Fe^{3+} -montmorillonite^{12b} and Fe^{3+} -gel^{12c} have been reported, and tedious work-up in their preparation and activation remained another problem to be resolved. In our process, $\text{Fe}_2(\text{SO}_4)_3 \cdot x\text{H}_2\text{O}$ is easily accessible, very cheap and highly efficient. In addition, its low solubility in some kinds of organic solvents means it can be used in a heterogeneous way, which means that many of the problems resulting from homogeneous $\text{Fe}(\text{III})$ catalysts can be resolved.

In view of a greener chemistry, efficient recovery and reuse of the catalyst are highly preferable. In our process, when the catalytic reaction was completed, $\text{Fe}_2(\text{SO}_4)_3 \cdot x\text{H}_2\text{O}$ could be recovered conveniently from the reaction mixture through filtration and subsequent washing with CH_2Cl_2 . Then, efforts were made on the examination of the reusability of $\text{Fe}_2(\text{SO}_4)_3 \cdot x\text{H}_2\text{O}$ by using benzaldehyde as a model substrate. The results are listed in Table 2 and show that successive reuses of

Table 2 Results of the study on the recovery and reusability of $\text{Fe}_2(\text{SO}_4)_3 \cdot x\text{H}_2\text{O}$

Round	Substrate	Catalyst recovered/g	Reaction time/Yield ^a min (%)
1	$\text{C}_6\text{H}_5\text{CHO}$	0.104	3 97
2	$\text{C}_6\text{H}_5\text{CHO}$	0.092	3 97
3	$\text{C}_6\text{H}_5\text{CHO}$	0.090	4 95
4	$\text{C}_6\text{H}_5\text{CHO}$	0.085	7 93
5	$\text{C}_6\text{H}_5\text{CHO}$	0.084	8 92
6	$\text{C}_6\text{H}_5\text{CHO}$	0.074	8 92
7	$\text{C}_6\text{H}_5\text{CHO}$	0.070	9 92

^a Isolated yields.

the recovered catalyst gave the product in yields almost as high as those of the first round. Even in the seventh round, reuse of the catalyst recovered from the sixth round can afford the corresponding product with a 92% yield (Table 2, entry 7).

In conclusion, with its high efficiency, low-cost, environmentally benign nature together with the mild and solvent-free reaction conditions, the present method may provide a green alternative for the preparation of acylals. Work on other uses of hydrated ferric sulfate as an efficient and green catalyst are currently ongoing in our laboratory.

Experimental

All the aldehydes and anhydrides were A. R. reagents. Hydrated ferric sulfate (Beijing Chemical Factory, A. R.) was also commercial reagent, and the content of $\text{Fe}(\text{III})$ was 21 ~ 23% (w/w).

Melting points were measured by a Kofler micro-melting point apparatus and were uncorrected. Infrared spectra were recorded on a Bruker Vector 22 spectrometer in KBr with absorption in cm^{-1} . ^1H NMR spectra were determined on a Bruker AC 400 spectrometer as CDCl_3 solutions. Chemical shifts (δ) were expressed in ppm downfield from the internal standard tetramethylsilane and coupling constants J were given in Hz. Mass spectra were recorded on a HP5989B mass spectrometer.

Typical procedure for the preparation of benzal diacetate

A mixture of benzaldehyde (10 mmol), freshly distilled acetic anhydride (12 mmol) and $\text{Fe}_2(\text{SO}_4)_3 \cdot x\text{H}_2\text{O}$ (0.20 mmol, 0.10 g) was stirred in a flask at ambient temperature. While stirring

continued, the mixture solidified gradually. When the conversion was completed as indicated by TLC, 1 mL CH₂Cl₂ was added to the mixture to dissolve the solid product. In the mean time, the catalyst remained as solid. Then, the catalyst was collected through filtration and washed with CH₂Cl₂ (2 × 1 mL) for further uses. The filtrate was concentrated under reduced pressure to give benzal diacetate as a white crystalline solid (2.02 g, 97%, m.p. 43–44 °C). Other acylal products can be obtained in a similar manner.

Physical and spectra data of selected products:

3e. m.p. 55–56 °C; ¹H NMR (CDCl₃, 400 MHz) δ: 7.98 (s, 1H), 7.56–7.26 (m, 4H), 2.14 (s, 6H); IR (KBr) ν: 3096, 3017, 2942, 1765, 1753, 1532, 1353, 1218, 1203, 993, 820, 742, 685 cm⁻¹; MS (EI): 207(M⁺–35, 83), 183(13), 165(36), 141(100), 123(23), 111(21), 77(23), 43(91).

3g. m.p. 78–79 °C; ¹H NMR (CDCl₃, 400 MHz) δ: 7.57 (s, 1H), 7.01–6.79 (m, 3H), 5.98 (s, 2H), 2.11 (s, 6H); IR (KBr) ν: 3014, 2913, 1764, 1749, 1609, 1477, 1370, 1237, 1201, 1037, 795, 675 cm⁻¹; MS (EI): 252(M⁺, 38), 193(10), 151(100), 121(10), 93(20), 43(23).

3j. m.p. 170–171 °C; ¹H NMR (CDCl₃, 400 MHz) δ: 7.68 (s, 2H), 7.56 (s, 4H), 2.12 (s, 12H); IR (KBr) ν: 3025, 2938, 1764, 1378, 1359, 1239 cm⁻¹; MS (EI): 338(M⁺, 1), 278(14), 235(100), 194(16), 176(40), 133(50), 77(10), 43(80).

3k. m.p. 102–103 °C; ¹H NMR (CDCl₃, 400 MHz) δ: 7.90 (s, 1H), 7.65–7.11 (m, 4H); 2.50 (s, 3H); 2.10 (s, 6H); IR (KBr) ν: 1755, 1748, 1614, 1373, 1251, 1212, 1194, 1011, 804, 767; MS (EI): 226 (M⁺, 1), 223(2), 164(18), 122(100), 43(41).

3l. m.p. 91–92 °C; ¹H NMR (CDCl₃, 400 MHz) δ: 7.65 (s, 1H), 7.14–7.04 (m, 3H), 3.86 (s, 3H), 2.32 (s, 3H), 2.13 (s, 6H); IR (KBr) ν: 2964, 2939, 2836, 1767, 1752, 1378, 1247, 1206, 1162, 994, 896, 784; MS (EI): 296(M⁺, 10), 254(71), 195(20), 153(100), 43(32).

Acknowledgement

This work was financially supported by the Natural Science Foundation of Education Commission of Henan Province of China under grant No. 1999150027.

References

- 1 K. S. Kochhar, B. S. Bal, R. P. Deshpande, S. N. Rajadhyaksha and H. W. Pinnick, *J. Org. Chem.*, 1983, **48**, 1765.
- 2 (a) R. E. Banks, J. A. Miller, M. J. Nunn, P. Stanley, T. J. R. Weakley and Z. Ullah, *J. Chem. Soc., Perkin Trans. 1*, 1981, 1096; (b) B. B. Snider and S. G. Amin, *Synth. Commun.*, 1978, **8**, 117.
- 3 T. W. Greene and P. G. M. Wuts, *Protective Groups in Organic Synthesis*, 3rd edn., Wiley, New York, 1999, p. 306.
- 4 (a) M. Tomita, T. Kikuchi, K. Bessho, T. Hori and Y. Inubushi, *Chem. Pharm. Bull.*, 1963, **11**, 1484; (b) F. Feeman and E. M. J. Karchevski, *Chem. Eng. Data*, 1977, **22**, 355; (c) W. Davey and J. R. Gwilt, *J. Chem. Soc.*, 1957, 1008.
- 5 (a) I. Scriabine, *Bull. Soc. Chim. Fr.*, 1961, 1194; (b) J. K. Michie and J. A. Miller, *Synthesis*, 1981, 824.
- 6 (a) V. K. Aggarwal, S. Fonquerna and G. P. Vennall, *Synlett*, 1998, 849; (b) N. Deka, D. J. Kalita, R. Borah and J. C. Sarma, *J. Org. Chem.*, 1997, **62**, 1563; (c) B. Karimi, H. Seradj and G. R. Ebrahimian, *Synlett*, 2000, 623; (d) N. Sumida, K. Nishioka and T. Sato, *Synlett*, 2001, 1921; (e) B. Karimi, G. R. Ebrahimian and H. Seradj, *Synth. Commun.*, 2002, **32**, 669.
- 7 (a) G. Zhang and H. Gong, *Synth. Commun.*, 1999, **29**, 1547; (b) G. Zhang, *Synth. Commun.*, 1999, **29**, 607.
- 8 The mol number of Fe₂(SO₄)₃ was calculated based on the formula: $M_{\text{Fe}_2(\text{SO}_4)_3} = 0.5 \times (W_{\text{Fe}_2(\text{SO}_4)_3 \cdot x\text{H}_2\text{O}} \times \text{Fe(III)\%} \div 55.8)$.
- 9 J. Lu and H. Ma, *Synlett*, 2000, 63.
- 10 B. Ganem and V. R. Small Jr., *J. Org. Chem.*, 1974, **39**, 3728.
- 11 B. M. Trost and C. B. Lee, *J. Am. Chem. Soc.*, 2001, **123**, 3671.
- 12 (a) Y. Q. Li, *Synth. Commun.*, 2000, **30**, 3913; (b) T. S. Li, Z. H. Zhang and Y. J. Gao, *Synth. Commun.*, 1998, **28**, 4665; (c) A. Fedel and J. Salaun, *Tetrahedron*, 1985, **41**, 1267.



Economic and environmental assessment of high-temperature water as a medium for terephthalic acid synthesis

Jennifer B. Dunn and Phillip E. Savage*

University of Michigan, Chemical Engineering Department Ann Arbor, MI 48109-2136, USA

Received 15th May 2003

First published as an Advance Article on the web 21st August 2003

Large-scale chemical processes to produce terephthalic acid typically use acetic acid as the reaction medium. Recent research has demonstrated the technical feasibility of synthesizing terephthalic acid in high-temperature water (HTW), a medium widely perceived as environmentally benign. We have developed an economic and environmental assessment of an HTW-based terephthalic acid synthesis process to determine whether such a process is economically competitive with and, in fact, more environmentally benign than the current process. We simulated four variations of an HTW-based process and calculated the energy requirements and the capital investment for each of these variations. A US Department of Energy report contained the corresponding energy consumption data for an acetic-acid-based process. The capital investment and energy requirement for an acetic-acid-based process were $\$250 \times 10^6$ and 19 MJ kg^{-1} terephthalic acid, respectively. The capital cost for an HTW-based process operating at $300 \text{ }^\circ\text{C}$ and 150 bar was $\$280 \times 10^6$; the energy intensity for this process was 17 MJ kg^{-1} terephthalic acid. Given the approximately 20% uncertainty typically associated with capital investment estimates, the capital costs of these two processes are approximately equal. Moreover, adoption of HTW would likely reduce methyl bromide emissions from terephthalic acid synthesis plants. With a capital investment equivalent to the current process and reduced energy and pollutant intensities, HTW shows economic and environmental promise as a replacement for acetic acid in terephthalic acid synthesis.

Introduction

Water as a reaction medium

A growing body of literature describing organic synthesis reactions in high-temperature water (HTW)^{1–4} is testament to this reaction medium's attractive qualities: environmental benignity and "tunable" properties under supercritical conditions. The density of supercritical water (SCW) is highly temperature and pressure dependent and therefore the density-dependent properties of SCW, such as its relative permittivity and dissociation constant, can be adjusted to accommodate a given reaction. Water is non-toxic, inexpensive and, from a life cycle perspective, offers limited pollution and energy expenditure associated with its preparation for use as a solvent.

Our recent work^{5,6} has focused on the synthesis of terephthalic acid in HTW *via* the partial oxidation of *p*-xylene. Terephthalic acid is a commercially important compound, serving as the raw material for polyethylene terephthalate (PET) manufacture. This polymer is a common component of injection-molded consumer products, such as soft drink bottles. The commercial process for terephthalic acid synthesis from *p*-xylene uses acetic acid as the reaction medium.⁷ In this process, the reaction occurs at a temperature of about $200 \text{ }^\circ\text{C}$ and pressures between 15 and 30 atm. The most common catalyst is the Mid-Century (MC) combination of manganese acetate, cobalt acetate, and hydrobromic acid. Fig. 1 illustrates the overall reaction.

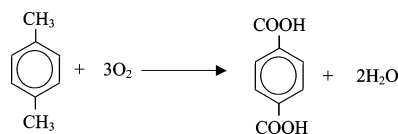


Fig. 1 Overall reaction of *p*-xylene partial oxidation to terephthalic acid.

The stream leaving the synthesis reactor is a slurry consisting of acetic acid, water that forms as a by-product of the reaction,

terephthalic acid, 4-carboxybenzaldehyde, and other impurities. Methyl bromide, a gaseous and environmentally harmful compound, also forms, predominantly from reaction between acetic acid and bromide. The slurry exiting the reactor is phase-separated; the liquid phase proceeds to a solvent dehydration tower that separates the acetic acid and water. To replace the acetic acid that burns off (oxidizes) in the reactor, fresh acetic acid is added to the solvent recycle stream leaving the solvent dehydration tower. Meanwhile, acetic acid and water vapor evaporate off the solid phase (crude terephthalic acid) in a residue still.

The crude terephthalic acid contains 4-carboxybenzaldehyde, an intermediate in the synthesis of terephthalic acid, which hinders terephthalic acid's polymerization.⁸ The two compounds are nearly equally soluble in water, making their separation *via* crystallization very difficult. To produce purified terephthalic acid, the crude product is mixed with water to form a 15 wt% slurry, heated to $260 \text{ }^\circ\text{C}$, and sent through a hydrogenation reactor (*N.B.* the current commercial process for terephthalic acid purification uses an HTW reaction medium). The 4-carboxybenzaldehyde is therein converted to *p*-toluic acid while the terephthalic acid remains unaltered. Subsequent crystallization steps isolate the purified terephthalic acid.

Green Context

The use of metrics in green chemistry is a critical element, which is often given less attention than it deserves. This paper investigates the conventional synthesis of terephthalic acid in comparison to a high temperature water route. The overall conclusion supports the water-based system – it is of similar cost, but has reduced emissions of MeBr and CO_2 , as well as being less energy intensive. *DJM*

Benefits of HTW substitution

Several potential benefits appear to accompany the adoption of HTW as the reaction medium for terephthalic acid synthesis. First, the solvent dehydration tower would be unnecessary. The azeotropic separation of acetic acid and water is energy-intensive, and its elimination from the process would reduce capital expenditure and energy requirements. Second, formation of methyl bromide from reaction between solvent and bromide would be avoided. Third, there would be no need for make-up solvent because HTW cannot be oxidized. In the current process, fresh acetic acid must replace the acetic acid that burns off in the reactor (approximately 0.07 kg of acetic acid per kg of terephthalic acid manufactured⁷). The production of this acetic acid results in added cost, energy expenditure, and pollution, which contribute to the current technology's environmental impact. Additionally, the replacement of acetic acid with water will eliminate fugitive emissions (*e.g.* from acetic acid storage tanks and transportation vessels) and risk of worker exposure to this chemical.

We have studied the synthesis of terephthalic acid in HTW to assess the technical feasibility of using this reaction medium. Such a process would embrace the principle of green chemistry⁹ mandating benign reaction media. The highest terephthalic acid molar yield we reported was $57 \pm 15\%$ at 380 °C, a batch holding time of 7.5 min, water density of 400 kg m⁻³, and initial concentrations of *p*-xylene, catalyst, and oxidant of 0.07 M, 7.7×10^{-3} M, and 0.58 M, respectively.⁶ This yield represents a lower bound, as it is based on the moles of *p*-xylene loaded to the reactor. If the terephthalic acid yield were based on the moles of material recovered from the reactor, values exceeding 90% were common. Additionally, Hamley *et al.*¹⁰ reported terephthalic acid yields of approximately 90% at 400 °C, 250 bar, a residence time of 0.15 min, and an oxygen : *p*-xylene molar feed ratio of 3.6 : 1. This research collectively shows that terephthalic acid synthesis in HTW is technically feasible.

Drawbacks of HTW substitution

Despite the potential economic and environmental improvements that may result from HTW substitution in the current process, adjustments in process conditions to accommodate this new reaction medium may increase the environmental impact of terephthalic acid production. For example, a reaction temperature of at least 300 °C is required to produce a satisfactory terephthalic acid yield in HTW. A higher process pressure accompanies this higher temperature to maintain the contents of the reactor in a liquid phase (below the critical temperature). This increase in the severity of reaction conditions will result in a higher energy requirement for the oxidation section of the process.

Necessity of quantitative evaluation

Qualitative examination of the acetic-acid-based process and a conceptual HTW-based process does not reveal which terephthalic acid synthesis process is more environmentally benign. To discern the environmentally superior process, a quantitative comparison of the environmental impacts of these two processes is necessary. Moreover, although HTW-based technology may reduce the environmental impact of terephthalic acid production, it will not replace the current technology unless it offers favorable economics.

To enable a quantitative evaluation of the benignity and economics of terephthalic acid production processes, we have developed simulations of four alternative HTW-based processes and conducted an environmental and economic assessment of this technology. The environmental assessment of the

HTW-based processes quantitatively considers two sustainability metrics: energy intensity and pollutant intensity.¹¹ While there are more sophisticated ways to analyze the environmental impact of a process (life cycle assessment,¹² optimization tools^{13,14}), sustainability metrics alone are useful tools to compare processes and are generally incorporated into more complex assessments. To measure economic feasibility, we developed capital cost estimates of the four HTW-based processes. This approach is primarily a Tier II environmental performance evaluation as described by Allen and Shonnard.¹⁵ Our economic analysis and brief consideration of the toxicity of process emissions are elements of Tiers I and III, respectively.

No report of such an analysis for terephthalic acid synthesis in HTW exists in the archival chemical literature. In fact, documented examples of the quantitative evaluation of new technologies' environmental impacts are relatively rare. The literature does contain several quantitative economic and environmental impact assessments of process design alternatives in the form of case studies.^{16–18} These studies typically demonstrate the effectiveness of various assessment techniques rather than assess a new technology's benignity or economic feasibility. Some researchers have developed a qualitative comparison of a new technology and the existing technology it may replace,¹⁹ and some present a limited quantitative economic and environmental impact analysis.^{20–22} The work presented herein is unique because it quantitatively examines, from a process systems perspective, both the economic feasibility and the environmental impact of a new, purportedly environmentally benign, technology. This analysis includes process steps upstream and downstream of the reactor, which has been the focus of previous laboratory research. With this approach, we can consider the advantages and disadvantages of HTW and acetic acid as possible solvents for this process and examine the effect of HTW on the benignity of the process as a whole. We seek to assess the potential value of our research, beyond scientific interest in reactions in HTW, to society and industry.

Methodology

Simulation parameters

We developed and carried out simulations of HTW-based processes with Aspen Plus[®] 11.1 software. The design basis was a production rate of 80 000 kg h⁻¹ of terephthalic acid, and we examined synthesis at both a subcritical (300 °C) and a supercritical (380 °C) temperature. In each case, the concentration of *p*-xylene in the reactor feed stream was 1.0 M, air was the oxidant, and the O₂ : *p*-xylene molar feed ratio was 3.5 : 1. Terephthalic acid and 4-carboxybenzaldehyde molar yields in each simulation were set at 99% and 1%, respectively. Previous experimental work¹⁰ demonstrates that this yield is realistic for the HTW-based process. Table 1 outlines the parameters that

Table 1 Design variables for process simulation

Parameter	Subcritical process	Supercritical process
Reaction temperature/°C	300	380
Reaction pressure/bar	150, 100	250
Water flow rate/kg h ⁻¹	346, 310	242, 170
Reactor residence time/min	30	0.20

differed between the sub- and supercritical processes. We selected the Redlich–Kwong–Soave equation of state with Huron–Vidal mixing rules as the thermodynamic property method for the simulations because it applies to polar non-

electrolyte solutions at high pressures.²³ It also satisfactorily predicted the phase behavior of pure water at the process conditions in the simulations. We were unable to include explicitly the catalyst (e.g. MnBr_2) in the simulations because Aspen's thermodynamic database did not contain adequate information about this compound. The catalyst : *p*-xylene molar feed ratio would be 0.1 : 1, as it has been in laboratory experiments,^{5,6} which results in a low (<3 wt%) catalyst concentration in the reactor. Its presence therefore is unlikely to affect greatly the macroscale thermodynamics of the process.

Simulation outline

Fig. 2 is a schematic of a conceptual subcritical HTW-based process. Water and *p*-xylene are pumped to the reaction pressure, mixed, and heated to the reaction temperature in a gas-fired furnace. In the stirred-tank reactor, compressed air at the reaction conditions mixes with the water and *p*-xylene. We also

simulated a process with an air separation step before the compression step such that only O_2 is compressed. The absence of N_2 allowed maintenance of a liquid phase in the reactor at a lower pressure of 100 bar, which was the reaction pressure used in the simulation of this process. Water boils and evaporates in the reactor to alleviate the heat of reaction, $2 \times 10^5 \text{ kJ kg}^{-1}$ *p*-xylene.⁷ This water is condensed and returned to the reactor. The water in the vapor stream leaving the reactor is condensed and mixed with the liquid stream also exiting the reactor to obtain an approximately 20 wt% solution of crude terephthalic acid. Next, this stream passes through an expansion valve to reduce its temperature and pressure to levels appropriate for the hydrogenation reaction. We did not simulate the hydrogenation or subsequent crystallization or purification steps because they were taken to be identical for both reaction media. Recall that in the acetic-acid-based process, the hydrogenation and subsequent crystallization steps are HTW-based.

Fig. 3 is a schematic of the HTW-based process with a supercritical reaction temperature (380 °C). This process uses

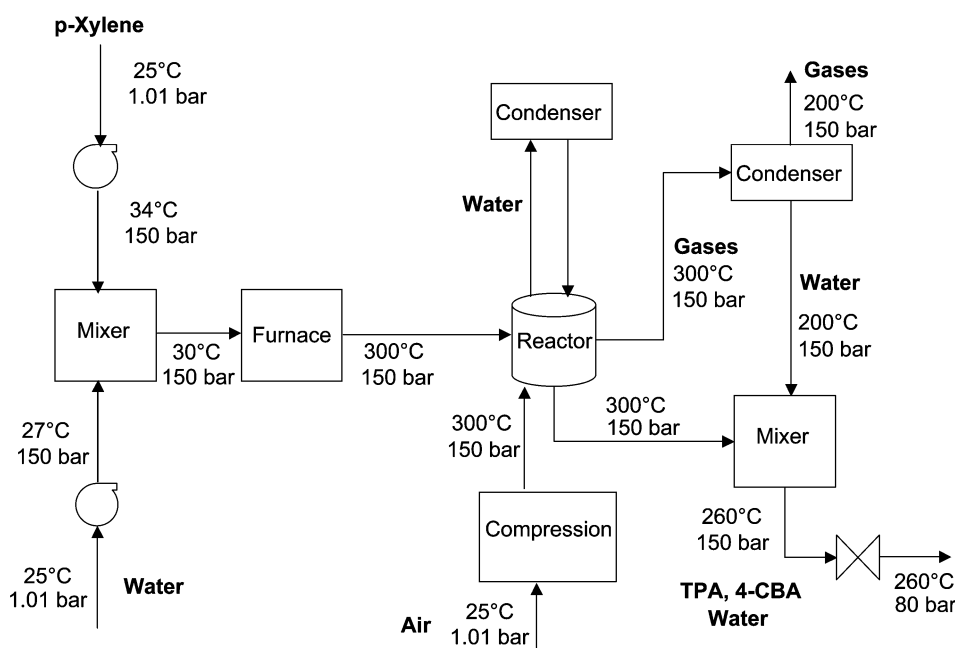


Fig. 2 Subcritical HTW-based process.

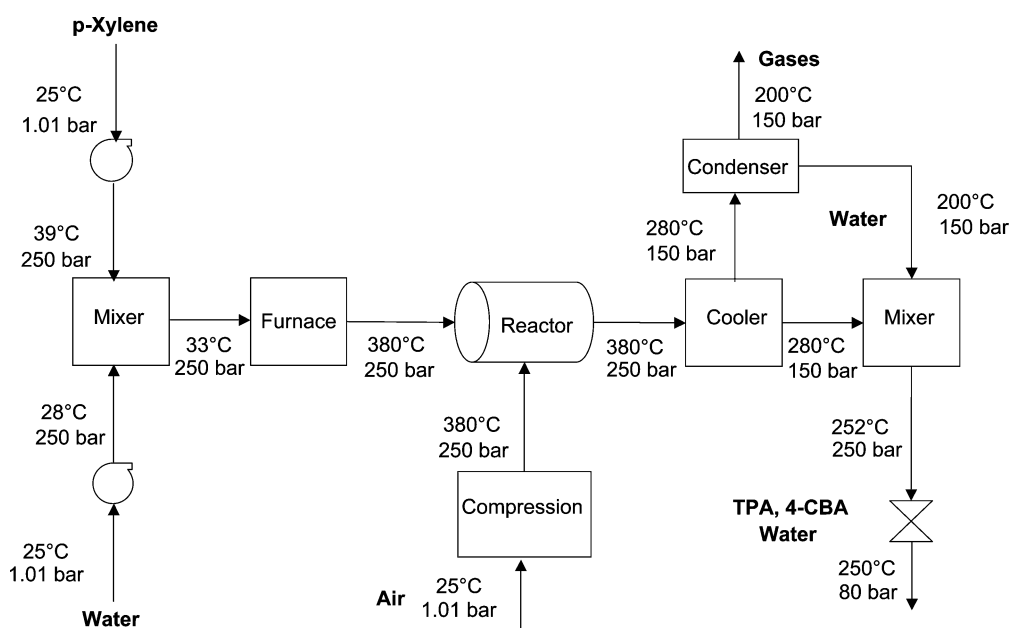


Fig. 3 Supercritical HTW-based process.

an isothermal tubular flow reactor rather than a stirred-tank reactor. The single, supercritical fluid stream leaving this reactor passes through a heat exchanger, which reduces its temperature. The water in the resulting vapor stream is condensed and mixed with the liquid stream that also leaves the heat exchanger. As in the subcritical process, flow through an expansion valve reduces the temperature and pressure of this combined stream to conditions suitable for hydrogenation. Although Fig. 2 and 3 do not include water recycle streams, water will separate easily from the terephthalic acid product during the crystallization steps and can then be recycled.

A simulation of reactant and solvent heating and pressurizing for the acetic-acid-based process provided data for estimating equipment sizes for this process. In this simulation, the reaction temperature, pressure, and residence time were 200 °C, 30 bar, and 1 h, respectively, based on published process information.⁷

Capital cost estimation

Volumetric flowrate and heat duty data from the simulations permitted calculation of process equipment sizes and capacities, the basis for capital cost estimation. The purchased equipment costs were estimated from correlations^{24,25} that relate equipment cost to an attribute such as capacity. Table 2 outlines the

Table 2 Basis for equipment cost estimations

Equipment	Cost basis	Material of construction
Pump	Capacity (gal min ⁻¹)	Carbon steel
Mixer	Capacity (gal)	Carbon steel
Furnace	Heat duty (MJ h ⁻¹)	Hastelloy C
Reactor	Capacity (gal)	Hastelloy C
Condenser	Surface area (ft ²)	Hastelloy C
Flash vessel	Capacity (gal)	Hastelloy C
Storage tank	Capacity (gal)	Carbon steel
Compression plant	Power (brake hp)	
Air separation plant	Capacity (t day ⁻¹)	

basis for the cost estimate for each piece of equipment, as well as the material of construction.

Bromide's corrosiveness mandates a special material of construction for high-temperature steps in the process. In the current process, the solvent dehydration tower and other process vessels are titanium-lined to prevent corrosion. Titanium, however, may not be an essential element of an HTW-based process. Hamley *et al.*¹⁰ state that bromide-induced corrosion is most problematic in regions with high thermal gradients. Therefore, the flow reactor in their experiments was Hastelloy, but they heated the aqueous MnBr₂ solution in a titanium mixing cross. Hastelloy might then be a suitable material of construction for the high-temperature vessels in the HTW-based processes, but some titanium sections of piping may be necessary. To account for the use of Hastelloy as well as elevated operating pressure, the equipment base costs were multiplied by appropriate adjustment factors. We updated the resulting costs to 2002 dollars with the Marshall and Swift Equipment Cost Index.²⁶

Estimating the sizes of the process equipment necessitated several assumptions. First, we assumed a holding time of 5 min for flash vessels and mixers.²⁷ We sized the *p*-xylene and water storage tanks to feed the process for 5 and 3 days, respectively.²⁸ The volume of each reactor was calculated as the product of the liquid volumetric flowrate entering the reactor and the residence time in the reactor plus an additional 15% of that product as head space for the vapor phase.²⁷ For supercritical reaction conditions, the reactor volume was simply the product of the volumetric flow rate and the residence time.

To calculate appropriate residence times, we used kinetics data that describe *p*-xylene conversion in HTW at different temperatures and residence times in a flow reactor.¹⁰ At 300 °C and a residence time of 2.43 min, the conversion of *p*-xylene was 75%. It reached 95% at 400 °C and a residence time of 0.15 min. From these data, we calculated pseudo-first-order rate constants at 300 °C and 400 °C and the corresponding Arrhenius parameters ($E = 110 \text{ kJ mol}^{-1}$, $\log(A/\text{min}^{-1}) = 10$). With these kinetics, 99% conversion occurs at a CSTR residence time of 30 min for reaction at 300 °C. A residence time of 0.20 min is required in the plug flow reactor at supercritical reaction conditions (380 °C).

Eqn. (1) provided the surface area of the condensers. The overall heat transfer coefficient was taken to be equal to that expected for heat transfer between water and condensing steam, 2270 W m⁻² K.²⁹

$$A = \frac{Q}{U \Delta T_{\text{lm}}} \quad (1)$$

where A = area of condenser, m²; U = overall heat transfer coefficient, W m⁻² K; ΔT_{lm} = log mean temperature difference, K.

Eqn. (2) provided the energy required to compress the air or oxygen for the process.³⁰ The compressor was assumed to operate adiabatically and with 80% efficiency. The compressor in the supercritical processes and the subcritical process without air separation comprises 4 stages whereas the unit in the subcritical process with air separation contains 3 stages. The compression ratio, p_b/p_a , was taken to be equal in each stage:

$$P_B = \frac{0.371 T_a \gamma q_0}{(\gamma - 1) \eta} \left[\left(\frac{p_b}{p_a} \right)^{1-\frac{1}{\gamma}} - 1 \right] \quad (2)$$

where P_B = power, kW; T_a = entrance temperature of gas, K; $\gamma = c_p/c_v = 1.39$ for normal air³¹; q_0 = volume of gas compressed evaluated at 0 °C and 1 atm, m³ s⁻¹; η = efficiency, 0.8; p_b = exit pressure, bar; p_a = entrance pressure, bar.

Energy intensities

HTW medium. The process simulations provided the heat duty of the furnace and the power requirements of the pumps. We used these data along with the power requirement for the compression plants from eqn. (2) to calculate the fuel energy intensity of each of the HTW-based processes from eqn. (3).

$$\text{Fuel energy intensity} = \frac{1}{0.8} \frac{\text{Furnace heat duty} \left[\frac{\text{MJ}}{\text{yr}} \right]}{\text{Production rate} \left[\frac{\text{kg}}{\text{yr}} \right]} + \sum \frac{1}{0.31} \frac{\text{Power requirement} \left[\frac{\text{MJ}}{\text{yr}} \right]}{\text{Production rate} \left[\frac{\text{kg}}{\text{yr}} \right]} \quad (3)$$

In this equation, the power requirement of each piece of equipment is divided by 0.31, the national average efficiency of the United States electricity grid.³² The furnace efficiency was taken to be 0.8.

Acetic acid medium. A report³² prepared by a United States Department of Energy (DOE) contractor provided the energy

intensity of the acetic-acid-based process. The report divided the acetic-acid-based process into three sections (oxidation, hydrogenation, and catalyst recovery) and reported energy intensities for each section. The HTW-based processes we simulated are most comparable to the oxidation section in the DOE report, which had an energy intensity of 5 MJ kg⁻¹ terephthalic acid. This intensity corresponded to a case in which the heat of reaction drove the reboiler for the solvent dehydration tower, which separates water and acetic acid. The HTW-based process simulations did not harness the heat of the oxidation reaction. Therefore, to place the HTW-based processes and the acetic-acid-based process on an equal footing (processes with no heat integration), we added the energy intensity of the heat of reaction, 7 MJ kg⁻¹ terephthalic acid, to the acetic-acid-based process energy intensity. Additionally, the oxidation section energy intensity in the DOE report does not account for heating the slurry of crude terephthalic acid and water to 260 °C prior to hydrogenation. The crude terephthalic acid stream in the HTW-based processes is prepared for hydrogenation and requires no additional heating. Therefore, we calculated the energy required to heat the crude terephthalic acid slurry from 200 °C (the oxidation reaction temperature) to 260 °C (the hydrogenation temperature) and added the result, 3 MJ kg⁻¹ terephthalic acid, to the acetic-acid-based process energy intensity. This calculation may underestimate the energy associated with heating the crude terephthalic acid because the solid may cool to below 200 °C before it is prepared for hydrogenation. The adjusted value for the oxidation section in the acetic-acid-based process is the sum of these three energy intensities, or 15 MJ kg⁻¹ terephthalic acid. These calculations and adjustments, however, still exclude the energy associated with producing acetic acid to replenish solvent lost to oxidation.

The DOE report also contains information about acetic acid production, which commonly occurs *via* the low-pressure carbonylation of methanol at 200 °C. The process employs a rhodium catalyst and produces carbon dioxide and propanoic acid as undesirable by-products. The total energy consumed in the product chain of acetic acid manufacture is 52 MJ kg⁻¹ acetic acid.³²

The energy intensity of providing replenishment acetic acid for the current process is then the product of the total energy consumed in the product chain of acetic acid manufacture and the 0.07 kg of fresh acetic acid supplied per kg of terephthalic acid manufactured.⁷ This figure may overestimate such losses, especially in newer plants. The resulting energy intensity is 4 MJ kg⁻¹ terephthalic acid. The total energy intensity of the acetic-acid-based process is then 19 MJ kg⁻¹ terephthalic acid. This figure served as the benchmark for comparing the energy intensities of the HTW-based processes.

Results and discussion

This section first presents the results of capital cost estimations for the acetic-acid-based process and the HTW-based process. Subsequent sections discuss the energy intensity and pollutant intensity of these two competing processes.

Purchased equipment costs

Table 3 contains estimates of the major equipment costs for the HTW- and acetic-acid-based processes. The costs of the pumps, mixers, condensers, and flash vessels contributed at most one million dollars to the total purchased equipment cost.

The furnace in each HTW-based process was the most expensive item. With less costly tubular flow reactors, the supercritical processes have lower total purchased equipment costs than the subcritical processes, which use stirred-tank

Table 3 Process summaries and equipment costs (million \$)

Process	HTW ₁	HTW ₂	HTW ₃	HTW ₄	Acetic acid
Reaction temperature/°C	300	300	380	380	200
Reactor pressure/bar	150	100	250	250	30
Air separation	No	Yes	No	Yes	No
Reactor residence time/min	30	30	0.20	0.20	60
Furnace cost	23	23	26	26	4
Reactor cost	7	7	0.3	0.3	10
Storage tanks cost	4	4	4	4	4
Distillation column cost					1
Total purchased equipment costs	35	34	31	30	20

reactors. The lower reaction temperature of the acetic-acid-based processes translates into a slower reaction and longer reactor residence time than in the HTW-based processes. As a result, the reactor volume and cost are larger than in the HTW-based processes. The distillation column that separates acetic acid and water, which is unnecessary in HTW-based processes, is generally titanium-lined. The estimated cost²⁵ of the 3 ft (0.9 m) diameter tower with 44 trays³³ spaced 24 inches (0.6 m) apart²⁷ is one million dollars. The acetic-acid-based process has a significantly lower purchased equipment cost than all of the HTW-based processes.

Capital cost analysis

Table 4 displays the capital cost estimates for all four HTW-based processes and the acetic-acid-based process. We estimated a capital cost for the HTW-based processes as the sum of air compression and separation plant cost estimates and the oxidation section capital investment, which was calculated as a fixed multiple (Lang Factor = 4.87) of the purchased equipment cost for that section.

Table 4 Capital cost analysis (million \$)

Process	HTW ₁	HTW ₂	HTW ₃	HTW ₄	Acetic acid
Oxidation section capital investment	170	170	150	150	96
Compression plant	390	53	470	100	150
Air separation plant		55		55	
Total capital investment	560	280	620	310	250

The cost of an air compression plant for an acetic-acid-based process is higher than that for HTW₂ and HTW₄. If solely oxygen were compressed, the cost of the compression plant and total capital investment would be \$5 million and \$220 million, respectively. Information about the current process,⁷ however, indicates air is generally the oxidant.

The nominal capital investment for an acetic-acid-based process is lower than the capital investment for all four HTW-based processes. A 20% uncertainty, however, is typically associated with the cost estimation procedure in this work.²⁴ Therefore, HTW₂, HTW₄, and the acetic-acid-based process have overlapping capital investments.

Operating costs

This work does not include a direct analysis of operating costs. The increased rate of reaction in HTW has a desirable effect on the capital cost of a terephthalic acid production plant. However, it comes at the expense of using more energy to heat the solvent and reactants to a higher reaction temperature. Operating costs of an HTW-based process may therefore exceed those of the current technology.

Energy intensities

Table 5 contains the energy intensities for major pieces of equipment in the HTW-based processes and compares the total energy intensities of these processes to the energy intensity of the acetic-acid-based process.

Table 5 Energy intensities (MJ kg⁻¹ of terephthalic acid) of HTW-based processes and acetic-acid-based process

Process	HTW ₁	HTW ₂	HTW ₃	HTW ₄	Acetic-acid-based
Furnace	9	9	10	10	
Compression plant	44	6	53	11	
Air separation plant ^a		2		2	
Total	53	17	63	23	19

^a 0.24 kW h per kg O₂ produced.³⁴

Air separation saves a great deal in energy intensity as air compression is the most energy intensive step in all the processes except HTW₂, the only process with a lower energy intensity than the acetic acid based-process.

Pollutant emissions

Toxics Release Inventory data available on the EPA website³⁵ allow calculation of the pollution intensity of methyl bromide for an acetic-acid-based process. BP's 1.3 billion kg/yr capacity³⁶ terephthalic acid plant in Cooper River, South Carolina emits 41 600 kg yr⁻¹ of methyl bromide after process gases are incinerated. Actual production of methyl bromide from the process is therefore greater than this figure. The majority of methyl bromide forming in the current process derives from acetic acid. HTW will not react with Br⁻ to form this pollutant and, consequently, one expects methyl bromide production in HTW to be significantly lower than in acetic acid.

Emissions of carbon dioxide from the process will also decrease with HTW substitution. If 0.07 kg of acetic acid per kg of terephthalic acid undergo oxidation in the reactor, then 0.10 kg of carbon dioxide per kg of terephthalic acid result from this oxidation of solvent.

Toxicity

The benignity of water relative to acetic acid provides a strong incentive for its adoption as solvent for terephthalic acid synthesis processes. Water is not toxic. Acetic acid is comparable to HCN in the sense that both compounds are restricted to a Permissible Exposure Limit of 10 ppm by volume of vapor at 25 °C and 1 atm.¹⁵ Moreover, acetic acid shares a 10 ppm Threshold Limit Value with chloroform and ethylene dichloride.¹⁵

Water intensity

An HTW-based process will require large amounts of water, and, if the water is not recycled, it will have a greater water intensity than the acetic-acid-based process. However, as terephthalic acid and other organic compounds involved in an HTW-based process easily separate from ambient liquid water, it is likely that the water can be recycled without much replenishment. Additionally, the chemical reaction generates two moles of water for every mole of terephthalic acid. Thus, there is a natural production of solvent during the reaction.

Safety

Safety concerns are a crucial consideration for any new technology. While water is naturally more benign than acetic acid and would not pose hazards to workers handling it at ambient conditions, the reaction conditions in an HTW-based process are more severe than in the current process and may pose a greater safety risk.

Conclusions

The economic and environmental assessment of terephthalic acid synthesis in HTW illustrates that a process based on this reaction medium is likely equally capital intensive, less energy intensive, and more environmentally benign than the current acetic-acid-based process. A subcritical process with air separation (HTW₂) emerges as the most promising of the HTW-based processes, of those we considered. Another attractive aspect of an HTW-based process is reduced emissions of methyl bromide and carbon dioxide. The safety concern of the increased severity of process conditions, however, must be weighed against the environmental benefits that HTW adoption offers. Nonetheless, the inherent benignity of water is a significant advantage of water-based technology.

Acknowledgments

We thank Barry Barkel of the University of Michigan and Phil Nubel of BP Research for helpful discussions. We also acknowledge financial support from BP, the National Science Foundation (CTS-9985456), and the donors of the Petroleum Research Fund (34644-AC9) which is administered by the American Chemical Society.

References

- 1 P. E. Savage, *Chem. Rev.*, 1999, **99**, 603.
- 2 L. U. Gron and A. S. Tinsley, *Tetrahedron Lett.*, 1999, **40**, 227.
- 3 K. Chandler, C. L. Liotta, C. A. Eckert and D. Schiraldi, *AIChE J.*, 1998, **44**, 2080.
- 4 F. Bigi, S. Carloni, L. Ferrari, R. Maggi, A. Mazzacani and G. Sartori, *Tetrahedron Lett.*, 2001, **42**, 5203.
- 5 J. B. Dunn and P. E. Savage, *Ind. Eng. Chem. Res.*, 2002, **41**, 4460.
- 6 J. B. Dunn, D. I. Urquhart, and P. E. Savage, *Adv. Synth. Catal.*, 2002, **344**, 385.
- 7 R. J. Sheehan, in *Ullmann's Encyclopedia of Industrial Chemistry*, Vol. A26, ed. B. Elvers, S. Hawkins and W. Russey, VCH, Weinheim, 1995.
- 8 A. K. Suresh, M. M. Sharma and T. Sridhar, *Ind. Eng. Chem. Res.*, 2000, **39**, 3958.
- 9 P. T. Anastas and J. C. Warner, *Green Chemistry: Theory and Practice*, Oxford University Press, New York, 1998.
- 10 P. A. Hamley, T. Ilkenhans, J. M. Webster, E. Garcia-Verdugo, E. Venardou, M. J. Clarke, R. Auerbach, W. B. Thomas, K. Whiston and M. Poliakov, *Green Chem.*, 2002, **4**, 235.
- 11 A. D. Curzons, D. J. C. Constable, D. N. Mortimer and V. L. Cunningham, *Green Chem.*, 2001, **3**, 1.
- 12 R. L. Lankey and P. T. Anastas, *Ind. Eng. Chem. Res.*, 2002, **41**, 4498.
- 13 S. K. Stefanis, A. G. Livingston and E. N. Pistikopoulos, *Comput. Chem. Eng.*, 1995, **19**(S1), S39.
- 14 J. A. Cano-Ruiz and G. J. McRae, *Annu. Rev. Energy Environ.*, 1998, **23**, 499.
- 15 D. T. Allen and D. R. Shonnard, *Green Engineering*, Prentice Hall, Upper Saddle River, NJ, 2002.
- 16 A. Azapagic and R. Clift, *Comput. Chem. Eng.*, 1999, **23**, 1509.
- 17 U. Fischer and K. Hungerbühler, *Chim.*, 2000, **54**, 494.
- 18 O. Jankowitsch, L. Cavin, U. Fischer and K. Hungerbühler, *Process Saf. Environ. Prot.*, 2001, **79**, 304.

- 19 E. J. Beckman, *Environ. Sci. Tech.*, 2002, **36**, 347A.
- 20 G. Carturan, R. Campostrini and R. Dal Monte, in *Green Chemistry, Challenging Perspectives*, ed. P. Tundo and P. Anastas, Oxford University Press, Oxford, 2000.
- 21 F. Rivetti, in *Green Chemistry, Challenging Perspectives*, ed. P. Tundo and P. Anastas, Oxford University Press, Oxford, 2000.
- 22 C. Roderick, *Chim.*, 2000, **54**, 508.
- 23 E. C. Carlson, *Chem. Eng. Prog.*, 1996, **92**, 35.
- 24 M. S. Peters and K. D. Timmerhaus, *Plant Design and Economics for Chemical Engineers*, 4th edition, McGraw-Hill, Inc., New York, 1991.
- 25 D. E. Garrett, *Chemical Engineering Economics*, Van Nostrand Reinhold, New York, 1989.
- 26 Economic Indicators, *Chem. Eng.*, 2002, **109**, 118.
- 27 W. D. Seider, J. D. Seader and D. R. Lewin, *Process Design Principles Synthesis, Analysis, and Evaluation*, 1st edn., Wiley, New York, 1999.
- 28 B. M. Barkel, personal communication, (Nov. 7, 2002).
- 29 C. J. Geankoplis, *Transport Processes and Unit Operations*, 3rd edition, Prentice Hall, Inc., Englewood Cliffs, NJ, 1993.
- 30 W. L. McCabe, J. C. Smith and P. Harriot, *Unit Operations of Chemical Engineering*, 5th edn., McGraw-Hill, New York, 1993.
- 31 Ingersoll-Rand, *Compressed Air and Gas Data*, 2nd Edition, Ingersoll-Rand Company, Woodcliff Lake, NJ, 1971.
- 32 BRIDGES to Sustainability, *A Pilot Study of Energy Performance Levels for the U.S. Chemical Industry*, US Department of Energy, Office of Industrial Technologies, Oak Ridge National Laboratory, June, 2001 (<http://www.oit.doe.gov/chemicals/tools.shtml>).
- 33 T. J. Mix, J. S. Dweck, M. Weinberg and R. C. Armstrong, *Chem. Eng. Prog.*, 1978, **74**, 49.
- 34 B. Heydorn, A. Leder, Y. Ishikawa and T. Hoffman, in *Chemical Economics Handbook*, SRI International, Menlo Park, CA, Nov 1999.
- 35 www.epa.gov/tri/. The zip code for Cooper River, South Carolina, required for obtaining data for the terephthalic acid plant, is 29492.
- 36 www.bpchemicals.com.



Hydrogenation of 2-butyne-1,4-diol to butane-1,4-diol in supercritical carbon dioxide

Fengyu Zhao,^{abc} Yutaka Ikushima^{*bc} and Masahiko Arai^{cd}

^a Japan Society for the Promotion of Science, Domestic Research Fellow, Daitokuikenohata1-1-1, MK-ikenohata 4F, Tokyo 110-0008, Japan; Fax: +81-03-3837-1867; Tel: +81-3837-1866

^b Supercritical Fluid Research Center, National Institute of Advanced Industrial Science and Technology, Sendai 983-8551, Japan. E-mail: y-ikushima@aist.go.jp; Fax: +81-22-237-5224; Tel: +81-22-237-5211

^c CREST, Japan Science and Technology Corporation (JST), Japan

^d Division of Materials Science and Engineering, Graduate School of Engineering, Hokkaido University, Sapporo 060-8628, Japan. E-mail: marai@eng.hokudai.ac.jp; Fax: +81-11-706-6594; Tel: +81-11-706-6594

Received 9th June 2003

First published as an Advance Article on the web 21st August 2003

Hydrogenation of 2-butyne-1,4-diol to butane-1,4-diol has been successfully conducted in supercritical carbon dioxide at 323 K with a high selectivity of 84% for butane-1,4-diol at 100% conversion. No catalysts are needed since the reaction is promoted by the stainless steel reactor wall.

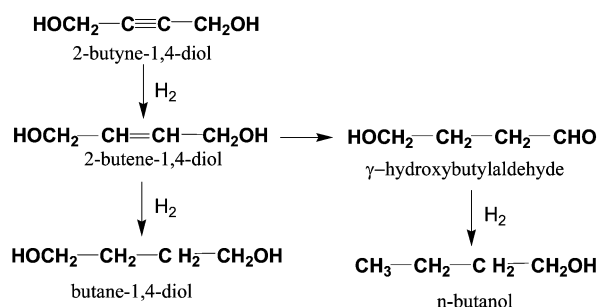
Introduction

Recently supercritical carbon dioxide has been playing an important role in the development of green chemical industrial processes due to its environmentally benign nature, nontoxicity, abundance, low cost and easy separation from products.^{1–4} It has become of interest that complete miscibility between hydrogen and scCO₂ is particularly beneficial for hydrogenation reactions since reactions in conventional solvents depend on the concentration of dissolved hydrogen and have frequently been limited by the rate of diffusion of hydrogen from the gaseous to the liquid phase. Furthermore, transition metal catalyzed heterogeneous reactions may be promoted by scCO₂ reaction medium, which would affect the nature of the transition metal particles, as suggested by a significant change of their optical absorption spectrum at high CO₂ pressures.⁵

Butane-1,4-diol is a useful intermediate in the manufacture of fine chemicals, such as polybutylene and polyurethane polymers, tetrahydrofuran and so on. Practical use of butane-1,4-diol may be greatly increased if it could be produced more cheaply. Traditional methods are based on catalytic hydrogenation of 2-butyne-1,4-diol (Scheme 1) with transition metal

butane-1,4-diol. High activity and selectivity to butane-1,4-diol were obtained with Pt/CaCO₃⁶ and Ru–Pd/C (Ru : Pd = 4 : 1)⁷ at 343 ~ 453 K as well as Pd/C and Pd/Al₂O₃ at 343 ~ 353 K in aqueous solution.⁸ Moreover, non-noble metal catalysts have also been known to contribute to butyne-1,4-diol hydrogenation in aqueous solution. Raney nickel catalyst containing 15 wt% copper⁹ exhibited a 83% yield to butane-1,4-diol at 333 ~ 373 K, and Ni–Cu–Mn supported on γ -alumina showed a 100% yield to butane-1,4-diol at a higher temperature of 433 K.¹⁰ Due to the presence of catalysts, promoters and conventional organic or aqueous solvents, an additional separation step should be essential and the catalysts would suffer from fast deactivation at high temperatures.

In this work, we have attempted the 2-butyne-1,4-diol hydrogenation using scCO₂ medium in a stainless steel reactor (SUS 316) without any catalyst, in which the reaction is greatly promoted by the stainless steel reactor wall. This is due to the materials of the reactor wall containing Ni and Mn metals which are the main active species for the 2-butyne-1,4-diol hydrogenation.^{9,10} To the best of our knowledge, we are the first to discover that hydrogenation reactions can be catalyzed by the reactor wall (SUS 316), especially in scCO₂. The present hydrogenation is an environmentally benign and “green” process as it is free of organic solvents, harmful catalysts and additives.



Scheme 1 2-Butyne-1,4-diol hydrogenation.

catalysts in aqueous solution or conventional organic solvents.^{6–10} Especially, noble metal supported catalysts such as Ru–Pd/C, Pt/CaCO₃, Pd/C and Pd/Al₂O₃ have been reported to be effective catalysts for 2-butyne-1,4-diol hydrogenation to

Green Context

Butane diol is produced by the hydrogenation of butyne-diol by catalytic reduction in a range of solvents. Here, a clever process is developed where the reaction is carried out in supercritical CO₂ (which means that hydrogen solubility is very high) avoiding the use of a volatile organic solvent, and the energy intensive separation of water required in the aqueous systems. Additionally, the walls of the reactor contain enough Ni and Mn to catalyze the reaction without the need for an added catalyst. *DJM*

Results and discussion

The visual observation of the reaction mixture gave estimates of the solubility of a substrate in the CO₂ phase.¹¹ The solubility of 2-butyne-1,4-diol in the gaseous phase has been estimated to be about 0.025 mmol mL⁻¹ at 4.0 MPa H₂ and 16 MPa CO₂ at 323 K. For the hydrogenation experiments under these conditions, the quantity of the substrate used corresponds to a nominal concentration of 0.1 mmol mL⁻¹. So, the substrate is distributed in both the liquid and gaseous phases. Under the present conditions, butane-1,4-diol and 2-butene-1,4-diol were the main products, with a minor product of n-butanol. Our concerns were the total conversion and selectivity with respect to these two main products.

The conversion of 2-butyne-1,4-diol in different solvents has been compared and the results obtained are shown in Table 1. The overall conversion increases with increasing H₂ pressure under solvent-free conditions (runs 1–3). Use of solvents can

Table 1 Hydrogenation of butyne-1,4-diol in different solvents

Entry	Solvent	H ₂ pressure/ MPa	Time/ min	Con- version (%)	Selectivity ^a (%)	
					Butan- diol	Butene- diol
1	—	2	180	9	—	100
2	—	4	180	38	11	87
3	—	6	180	62	10	85
4	CO ₂ 6.0 MPa	4	180	53	11	89
5	CO ₂ 7.0 MPa	4	180	65	20	78
6	CO ₂ 8.5 MPa	4	180	90	29	62
7	CO ₂ 12.0 MPa	4	180	100	43	57
8	CO ₂ 16.0 MPa	4	60	66	18	79
9	CO ₂ 16.0 MPa	4	90	98	37	50
10	CO ₂ 16.0 MPa	4	120	100	74	—
11	CO ₂ 16.0 MPa	4	180	100	84	—
12	N ₂ 8.5 MPa	4	180	65	10	85
13	Ethanol	4	60	96	48	44
14	Ethanol	4	90	100	52	30
15	Ethanol	4	120	100	64	19
16	Ethanol	4	180	100	77	—
17	Hexane	4	180	30	17	83
18	Toluene	4	180	26	11	89
19	Water	4	180	100	13	87

Reaction conditions: butyne-diol 5 mmol (0.1 mmol per 1 mL of reactor, 0.5 mmol per 1 mL of organic solvents or water), organic solvent or water 10 mL, temperature 323 K.^a Selectivity of A = (moles of A produced)/(moles of butyne-diol reacted). During the reaction n-butanol as a byproduct was produced in a minor amount.

enhance the conversion, and polar solvents like ethanol and water are more effective compared with hexane and toluene (runs 16–19). Apolar CO₂ was found to be an effective medium when the pressure was raised up to the supercritical region (higher than 7.3 MPa). Supercritical CO₂ is also effective, similar to ethanol and water, under the reaction conditions used and, moreover, the selectivity to butane-1,4-diol is higher in scCO₂ than in these polar solvents at 100% conversion (runs 11,16,19). The conversion decreased when N₂ (8.5 MPa) was used instead of CO₂, indicating that the conversion depends on not only the total pressure but also the nature of reaction medium (runs 6,12). The total conversion and selectivity to butane-1,4-diol increased for longer reaction times in both scCO₂ and ethanol (runs 8–11,13–16). The initial conversion in ethanol was higher than that in scCO₂; however, the selectivity to butane-1,4-diol in scCO₂ increased with reaction time faster than that in ethanol, which means that in scCO₂ the first step hydrogenation of C≡C to C=C is slower but the second-step hydrogenation of C=C to C–C is faster compared to the reaction in ethanol.

It was recently reported that a stainless steel reactor wall could catalyze oxidation reactions of olefins.^{12–14} The effect of

the reactor wall has also been examined for the present hydrogenation reactions by using just an inner glass tube, an inner glass tube with stainless steel shavings and a Teflon cell instead of using an SUS 316 autoclave. The total conversion data are shown in Fig. 1. For ethanol, almost no reaction

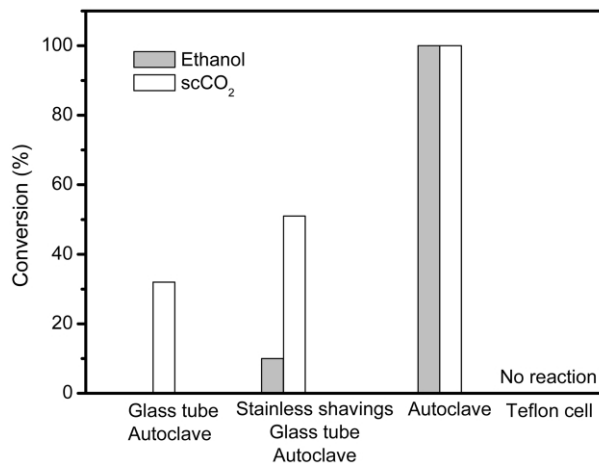


Fig. 1 Hydrogenation of butyne-diol in scCO₂ and in ethanol in the absence and presence of an inner glass tube and/or stainless steel shavings. Reaction conditions: butyne-diol 5 mmol (0.1 mmol mL⁻¹ reactor volume, 0.5 mmol mL⁻¹ ethanol), ethanol 10 mL, CO₂ 16.0 MPa, H₂ 4.0 MPa, temperature 323 K, time 2 h, stainless steel shavings 0.2 g (if necessary).

occurred when the inner glass tube was used inside the autoclave reactor, in contrast to 100% conversion in the autoclave. For scCO₂, when the inner glass tube was used, the conversion decreased to 32% from 100% (in the autoclave). When 0.5 g of stainless steel shavings was added to the glass tube, the reaction was promoted both in ethanol and scCO₂ compared with the reactions in the glass tube. *In situ* high-pressure NMR indicated that no hydrogenation products could be detected in the Teflon reaction-cell under identical reaction conditions as those in the stainless steel reactor. These results clearly demonstrate that the stainless steel reactor wall (SUS 316) promoted 2-butyne-1,4-diol hydrogenation in scCO₂ and in ethanol. The reactor wall (SUS 316) contains Ni, Cr and Mn components which can act as catalyst in the present hydrogenation reactions. It has already been reported that hydrogenation of butyne-1,4-diol can be catalyzed by Raney type nickel catalysts⁹ or Ni–Cu–Mn supported on γ -alumina catalyst.¹⁰ In the case of scCO₂, the substrate can be soluble in the gaseous phase to some extent, and it may be easy for direct contact between the reaction mixture and the reactor wall to occur. This could be a reason for the enhanced conversion observed in scCO₂ even when the inner glass tube is used, and such a direct interaction is not possible in ethanol at a lower reaction temperature of 323 K.

To certify the influence of phase behavior on the hydrogenation in scCO₂, the phases of the reaction mixture have been examined with a high-pressure view-cell. We observed two phases of solid (2-butyne-1,4-diol) and gas under ambient atmosphere and under 8.5 MPa N₂ at 323 K. It is interesting, in contrast, that two phases of liquid (not solid) and gas exist under a pressurized CO₂ atmosphere at 8.5 MPa and at a slightly lower temperature of 320 K, where the liquid phase is 2-butyne-1,4-diol and the CO₂ gas phase may include some 2-butyne-1,4-diol. The normal boiling point of 2-butyne-1,4-diol is 323 K,¹⁵ but, in the presence of 8.5 MPa scCO₂, to some extent, it is easier for its melting to occur compared with ambient atmosphere and pressurized N₂. Fulton *et al.* had suggested the existence of an interaction between alcohol and scCO₂, which could affect the intermolecular hydrogen bonding between alcohol molecules in scCO₂.^{16,17} It was further suggested that such a solute–solvent interaction would enhance the solubility

of materials in scCO₂ and result in remarkable variation of physical properties.¹⁸

It is important that, after depressurization, the reaction mixture only includes the products and/or the substrate in a single liquid phase at a lower temperature. At 100% conversion, only the products exist in the reactor, and so no separation from catalysts and organic solvents is necessary.

Conclusions

ScCO₂ is an ideal replacement for organic solvents in the hydrogenation of 2-butyne-1,4-diol to butane-1,4-diol. The reaction can be effective by a very mild and environmentally friendly process, free of catalysts as well as organic solvents, with a catalytic action of the stainless steel reactor wall. Even at such a low temperature as 323 K, a high selectivity of 84% for butane-1,4-diol is achieved at 100% total conversion.

Experimental

Hydrogenation

The hydrogenation reactions were carried out in a 50 mL SUS316 stainless steel autoclave. Five mmol 2-butyne-1,4-diol (0.1 mmol per 1 mL reactor) was charged into the reactor and the reactor was flushed with 2.0 MPa CO₂ three times. The reactor was then heated up to the desired temperature of 323 K and H₂ and compressed liquid CO₂ were introduced to the desired pressure with a high-pressure liquid pump. The reaction runs were conducted while stirring with a magnetic stirrer. The composition of the reaction mixture was analyzed by a gas chromatograph using a flame ionization detector.

Phase behavior

The examination of phase behavior is important to study whether the reaction in scCO₂ is taking place homogeneously in

a single phase or heterogeneously in two or more phases. A 10 mL high-pressure sapphire-windowed view cell was used to observe the phases present under ambient atmosphere and pressurized N₂ and CO₂. The phase behavior observation was also used to estimate the solubility of the substrate in compressed CO₂ and H₂.¹¹ A certain amount of 2-butyne-1,4-diol was added to a view cell followed by introduction of the gases. Then, stirring of the mixture was started and the state of the reaction mixture was inspected by naked eye from the windows several times within 30 min.

References

- 1 W. Leitner, *Acc. Chem. Res.*, 2002, **35**, 746.
- 2 A. Baiker, *Chem. Rev.*, 1999, **99**, 453.
- 3 *Chemical Synthesis Using Supercritical Fluids*, ed. P. G. Jessop and W. Leitner, Wiley-VCH, Weinheim, 1999.
- 4 J.-D. Grunwaldt, R. Wandeler and A. Baiker, *Catal. Rev. Sci. Eng.*, 2003, **45**, 1.
- 5 M. Arai, Y. Nishiyama and Y. Ikushima, *J. Supercrit. Fluids*, 1998, **13**, 149.
- 6 R. V. Chaudhari, C. V. V. Road, R. Jaganathan, M. M. Telkar and V. H. Rane, US Pat. 2002, 6469221B1.
- 7 F. Codignola, US. Pat. 1984, 4438285.
- 8 F. Y. Zhao, C. Wang and X. Hua, *Chin. J. Petrochem. Technol.*, 1993, **22**, 650.
- 9 V. H. Eugene and N. J. Westfield, US Pat. 1960, 2953605.
- 10 S. R. Elizabeth and W. D. Parsippany, US Pat. 1976 3950441.
- 11 F. Y. Zhao, Y. Ikushima, M. Chatterjee, O. Sato and M. Arai, *J. Supercrit. Fluids*, in press.
- 12 F. Loeker and W. Leitner, *Chem. Eur. J.*, 2000, **6**, 2011.
- 13 U. Shah, S. M. Mahajani, M. M. Sharma and T. Sridhar, *Chem. Eng. Sci.*, 2000, **55**, 25.
- 14 B. C. Ranu, S. S. Dey and A. Hajra, *Green Chem.*, 2003, **5**, 44.
- 15 D. R. Lide, Ed., *CRC Handbook of Chemistry and Physics*, CD-ROM Version 2003.
- 16 J. L. Fulton, G. G. Yee and R. D. Smith, *J. Am. Chem. Soc.*, 1991, **113**, 8327.
- 17 G. G. Yee, J. L. Fulton and R. D. Smith, *J. Phys. Chem.*, 1992, **96**, 6172.
- 18 Y. Wang and P. B. Balbuena, *J. Phys. Chem. A*, 2001, **105**, 9972.



Continuous synthesis of zinc oxide nanoparticles in supercritical water

Kiwamu Sue, Kenji Murata, Kazuhito Kimura and Kunio Arai*

Graduate School of Environmental Studies, Tohoku University, 07 Aoba Aramaki-Aza, Aoba-ku, Sendai 980-8579, Japan. E-mail: karai@arai.che.tohoku.ac.jp; Fax: +81-22-217-7246; Tel: +81-22-217-7246

Received 11th June 2003

First published as an Advance Article on the web 27th August 2003

Hydrothermal synthesis of nano-size zinc oxide particles was conducted using a flow type apparatus for rapid heating of zinc nitrate and potassium hydroxide aqueous solution to supercritical conditions at 30 MPa and temperatures ranging from 573 to 673 K.

Introduction

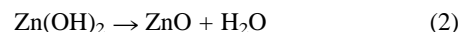
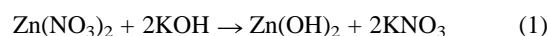
Zinc oxide (ZnO) is used in various technologies such as varistor, gas-sensor, catalyst, phosphor, and other applications. ZnO particles can be produced by several techniques such as precipitation,^{1–3} spray pyrolysis,⁴ thermal decomposition,⁵ and hydrothermal synthesis.^{6–8} In particular, hydrothermal synthesis is well known as an environmentally safe and simple process, since it does not require any organic solvents and additional processing such as comminution or calcination.

Typically, hydrothermal synthesis is conducted with a batch type apparatus.^{6–8} An aqueous solution is heated up slowly to 373–573 K and then aged for several hours or days. During the heat-up time, hydrothermal reaction takes place to produce nuclei and then crystals grow. As ZnO becomes more soluble in water compared with the other metal oxides such as TiO₂ and ZrO₂,^{9,10} hydrothermal synthesis of nano-size fine particles is an especially difficult problem without any surfactants.

Over the past ten years, continuous hydrothermal synthesis methods have been established for forming micro or nano-size metal oxide fine particles in supercritical water.^{11–15} In this method, the starting materials at ambient temperature are pressurized and fed as aqueous solutions into a mixing tee that combines the reactants with preheated water at high pressure. This rapidly heats the reactants to the desired temperature and allows continuous hydrothermal reactions to take place. When water in its near-critical or supercritical state is used, the hydrothermal reaction rate and metal oxide solubility can be controlled by changing temperature and pressure since the reaction solvent properties are strongly dependent on the conditions in these regions. Further, since supercritical water forms homogeneous phases with oxygen and hydrogen, redox reactions can be also controlled. Therefore, the continuous hydrothermal synthesis method can be used to possibly change particle size, morphology, and crystal structure. Generally, at 30 MPa, the reaction rate of hydrothermal synthesis above the critical temperature ($T_C = 647$ K) is a few orders of magnitude higher than that under T_C .¹¹ In contrast, metal oxide solubilities above T_C are a few orders of magnitude lower than that under T_C .^{11,16} Thus, the continuous hydrothermal synthesis method has great potential for producing nano-size metal oxide fine particles. This work focuses on the continuous production of nano-size ZnO fine particles in supercritical water by using a flow-through apparatus for rapid heating of an aqueous solution.

Experimental

The solution was prepared by dissolving precise amounts of zinc nitrate (Zn(NO₃)₂·6H₂O, Wako Pure Chemicals, Osaka, Japan) and potassium hydroxide (KOH, Wako Pure Chemicals, Osaka, Japan) crystals in distilled water. The concentrations of Zn(NO₃)₂ and KOH are summarized in Table 1. In this study, hydrothermal reaction is represented in terms of two reaction steps; zinc hydroxide sol formation (1) and dehydration from the sol (2):



The crystal structures of the products were analyzed by powder X-ray diffractometry (XRD) (RINT-2200, Rigaku), using CuK α radiation. Observation of these products was performed by transmission electron microscopy (TEM) (LEO-912-OMEGA, Karl Zeiss). Particle size distribution and average particle size with standard deviation (S.D.) were determined based on the diameter of about 200 particles measured from TEM results. The concentrations of remaining Zn ion in the recovered aqueous solution were measured by inductively coupled plasma (ICP) emission spectroscopy (SPS-7800, Seiko). Conversion of Zn ion to solid product was defined as follows:

$$X = (1 - C/C_0) \times 100 \quad (3)$$

where C and C_0 are molal concentrations of the Zn species in the recovered and feed solutions, respectively.

Green Context

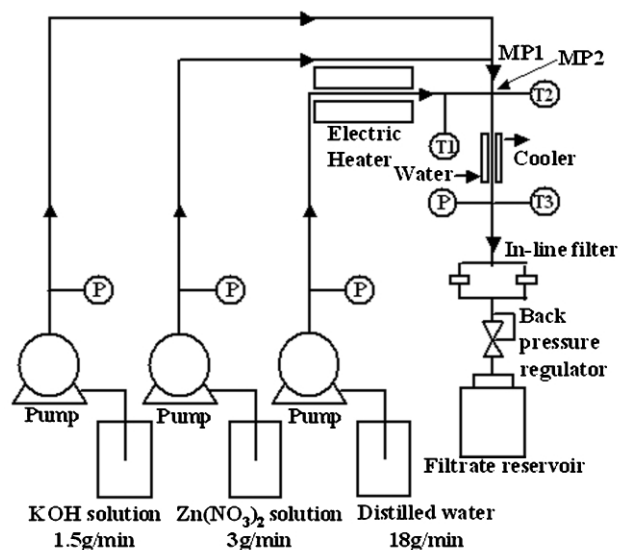
The synthesis of nanoparticles can be a tricky and complex business. The initial synthesis often needs to be followed by calcination and then by a step to reduce the size of particles, often present as clusters. Here, supercritical water is shown to be a clean synthesis environment for the primary syntheses, but has the added advantages that no calcination is required, nor is comminution necessary, since the size distribution of the nanoparticles is controlled by the large changes to reaction rates and solubilities around the critical point.

DJM

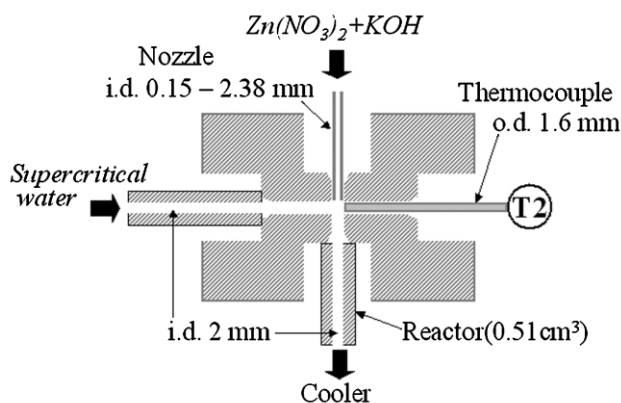
Table 1 Experimental results

Run no.	Zn(NO ₃) ₂ /mol kg ⁻¹	KOH/mol kg ⁻¹	Temperature/K	Residence time/s	Conversion (%)	Average particle size/nm	S.D./nm	Nozzle i.d./mm
1 (flow)	5 × 10 ⁻²	10 ⁻¹	673	0.5	97	45	14	0.59
2 (flow)	5 × 10 ⁻²	10 ⁻¹	657	0.7	100	44	15	0.59
3 (flow)	5 × 10 ⁻³	10 ⁻²	663	0.6	98	28	11	0.59
4 (flow)	5 × 10 ⁻³	10 ⁻²	573	1.0	92	31	14	0.59
5 (flow)	5 × 10 ⁻³	10 ⁻²	662	0.7	99	57	26	2.38
6 (flow)	5 × 10 ⁻³	10 ⁻²	663	0.6	90	23	10	0.15
7 (flow)	5 × 10 ⁻⁴	10 ⁻³	658	0.7	63	49	62	0.59
8 (flow)	5 × 10 ⁻⁴	2 × 10 ⁻³	658	0.7	100	27	11	0.59
9 (batch)	5 × 10 ⁻²	10 ⁻¹	673	600	100	447	252	—

A schematic diagram of experimental flow apparatus is shown in Fig. 1. Zn(NO₃)₂ and KOH aqueous solutions were fed with two pumps at a flow rate of 3 g min⁻¹ and 1.5 g min⁻¹,

**Fig. 1** A flow-through experimental apparatus.

respectively. In this system, to reduce nucleation and particle growth at room temperature after zinc hydroxide sol formation by mixing Zn(NO₃)₂ and KOH aqueous solutions at mixing point 1 (MP1), the sol was quickly fed to mixing point 2 (MP2) by a nozzle made of stainless steel tube (i.d. 0.15, 0.59, and 2.38 mm, and 15 mm length). The solution was mixed at mixing point 2 (MP2) (inner volume 0.012 cm³) with preheated water fed at a flow rate of 18 g min⁻¹ and then the mixture was rapidly heated to the reaction temperature within a few seconds by the micro mixing unit. The details of this unit (MP2) are shown in Fig. 2. The reactor was made of Hastelloy C276 tube (i.d. 2 mm)

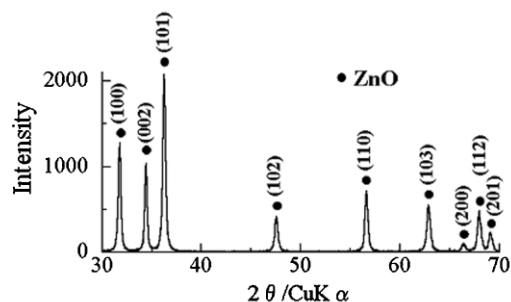
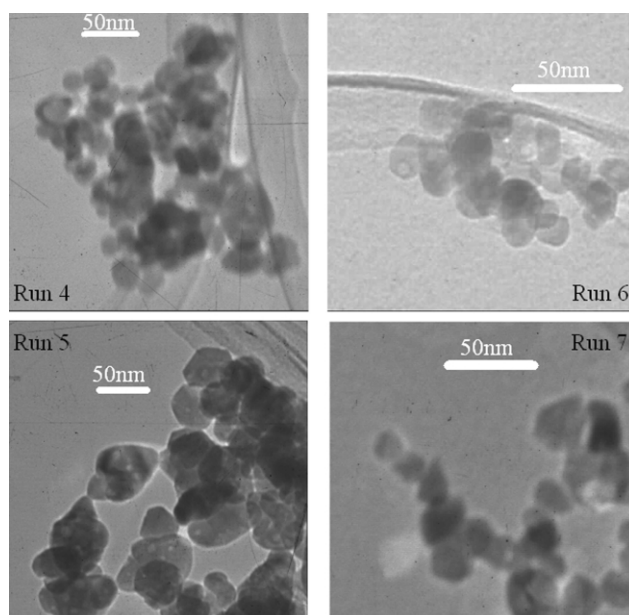
**Fig. 2** Details of mixing point (MP2).

and it has a volume of 0.51 cm³. Reaction temperature was defined as the temperature in MP2 (T₂). Residence time, *t*, was

calculated using eqn. (4), from the density of pure water¹⁷ at the reaction temperature and pressure as follows:

$$\tau = V/(F(\rho_{298}/\rho_{T2})) \quad (4)$$

where *F* is the total flow rate and *V* is the reactor volume; ρ_{298} and ρ_{T2} are the densities of pure water at room and given temperature, respectively. At the exit of the reactor the fluid was quenched with an external water jacket. The temperature was measured with a K-type thermocouple. The system pressure was maintained to 30 ± 0.1 MPa by using a back pressure regulator that was placed after the cooler. Particles were removed by using an in-line filter to minimize plugging at the back pressure regulator. When the system achieved steady state, as judged by the temperature, produced particles were collected by diverting the flow to a parallel in-line filter with a three-way valve.

**Fig. 3** Typical XRD pattern of product (Run 1).**Fig. 4** TEM observations.

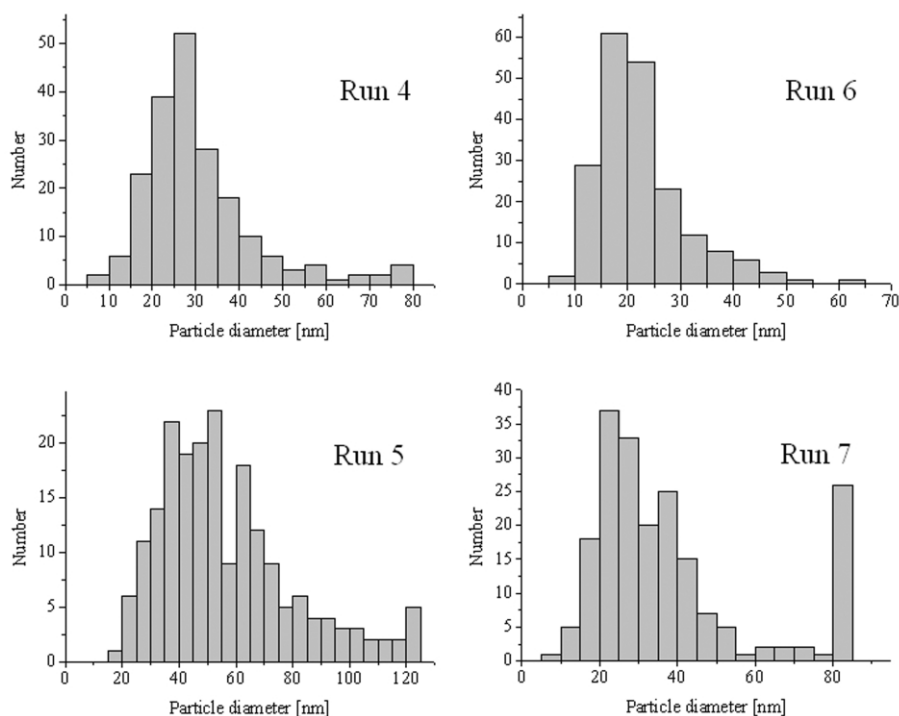


Fig. 5 Particle size distributions.

To investigate particle production over longer reaction times, an experiment with a batch type reactor was also conducted. $\text{Zn}(\text{NO}_3)_2$ and KOH aqueous solutions were loaded into a 153 cm^3 reactor made of a Ti alloy. The temperature was measured with a K-type thermocouple that was inserted into the reactor. Reactor load water density was about 0.35 g cm^{-3} , which corresponds to 30 MPa at a reaction temperature of 673 K. The batch reactor was heated by immersion into a temperature-controlled molten-salt bath. Approximately 5 min was required for the batch reactor to reach the reaction temperature. Reaction time was 10 min, which includes heating up time. The reactor was quenched in a water bath, which was kept to room temperature.

Experimental conditions are summarized in Table 1. The molal concentration ratio of $\text{Zn}(\text{NO}_3)_2$ to KOH after mixing was kept at a constant value of 0.5 and 1.0.

Results and discussion

Fig. 3 shows a typical XRD pattern of the product (Run 1). All peaks could be assigned to ZnO. The particles obtained in this work were also a single phase of ZnO. Typical results of TEM observation and particle size distribution are shown in Figs. 4 and 5, respectively. Average particle diameter with S.D. and conversion are summarized in Table 1

Firstly, particle size of the flow experiment (Run 1) was 45 nm, which was about 10 times smaller than that of the batch experiments (Run 9). The difference in heat-up time between the flow apparatus and the batch apparatus probably accounted for the small particles produced. Secondly, for temperatures increasing from 657 K (Run 2) to 673 K (Run 1) and from 573 K (Run 4) to 663 K (Run 3), no significant difference in particle size and conversion was observed. Thirdly, with increasing nozzle inner diameter from 0.15 mm (Run 6) to 2.38 mm (Run 5), particle size increased from 23 nm to 57 nm. This increase of particle size seemed to be related to the increase in heat-up time from the mixing point of $\text{Zn}(\text{NO}_3)_2$ and KOH (MP1) to the mixing point with preheated water (MP2). Finally, for initial $\text{Zn}(\text{NO}_3)_2$ concentrations decreasing from $5 \times 10^{-2} \text{ mol kg}^{-1}$ (Run 2) to $5 \times 10^{-3} \text{ mol kg}^{-1}$ (Run 3), particle size decreased

from 44 (S.D.15) nm to 28 nm (S.D.11) and no significant difference of conversion was observed. For the case where initial reactant concentrations are a few orders of magnitude higher than metal oxide solubility at the given reaction conditions, a decrease in the initial reactant concentration usually results in the formation of smaller particles.¹⁵ In contrast, in our results, reducing the initial $\text{Zn}(\text{NO}_3)_2$ concentrations from $5 \times 10^{-3} \text{ mol kg}^{-1}$ (Run 3) to $5 \times 10^{-4} \text{ mol kg}^{-1}$ (Run 7) caused the particle sizes to increase to 49 nm (S.D.62) and the conversion to decrease to 63%. For this case, the decrease in initial $\text{Zn}(\text{NO}_3)_2$ concentration and the approach of the initial concentration to the zinc oxide solubility limit apparently promoted dissolution and precipitation, which resulted in the formation of polydispersion particles (larger S.D.) and low conversion. Further, for increasing the KOH concentration from $1 \times 10^{-3} \text{ mol kg}^{-1}$ (Run 7) to $2 \times 10^{-3} \text{ mol kg}^{-1}$ (Run 8), particle size decreased and conversion increased. This can be explained by the probable increase in KOH species under a neutral pH region that tends to lower ZnO solubility¹⁰ and as a result, smaller particles were produced with high conversion. In conclusion, continuous hydrothermal synthesis of nano-size ZnO fine particles *via* a flow-through apparatus could be established at supercritical conditions.

Acknowledgements

This research was partially supported by the Ministry of Education, Science, Sports and Culture, Grant-in-Aid for Scientific Research, No.15360416, 2003.

References

- 1 S. M. Haile, D. W. Johnson, G. H. Wiseman and H. K. Bowen, *J. Am. Ceram. Soc.*, 1989, **72**, 2004.
- 2 M. E. V. Costa and J. L. Baptista, *J. Eur. Ceram. Soc.*, 1993, **11**, 275.
- 3 T. Trindade, J. D. Pedrosa de Jesus and P. O'Brien, *J. Mater. Chem.*, 1994, **4**, 1611.

- 4 T. Q. Liu, O. Sakurai, N. Mizutani and M. Kato, *J. Mater. Sci.*, 1986, **21**, 3698.
- 5 M. Andrés-Vergés and M. Martínez-Gallego, *J. Mater. Sci.*, 1992, **27**, 3756.
- 6 H. Nishizawa, T. Tani and K. Matsuoka, *J. Am. Ceram. Soc.*, 1984, **67**, 98.
- 7 A. Chittofrati and E. Matijevic, *Colloids Surf.*, 1990, **48**, 65.
- 8 C. H. Lu and C. H. Yeh, *Ceram. Int.*, 2000, **26**, 351.
- 9 S. E. Ziemniak, M. E. Jones and K. E. S. Combs, *J. Solution Chem.*, 1993, **22**, 601.
- 10 P. Bénézeth, D. A. Palmer and D. J. Wesolowski, *Geochim. Cosmochim. Acta*, 1999, **63**, 1571.
- 11 T. Adschiri, Y. Hakuta, K. Sue and K. Arai, *J. Nanopart. Res.*, 2001, **3**, 227.
- 12 Y. Hakuta, T. Haganuma, K. Sue, T. Adschiri and K. Arai, *Mater. Res. Bull.*, 2003, **38**, 1257.
- 13 A. Cabanas and M. Poliakoff, *J. Mater. Chem.*, 2001, **11**, 1408.
- 14 R. Viswanathan and R. M. Gupta, *J. Supercrit. Fluids*, 2003, in press.
- 15 Y. Hao and A. S. Teja, *J. Mater. Res.*, 2003, **18**, 415.
- 16 K. Sue, Y. Hakuta, R. L. Smith Jr., T. Adschiri and K. Arai, *J. Chem. Eng. Data*, 1999, **44**, 1422.
- 17 W. Wagner and A. Pruss, *J. Phys. Chem. Ref. Data*, 2002, **31**, 387.



The catalytic opportunities of near-critical water: a benign medium for conventionally acid and base catalyzed condensations for organic synthesis

Shane A. Nolen,^a Charles L. Liotta,^a Charles A. Eckert^{*a} and Roger Gläser^b

^a Schools of Chemical Engineering and Chemistry and the Specialty Separations Center, Georgia Institute of Technology, Atlanta, Georgia 30332-0100

^b Institute of Chemical Technology, University of Stuttgart, D-70550 Stuttgart, Germany

Received 22nd July 2003

First published as an Advance Article on the web 3rd September 2003

Near-critical water (NCW; 250–350 °C, 40–90 bar) provides an environmentally benign alternative medium for conducting organic synthesis. The Claisen–Schmidt condensation of benzaldehyde with 2-butanone was investigated and is used to demonstrate the ability to conduct conventionally acid or base catalyzed reactions homogeneously using NCW without the addition of a catalyst. Kinetic investigations of the Claisen–Schmidt condensation yielded activation energies of 24.7 and 22.6 kJ mol⁻¹ for the formation of products consistent with those formed under classical acidic and basic conditions, respectively. Investigations of other conventionally base catalyzed condensations were performed in uncatalyzed NCW for completeness, including the self-condensation reaction of butyraldehyde, the benzaldehyde–acetone cross-aldol condensation, the intramolecular Claisen condensations of ethyl-4-acetylbutyrate and ethyl levulinate, as well as the intramolecular Dieckmann condensation of diethyl adipate.

Introduction

Approximately 70% of the Earth's surface is comprised of water making water the most abundantly available liquid solvent with $\sim 1.36 \times 10^{18}$ metric tons available for chemical process applications.¹ Not only is water readily available at low cost, it is also environmentally benign providing opportunities for clean processing and pollution prevention. Liquid water in the "near-critical regime" (250–350 °C, 40–90 bar) can serve as a reactive medium for organic synthesis as a result of the changes that occur to its chemical and physical properties at elevated temperature. The dielectric constant of saturated liquid water decreases with increasing temperature from 80, at ambient conditions, to 20, at 275 °C. Similarly, the density decreases from 1 to 0.7 g cm⁻³. These changes influence the solvent properties of near-critical water (NCW; $T_c = 374$ °C, $P_c = 221$ bar) making it similar to room temperature polar organic solvents, like acetone. Polar organics are completely miscible in NCW, while the solubility of non-polar organics increases dramatically in comparison to the ambient temperature solubility.² The relative permittivity also remains high enough to dissolve and ionize ionic species giving NCW a wide range of synthetic applications.

Similar to the other physical properties of water, the ionization constant changes as a function of temperature reaching a maximum near 250 °C. The result is a 3-fold increase in the dissociation of saturated liquid water into hydronium and hydroxide ions allowing acid or base catalyzed reactions to be performed without the addition of acids or bases. The ionization constant is a very tunable property that can be further increased by several orders of magnitude with a subsequent increase in pressure. This naturally occurring *in situ* form of catalysis eliminates the need for post reaction neutralization, which is a common practice with the use of many conventional acids and bases. This is significant since the production of waste salts from neutralizations can be as great as several kg/kg of product.³

In addition to eliminating the use of hazardous organic solvents and acid and base catalyst additions, the properties of NCW are easily tuned by variations of temperature and pressure. This results in a number of processing benefits including reduced or eliminated mass transfer limitations and improved product selectivity. Facile separation of the organic products from water is also achieved due to the natural phase separation that occurs upon cooling from reaction temperatures to ambient conditions. This free separation can result in tremendous cost savings since separations can contribute to as much as 50–80% of the total capital and operating expense of an industrial process.

Although numerous reactions have been investigated in NCW, the primary focus to date has been on providing examples of the ability to synthesize compounds formed under classical acidic conditions using uncatalyzed NCW. The research groups of Siskin and Katritzky,^{4,5} Strauss and Trainor,^{6–8} and Liotta and Eckert,^{9–12} have contributed extensively in this area. Comprehensive reviews of the reactions conducted in near and supercritical water have been provided by Savage,¹³ as well as Siskin and Katritzky^{14,15}.

NCW has equal concentrations of hydronium and hydroxide ions; however, no definitive investigations have been performed

Green Context

Water is widely regarded as a very attractive medium for organic reactions since it is safe to handle, inexpensive and environmentally compatible. One of the drawbacks is the poor solubility of many organic compounds but increasing the temperature of water towards supercritical conditions causes dramatic effects to the properties of the liquid including much-improved organophilicity. Here we see this effectively exploited in various acid and base catalyzed organic reactions. *JHC*

showing whether a reaction occurs strictly *via* a mechanism involving hydroxide ions. Investigations of the hydrolysis of anisoles in NCW have been studied and show that even though direct attack of hydroxide ions to the anisole methyl group may play a role in the reaction, the dominant mechanism involves the S_N2 substitution of water to the methyl group.¹⁶

Investigations of classically base catalyzed reactions have also been briefly explored in uncatalyzed supercritical water. Benzaldehyde was found to form benzyl alcohol and benzoic acid by an oxidative–reductive mechanism consistent with a classical Cannizzaro reaction, which is usually performed in strong aqueous base.¹⁷ It should be emphasized that in contrast to supercritical water, NCW is a more diverse medium for organic synthesis since (1) it can solubilize ionic species in addition to organics and (2) since the temperatures and pressures are less extreme favoring carbon–carbon bond formations over destruction. As a consequence of the more process friendly nature of NCW, we have explored a variety of condensation reactions in this medium. In particular, we have conducted detailed studies of the Claisen–Schmidt condensation between benzaldehyde and 2-butanone to form α,β -unsaturated ketones along with the self-condensation of butyraldehyde, the intramolecular condensations of ethyl-4-acetylbutyrate, ethyl levulinate, and diethyl adipate, as well as the cross aldol condensation between benzaldehyde and acetone.

The main focus of this work is the Claisen–Schmidt condensation, which forms two products due to the asymmetry of 2-butanone with respect to the carbonyl functionality (Fig. 1).

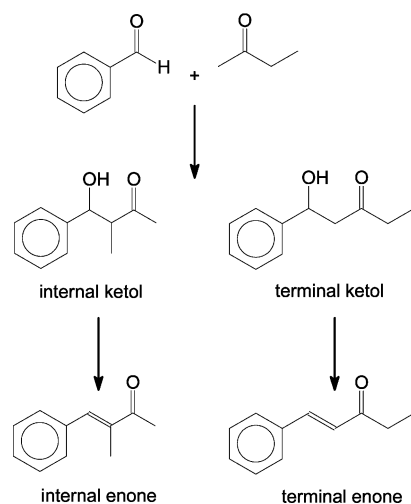


Fig. 1 Claisen–Schmidt reaction of benzaldehyde with 2-butanone showing the two possible condensation products 4-phenyl-3-methyl-3-buten-2-one (internal enone) and 1-phenyl-1-penten-3-one (terminal enone), as well as their precursor intermediate ketols.

It has been reported that under traditional acidic conditions the terminal enone condensation product (1-phenyl-1-penten-3-one) is selectively formed, while under basic conditions, the internal enone condensation product (4-phenyl-3-methyl-3-buten-2-one) is selectively formed.¹⁸ Although it is possible for both products to be formed *via* acid or base catalysis, a single dominant species is favored for each set of conditions.¹⁹ Stiles *et al.* verified this through a series of investigations conducted at ambient temperatures in which the ketol intermediates (Fig. 1) were subjected to conventional acidic and basic conditions to determine if the ketols dehydrate to form their corresponding unsaturated products or are cleaved to form the starting materials. It was found that under basic conditions, the internal ketol is unstable and decomposes to form the starting materials, while the terminal ketol is dehydrated to form a single product, the terminal enone product.²⁰ Under acidic conditions, both ketols result in the formation of their corresponding α,β -

unsaturated carbonyl products; however, within an acidic environment, the internal enol intermediate of 2-butanone (Fig. 2) is more stable than the terminal enol intermediate resulting in

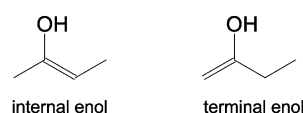


Fig. 2 Internal and terminal enols of 2-butanone.

the preferential formation of the internal ketol and therefore internal enone product.²⁰ The only deviation from this trend is observed under very strongly acidic or basic conditions where both α,β -unsaturated carbonyl products are formed. Even under these extreme conditions, the product derived from the more stable enol for the given set of conditions is favored by as much as 9 to 1 over the product derived from the less stable enol.^{21,22}

Experimental

Materials

The following reactants and reagents, 2-butanone (HPLC grade, >99.5%), benzaldehyde (>99.5%), butyraldehyde (99%), ethyl-4-acetylbutyrate (98%), diethyl adipate (99%), and water (HPLC grade) were purchased from Sigma-Aldrich, while hydrochloric acid (37 wt%, certified A.C.S. plus grade) was obtained from Fisher Scientific, and ethyl levulinate (98%) was obtained from TCI. The product compound, 2-ethylhexanal (97%), was obtained from Fluka, while 2-ethyl-2-hexenal (99%) was obtained from TCI, and *trans*-4-phenyl-3-buten-2-one (99%) and *trans,trans*-dibenzylidene acetone were purchased from Sigma-Aldrich. Additionally, 4-phenyl-3-methyl-3-buten-2-one (>99%) was synthesized from benzaldehyde and 2-butanone according to the literature method of Kawai *et al.*²³ Acetone (Sigma-Aldrich, HPLC grade) was used during post-reaction processing for sample dilutions prior to analysis, with the exception of the benzaldehyde–acetone condensation in which *N,N*-dimethylformamide (Sigma-Aldrich, >99.9% HPLC grade) was used. All chemicals were used as obtained without further purification, except for water, which was degassed using nitrogen (High Purity Grade) obtained from Air Product and Chemicals, Inc. for a minimum of 30 min.

Experimental apparatus and procedures

Reactions were conducted in 3.0 ± 0.2 mL (5/16 inch I.D., 5/8 inch O.D., $2\frac{1}{2}$ inch long) constant volume titanium batch reactors. These reactors were designed and produced in-house and were sealed with titanium NPT plugs. Titanium was used as the material of construction due to the very low level of transition metals and corrosion resistance of the metal. The transition metals present in 316 stainless steel have been found to catalyze unwanted side reactions during investigations conducted within our research group. The reactors were heated using a thermostated aluminium block designed to hold 10 batch reactors (Fig. 3). The temperature of the block varied by ± 1 °C along the length of the block and was maintained to within ± 1 °C by a series of four cartridge heaters (Omega Technologies) and an Omega Model CN8500 temperature controller. An over-temperature controller (I²R Model OTP-1500) was also employed as a safety precaution to prevent the block from over heating in the case of a temperature controller failure.

These reactors provided numerous advantages over other types of reaction vessels. The time required to heat the contents

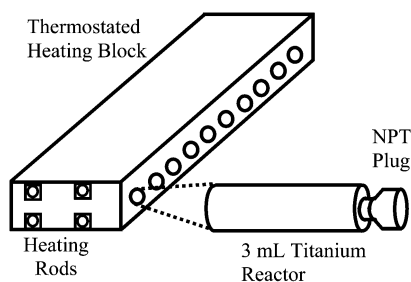


Fig. 3 Titanium batch reactor and thermostated aluminium heating block.

of a reactor to the desired reaction temperature was 5–7 min., while cooling back to ambient conditions, took ~2 min.¹⁰ Cooling was achieved by quenching the reactors in a room temperature water bath. Because of their size, numerous reactions could be performed at the same time. This allowed various parameters to be tested relatively quickly, providing mechanistic insight into the reactions, while still allowing for the elucidation of the reaction kinetics.

In all experiments, solid reactants were weighed and loaded prior to the addition of any liquids. Liquids were loaded using Eppendorf Reference Standard adjustable pipettors. Reactor loading was performed under a nitrogen atmosphere to prevent oxygen from being present within the reactor, which could have resulted in unwanted oxidations. Upon experimental completion, the reactor contents were transferred into a 10 mL volumetric flask. Acetone was then used to wash the reactor and the washings were added to the volumetric flask. This procedure was repeated until the volumetric flask was full, resulting in a single homogeneous phase. Analysis was performed by GC-MS and GC-FID. GC-MS (EI mode) was used for qualification, while GC-FID was used for quantification. External standards of known concentration of the reactants and products were used to calibrate the GC-FID for quantification. Error analysis of the results was assessed through experiments performed in triplicate under analogous conditions.

Results and discussion

Claisen–Schmidt condensation in NCW

In order to elucidate the capability of NCW to act as a medium suitable for performing conventionally acid and base catalyzed organic synthesis without the use of a catalyst, the Claisen–Schmidt condensation of benzaldehyde with 2-butanone was investigated. Employing conventional synthetic techniques, the formation of 4-phenyl-3-methyl-3-buten-2-one (internal enone product) is favored under acidic conditions, while the formation of 1-phenyl-1-penten-3-one (terminal enone product) is favored under basic conditions.²⁰ Since near-critical water has equal concentrations of both hydronium and hydroxide ions, it was anticipated that both products should be formed within this pH neutral medium.

Investigations of the Claisen–Schmidt reaction were conducted in NCW over a temperature range of 250 to 300 °C without the addition of any acid or base. The autogenic pressure of the reactions was between 40 and 90 bar and was strongly dependent upon the temperature used during each experiment and the corresponding vapor pressure of water. A narrow temperature range was used due to the change that would occur to the physical and chemical properties of NCW, particularly the ability to form and support hydronium and hydroxide ions over a broader temperature range. Under the conditions investigated, the reactions occurred homogeneously within a saturated liquid water phase since experiments were performed above the upper critical solution temperature of 2-butanone

(UCST_{2-butanone} = 150 °C)²⁴ and above the UCST for acetophenone (UCST_{acetophenone} = 228 °C),²⁵ which is less polar, and therefore should be less soluble than benzaldehyde.

Following the observations of Gettler and Hammett, a 10 fold molar excess of 2-butanone to benzaldehyde was used during these investigations in an attempt to minimize the formation of higher adducts resultant from continued reaction between the primary condensation products and the starting materials.¹⁹ The results for reactions performed at temperatures of 250, 275, and 300 °C are shown in Fig. 4, 5, and 6 respectively. Both

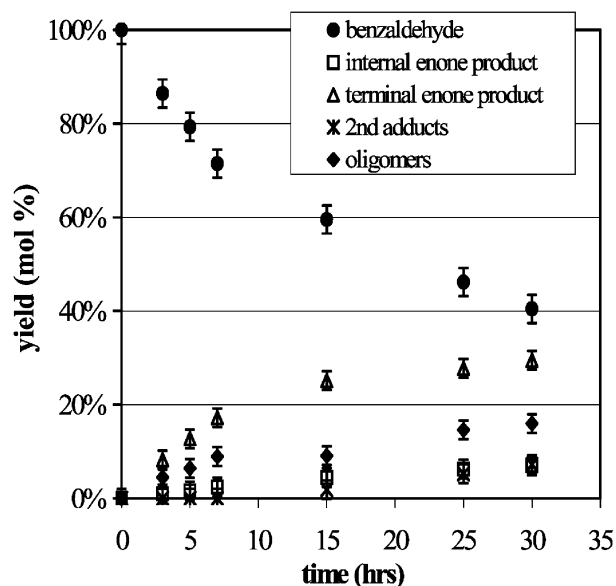


Fig. 4 Production of 1-phenyl-1-penten-3-one (terminal enone product) and 4-phenyl-3-methyl-3-buten-2-one (internal enone product) from the Claisen–Schmidt condensation of benzaldehyde with 2-butanone as a function of time at 250 °C. Formation of secondary condensation products and higher addition products (oligomers) is also shown. The reactant molar ratio (benzaldehyde : 2-butanone : water) was 1 : 10 : 55.

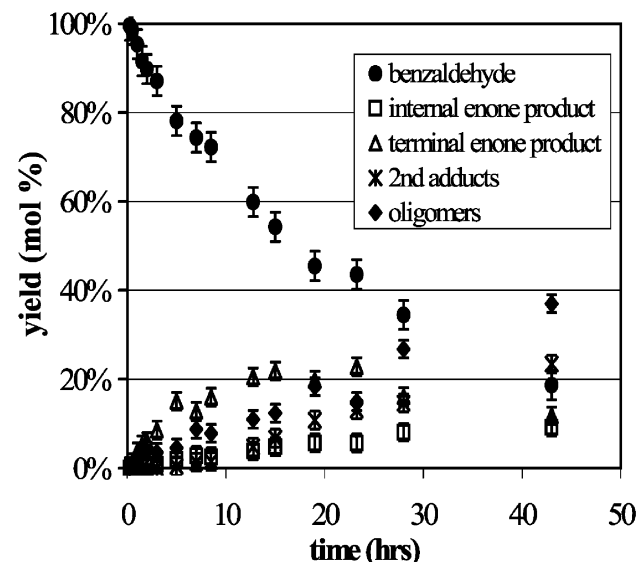


Fig. 5 Production of 1-phenyl-1-penten-3-one (terminal enone product) and 4-phenyl-3-methyl-3-buten-2-one (internal enone product) from the Claisen–Schmidt condensation of benzaldehyde with 2-butanone as a function of time at 275 °C. Formation of secondary condensation products and higher addition products (oligomers) is also shown. The reactant molar ratio (benzaldehyde : 2-butanone : water) was 1 : 10 : 55.

4-phenyl-3-methyl-3-buten-2-one and 1-phenyl-1-penten-3-one were formed indicating that products consistent with classical acid and base catalyzed reactions can be formed using

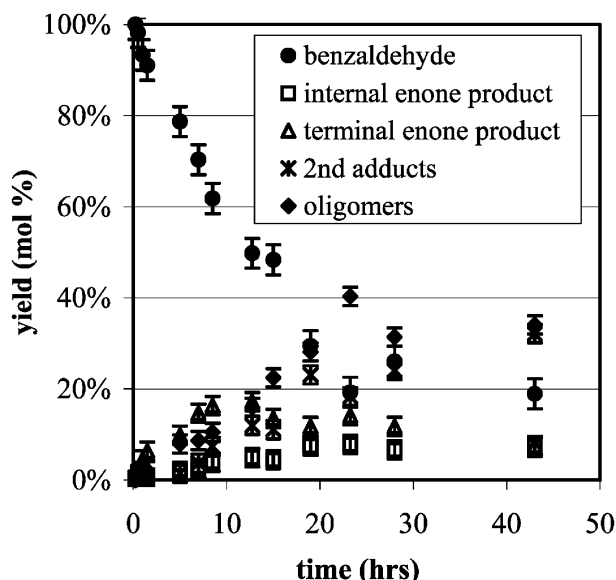


Fig. 6 Production of 1-phenyl-1-penten-3-one (terminal enone product) and 4-phenyl-3-methyl-3-buten-2-one (internal enone product) from the Claisen-Schmidt condensation of benzaldehyde with 2-butanone as a function of time at 300 °C. Formation of secondary condensation products and higher addition products (oligomers) is also shown. The reactant molar ratio (benzaldehyde : 2-butanone : water) was 1 : 10 : 55.

uncatalyzed NCW. Secondary adducts resulting from the addition of another benzaldehyde or 2-butanone molecule to the primary adducts, 4-phenyl-3-methyl-3-buten-2-one and 1-phenyl-1-penten-3-one, were also detected as shown in the figures. Additionally, although not chemically identified, it is speculated that oligomers result from even further condensations occurred. The concentration of these compounds is reported in Fig. 4, 5, and 6. It is interesting to note that the formation of 1-phenyl-1-penten-3-one is dominant over the formation of 4-phenyl-3-methyl-3-buten-2-one. The error bars shown in Fig. 4, 5, and 6 represent the 95% confidence interval determined through triplicate investigations under analogous conditions.

A comparison between the selectivities of the internal and terminal enone products is shown in Fig. 7 for all three

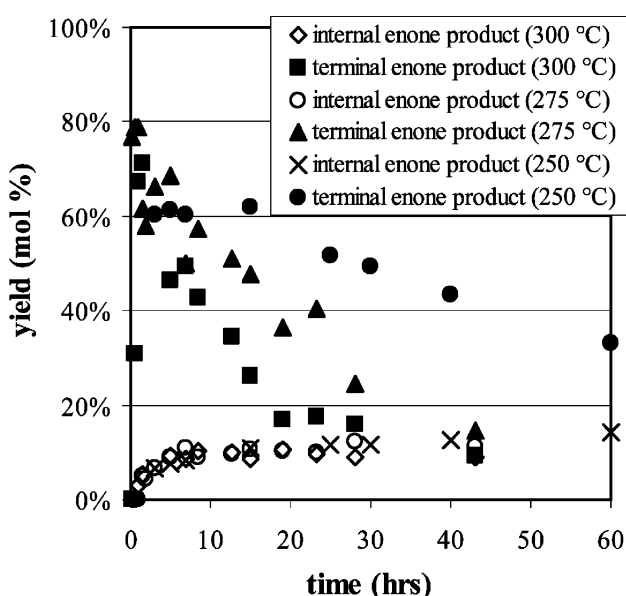


Fig. 7 Selectivity comparison between the internal and terminal enone products at 250, 275, and 300 °C. The reactant molar ratio (benzaldehyde : 2-butanone : water) was 1 : 10 : 55.

temperatures investigated. The selectivity of the terminal enone product is shown to decrease with increasing temperature, while

the selectivity of the internal enone product remains fairly constant over all three temperatures.

Product stability investigation

The products of the Claisen-Schmidt condensation are α,β -unsaturated ketones, which are formed through dehydration of the ketol intermediates resulting in a stoichiometric formation of water. Previous investigations of alkylations and acylations in NCW, which also produce water as a byproduct, were found to be equilibrium limited in accordance with Le Chatelier's Principle since water is the reaction solvent and therefore present in large concentrations.^{9,12,26} For these reasons, studies were performed to determine if an equilibrium limitation exists for the Claisen-Schmidt condensation. This was achieved by monitoring the stability of 4-phenyl-3-methyl-3-buten-2-one in NCW at 250 °C over a period of 30 hrs.

The results (Fig. 8) show that small concentrations of benzaldehyde and 2-butanone were formed along with a large

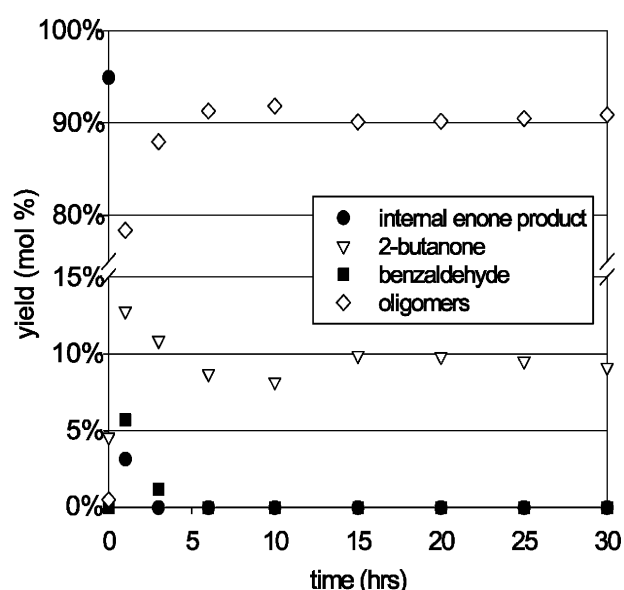


Fig. 8 Claisen-Schmidt condensation back reaction of 4-phenyl-3-methyl-3-buten-2-one (internal enone product) in NCW at 250 °C. The reactant molar ratio (internal enone product : water) was 1 : 55.

concentration of other unidentified products. The unidentified products are attributed to the oligomerization of 4-phenyl-3-methyl-3-buten-2-one with itself, as well as with the starting materials produced from 4-phenyl-3-methyl-3-buten-2-one decomposition. This oligomerization is much more pronounced in the back reaction investigation than it was in the forward reaction, which may be a result of the higher concentrations of 4-phenyl-3-methyl-3-buten-2-one present during the back reaction investigation. The cleavage of 4-phenyl-3-methyl-3-buten-2-one would also result in a stoichiometric ratio of benzaldehyde and 2-butanone to 4-phenyl-3-methyl-3-buten-2-one, which has been reported to increase the formation of higher condensation products.¹⁹ A 10-fold molar excess of 2-butanone was used in the forward reaction to minimize this effect; however, no experiments were performed with an excess of 2-butanone during investigation of the reverse reaction.

It is important to note that no 1-phenyl-1-penten-3-one was detected during investigations of the back reaction indicating that isomerization does not occur between internal and terminal enone products. This finding is in agreement with the research reported by Stiles *et al.*²⁰ Since the oligomerization reactions are much faster than the cleavage of 4-phenyl-3-methyl-3-buten-2-one to benzaldehyde and 2-butanone, the kinetics of

the back reaction were neglected in modeling the condensation, which will be discussed shortly.

Influence of added acid

Investigations of the Claisen–Schmidt condensation were performed with the addition of HCl to further elucidate that reactions involving both hydronium and hydroxide ion catalyzed mechanisms were occurring within NCW. It was theorized that an increase in hydronium ion concentration would lead to an increased production of 4-phenyl-3-methyl-3-buten-2-one, which would be opposite to the trend observed in NCW without the addition of HCl. This theory was tested with a 0.1 : 1 molar addition of HCl to benzaldehyde at 250 °C. The results (Fig. 8 and 9) show a significant increase in the

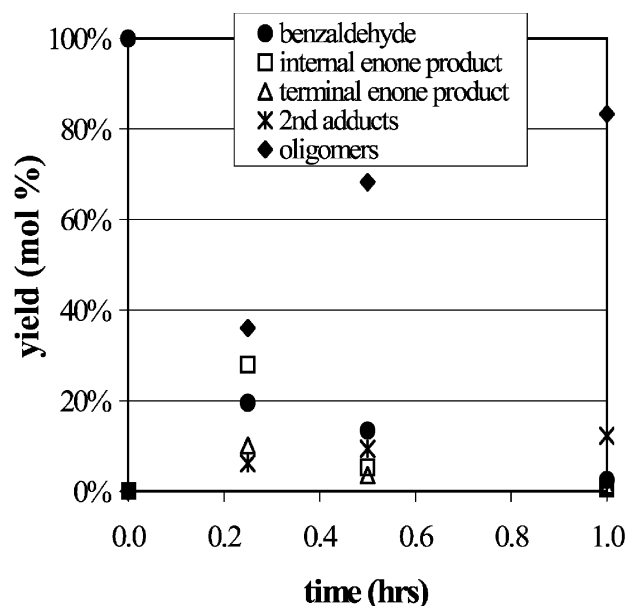


Fig. 9 Investigation of the influence of added HCl on the formation of 1-phenyl-1-penten-3-one (terminal enone product) and 4-phenyl-3-methyl-3-buten-2-one (internal enone product) from the Claisen–Schmidt condensation of benzaldehyde with 2-butanone over short times at 250 °C. Formation of secondary condensation products and higher addition products (oligomers) are also shown. The reactant molar ratio (benzaldehyde : 2-butanone : water : HCl) was 1 : 10 : 55 : 0.1.

production of 4-phenyl-3-methyl-3-buten-2-one. After 15 min, the yield of 4-phenyl-3-methyl-3-buten-2-one was 30 mol% with the addition of HCl as opposed to 0 mol% without HCl. Although the production of 4-phenyl-3-methyl-3-buten-2-one was dominant with the addition of HCl, there was also a pronounced increase in the concentration of 1-phenyl-1-penten-3-one; 10 mol% with HCl as compared to 1 mol% without HCl.

The increase in 1-phenyl-1-penten-3-one production was unexpected, but can be explained by the difference in acid concentrations between investigations with and without HCl. The concentration of hydronium ions in the reaction with HCl (0.04 M) was 15,000 times greater than in NCW without added HCl (3.0×10^{-6} M). At such a high hydronium ion concentration, reactions involving both the favored internal enol and unfavored terminal enol of 2-butanone occur at higher rates. This was verified by Noyce and Snyder through their investigations of the room temperature condensation of anisaldehyde with 2-butanone in 0.3 M acidic solutions.²² Beside the enhancement observed in the formation of the primary condensation products, there is also a considerable enhancement in the rate of formation of secondary adducts and higher condensation products. The formation of these higher adducts comes at the expense of the primary condensation products,

which are only seen in appreciable concentration at very short times (Fig. 9 and 10).

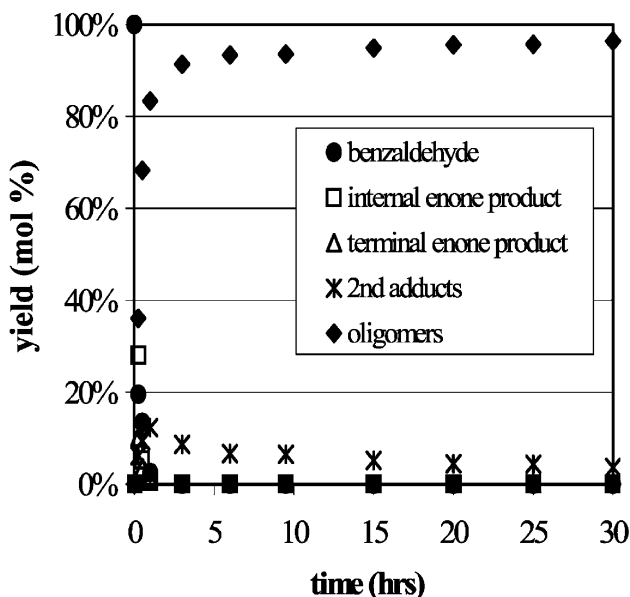


Fig. 10 Investigation of the influence of added HCl on the formation of 1-phenyl-1-penten-3-one (terminal enone product) and 4-phenyl-3-methyl-3-buten-2-one (internal enone product) from the Claisen–Schmidt condensation of benzaldehyde with 2-butanone as a function of time at 250 °C. Formation of secondary condensation products and higher addition products (oligomers) are also shown. The reactant molar ratio (benzaldehyde : 2-butanone : water : HCl) was 1 : 10 : 55 : 0.1.

Kinetic investigation

The reaction kinetics for the condensation of benzaldehyde with 2-butanone are described using first order rate models for the formation of each of the primary condensation products (eqn. 1, 2, and 3). Because 2-butanone was used in large excess, it was assumed that the reaction kinetics would be pseudo-first order in benzaldehyde. The parameters in eqn. 1, 2, and 3 are defined as follows: k'_1 is the pseudo-first order rate constant for the formation of 1-phenyl-1-penten-3-one, k'_2 is the pseudo-first order rate constant for the formation of 4-phenyl-3-methyl-3-penten-2-one, C_{Bz} is the concentration of benzaldehyde, and C_{Bu} is the concentration of 2-butanone. Determination of the rate constants was performed by fitting the data collected at short times, since the formation of higher condensation products is significant at longer times and will affect the kinetics of the primary adducts.

$$-r_{Bz} = k'_1 C_{Bz} + k'_2 C_{Bz} \quad (1)$$

therefore

$$r_{\text{terminal enone}} = k'_1 C_{Bz} \quad (2)$$

$$r_{\text{internal enone}} = k'_2 C_{Bz} \quad (3)$$

where

$$k'_1 = k_1 C_{Bu}$$

$$k'_2 = k_2 C_{Bu}$$

Least squares analysis of the data was found to agree with the pseudo-first order reaction rate assumption for the three temperatures investigated resulting in the rate constants shown in Table 1. The activation energies were calculated through an Arrhenius investigation (Fig. 11) and found to be 22.66 kJ mol⁻¹ for the formation of 1-phenyl-1-penten-3-one and 24.7 kJ mol⁻¹ for the formation of 4-phenyl-3-methyl-3-buten-2-one. The activation energy for the formation of 1-phenyl-

Table 1 Rate constants for the formation of 1-phenyl-1-penten-3-one (terminal enone product, k_1) and 4-phenyl-3-methyl-3-buten-2-one (internal enone product, k_2) from the Claisen–Schmidt condensation of benzaldehyde with 2-butanone

$T/^\circ\text{C}$	k_1/s^{-1}	$k_1/\text{L mol}^{-1}\text{s}^{-1}$	k_2/s^{-1}	$k_2/\text{L mol}^{-1}\text{s}^{-1}$
250	190.15	38.03	21.26	4.25
275	219.29	43.86	28.36	5.67
300	299.94	59.99	34.72	6.94

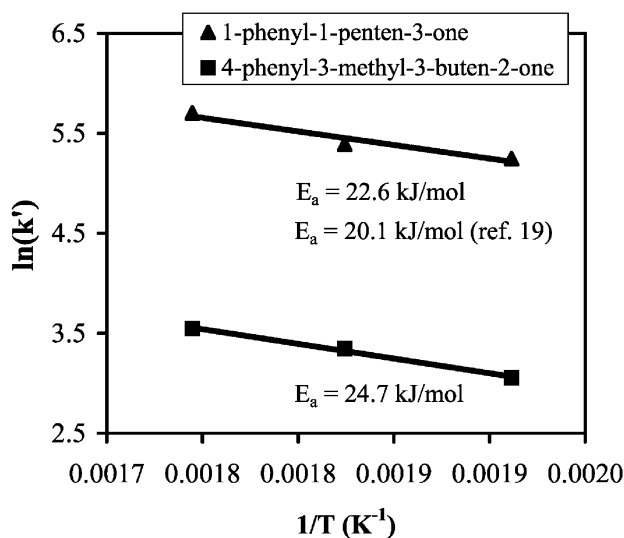


Fig. 11 Arrhenius plot for the formation of 1-phenyl-1-penten-3-one and 4-phenyl-3-methyl-3-buten-2-one from the Claisen–Schmidt condensation of benzaldehyde with 2-butanone over a temperature range of 250–350 °C.

1-penten-3-one is in good agreement with the value reported by Gettler and Hammett ($E_a = 20.1 \text{ kJ mol}^{-1}$) for an investigation conducted in a basic dioxane : water solution (70 : 30, by weight) over a temperature range of 25–50 °C.¹⁹

Additional examples of classic base catalyzed condensations performed in NCW

In addition to the investigations of the Claisen–Schmidt condensation, studies of several reactions that are conventionally performed under basic conditions were conducted in NCW without the addition of a base. The reactions investigated include the butyraldehyde self-condensation reaction, the cross-aldol condensation of benzaldehyde with acetone, the intramolecular Claisen condensations of ethyl-4-acetylbutyrate and of ethyl levulinate, and the intramolecular Dieckmann condensation of diethyl adipate. These investigations are a continuation of the work reported by Gläser *et al.*¹⁰ No condensation products were detected during investigations of the Claisen and Dieckmann reactions due to the dominance of hydrolysis, which is consistent with the findings reported by Patrick (a.k.a. Lesutis) *et al.*^{11,16}

The butyraldehyde self-condensation reaction is an industrially interesting reaction that yields a number of products including 2-ethyl-2-hexenal, 2-butyl-2-butenal, and 2-ethylhexenal. These products, once hydrogenated, can be esterified with phthalic acid to yield the plasticizer, dioctylphthalate (DOP), which has a demand of over 6×10^6 metric tons yr^{-1} .²⁷ The results from the condensation of butyraldehyde indicate that a 40 mol% yield of 2-ethyl-2-hexenal is achieved before the formation of byproducts become dominant (Fig. 12). In addition to the formation of byproducts, investigations of the back reaction of 2-ethyl-2-hexenal show that a pronounced equilibrium limitation exists for this reaction (Fig. 13). This equilib-

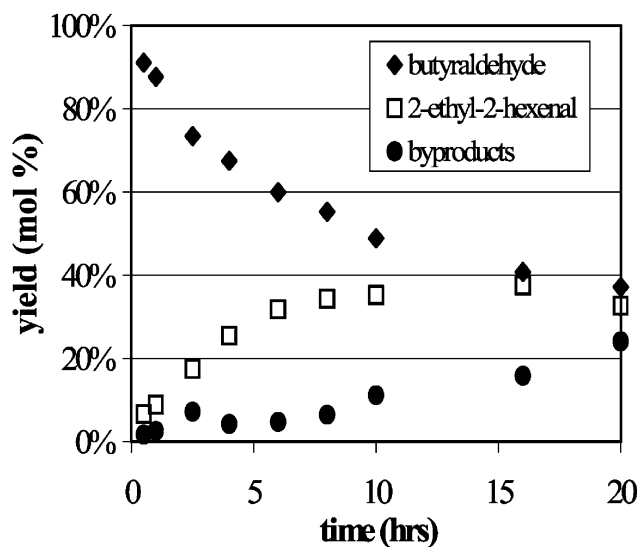


Fig. 12 Butyraldehyde self-condensation reaction in NCW at 250 °C. The reactant molar ratio (butyraldehyde : water) was 1 : 47.

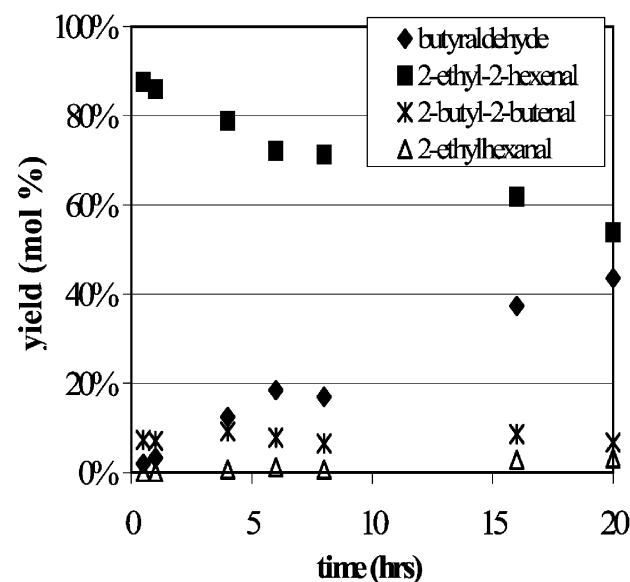


Fig. 13 The butyraldehyde condensation back reaction of the product compound 2-ethyl-2-hexenal at 250 °C. The reactant molar ratio (2-ethyl-2-hexenal : water) was 1 : 47.

rium limitation, as explained earlier, is attributed to the combined effects of the water formed during the condensation reaction and the large water concentrations present in the system, since water is the reaction solvent.

Investigations of the cross aldol condensation of benzaldehyde with acetone were also performed in NCW at 250 °C. This reaction is very similar to the reaction between benzaldehyde and 2-butanone, with the exception that acetone is a symmetrical ketone and therefore only capable of forming a single product. The results (Fig. 14) show that a small yield of the primary condensation product is formed as well as a much smaller proportion of the secondary condensation product. The low yields are an indication that this reaction could be equilibrium limited.

Conclusions

Near-critical water is an environmentally benign medium with properties conducive to organic synthesis at temperatures of 250–350 °C. In this temperature range, saturated liquid water has solvent properties (density and dielectric constant) compa-

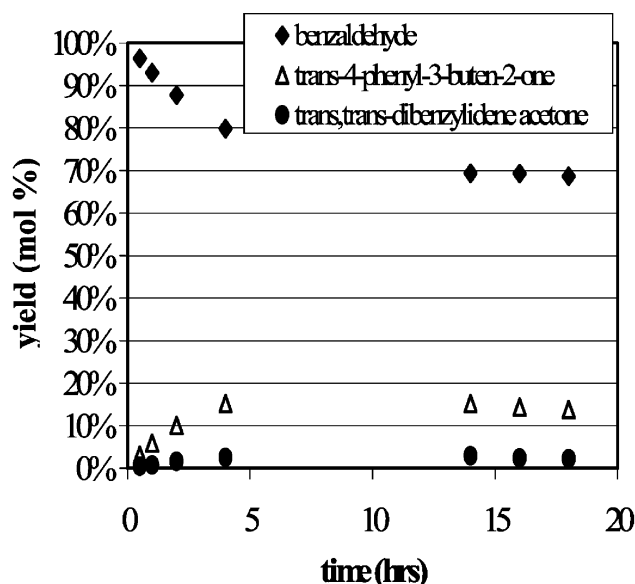


Fig. 14 The benzaldehyde–acetone mixed aldol condensation at 250 °C as a function of time. The reactant molar ratio (benzaldehyde : acetone : water) was 1 : 1 : 47.

rable to ambient acetone and is able to act as a solvent for both organics and ionics. Since the ionization constant of NCW is three orders of magnitude higher than ambient water, NCW should be capable of performing traditional acid and base catalyzed reactions without acid or base additions. Investigations of the Claisen–Schmidt condensation of benzaldehyde with 2-butanone in NCW yielded results consistent with conventional acid and base catalyzed reactions. Support for these findings was provided through investigations of the primary condensation product stabilities as well as the influence of added acid. Through kinetic investigations of the Claisen–Schmidt condensation, the activation energy for the formation of 1-phenyl-1-penten-3-one in NCW was determined and found to agree with the value reported by Gettler and Hammett for a reaction conducted in an aqueous–organic solvent system near room temperature. Investigation of several other condensation reactions, including the butyraldehyde self-condensation reaction and benzaldehyde–acetone cross aldol condensation, were performed to demonstrate the capacity of NCW to be used as a reactive medium for conventionally base catalyzed reactions. Although these reactions did not produce yields of industrial interest, this work demonstrates that NCW is a medium with great potential for performing organic synthesis, including carbon–carbon bond forming reactions without the addition of acids or bases.

Acknowledgements

The authors thank the EPA (Grant Nos. R-82813001-0 and R825325) and the NSF (Grant No. CTS-9613063) for their

financial support. R. G. thanks the Dr. Leni Schoeninger Foundation for a habilitation stipend. The authors also thank Jonathan McCarney for his assistance in synthesizing the 4-phenyl-3-methyl-3-buten-2-one and Greg Robbins for his laboratory assistance.

References

- 1 *How Much Water is There on (and in) the Earth*, <http://ga.water.usgs.gov>, ed. USGS, 2001, vol. 2001.
- 2 J. F. Connolly, *J. Chem. Eng. Data*, 1966, **11**, 13–16.
- 3 C. B. Dartt and M. E. Davis, *Ind. Eng. Chem. Res.*, 1994, **33**, 2887–2899.
- 4 M. Siskin and A. R. Katritzky, series of 18 publications in *Energy Fuels*, 1990, **4**, 475–484.
- 5 A. R. Katritzky and S. M. Allin, *Acc. Chem. Res.*, 1996, **29**, 399–406.
- 6 C. R. Strauss and R. W. Trainor, *Aust. J. Chem.*, 1995, **48**, 1665–1692.
- 7 L. Bagnell, T. Cablewski, C. R. Strauss and R. W. Trainor, *J. Org. Chem.*, 1996, **61**, 7355–7359.
- 8 J. An, L. Bagnell, T. Cablewski, C. R. Strauss and R. W. Trainor, *J. Org. Chem.*, 1997, **62**, 2505–2511.
- 9 K. Chandler, F. Deng, A. K. Dillow, C. L. Liotta and C. A. Eckert, *Ind. Eng. Chem. Res.*, 1997, **36**, 5175–5179.
- 10 R. Gläser, J. S. Brown, S. A. Nolen, C. L. Liotta and C. A. Eckert, *Prepr. Symp. - Am. Chem. Soc., Div. Fuel Chem.*, 1999, **44**, 385–388.
- 11 H. P. Lesutis, R. Gläser, C. L. Liotta and C. A. Eckert, *Chem. Commun.*, 1999, 2063–2064.
- 12 J. S. Brown, R. Gläser, C. L. Liotta and C. A. Eckert, *Chem. Commun.*, 2000, 1295–1296.
- 13 P. E. Savage, *Chem. Rev.*, 1999, **99**, 603–621.
- 14 M. Siskin and A. R. Katritzky, *Chem. Rev.*, 2001, **101**, 825–835.
- 15 A. R. Katritzky, D. A. Nichols, M. Siskin, R. Murugan and M. Balasubramanian, *Chem. Rev.*, 2001, **101**, 837–892.
- 16 H. R. Patrick, R. Gläser, K. Griffith, C. L. Liotta and C. A. Eckert, *Ind. Eng. Chem. Res.*, 2001, **40**, 6063–6067.
- 17 Y. Ikushima, K. Hatakeda, O. Sato, T. Yokoyama and M. Arai, *Angew. Chem., Int. Ed.*, 2001, **40**, 210–213.
- 18 F. A. Carey and R. J. Sundberg, *Advanced Organic Chemistry, Part B: Reactions and Synthesis*, 3rd edn., Plenum Press, New York, 1990.
- 19 J. D. Gettler and L. P. Hammett, *J. Am. Chem. Soc.*, 1943, **65**, 1824–1829.
- 20 M. Stiles, D. Wolf and G. V. Hudson, *J. Am. Chem. Soc.*, 1959, **81**, 628–632.
- 21 S. A. Fine and P. D. Pulaski, *J. Org. Chem.*, 1973, **38**, 1747–1749.
- 22 D. S. Noyce and L. R. Snyder, *J. Am. Chem. Soc.*, 1958, **80**, 4033–4037.
- 23 Y. Kawai, K. Saitou, K. Hida, D. H. Dao and A. Ohno, *Bull. Chem. Soc. Jpn.*, 1996, **69**, 2633–2638.
- 24 J. M. Sørensen and W. Arlt, *Liquid–Liquid Equilibrium Data Collection*, Deutsche Gesellschaft für Chemisches Apparatewesen, Frankfurt/Main West Germany, 1979, **Vol. V**, Part I.
- 25 J. S. Brown, J. P. Hallett, D. Bush and C. A. Eckert, *J. Chem. Eng. Data*, 2000, **45**, 846–850.
- 26 K. Chandler, C. L. Liotta and C. A. Eckert, *AIChE J.*, 1998, **44**, 2080–2087.
- 27 K. Weissmermel and H.-J. Arpe, *Industrial Organic Chemistry*, 3rd edn. VCH, Weinheim, Germany, 1997.



Deuteration of 2-methylnaphthalene and eugenol in supercritical and pressurised hot deuterium oxide

Jarno Kalpala, Kari Hartonen,* Maarit Huhdanpää and Marja-Liisa Riekkola

Laboratory of Analytical Chemistry, Department of Chemistry, P.O.Box 55, FIN-00014 University of Helsinki, Finland

Received 9th April 2003

First published as an Advance Article on the web 16th September 2003

The dramatic changes in the properties of water (*e.g.* density, relative permittivity, ionic product) near its critical point make high temperature water an attractive reaction medium in place of organic solvents. The suitability of deuterium oxide (D_2O) at high temperatures (200–450 °C) for the deuteration of eugenol and 2-methylnaphthalene was studied in this work. Deuteration was performed with pure D_2O and with D_2O containing several acid, base, salt and metal catalysts. As well, deuterium chloride and sodium deuterioxide were tested as catalysts. Reactions were carried out in batch-type reactors made of stainless steel or Hastelloy® C-22. Gas chromatography-mass spectrometry (GC-MS) was used for the determination of reaction products. With 2-methylnaphthalene deuteration efficiencies were as high as 100% at 450 °C. Reactions with NaOH, NaOD and Na_2CO_3 catalysts produced most repeatable results (in the best conditions RSD < 5%). In the case of eugenol, relatively good deuteration efficiency was achieved at lower temperatures, with use of D_2O alone, without any catalyst. With both compounds, small amounts of by-products were occasionally detected in the total ion chromatogram of GC-MS.

1 Introduction

Decreasing the chemical load to the environment is an essential goal today. Chemists are in a key position to cut pollution, both in industry and in research. One area where environmentally friendly solutions are keenly sought is separation and reaction science and the related industrial processes. The “green chemistry” approach aims to reduce the production and use of harmful products and chemicals, seeking, for example, alternative reagents and solvents. Supercritical fluids, such as carbon dioxide and water, and water at high temperature (but below critical temperature), have attracted increasing attention as substitutes for harmful organic solvents.

The properties of a solvent are typically determined by polarity, dipole moment, relative permittivity (dielectric constant) and the solubility parameter value, all of which are highly sensitive to temperature. Water at room temperature is highly polar, with high dipole moment, high relative permittivity (dielectric constant) and high solubility parameter value. An increase in the temperature of water decreases the relative permittivity and solubility parameter value and results in lower viscosity and surface tension, less hydrogen bonding and generally better solubility of less polar compounds. Near the critical temperature of water, dramatic changes occur in density and the ionic product of water. Above the critical temperature, with pressure held constant, pK_w increases with temperature.¹ Below the critical temperature, however, pK_w decreases as temperature increases.¹ These relationships can be exploited to obtain enhanced reaction and extraction rates.

Supercritical water, *i.e.* $T > T_c$ (374.1 °C) and $P > P_c$ (218.3 atm), is an excellent solvent in which a variety of organic compounds and gases are fully soluble. This makes it of special interest as a reaction medium where reactions can be conducted in one phase. Supercritical water can also act as a reagent and catalyst in reactions. At the same time, it must be remembered that the higher the temperature, the more destructive (oxidative) are the conditions in water. Corrosion must not be overlooked either; water itself is corrosive. At high temperatures and pressures,^{2,3} especially under very basic or acidic conditions, a high concentration of dissolved oxygen or the presence of

inorganic species such as Cl^- -ions makes water a highly corrosive medium. Corrosion-based degradation is maximal at near critical temperatures, between approximately 345 and 370 °C.⁴

Similarly to H_2O , deuterium oxide (D_2O) can be used as a reaction solvent at high temperatures and pressures. Compared with water D_2O has slightly higher melting and boiling points (3.8 °C and 101.4 °C, respectively), but lower critical temperature (371.5 °C) and pressure (214.4 atm). Concentrations of DO^- and D_3O^+ ions are increased with temperature,^{5,6} which means that certain acid- or base-catalysed reactions that are not possible under normal conditions may take place under supercritical or near critical conditions.^{5,6} H–D exchange reactions for example, are easily performed in pressurised hot deuterium oxide and supercritical deuterium oxide.^{5–7} Deuterated compounds are generally employed as analytical standards when mass spectrometry (MS) is used for detection, and deuterated solvents are essential in nuclear magnetic resonance spectroscopy (1H -NMR). Labelled reagents can also be of good aid in synthetic chemistry, when studying reaction mechanisms. Advantages of deuteration in pressurised hot D_2O and supercritical D_2O are short reaction times,⁷ relatively low cost⁸ and the possibility to selectively deuterate⁹ or perdeuterate^{7,10} different organic compounds in high yield with insignificant by-product formation.^{7,9,11} It may also be possible to affect the reaction efficiency, reaction rate and selectivity by adjusting the temperature^{5,12} (affecting the relative permittivity),¹³ pressure (or rather density)^{6,14} or pH^{6,8,9,12} or by introducing a catalyst.⁸

Green Context

Deuteration of compounds is both synthetically useful and a probe of the properties of different reaction media. Here, the behaviour of supercritical D_2O is examined under various operating conditions, and with a range of catalysts. Deuteration could be achieved readily under conditions where few other destructive reactions took place. *DJM*

Normally with organic compounds, the H–D exchange occurs through electrophilic substitution or bond cleavage.¹⁵ The resulting deuterated compounds are more stable since more energy is needed to break the C–D bond than the C–H bond.

In this work, deuterium oxide at high temperatures (200–450 °C) was used to study the deuteration of eugenol and 2-methylnaphthalene. These compounds were chosen purely to see the capability to exchange differently located hydrogen atoms, since these are not generally the compounds used as deuterated standards. However, similar reaction conditions could then be used for other compounds as well. Deuteration of the two compounds was carried out with pure D₂O and with D₂O containing several acid, base, salt or metal catalysts under different reaction conditions. Deuterium chloride and sodium deuterioxide were also tested as catalysts. Reactors used in this laboratory scale study were of three different types.

2 Experimental

2.1 Chemicals

Deuterium oxide (99.9%) was from Cortec (Paris, France) and 2-methylnaphthalene (98%) and eugenol were from Aldrich (Milwaukee, USA) and Sigma (St. Louis, USA), respectively. Sodium deuterioxide (40 wt% solution in D₂O, 99+ atom% D) and deuterium chloride (37 wt% solution in D₂O, 99.5 atom% D) were from Aldrich (Milwaukee, USA). HPLC grade n-heptane and solid NaOH, KOH, Na₂CO₃ and Na₂SO₄ (p.a., 10–60 mesh) were from Merck (Darmstadt, Germany). Dichloromethane (HPLC grade) and concentrated HCl (36–38%) were from J.T. Baker (Deventer, Holland), ammonium solution (25%) and ammonium carbonate were from Riedel-de Haën (Seelze, Germany), zinc powder was from Adlershof (Berlin, Germany) and platinum (99.99%) was from Koch-Light laboratories Ltd. (Colnbrook Bucks, England). Palladium on activated charcoal (10% Pd) was from Fluka, Buchs, Switzerland. CaCO₃, Dewarda's alloy, Ti–Si–Al powder, zinc chips, magnesium and nickel were from the chemical storage of the laboratory.

2.2 Deuteration

2.2.1 Equipment. Deuteration reactions were performed with two different systems, (A) and (B). Different types of reactors and different ovens were used in two systems and there were minor differences in analytical procedure.

In system (A), H–D exchange reactions were performed in fully closed 2.2 ml extraction vessels made of stainless steel (Keystone Scientific, Bellefonte, PA, USA). Vessels containing reagents were heated in a Fractovap series 2150 gas chromatographic oven (Carlo Erba Strumentazione) for the desired time at the selected temperature. Temperature of the oven air was monitored *via* an additional thermocouple, which was connected to a thermometer having digital readout. Continuous closing (tightening) and opening of the lid in the commercial reactor (Keystone Scientific) damaged the sealing surfaces and resulted in frequent leaking. For this reason, and because the Keystone reactor was no longer available, other reactors¹⁶ and reactor materials were sought.

In system (B), deuteration reactions were performed in self-made batch-type reactors. The first reactors were made of stainless steel (AISI316L) and the second of Hastelloy® C-22 Ni-based alloy. Volumes of the reactors were approximately 3 ml and the amounts of the reagents were proportioned (using accurate reactor volumes) to correspond to the amounts used with the 2.2 ml reactor in system (A). Reactors with the reagents were heated in a Perkin-Elmer F22 gas chromatograph oven. Oven temperatures were monitored *via* two separate thermo-

couples, both connected to an external thermometer. The other ends of the thermocouples were connected to an empty reactor and to one of the reactors with reagents inside.

2.2.2 Deuteration procedure. In both systems the procedure began with weighing and pipetting the studied compound, deuterium oxide and additives into the reactor. To avoid very high pressures the maximum amount of D₂O was 45% of the reactor volume (pressure builds up in a heated closed container). For the same reason, the amount of D₂O and the amounts of other reagents were decreased to half (23%) in reactions made at 450 °C. Tables 1 and 2 list the studied parameters and reagents used in the experiments. After measuring of the reagents, the reactor was closed and placed in the oven.

Table 1 Reaction parameters investigated and their values in 2-methylnaphthalene deuteration

Parameter	Values examined
Reaction temperature/°C	250, 300, 350, 400, 450
Reaction time/h	2, 4, 6
Amount of D ₂ O/ml	1.0
Amount of 2-methylnaphthalene/mg	5, 50, 500
Volume of the reactor/ml	2.2, 3
Catalyst	HCl, DCl, NaOH, NaOD, KOH, Na ₂ CO ₃ , CaCO ₃ , KOH + NH ₃ , NaOH + DMSO, (NH ₄) ₂ CO ₃ , Pt, Pd, Dewarda's alloy (45% Al, 50% Cu and 5% Zn), Ti–Si–Al alloy (36% Ti, 6% Si and 4% Al), Mg, Ni, Zn
Reactor material	Keystone Scientific (unknown stainless steel), Self constructed (AISI316L stainless steel), Self constructed (Hastelloy® C22)

Table 2 Reaction parameters investigated and their values in eugenol deuteration

Parameter	Values examined
Volume of the reactor/ml	2.2, 3
Reaction temperature/°C	200, 250, 300, 350
Reaction time/h	2, 4, 6
Amount of eugenol/mg	5, 50, 500
Amount of D ₂ O/ml	0.1, 0.2, 0.5, 1.0
Catalyst	HCl, Na ₂ CO ₃
Reactor material	Keystone Scientific (unknown stainless steel), Self constructed (AISI316L stainless steel), Self constructed (Hastelloy® C22)

In system (A), measurement of the reaction time was started after the set oven (reaction) temperature was reached. In system (B), the oven with the empty reactor was first heated to 250 °C (measured by thermocouple in the empty reactor) and after that the reactors were quickly put into the oven and the other thermocouple was connected to one of the reactors. Heating was continued until the desired reactor temperature was achieved. The reaction time count was started and the reactor (plus oven) temperature was kept constant during the whole reaction time. The pressure of the reaction mixture at high temperatures inside the closed reactor was calculated with the NIST/ASME Steam Properties program (Formulation for General and Scientific Use, Standard Reference Database 10 Version 2.01, USA).

After the sample had cooled, it was extracted with 5 ml of solvent and dried with Na₂SO₄. For GC-MS analysis, deuterated eugenol was extracted and diluted with dichloromethane and deuterated 2-methylnaphthalene with n-heptane. Each experiment was repeated three times ($n = 3$).

2.3 GC-MS analysis

A Hewlett-Packard model 5890 gas chromatograph connected to HP model 5989A mass spectrometer was used for identification of the reaction products. The analytical column was a 25 m HP-5 (Agilent Technologies, Karlsruhe, Germany) with 0.2 mm i.d. and 0.11 μm film thickness. A 2.5 m DPTMDS-deactivated retention gap (i.d. 0.53 mm, Agilent Technologies, USA) was used in front of the analytical column. All on-column injections were done with an HP 7673 auto sampler and with oven tracking for injector temperature. Helium (99.996%, Oy Aga Ab, Espoo, Finland) was used as carrier gas and GC runs were done in constant pressure (100 kPa) mode. The GC oven temperature was programmed from 80 $^{\circ}\text{C}$ (2 min) to 280 $^{\circ}\text{C}$ (5 min) at 20 $^{\circ}\text{C min}^{-1}$ for 2-methylnaphthalene and from 30 $^{\circ}\text{C}$ (2 min) to 280 $^{\circ}\text{C}$ (5 min) at 20 $^{\circ}\text{C min}^{-1}$ for eugenol. The temperature of the GC-MS transfer line was 300 $^{\circ}\text{C}$.

MS was operated in scan mode with EI (70 eV) ionisation. Scanned mass ranges were 50–160 for 2-methylnaphthalene and 50–200 for eugenol. MS ion source and quadrupole analyser temperatures were 250 $^{\circ}\text{C}$ and 120 $^{\circ}\text{C}$, respectively. The GC-MS system was controlled with the HP ChemStation program. Analyte concentration in the samples subjected to GC-MS was *ca.* 1 $\mu\text{g ml}^{-1}$. Ion chromatograms subtracted from the total ion chromatogram (TIC) were used to calculate the degree of deuteration and the TIC was used to estimate the amount of deuteration by-products.

3 Results and discussion

3.1 Reactor material and corrosion

Hastelloy C-22 was found to be an excellent reactor material because the stainless steel reactors suffered from severe corrosion. The corrosion was probably due to the acidic and basic conditions together with Cl^{-} -ions at high temperature and high pressure D_2O . These conditions can damage the passive layer, which under milder conditions protects stainless steel from corrosion. Failing of this protective layer exposes steel for pitting and crevice corrosion, which would explain small holes and micro fissures observed in the reactors. Probably stress corrosion also had some effect on the stainless steel reactor failure. Because of the harmfulness of Cl^{-} -ions, dilute HCl wash of reactors was left out from the procedure. Hastelloy C-22 reactors proved to be much more resistant against corrosion and a much longer lifetime is expected without any damage to induce leaking.

Because of differences in the structure of the reactors and in the density of stainless steel and Hastelloy C-22, heating times were also different. Heating procedures were discussed pre-

viously in the experimental section and all similar reactors were presumed to reach the reaction temperature in the same time despite small mass variation. The effect of reactor walls on reaction efficiency under certain conditions was not investigated in detail, but it was presumed to be constant with the same reactor material and reactor cleaning procedure. However, small differences were obtained between new and used (oxidised) reactors. This is why pre-treatment of the new reactor under reaction conditions is recommended before actual use.

3.2 2-Methylnaphthalene

The effects of reaction time and reaction temperature on deuteration efficiencies were first investigated with 2-methylnaphthalene. Also the effects of different catalysts and the amount of 2-methylnaphthalene were examined (Table 1).

Reaction time had only a minor influence on the deuteration efficiency. Deuteration of 2-methylnaphthalene at 350 $^{\circ}\text{C}$ with different reaction times (2, 4 and 6 h) in the presence of HCl catalyst led to almost identical deuteration distribution (data not shown). However, the repeatability was much worse with a 2 h reaction time (RSD generally 15–70%) than with a 4 or 6 h reaction time (RSD <6%). With all reaction times tested, heptadeuterated 2-methylnaphthalene was the main reaction product and octadeuterated 2-methylnaphthalene the highest deuteration level. In no case was undeuterated or mono-deuterated 2-methylnaphthalene obtained.

2-Methylnaphthalene was stable in the whole temperature range investigated (250–450 $^{\circ}\text{C}$). To avoid too high pressures and consequently a reactor breakdown, the amounts of D_2O and other reagents were reduced to half at 450 $^{\circ}\text{C}$. Increase in temperature clearly improved the deuteration efficiency of 2-methylnaphthalene and moved the deuteration distribution towards higher deuteration levels (Fig. 1). This was true even at 450 $^{\circ}\text{C}$, where the density was half of that at lower temperatures. The positive effect of increasing temperature on reaction efficiency is a consequence of changes in the self-ionisation constant of water near the critical point. The effect of differences in ionic product is indicated by the general acid–base reaction (1) presented by Yao and Evilia:⁶



The equilibrium constant of reaction (1) can be written as K_a/K_w , where K_a is the acidic ionisation constant of the weak organic acid RH, and K_w is the self-ionisation constant of D_2O . The equilibrium constant of reaction (1) increases with temperature, because beyond the critical temperature and at constant pressure pK_w enhances as temperature increases. pK_w has a similar effect on the equilibrium constant of reaction (2):

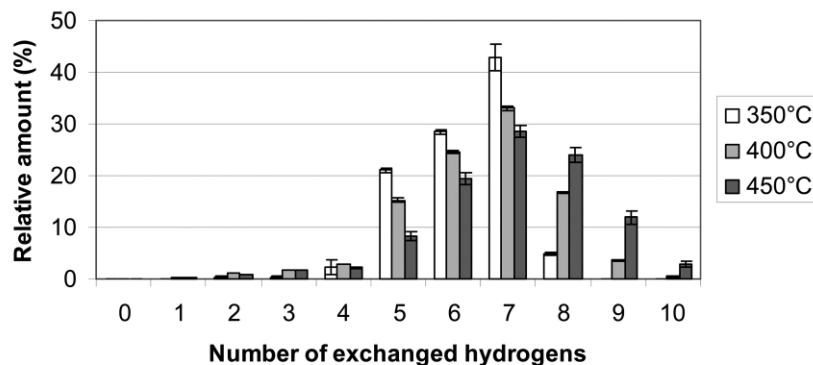
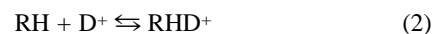


Fig. 1 Effect of reaction temperature on deuteration distribution of 2-methylnaphthalene. At 350 $^{\circ}\text{C}$ and 400 $^{\circ}\text{C}$ $t_r = 2$ h, $m(2\text{-methylnaphthalene}) = 50$ mg, $V(\text{HCl}) = 5$ μl and $V(\text{D}_2\text{O}) = 1.0$ ml. At 450 $^{\circ}\text{C}$ amounts were halved. $n = 3$ and system (B) with stainless steel reactor was used for the reaction. Error bar represents $\pm\text{SD}$.

The ΔH of many weak acid and base ionisation reactions is positive,⁶ and therefore, an increase in temperature enhances reaction efficiencies of such reactions. In this respect, the deuteration reaction of 2-methylnaphthalene is more efficient in one phase (supercritical) than in two phases (liquid and gas).

Because deuteration is an equilibrium reaction, it is conceivable that the amount of 2-methylnaphthalene relative to the amount of D_2O would affect the deuteration efficiency. The effect of the amount of 2-methylnaphthalene on the deuteration efficiency was explored with three amounts of 2-methylnaphthalene 5 mg, 50 mg and 500 mg. With decreasing amount of 2-methylnaphthalene in reactions without catalysts, the deuteration distribution (and reaction equilibrium) was shifted towards higher deuteration states in reactions (Fig. 2). The same phenomenon was seen to a lesser degree in the presence of an acid catalyst (Fig. 2). In the presence of catalyst, the difference between 5 and 50 mg is very small, indicating that under these conditions the equilibrium cannot be pushed much further by decreasing the amount of 2-methylnaphthalene.

Some of the catalysts tested (Table 1) clearly improved the deuteration efficiency and moved the deuteration distribution toward higher deuteration levels. With acid and base catalysts, the reaction equilibrium was easily pushed towards more complete deuteration. Reactions with deuterated acid and base catalysts instead of the regular ones generally had the same effect on the deuteration distribution. However, at optimised conditions (as can be seen from Fig. 3), similar results can be obtained with HCl compared to DCl, and reactor material can cause more dramatic changes on the reaction efficiency. With acid catalyst, the deuteration reaction occurs *via* an arenium ion mechanism. In the first step, D^+ -ion attacks the aromatic compound, giving rise to a positively charged intermediate (the arenium ion),¹⁷ and in the second step the leaving group (hydrogen) departs. Acids catalyse this reaction. With base

catalyst, the leaving group (hydrogen) is removed by the base before the electrophile (D^+) arrives and the reaction follows the S_{E1} mechanism.¹⁷

With acid catalysts, the amount of acid had only a minor effect on the deuteration distribution. However, in reactions with 1 μ l, 3 μ l and 5 μ l of HCl, the highest deuteration level (octadeuterated 2-methylnaphthalene) was more evident with 5 μ l than with 1 μ l and 3 μ l HCl (data not shown). The best repeatability (RSD < 11%) was achieved with a 3 μ l amount of HCl catalyst. With NaOH catalyst amounts of 20 and 40 mg, a much narrower distribution and a more complete deuteration were obtained than with 1.5 mg, and over 30% of perdeuterated 2-methylnaphthalene was gained (data not shown). No clear differences in deuteration efficiency could be seen with these two highest NaOH amounts.

Reactions in the presence of base catalysts resulted in more highly deuterated 2-methylnaphthalene than reactions in the presence of acid catalysts. A single experiment with KOH catalyst (data not shown) gave a similar deuteration distribution to reactions in D_2O with NaOH and Na_2CO_3 catalysts at 350 °C (Fig. 4). The similarity in the reaction efficiency with these catalysts can be understood from the reaction of Na_2CO_3 with water, where NaOH and $NaHCO_3$ are formed as reaction products¹⁸ and NaOH acts as the final catalyst. With $CaCO_3$ catalyst (single experiment, data not shown), most of the 2-methylnaphthalene remained unreacted and only small amounts of mono- and dideuterated 2-methylnaphthalene were obtained. $CaCO_3$ is almost insoluble in water, but in the presence of acid it releases CO_2 .¹⁸ Taking this and our own results without catalyst into account, it seems clear that $CaCO_3$ does not take part in the reaction, and mono- and dideuterated 2-methylnaphthalene are achieved solely because of D_2O .

Some other catalysts and catalyst mixtures were also tested. When KOH and NH_3 ($m(KOH) = 0.2$ mg and $V(NH_3, 25\%) =$

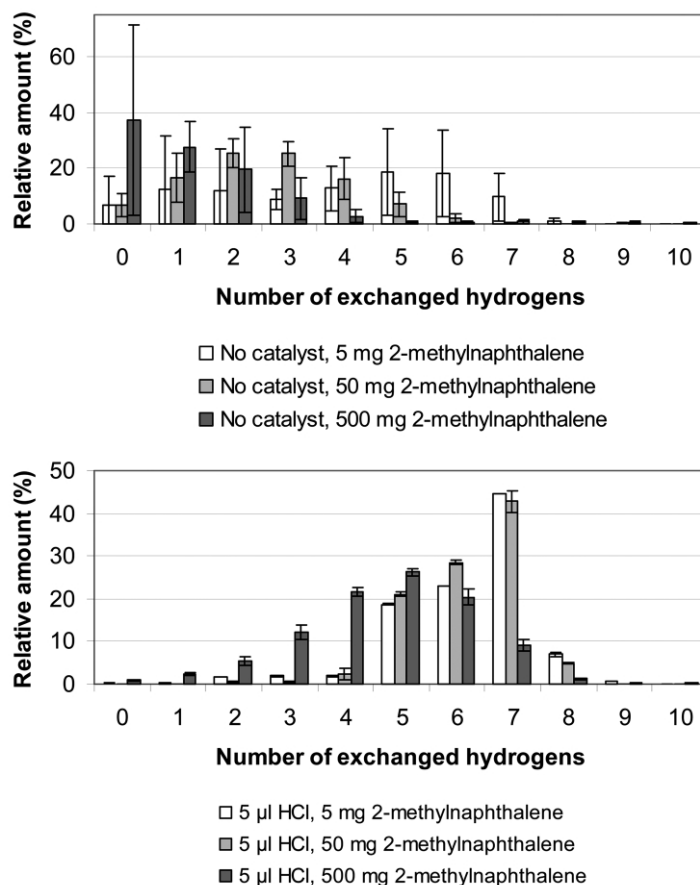


Fig. 2 Effect of 2-methylnaphthalene amount on deuteration efficiency without catalyst and with HCl catalyst. $T = 350$ °C, $t_r = 2$ h, $n = 3$ and system (B) with stainless steel reactor was used for the reaction. Error bar represents \pm SD.

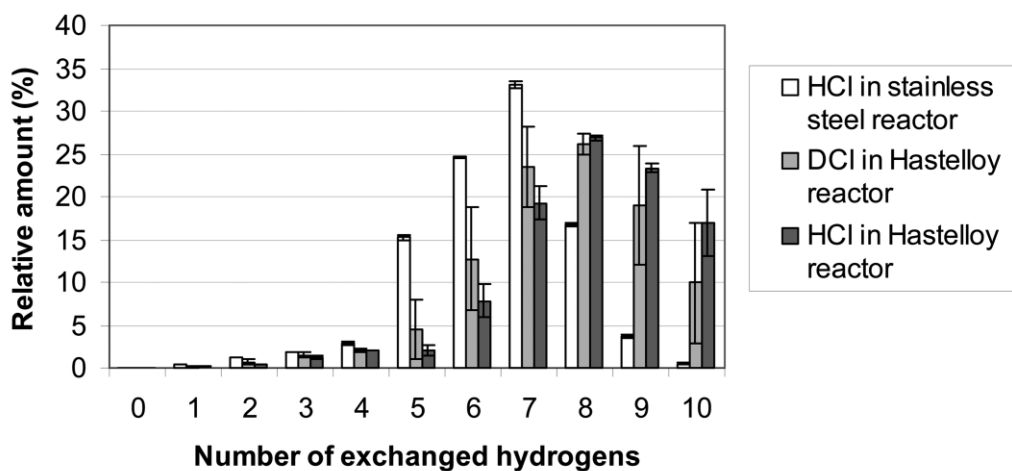


Fig. 3 The deuteration distributions of 2-methylnaphthalene with HCl catalyst (Stainless steel and Hastelloy reactors) and DCl catalyst (Hastelloy reactor). $T = 400\text{ }^{\circ}\text{C}$, $t_r = 2\text{ h}$, $V(\text{D}_2\text{O}) = 1\text{ ml}$, $m(2\text{-methylnaphthalene}) = 50\text{ mg}$, $V(\text{HCl}) = V(\text{DCl}) = 5\text{ }\mu\text{l}$, $n = 3$ and system (B) was used for the reaction. Error bar represents $\pm\text{SD}$.

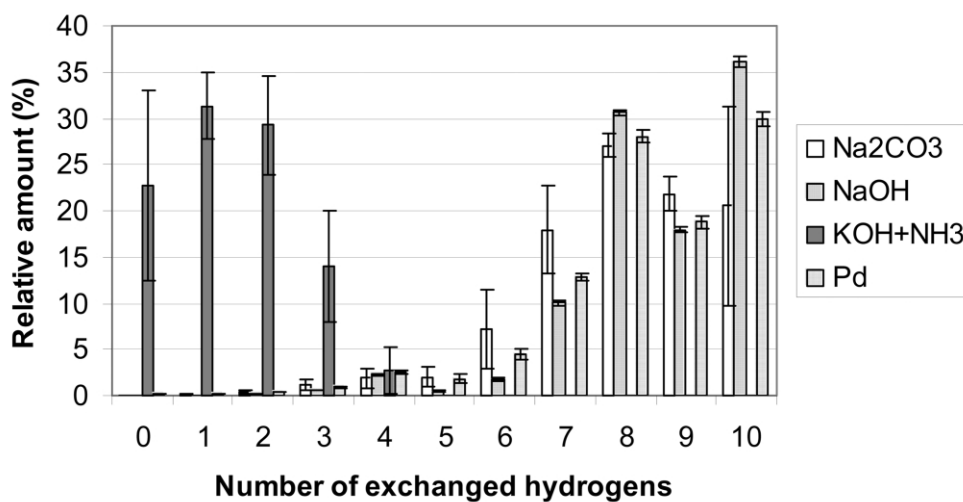


Fig. 4 The deuteration distribution of 2-methylnaphthalene with Na_2CO_3 , NaOH, KOH + NH_3 and Pd catalysts. $T = 350\text{ }^{\circ}\text{C}$, $t_r = 2\text{ h}$, $V(\text{D}_2\text{O}) = 1.0\text{ ml}$, $m(2\text{-methylnaphthalene}) = 50\text{ mg}$, $m(\text{KOH}) = 0.2\text{ mg}$, $V(\text{NH}_3, 25\%) = 5\text{ }\mu\text{l}$, $m(\text{NaOH}) = 20\text{ mg}$, $m(\text{Na}_2\text{CO}_3) = 2\text{ mg}$, $m(\text{Pd}, 10\%\text{ Pd in active carbon}) = 60\text{ mg}$ and $n = 3$. System (A) was used with KOH + NH_3 and system (B) with Na_2CO_3 , NaOH and Pd. Stainless steel reactor was used with system B except for Pd (Hastelloy reactor). Error bar represents $\pm\text{SD}$.

5 μl) were used together as catalyst (Fig. 4), monodeuterated 2-methylnaphthalene was obtained as main product and the deuteration distribution ranged from undeuterated to tetra-deuterated 2-methylnaphthalene. This was a quite different result from that with KOH alone and it is concluded that KOH had only a minor effect on the deuteration efficiency here. With NaOH + DMSO, on the other hand, NaOH made a decisive contribution, and the reaction efficiency and deuteration distribution were similar to that obtained with pure NaOH (Fig. 4). The reaction including the $(\text{NH}_4)_2\text{CO}_3$ catalyst gave a similar deuteration distribution to the reaction including KOH + NH_3 catalyst. In this case the similarity was probably due to the formation of NH_3 in the reaction of $(\text{NH}_4)_2\text{CO}_3$ with hot water.¹⁸

With two exceptions, all tested metal catalysts (Table 1) gave relatively poor deuteration efficiencies and the percentage of undeuterated 2-methylnaphthalene was 32–92%. Better reaction efficiencies were obtained only with the smallest amount of Pt tested (5 mg) and with the palladium catalyst (Fig. 4). With Pt catalyst (data not shown) the main product was tetra-deuterated 2-methylnaphthalene, and heptadeuterated 2-methylnaphthalene was the highest deuteration level. Excellent reaction efficiency and repeatability were achieved with palladium catalyst even at 350 $^{\circ}\text{C}$. The deuteration distribution

was almost identical to that obtained with NaOH-catalyst at the same temperature (Fig. 4).

With optimal reaction conditions and with NaOD as catalyst, over 50% of the initial 2-methylnaphthalene was perdeuterated (Fig. 5). As can be seen also from Fig. 5, an identical deuteration distribution was achieved with Na_2CO_3 as catalyst, but at 400 $^{\circ}\text{C}$ rather than the 450 $^{\circ}\text{C}$ used with the NaOD catalyst. Fig. 5 also shows the excellent repeatability obtained (error bars difficult to see). RSD with NaOH, NaOD and Na_2CO_3 catalysts were generally less than 5%.

3.3 Eugenol

With eugenol, study was made of the effects on deuteration efficiency of reaction temperature, reaction time, amount of D_2O , different reactors, and HCl and Na_2CO_3 catalysts (Table 2).

Reaction temperatures 200, 250, 300 $^{\circ}\text{C}$ were investigated in system (A) and 350 $^{\circ}\text{C}$ with system (B). At the lowest temperature, at least monodeuterated eugenol (Fig. 6) was produced, most likely indicating that hydrogen in the hydroxy group was exchanged. At 250 and 300 $^{\circ}\text{C}$, higher deuteration levels (tri- and tetra-deuterated) for eugenol were obtained as

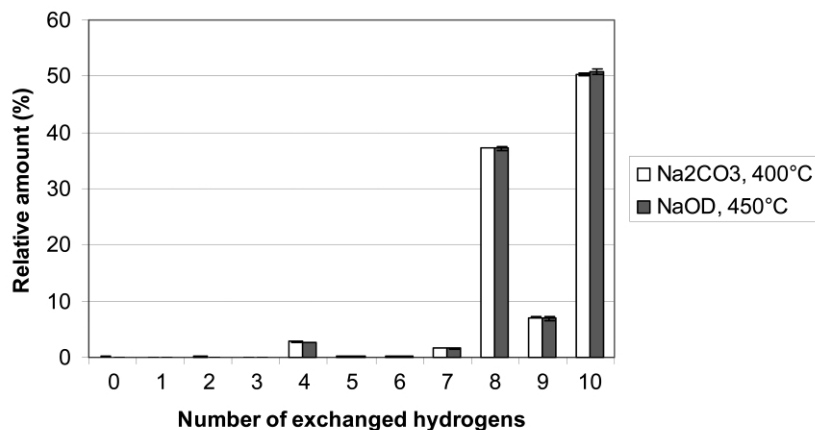


Fig. 5 The deuteration distribution of 2-methylnaphthalene with NaOD catalyst and Na₂CO₃ catalyst. With NaOD $T = 450\text{ }^{\circ}\text{C}$, $t_r = 2\text{ h}$, $V(\text{D}_2\text{O}) = 0.5\text{ ml}$, $m(2\text{-methylnaphthalene}) = 2.5\text{ mg}$, $V(\text{NaOD}_{40\%}) = 16.3\text{ }\mu\text{l}$ and system (B) with Hastelloy reactor was used for the reaction. With Na₂CO₃ $T = 400\text{ }^{\circ}\text{C}$, $t_r = 2\text{ h}$, $V(\text{D}_2\text{O}) = 1.0\text{ ml}$, $m(2\text{-methylnaphthalene}) = 5.0\text{ mg}$, $m(\text{Na}_2\text{CO}_3) = 2\text{ mg}$, $n = 3$ and system (B) with stainless steel reactor was used for the reaction. Error bar represents $\pm\text{SD}$.

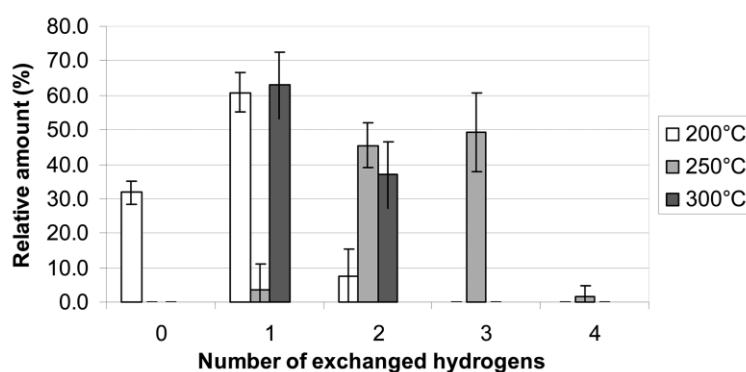


Fig. 6 Effect of reaction temperature on the deuteration distribution of eugenol. Reaction time 2 h, $m(\text{eugenol}) = 50\text{ mg}$, $V(\text{D}_2\text{O}) = 1\text{ ml}$ and $n = 3$. System (A) was used for the reaction. Error bar represents $\pm\text{SD}$.

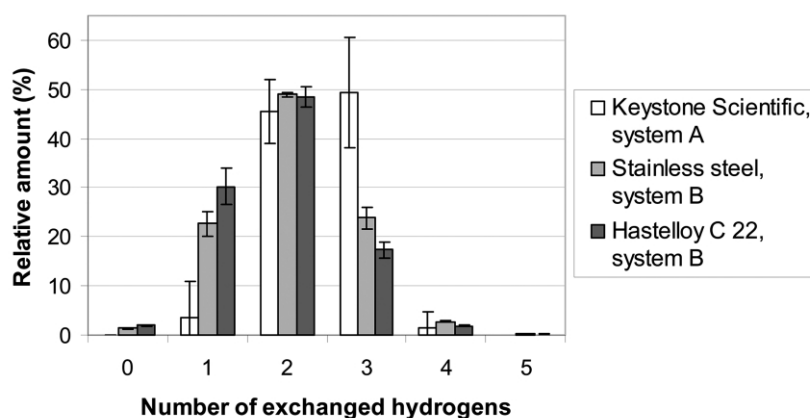


Fig. 7 Effect of different reactors on the deuteration distribution of eugenol. Reaction time 2 h, $m(\text{eugenol}) = 50\text{ mg}$, $T = 250\text{ }^{\circ}\text{C}$, $V(\text{D}_2\text{O}) = 1\text{ ml}$ and $n = 3$. Error bar represents $\pm\text{SD}$.

well, indicating that some other hydrogens were also exchanged. Raising the reaction temperature thus moved the deuteration level distribution towards higher deuteration degree. Because of the narrow deuteration distribution, one to three hydrogens could easily be exchanged selectively without any catalyst. At the highest temperature (350 °C), eugenol decomposed.

As with 2-methylnaphthalene, reaction time had only a minor impact on the deuteration efficiency of eugenol. With 2, 4 and 6 hours reaction times at 250 °C, deuteration distributions and profiles were very similar (data not shown). In all cases, all of the initial eugenol was deuterated and, taking the RSD-values into consideration, the deuteration reaction reached equilibrium in less than two hours.

The relative amount of D₂O logically had a great effect on the deuteration efficiency (data not shown). With lower D₂O volumes (0.1 and 0.2 ml), the amount of D₂O is limiting the reaction and the deuteration efficiency was low with descending deuteration distribution profile. With higher D₂O volumes (0.5 and 1.0 ml), the profile became ascending and the distribution moved towards higher deuteration levels.

As already seen in Fig. 3, possible variations to the results could be caused by different reactor materials, reactor designs and heating systems used. This was checked with eugenol at 250 °C. The two self-made reactors (made of stainless steel and Hastelloy) used with system (B), gave almost identical deuteration efficiencies and profiles (Fig. 7). Dideuterated eugenol was the main reaction product. With the commercial

Keystone Scientific reactor, used in system (A), the deuteration reaction gave mostly trideuterated eugenol. These small differences between the self-made and the commercial reactor were probably due to the different reactor materials, the acid wash used with the commercial reactor or the differences in the heating procedures between systems (A) and (B). Because we did not know the composition of the Keystone Scientific reactor, the exact cause of the difference remains unclear.

For eugenol with pure D₂O, up to four hydrogens were exchanged with deuterium. The effects of HCl and Na₂CO₃ catalysts on deuteration efficiency of eugenol were quickly evaluated. These acid and base catalysts, however, caused eugenol to decompose.

3.4 Repeatability

As discussed already earlier, excellent repeatability was generally obtained for the deuteration of 2-methylnaphthalene with base catalysts NaOH, NaOD and Na₂CO₃. Deuteration of eugenol was usually much less repeatable. Repeatability was greatly affected by the reaction time, reagent (catalyst) amount and catalyst nature. Normally, the RSD values were high for the reaction without the catalyst for both substrates studied. Also the reaction system and the reactor material had an effect on the repeatability.

With system (A) and the commercial reactor, the average RSD for reactions with 2-methylnaphthalene was 25%, ranging from 0.1% to 202%. The repeatability for reactions with eugenol was much poorer (average RSD 102%, ranging from 7 to 265%). With system (B) and the self-made stainless steel reactor, the average RSD with 2-methylnaphthalene was 33%, ranging from 0.1 to 205%. With eugenol the average RSD was just 9% ranging from 1 to 52%. Reactions in Hastelloy C 22 reactors gave 26% as average RSD for 2-methylnaphthalene, ranging from 0.7 to 139%, and 26% for eugenol, ranging from 4 to 68%. Normally, the very high RSD values (*ca.* 150–250%) were achieved in cases where the relative amount of deuterated isotope was very small. These results also showed that the effect of the reactor wall on the repeatability should not be underestimated. In this respect, the Hastelloy seemed to work well.

4 Conclusions

Supercritical and pressurised hot water are effective reaction media for acid–base reactions. The possibility to affect the solvent properties, especially the self-ionisation constant, by controlling temperature and pressure enables the control of the magnitude of the reaction equilibrium constant and thereby the reaction efficiency and selectivity.

Fast deuteration with deuterium oxide at high temperature and pressure was achieved for both 2-methylnaphthalene and eugenol. With eugenol, one to three hydrogens were easily and selectively exchanged in the absence of catalyst. Base and acid catalysts caused eugenol to decompose.

Unlike eugenol, the deuteration of 2-methylnaphthalene was clearly enhanced by acid, base and Pd catalysts and the selectivity could be tuned with the catalysts. Even better results were obtained by using hydrogen-free reagents such as Na₂CO₃ or NaOD and DCl in place of NaOH and HCl. Slightly better deuteration efficiencies were achieved with base and palladium catalysts than with acid catalysts. The selectivity could be modified through a combination of two bases and totally

different deuteration distributions were gained with various combinations. A pronounced effect on selectivity was also observed with various carbonates as catalyst. Studies carried out with metal catalysts other than Pt and Pd generally resulted in poor deuteration efficiencies.

With both compounds studied, reaction time had only a minor impact on the deuteration efficiency (but a larger impact on repeatability) and the deuteration reaction reached equilibrium in less than two hours. This is less than the reaction times generally used in conventional deuteration with organic solvents. The relative amount of substrate had a noticeable effect on the deuteration efficiency: a decrease in the amount of 2-methylnaphthalene or increase of the amount of D₂O with eugenol moved the reaction equilibrium towards higher deuteration levels in both cases.

All hydrogen atoms of 2-methylnaphthalene were easily exchanged with deuterium when base catalyst was employed. With both 2-methylnaphthalene and eugenol, only small amounts of by-products were detected in total ion chromatograms of GC-MS, and only occasionally. At best, 0.1% RSD values were obtained in reactions. Reactions with NaOH, NaOD and Na₂CO₃ catalysts produced most repeatable results (RSD < 5%). However, it seems that the equilibrium of the reaction regulates the reaction so that it is not possible to perdeuterate 2-methylnaphthalene with 100% efficiency even under optimal reaction conditions.

5. Acknowledgements

Funding for the research (SUNARE project no. 52746) was obtained from the Academy of Finland. Pekka Tarkiainen is thanked for technical assistance.

References

- 1 W. L. Marshal and E. U. Franck, *J. Phys. Chem. Ref. Data*, 1981, **10**(2), 295.
- 2 E. F. Gloyna and L. ja Li, *Environ. Prog.*, 1995, **14**(3), 182.
- 3 D. B. Mitton, J. C. Orzalli and R. M. Latanision, in *Innovations in Supercritical Fluids, ACS Symp. Ser. 608*, ed. K. W. Hutchenson and N. R. Foster, American Chemical Society, Washington, DC, 1995, ch. 22, 327.
- 4 D. B. Mitton, J.-H. Yoon, J. A. Cline, H.-S. Kim, N. Eliaz and R. M. Latanision, *Ind. Eng. Chem. Res.*, 2000, **39**, 4689.
- 5 B. Kuhlmann, E. M. Arnett and M. Siskin, *J. Org. Chem.*, 1994, **59**, 3098.
- 6 J. Yao and R. F. Evilia, *J. Am. Chem. Soc.*, 1994, **116**, 11229.
- 7 T. Junk and W. J. Catallo, *Tetrahedron Lett.*, 1996, **37**(20), 3445.
- 8 T. Junk and W. J. Catallo, *Chem. Soc. Rev.*, 1997, **26**, 401.
- 9 C. Boix and M. Poliakoff, *Tetrahedron Lett.*, 1999, **40**, 4433.
- 10 T. Junk, W. J. Catallo and J. Elguero, *Tetrahedron Lett.*, 1997, **38**(36), 6309.
- 11 S. Bai, B. J. Palmer and C. R. Yonker, *J. Phys. Chem. A*, 2000, **104**, 53.
- 12 Y. Yang and R. F. Evilia, *J. Supercrit. Fluids*, 1999, **15**, 165.
- 13 E. U. Franck, *Endeavour*, 1968, **27**(101), 55.
- 14 M. M. Hoffmann and M. S. Conradi, *J. Supercrit. Fluids*, 1998, **14**, 31.
- 15 A. F. Thomas, *Deuterium Labeling in Organic Chemistry*, Meredith Corporation, USA, 1971, 1.
- 16 T. Andersson, K. Hartonen, T. Hyötyläinen and M.-L. Riekkola, *Analyst*, 2003, **128**, 150.
- 17 M. B. Smith and J. March, *March's Advanced Organic Chemistry*, 5th edn., John Wiley & Sons, Canada, 2001, 675–677 and 695–696.
- 18 E. M. Karamäki, *Epäorgaaniset kemikaalit, Inorganic Chemicals* (in Finnish) 1st edn., Tietoteos, Finland, 1983, 362–369.



Letter

Ionic liquids and their heating behaviour during microwave irradiation – a state of the art report and challenge to assessment. Letter and reply

Letter: Nicholas Leadbeater^{*a} and **Reply:** Bernd Ondruschka^{*b}

^a Department of Chemistry, King's College London, Strand, London, UK WC2R 2LS. E-mail: nicholas.leadbeater@kcl.ac.uk

^b Institute of Technical Chemistry and Industrial Chemistry, Friedrich Schiller University Jena, Lessingstr. 12, D-07743 Jena, Germany. E-mail: bernd.ondruschka@uni-jena.de

Received 20th August 2003

First published as an Advance Article on the web 22nd September 2003

Letter

I write in connection with the communication by Ondruschka and co-workers recently published in *Green Chemistry* entitled 'Ionic liquids and their heating behaviour during microwave irradiation – a state of the art report and challenge to assessment' (2003, **5**, 296–299). In their communication the authors present the idea of using ionic liquids in conjunction with microwave heating, and in addition their use as heating agents for non-polar solvents in conjunction with microwave irradiation. They fail, however, to reference or acknowledge the work published by our group and also others who have presented similar findings previously.

In 2002, we published a paper in the *Journal of Organic Chemistry* (2002, **67**, 3145) in which we studied the ionic liquid mediated microwave heating of organic solvents. This was an in-depth study and built on a paper by Ley and co-workers in *Journal of the Chemical Society, Perkin Transactions 1* (2001, 358) and a patent by Westman (WO0072956). In their microwave assisted synthesis of thiocarbonyls using a polymer-supported thionating reagent, Ley *et al.* show that addition of a small quantity of an ionic liquid to a toluene solution can greatly increase the rate and yields of reaction. In our paper we built on the idea and showed that hexane and toluene as well as THF and dioxane can be heated way above their boiling point very rapidly in sealed vessels using a small quantity of an ionic liquid thereby allowing them to be used as media for microwave-assisted chemistry. Our attention focused not only on the heating effects but also on studying the contamination, if any, of the parent solvent with the ionic liquid or any decomposition products formed as they are heated. We screened a range of ionic liquids of the 1,3-dialkylimidazolium type. We also showed the use of this heating methodology in three reactions, these indicating the scope and also the limitations of the methodology. We and others have gone on further to use this protocol for synthesis. In 2003 we reported the use of ionic liquids as reagents and solvents in conjunction with microwave heating, focusing on the rapid synthesis of alkyl halides from alcohols and nitriles from aryl halides (*Tetrahedron*, 2003, **59**, 2253). Van der Eycken and co-workers used the methodology in their microwave promoted hetero-Diels–Alder reactions of 2(1*H*)-pyrazinones (*J. Org. Chem.*, 2002, **67**, 7904). There are also numerous other papers published over the last year or two where ionic liquids are used as solvents themselves in microwave-promoted chemistry. For example, Kiddle and co-workers use ionic liquids as solvents for microwave-promoted ring-closing metathesis reactions (*Org. Lett.*, 2002, **4**, 1567). Schotten and co-workers presented the microwave-promoted catalytic transfer hydrogenation of different homo- and hetero-nuclear organic compounds in an ionic liquid as solvent

(*Synlett*, 2002, 1607) and Vallin and co-workers have reported high-speed Heck reactions in an ionic liquid solvent with controlled microwave heating (*J. Org. Chem.*, 2002, **67**, 6243). I stress these are not the only examples found in the recent literature.

In the light of the above, I believe that the authors of the communication should have cited previous work in the field.

Reply

I would like to reply to Nicholas Leadbeater's letter to the Editor concerning our recently published communication in *Green Chemistry* (2003, **5** (3), 296; 'Ionic liquids and their heating behaviour during microwave irradiation – a state of the art report and challenge to assessment'). In his letter, Mr. Leadbeater concluded that the authors (J. Hoffmann, M. Nüchter, B. Ondruschka and P. Wasserscheid) "(had) fail(ed) to cite or acknowledge the work published by his group and also others who have presented similar findings previously."

With respect to our article in question, this conclusion is not true. In the footnote on page 296, we clearly indicated that the content of our communication was already published as a last-minute-poster at the annual 221st ACS Meeting at San Diego, USA, in April 2002, entitled 'Greener Industrial Applications of Ionic Liquids'. After the conference, this poster could and still can be downloaded from the webpage of our institute at <http://www.ituc.uni-jena.de>. The investigations that are reported in the poster as well as in the communication are results from the diploma thesis of J. Hoffmann from 2001 (J. Hoffmann, 'Ionic Liquids in the Microwave Field', Diploma Thesis, University Jena, Jena 2001). Furthermore, physical–chemical aspects of the heating of solvents (including ionic liquids) in the microwave field were discussed at an invited lecture given by B. Ondruschka at the 8th Ampere Meeting in Bayreuth (Germany) in 2001. The manuscript of this lecture has been published in the meantime (unfortunately with a significant delay): J. Hoffmann, A. Tied, M. Nüchter and B. Ondruschka, 'Conventional and New Solvent Systems for Microwave Chemistry', in: *Advances in Microwave and Radio Frequency Processing*, ed. M. Willert-Proada, Springer, Berlin-Heidelberg, 2003, 402.

Apparently, Leadbeater ignored the fact that reference 10 (*Tetrahedron*, 2001, **57**(45), 9225, 'Microwave Assisted Organic Synthesis – A Review') in our article is almost exactly identical, including the figure, to the patent of Westman (WO 00/72956) mentioned by Leadbeater. Therefore, we did not include the patent in our list of references.

It is correct that the works of Leadbeater *et al.* (*J. Org. Chem.*, 2002, **67** (9), 3145) and Ley *et al.* (*J. Chem. Soc., Perkin Trans.*

1, 2001, 358) could have been cited. In the following sections, I would like to explain why they were not cited in our article.

In this context, a database search with SciFinder Scholar (keywords: ionic liquids and microwaves) from 25 July 2003 generated 60 (or 62) hits, whereas a majority of these hits proved to be irrelevant to our topic after reading their abstracts. Otherwise, the results obtained with those two keywords can be subdivided into three fields. First, investigations on the synthesis of ionic liquids using microwaves (*e.g.* R. S. Varma *et al.*, *Chem. Commun.*, 2001, 643; *Tetrahedron Lett.*, 2002, **43** (31), 5381). Second, investigations in which ionic liquids are used as solvents for syntheses in the microwave field (*e.g.* Lee *et al.*, *Bull. Korean Chem. Soc.*, 2002, **23** (5), 667). Third, investigations in which ionic liquids and other co-solvents are used for a systematic synthesis planning in the microwave field. In the latter field, the work of Leadbeater and his co-workers must be mentioned (*e.g.* *Tetrahedron*, 2003, **59** (13), 2253) along with the work of Van der Eycken *et al.* (*J. Org. Chem.*, 2002, **67** (22), 7904).

These works (including research done by personal chemistry) have in common the goal to rapidly heat solvents such as toluene, hexane, THF or dioxane, which do not or do only poorly absorb microwave radiation due to their chemical structure, by adding small amounts (<5 vol%, *cf.* Westman, WO 00/72956, p. 7) of ionic liquids to allow for an optimal synthesis planning. Leadbeater demonstrates several interesting example syntheses in this context. He also mentions,

without providing a thorough explanation, the complex interaction between the planning and the realisation of the physical–chemical environment of such syntheses. The molar amounts of the batches that he investigated in his studies, however, remain limited to (very) small reactor volumes due to the microwave equipment used by his group. The aim of our work (*Green Chem.*, 2003, **5** (3), 296) was to demonstrate that these heating phenomena (ionic liquids in combination with non-polar solvents: toluene or cyclohexane) also prevail on the larger scale of up to 0.5 mol. For heating experiments of non-polar solvents up to high molar amounts see M. Nüchter *et al.*, *Chem. Ing. Tech.*, 2002, **74** (7), 910. Our own experiments in which we carried out synthetic reactions under these conditions are not reported yet (*cf.* ref. [20] in *Green Chem.* 2003, **5** (3), 296). In conclusion, the aforementioned publications by our group deal with physical and reaction engineering problems. Therefore, we believe that articles with this intention do not require a complete reflection of all work that has been carried under the scope of synthesis planning in the microwave field.

In connection with the aforementioned arguments, I am convinced that Leadbeater's Letter to the Editor and my answer point out the importance of the interaction of the two 'green' tools – ionic liquids and microwaves. I would also like to stress the importance of the knowledge of common scientific quotation customs and the somewhat randomness inherent to all database searches.